frontiers | Research Topics

Plant responses to salt stress

Edited by
Keni Cota-Ruiz, Zulfiqar Ali Sahito and
Adalberto Benavides-Mendoza

Published in
Frontiers in Plant Science

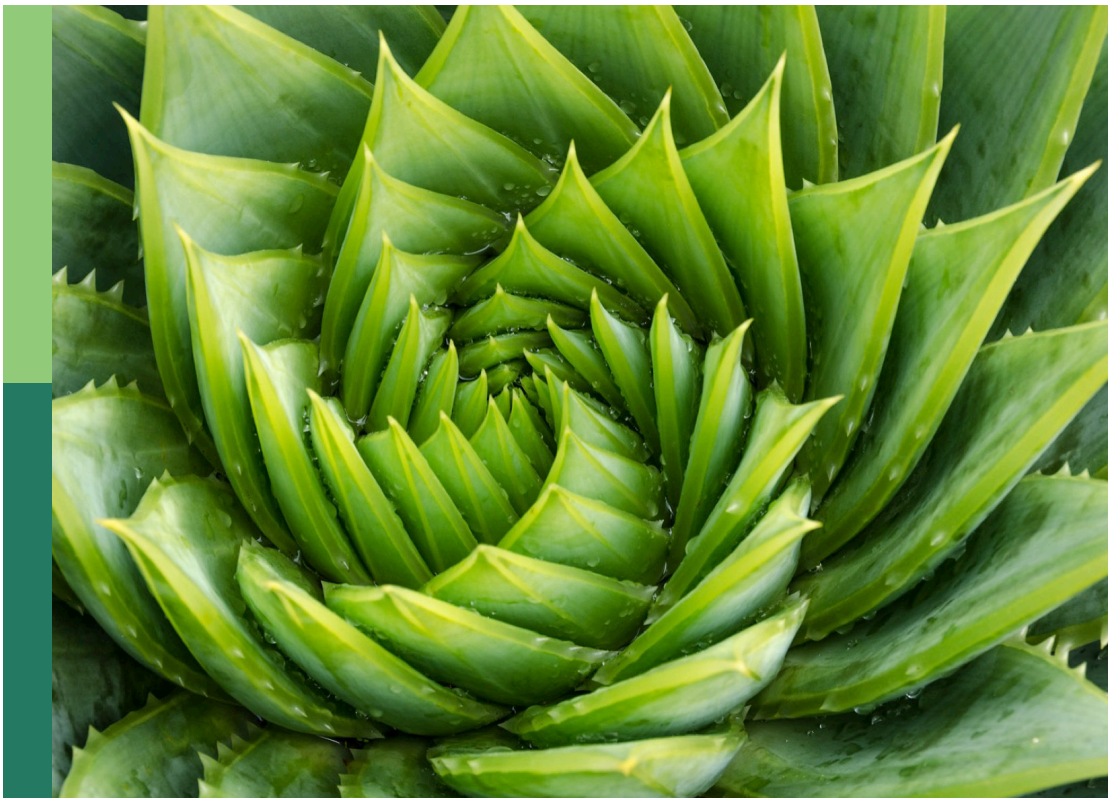

ISSN 1664-8714
ISBN 978-2-8325-5424-1
DOI 10.3389/978-2-8325-5424-1

About Frontiers

Frontiers is more than just an open access publisher of scholarly articles: it is a pioneering approach to the world of academia, radically improving the way scholarly research is managed. The grand vision of Frontiers is a world where all people have an equal opportunity to seek, share and generate knowledge. Frontiers provides immediate and permanent online open access to all its publications, but this alone is not enough to realize our grand goals.

Frontiers journal series

The Frontiers journal series is a multi-tier and interdisciplinary set of open-access, online journals, promising a paradigm shift from the current review, selection and dissemination processes in academic publishing. All Frontiers journals are driven by researchers for researchers; therefore, they constitute a service to the scholarly community. At the same time, the *Frontiers journal series* operates on a revolutionary invention, the tiered publishing system, initially addressing specific communities of scholars, and gradually climbing up to broader public understanding, thus serving the interests of the lay society, too.

Dedication to quality

Each Frontiers article is a landmark of the highest quality, thanks to genuinely collaborative interactions between authors and review editors, who include some of the world's best academicians. Research must be certified by peers before entering a stream of knowledge that may eventually reach the public - and shape society; therefore, Frontiers only applies the most rigorous and unbiased reviews. Frontiers revolutionizes research publishing by freely delivering the most outstanding research, evaluated with no bias from both the academic and social point of view. By applying the most advanced information technologies, Frontiers is catapulting scholarly publishing into a new generation.

What are Frontiers Research Topics?

Frontiers Research Topics are very popular trademarks of the *Frontiers journals series*: they are collections of at least ten articles, all centered on a particular subject. With their unique mix of varied contributions from Original Research to Review Articles, Frontiers Research Topics unify the most influential researchers, the latest key findings and historical advances in a hot research area.

Find out more on how to host your own Frontiers Research Topic or contribute to one as an author by contacting the Frontiers editorial office: frontiersin.org/about/contact

Plant responses to salt stress

Topic editors
Keni Cota-Ruiz — Utica University, United States
Zulfiqar Ali Sahito — Zhejiang University, China
Adalberto Benavides-Mendoza — Universidad Autónoma Agraria Antonio Narro, Mexico

Citation
Cota-Ruiz, K., Sahito, Z. A., Benavides-Mendoza, A., eds. (2024). *Plant responses to salt stress*. Lausanne: Frontiers Media SA. doi: 10.3389/978-2-8325-5424-1

Table of contents

frontiers | Frontiers in Plant Science

TYPE Editorial
PUBLISHED 02 September 2024
DOI 10.3389/fpls.2024.1475599

OPEN ACCESS

EDITED AND REVIEWED BY
Shalini Tiwari,
South Dakota State University, United States

*CORRESPONDENCE
Keni Cota-Ruiz
akcotaru@utica.edu

RECEIVED 04 August 2024
ACCEPTED 21 August 2024
PUBLISHED 02 September 2024

CITATION
Sahito ZA, Benavides-Mendoza A and Cota-Ruiz K (2024) Editorial: Plant responses to salt stress.
Front. Plant Sci. 15:1475599.
doi: 10.3389/fpls.2024.1475599

Editorial: Plant responses to salt stress

Zulfiqar Ali Sahito[1], Adalberto Benavides-Mendoza[2] and Keni Cota-Ruiz[3]*

[1]Industrial Crops Research Institute, Yunnan Academy of Agricultural Sciences (YAAS), Kunming, Yunnan, China, [2]Universidad Autónoma Agraria Antonio Narro, Department of Horticulture, Saltillo, Mexico, [3]Biology Department, Utica University, Utica, NY, United States

KEYWORDS

agriculture, salt stress, salt tolerance, antioxidants, osmolyte accumulation

Editorial on the Research Topic
Plant responses to salt stress

As the world population is increasing, food production largely depends on agriculture. However, crops are under pressure from biotic and abiotic stressors such as climate change, excess agrochemicals, pests, diseases, and soil salinization. The expansion of irrigation practices has led to higher salt contents in agricultural lands, impairing plant function and reducing yields. Hence, investigating how plants behave against salt stress is imperative. Furthermore, a clearer mechanistic understanding of those responses is fundamental to leveraging proactive responses and developing technologies to improve plant fitness and productivity. The articles published in our Research Topic summarize cutting-edge research on the effects of salt stress on several plant species. These studies explore the genetic, physiological, and biochemical responses of plants to salt stress. Below, we contextualize the findings of each article and briefly discuss their impact.

Taybi and Alyahya examined how bread wheat plants cope with salt in their roots and shoots. A comparative RNA sequencing analysis was conducted on bread wheat (Najran cultivar) under unstressed and salt-stressed conditions. The authors reported that more genes were affected in the roots than in the shoots. This study highlighted the potential involvement of glutathione metabolism, secondary metabolite biosynthesis, and galactose metabolism in wheat salt tolerance. These findings could help scientists find ways to make wheat more tolerant to salt, which would be very important for growing enough food.

Meena et al. investigated the potential of the ACC deaminase producer Nocardioides sp. in enhancing wheat growth in saline environments. This research aimed to elucidate the molecular mechanisms that control Nocardioides sp.-facilitated salinity tolerance in wheat. The authors reported that Nocardioides sp. inoculation improved wheat growth under saline conditions and increased biomass. It also increased antioxidant potential and promoted elevated stress-responsive gene transcripts. These findings suggest the potential of Nocardioides sp. to increase wheat tolerance to salinity stress, with implications for agricultural sustainability in saline-prone regions.

Zhang et al. provided a thorough overview of how *Dunaliella salina* responds to salt stress at the transcriptomic level, highlighting the major cellular biological processes that are regulated. The authors revealed the extensive upregulation of genes involved in DNA repair, protein folding, and cell redox homeostasis in response to salt stress. As noted by the

authors, these findings indicate that *D. salina* has developed important mechanisms to survive under salt stress, which were previously overlooked by other researchers. This study encourages a need for further in-depth study in this area.

Ma et al. sequenced libraries prepared from *Suaeda dendroides* plants subjected to both optimal salt and high salt concentrations. This approach resulted in the discovery of differentially expressed genes. The data revealed significant upregulation of genes associated with plant hormone signal transduction, cell wall biosynthesis and modification, organic osmolyte accumulation, ion homeostasis, and reactive oxygen species detoxification in response to high-salt treatment. The relevance of this study lies in its contribution to our understanding of how halophytes adapt to high salinity.

Xu et al. researched the effectiveness of the phytochemical eugenol in promoting salt tolerance in tobacco seedlings through histochemical, physiological, and biochemical methods. They found that eugenol reduces the obstructing effects of salt stress on seedling growth in a dose-dependent manner and that this effect is optimal at 20 μM. Eugenol treatment reduced the accumulation of reactive oxygen species, lipid peroxidation, and osmoprotectant content in salt-stressed seedlings. This study showed that eugenol can increase plant growth in salty soils. This could lead to new ways to help plants thrive in harsh conditions.

Rajabi Dehnavi et al. explored the responses of ten sorghum genotypes to varying salt stress levels. They successfully identified key indicators for salt tolerance, including the K/Na ratio, MDA, MSI, and proline contents, and SOD activity, which proved to be effective in differentiating between tolerant and sensitive genotypes. These findings provide valuable insights for sorghum breeding. The authors emphasized the potential for enhancing salt tolerance in sorghum to support sustainable production in saline environments. The identified salt-tolerant sorghum genotypes, such as Pegah and GS4, are promising candidates for further evaluation in salt-affected environments, with potential benefits for agriculture and food security.

Song et al. identified salt-tolerant and salt-sensitive genotypes of smooth bromegrass. The salt-tolerant genotype, Q25, presented a better performance in diverse characteristics, such as leaf relative water content, photosynthetic performance, and proline content, compared to the salt-sensitive genotype, Q46. KEGG analysis identified genes involved in plant hormone signal transduction and the MAPK signaling pathway responsible for the salt response differences between the two genotypes. This study also uncovered candidate genes associated with salt tolerance, including zinc finger transcription factors. This research offers valuable insights into critical genes linked to salt tolerance, which could help develop salt-tolerant crop varieties to address the adverse effects of salinity on crop yield.

Mi et al. demonstrated distinctive responses of *Astragalus membranaceus* and *Medicago sativa* during seedling growth under salt stress. Their study revealed that salinity directly affects plant characteristics and physiological indices and indirectly impacts leaf succulence. Additionally, the study noted variations in the activity of specific protective enzymes in response to salt stress between the two legumes. This research has implications for agriculture because it helps us understand how legume species respond to salt stress. This is particularly interesting in the context of restoring and utilizing salinized grasslands.

Li et al. examined the genetic factors affecting salt tolerance in maize. They found a specific allele, ZmSC IL76, derived from *Zea perennis*, which increased salt tolerance in maize. This allele had a non-synonymous mutation that improved salt tolerance compared to the ZmSC Z58 allele. Additionally, this study identified ZmSC as a potential regulator of salt tolerance pathways, notably playing a role in controlling ABA content and downstream gene expression. These findings offer valuable insights for further molecular breeding and genetic engineering research to enhance salt tolerance in maize and likely other crops.

Tang et al. focused on assessing the ability of *Miscanthus sacchariflorus* and *M. lutarioriparius* to grow in saline soils for bioenergy production. This study revealed a wide range of salt tolerances among different genotypes, with salt-tolerant variants exhibiting relatively low Na+ levels and a positive relationship between K^+ and Na^+ contents. Additionally, the research highlighted the different mechanisms these plants employ to adapt to salt stress, including regulating ion balance, increasing K^+ absorption, excluding Na^+ from the shoot, and storing Na+ in shoot vacuoles. By establishing a mini-core elite collection for salt tolerance, this study provides a valuable gene pool for future investigations of salt tolerance mechanisms in Miscanthus.

Duan et al. revealed that tetraploid *Plumbago auriculata* plants have an increased tolerance to salt by selectively secreting more sodium (Na^+) compared to diploids when exposed to salt stress. This increased Na+ secretion in tetraploids was associated with increased salt gland calcium (Ca^{2+}) content. The research also investigated the effects of the addition of calcium, inhibition of H_2O_2 generation, and H^+-ATPase activity on sodium and potassium (K^+) secretion rates in both diploid and tetraploid plants under salt stress. These findings provide insights into the mechanisms of salt tolerance in plants, particularly how tetraploid plants may adapt to salt stress by enhancing selective sodium secretion through the modulation of salt gland calcium content.

Author contributions

ZS: Writing – original draft, Writing – review & editing, Conceptualization. AB-M: Writing – original draft, Writing – review & editing. KC-R: Writing – original draft, Writing – review & editing.

Acknowledgments

Grammarly and its AI tool were used to edit and improve the readability of the content.

Conflict of interest

The authors declare that the research was conducted in the absence of any commercial or financial relationships that could be construed as a potential conflict of interest.

Publisher's note

frontiers | Frontiers in Plant Science

TYPE Original Research
PUBLISHED 28 July 2023
DOI 10.3389/fpls.2023.1225541

OPEN ACCESS

EDITED BY
Keni Cota-Ruiz,
Michigan State University, United States

REVIEWED BY
Mohd. Kamran Khan,
Selçuk University, Türkiye
Antonio Lupini,
Mediterranea University of Reggio Calabria, Italy

*CORRESPONDENCE
Tahar Taybi
Tahar.Taybi@newcastle.ac.uk

†These authors have contributed equally to this work

RECEIVED 19 May 2023
ACCEPTED 28 June 2023
PUBLISHED 28 July 2023

CITATION
Alyahya N and Taybi T (2023) Comparative transcriptomic profiling reveals differentially expressed genes and important related metabolic pathways in shoots and roots of a Saudi wheat cultivar (Najran) under salinity stress.
Front. Plant Sci. 14:1225541.
doi: 10.3389/fpls.2023.1225541

Comparative transcriptomic profiling reveals differentially expressed genes and important related metabolic pathways in shoots and roots of a Saudi wheat cultivar (Najran) under salinity stress

Norah Alyahya[1,2†] and Tahar Taybi[1*†]

[1]School of Natural and Environmental Sciences, Newcastle University, Newcastle upon Tyne, United Kingdom, [2]Department of Biology, Faculty of Science, King Khalid University, Abha, Saudi Arabia

High salinity of soil is a threatening constraint for agricultural output worldwide. The adverse effects of salt stress on plants can be revealed in different manners, from phenotypic to genetic changes. A comparative RNA-Sequencing analysis was done in roots and shoots of bread wheat, Najran cultivar between plants grown under unstressed control condition (0 mM NaCl) and salt treatment (200 mM NaCl). More than 135 million and 137 million pair-end reads were obtained from root and shoot samples, respectively. Of which, the mapped reads to *Triticum aestivum* genome IWGSC_V51 ranged from 83.9% to 85% in the root and 71.6% to 79% in the shoot. Interestingly, a comparison of transcriptomic profiling identified that total number of significantly differentially expressed genes (DEGs) examined in the roots was much higher than that found in the shoots under NaCl treatment, 5829 genes were differentially expressed in the roots whereas 3495 genes in the shoots. The salt-induced change in the transcriptome was confirmed by RT-qPCR using a set of randomly selected genes. KEGG enrichment analysis classified all DEGs in both roots and shoots into 25 enriched KEGG pathways from three main KEGG classes: Metabolism, organismal systems and genetic information processing. According to that, the most significantly regulated pathways in the root and shoot tissues were glutathione metabolism and biosynthesis of secondary metabolites such as phenylpropanoids and galactose metabolism suggesting that these pathways might participate in wheat salt tolerance. The findings highlight the importance of the control of oxidative stress via Glutathione and phenylpropanoids and the regulation of galactose metabolism in the roots and shoots for salt-tolerance in wheat. They open promising prospects for engineering salt-tolerance in this important crop via targeted improvement of the regulation of key genes in the production of these compounds.

KEYWORDS

salt stress, salt-tolerance, wheat, RNA-seq, differentially expressed genes (DEGs), salt enrichment pathways, Glutathione and phenylpropanoids

1 Introduction

Environmental stresses including water-stress and salt-stress represent a serious challenge to plant growth and crop productivity. It has been estimated that salt stress could severely restrict the productivity of about 30% arable land by 2050 (Wang et al., 2018). Ranked as the third most important crop, wheat (*Triticum aestivum*) is the staple food in many parts of the world. Unfortunately wheat production, is currently challenged by salinity stress that causes up to 40% yield loss, seriously compromising global food security (Singh et al., 2020).

A considerable number of studies has examined the harmful effects of salt stress on plant life (Borrelli et al., 2018; Hniličková et al., 2019; Tanveer et al., 2020). These harmful effects result first in growth inhibition, then accelerated development, senescence, and ultimately plant death. Accumulation of salts in soil causes a reduction in soil water potential leading to a hyperosmotic and hyper-ionic environment. High levels of salt cause a reduction in the amount of water and essential minerals that plant roots can take up from the soil (Seleiman et al., 2021). Consequently, reduced uptake of mineral nutrients results ultimately in nutritional deficiencies which eventually affect plant growth and reduce crop yield (Hajihashemi et al., 2009). Accumulation of toxic salts in the cell causes inhibition of enzymes which together with stomatal closure result in reduced photosynthetic efficiency, reduced cell elongation and division and thereby decreased biomass accumulation. Stomatal closure under stress results in the generation of reactive oxygen species (ROS), which are very harmful to cells at high concentrations. ROS toxicity causes cellular damage in the form of DNA mutations, protein degradation or lipid peroxidation (Apel & Hirt, 2004; Ahmad et al., 2010). Plants respond to oxidative stress, by synthesizing a variety of protective enzymes that act as an antioxidant scavenging systems (Ayvaz et al., 2016). Extensive research has indicated remarkable increases in the activity levels of scavenging enzymes, such as ascorbate peroxidase, guaiacol peroxidase, glutathione reductase, superoxide dismutase and catalase, in different wheat cultivars to mitigate against ROS-induced oxidative stress (Mandhania et al., 2006; Esfandiari et al., 2007; Rao et al., 2013). Other plant's responses to salt-stress include osmotic adjustment, increased biosynthesis of secondary metabolites, which help plants stay hydrated and maintain ion homeostasis under stress conditions (Ashraf et al., 2008). All the above responses implicate thousands of genes which may be directly or indirectly involved in plant salt tolerance by regulating ion influx and efflux (Li et al., 2020), production and accumulation of osmotica or compatible solutes (Singh et al., 2018), biosynthesis of signaling and regulatory enzymatic and nonenzymatic elements (Thabet et al., 2021). To understand the complexity of the various plant's responses to salt stress, gene expression profiling can be used to identify salt-responsive genes. Many studies used transcriptomics to unravel the genes and associated metabolic pathways and biological functions involved in tolerance of environmental stress in wheat (Goyal et al., 2016; Amirbakhtiar et al., 2019; Luo et al., 2019). Despite the latest interest in transcriptome analysis in wheat under salt stress, all available studies have focused either on roots or shoots. No research has analyzed the effect of salt-stress on gene expression in both roots and shoots simultaneously. In this study, a global RNA-Seq analysis was done in the roots and shoots of a salt-tolerant wheat cultivar (Najran) under two conditions: control (0 mM NaCl) and salt treatment (200 mM NaCl). The current study identified differentially expressed genes revealing key biological pathways and processes involved in wheat responses to salt stress in root and shoot tissues, providing important insights into the molecular mechanisms underlying salt tolerance in this species. To our knowledge this is the first work where salt-induced changes in the transcriptome were analyzed in roots and shoots of the same wheat plants at the same time providing an integrated view of the response of wheat plants to salt-stress. The findings show that the control of oxidative stress via the production of antioxidants including glutathione and phenylpropanoids and galactose metabolism in roots and shoots are key pathways in the salt-tolerance trait in wheat. They offer a promising avenue for developing salt-tolerance in wheat via marker-assisted breeding or via genetic engineering technologies including gene editing to optimize the expression of targeted genes in these pathways.

2 Material and methods

2.1 Plant growth and salt stress treatment

Seeds of Najran wheat cultivar (accession No. 193) were obtained from Ministry of Environment, Water & Agriculture, Saudi Arabia. Cold-stratified seeds were germinated as three seeds per pot in 2L pots filled with 2:1:1 (v/v/v) mix of John Innes soil compost No. 2, vermiculite, and grit sand, respectively. After germination plants were divided into two groups, each group having a salt-treated batch and water-control batch.

The first group consisted of (1) unstressed control plants, watered with tap water and (2) salt-treated plants, watered with 200 mM NaCl solution. These plants were grown for 4 weeks from germination to full vegetative growth. Plants from this group were used to measure growth and extract RNA for sequencing.

The second group consisted of (1) unstressed control plants, watered with tap-water and (2) salt-treated plants watered with 100 mM NaCl solution. These plants were grown until flowering and seed production. Spikes were harvested when seeds became dry.

All plants were watered every other day and kept under controlled conditions; 16 h light at 20°C, 8 h dark at 15°C and 70% humidity.

2.2 Growth and yield analysis

Roots and shoots were harvested separately at midday, and roots washed thoroughly to remove soil and dried with paper towel. Different growth parameters including root and shoot fresh weight, dry weight and length were recorded. Roots and shoots were grouped into three replicates (each sample had a duplicate of plants), snap frozen in liquid nitrogen and stored at -80°C, they were later ground to a fine powder under liquid nitrogen to be used

in RNA extraction. Dry weight was determined after drying plant tissues in an oven at 80°C for 7 days. To evaluate the impact of salt-stress on yield, the number of spikes and seeds was determined, and seed weight measured in control and salt-treated plants. Root and shoot Dry weight and number of spikes per plant and number of seeds per plant obtained.

2.3 RNA extraction and qualification

Total RNA was extracted from twelve root and shoot samples using Plant/Fungi Total RNA Purification Kit, according to the manufacturer's instructions (Cat. 25800, Norgen, Canada) and treated with RNase-Free DNase I (Cat. 25710, Norgen) during RNA purification. RNA purity and quality were assessed using NanoDrop 1000 spectrophotometer whereas its integrity was examined by RNA 6000 Nano Kit for Agilent 2100 Bioanalyzer (Agilent Technologies, Waldbronn, Germany). High quality RNA samples with RIN ≥ 7.2 were sent to Admera Health LLC (New Jersey, USA) for cDNA library construction and sequencing.

2.4 Illumina library construction and transcriptome sequencing

According to Admera Health LLC, the quality of 20 µl RNA samples was assessed by High Sensitivity RNA Tapestation (Agilent Technologies Inc., California, USA) and quantified by Qubit 2.0 RNA HS assay (ThermoFisher, Massachusetts, USA). Paramagnetic beads coupled with oligo d(T)25 were combined with total RNA to isolate poly (A)+ transcripts based on NEBNext® Poly(A) mRNA Magnetic Isolation Module manual (New England BioLabs Inc., Massachusetts, USA). Prior to first strand synthesis, samples were randomly primed (5′ d(N6) 3′ [N=A,C,G,T]) and fragmented based on manufacturer's recommendations. The first strand was synthesized with the Protoscript II Reverse Transcriptase with a longer extension period, approximately 40 minutes at 42°C. All remaining steps for library construction were done according to the NEBNext® Ultra™ II *Non-Directional* RNA Library Prep Kit for Illumina® (New England BioLabs Inc., Massachusetts, USA). Final libraries quantity was assessed by Qubit 2.0 (ThermoFisher, Massachusetts, USA) and quality was assessed by TapeStation D1000 ScreenTape (Agilent Technologies Inc., California, USA). Final library size was about 430bp with an insert size of about 300bp. Illumina® 8-nt dual-indices were used. Equimolar pooling of libraries was performed based on QC values and sequenced on an Illumina® Novaseq S4 (Illumina, California, USA) with a read length configuration of 150 PE for *40*M total reads per sample (*20*M in each direction).

2.5 RNA-seq data analysis

The workflow of RNA-Seq data analysis started with the pre-processing of the raw reads and ended with identifying enriched KEGG pathways for the DEGs (Figure S1). All data presented and discussed in this study have been deposited in NCBI's Gene Expression Omnibus and are accessible through GEO Series accession number GSE225565 (https://www.ncbi.nlm.nih.gov/geo/query/acc.cgi?acc=GSE225565).

2.5.1 Quality control and read quantification

Raw sequences from FASTQ files generated by Illumina were assessed with FastQC (version 11.8, http://www.bioinformatics.babraham.ac.uk/projects/fastqc). A total of 136281942 and 138608660 paired-end reads were obtained from twelve control and salt stressed samples of root and shoot tissues, respectively (Table 1). Trimmomatic (version 0.36, http://www.usadellab.org/cms/?page=trimmomatic) was used for trimming out contaminating adaptor sequences and producing filtered reads (Bolger et al., 2014).

TABLE 1 Summary of sequencing output, clean reads and mapping on the genome. R indicates root and S indicates shoot.

Sample	Total reads	High quality reads	Mapped reads
Ctrl_R_1	23001104	22838034	19425012
Ctrl_R_2	26022495	25836862	21983090
Ctrl_R_3	21950892	21726586	18437481
Salt_R_1	24008611	23818150	20066908
Salt_R_2	20462131	20265845	17006769
Salt_R_3	20836709	20702466	17395220
Ctrl_S_1	20340235	20188148	14449739
Ctrl_S_2	27874023	27720205	21256010
Ctrl_S_3	26033823	25804393	19259820
Salt_S_1	20727638	20590369	15766118
Salt_S_2	20869668	20721980	16374493
Salt_S_3	22763273	22575139	17764005

High-quality reads were quantified against transcripts derived from the Ensembl *T. aestivum* genome (version 51, https://plants.ensembl.org/Triticum_aestivum/Info/Index). Salmon (version 0.12.0, https://combine-lab.github.io/salmon); a tool which performs 'quasi-alignment' was used to quantify expression of transcripts from RNA-Seq data via read abundances. To quantify the levels of gene expression (gene-level counts), the R package 'tximport' (version 1.18.0, http://bioconductor.org/packages/release/bioc/html/tximport.html) was used.

2.5.2 Differential gene expression analysis

Differentially expressed genes (DEGs) were identified using the R package DESeq2 (version 1.30.1, http://bioconductor.org/packages/devel/bioc/vignettes/DESeq2/inst/doc/DESeq2.html). DESeq2 estimates fold change between experimental conditions (Table 2) in the root and shoot samples using a Negative Binomial GLM (General Linear Model) with a logarithmic link function. According to that, genes which have base 2 logarithmic fold change ≥1 and a cut-off of adjusted P-value (false discovery rate (FDR)) < 0.01 were considered as upregulated genes, whereas genes with a fold-changes ≤ −2 ($Log_2 \leq -1$) have been indicated as downregulated genes.

2.5.3 GO terms analysis

The GO terms enrichment analysis was done by searching the Gene Ontology resource (http://geneontology.org/) using the obtained DEGs against the wheat repository. Testing for enriched GO terms was carried out using the hyper GTest function from the R package GO stats, with a p-value test at cut-off of 0.05.

2.5.4 Functional enrichment analysis

The Kyoto Encyclopedia of Genes and Genomes (KEGG) was searched to identify enriched KEGG pathways for the DEGs. KEGG pathways for *T. aestivum* were obtained using the R package 'KEGGREST' (version 1.34.0, https://bioconductor.org/packages/release/bioc/html/KEGGREST.html). Protein sequences for wheat genes were downloaded in FASTA format using the ID mapping tool from UniProt (https://www.uniprot.org/uploadlists/). KEGG's 'GhostKOALA' search (https://www.kegg.jp/ghostkoala) was used to find KEGG orthology IDs for wheat genes based on the UniProt FASTA download. The KEGG orthology numbers enabled a mapping from wheat genes to KEGG pathways. Enriched KEGG pathways for the lists of significantly DEGs were calculated using a hypergeometric test with the corrected P-value < 0.05.

2.6 Validation of RNA-sequencing results using quantitative real-time PCR analysis

To validate the gene expression profiles obtained from the analysis of RNA-Seq data, eight genes differentially expressed under salt-stress were randomly chosen and their transcript levels monitored by RT-qPCR using the same RNA samples to RNA-Seq. The genes included four genes upregulated in both roots and shoots, two genes down-regulated in roots and shoots, one gene upregulated in roots and downregulated in shoots and one gene down regulated in roots and up-regulated in shoots (Table S1). Gene-specific primers (Table S2) for RT–qPCR (18–21 bp) were designed using Primer3(v. 0.4.0). cDNA was synthesized from twelve purified RNA samples using Tetro^{TM} cDNA Synthesis Kit (Bioline, UK) according to the manufacturer's procedure using Oligo dT primer. The SensiFAST^{TM} SYBR Hi-ROX Kit (Bioline, UK) was used to perform qPCR in Rotor Gene Q5 & Qiagility Robot instrument (Qiagen, UK) based on the manual of SYBR Hi-ROX Kit (Bioline, UK) using cDNA as template. Normalization of gene expression level was done using CJ705892 gene as a housekeeping (internal control) gene from wheat (Dudziak et al., 2020). Primer efficiency was determined using serial dilutions of the cDNA for each gene, it ranged from 95% to 103%. Relative gene transcript levels of the target genes were quantified using the standard $2^{-(\delta\delta Ct)}$ method (Livak & Schmittgen, 2001).

3 Results

3.1 Plant growth and yield

Salt stress resulted in important reductions in all growth parameters tested in this study. Plants subjected to salt-stress (200 mM NaCl) have shown 8.3-, 7.8-fold decrease in their root and shoot fresh weight, respectively (Figure 1A). Similarly, salt-stress caused a 9.3- and 8.7-fold decrease in the root and shoot dry weight, respectively in these plants (Figure 1B). Salt stress also affected plant's height, as shown in Figure 1C salt-stressed plants have shown approximately 39% and 36% decline in the length of roots and shoots respectively.

Interestingly, despite the negative effect on plant growth, salt-stress with 100 mM NaCl resulted in increased number of spikes and seeds per plant. As shown in Figure 2A, spike number per plant increased to more than two-folds under salt-stress compared to control plants (P < 0.01). Similarly, seed number per plant increased under salt-stress by 62.5% (Figure 2B). In contrast, the weight of seeds (0.21 g) decreased by 84% of the control (1.33 g) (P < 0.001) under saline conditions (Figure 2C)

3.2 Transcriptome profiling and sequencing statistics

In order to investigate the regulatory mechanism of wheat responses to salinity stress at transcriptional level, RNA sequencing was carried out in the root and shoot tissues of Najran cultivar. Three biological replicates for each tissue and treatment were used in Illumina high-throughput sequencing. The number of raw reads obtained varied from 20.34 million to 27.87 million for 12 samples with a mean of 22.90 million. A total of 272788177 high-quality pair-end reads (99% of the raw reads) were generated from all samples; 135187943 and 137600234 reads from roots and shoots (Table 1), respectively. All the clean reads were quantified against transcripts of *T. aestivum* genome IWGSC_V51 (accessed Nov. 2021), resulting in mapped reads ranging from

TABLE 2 Number of total differentially expressed genes (DEGs) and up/down-regulated genes in the root and shoot tissues of Najran wheat cultivar under 0 mM NaCl (control) and 200 mM NaCl (salt treatment) conditions.

	Total DEGs	Up-regulated	Down-regulated	Up_differences % ratio	Down_differences % ratio
Salt treated Root vs Control Root	5829	2226	3603	38.19	61.81
Salt treated Shoot vs Control Shoot	3495	1473	2022	42.15	57.85

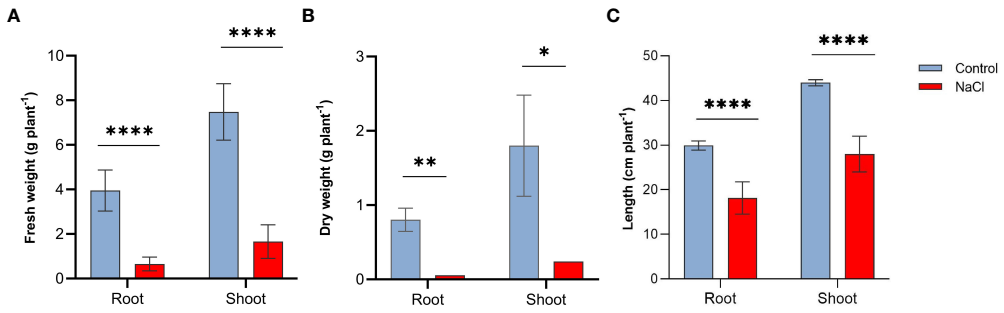

FIGURE 1
Effect of salt-stress on **(A)** fresh weight, **(B)** dry weight, and **(C)** lengths of the root and shoot of wheat *(Triticum aestivum)* (n=6 +/- S.E) plants subjected to salt-stress (200mM NaCl) or watered with tap water only (control). Columns with asterisks refer to the significant difference between control and salt stressed samples assigned using Independent T-Test ($P \leq 0.05$). ns means P-value > 0.05, * means $P \leq 0.05$, ** means $P \leq 0.01$, **** means $P \leq 0.0001$.

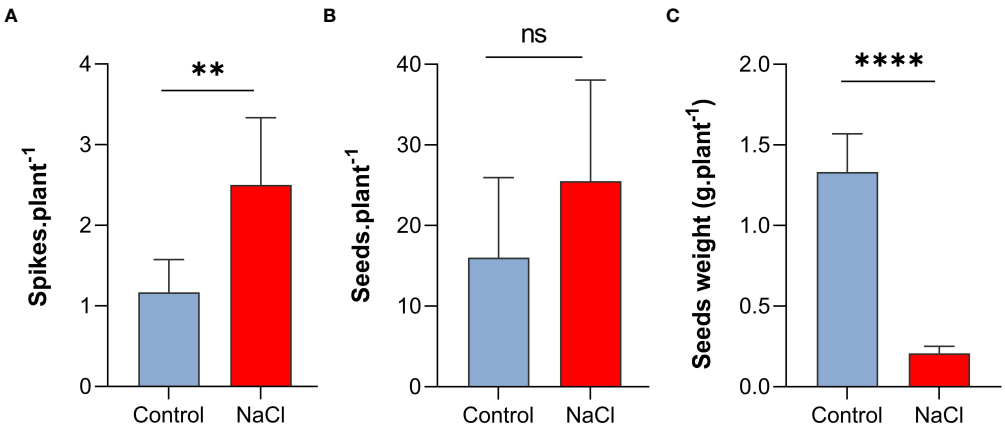

FIGURE 2
Effect of salt-stress on **(A)** spikes number, **(B)** seeds number, and **(C)** seeds weight of wheat *(Triticum aestivum)* (n=6 +/- S.E). plants subjected to salt-stress (200mM NaCl) or watered with tap water only (control). Columns with asterisks refer to the significant difference between control and salt stressed samples assigned using Independent T-Test ($P \leq 0.05$). ns means P-value > 0.05, * means $P \leq 0.05$, ** means $P \leq 0.01$, **** means $P \leq 0.0001$.

83.9% to 85% (17006769 to 21983090 reads) in the root and 71.6% to 79% (14449739 to 16374493 reads) in the shoot (Table 1).

3.3 Differential gene expression analysis

Transcript abundance of each gene expressed under 0 or 200 mM NaCl conditions and mapped was normalized, then the significance of difference in transcript abundance in the root and shoot tissues was determined based on the thresholds of adjusted P-value (FDR < 0.01). Interestingly, a total of 5829 genes were differentially expressed in the roots under salt treatment, including 38.19% up-regulated genes and 61.81% down-regulated genes (as obviously depicted in the volcano plot Figure 3A). On the other hand, 3495 DEGs were revealed between the control and salt treated shoots; 42.15% of them were up-regulated, while 57.85% were down-regulated (Figure 3B). Only 1205 from 5829 genes expressed in roots and 733 from 3495 genes in shoots had annotated functions (Table 2).

The number of genes that were identified as DEGs in roots and shoots was compared and the overlap of DEGs in the two organs analyzed using a Venn diagram (Figure 4). The Venn diagram

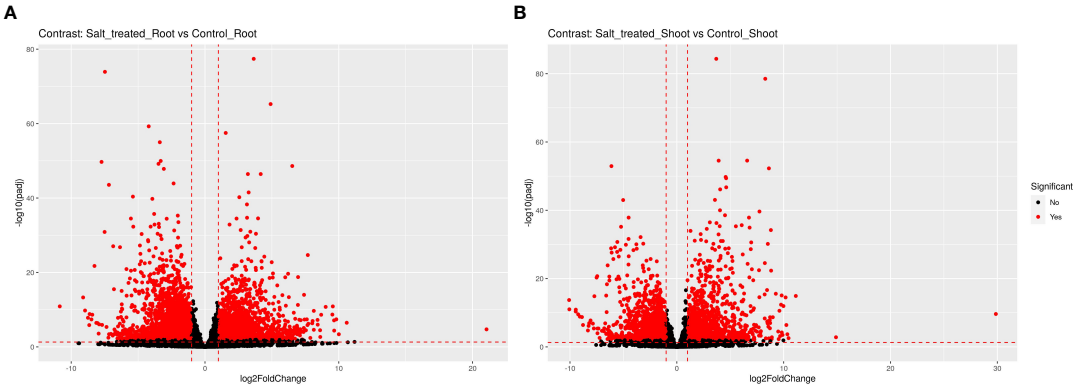

FIGURE 3
The volcano plot (log_2 FC ≥1 or ≤ -1, p-adj ≤ 0.01) of differentially expressed genes in roots and shoots of Wheat (Najran) under salt-stress (200mM NaCl). DEGs in **(A)** salt-treated root versus control root, **(B)** salt-treated shoot versus control shoot. Red dotes towards the right indicate statistically significant-upregulated genes, red dotes towards the left indicate statistically significant-downregulated genes and black dotes indicate non-significant genes.

showed that only 1158 genes were overlapping genes expressed in roots and shoots under salt-stress conditions.

3.4 Cluster analysis of RNA-sequencing data

To have an overview of the relationship of expression patterns between the control and salt stressed samples as well as between the roots and shoots, Principal Component Analysis (PCA) and hierarchical clustering methods were used. PCA, showed that 98% variance was observed between the root and shoot samples (Figure 5A). Moreover, these two distinct groups formed based on their expression profile; one group comprised control and salt-treated roots and the other group comprised shoots from non-stressed and stressed plants. On the other hand, the PCA plot in Figure 5A demonstrated that the outlier (Salt-treated root) at the middle west of the plot is almost entirely responsible for the variation seen in the second principal component (1% of the variation in the entire dataset).

The heatmap visualization of gene expression, combined with clustering method grouped the 12 samples based on similarity of their gene expression pattern and these classifications were consistent with the PCA findings. The color and intensity of heat map boxes was used to represent the similarity in gene expression, the darker the blue color, the more similarity between samples. The heatmap analysis indicated the notable difference between the control and salt treated samples in both roots and shoots and a massive difference between the gene expression profiles of the roots and shoots (Figure 5B). These variations in gene expression patterns among wheat samples are a result of exposing plants to salt stress as well as differences in plant organs.

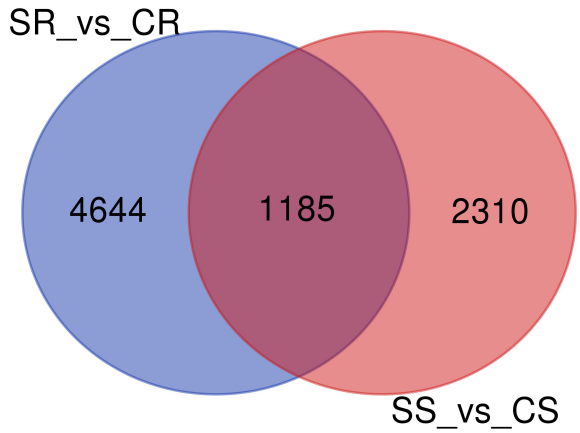

FIGURE 4
Venn diagram of differentially expressed genes (DEGs)in roots and shoots of Najran wheat *(Triticum aestivum)* under salt-stress (200mM NaCl). The numbers in the Venn diagram indicate DEGs in salt treated-roots vs. control-roots (SR_vs_CR), root and salt-treated shoots vs. control-shoots; (SS_vs_CS).

3.5 GO terms enrichment of DEGs

To determine the functional meaning of the salt-induced changes in the transcriptome in roots and shoots of Najran Wheat, we performed the GO terms enrichment for the DEGs in the two organs.

As shown in the heatmap of Figure 6, the DEGs in roots and/or shoots were associated with 76 functional categories in total. The DEGs were associated with 48 “biological process” categories, 19 “molecular function” categories and 9 “cellular component” categories. Exactly 35 categories were present only in roots and 16 were present only in shoots while 25 categories were present in both organs. Among the categories enriched in roots there were processes involved in cell ionic homeostasis, oxidative stress responses including Glutathione synthesis, osmotic stress response, hormonal signaling, carbohydrate transport etc. Among the categories enriched in shoots there were protein folding, photosynthesis, synthesis of secondary metabolites, response to Abscisic acid, hormonal-signaling. Among the categories enriched

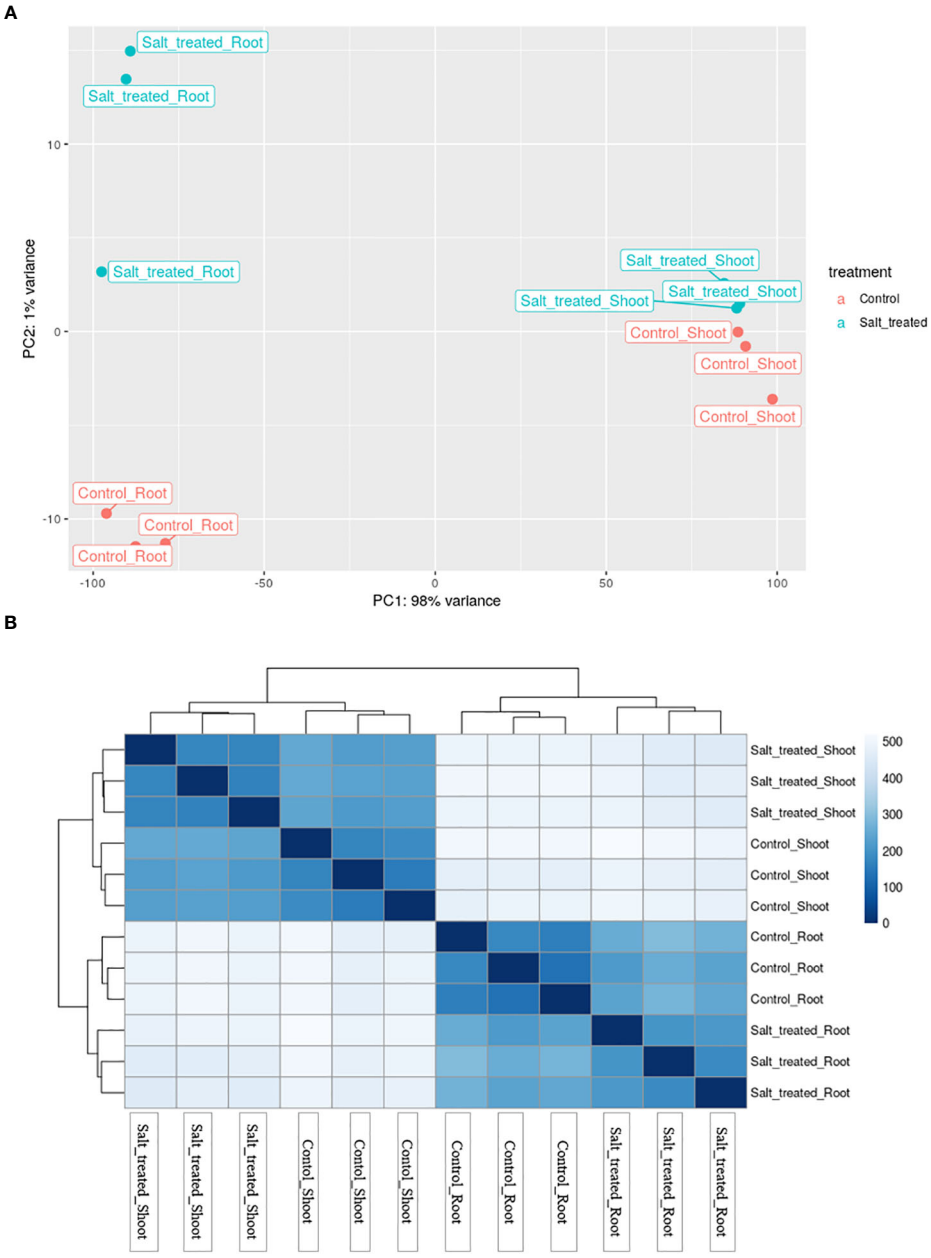

FIGURE 5
(A) Principal component analysis (PCA) of differential gene expression in Najran wheat (*Triticum aestivum*) subjected to salt-stress (200mM NaCl). Samples showing the relationship between salt stressed and control roots and shoots. Blue color refers to control samples and orange color to salt treated samples. **(B)** Heatmap showing the clustering and relationship of gene expression in salt-stressed and control roots and shoots, each sample being represented by three replicates. Darker color refers to more similarity between samples.

in both organs we find response to oxidative stress response, glutathione synthesis and carbohydrate transport.

3.6 KEGG enrichment analysis of DEGs and functional annotations

To identify which biological pathways for the DEGs were potentially enriched in the roots and shoots of Najran cultivar transcriptome, KEGG enrichment analysis was done for all pairwise comparisons. The KEGG analysis revealed that all DEGs in both roots and shoots could be classified into 25 enriched KEGG pathways which located in three main KEGG classes; metabolism, organismal systems; environmental adaptation and Genetic information processing; folding, sorting and degradation (Figure 7A, Tables S3, S4). Among them, the number of DEGs was the largest in metabolism category, which included 4044 genes involved in different pathways such as biosynthesis of secondary metabolites, Amino acid metabolism, Carbohydrate metabolism, Metabolism of cofactors and vitamins and other compounds.

Pathways relating to glutathione metabolism, galactose metabolism and thiamine metabolism were significantly

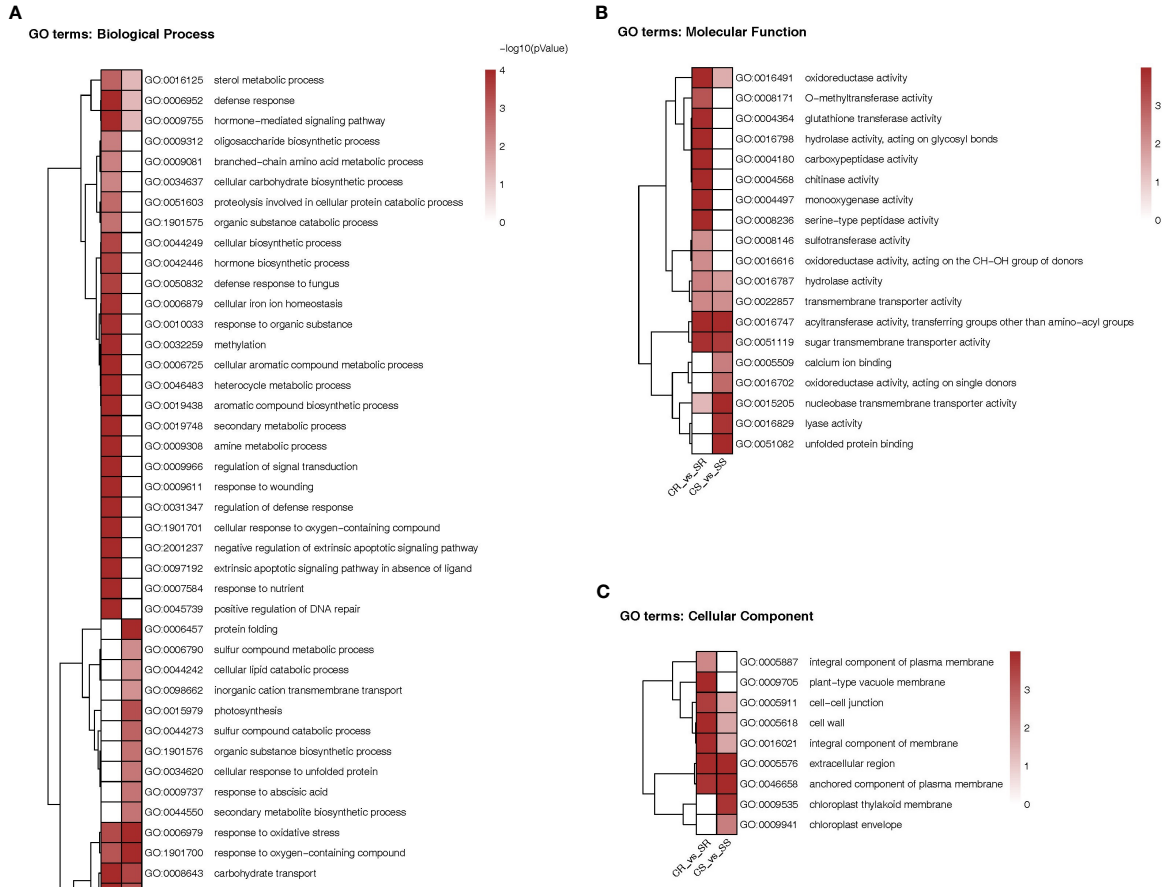

FIGURE 6
Heatmap comparison of Gene Ontology classifications of DEGs in roots and shoots of Najran Wheat plants under salt stress (200 mM NaCl) versus unstressed control. The heatmaps representing GO terms based on **(A)** biological process (45 categories), **(B)** molecular function (19 categories) and **(C)** cellular component (9 categories). The color scale indicates different levels of significance of enriched terms (P-value < 0.05).

upregulated in the roots under salt stress (Figure 7B), where glutathione metabolism had the highest number of DEGs (Figure S2). In contrast, the significantly enriched pathways in the salt treated shoot were biosynthesis of secondary metabolites, protein processing in endoplasmic reticulum, starch and sucrose metabolism, phenylpropanoid biosynthesis, galactose metabolism and phenylalanine metabolism pathways (Figure 7C). Most of DEGs were related to biosynthesis of secondary metabolites such as genes associated with phenylpropanoids (Figure S3).

Comparing salt-stress to control plants revealed three and six different pathways preferably enriched in salt treated roots vs control roots and salt treated shoots vs control shoots, respectively (Table S4). Interestingly, the only common pathway between salt treated roots vs control roots and salt treated shoots vs control shoots was galactose metabolism (Figure S4), which is part of carbohydrate metabolism and has been reported to have a role in salt tolerance (Darko et al., 2019).

3.7 Validation of RNA-seq results using quantitative real-time PCR analysis

To validate the change in transcript-levels revealed by RNA-Seq data, transcript levels of eight DEGs in both roots and shoots of Najran wheat were measured by RT-qPCR. The results of this analysis (Figure 8) confirmed that change (up or down-regulation depending on gene) in transcript levels was consistent with that obtained by RNA-Seq for the selected genes including heat shock protein 90, dirigent protein, delta-1-pyrroline-5-carboxylate synthase, flavin-containing monooxygenase, glutamate receptor, lipoxygenase,

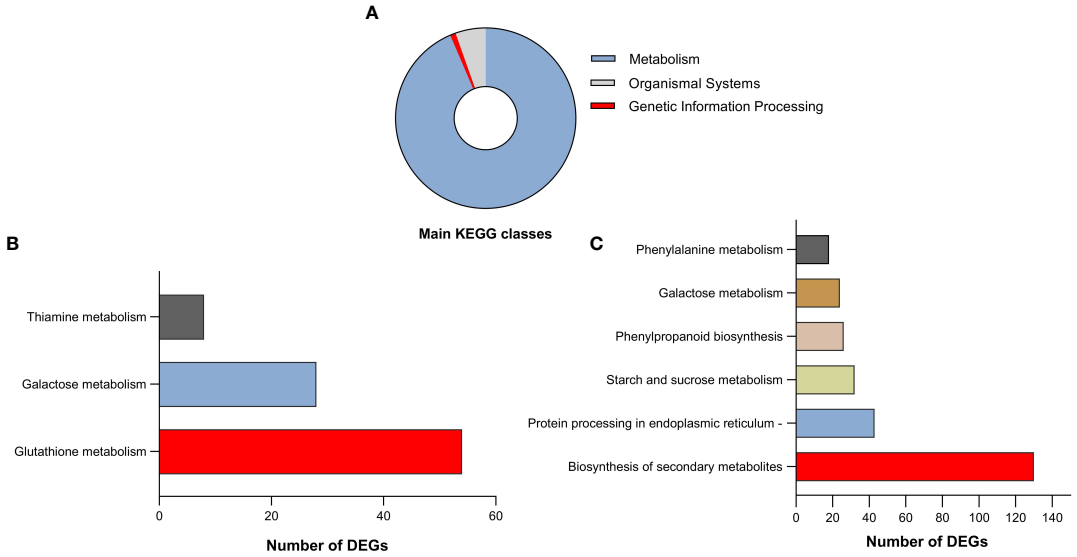

FIGURE 7
(A) Categorization of the identified differentially expressed genes in both roots and shoots of Najran wheat (*Triticum aestivum*) in three chief KEGG classes. The top significantly enriched pathways of identified DEGs in roots **(B)** and shoots **(C)** in response to salinity stress.

bidirectional sugar transporter SWEET and ABA inducible protein. The log2 fold change in transcript levels for the eight randomly selected genes measured by RT-qPCR and RNA-Seq is shown in Figure 8.

4 Discussion

4.1 Growth and yield

Salt-stress caused a significant reduction in root and shoot growth of Najran wheat. This decrease in growth and biomass is common to most non-halophytic plants including wheat which is considered as a salt-tolerant non halophyte. A previous study compared the effect of salt-stress on the growth of three wheat cultivars from Saudi Arabia including Najran, Qiadh, Mebiah, the results concluded that among the three cultivars, Najran was the least impacted by salinity (Alyahya and Taybi unpublished). Similarly, Alfagham (2021) compared the effect of water-stress on the growth of six wheat cultivars including Najran, Jaizan, Sama, Rafha, Ma'ayah and Najd and concluded that Najran was the least impacted by water-stress. In contrast to growth and biomass, salinity has increased the number of spikes and seeds per plant in Najran wheat. Although the seeds were smaller, they maintained a full-germination rate compared to seeds obtained from unstressed plants. This response clearly suggests a high degree of adaptability of this wheat cultivar to survive and maintain itself under stressful conditions. Dadshani et al. (2019) have shown that salt-stress decreases root and shoot growth (dry weight and length) in three wheat genotypes, SBLs, Zentos, Syn86. Moreover, high soil concentrations of some mineral

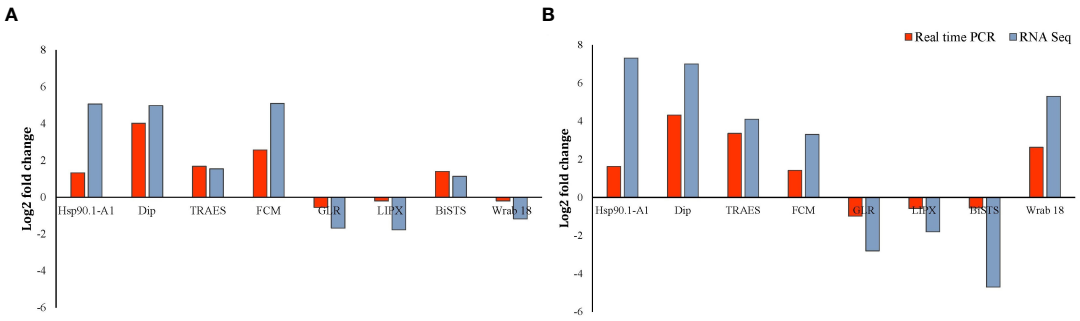

FIGURE 8
RT-qPCR validation of the salt-induced transcript change in Najran wheat (*Triticum aestivum*) subjected to salt- stress (200 mM NaCl). Log2 fold change in transcript levels is shown in root **(A)** and shoot **(B)** for eight genes including four up-regulated genes in roots and shoots (TaHSP 90, TaDip, Tres CFD, TaCFM), two genes down regulated in roots and shoots (TaGLR and Ta LIPX), one gene upregulated in roots and down regulated in shoots (taBiSTS) and one gene down regulated in roots and up-regulated in shoots (TaWrab18). Red bars represent qPCR results, whereas blue bars represent the results of RNA sequencing.

nutrients like Boron, impact negatively growth in different wheat cultivars (Pandey et al., 2022; Khan et al., 2023).

4.2 Differential gene expression

Global profiling of the transcriptome of roots and shoots of Najran wheat revealed profound changes in gene expression under salt-stress as shown by the high number of DEGs. The expression of about 6.5% and 3.9% of the estimated 90000 wheat genes changed in roots and shoots respectively under salt-stress. Among the identified DEGs, candidate genes related to key pathways with important roles in adaptation and responses to salt stress were identified. It is worth noting the levels of transcriptional changes under abiotic stresses vary between plant tissues, this being observed to a greater extent in tissues sensing stress early rather than those subsequently detecting it. Roots of drought-treated Arabidopsis plants, undergo higher levels of transcriptional alterations compared to shoots under water-stress, suggesting that the physiological adjustments induced in roots were deeper to those induced in shoots (Bashir et al., 2018). Goyal et al. (2016) have shown that 17,911 genes were differentially expressed under salt-stress in roots of Kharchia wheat. Similarly, Amirbakhtiar et al. (2019) have shown that 5128 were differentially expressed under salt-stress in roots of Arg wheat. Among these genes, there were genes for sensing and signaling of salt stress such as genes that encode calcium transporters (Ta.ANN4, Ta.ACA7, Ta.NCL2 and Ta.GLR) and SOS1 (Na^+/H^+ antiporter), genes coding for transcriptional regulators such as transcription factors (MYB, bHLH, AP2/ERF, WRKY, NAC, and bZIPs) as well as genes related to salt stress adaptation, including genes coding for LEA proteins, Aquaporins, P5CS, dehydrins, ABA and K+ transporters (Ta.ABAC15, Ta.HAK25), catalases, glutathione-S-transferases.

Roots as the first organ encountering salinity in the surrounding media often respond by deploying specific responses to maintain water and nutrient uptake while limiting the uptake of toxic ions and potentially extruding them (Rajaei et al., 2009). On contrast, plant shoots detect and respond to salt-stress at a later stage, they might deploy specific responses to keep cells hydrated and protect metabolism from inhibition including photosynthetic reactions to keep growth. Shoots have higher sensitivity to salinity than the roots (Esechie et al., 2002).

4.3 Functional enrichments of the DEGS

Functional enrichment of the DEGs in roots and shoots of Najran wheat revealed important biological and molecular functions that may be key to the survival and development of this wheat cultivar under salinity. Genes associated with glutathione metabolism, galactose metabolism and thiamine metabolism were differentially regulated in roots of salt treated Najran wheat compared to the control. The highest number of DEGs was in glutathione metabolism pathway. These DEGS included fifty genes coding for glutathione S-transferase (GST) and one gene coding for glutathione dehydrogenase. Three genes encoded glutathione synthase (GSS) were however downregulated in response to salinity stress. Exposure of plants to salt stress may increase the production of reactive oxygen species (ROS) which might lead to cellular damage via protein denaturation, peroxidation of membrane lipids, DNA mutation, pigment breakdown and carbohydrate oxidation (Noctor and Foyer, 1998; Ahmad et al., 2010). To alleviate ROS-destructive effects, plants have evolved ROS-scavenging systems, including regulatory enzymes eg. glutathione transferase (GT), ascorbate peroxidase (APX), catalase (CAT), and nonenzymatic elements (metabolites such as phenolics, glutathione, flavonoids, ascorbic acid, carotenoid). The detoxifying role of these enzymes and antioxidants has been reported to enhance salt tolerance in many plants such as GST in Arabidopsis (Qi et al., 2010), glutathione peroxidase (GPX) in rice (Paiva et al., 2019), phenolic acids in cabbage (Linić et al., 2019), APX, CAT, superoxide dismutase (SOD) and peroxidase (POD) in Tobacco (Li C et al., 2020) and flavonoids in *Ginkgo biloba* (Xu et al., 2020). The significantly enriched pathways in shoots of salt-treated plants included biosynthesis of secondary metabolites, protein processing in endoplasmic reticulum, starch and sucrose metabolism, phenylpropanoid biosynthesis, galactose metabolism and phenylalanine metabolism pathways. Most DEGs in shoots of Najran wheat were related to biosynthesis of secondary metabolites pathway. Secondary metabolites play important roles in plants acclimation to different environmental stresses. In this study, genes associated with phenylpropanoid, galactose metabolism, fatty acid elongation, flavonoid biosynthesis, starch and sucrose metabolism and lignin synthesis pathways were shown to be significantly regulated in shoots under NaCl stress. As an example of the salt-regulated genes in phenylpropanoid biosynthesis there were genes encoding phenylalanine ammonia-lyase (PAL), two isogenes encoding for caffeoyl shikimate esterase (CSE), one isogene encoding for cinnamoyl-CoA reductase (CCR) and one isogene encoding ferulate-5-hydroxylase (CYP84A). All these genes have previously been documented to participate in salt tolerance in (Amirbakhtiar et al., 2021; Kong et al., 2021). In phenylpropanoid biosynthesis, PAL is involved in the first step of synthesizing trans-cinnamate from L-phenylalanine and acts as one of the antioxidative components produced under stress to minimize oxidative damage induced by salt stress (Gholizadeh and Kohnehrouz, 2010). The final products in this metabolic pathway are lignin components, including syringyl lignin, 5-hydroxy-guaiacyl-lignin and guaiacyl lignin. It is widely known that plants synthesize lignin to maintain the structural integrity of cell wall and the rigidity of the stem helping the plants to cope with various environmental stresses (Rao et al., 2017). More recent work highlighted the important regulatory role of NAC transcription factor (AgNAC1) in lignin biosynthesis which ultimately enhances salt tolerance in *Arabidopsis thaliana* plants (Duan et al., 2020). In the present study, one NAC domain-containing gene was significantly up-regulated in wheat shoots and five genes were down-regulated in the roots. Another study conducted on *Betula platyphylla* suggested the positive correlation between overexpression of BpNAC012 and lignin biosynthesis and its crucial role in the tolerance of both salt and osmotic stresses (Hu et al., 2019).

Luo et al. (2019) carried out functional enrichment analysis for DEGs induced under salinity stress in new leaf, old leaf, and root

tissues of two wheat varieties, Zhongmai 175 and Xiaoyan 60, they found that metabolic pathways including those for phenylpropanoid biosynthesis, biosynthesis of secondary metabolites, benzoxazinoid biosynthesis and starch and sucrose metabolism were significantly enriched in the three organ types. DEGs under drought were classified into 5 key categories of KEGG pathways in roots (Amirbakhtiar et al., 2019) and leaves (Amirbakhtiar et al., 2021) of Arg wheat cultivar namely metabolism, genetic information processing, environmental information processing, cellular processes and organismal systems. Metabolism in these studies has been reported to have the greatest enrichment, far larger than the other enriched pathways. Similarly, our findings revealed that most DEGs in the roots and shoots were enriched in three main KEGG classes: metabolism, organismal systems and genetic information processing pathways. Among them, the number of DEGs was largest in metabolism category, including 4044 genes involved in different pathways such as biosynthesis of secondary metabolites, amino acid metabolism, carbohydrate metabolism, metabolism of cofactors and vitamins.

Abiotic stresses including salt stress usually result in high accumulation of sugars such as glucose, sucrose and galactose which has a great role in osmoregulation, homeostasis, stabilization of protein structure and carbon storage (Singh et al., 2015; Sami et al., 2016). Darko et al. (2019) investigated the content of different metabolites in wheat seedlings and found that plants exposed to NaCl exhibited higher levels of sucrose and galactose in root and shoot tissues, suggesting the participation of L-galactose in ascorbic acid pathway. Ascorbic acid has been shown to protect plants from stress-induced oxidative damage, acting as an antioxidant, and to enhance the growth and development of plants (Zhang et al., 2015). The results obtained in this study confirm these findings where two genes involved in galactose metabolism, and which encode beta-fructofuranosidase (INV) and raffinose synthase were identified to be regulated in the roots and shoots of Najran wheat under NaCl stress.

5 Conclusions

This investigation used RNA sequencing to profile salt-induced changes in the transcriptome of roots and shoots of a salt-tolerant wheat, the Najran Cultivar from Saudi Arabia. Previous studies used the same approach to study changes in the transcriptome of roots or shoots of different wheat plants under salt-stress or water-stress, to our knowledge no previous study analyzed these changes simultaneously in roots and shoots of same wheat plants. Our results, show that roots respond to a higher extent than shoots to salt-stress and that salt-stress induces organ specific responses as well as responses that are common to roots and shoots. These results suggest that an efficient attempt to improve tolerance to salt-stress should consider starting with optimizing antioxidants responses including the production of glutathione and phenolics particularly phenylpropanoids as well as galactose metabolism in roots and shoots. A transcriptomic approach such as the one used in this work is vital to map the global changes induced by salt-stress to the cellular functions and metabolic pathways. This needs however to be complemented with detailed expression- and functional analysis of key genes of these functions and pathways to inform an integrated and efficient approach to improve salt-tolerance in wheat and potentially other plant species.

Data availability statement

The datasets presented in this study can be found in online repositories. The names of the repository/repositories and accession number(s) can be found in the article/Supplementary Material.

Author contributions

These two authors contributed equally to this work and share first authorship, the inception of the project was made by TT, the two authors contributed to the design and implementation of the experiments as well as the analysis and interpretation of the results. NA wrote the first draft of the manuscript which was revised into its final version by TT. The two authors agree to be accountable for the content of the work. All authors contributed to the article and approved the submitted version.

Funding

The work was supported by a grant from King Khalid University, Kingdom of Saudi Arabia.

Acknowledgments

The authors would like to thank John Casement from the Bioinformatics Unit, Newcastle University, UK for assisting with the analysis of RNA-seq data and the University of King Khalid, Saudi Arabia for providing financial support to NA.

Conflict of interest

The authors declare that the research was conducted in the absence of any commercial or financial relationships that could be construed as a potential conflict of interest.

Publisher's note

Supplementary material

The Supplementary Material for this article can be found online at: https://www.frontiersin.org/articles/10.3389/fpls.2023.1225541/full#supplementary-material

References

Ahmad, P., Jaleel, C. A., Salem, M. A., Nabi, G., and Sharma, S. (2010). Roles of enzymatic and nonenzymatic antioxidants in plants during abiotic stress. *Crit. Rev. Biotechnol.* 30, 161–175. doi: 10.3109/07388550903524243

Alfagham, A. (2021). *Physiological and molecular responses to water-stress in local Saudi wheat cultivars* (Robinson library: Newcastle University, UK), 46–53.

Amirbakhtiar, N., Ismaili, A., Ghaffari, M. R., Firouzabadi, F. N., and Shobbar, Z.-S. (2019). Transcriptome response of roots to salt stress in a salinity-tolerant bread wheat cultivar. *PloS One* 14, e0213305. doi: 10.1371/journal.pone.0213305

Amirbakhtiar, N., Ismaili, A., Ghaffari, M.-R., Mirdar Mansuri, R., Sanjari, S., and Shobbar, Z.-S. (2021). Transcriptome analysis of bread wheat leaves in response to salt stress. *PloS One* 16 (7), e0254189. doi: 10.1371/journal.pone.0254189

Apel, K., and Hirt, H. (2004). Reactive oxygen species: metabolism, oxidative stress, and signal transduction. *Annu. Rev. Plant Biol.* 55, 373–399. doi: 10.1146/annurev.arplant.55.031903.141701

Ashraf, M., Athar, H., Harris, P., and Kwon, T. (2008). Some prospective strategies for improving crop salt tolerance. *Adv. Agron.* 97, 45–110. doi: 10.1016/S0065-2113(07)00002-8

Ayvaz, M., Guven, A., Blokhina, O., and Fagerstedt, K. V. (2016). Boron stress, oxidative damage and antioxidant protection in potato cultivars (Solanum tuberosum l.). *Acta Agricul. Scandinavica Section B—Soil Plant Sci.* 66, 302–316. doi: 10.1080/09064710.2015.1109133

Bashir, K., Rasheed, S., Matsui, A., Iida, K., Tanaka, M., and Seki, M. (2018). Monitoring transcriptomic changes in soil-grown roots and shoots of arabidopsis thaliana subjected to a progressive drought stress. *In Root Develop. Springer.* 1761, 223–230. doi: 10.1007/978-1-4939-7747-5_17

Bolger, A. M., Lohse, M., and Usadel, B. (2014). Trimmomatic: a flexible trimmer for illumina sequence data. *Bioinformatics* 30, 2114–2120. doi: 10.1093/bioinformatics/btu170

Borrelli, G. M., Fragasso, M., Nigro, F., Platani, C., Papa, R., Beleggia, R., et al. (2018). Analysis of metabolic and mineral changes in response to salt stress in durum wheat (Triticum turgidum ssp. durum) genotypes, which differ in salinity tolerance. *Plant Physiol. Biochem.* 133, 57–70. doi: 10.1016/j.plaphy.2018.10.025

Dadshani, S., Sharma, R. C., Baum, M., Ogbonnaya, F. C., Léon, J., and Ballvora, A. (2019). Multi-dimensional evaluation of response to salt stress in wheat. *PloS One* 14 (9), e0222659. doi: 10.1371/journal.pone.0222659

Darko, E., Végh, B., Khalil, R., Marček, T., Szalai, G., Pál, M., et al. (2019). Metabolic responses of wheat seedlings to osmotic stress induced by various osmolytes under iso-osmotic conditions. *PloS One* 14, e0226151. doi: 10.1371/journal.pone.0226151

Duan, A.-Q., Tao, J.-P., Jia, L.-L., Tan, G.-F., Liu, J.-X., Li, T., et al. (2020). AgNAC1, a celery transcription factor, related to regulation on lignin biosynthesis and salt tolerance. *Genomics* 112, 5254–5264. doi: 10.1016/j.ygeno.2020.09.049

Dudziak, K., Sozoniuk, M., Szczerba, H., Kuzdraliński, A., Kowalczyk, K., Börner, A., et al. (2020). Identification of stable reference genes for qPCR studies in common wheat (Triticum aestivum l.) seedlings under short-term drought stress. *Plant Methods* 16, 1–8. doi: 10.1186/s13007-020-00601-9

Esechie, H., Al-Barhi, B., Al-Gheity, S., and Al-Khanjari, S. (2002). Root and shoot growth in salinity-stressed alfalfa in response to nitrogen source. *J. Plant Nutr.* 25, 2559–2569. doi: 10.1081/PLN-120014713

Esfandiari, E., Shekari, F., Shekari, F., and Esfandiari, M. (2007). The effect of salt stress on antioxidant enzymes' activity and lipid peroxidation on the wheat seedling. *Notulae Botanicae Horti Agrobotanici Cluj-Napoca* 35, 48. doi: 10.15835/nbha.35.1.251

Gholizadeh, A., and Kohnehrouz, B. B. (2010). Activation of phenylalanine ammonia lyase as a key component of the antioxidative system of salt-challenged maize leaves. *Braz. J. Plant Physiol.* 22, 217–223. doi: 10.1590/S1677-04202010000400001

Goyal, E., Amit, S. K., Singh, R. S., Mahato, A. K., Chand, S., and Kanika, K. (2016). Transcriptome profiling of the salt-stress response in triticum aestivum cv. kharchia local. *Sci. Rep.* 6, 1–14. doi: 10.1038/srep27752

Hajihashemi, S., Kiarostami, K., Enteshari, S., and Saboora, A. (2009). Effect of paclobutrazol on wheat salt tolerance at pollination stage. *Russian J. Plant Physiol.* 56, 251–257. doi: 10.1134/S1021443709020149

Hniličková, H., Hnilička, F., Orsák, M., and Hejnák, V. (2019). Effect of salt stress on growth, electrolyte leakage, na+ and k+ content in selected plant species. *Plant Soil Environ.* 65, 90–96. doi: 10.17221/620/2018-PSE

Hu, P., Zhang, K., and Yang, C. (2019). BpNAC012 positively regulates abiotic stress responses and secondary wall biosynthesis. *Plant Physiol.* 179, 700–717. doi: 10.1104/pp.18.01167

Khan, M. K., Pandey, A., Hamurcu, M., Rajpal, V. R., Vyhnanek, T., Topal, A., et al. (2023). Insight into the boron toxicity stress-responsive genes in boron-tolerant triticum dicoccum shoots using RNA sequencing. *Agronomy* 13, 631. doi: 10.3390/agronomy13030631

Kong, Q., Mostafa, H. H., Yang, W., Wang, J., Nuerawuti, M., Wang, Y., et al. (2021). Comparative transcriptome profiling reveals that brassinosteroid-mediated lignification plays an important role in garlic adaption to salt stress. *Plant Physiol. Biochem.* 158, 34–42. doi: 10.1016/j.plaphy.2020.11.033

Li, C., Ji, J., Wang, G., Li, Z., Wang, Y., and Fan, Y. (2020). Over-expression of LcPDS, LcZDS, and LcCRTISO, genes from wolfberry for carotenoid biosynthesis, enhanced carotenoid accumulation, and salt tolerance in tobacco. *Front. Plant Sci.* 11, 119. doi: 10.3389/fpls.2020.00119

Linić, I., Šamec, D., Grúz, J., Vujčić Bok, V., Strnad, M., and Salopek-Sondi, B. (2019). Involvement of phenolic acids in short-term adaptation to salinity stress is species-specific among brassicaceae. *Plants* 8, 155. doi: 10.3390/plants8060155

Livak, K. J., and Schmittgen, T. D. (2001). Analysis of relative gene expression data using real-time quantitative PCR and the 2– ΔΔCT method. *Methods* 25, 402–408. doi: 10.1006/meth.2001.1262

Luo, Q., Teng, W., Fang, S., Li, H., Li, B., Chu, J., et al. (2019). Transcriptome analysis of salt-stress response in three seedling tissues of common wheat. *Crop J.* 7, 378–392. doi: 10.1016/j.cj.2018.11.009

Mandhania, S., Madan, S., and Sawhney, V. (2006). Antioxidant defense mechanism under salt stress in wheat seedlings. *Biol. Plantarum* 50, 227–231. doi: 10.1007/s10535-006-0011-7

Noctor, G., and Foyer, C. H. (1998). Ascorbate and glutathione: keeping active oxygen under control. *Annu. Rev. Plant Biol.* 49, 249–279. doi: 10.1146/annurev.arplant.49.1.249

Paiva, A. L. S., Passaia, G., Lobo, A. K. M., Jardim-Messeder, D., Silveira, J. A., and Margis-Pinheiro, M. (2019). Mitochondrial glutathione peroxidase (OsGPX3) has a crucial role in rice protection against salt stress. *Environ. Exp. Bot.* 158, 12–21. doi: 10.1016/j.envexpbot.2018.10.027

Pandey, A., Khan, M. K., Hamurcu, M., Brestic, M., Topal, A., and Gezgin, S. (2022). Insight into the root transcriptome of a boron-tolerant triticum zhukovskyi genotype grown under boron toxicity. *Agronomy* 12 (10), 2421. doi: 10.3390/agronomy12102421

Qi, Y., Liu, W., Qiu, L., Zhang, S., Ma, L., and Zhang, H. (2010). Overexpression of glutathione s-transferase gene increases salt tolerance of arabidopsis. *Russian J. Plant Physiol.* 57, 233–240. doi: 10.1134/S102144371002010X

Rajaei, S., Niknam, V., Seyedi, S., Ebrahimzadeh, H., and Razavi, K. (2009). Contractile roots are the most sensitive organ in crocus sativus to salt stress. *Biol. Plantarum* 53, 523–529. doi: 10.1007/s10535-009-0095-y

Rao, A., Ahmad, S. D., Sabir, S. M., Awan, S. I., Shah, A. H., Abbas, S. R., et al. (2013). Potential antioxidant activities improve salt tolerance in ten varieties of wheat (Triticum aestivum l.). *Am. J. Plant Sci.* 4, 69–76. doi: 10.4236/ajps.2013.46A010

Rao, X., Shen, H., Pattathil, S., Hahn, M. G., Gelineo-Albersheim, I., Mohnen, D., et al. (2017). Dynamic changes in transcriptome and cell wall composition underlying brassinosteroid-mediated lignification of switchgrass suspension cells. *Biotechnol. Biofuels* 10, 1–18. doi: 10.1186/s13068-017-0954-2

Sami, F., Yusuf, M., Faizan, M., Faraz, A., and Hayat, S. (2016). Role of sugars under abiotic stress. *Plant Physiol. Biochem.* 109, 54–61. doi: 10.1016/j.plaphy.2016.09.005

Seleiman, M. F., Aslam, M. T., Alhammad, B. A., Hassan, M. U., Maqbool, R., Chattha, M. U., et al. (2022). Salinity stress in wheat: effects, mechanisms and management strategies. *Phyton Int. J. Experimental. Botany* 91 (4), 667–694. doi: 10.32604/phyton.2022.017365

Singh, M., Kumar, J., Singh, S., Singh, V. P., and Prasad, S. M. (2015). Roles of osmoprotectants in improving salinity and drought tolerance in plants: a review. *Rev. Environ. Sci. Bio/Technol.* 14, 407–426. doi: 10.1007/s11157-015-9372-8

Singh, P., Mahajan, M. M., Singh, N. K., Kumar, D., and Kumar, K. (2020). Physiological and molecular response under salinity stress in bread wheat (Triticum aestivum l.). *J. Plant Biochem. Biotechnol.* 29, 125–133. doi: 10.1007/s13562-019-00521-3

Singh, V., Singh, A. P., Bhadoria, J., Giri, J., Singh, J., TV, V., et al. (2018). Differential expression of salt-responsive genes to salinity stress in salt-tolerant and salt-sensitive rice (Oryza sativa l.) at seedling stage. *Protoplasma* 255, 1667–1681. doi: 10.1007/s00709-018-1257-6

Tanveer, K., Gilani, S., Hussain, Z., Ishaq, R., Adeel, M., and Ilyas, N. (2020). Effect of salt stress on tomato plant and the role of calcium. *J. Plant Nutr.* 43, 28–35. doi: 10.1080/01904167.2019.1659324

Thabet, S. G., Alomari, D. Z., and Alqudah, A. M. (2021). Exploring natural diversity reveals alleles to enhance antioxidant system in barley under salt stress. *Plant Physiol. Biochem.* 166, 789–798. doi: 10.1016/j.plaphy.2021.06.030

Wang, N., Qian, Z., Luo, M., Fan, S., Zhang, X., and Zhang, L. (2018). Identification of salt stress responding genes using transcriptome analysis in green algae chlamydomonas reinhardtii. *Int. J. Mol. Sci.* 19, 3359. doi: 10.3390/ijms19113359

Xu, N., Liu, S., Lu, Z., Pang, S., Wang, L., Wang, L., et al. (2020). Gene expression profiles and flavonoid accumulation during salt stress in ginkgo biloba seedlings. *Plants* 9, 1162. doi: 10.3390/plants9091162

Zhang, G.-Y., Liu, R.-R., Zhang, C.-Q., Tang, K.-X., Sun, M.-F., Yan, G.-H., et al. (2015). Manipulation of the rice l-galactose pathway: evaluation of the effects of transgene overexpression on ascorbate accumulation and abiotic stress tolerance. *PloS One* 10, e0125870. doi: 10.1371/journal.pone.0125870

frontiers | Frontiers in Plant Science

TYPE Original Research
PUBLISHED 13 September 2023
DOI 10.3389/fpls.2023.1249600

OPEN ACCESS

EDITED BY
Zulfiqar Ali Sahito,
Zhejiang University of Technology, China

REVIEWED BY
Krishan K. Verma,
Guangxi Academy of Agricultural Sciences, China
Waheed Akram,
University of the Punjab, Pakistan

*CORRESPONDENCE
Kamlesh K. Meena
kk.meena@icar.gov.in

†These authors have contributed equally to this work

RECEIVED 28 June 2023
ACCEPTED 21 August 2023
PUBLISHED 13 September 2023

CITATION
Meena KK, Sorty AM, Bitla U, Shinde AL, Kumar S, Wakchaure GC, Kumar S, Kanwat M and Singh DP (2023) Stress-responsive gene regulation conferring salinity tolerance in wheat inoculated with ACC deaminase producing facultative methylotrophic actinobacterium. *Front. Plant Sci.* 14:1249600. doi: 10.3389/fpls.2023.1249600

Stress-responsive gene regulation conferring salinity tolerance in wheat inoculated with ACC deaminase producing facultative methylotrophic actinobacterium

Kamlesh K. Meena[1*†], Ajay M. Sorty[2,3†], Utkarsh Bitla[2], Akash L. Shinde[2], Satish Kumar[2,4], Goraksha C. Wakchaure[2], Shrvan Kumar[1], Manish Kanwat[1] and Dhananjaya P. Singh[5]

[1]Division of Integrated Farming System, Indian Council of Agricultural Research (ICAR)-Central Arid Zone Research Institute, Jodhpur, India, [2]School of Soil Stress Management, Indian Council of Agricultural Research (ICAR)-National Institute of Abiotic Stress Management, Baramati, India, [3]Department of Environmental Science–Environmental Microbiology, Aarhus University, Roskilde, Denmark, [4]Department of Biochemistry, Indian Council of Agricultural Research (ICAR)-Directorate of Onion and Garlic Research, Pune, India, [5]Indian Council of Agricultural Research (ICAR)-Crop Improvement Division, Indian Institute of Vegetable Research, Varanasi, India

Microbes enhance crop resilience to abiotic stresses, aiding agricultural sustainability amid rising global land salinity. While microbes have proven effective via seed priming, soil amendments, and foliar sprays in diverse crops, their mechanisms remain less explored. This study explores the utilization of ACC deaminase-producing *Nocardioides* sp. to enhance wheat growth in saline environments and the molecular mechanisms underlying *Nocardioides* sp.-mediated salinity tolerance in wheat. The *Nocardioides* sp. inoculated seeds were grown under four salinity regimes *viz.*, 0 dS m^{-1}, 5 dS m^{-1}, 10 dS m^{-1}, and 15 dS m^{-1}, and vegetative growth parameters including shoot-root length, germination percentage, seedling vigor index, total biomass, and shoot-root ratio were recorded. The *Nocardioides* inoculated wheat plants performed well under saline conditions compared to uninoculated plants and exhibited lower shoot:root (S:R) ratio (1.52 $\pm$ 0.14 for treated plants against 1.84 $\pm$ 0.08 for untreated plants) at salinity level of 15 dS m^{-1} and also showed improved biomass at 5 dS m^{-1} and 10 dS m^{-1}. Furthermore, the inoculated plants also exhibited higher protein content *viz.*, 22.13 mg g^{-1}, 22.10 mg g^{-1}, 22.63 mg g^{-1}, and 23.62 mg g^{-1} fresh weight, respectively, at 0 dS m^{-1}, 5 dS m^{-1}, 10 dS m^{-1}, and 15 dS m^{-1}. The mechanisms were studied in terms of catalase, peroxidase, superoxide dismutase, and ascorbate peroxidase activity, free radical scavenging potential, *in-situ* localization of H_2O_2 and superoxide ions, and DNA damage. The inoculated seedlings maintained higher enzymatic and non-enzymatic antioxidant potential, which corroborated with reduced H_2O_2 and superoxide localization within the tissue. The gene expression profiles of 18 stress-related genes involving abscisic acid signaling, salt overly sensitive (SOS response), ion transporters, stress-related transcription factors, and antioxidant enzymes were also analyzed. Higher levels of stress-responsive gene transcripts, for instance,

TaABARE (~+7- and +10-fold at 10 dS m^{-1} and 15 dS m^{-1}); TaHAk1 and hkt1 (~+4- and +8-fold at 15 dS m^{-1}); antioxidant enzymes *CAT*, *MnSOD*, *POD*, *APX*, *GPX*, and *GR* (~+4, +3, +5, +4, +9, and +8 folds and), indicated actively elevated combat mechanisms in inoculated seedlings. Our findings emphasize *Nocardioides* sp.–mediated wheat salinity tolerance via ABA-dependent cascade and salt-responsive ion transport system. This urges additional study of methylotrophic microbes to enhance crop abiotic stress resilience.

KEYWORDS

salinity stress, ACC deaminase, *Nocardioides*, methylotrophic bacteria, mitigation, wheat, ABA, Mitigation

1 Introduction

Agricultural productivity is vulnerable to ever-intensifying abiotic stresses under the current scenario of climate change. Salinization of agricultural lands is becoming one of the greatest threats to global crop yields. Attempts made to improve the agricultural losses due to salinity stress through breeding and genetic improvement programs have met limited success and are significantly time, cost, and labor intensive. Hence, a need to develop new strategies based on utilizing microbial capacities to strengthen biosaline agriculture has been proposed. Despite the significant progress already made in the area of microbial management of salinity stresses in crop plants (Kumar and Verma, 2018), there exists a bottleneck on wider applicability of plant biologicals under saline conditions typically due to underlying mechanisms of microbe-mediated salinity tolerance in plants. Majority of the currently available microbial inputs originate from different agricultural ecosystems, wild, stress-prone habitats, or from the plant's phyllosphere region where the microbes form native communities (Dong et al., 2019; Xu et al., 2022) and are involved in beneficial plant interactions leading to stress tolerance (Inbaraj, 2021); however, their efficiency significantly differs due to differing mechanisms of action. For instance, the facultative methylotrophic bacteria from epiphytic habitat utilize single carbon (C1) substrates and produce a range of plant beneficial biomolecules including growth hormones (Meena et al., 2012). Inherent resilience of the methylotrophic bacteria merit them to thrive in constantly changing stressful microhabitat on the plant surface, particularly on the leaves, where methanol is abundant (Srivastava et al., 2022). Therefore, due to the characteristic resilience and beneficial bio-molecules production, methylotrophs make an important tool to maintain plant fitness under stressful conditions. Furthermore, inoculation of resilient microbes in agro-ecosystem is advantageous owing to their higher probabilities of survival and establishment, which reduces the chances of inoculum failure. Therefore, methylotrophic bacteria are of major interest in biosaline agriculture (Meena et al., 2020). Additionally, physiology of methylotrophic bacteria aligns with the criteria for proposed microbe-based stress management in plants (Meena et al., 2017; Munir et al., 2022). For instance, supra-optimal levels of ethylene under stress conditions could be efficiently regulated through 1-aminocyclopropane-1-carboxylic acid (ACC) deaminase, (Gupta and Pandey, 2019; Riyazuddin et al., 2020) while simultaneously produced growth hormones could sustain the plant growth and development.

Synthesis of ACC deaminase enzyme seems to be a rare characteristic among the known methylotrophic bacteria, with a few examples available such as *Methylobacterium fujisawaense* and *M. oryzae* (Madhaiyan et al., 2004). A positive influence of phytohormones producing and nitrogen fixing methylotrophs on plant growth and development is also documented (Fedorov et al., 2011; Meena et al., 2012). Consequently, such strains can have a high applicability as plant biologicals under stress conditions. However, despite the available knowledge on plant beneficial capabilities of methylotrophic bacteria (Ivanova et al., 2001; Subhaswaraj et al., 2017), their applicability as plant biologicals is limited due to the lack of knowledge on their specific plant interactions under stress conditions. Therefore, this study was designed to unfold the mechanistic interactions of wheat and an ACC deaminase producing methylotrophic bacterium under saline conditions. The major emphasis was to investigate post-methylotrophs inoculation changes at physicochemical and molecular level involving expression profile of stress-responsive enzymes and genes conferring salinity tolerance in wheat.

2 Materials and methods

2.1 Description of bacterial strain

The bacterial strain used in the study was originally isolated from soybean leaf and was identified as *Nocardioides* sp. by 16S rRNA gene sequencing (LC140963). The details of leaf-epiphytic methylotrophic bacterium *Nocardioides* sp. and its functional characteristics have been described earlier (Meena et al., 2020).

2.2 ACC deaminase activity

ACC deaminase activity was measured by the method described by Honma and Shimomura (1978), where the quantitation was achieved using a standard curve of the deamination product α-

ketobutyrate in the range 0.1 µM to 1.0 µM. Briefly, the *Nocardioides* strain was initially grown in Luria Broth medium. The overnight grown cells were harvested, washed with sterile phosphate buffer saline (pH 7.0), and inoculated into the DF (Dworkin and Foster's) medium (Dworkin and Foster, 1958) having ACC as sole nitrogen source and allowed to grow until late log phase was achieved. The cells were harvested, washed with tris-HCl (100 mM; pH 7.6), added with 5% toluene (v/v), and finally vortexed for 30 s to labilize the cells (Senthilkumar et al., 2021). The 50 µL of labilized cell suspension was then incubated with 5 µL of 0.3 M ACC for 30 min. The labilized cell suspension without ACC served as a negative control, while 0.1 M tris-HCl (pH 8.5) with 5 µL of 0.3M ACC served as a blank. The cell suspension was mixed thoroughly with 500 µL of 0.56N HCl by vortexing and cell debris were removed by centrifugation at 12,000 rpm for 5 min, a 500 µL of which was then mixed with 400 µL of 0.56 N HCl and 150 µL of DNF (2,4-dinitrophenylhydrazine in 100 ml of 2 N HCl) solution and incubated at 28°C for 30 min. One milliliter of 2N NaOH was added to the sample and the absorbance was recorded at 540 nm using a double beam spectrophotometer. The lysed cell suspension was used for estimation of protein content using Bradford assay (Bradford, 1976). Finally, the activity was calculated in terms of the nanomoles of α-ketobutyrate formed per milligram of protein in 1 hr.

2.3 Preparation of inoculum and impact assessment on wheat

The strain was cultivated in DF medium with ACC as nitrogen source at 30°C ± 2°C at 150 rpm for 72h. The cells were pelleted at 7830 rpm using centrifugation (Eppendorf *5430R*) and were washed with sterile phosphate-buffered saline (PBS), re-suspended in sterile PBS to obtain a CFU equivalent of 10^9 ml^{-1}. The inoculum was then used for priming wheat seeds.

Efficiency of the strain to mitigate salinity stress in wheat was evaluated in a gnotobiotic pot-experiment. Wheat seeds (*var. Lok*I) were treated with 5% sodium hypochlorite solution (Sauer et al., 1986) followed by several times washing with sterile milli-Q water to remove residual hypochlorite. The seeds were then treated with the inoculum (~10^9cfu ml^{-1}) in 0.1% carboxymethyl cellulose (CMC), dried aseptically in a laminar hood and finally sown into the pots filled with autoclave-sterilized garden-soil pre-adjusted to salinity levels of 0 dS m^{-1}, 5 dS m^{-1}, 10 dS m^{-1}, and 15 dS m^{-1}, respectively using crude salt (NaCl) solution. The pots were kept in dark for 72h at 20°C followed by 12h dark and light cycle till 28 days. Uninoculated seeds served as control.

2.4 Phenotypic characteristics of the wheat seedlings

The germination parameters *viz.* shoot-root length, germination percentage, seedling vigor index, total biomass, and shoot-root ratio were obtained from the freshly harvested 28 days old seedlings.

2.5 Biochemical analysis of wheat seedlings

2.5.1 Preparation of enzyme extract

Enzyme extract was prepared from freshly harvested tissues by crushing in ice-cold phosphate buffer (100 mM; 0.5 mM ethylene diamine tetraacetic acid (EDTA); pH 7.5). Tissue debris was removed by centrifugation at 14000 rpm/10 min. The supernatant so obtained was stored at −20°C for further use as crude enzyme, and an aliquot of the extract was also used to determine the protein content. Ascorbic acid (1.0 mM) was added to the buffer while preparing the enzyme extract for determination of ascorbate peroxidase (Nakano and Asada, 1981).

2.5.2 Antioxidant enzymes activity

Superoxide dismutase activity in the enzyme extract was assayed by measuring its ability to inhibit the photochemical reduction of Nitroblue tetrazoliumn by the method of Dhindsa et al. (1981). Briefly, 3 mL of reaction cocktail contained methionine (13.33 mM), EDTA (0.1 mM), phosphate buffer (50 mM, pH 7–8), sodium carbonate (50 mM), nitro blue tetrazolium chloride (NBT) (75 µM) and crude enzyme extract (10.0 µL) was added with riboflavin (2.0 µM). The reaction was started by illuminating the reaction mixture for 10 min under two white fluorescent lamps (15 W each). The reaction was stopped by shifting the reaction mixture in dark for 15 min. The absorbance was measured at 560 nm. A non-illuminated reaction mixture with no color served as control. The reaction mixture with no enzyme extract developed the maximum color, which decreased with the increase in the amount of added enzyme extract. Volume of enzyme extract corresponding to 50% inhibition reaction was considered as one enzyme unit.

Catalase activity was determined by monitoring the decrease in A_{240} resulting from the elimination of H_2O_2 as per the method described by Luck (1971). The standard reaction mixture contained (3.0 mL) potassium phosphate buffer (50 mM, pH 7.0), H_2O_2 (12.5 mM) and crude enzyme extract (50 µL). The decrease in absorbance was noted every 30s up to 3 min. The extinction coefficient of H_2O_2 at 240 nm was assumed to be 0.036 µm/ml. One unit (U) of the catalase activity was defined as the amount of enzyme required to degrade 1 µM mL^{-1} of H_2O_2.

Peroxidase activity was calculated according to Putter (Putter, 1974). Briefly, 3.0 mL of reaction mixture contained potassium phosphate buffer (50 mM; pH 6.1), guaiacol (16 mM), H_2O_2 (2.0 mM), and the crude enzyme extract (100 µL). The rate of formation of oxidized guaiacol in the guaiacol assay was measured at 436 nm.

Ascorbate peroxidase activity was estimated as described by Nakano and Asada (1981). Three milliliter of reaction mixture containing potassium phosphate buffer (50 mM; pH 7.0), ascorbic acid (0.5 mM), EDTA (0.1 mM), H_2O_2 (0.1 mM), and the enzyme extract (100 µL) was prepared. The reaction kinetics was monitored in terms of decreasing absorbance at 290 nm for 30 s. The oxidation of ascorbate was followed by the decrease in absorbance at 290 nm. The enzyme activity was calculated as µmol of ascorbic acid decomposed per minute with the absorbance coefficient 2.8 mM^{-1} cm^{-1} at 290 nm.

2.5.3 Total sugars

The total sugar content from shoot and roots of the seedlings was estimated using anthrone reagent (Yemm, 1954). Briefly, 50 mg of sample was treated with 2.5M HCl in boiling water bath for 3h. The acid was neutralized with excess sodium carbonate and diluted to 50 mL. The debris was removed by centrifugation at 7830 rpm and 1.0 mL of supernatant was mixed with 4.0 mL of freshly prepared, ice-cold anthrone reagent (0.2% anthrone in 95% H_2SO_4). The contents were mixed thoroughly and kept in boiling water bath for 10 min, cooled under ambient condition, and read at 630 nm in terms of glucose equivalents.

2.5.4 Phenolic compounds

The content of phenolic compounds was determined according to Singleton and Rossi (1965). For this, 100 mg of tissue samples were ground in 2.0 mL of chilled, 80% methanol. Debris was removed by centrifugation at 14000 rpm for 15 min, and 100 µL from the saved supernatant was mixed with Folin Ciocalteau reagent (1.0 N) under alkaline conditions. The reaction mixture was kept in boiling water bath for 1.0 min, cooled, and read at 650 nm. The Catechol was used as standard, and results were expressed in terms of mg CE g^{-1} fresh weight.

2.5.5 Free radicle scavenging activity

Free radicle scavenging activity (FRSA) of the extract was estimated using 2,2-diphenyl-1-picrylhydrazyl (DPPH) radicle assay. Briefly, 1.0 ml aliquot of methanolic extract was mixed with 4.0 ml of DPPH reagent (40 µg ml^{-1} in methanol), and the initial absorbance was recorded at 517 nm. The tubes were then kept in dark under ambient conditions for 30 min followed by recording the post-reaction absorbance. The DPPH dissolved in methanol with no added plant extract served as control. Radical scavenging activity was expressed in terms of % antioxidant activity based on the decrease in absorbance at 517 nm using the formula-

$$\%\ \textbf{antioxidant activity} = \frac{\textbf{Abs(control)} - \textbf{Abs (sample)}}{\textbf{Abs(Control)}} \times 100$$

2.5.6 Total proteins

Protein content from the tissue was measured according to Bradford (1976). The tissue extracts obtained for enzyme estimation were mixed with Bradford reagent, allowed to react in dark for 15 min, and the absorbance was recorded at 595 nm. Proteins were quantified using the standard curve of bovine serum albumin.

2.5.7 2-Deoxyribose degradation assay

The hydroxyl (OH) radical-scavenging activity plant extract was measured using deoxyribose degradation assay modified by Li et al, (2013) to assess the extent of DNA damage. Briefly, the shoot samples were washed with distilled water and shade dried at 40°C. The dried samples were extracted with 100% ethanol, filtered and vacuum dried. The extracts were solubilized in dimethyl sulfoxide and diluted with sterile water to obtain varying concentrations. Hydroxyl radical were generated by adding H_2O_2 (1 mM) to the 1 ml of final reaction mix containing phosphate buffer (pH 7.2) (25 mM), EDTA (100 µM), $FeCl_3$ (100 µM), 100 µl DNA (3 mM), and varying concentration of plant extract. Reaction mix was incubated at 37°C for 1h, followed by mixing with 100 µl of 2% trichloroacetic acid (TCA) and 100 µl of 1% thiobarbituric acid (TBA) and heating for 15 min at 100°C. The absorbance was read at 532 nm. Hydroxyl radical inhibition potential was expressed in terms of "%inhibition" (Li, 2013) using the formula -

$$\%\ \textbf{inhibition} = \frac{\textbf{Ao} - \textbf{A}}{\textbf{Ao}} \textbf{x}\ 100$$

Here, Ao is the absorbance of reaction mixture without plant extract and A is the absorbance of reaction mixture added with plant extract.

2.5.8 Localization of oxidative radicles in wheat leaves

Localization of H_2O_2 and superoxide radicles in the leaves was analyzed using specific high-affinity dye. H_2O_2 localization was determined according to the method of Thordal-Christensen et al. (1997) with few modifications. Briefly, fresh leaves were immersed in freshly prepared 3,3′-diaminobenzidine (DAB) reagent (1.0 mg mL^{-1} DAB; 0.05% v/v Tween 20 and 10 mM Na_2HPO_4) and were subjected to vacuum infiltration for 15 min followed by leaving them for overnight for adequate staining. After decolorizing the leaves multiple times in ethanol:aceticacid:glycerol (3:1:1; v/v) in water bath for 10 min to remove chlorophyll, the decolorized leaves were kept on 60% glycerol-bed. Development of dark brown stain indicated the localization and distribution of reactive oxygen species (ROS) in the leaf tissues.

Similarly, localization of superoxide radicle was studied using NBT reagent (Jabs et al., 1996). Freshly harvested leaves were immersed in NBT reagent (0.2% NBT in 50 mM phosphate buffer; pH 7.5). Vacuum infiltration, decolorization, and the process of observation were identical to that of DAB staining.

2.6 Gene-expression profiling of the wheat seedlings

Freshly harvested tissues were immediately frozen in liquid nitrogen and subjected to RNA extraction using RNeasy plant mini kit (Qiagen, the Netherlands) following the manufacturer's instructions. Immediately, synthesis of cDNA was done using Verso cDNA synthesis kit (Thermo Fisher Scientific, USA) as per manufacturer's instructions.

Reference and target genes were quantitatively amplified in a 96-well cfx96 real-time PCR system (BioRad, USA), using DyNAmo Color Flash SYBR Green qPCR master mix (Thermo Fisher Scientific, USA). PCRs were carried out in a total volume of 20 µl containing 800 ng of cDNA, and 400 nM of each primer along with 1× of DyNAmo Colo rFlash SYBR Green qPCR master mix. Each reaction was carried out in three technical replicates along with a blank with sterile PCR-water serving as no template control (NTC). The reaction program in CFX manager (Version 3.1.1517.0823) consisted of 2 min at 50°C; 10 min at 95°C; 40 cycles of 30 s at 95°C and 1 min at annealing temperature of 60°C and 30 s at 72°C.

Melting curves were plotted through the range 65°C –95°C during which the fluorescence was recorded in steps of 0.5°C. The actin (*Act*) and beta-tubulin (β-tubulin) genes served as reference gene for normalization of the real-time qPCR data. The fold-change expression of transcript accumulation of target genes was quantified using the comparative $2^{-\Delta\Delta Ct}$ method. The primers used for quantification of 18 stress-responsive genes are depicted in the (Supplementary Table S1).

2.7 Statistical analyses

All the data were presented in mean values. All the numerical data were statistically analyzed using analysis of variance (ANOVA) with *post-hoc* Duncan's multiple range test (DMRT), principal component, and clustering analysis was performed using SPSS 16.0 (Windows 8.0; SPSS Inc., www.spss.com/), Plotly (https://www.statskingdom.com/), and R 3.6.1 (Windows 10; www.cran.r-project.org/). The differences at the 95% confidence level were considered significant.

3 Results

The *Nocardioides* sp. (LC140963) exhibited positive reaction toward ACC deamination under *in vitro* conditions. The quantitative assay revealed the production of 1257 nM ± 72 nM of α-ketobutyrate mg^{-1} protein h^{-1}. The scope of application of the actinobacterial strain was explored in this study through investigations on the mechanism of salt stress mitigation in wheat at phenotypic, biochemical, and molecular level. The results established a relationship among the physicochemical and molecular dynamics of wheat under saline conditions and mitigation induced by ACC deaminase producing bacterium.

3.1 Effect of bacterial application on physicochemical characteristics of wheat

Development of roots was influenced by the inoculation. Saline conditions indeed restricted root development, which was clearly evident from a higher S:R ratio; however, under the similar scenario, the inoculation of *Nocardioides* sp. significantly lowered the S:R ratio, thereby, confirming that the root development was successfully sustained from 5 dS m^{-1} to 15 dS m^{-1} (Figures 1A, 2D). Lower S:R ratio of 1.52 ± 0.14 of the treated seedlings as against 1.84 ± 0.08 for the untreated ones at salinity level of 15 dS m^{-1}. Root development was stimulated predominantly at low (5 dS m^{-1}) and high (15 dS m^{-1}) levels of salinity stress, although there was moderate improvement at 10 dS m^{-1} (Figure 1A). Similarly, the highest average biomass of 0.041 ± 0.03 g $seedling^{-1}$ was recorded under non-saline conditions, but the bacterial application significantly improved the biomass at 5 dS m^{-1} and 10 dS m^{-1}. However, the effect of bacterial application on biomass remained non-significant at 15dS m^{-1} (Figure 1B).

Biochemical parameters of wheat seedlings were also significantly influenced by the inoculation. Activity of oxidative stress management characteristics showed critical responsiveness toward the bacterial inoculation. Catalase, peroxidase, and ascorbate peroxidase activities revealed increasing trend with increasing salinity stress. Ascorbate peroxidase and catalase activity in inoculated seedlings increased mainly at higher salinity levels of 10 dS m^{-1} and 15 dS m^{-1} (Figures 2C, F). The peroxidase activity, however, remained almost steady up to 10 dS m^{-1} but eventually increased significantly at 15 dS m^{-1} (Figure 2G). The SOD activity declined markedly in control at 15 dS m^{-1} and remained stable at all the three stress levels with peak activity in seedlings with no stress (0 dS m^{-1}) (Figure 2E). In treated groups also, the SOD activity remained almost stable at all the salinity stress levels. The *in-situ* localization of H_2O_2 and O^+radicals was also likely to be linked to the activity of oxidative stress management machinery (Figures 2A, B). Elevated levels of oxidative radicals were noted in control compared to the treated seedlings especially making substantial difference at higher salinity stress levels of 10 dS $m^{-1}$and 15 dS m^{-1}.

Free radical scavenging activity of seedling extract, as evaluated by DPPH assay, showed effective neutralization of the free radicals by the extract. Among all the salinity stress levels (5 dS m^{-1} to 15 dS m^{-1}), including no stress (0 dS m^{-1}) the free radical scavenging activity of extract was higher in treated samples compared to the control, indicating stimulation of the antioxidant mechanism in the inoculated wheat seedlings (Table 1). The effect of inoculation on antioxidant activity was much higher in treated plants (26.68%) as compared to control (21.67%) at 5 dS m^{-1}.

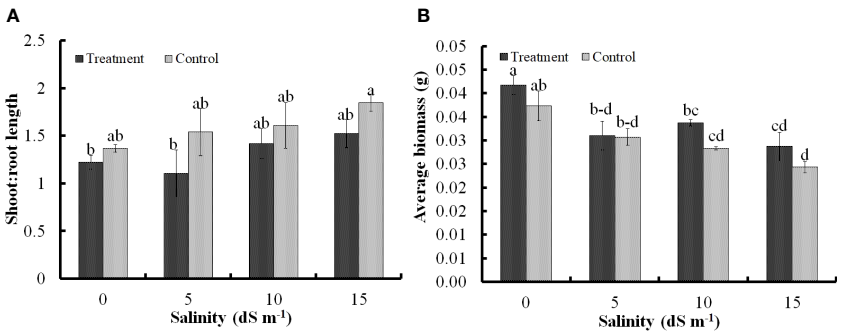

FIGURE 1
Impact of *Nocardioides* sp. on development of shoot and root of wheat seedlings in terms of shoot:root ratio **(A)**; and biomass accumulation **(B)** under saline conditions. Values in the same data series with different letters indicate significant difference (p less than or equal to 0.05) in the Duncan's multiple range test.

10.3389/fpls.2023.1249600

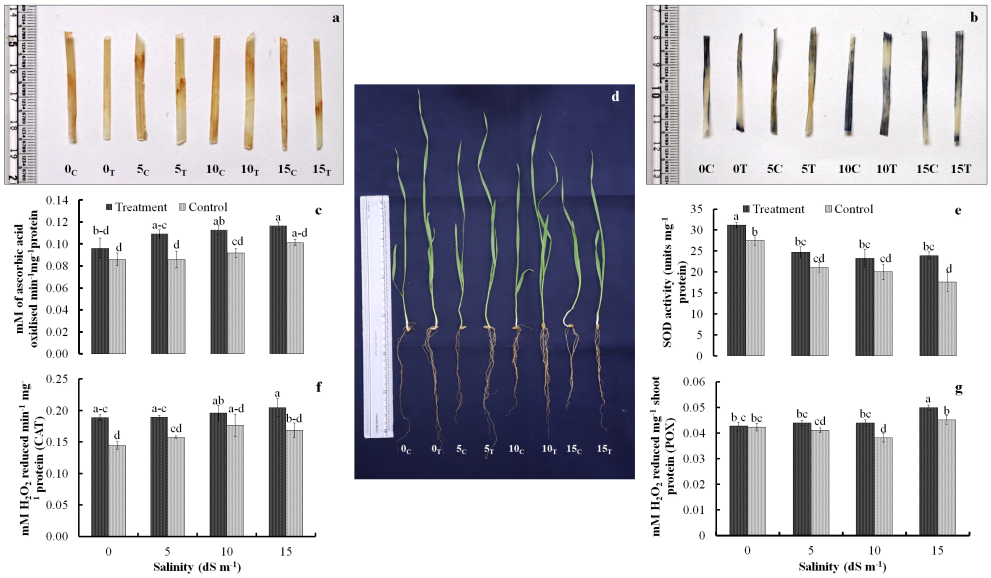

FIGURE 2
Localization of H_2O_2 radicals **(A)** and superoxide radicals **(B)** in treated and non-treated seedlings; trends of antioxidant enzymes ascorbate peroxidase **(C)**, superoxide dismutase **(E)**, catalase **(F)**, and peroxidase **(G)** activity as affected by salinity stress and *Nocardioides* sp. inoculation; and appearance of treated and untreated wheat seedlings under the influence of increasing salinity stress **(D)**. Values in the same data series with different letters indicate significant difference (p less than or equal to 0.05) in the Duncan's multiple range test.

Predominant biochemical traits comprising the contents of protein, sugars, and plant phenolics were assessed to generate an overview of cellular homeostasis of the inoculated seedlings. The protein content in inoculated seedlings remained significantly higher over the control with steady trend (22.13 mg g^{-1}, 22.10 mg g^{-1}, and 22.63 mg g^{-1} fresh weight, respectively) at 0 dS m^{-1}, 5 dS m^{-1}, and 10 dS m^{-1}. However, a marked rise in protein content (23.62 mg g^{-1} fresh weight in inoculated plants compared to 17.50 mg g^{-1} fresh weight in control) at 15 dS m^{-1} was also observed (Table 1). The difference in sugar and plant phenolics content in treated and control remained statistically insignificant at 0 dS m^{-1} and 5 dS m^{-1}, but sugar content was significantly increased at 10 dS m^{-1} and 15 dS m^{-1} (Table 1). The phenolic content in inoculated wheat seedlings was significantly higher under saline conditions (at 5 dS m^{-1}, 10 dS m^{-1}, 15 dS m^{-1} EC) compared to 0 dS m^{-1}. The difference in plant phenolics content was insignificant for three salinity stress levels.

The ability of extracts to inhibit the degradation of 2-deoxy-D-ribose, a nucleotide sugar was also investigated as a protective indicator of the DNA damage. Except for the treatment at 0 dS m^{-1} the inoculated seedlings exhibited significantly higher ability to inhibit the hydroxyl radical-mediated degradation of 2-deoxy-D-ribose sugar in DNA, which was evident by higher % inhibition of 21.08%, 22.53%, and 25.31% recorded for inoculated seedling grown at 5 dS m^{-1}, 10 dS m^{-1}, and 15 dS m^{-1}, respectively, as against the

TABLE 1 Biochemical attributes of the wheat seedling tissues under the influence of *Nocardioides* sp.

Salinity (dS m^{-1})	Treatment	Protein[#]	Sugar*	Phenolics[£]	DPPH[†]	Deoxy ribose protection[‡]
0.0	Inoculated	**22.13 ± 1.87^{ab§}**	24.97 ± 1.23^{c}	2.99 ± 0.37^{b}	**24.74 ± 1.12^{ab}**	12.57 ± 2.44^{d}
	Control	18.34 ± 2.11^{c}	24.51 ± 0.73^{c}	2.89 ± 0.19^{b}	22.44 ± 2.02^{bc}	13.26 ± 1.92^{d}
5.0	Inoculated	**22.10 ± 1.87^{ab}**	26.28 ± 1.19^{c}	3.39 ± 0.66^{ab}	**26.68 ± 2.02^{bc}**	**21.08 ± 1.18^{bc}**
	Control	20.53 ± 1.83^{a-c}	24.67 ± 1.38^{c}	3.15 ± 0.68^{ab}	21.67 ± 1.50^{cd}	18.47 ± 1.63^{c}
10.0	Inoculated	**22.63 ± 1.96^{ab}**	**30.33 ± 1.16^{b}**	**3.83 ± 0.29^{a}**	**24.63 ± 0.75^{ab}**	**22.53 ± 1.76^{ab}**
	Control	19.32 ± 1.85^{bc}	25.75 ± 1.61^{c}	3.19 ± 0.39^{ab}	21.66 ± 1.48^{cd}	17.92 ± 1.61^{c}
15.0	Inoculated	**23.62 ± 1.83^{a}**	**32.77 ± 1.34^{a}**	**3.85 ± 0.47^{a}**	**23.36 ± 1.60^{bc}**	**25.31 ± 1.45^{a}**
	Control	17.50 ± 1.79^{c}	28.45 ± 1.06^{b}	3.03 ± 0.44^{ab}	19.22 ± 1.17^{d}	20.43 ± 1.72^{bc}

[#]Protein content.
*Total sugars.
[£]Total phenolic compounds expressed in mg g^{-1} fresh weight.
[†]Percent reduction of DPPH dye by the phenolic compounds from wheat seedlings.
[‡]Percent inhibition of 2-deoxy-D- ribose decomposition in presence of tissue extract of wheat seedlings.
[§]Values in the same data series superscripted by different letters indicate significant difference at p = 0.05 in Duncan's multiple range test.
Significantly induced values are marked in bold.

18.47%, 17.92%, and 20.43% inhibition recorded for uninoculated control seedlings at similar salinity levels (Table 1). These results indicated the presence of more efficient mechanisms to protect salinity-induced DNA damage into the inoculated seedlings.

3.2 Localization of H_2O_2 and superoxide radicals

The DAB- and NBT-based histochemical staining assays were used for *in-situ* localization of H_2O_2 and superoxide radicals, respectively. The development of reddish and purple color patches indicated the presence of H_2O_2 and superoxide radicals in the leaf tissues. A greater number of radish color patches developed in the leaves of uninoculated control wheat seedlings at no salinity stress (0 dS m^{-1}) and also at all salinity stress levels (5 dS m^{-1}, 10 dS m^{-1}, and15 dS m^{-1}) (Figure 2A). Similarly, the localization of superoxide radicals was inferred by development of purple color patches in NBT staining. Higher abundance of purple color spots was seen in leaves of uninoculated control wheat plants at no salinity stress (0 dS m^{-1}) and also at all salinity stress levels (5 dS m^{-1}, 10 dS m^{-1}, and 15 dS m^{-1}) (Figure 2B). The sharp differences were observed in purple color development in inoculated and uninoculated plants at salinity level of 5 dS m^{-1} and 10 dS m^{-1}. However, the results at higher salinity level of 15 dS m^{-1} were not so obvious.

3.3 qPCR-based quantification of wheat genes implicated under salinity stress

We used qRT-PCR to study the expression of 18 genes known to confer plant stress-response against salinity conditions. These genes were related to abscisic acid signaling (*TaABARE* and *TaOPR1*), SOS response genes (*TaSOS1* and *TaSOS4*), and the genes for stress-related transcription factors (*TaWRKY10*, *TaWRKY17*, *TaMYB33*, and *TaST*), ion transporters (*TaHKT*, *TaNHX*, and *TaHAK1*), genes for antioxidant enzymes (*POD*, *CAT*, *MnSOD*, *APX*, *GR*, and *GPX*). Figure 3A details the trends of the studied gene transcripts at different salinity levels. The qPCR-based expression studies revealed around 7- and 10-fold higher expression of *TaABARE* gene in inoculated plants at higher salinity levels of 10 dS m^{-1} and 15 dS m^{-1}, respectively compared to unstressed plants at 0 dS m^{-1}. Minor differences were observed in *TaOPR1* transcripts of inoculated plants at all salinity levels. Similarly, the expression profiling of two genes (*TaSOS1* and *TaSOS4*) of salt overly sensitive (SOS) pathway showed around twofold and fivefold higher expression of *TaSOS1* at salinity stress of 10 dS m^{-1} and 15 dS m^{-1}, respectively; however, change in gene expression of *TaSOS4* at all salinity stress levels was non-significant. Among the transcripts of the three-transcription factor-linked genes, namely, *TaWRKY10*, *TaWRKY17*, and *TaMYB33* showed a higher expression of *TaWRKY17* with the increasing salinity stress levels. The expression of *TaWRKY10* and *TaMYB33* also increased with increasing salinity stress, but the differences were non-significant for 10 dS m^{-1} and 15 dS m^{-1}. The three ion transporter genes *TaHKT*, *TaNHX*, and *TaHAK1* also showed increased expression at higher salinity stress levels. The expression of *TaHAK1* and *HKT1* was fourfold and eightfold higher, respectively, in inoculated plants at 15 dS m^{-1}. A higher expression of genes (*POD*, *CAT*, *MnSOD*, *APX*, *GR*, and *GPX*), coding antioxidant enzymes was observed in inoculated plants compared to uninoculated plants and the differences were more obvious at higher salinity (15 dS m^{-1}), except for *MnSOD*, whose expression did not increase with salinity stress. The change in expression of GR and GPX was highest with eight and ninefold higher, respectively, in inoculated plants compared to their uninoculated counterparts at 15 dS m^{-1}. Principal component analysis (PCA) vectors of the seedlings grown in 0 dS m^{-1} and 5 dS m^{-1} indicated relatedness in gene expression trends (Figure 3B). However, those of 10 dS m^{-1} and 15 dS m^{-1} remained significantly diverging in patterns. Thus, in general, a characteristic expression of salinity-induced genes appeared more prominent at the salinity levels above 5 dS m^{-1} (Figure 3A). The increasing expression trends typically above 5 dS m^{-1} indicated perception and mounting of indigenous responses by the plants. However, microbial amendment incorporated an additive effect to the indigenous plant responses, thereby improving the physiochemical performance of the seedlings over the control. The alignments of gene expression trends were further corroborated by specific clustering of 0–5; and 10–15 dS m^{-1} regimes (Figure 4).

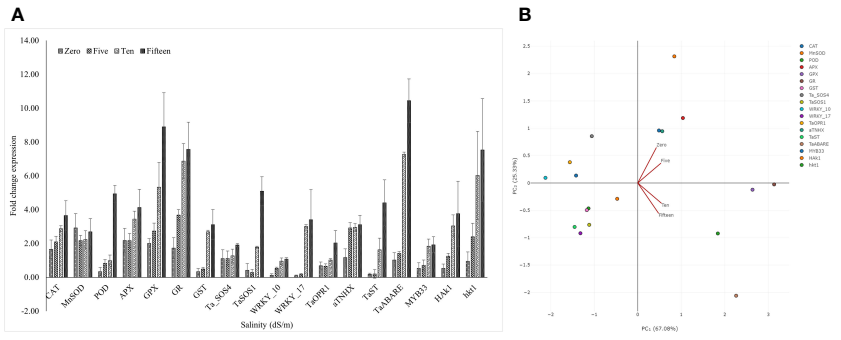

FIGURE 3
Status of different stress responsive gene transcripts at different salinity levels **(A)**. Principle component analysis of gene expression trends under saline conditions **(B)**. Note the relatively aligning trends of expression, respectively, under low intensity (0 dS m^{-1} to 5 dS m^{-1}) and higher intensity (10 dS m^{-1} to 15 dS m^{-1}) of salinity stress.

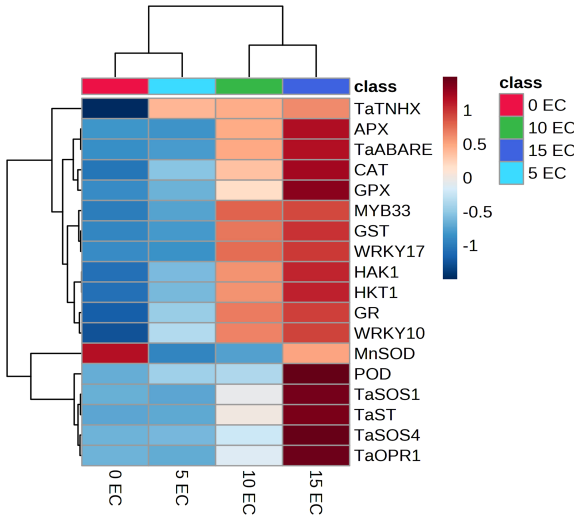

FIGURE 4
Clustered heat map showing specific expression trends of salt-responsive genes in wheat. Note the gradually increasing expression trends from no stress to highest stress regime.

4 Discussion

Many bacterial genera of phylum Actinobacteria, such as *Arthrobacter*, *Frankia*, *Streptomyces*, *Micromonospora*, *Micrococcus*, and *Kocuria*, are widely reported to exhibit plant growth promotion activities (Mitra et al., 2022). The application of BCFE (bacterial culture filtrate extract) derived from actinobacterial genus *Nocardioides* and its positive influence on wheat growth parameters under saline condition was reported in our earlier report (Meena et al., 2020). On similar lines, the *Nocardioides* sp. KNC-3 isolated from Moroccan sites showed the ability to grow on N-free medium indicative of its nitrogen fixing ability (Nafis et al., 2019). The antinobacterial methylotrophic strain *Nocardioides* sp. NIMMe6 used in this study was able to degrade ACC and thereby utilizing sole nitrogen source in the selective media (indicative of its ability to downregulate the ethylene production under stress conditions by sequestering and cleaving plant-produced ACC, which is the biochemical precursor for the ethylene biosynthesis, thereby sinking the excess ethylene to protect the plant from its inhibitory effect. Ethylene, being a gaseous hormone, is involved in plant response to diverse environmental stresses and its synthesis is reported to be induced under salinity stress conditions (Yang et al., 2009). Reduced ethylene levels lead to increased stress tolerance in plants to a wide range of environmental stresses (Glick, 2005). In our study, the inoculated seeds with *Nocardioides* sp. resulted in better root growth (lower S:R ratio) and a superior biomass at higher salinity levels compared to the uninoculated control, which indicated that the inoculated plants better tolerated the negative impact of salinity stress. The negative impact of higher ethylene level on root growth have also been reported in other crops like groundnut (Saravanakumar and Samiyappan, 2007) and *Pisum Sativum* (Barnawal et al., 2014, Gupta et al, 2021).

Exposure to salinity stress leads to increased ROS production in plants stimulating oxidative damage to cell membranes (Talaat, 2019). The ROS so produced are neutralized by non-enzymatic and enzymatic detoxification systems to protect the plants from oxidative damage (Zhang et al., 2022). In this study, the inoculated plants displayed a higher activity of antioxidant enzymes at all salinity levels compared to the uninoculated control plants indicating the positive influence of *Nocardioides* inoculation on enzymatic antioxidant system in wheat. The results of qPCR-based gene expression experiment also confirmed increased expression of CAT (encoding subunit of catalase), POD (gene encoding peroxidase), and APX (gene encoding for ascorbate peroxidase) genes under salinity stress conditions. The increase in gene expression levels CAT, POD, and APX suggest that the *Nocardioides* sp. inoculation resulted in effective scavenging of ROS species by increasing the *de novo* synthesis of antioxidant enzymes at transcription level. The increased activities of peroxidase (POD) and catalase (CAT) in plant growth promoting rhizobacteria (PGPR)-inoculated wheat plants are in agreement with previous report of Haroon and coworkers (Harron et al., 2021), where *B. tequilensis* inoculated plants showed significant increase in activity of POD and CAT at 100 mM salinity compared to uninoculated control. The *in-situ* localization of H_2O_2 and superoxide radicles was also confirmed by DAB reagent-based assay (Thordal-Christensen et al., 1997) and NBT-based assay (Jabs et al., 1996), respectively. Using both the free radicle localization assays, we showed the lower production of H_2O_2 and superoxide radicle in inoculated plants and, hence, supposedly leads to lesser damage to cellular membranes and, thus, leading to high

salt stress tolerance in *Nocardioides* sp. inoculated plants. The higher expression of GPX gene (glutathione peroxidase gene) and GR (Glutathione reductase) was noted in inoculated plants at higher salinity level (10 dS m^{-1} to 15 dS m^{-1}). Glutathione peroxidase catalyses the reduction of hydrogen peroxide (H_2O_2) to water (H_2O), using glutathione (GSH) as a reducing agent. The GR gene encodes the glutathione reductase enzyme, which catalyzes the reduction of oxidized glutathione (GSSG) to reduced glutathione (GSH) using NADPH as a cofactor. The higher expression of GPX and GR genes at higher salinity stress (15 dS m^{-1}) indicates the important role of ascorbate-glutathione antioxidant system in scavenging free radicles produced due to the salinity stress.

We also assessed the FRSA of extracted phenolic compounds using DPPH assay. Phenolic compounds are the most crucial non-enzymatic antioxidants for scavenging the excessive ROS that is generated during stress conditions (Kiani et al., 2021). Our results indicate higher phenolics content in inoculated wheat seedlings compared to the untreated control, and our results also corroborated well with higher DPPH scavenging activity observed in inoculated wheat seedlings. Among various types of ROS produced under stress, the hydroxyl radical ($^{\bullet}OH$) occupies an exceptional position because of its extreme reactivity and its ability to attack even the inert compounds like alkanes, which are otherwise considered to be stable under physiological conditions (Wilson et al., 2006). We used a modified deoxyribose degradation method to assess the DNA damage protection ability of wheat seedlings extract. The hydroxyl radicals were generated *in vitro* in the reaction mix by Fenton reaction and wheat seedling extracts were added to scavenge the hydroxyl radicals causing DNA damage. Our results indicated that the *Nocardioides* sp. inoculated plants showed a higher ability to scavenge hydroxyl radical ($^{\bullet}OH$), thereby minimizing the hydroxyl radical-induced DNA damage under salinity stress conditions. The non-structural polyphenolic compounds and flavonoids are reported to be involved in scavenging the Hydroxyl radicals produced during stress conditions (Kaur et al., 2017). The hydroxyl radical scavenging activity in salt stressed wheat is reported to increase with addition of the exogenously supplied phenolic acids compared to the seedling grown without phenolics application. When plants are subjected to salt stress, one of the most common biological and physiological effects is an increase in the generation of ROS, which include hydroxyl radical (OH), superoxide radical (O_2), and hydrogen peroxide (H_2O_2). Our observations pertaining to antioxidant enzymatic activity assay, DPPH assay and hydroxyl radical scavenging activity assay clearly show that the *Nocardioides* sp. inoculated plants effectively neutralized the free radicals produced and maintained a good redox homeostasis under saline conditions, thereby avoiding damage to cellular membranes and thus registered better growth parameters. These results also corroborated well with the results obtained for H_2O_2 and superoxide radical localization assays performed on intact wheat leaf tissue for inoculated and uninoculated control plants using DAB reagent and NBT reagent, respectively. The *in-situ* localization of free radicals clearly indicated that the accumulation of H_2O_2 and superoxide radical was much lower in inoculated plants even at higher salinity of 15 dS m^{-1} compared to the uninoculated control plants (Figures 2A, B). The DAB used for H_2O_2 localization polymerizes into a radish brown polymer immediately at sites of peroxidase activity as soon it comes into contact with H_2O_2 (Thordal-Christensen et al., 1997). The development of smaller and less prominent patches of radish color in treated inoculated plants at all salinity levels indicated that the production of $H_2O_2$was lesser in inoculated plants compared to uninoculated control. Similarly, the NBT staining was used to localize the superoxide radicals, whose presence was indicated by the development of purple precipitate in the target leaf tissue (Figure 2B). The lesser number of purple lesions developed in inoculated plants indicated lesser superoxide ions produced under salinity stress in *Nocardioides* sp. inoculated wheat plants. In addition to enhancing ROS scavenging abilities and antioxidant enzyme activities, the improved regulation of ion balance contributed to the enhanced salt tolerance observed in inoculated plants.

The increased expression of *TaSOS1* gene in inoculated plants at higher salinity implies better regulation of ion homeostasis through SOS pathway. The SOS pathway involves a series of signaling events that result in the activation of plasma membrane ion transporters, such as Na^+/H^+antiporter, which pumps excess Na^+ ions out of the cell and helps to maintain a favorable cytosolic Na^+/K^+ ratio (Zhu, 2016). SOS1 is a plasma membrane Na^+/H^+ anti-porter, which plays a crucial role in regulating long-distance Na^+ transport from root to shoot, contributing to salt tolerance. On the other hand, SOS4 encodes pyridoxal kinase, which is involved in the biosynthesis of pyridoxal-5-phosphate, an essential cofactor for numerous cellular enzymes (Nidhi et al., 2016). A higher expression of *TaTNHX*, HAK1, and *HKT1* genes which encodes for "vacuolar cation/proton exchanger," "potassium transporter," and "high-affinity sodium transporter," respectively was observed in inoculated plants compared to their uninoculated counterparts suggesting that the increased salt stress tolerance in inoculated plants was mediated through the increased activity of ion transporters. The over expression of *TaTNHX* has been shown to enhance salt tolerance in plants such as *Arabidopsis* by reducing the accumulation of toxic Na^+ ions in the cytoplasm and thereby increasing the sequestration of Na^+ ions into the vacuoles (Li et al., 2019). Similarly, the over expression of *HAK1* gene in *Arabidopsis thaliana* and bread wheat has been linked to improved salt tolerance in both plants (Li et al., 2021). The over expression of wheat HKT1 gene in transgenic alfalfa resulted in improved salt tolerance suggesting that the regulation of HKT1 expression and activity is a key factor in improving plant salt tolerance (Zhang et al., 2018). In this study, we also studied the expression profile of genes encoding for transcription factors such as WRKY10, WRKY17, and MYB33 in inoculated and uninoculated plants. Transcription factor genes are known to play a crucial role in the regulation of various stress-responsive genes that are involved in salt stress tolerance mechanisms in plants. We noted a higher expression of WRKY17 in inoculated plants at higher salinity suggesting its critical role in regulating salt stress-response in wheat seedlings. WRKY17 over expression was found to up

regulate the expression of various stress-responsive genes, including those involved in ion transport and osmotic adjustment (Wang et al., 2019).

5 Conclusion

The results clearly underscore the applicability of methylotrophic bacteria for enhancing salinity stress tolerance in wheat. *Nocardioides* sp. used in this study implies major modes of action include ABA-mediated cascades, subsequent enhanced enzyme and non-enzyme-based oxidative stress management, cellular osmolytes, and important membrane proteins involved in ionic interactions to manage cellular Na^+ levels. The transcript profiles indicate involvement of ABA as predominantly functioning pathway for *Nocardioides* sp.–mediated salt stress management in early wheat. With these newly available mechanisms, an investigation of the *Nocardioides* strain under naturally stressed conditions is required to validate its capabilities as a biological input to mitigate salinity (and potentially drought) stress in wheat.

Data availability statement

The data presented in the study are deposited in the DDBJ-GenBank repository, and can be accessed at https://www.ncbi.nlm.nih.gov/nucleotide/ with the accession number LC140963.

Author contributions

KM: conceptualization; KM and AMS: experimental design; AMS, UB, ALS, and SaK: experimental implementation; UB, AMS, GW, and SaK: results compilation and statistical analyses; AMS, KM, and UB: initial draft preparation; SaK, MK, ShK, and DS: copy editing and improvements. All authors contributed to the article and approved the submitted version.

Acknowledgments

Authors are grateful to ICAR-Central Arid Zone Research Institute, India; and ICAR-National Bureau of Agriculturally Important Microorganisms – India for financial support through the network project on Application of Microorganisms in Agriculture and Allied Sectors.

Conflict of interest

The authors declare that the research was conducted in the absence of any commercial or financial relationships that could be construed as a potential conflict of interest.

Publisher's note

Supplementary material

The Supplementary Material for this article can be found online at: https://www.frontiersin.org/articles/10.3389/fpls.2023.1249600/full#supplementary-material

References

Barnawal, D., Bharti, N., and Maji, D. (2014). ACC deaminase-containing Arthrobacterprotophormiae induces NaCl stress tolerance through reduced ACC oxidase activity and ethylene production resulting in improved nodulation and mycorrhization in Pisumsativum. *J. Plant Physiol.* 171, 884–894. doi: 10.1016/j.jplph.2014.03.007

Dhindsa, R. S., Plumb-Dhindsa, P., and Thorpe, T. A. (1981). Leaf senescence: correlated with increased levels of membrane permeability and lipid peroxidation, and decreased levels of superoxide dismutase and catalase. *J. Exp. Bot.* 32, 93–101. doi: 10.1093/jxb/32.1.93

Dong, C. J., Wang, L. L., Li, Q., and Shang, Q. M. (2019). Bacterial communities in the rhizosphere, phyllosphere and endosphere of tomato plants. *PloS One* 14 (11), e0223847. doi: 10.1371/journal.pone.0223847

Dworkin, P., and Foster, R. (1958). Experiments with some microorganisms which utilize ethane and hydrogen. *J. Bacteriol.* 75, 592–604.

Fedorov, D. N., Doronina, N. V., and Trotsenko, Y. A. (2011). Phytosymbiosis of aerobic methylobacteria: New facts and views. *Microbiology* 80, 443–454. doi: 10.1134/S0026261711040047

Glick, B. R. (2005). Modulation of plant ethylene levels by the bacterial enzyme ACC deaminase. *FEMS Microbiol. Lett.* 251 (1), 1–7. doi: 10.1016/j.femsle.2005.07.030

Gupta, S., and Pandey, S. (2019). ACC deaminase producing bacteria with multifarious plant growth promoting traits alleviates salinity stress in french bean (Phaseolus vulgaris) plants. *Front. Microbiol.* 10. doi: 10.3389/fmicb.2019.01506

Honma, M., and Shimomura, T. (1978). Metabolism of 1-aminocyclopropane-1-carboxylic acid. *Agril Biol. Chem.* 42, 1825–1831.

Inbaraj, M. P. (2021). Plant-microbe interactions in alleviating abiotic stress—a mini review. *Front. Agron.* 3, 667903. doi: 10.3389/fagro.2021.667903

Ivanova, E. G., Doronina, N. V., and Trotsenko, Y. A. (2001). Aerobic methylobacteria are capable of synthesizing auxins. *Microbiology* 70, 392–397. doi: 10.1023/A:1010469708107

Jabs, T., Dietrich, R. A., and Dangl, J. L. (1996). Initiation of runaway cell death in an *Arabidopsis* mutant by extracellular superoxide. *Science* 273 (5283), 1853–1856.

Kaur, H., Bhardwaj, R. D., and Grewal, S. K. (2017). Mitigation of salinity-induced oxidative damage in wheat (*Triticum aestivum* L.) seedlings by exogenous application of phenolic acids. *Acta Physiologiae Plantarum* 39, 1–15. doi: 10.1007/s11738-017-2521-7

Kiani, R., Arzani, A., and Mirmohammady Maibody, S. A. M. (2021). Polyphenols, flavonoids, and antioxidant activity involved in salt tolerance in wheat, Aegilopscylindrica and their amphidiploids. *Front. Plant Sci.* 12, 646221. doi: 10.3389/fpls.2021.646221

Kumar, A., and Verma, J. P. (2018). Does plant-Microbe interaction confer stress tolerance in plants: A review? *Microbiol. Res.* 207, 41–52. doi: 10.1016/j.micres.2017.11.004

Li, X. (2013). Solvent effects and improvements in the deoxyribose degradation assay for hydroxyl radical-scavenging. *Food Chem.* 141 (3), 2083–2088. doi: 10.1016/j.foodchem.2013.05.084

Li, Z., Li, B., Tong, Y., Zhang, A., Wang, T., Li, Y., et al. (2021). Over expression of wheat HAK1 improves salt tolerance of Arabidopsis thaliana and bread wheat. *Front. Plant Sci.* 12. doi: 10.3389/fpls.2021.667847

Li, H., Zhang, X., Chen, J., Liang, J., Li, J., Wang, Y., et al. (2019). Over expression of wheat vacuolar Na+/H+ antiporter gene (*TaNHX3*) enhances tolerance to salt stress in Arabidopsis thaliana. *Plant Physiol. Biochem.* 143, 153–162. doi: 10.1016/j.plaphy.2019.08.018

Luck, H. (1971). "Catalase". in *Methods of enzymatic analysis.* Ed, B. Hu 3, 279.

Madhaiyan, M., Poonguzhali, S., Senthilkumar, M., Seshadri, S., Chung, H., Wang, J. Y., et al. (2004). Growth promotion and induction of systemic resistance in rice cultivar Co-47 (*Oryza sativa* L.) by Methylobacterium spp. *Bot. Bull. Acad. Sin.* 45, 315–324.

Meena, K. K., Sorty, A. M., Bitla, U. M., Choudhary, K., Gupta, P., Pareek, A., et al. (2017). Abiotic stress responses and microbe-mediated mitigation in plants: the omics strategies. *Front. Plant Sci.* 8, 172. doi: 10.3389/fpls.2017.00172

Meena, K. K., Bitla, U. M., Sorty, A. M., Singh, D. P., Gupta, V. K., Wakchaure, G. C., et al. (2020). Mitigation of salinity stress in wheat seedlings due to the application of phytohormone-rich culture filtrate extract of methylotrophic actinobacterium Nocardioides sp. NIMMe6. *Front. Microbiol.* 11, 2091. doi: 10.3389/fmicb.2020.02091

Meena, K. K., Kumar, M., Kalyuzhnaya, M. G., Yandigeri, M. S., Singh, D. P., Saxena, A. K., et al. (2012). Epiphytic pink-pigmented methylotrophic bacteria enhance germination and seedling growth of wheat (*Triticum aestivum*) by producing phytohormone. *Antonie Van Leeuwenhoek* 101, 777–786. doi: 10.1007/s10482-011-9692-9

Mitra, D., Mondal, R., Khoshru, B., Senapati, A., Radha, T. K., Mahakur, B., et al. (2022). Actinobacteria-enhanced plant growth, nutrient acquisition, and crop protection: Advances in soil, plant, and microbial multifactorial interactions. *Pedosphere* 32 (1), 149–170. doi: 10.1016/S1002-0160(21)60042-5

Munir, N., Hanif, M., Abideen, Z., Sohail, M., El-Keblawy, A., Radicetti, E., et al. (2022). Mechanisms and strategies of plant microbiome interactions to mitigate abiotic stresses. *Agronomy* 12), 2069. doi: 10.3390/agronomy12092069

Nafis, A., Raklami, A., Bechtaoui, N., El Khalloufi, F., El Alaoui, A., Glick, B. R., et al. (2019). Actinobacteria from extreme niches in Morocco and their plant growth-promoting potentials. *Diversity* 11 (8), 139. doi: 10.3390/d11080139

Nidhi, B., Pandey, S. S., Deepti, B., Patel, V. K., and Alok, K. (2016). Plant growth promoting rhizobacteria Dietzia natronolimnaea modulates the expression of stress responsive genes providing protection of wheat from salinity stress. *Sci. Rep.* 6 (1), 34768.

Putter, J. (1974). "Peroxidases," in *Methods of enzymatic analysis* (San Diego: Academic), 685–690.

Riyazuddin, R., Verma, R., Singh, K., Nisha, N., Keisham, M., Bhati, K. K., et al. (2020). Ethylene: a master regulator of salinity stress tolerance in plants. *Biomolecules.* 10 (6), 959. doi: 10.3390/biom10060959

Senthilkumar, M., Amaresan, N., and Sankaranarayanan, A. (2021). "Estimation of ACC deaminase activity in bacterial cells," in *Plant-microbe interactions* (Humana, New York, NY: Springer Protocols Handbooks). doi: 10.1007/978-1-0716-1080-0_18

Singleton, V. A., and Rossi, J. A. (1965). Colorimetry of total phenolics with phosphomolybdic-phosphotungstic acid reagents. *Am. J. Enol Vitic* 16 pp, 144–158. doi: 10.5344/ajev.1965.16.3.144

Srivastava, A., Dixit, R., Chand, N., and Kumar, P. (2022). Overview of methylotrophic microorganisms in agriculture. *Bio Sci. Res. Bull.* 38 (1), 65–71. doi: 10.5958/2320-3161.2022.00009.8

Subhaswaraj, P., Jobina, R., Parasuraman, P., and Siddhardha, B. (2017). Plant growth promoting activity of pink pigmented facultative methylotroph-methylobacterium extorquens mm2 on lycopersicon esculentum l. *J. App. Biol. Biotech.* 5 (01), 042–046. doi: 10.7324/JABB.2017.50107

Thordal-Christensen, H., Zhang, Z., Wei, Y., and Collinge, D. B. (1997). Subcellular localization of H_2O_2 in plants. H_2O_2 accumulation in papillae and hypersensitive response during the barley—powdery mildew interaction. *Plant J.* 11 (6), 1187–1194.

Wang, X., Chen, X., Liu, Y., and Shen, W. (2019). Over expression of the WRKY17 gene enhances the salt tolerance of *Arabidopsis thaliana*. *J. Plant Physiol.* 234, 93–105. doi: 10.1016/j.jplph.2019.02.019

Wilson, E. W., Hamilton, W. A., Kennington, H. R., Evans, B., Scott, N. W., and DeMore, W. B. (2006). Measurement and estimation of rate constants for the reactions of hydroxyl radical with several alkanes and cycloalkanes. *J. Phys. Chem. A* 110 (10), 3593–3604. doi: 10.1021/jp055841c

Xu, N., Zhao, Q., Zhang, Z., Zhang, Q., Wang, Y., Qin, G., et al. (2022). Phyllosphere microorganisms: sources, drivers, and their interactions with plant hosts. *J. Agric. Food Chem.* 70 (16), 4860–4870. doi: 10.1021/acs.jafc.2c01113

Yang, J., Kloepper, J. W., and Ryu, C. ,. M. (2009). Rhizosphere bacteria help plants tolerate abiotic stress. *Trends Plant Sci.* 14, 1–4. doi: 10.1016/j.tplants.2008.10.004

Zhang, H., Liu, W., Wan, L., Liu, T., and Li, L. (2018). Increased expression of the wheat HKT1 gene enhances salt tolerance in transgenic alfalfa (*Medicago sativa* L.). *Plant Sci.* 272, 277–286. doi: 10.1016/j.plantsci.2018.03.023

Zhang, Y., Zheng, L., Yun, L., Ji, L., Li, G., Ji, M., et al. (2022). Catalase (CAT) Gene family in wheat (*Triticum aestivum* L.): evolution, expression pattern and function analysis. *Int. J. Mol. Sci.* 23 (1), 542.

Zhu, J. K. (2016). Abiotic stress signaling and responses in plants. *Cell* 167 (2), 313–324. doi: 10.1016/j.cell.2016.08.029

frontiers | Frontiers in Plant Science

TYPE Original Research
PUBLISHED 04 December 2023
DOI 10.3389/fpls.2023.1278954

OPEN ACCESS

EDITED BY
Keni Cota-Ruiz,
Utica University, United States

REVIEWED BY
Manoj Kumar Solanki,
University of Silesia in Katowice, Poland
Satish Kumar,
Directorate of Onion and Garlic Research (ICAR), India

*CORRESPONDENCE
Qinghua He
demeatry@gmail.com
Qinglian Zhang
qlzhang80@163.com

†These authors have contributed equally to this work

RECEIVED 17 August 2023
ACCEPTED 10 November 2023
PUBLISHED 04 December 2023

CITATION
Zhang B, Deng C, Wang S, Deng Q, Chu Y, Bai Z, Huang A, Zhang Q and He Q (2023) The RNA landscape of *Dunaliella salina* in response to short-term salt stress. *Front. Plant Sci.* 14:1278954. doi: 10.3389/fpls.2023.1278954

The RNA landscape of *Dunaliella salina* in response to short-term salt stress

Bingbing Zhang[1†], Caiyun Deng[2†], Shuo Wang[1], Qianyi Deng[1], Yongfan Chu[3], Ziwei Bai[3], Axiu Huang[2], Qinglian Zhang[2*] and Qinghua He[3*]

[1]The Research Institute of Qinghai-Tibet Plateau, Southwest Minzu University, Chengdu, China, [2]School of Laboratory Medicine, Chengdu Medical College, Chengdu, China, [3]Key Laboratory of Qinghai-Tibet Plateau Animal Genetic Resource Reservation and Utilization, Southwest Minzu University, Chengdu, China

Using the halotolerant green microalgae *Dunaliella salina* as a model organism has special merits, such as a wide range of salt tolerance, unicellular organism, and simple life cycle and growth conditions. These unique characteristics make it suitable for salt stress study. In order to provide an overview of the response of *Dunaliella salina* to salt stress and hopefully to reveal evolutionarily conserved mechanisms of photosynthetic organisms in response to salt stress, the transcriptomes and the genome of the algae were sequenced by the second and the third-generation sequencing technologies, then the transcriptomes under salt stress were compared to the transcriptomes under non-salt stress with the newly sequenced genome as the reference genome. The major cellular biological processes that being regulated in response to salt stress, include transcription, protein synthesis, protein degradation, protein folding, protein modification, protein transport, cellular component organization, cell redox homeostasis, DNA repair, glycerol synthesis, energy metabolism, lipid metabolism, and ion homeostasis. This study gives a comprehensive overview of how *Dunaliella salina* responses to salt stress at transcriptomic level, especially characterized by the nearly ubiquitous up-regulation of the genes involving in protein folding, DNA repair, and cell redox homeostasis, which may confer the algae important mechanisms to survive under salt stress. The three fundamental biological processes, which face huge challenges under salt stress, are ignored by most scientists and are worth further deep study to provide useful information for breeding economic important plants competent in tolerating salt stress, other than only depending on the commonly acknowledged osmotic balance and ion homeostasis.

KEYWORDS

salt stress, *Dunaliella salina*, comparative transcriptomic analysis, protein Folding, DNA repair, cellular redox homeostasis

1 Introduction

Salt stress of plants is an active area of research. A lots of researches have been carried out using the model plant *Arabidopsis thaliana* (Møller and Tester, 2007), partially because that *Arabidopsis thaliana* has a clear genetic background and is from the same family *Brassicaceae* as some economic important crops and vegetables, such as rapeseed, cabbage, radish et al., and the response mechanisms of *Arabidopsis thaliana* under salt stress may better reflect those of related crops (Kowalski et al., 1994).

Dunaliella salina is an extremely halotolerant, unicellular, eukaryotic, photosynthetic green microalgae, which is unique in its remarkable ability to survive in media containing NaCl at a wide range of concentrations, from about 0.05 M to 5.5 M (Ben-Amotz and Avron, 1973). *Dunaliella salina* can grow easily in aqueous media in a flask, which makes it very convenient to apply salt stress and other abiotic stresses, such as heavy metal, nutrition, temperature and light stress, on it for study. Compared with *Arabidopsis thaliana*, *Dunaliella salina* is unicellular, cells in log phase are highly homogeneous. For this reason, it is hopefully to find some of the fundamental and conserved mechanisms that remain uncovered due to cellular heterogeneity of study materials. These characteristics make *Dunaliella salina* a very good model organism for studying salt stress response and tolerance (Ben-Amotz and Avron, 1973).

Omics methods, such as methods of genomics, transcriptomics and proteomics, are powerful tools to reveal the mechanisms of salt tolerance and can give an overview of the response of plants to salt stress because omics aims at the collective characterization and quantification of pools of biological molecules (Mangelsen et al., 2011; Marco et al., 2011; Kang et al., 2020). With the development of high throughput sequencing technology, comparative transcriptomic analysis becomes an efficient and powerful method to reveal the response of plants to all kinds of stress at a global level, and some papers reported using this method to study the response of *Dunaliella salina* to salt stress (He et al., 2020a; Gao et al., 2021; Lv et al., 2021; Panahi and Hejazi, 2021). Considering that morphological change and glycerol synthesis in *Dunaliella salina* are almost accomplished in about 2 hours after salt stress (Chitlaru and Pick, 1989; Oren, 2005), it is universally acknowledged that most of the adaptive changes of *Dunaliella salina* should occur within about 2 hours under salt stress. Lv et al. (Lv et al., 2021) reported the transcriptomes at 15, 30, 60, and 120-min under salt stress of 4.5 M NaCl, finding that GO (Gene Ontology) terms of "chromosome and associated proteins", "transporters", and "cytoskeleton proteins" were enriched by differentially expressed genes (DEGs). They also analyzed the expression of enzymes in the core carbon metabolism pathway, such as starch catabolism, glycolysis, Calvin cycle and glycerol metabolic pathways. However, except the core carbon metabolism pathway, other biological processes and pathways weren't analyzed in detail. He et al. (He et al., 2020a) reported the transcriptomes at 30, 60, and 120-min under salt stress of 2.5M NaCl, found that some biological processes, such as photosynthesis, lipid metabolism, amino acids and protein metabolism, starch and sucrose metabolism and glycerol synthesis, were enriched by the DEGs. They also constructed for the first time the carbon metabolism pathway from starch to glycerol in *Dunaliella salina*. In that study, the transcripts from the third-generation sequencing (PacBio sequencing) was used as the reference genes for gene expression quantification analysis due to there was no genome data of *Dunaliella salina* strain CCAP 19/30 available at the moment. Although this method has the advantage to detect alternatively spliced transcripts, there exist obvious drawbacks, since artificially spliced transcripts generated during incomplete reverse transcription could interfere the expressional quantification of the genes and the potential loss of low-abundance mRNAs could lower genome coverage (Van Dijk et al., 2018). Recently we sequenced the whole genome of *Dunaliella salina* strain CCAP 19/30 by PacBio sequencing, which gave a total of 13509 genes by annotation. Using this high-quality genome sequence as the reference, we redo in this study the comparative transcriptomic analysis for *Dunaliella salina* strain CCAP 19/30 under salt stress of 2.5 M NaCl within 2 hours duration. In addition to helping to focus on identifying and analyzing the major biological processes being regulated to reflect the responses of *Dunaliella salina* to salt stress at a global level, the high-quality reference genome also enables us to analyze the specific pathways, the glycerol synthesis, the fatty acid synthesis, and the TAG synthesis pathway in detail, especially the key enzymes that regulate a specific pathway. This work gives an overview of the response of *Dunaliella salina* to salt stress at transcriptomic level. The nearly ubiquitous up-regulation of the genes involved in protein folding, DNA repair, and cell redox homeostasis characterizes the expression profile of *Dunaliella salina* when confronting salt stress, which may be important mechanisms to enable the algae to survive under salt stress.

2 Materials and methods

2.1 Algae and culture conditions

Dunaliella salina strain CCAP 19/30 was obtained from Mariela A. González and Thomas Pröschold. The algae grew in a controlled-environment chamber with 16 h lighting (17500 lx) and 8 h darkness at 20 °C. The growth medium contains 1 M NaCl, 5.0 mM $NaNO_3$, 5.0 mM $MgSO_4 \cdot 7H_2O$, 0.1 mM $NaH_2PO_4 \cdot 2H_2O$, 1.0 mM KCl, 10.0 mM $NaHCO_3$, 0.3 mM $CaCl_2 \cdot 2H_2O$, 4.6 uM H_3BO_3, 0.9 uM $MnCl_2.4H_2O$, 0.08 uM $ZnSO_4.7H_2O$, 0.03 uM $CuSO_4.5H_2O$, and 0.02 uM $Na_2MoO_4.2H_2O$. Briefly, the algae grew in growth medium containing 1 M NaCl. Salt stress was applied by adding equal volume of high-salt medium (containing 4M NaCl) to the growth medium containing algae in log phase (1×10^6 cells/ml), which resulted in an increasing of salt concentration from 1 M to 2.5 M. Then the algae were collected at the time points of 0.5 h, 1 h and 2 h after the applying of salt stress, respectively, for RNA extraction. The algae were also collected before stress for RNA extraction to serve as the control. The salt stress and RNA extraction experiments were performed in triplicate.

2.2 Genome sequencing, assembling, and annotation

The genomic DNA was extracted using plant genomic DNA extraction kit (DP305, TIANGEN, China) by omitting the step of tissue homogenization by liquid nitrogen. Following genomic DNA extraction, libraries were generated and sequenced by using either the Illumina (insert size 350 bp) or the PacBio platforms. Totally, 102.65 Gbp were produced including 25.44 Gbp Illumina data (sequencing depth is 92.7 × and 77.21 Gbp PacBio data (sequencing depth is 281.4 × The sequencing coverage is 99.38%. The genome was assembled using overlap-layout-consensus algorithm (Lieberman-Aiden et al., 2009). The main genome assembly is about 223.7 Mbp with contig N50 = 2.93 Mbp, scaffold N50 = 13.13 Mbp. Using the RNA-Seq data of *Dunaliella salina* strain CCAP 19/30 and the published genomic data of closely related algae, 13509 protein-coding genes were found in the genome and used for comparative transcriptomic analysis.

2.3 RNA-Seq and gene expression analysis

Total RNA was extracted with Trizol (Invitrogen, USA) by following the user manual for suspension cell culture. Briefly, the algae cells from salt stress treatment group and control group were collected immediately by centrifugation at room temperature for 5 min at 4000 × g, and quickly lysed by adding 1 ml Trizol. The time from centrifugation to lysing should be as short as possible to avoid additional stress. The remaining steps are the same as the manual recommends. The RNA pellets were kept in 75% ethanol and stored at -80°C before library construction. For library construction, mRNA was purified from total RNA and fragmented to perform cDNA synthesis. The cDNA was used to construct library with insert size of 350 bp. The libraries were sequenced by HiSeq 2000 platform to generate paired-end reads of 150 bp. The raw reads were processed to generate clean reads by removing adapter sequences, excluding reads contain >10% ambiguous bases N and > 50% bases with Qphred ≤20. The clean reads were used to quantify the values of expression of the reference genes from genome annotation of *Dunaliella salina* CCAP 19/30. Briefly, read count of each gene was calculated by mapping the clean reads from each RNA sample to the full-length coding sequence of the reference gene using HTSeq v0.6.1 (Anders et al., 2015). And then FPKM (expected number of Fragments per Kilobase of transcript sequence per Millions base pairs sequenced) of the genes was calculated by involving parameters of gene length, reads count and sequencing depth (Trapnell et al., 2010).

Differential expression analysis of the genes from two groups was performed by using the DESeq R package with the read counts of the genes (Anders and Huber, 2010). The resulting P values from DESeq were adjusted using the Benjamini and Hochberg's approach for controlling the false discovery rate. Those with an adjusted P-value below 0.05 were considered as differentially expressed genes (DEGs). Heatmaps were made using online tool Chiplot (https://www.chiplot.online).

2.4 Functional enrichment analysis

Functional categorization of the DEGs was performed by using Gene Ontology (GO) database and Kyoto Encyclopedia of Genes and Genomes (KEGG) database. GO enrichment analysis of DEGs was performed by using the BLAST2GO platform (Conesa et al., 2005) and the GOseq R package (Young et al., 2010). GO terms with corrected P value below 0.05 were considered significantly enriched. KEGG enrichment analysis of DEGs was performed by using the KEGG Automatic Annotation Server (Moriya et al., 2007) and KOBAS software (Mao et al., 2005). KEGG terms with false discovery rate (FDR) below 0.05 were considered significantly enriched.

2.5 Quantitative real-time PCR

In order to confirm the genes expression profiles resulting from high throughput RNA-seq analysis, we performed real-time PCR to analyze the expressions of the key genes from each pathway or functional group. The real-time PCR kit was from QIAGEN (208054, Germany). The primers used in real-time PCR were in the Supplementary Materials (Supplementary File 2). The reference genes used in real-time PCR were elongation factor 1-alpha. The relative expression quantification was calculated by the $2^{-\Delta\Delta Ct}$ method (Livak and Schmittgen, 2001).

3 Results

3.1 Overview of the transcriptomic response

There were 13509 genes annotated in the genome of *Dunaliella salina*. Among the 9537 genes annotated by the GO database, the number of differently regulated genes (DEGs) increased from 4142 at 0.5-hour under stress, to 4568 at 1-hour, and to 6577 at 2-hour, accounting for about 31%, 34%, and 49% of the total genes. The number of DEGs increased with the increasing of stress time. By using GO enrichment analysis, most of these differently regulated genes (DEGs) can be clustered into some biological processes. These biological processes reflect the responses during the first two hours of *Dunaliella salina* when confronting salt stress at a more global level, include transcription, protein synthesis, protein degradation, protein folding, protein modification, protein transport, cellular component organization, cell redox homeostasis, DNA repair, glycerol synthesis, energy metabolism, lipid metabolism, and ion homeostasis. Among them, protein folding, DNA repair, and cell redox homeostasis are the three eye-catching ones characterized by the nearly ubiquitous up-regulation of the genes involved in them. All the biological processes are analyzed and discussed in the following sections.

3.2 Biological processes being regulated under salt stress

3.2.1 Transcription

3.2.1.1 Regulation of transcription initiation

There were 33 genes encoding subunits of DNA-directed RNA polymerases (RNAP) annotated in the genome of *Dunaliella salina*. Twenty-two of them were differentially expressed, including the largest and catalytic core components of RNAP I, II and III (subunit rpa1, subunit 1, and subunit rpc1 respectively), the second largest components of RNAP II and III (subunit RPB2 and subunit RPC2), components of RNAP II, IV and V (subunit 11 and 12), and other subunits of RNAPs. The chloroplastic/mitochondrial specific RNA polymerase 2 was also included (Supplementary File 1: Figure S1).

Lots of transcription factors (TFs) were differentially expressed, including general transcription factors and gene specific transcription factors. The general TFs included subunits of RNA polymerase II transcription factor B, transcription factor IIH subunit 2, transcription termination factor MTERF9, mediator of RNA polymerase II transcription subunit 6, etc. The gene specific TFs, which regulate specific genes, included ethylene-responsive transcription factor AIL1, transcription factor VIP1, heat stress transcription factor A-1d, leucine zipper transcription factor-like protein 1, etc. (Supplementary File 1: Figure S2). Previous studies show that these TFs participated in variety of biologic processes including response to abiotic stresses (salt, osmotic, and heat stress), DNA repair, cell cycle, lipid accumulation, protein transport, etc. (Table 1).

3.2.1.2 Pre-initiation regulation of transcription

Besides the TFs involved in regulations of transcription, some genes involved in chromatin remodeling and histone modification were also differentially expressed, including histone-lysine N-methyltransferases, histone acetyltransferases, CHD3-type chromatin-remodeling factor PICKLE, protein chromatin remodeling 20, bromodomain-containing protein 7, etc. The regulation of these genes reflects pre-initiation regulations of transcription which affect the binding of the core transcriptional machinery proteins to the core promoter sequence on the coding region of the DNA.

3.2.1.3 Post-transcriptional regulation

Some genes involved in post-transcriptional regulations (RNA processing) were also differentially expressed, including pre-mRNA splicing factors, mRNA decapping enzymes, tRNA & rRNA methyltransferases, Zinc phosphodiesterases, Component of the SSU processome, RAP domain-containing protein, etc. These DEGs can be classified by function into groups of pre-mRNA splicing, mRNA decay, and tRNA and rRNA processing.

3.2.2 Protein synthesis and degradation

3.2.2.1 Protein synthesis

The GO term of peptide biosynthetic process was significantly enriched by DEGs. Lots of genes encoding ribosomal proteins were up-regulated, including chloroplast, mitochondrial, and cytosolic ribosomal protein genes (Supplementary File 1: Figure S3). Most of

TABLE 1 Differently expressed transcription factors and their reported function.

Gene ID	Name	Function
General TFs		
DsaChr060759	Mediator of RNA polymerase II transcription subunit 6	A coactivator involved in the transcription of RNAP II-dependent genes. 10.1128/MCB.17.8.4622
DsaChr090323	Transcription termination factor MTERF9, chloroplastic	Required for processing and steady-state levels of plastid transcripts. Involved in response to abiotic stresses. 10.1111/ppl.12307
DsaChr020919	General transcription factor IIH subunit 2	Component of TFIIH core complex, which is involved in DNA repair and transcription by RNAP II. (PubMed: 16623910).
DsaChr090639	Probable RNA polymerase II transcription factor B subunit 1-1	Component of TFIIH core complex, which is involved in DNA repair and transcription by RNAP II. PMID: 8194529
DsaChr160111	RNA polymerase II transcription factor B subunit 2	Component of TFIIH core complex, which is involved in DNA repair and transcription by RNAP II. PMID: 8194529
DsaChr050631	RNA polymerase II transcription factor B subunit 4	Component of TFIIH core complex, which is involved in DNA repair and transcription by RNAP II. PMID: 8194529
DsaChr030808	Transcription factor IIIB 90 kDa subunit	Involved in the transcription of tRNA, 10.1128/mcb.11.10.5181-5189.1991
Gene specific TFs		
DsaChr130238	Leucine zipper transcription factor-like protein 1	Response to salt stress, 10.1016/j.gene.2005.04.014
DsaChr010232	Transcription factor VIP1	Involved in osmosensory response, (PubMed: 25093810).
DsaChr030409	Heat stress transcription factor A-1d	High light and heat stress, 10.1093/pcp/pcr045
DsaChr120169	Nuclear transcription factor Y subunit C-2	Activated by Photooxidative Stress, 10.3390/ijms13033458
DsaChr040243	AP2-like ethylene-responsive transcription factor AIL1	Involved in biotic and abiotic stress, 10.3389/fpls.2019.00228
DsaChr100475	Nascent polypeptide-associated complex subunit beta	Play a central role as a proteostasis sensor, control translational activity in response to stress, 10.1038/emboj.2013.87
DsaChr030772	Transcription factor bHLH140	Involved DNA repair, 10.1093/bib/bbr042
DsaChr060567	Transcription factor Pur-alpha 1	Involved in cell cycle and DNA repair 10.4161/cc.8.3.7585

(Continued)

TABLE 1 Continued

Gene ID	Name	Function
DsaChr050740	Paired amphipathic helix protein Sin3b	Acts as a transcriptional repressor, regulates cell cycle progression (PubMed: 22476904).
DsaChr070147	Transcription factor BOA	Transcription factor that is a critical component of the regulatory circuit of the circadian clock. 10.1105/tpc.111.084293
DsaChr060003	Transcription factor MYB1	Lipid accumulation, 10.1111/nph.18141
DsaChr110109	Ankyrin repeat domain-containing protein 26	Acts as a regulator of adipogenesis.10.1371/journal.pone.0038130
DsaChr060686	Ankyrin repeat domain-containing protein 50	Involved in protein transport (PubMed: 25278552).
DsaChr090477	Helicase-like transcription factor CHR27	Involved in transcriptional gene silencing. (PubMed: 25420628).
DsaChr040325	Protein BFR2	Involved in 18S ribosomal RNA processing, 10.1093/nar/gkt1293
DsaChr120929	Putative transcription elongation factor SPT5 homolog 1	Enhances transcription, 10.1128/MCB.00609-09
DsaChr030474	Transcription factor 25	May play a role in cell death control. 10.1016/j.bbrc.2006.02.187
DsaChr020321	Transcription factor A, mitochondrial	DNA packaging factor in mitochondria regulating mitochondria gene expression, 10.1073/pnas.1119738109
DsaChr050461	Transcription factor DIVARICATA	Involved in the dorsovental asymmetry of flowers. Promotes ventral identity, flower development, 10.1101/gad.221002.

the 40S and 60S ribosomal proteins showed up-regulation at 0.5-hour and 1-hour under stress, and return to normal level at 2-hour under stress, on the other side, most of the 30S and 50S ribosomal proteins showed up-regulation at 2-hour of stress (Supplementary File 1: Figure S3). Lots of aminoacyl-tRNA ligases, translation initiation factors, and translation elongation factors were also up-regulated (Supplementary File 1: Figure S4). The up-regulation of these genes possibly reflect the accelerating of protein synthesis. The child term glycoprotein biosynthetic process was also enriched, subunits of dolichyldiphosphooligosaccharide-protein glycosyltransferase, Exostosin-like 2 & 3, and UDP-glucose: glycoprotein glucosyltransferase were up-regulated, which may reflect the regulation of glycoprotein synthesis.

3.2.2.2 Protein degradation

On the other side, the GO term of ubiquitin-dependent protein catabolic process was enriched. Lots of ubiquitin-protein ligases, ubiquitin-conjugating enzymes (Supplementary File 1: Figure S5), and subunits of 26S proteasome were up-regulated (Supplementary File 1: Figure S6). The up-regulation of the genes possibly suggest the acceleration of protein degradation by ubiquitin proteasome system (UPS).

The accelerating of both protein synthesis and ubiquitin-dependent protein degradation possibly reflect the accelerating of protein dynamic change under salt stress.

3.2.3 Protein folding

In cytosol, protein folding starts with the help of a first tier of ribosome-associated chaperones (mainly Hsp70 and Hsp40 which stabilize the nascent polypeptides) which form complex with ribosome called ribosome-associated complex (RAC), then a second tier of components including chaperonins and Hsp90 act downstream in completing the folding process (Vabulas et al., 2010). The ubiquitous up-regulation of Hsp40s (also called chaperone protein DnaJ), Hsp70s, and Hsp90s were observed (Supplementary File 1: Figure S7). The subunits of T-complex protein 1 (the group II chaperonin) and prefoldin were also up-regulated (Supplementary File 1: Figure S7).

In endoplasmic reticulum, protein folding participants include luminal binding proteins (BiPs) which bind to nascent polypeptides to prevent their aggregation, ER-localized DNAJ domain-containing proteins (ERdj proteins) which are BiP cochaperones that assist protein folding, calreticulin (CRT, folding apparatus) which sequester nascent glycoproteins to facilitate folding, UDP-glucose: glycoprotein glucosyltransferase (UGGT) which tells CRT if the glycoprotein needs another round of folding by adding a terminal glucose to the glycoprotein, and protein disulfide isomerases (PDIs) which catalyzes the breaking and reforming of disulfide bonds (Liu and Howell, 2016). These genes were all up-regulated except one ERdj gene (the other ERdj was up-regulated) (Supplementary File 1: Figure S7). Besides the genes mentioned above, there were as much as 37 genes encoding peptidyl-prolyl cis-trans isomoerases, only 3 of them do not showed up-regulation (Supplementary File 1: Figure S8). We speculate that the non-up-regulated genes possibly been up-regulated before 0.5-hour of stress. The expressional profiles of these genes suggest that protein folding was strongly enhanced under salt stress.

3.2.4 Protein modification

Lots of DEGs were enriched in protein modification processes including phosphorylation, glycosylation, ubiquitination, lipidation, dephosphorylation, methylation, alkylation, acetylation, and mannosylation. Among these modifications, protein phosphorylation was the most eye-catching one with the largest number of DEGs involved, accounting for about 60% of the total DEGs of protein modification. A lot of protein kinases enriched in protein phosphorylation, included serine/threonine-protein kinases, cyclin-dependent kinases, calcium-dependent protein kinases, mitogen-activated protein kinases, subunits of cAMP-dependent protein kinases, etc. By GO enrichment analysis, these kinases participate in a variety of cellular biological processes including response to abiotic stress (including salt, osmotic, drought, oxidative, and cold stress), response to DNA damage and lead to cell cycle control, response to unfolded protein, RNA processing, carbohydrate metabolism, photosystem II regulating, microtubule organization, and chloroplast protein import (Table 2).

TABLE 2 Selected kinases and the related biological processes.

BP/Gene ID	Gene name	Reference (PMID)
Salt stress		
DsaChr020159	Calcium-dependent protein kinase 12	21883553
DsaChr060221	Serine/threonine-protein kinase AtPK2/ AtPK19	29084871
Osmotic/drought stress		
DsaChr100125	Serine/threonine-protein kinase SRK2C	15561775
DsaChr010085	Serine/threonine-protein kinase SRK2E	30361234
Oxidative stress		
DsaChr030312	Mitogen-activated protein kinase kinase kinase ANP1	10717008
Cold stress		
DsaChr080233	CBL-interacting serine/threonine-protein kinase 7	21600398
DsaChr060221	Serine/threonine-protein kinase AtPK2/ AtPK19	29084871
Response to unfolded protein		
DsaChr130345	Serine/threonine-protein kinase ppk4	23066505
DsaChr110405	Serine/threonine-protein kinase/ endoribonuclease IRE1	11779464
DsaChr050352	Serine/threonine-protein kinase/ endoribonuclease IRE1	22050533
DNA damage/cell cycle control		
DsaChr090603	Cyclin-dependent kinase 7	10024882
DsaChr060653	Serine/threonine-protein kinase ATM	12509526
DsaChr010826	Serine/threonine-protein kinase Nek1	20230784
DsaChr010422	Serine/threonine-protein kinase Nek4	22851694
RNA processing		
DsaChr100614	Serine/threonine-protein kinase SMG1	15175154
DsaChr020456	Serine/threonine-protein kinase RIO1	22072790
Microtubule/cytoskeleton organization		
DsaChr010549	Mitogen-activated protein kinase 4	20215588
DsaChr060318	Mitogen-activated protein kinase kinase kinase 11	12529434
DsaChr070114	Mitogen-activated protein kinase kinase kinase 2	20215588
DsaChr010906	Serine/threonine-protein kinase phg2	15194808
DsaChr120313	Serine/threonine-protein kinase RUNKEL	19268593
Carbohydrate metabolism		
DsaChr120587	SNF1-related protein kinase catalytic subunit alpha KIN10	17671505
Chloroplast protein import		
DsaChr110313	Serine/threonine-protein kinase STY17	17090544
DsaChr100019	Serine/threonine-protein kinase STY46	17090544
DsaChr020711	Serine/threonine-protein kinase STY8	17090544
Photosystem II regulating		
DsaChr050007	Serine/threonine-protein kinase STN8, chloroplastic	16040609
DsaChr130132	Serine/threonine-protein kinase stt7, chloroplastic	12624266

These biological processes, except the response to abiotic stress which is a general expression, represent most of the aspects of this paper that are discussed or will be discussed in the following sections. Upon the whole, the regulation of these kinases suggests that most of the biological processes of *Dunaliella salina* in response to salt stress are carried out through the way of protein phosphorylation by kinases.

3.2.5 Protein transport

There are two kinds of protein transport, co-translational transport (vesicle-mediated transport) and post-translational transport (non-vesicular transport) (Jungnickel et al., 1994). Compared to post-translational transport, co-translational transport is reported to involve in abiotic stress response (Wang et al., 2020), so we analyze only co-translational transport here. The co-translational transport pathway utilizes the signal recognition particle (SRP) to deliver proteins to the ER membrane while they are still being synthesized by ribosomes (Nyathi et al., 2013). On ER membrane with the help of Sec translocon (Sec61 complex), the nascent polypeptides enter the lumen of ER where they fold to their final conformation (Denks et al., 2014). Then the protein cargos can be transported from ER to Golgi, subsequentially from Golgi to Lysosome, to Plasma membrane, or to out of cell by vesicles. Protein cargos can also be transported from Golgi back to ER, or from Plasma membrane to Lysosome by vesicles (Paez Valencia et al., 2016). During the process, there are proteins and protein machineries work together to create vesicles from donor membranes, to target the vesicles to different destinations, and to fuse vesicles to target membranes (Paez Valencia et al., 2016). In *Dunaliella salina*, the genes encoding the proteins and the subunits of the machineries that involved in vesicle-mediate transport are summarized in Table 3. The SRP proteins including the SRP54 protein which carries the core function, the alpha and gamma subunits of sec61 translocon, and the subunits of coat proteins including COPI (required for vesicles formation from cis Golgi membrane), COPII (required for vesicles formation from ER membrane), and Clathrin (required for vesicles formation from trans Golgi membrane and plasma membrane), were up-regulated.

10.3389/fpls.2023.1278954

TABLE 3 Genes participate in vesicle-mediate protein transport.

Gene ID	Gene name	log_2(FoldChange)		
		0.5 h *VS* 0 h	1 h *VS* 0 h	2 h *VS* 0 h
SRP				
DsaChr110350	SRP 9 kDa	UP	UP	FALSE
DsaChr120098	SRP 14 kDa	UP	FALSE	FALSE
DsaChr110363	SRP 43 kDa	UP	UP	DOWN
DsaChr120629	SRP protein	UP	UP	UP
DsaChr100436	SRP subunit SRP72	FALSE	FALSE	UP
DsaChr020098	SRP 54 kDa protein 1	FALSE	FALSE	UP
Translocon				
DsaChr080295	Sec61 subunit alpha	UP	UP	UP
DsaChr070622	Sec61 subunit gamma	UP	FALSE	DOWN
COPI				
DsaChr010839	Coatomer subunit alpha-1	UP	UP	FALSE
DsaChr050350	Coatomer subunit zeta-2	FALSE	FALSE	UP
DsaChr080298	Coatomer subunit beta'-1	UP	UP	UP
DsaChr120756	Coatomer subunit beta-1	UP	UP	UP
DsaChr060027	Coatomer subunit gamma-2	UP	UP	UP
DsaChr040552	Coatomer subunit epsilon-1	UP	UP	FALSE
DsaChr050508	Coatomer subunit delta-1	UP	FALSE	UP
COPII				
DsaChr090410	Protein transport protein Sec24-like CEF	UP	UP	FALSE
DsaChr020331	Protein transport protein SEC13 homolog A	FALSE	FALSE	UP
DsaChr050599	Protein transport protein Sec24-like At3g07100	FALSE	UP	UP
DsaChr120331	Protein transport protein SEC31 homolog B	FALSE	UP	UP
DsaChr030638	GTP-binding protein SAR1A	FALSE	FALSE	UP
Clathrin				
DsaChr140276	Clathrin heavy chain 2	UP	UP	UP
DsaChr030331	Clathrin assembly protein At1g14910	UP	UP	DOWN
Adaptor				
DsaChr020052	Beta-adaptin-like protein A	UP	UP	DOWN
DsaChr121169	Beta-adaptin-like protein C	UP	UP	UP
DsaChr060511	AP-4 complex subunit epsilon	FALSE	FALSE	UP
DsaChr060511	AP-4 complex subunit epsilon	FALSE	FALSE	UP
DsaChr030303	AP-1 complex subunit gamma-2	FALSE	FALSE	UP
DsaChr050143	AP-2 complex subunit alpha-1	UP	UP	FALSE
Syntaxin				
DsaChr050130	Syntaxin-132	FALSE	FALSE	UP
DsaChr060051	Syntaxin-32	DOWN	DOWN	UP
DsaChr010717	Syntaxin-22	FALSE	FALSE	UP
DsaChr060183	Syntaxin-52	DOWN	DOWN	UP
VPS				
DsaChr010788	VPS29	UP	FALSE	DOWN
DsaChr010952	VPS26B	UP	UP	UP
DsaChr150146	VPS32 homolog 2	UP	UP	UP
DsaChr020689	VPS24 homolog 1	FALSE	DOWN	UP
DsaChr070483	VPS55 homolog	FALSE	DOWN	FALSE
DsaChr050295	VPS16 homolog	UP	UP	DOWN
DsaChr010029	VPS33A	UP	UP	DOWN
DsaChr140366	VPS28 homolog 2	DOWN	DOWN	FALSE
DsaChr080378	VPS18 homolog	DOWN	FALSE	DOWN
DsaChr010762	VPS35A	UP	UP	UP
DsaChr121235	VPS51	FALSE	FALSE	DOWN
DsaChr121048	VPS2 homolog 3	FALSE	FALSE	UP
DsaChr060632	VPS22 homolog 1	FALSE	DOWN	DOWN
DsaChr100474	VPS41 homolog	FALSE	UP	DOWN
DsaChr110426	VPS9A	FALSE	UP	FALSE
DsaChr110193	VPS13a	UP	UP	UP
DsaChr130018	VPS36	UP	UP	UP
DsaChr010386	VPS53 A	FALSE	FALSE	DOWN
DsaChr020102	VPS25	FALSE	DOWN	FALSE

(Continued)

TABLE 3 Continued

Gene ID	Gene name	log_2(FoldChange)		
		0.5 h *VS* 0 h	1 h *VS* 0 h	2 h *VS* 0 h
DsaChr020245	VPS2 homolog 1	FALSE	FALSE	UP
DsaSca0152	VPS45 homolog	DOWN	FALSE	FALSE
DsaChr160069	VPS11 homolog	FALSE	UP	UP
DsaChr010996	VPS23	FALSE	FALSE	UP
DsaChr130098	LIP5	FALSE	UP	UP
DsaChr150326	SKD1	FALSE	FALSE	UP
Novelgene0862	ESCRT-related protein CHMP1B	FALSE	FALSE	UP
SNARE				
DsaChr110201	Vesicle transport v-SNARE 11	DOWN	FALSE	UP
DsaChr030800	Golgi SNAP receptor complex member 1-2	FALSE	DOWN	DOWN
DsaChr090438	R-SNARE, Tomsyn-like family	UP	UP	UP
DsaChr040011	Qb-SNARE protein, Sec20-family	UP	FALSE	UP
DsaChr110432	Qc-SNARE protein, USE1 family	FALSE	FALSE	DOWN
DsaChr121024	Qc-SNARE protein, Bet1/mBET1 family	FALSE	DOWN	FALSE
DsaChr070004	Vesicle-associated membrane protein 727	DOWN	FALSE	UP
DsaChr030249	Qc-SNARE protein, SFT1 family	FALSE	FALSE	DOWN
DsaChr070004	Vesicle-associated membrane protein 727	DOWN	FALSE	UP
DsaChr020111	Vesicle-associated membrane protein 714	DOWN	DOWN	UP
DsaChr030329	Vesicle transport protein GOT1	FALSE	FALSE	DOWN

"FALSE" means no significant up- or down-regulation, "UP" and "DOWN" means significant up-regulation and down-regulation respectively.

The adaptor proteins and syntaxins were also up-regulated. The up-regulation of these genes suggests the enhancing of vesicle-mediated protein transport under salt stress. Lots of vacuolar protein sorting-associated proteins (VPS), including components of ESCRT-I, ESCRT-II, and ESCRT-III complex which involved in ubiquitin tagged proteins sorting and delivery to the endosome for degradation, were differently regulated. The SNARE proteins, which drive membrane fusion, were also differently regulated. Studies report that Sec31 (coat protein) (Chung et al., 2016), Sar1a (small GTPase, mediating COPII vesicle formation) (Zeng et al., 2021), Vps23 (component of ESCRT-I) (Yu et al., 2016), LIP5 (accessory protein mediating endosomal sorting) (Wang et al., 2015), and SKD1 (AAA-type ATPase mediating endosomal sorting) (Ho et al., 2010) participated in abiotic stress including drought and salt stress. The homologs of the five genes in *Dunaliella salina* were also up-regulated, which reflects the conservation of the response mechanism between the algae and *Arabidopsis thaliana* (Table 3).

3.2.6 Cellular component organization

When confronting salt stress, the *Dunaliella* cells decrease their volume quickly due to high extracellular osmotic pressure, and then gradually increase their cell volume by increasing the intracellular glycerol content to balance the osmotic pressure across plasma membrane. The whole process accomplishes in about 2 hours (Ben-Amotz and Avron, 1973). During the process, cellular component organization is a must. GO terms, such as membrane organization, endomembrane system organization, cytoskeleton organization, chromosome organization, protein-containing complex organization, etc., were enriched (Supplementary File 1: Figure S9). Here we only discuss membrane organization, endomembrane system organization, and cytoskeleton organization. The rest GO terms will not be discussed due to the limits of paper length. For membrane organization, it is well-known that autophagy, which was enriched in our study, involves organization of plasma membrane and reported to be induced by salt stress (Liu and Bassham, 2012). For endomembrane system organization, it is known that the vesicle-mediated protein trafficking is carried out by the way of endomembrane system organization as described in the section of protein transport. Besides membrane and endomembrane system organization, the other eye-catching GO term is cytoskeleton organization containing the most DEGs among the child terms of organelle organization ((Supplementary File 1: Figure S9).

3.2.7 Glycerol synthesis and energy metabolism

3.2.7.1 Glycerol synthesis

When confronting salt stress, *Dunaliella* cells rapidly shrink, then gradually recover its original volume by intracellular glycerol synthesis to balance the extracellular osmotic pressure (Ben-Amotz and Avron, 1973; Baek et al., 2011). The whole process finished in about 2 hours. Studies report that *Dunaliella* cells grown in 4 M NaCl contain about 8 M glycerol (Chitlaru and Pick, 1989; Oren, 2005). These studies indicate that rapid high-yield biosynthesis of glycerol is a special mechanism of *Dunaliella* to tolerate salt stress. In the last century, scientists suggested that the reserve starch pool is a carbon source of glycerol synthesis (Ben-Amotz and Avron, 1973), and proposed the glycerol cycle pathway which suggested that glycerol can be synthesized from and converted to DHAP (dihydroxyacetone phosphate or glycerone-phosphate) which is an intermediate metabolite of glycolysis (Haus and Wegmann, 1984) However a complete synthesis pathway from starch to glycerol was absent, here we propose a pathway from starch to glycerol based on our genomic data and the published papers (He et al., 2020b), the input of energy and reducing equivalents are also indicated (Figure 1A). The expressions of the enzymes were all up-

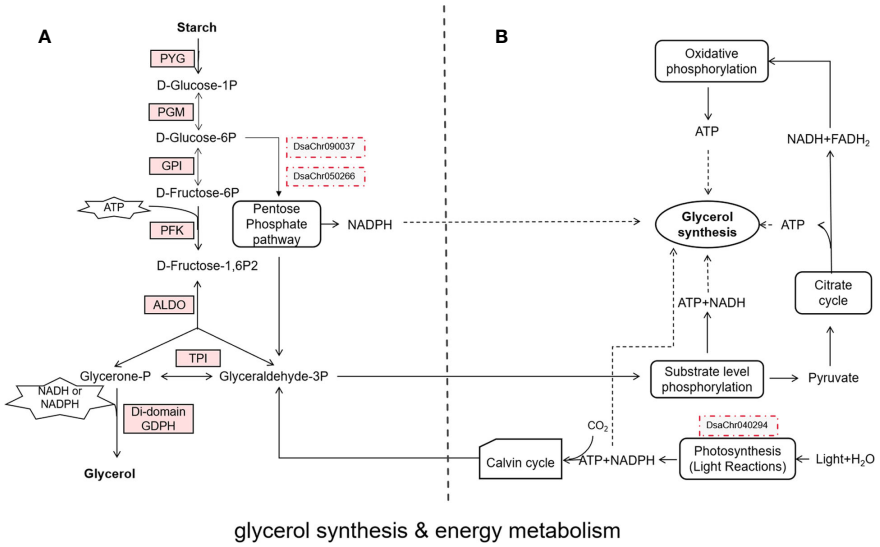

FIGURE 1
Glycerol synthesis & energy metabolism. **(A)** the glycerol synthesis pathway from starch to glycerol, the enzymes on the pathway are shown by rectangles, the up-regulated enzymes are indicated by light red background, the two red dotted boxes indicate the two key genes of pentose phosphate pathway confirmed by real-time PCR; **(B)** the possible sources (rounded rectangles) of ATP and reducing equivalents (NADH or NADPH) for glycerol synthesis, the dotted arrows indicate the ATP and reducing equivalents could be used for glycerol synthesis, the red dotted box indicates the gene confirmed by real-time PCR.

regulated, the key enzymes are PYG, PFK, and the di-domain GPDH, which catalyze the three irreversible reactions.

Study also showed that photosynthesis is also a carbon source of glycerol synthesis (Goyal, 2007). In our study, the up-regulated genes enriched in the term photosynthesis included photosystem I reaction center subunits, photosystem II reaction center proteins, chlorophyII a-b binding proteins, oxygen-evolving enhancer proteins, PsbP domain-containing proteins, thylakoid luminal proteins, etc. We can see most of the genes showed a quick up-regulation of expression at 0.5 and 1-hour under stress followed by a down-regulation of expression at 2-hour under stress (Supplementary File 1: Figure S10). The expressional profiles of these genes suggest that photosynthesis was transiently up-regulated by salt stress.

3.2.7.2 Energy metabolism

Study report that photosynthesis and reserved starch are the carbon source of glycerol synthesis, and reserved starch is the main source (Goyal, 2007). From the glycerol synthesis pathway that we proposed, synthesis of one molecule of glycerol needs 0.5 molecule of ATP and one molecule of NADH or NADPH (reducing equivalents) (Figure 1A). So, synthesis of large amount of glycerol needs large amount of ATP and reducing equivalents. Where do these ATP and reducing equivalents come from the GO enrichment analysis, glycolysis, TCA cycle and oxidative phosphorylation, which can generate ATP or NADH or both of them, were enriched. It is worth noting that pentose phosphate pathway (PPP) was also enriched. Glucose-6-phosphate dehydrogenase, the rate-controlling enzyme of PPP, was significantly up-regulated (Stryer and Co, 1995). 6-phosphogluconate dehydrogenase, the second NADPH producing enzyme in PPP, was also significantly up-regulated. Since generation of NADPH is one of the outcomes of PPP, the up-regulation of PPP could be a source of reducing equivalents for glycerol synthesis. From the starch catabolism pathway (Figure 1A), the carbon flux branches at the point of fructose 1, 6-biphosphate, some carbon goes to glycerol synthesis, the other goes to TCA cycle and oxidative phosphorylation to generate NADH and ATP which can be used for glycerol synthesis. Taking together, it seems that the large amount of ATP and reducing equivalents needed for glycerol synthesis could be provided by starch catabolism through glycolysis, pentose phosphate pathway, TCA cycle and oxidative phosphorylation (Figure 1B).

3.2.8 Cell redox homeostasis

Efficient flux of electrons is vital for photosynthesis and respiration of plant cells. Efficient flux of electrons also means that the oxidized and reduced forms of electron carriers in electron transport chains must be balanced, which is called redox homeostasis (Foyer and Noctor, 2005). However, salt stress can disrupt the balance and induce the rise of reactive oxygen species (ROS) and lead to oxidative stress. To survive, organisms need to regain cell redox homeostasis by getting the excessive ROS reduced by small molecule antioxidants, such as ascorbate, glutathione (GSH), and tocopherol. The genes involved in regeneration of these antioxidants, such as monodehydroascorbate reductase and glutathione reductase, were mostly up-regulated at 0.5-hour under stress (Supplementary File 1: Figure S11). Another type of antioxidants is antioxidative proteins, such as thioredoxins, glutaredoxins, and peroxiredoxins. Most of the genes encoding antioxidative proteins were up-regulated at 0.5-hour under stress (Supplementary File 1: Figure S11). The genes involved in regeneration of these antioxidative proteins, such as thioredoxin reductase and methionine sulfoxide reductase, were also up-

regulated at 0.5-hour under stress. Taken together, the genes involved in cell redox homeostasis responded quickly and strongly to salt stress by up-regulation of their expressions.

3.2.9 DNA repair

Salt stress induces the rise of ROS. ROS have strong oxidizing potential and lead to DNA damage. When DNA damage happens, cells stop cell cycle and activate DNA repair mechanisms to repair DNA. If DNA repairs are successful, cell cycle is reactivated. On the contrary, if the repairs fail and DNA lesions accumulate, cells undergo apoptosis (Hu et al., 2016) From this perspective, the strength of ability of DNA repair influences the degree of salt tolerance of an organism. Although we know that *Dunaliella salina* is extremely salt tolerant, it was still astonishing to see that so many genes involved in DNA repair were up-regulated by salt stress. The DEGs included DNA repair proteins, DNA repair ligases, DNA repair helicases, endonucleases, glycosylases, DNA polymerases, replication factor C subunits, recombinases, and DNA methyltransferases, etc. Most of these genes were up-regulated at 0.5-hour and 1-hour under stress (Supplementary File 1: Figure S12).

3.2.10 Lipid metabolism

In general, the up-regulation of the key genes in the biosynthetic pathways indicates the acceleration of *de novo* fatty acid synthesis and TAG synthesis under salt stress. The up-regulation of the desaturases indicates that the fatty acids and lipids undergo desaturation.

3.2.10.1 Fatty acid metabolism

The chloroplastic acetyl-CoA carboxylase (heteromeric ACC) catalyzing the irreversible carboxylation of acetyl-CoA to produce malonyl-CoA, which is involved in *de novo* fatty acid synthesis in plants (Konishi et al., 1996), is composed of four independent polypeptides: biotin carboxyl carrier protein (BCCP), biotin carboxylase (BC), α carboxyl transferase, and β carboxyl transferase. The four subunits were all significantly up-regulated at 0.5-hour and 1-hour under salt stress. The cytosolic acetyl-CoA carboxylase (homomeric ACC) was also significantly up-regulated. The malonyl-CoA-ACP transacylase (FabD) and the other subunits of type II fatty acid synthase (FAS) including 3-ketoacyl-ACP synthase II and III (KAS II or FabF and KAS III or FabH), 3-oxoacyl-ACP reductase (FabG), 3-hydroxyacyl-ACP dehydratase (FabZ), and enoyl-ACP reductase (FabI), were all significantly up-regulated at 0.5-hour and 1-hour under salt stress (Figure 2). The expression of the biotin carboxylase and cytosolic acetyl-CoA carboxylase were confirmed by real-time PCR (Figure 3; Supplementary File 2). The up-regulation of these genes reflects the acceleration of *de novo* fatty acid synthesis under salt stress. Acyl-protein thioesterases and long chain acyl-CoA synthetases were also up-regulated, which possibly suggest the synthesized acyl-CoA could be used for lipid synthesis (Ohlrogge and Browse, 1995).

3.2.10.2 Glycerolipid metabolism

Glycerol-3-phosphate acyltransferase (EC: 2.3.1.15) and 1-acylglycerol-3-phosphate O-acyltransferase (EC: 2.3.1.51) were up-regulated at 0.5-hour under stress, which possibly suggest the acceleration of phosphatidic acid (PA) synthesis. The up-regulation of phosphatidate phosphatase (EC: 3.1.3.4) was detected at 10-min under stress by qPCR (Figure 3; Supplementary File 2). The up-regulation of the chloroplastic lipid phosphate phosphatase 3, which may exhibit phosphatidate phosphatase activity (Pierrugues et al., 2001; Nakamura et al., 2007), was also observed at 2-hour under stress. The expression of diacylglycerol O-acyltransferases (EC: 2.3.1.20) and phospholipid:diacylglycerol acyltransferase (EC: 2.3.1.158) were up-regulated at 10-min and 30-min under stress (Figures 3, 4). Taken together, the expression profiles of these genes possibly suggest the acceleration of triacylglycerol (TAG) synthesis under stress.

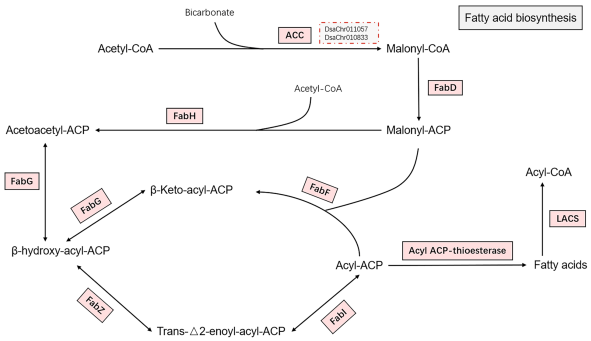

FIGURE 2
Fatty acid biosynthesis. The pathway of fatty acid biosynthesis from acetyl-CoA to fatty acids are shown in the figure. Enzymes catalyzing the reactions on the pathway are shown by rectangles. The enzymes were all up-regulated as indicated by light red background. The two red dotted boxes indicate the two key genes (biotin carboxylase and acetyl-CoA carboxylase) confirmed by real-time PCR. The full name of the enzymes are acetyl-CoA carboxylase (ACC), malonyl-CoA-ACP transacylase (FabD), 3-ketoacyl-ACP synthase II and III (FabF and FabH), 3-oxoacyl-ACP reductase (FabG), 3-hydroxyacyl-ACP dehydratase (FabZ), and enoyl-ACP reductase (FabI), acyl-protein thioesterase, and long chain acyl-CoA synthetase (LACS).

Many desaturases were up-regulated under salt stress, including stearoyl-[acyl-carrier-protein] 9-desaturase (EC: 1.14.19.2), acyl-lipid omega-3 desaturase (chloroplastic, EC: 1.14.19.25), Delta12 fatty acid desaturase (EC: 1.14.19.6), Delta7-sterol 5(6)-desaturase (EC: 1.14.19.20), Palmitoyl-monogalactosyldiacylglycerol delta-7 desaturase (chloroplastic, EC: 1.14.19.42), Acyl-lipid (7-3)-desaturase (chloroplastic, EC: 1.14.19.31), and acyl-lipid omega-3 desaturase (chloroplastic, EC: 1.14.19.25) (Supplementary File 1: Figure S13). Upon the whole, the up-regulation of these desaturases suggest the desaturation of lipids under salt stress.

3.2.11 Ion homeostasis

Studies report that Na^+/H^+ antiporters (or exchangers) located on plasma membrane are responsible for sodium ion extrusion, while Na^+/H^+ exchangers located on vacuolar membrane are for sodium ion sequestration in vacuole (Zhu, 2003). There is one gene, named as *DsaChr110059* and showing sequence similarity with Na^+/H^+ antiporter 7 of *Arabidopsis thaliana* (SOS1) which was reported to be responsible for Na^+ and Li^+ extrusion across plasma membrane (Wu et al., 1996; Shi et al., 2000), was significantly up-regulated at 0.5-hour and 1-hour under stress (Figure 3; Supplementary File 2). There are two genes, named as

10.3389/fpls.2023.1278954

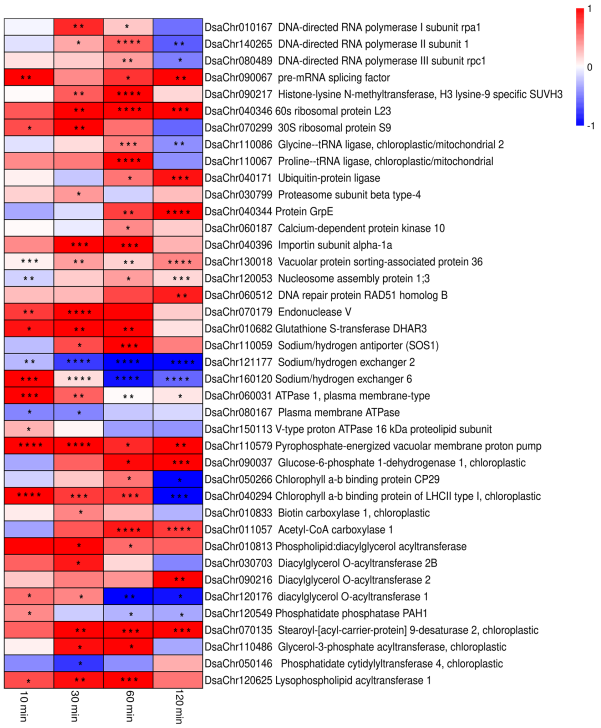

FIGURE 3
Heatmap of the expressions from real-time PCR of the selected key genes in the biological processes. The colors from blue to red represent the gene expression values from low to high. Values of $\log_2$ (Fold change) are used to generate the heatmap. The significance is indicated by asterisks in the heatmap (* P<0.05,** P< 0.01, *** P< 0.001,**** P < 0.0001).

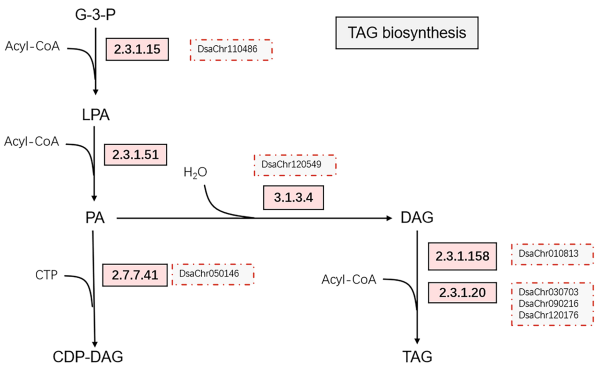

FIGURE 4
Simplified triacylglycerol biosynthesis pathway. The up-regulated enzymes catalyzing the reactions on the pathway are indicated by rectangles with light red background, the red dotted boxes indicate the genes confirmed by real-time PCR. The enzymes are glycerol-3-phosphate acyltransferase [2.3.1.15], 1-acylglycerol-3-phosphate O-acyltransferase [2.3.1.51], phosphatidate phosphatase [3.1.3.4], diacylglycerol O-acyltransferases [2.3.1.20], phospholipid: diacylglycerol acyltransferase [2.3.1.158], and phosphatidate cytidylyltransferases [2.7.7.41].

DsaChr121177 and *DsaChr160120*, that show sequence similarities with Na^+/H^+ exchanger 2 and 6 of *Arabidopsis thaliana*, respectively, which are reported to be involved in vacuolar sodium ion compartmentalization (Yokoi et al., 2002; Bassil et al., 2011). Real-time PCR show that *DsaChr160120* was up-regulated at 10-min under stress, but *DsaChr121177* was not up-regulated (Figure 3; Supplementary File 2).

Studies also report that plasma membrane-type and vacuolar-type proton ATPase are responsible for creating proton gradient across plasma membrane and vacuolar membrane respectively, which could benefit Na^+ efflux and sequestration by Na^+/H^+ antiporters and Na^+/H^+ exchangers (Yang and Guo, 2018). There are two genes, named as *DsaChr060031* and *DsaChr080167*, which show sequence similarities with plasma membrane ATPase 1 of *Arabidopsis thaliana* and plasma membrane ATPase of *Dunaliella bioculata*, respectively. *DsaChr060031* showed up-regulation at 10-min and 30-min under stress, but *DsaChr080167* didn't show up-regulation (Figure 3; Supplementary File 2). There are 13 genes encoding subunits of vacuolar-type proton ATPase, 5 of them showed significant up-regulation. Besides the vacuolar-type proton ATPases, a gene encoding pyrophosphate-energized vacuolar membrane proton pump which also contributes to the proton gradient across vacuolar membrane showed up-regulation (Segami et al., 2018). The up-regulation of the vacuolar-type proton ATPases and the pyrophosphate-energized vacuolar membrane proton pump would lead to acidation of the vacuoles and benefit for Na^+ sequestration.

Taken together, We did saw the up-regulation of a plasma membrane-type Na^+/H^+ antiporter (*DsaChr110059*), which shows sequence similarity with the well-studied SOS1 of *Arabidopsis thaliana* which was the main player of Na^+ extrusion under salt stress (Zhu, 2003). We also saw the up-regulation of a vacuolar-type Na^+/H^+ exchanger (*DsaChr160120*) together with the up-regulation of some of the subunits of vacuolar-type proton ATPase and the up-regulation of a pyrophosphate-energized vacuolar membrane proton pump.

4 Discussion

This research gives a more comprehensive overview of how *Dunaliella* cells response to salt stress than the previous published papers do (Li et al., 2019; Lv et al., 2021; Panahi and Hejazi, 2021) due to high quality genomic data of this algae and appropriated stress time course setting. From the point of evolution, all plant cells, including higher plants, lower plants, and green algae, have similar cellular structure and respond to environmental stress similarly (Chapin, 1991), so this is also an overview of how photosynthetic cells response to salt stress. Although this overview is only at transcriptomic level, there are published papers to support most of the biological processes being discussed in this research, which also suggests that the regulations of the biological processes are conserved mechanisms of plants in response to salt stress.

The basic way of a plant cell to response to environmental changes is the regulation of gene expression. Besides the expressional regulations of the core components of transcription machineries, lots of the TFs were regulated in response to salt stress, many of them were reported to participate in abiotic stress response (Table 1). Moreover, the regulations at pre-initiation of transcription and post-transcriptional levels were also indicated

by the DEGs, some of the DEGs were reported to be involved in salt tolerance of *Arabidopsis thaliana*, such as histone-lysine N-methyltransferase, histone acetyltransferase GCN5, and pre-mRNA splicing factors (Baek et al., 2011; Zheng et al., 2019).

Gene expression includes not only the transcription process, but also the translation process. The functional enrichment analysis of the DEGs indicates that the protein synthesis process was enhanced. This is reasonable because cells need to synthesize new proteins to adapt to salt stress. There are studies reported the association of glycoprotein with salt tolerance in *Arabidopsis* (Frank et al., 2008; Kang et al., 2008; Nagashima et al., 2018). What is interesting is that protein degradation was also enriched. In the last century, scientists found that mammal cells exhibit increased rates of proteolysis following exposure to oxidative stress (Pacifici et al., 1989; Grune et al., 1997) and proposed that ubiquitin proteasome system (UPS) is a major way for protein degradation (Hershko and Ciechanover, 1992). In plants, scientists found many homologs of mammal UPS, and suggested that UPS is also a major way for protein degradation (Smalle and Vierstra, 2004), however published works that report protein degradation induced by abiotic stress are rare (Ferguson et al., 1990; Neelam and Subramanyam, 2013). Here our data show that lots of ubiquitin-protein ligases, ubiquitin-conjugating enzymes, and subunits of 26S proteasome were up-regulated under salt stress, which indicate that UPS plays an important role in protein degradation under salt stress.

The protein folding process accompanies the translation process. Salt stress disrupts protein folding in ER and lead to ER stress. ER stress activates signal transduction pathway to up-regulate the expression of genes that aid in protein folding, such as chaperones, peptidyl prolyl isomerases, prefoldins, etc. (Liu and Howell, 2016). We saw the nearly ubiquitous up-regulation of the genes involved in protein folding, which indicates the process was strongly enhanced. However, reports of genetic engineering of protein folding to increase salt tolerance are rare (Wang et al., 2004). There are lots of molecular chaperones and enzymes that aid in protein folding, it is not likely to randomly choose a target that will lead to significant improvement of salt tolerance.

In eukaryotic cells, many newly synthesized proteins go to the post-translational modification process to become functional forms. There are two kinds of protein modifications that obviously related to salt stress response, one is ubiquitination, as mentioned above, the misfolded or damaged proteins must be attached the tag of ubiquitin before degradation. The other is protein phosphorylation, protein phosphorylation usually plays important role in signal transduction of stress sensing and response. To modulating signal transduction of salt stress response is a hopeful way to increase salt tolerance by changing phosphorylation state of key component of signal cascade. For example, the activity of Na^+/H^+ antiporter (SOS1) in salt overly sensitive (SOS) pathway is control by phosphorylation (Shi et al., 2000; Dittmore et al., 2016). Phosphorylation can activates SOS1 and might increase Na^+ exclusion and lead to improvement of salt tolerance. Besides ubiquitination and phosphorylation, reactive oxygen species (ROS) and reactive nitrogen species (RNS) were reported to regulate ion transporters by protein modifications. These modifications include cysteine oxidation, methionine oxidation, cysteine S-nitrosylation, and tyrosine nitration (Nieves-Cordones et al., 2019; Sandalio et al., 2023). Salt stress can induce the rise of ROS and probably RNS, which could lead to oxidation or nitration of the residues of ion transporters and regulate their activities. Garcia-Mata et al. (Garcia-Mata et al., 2010) demonstrated that the residue Cys168 of SKOR K^+ Channel was essential for sensitivity to H_2O_2. However more experiments on other transporters at protein molecular or structural level are still needed to show how ROS and RNS regulate the activities of transporters through residues oxidation or nitration in response to salt stress.

Since proteins are synthesized far away from their functional sites, protein transport is a fundamental cellular process that can be regulated in response to environmental changes. The vesicle-mediated protein transport involves ER as the very important departure station of protein cargos. Salt stress disrupt protein folding in ER, leading to accumulation of unfolded or misfolded proteins in ER which is also called ER stress (Liu et al., 2010). ER needs to activate signal transduction pathway to up-regulate the expression of genes that aid in protein folding, such as chaperones, and to send the unfolded proteins cargos to degradation. This is how salt stress intersects protein transport. By loss of function mutation techniques, researchers identified some participators of vesicle-mediated protein transport involved in salt stress response. Loss of function mutants were sensitive to salt stress compare to wild type plants (Wang et al., 2020). Although we know that protein transport is tightly linked to salt stress response, the underlying mechanisms are largely unknown.

Cellular component organization plays an essential role in a variety of biological processes, such as vesicle-mediated protein transport, cytoskeleton dynamics, autophagy, etc. Autophagy is a bulk degradation pathway that is essential for cell survival under nutrient-limiting conditions (Levine and Klionsky, 2004). Later scientists found that autophagy helps maintain cellular homeostasis under oxidative stress by degradation and recycling of the oxidized proteins and other cellular components (Bassham, 2007). Studies showed directly that salt stress induced autophagy of *Arabidopsis* within 30 min and mutants defective in autophagy were sensitive to salt stress (Leshem et al., 2007; Luo et al., 2017). These studies indicate that autophagy plays an important role in plant response to salt stress. Leshem et al. also reported that phosphoinositide signaling pathway is involved in autophagy under salt stress (Leshem et al., 2007). Considering that phosphoinositide signaling is also involved in the organization of cytoskeleton (Yin and Janmey, 2003) and the regulation of vesicle trafficking (Roth, 2004), we speculate that these biological processes might be coordinated by phosphoinositide signaling pathway in response to salt stress. However more work needed to elucidate how they can be regulated.

Salt stress induces rise of ROS and leads to disruption of redox homeostasis which is vital for proper cellular function. To survive, cells need to regain redox homeostasis by removing the excessive ROS. We saw most of the genes involved in cellular redox homeostasis were up-regulated at 0.5-hour under stress and last to 2-hour under stress, which indicates that the process was quickly and strongly enhanced. The quick and strong type of response of these genes also reflects the strong ability of *Dunaliella salina* to maintain cell redox homeostasis under salt stress. Overexpression of the genes encoding antioxidative enzymes led to improved salt

tolerance (Agarwal et al., 2013; Wang et al., 2020), which indicates the importance of redox homeostasis in response to salt stress.

The rise in ROS also brings another serious consequence that is DNA damage. When DNA damage happens, cells activate DNA repair mechanisms to repair DNA (Hu et al., 2016). We saw that most of the genes involved in DNA repair were up-regulated at 0.5-hour and 1-hour under stress, which reflects the quick and strong response of *Dunaliella salina* to maintain DNA correctness under salt stress. *Dunaliella salina* can survive in medium containing NaCl as high as 5.5 M, so it is unexpected that salt stress of 2.5 M NaCl would cause such a strong response. On the other side, the strong response of DNA repair possibly reflects the high efficiency of DNA repair, which may be a major reason for the algae to survive in hypersaline environment.

There are studies reported that salt stress induced synthesis of fatty acid and total lipids in some microalgae (Takagi et al., 2006; El Arroussi et al., 2015; Pandit et al., 2017), and desaturation of fatty acids were reported in a few species(López-Pérez et al., 2009; Harrathi et al., 2011; Sui and Han, 2014). In our study, we see the up-regulation of the key enzymes ACCs (both the chloroplastic form and the cytosolic form) of the *de novo* fatty acid synthesis pathway and the enzymes in TAG synthesis pathway, which indicates the synthesis of fatty acids and TAG. The TAG contents were indeed increased (our unpublished data) under salt stress. We also see the up-regulation of the fatty acids desaturases, which indicates the lipids undergo desaturation under salt stress. Our data are in consistent with the previous studies. Moreover, Overexpression of *des*A encoding Δ12 acyl-lipid desaturase in *Synechococcus* led to improved salt tolerance (Allakhverdiev et al., 2001). Although these studies indicate that lipid metabolism is relevant to salt stress response, the underlying mechanism is unclear. Scientists speculate that unsaturated fatty acids can act as modulators of cellular membrane to increasing the fluidity of membrane under salt stress (He and Ding, 2020), and they also suggested that glycerolipids can work as carbon and energy reservoir under stress (He and Ding, 2020).

Besides the above discussed aspects, salt stress has two direct impacts on plant cells, one is that high salt content can alter the osmotic potential across plasma membrane and results in dehydration of plasma. The rapid high-yield biosynthesis of glycerol is a special mechanism of *Dunaliella* to cope with osmotic stress (Chitlaru and Pick, 1989; Oren, 2005). Based on our data, we propose a pathway from starch to glycerol, and suggest that PYG, PFK, and the di-domain GPDH are the three rate-limiting enzymes of the glycerol synthesis pathway. Our published paper showed that the di-domain GPDH can convert DHAP directly to glycerol whereas a separate phosphatase protein is required for this conversion process in most organisms, and the homotetramer structure of di-domain GPDH likely contributes to the rapid biosynthesis of glycerol (He et al., 2020b).

The other impact is that under high salt content, Na^+ enters cell more easily, which will disrupt the intrinsic homeostasis of high concentration of K^+ and low concentration of Na^+, which is vital for diverse cellular processes. We find in *Dunaliella* the up-regulation of the homolog of SOS1 of *Arabidopsis* which is the main player of Na^+ extrusion under salt stress (Zhu, 2003). We also find the up-regulation of a vacuolar-type Na^+/H^+ exchanger, some of the subunits of vacuolar-type proton ATPase, and a pyrophosphate-energized vacuolar membrane proton pump. The up-regulation of these genes is consistent with the

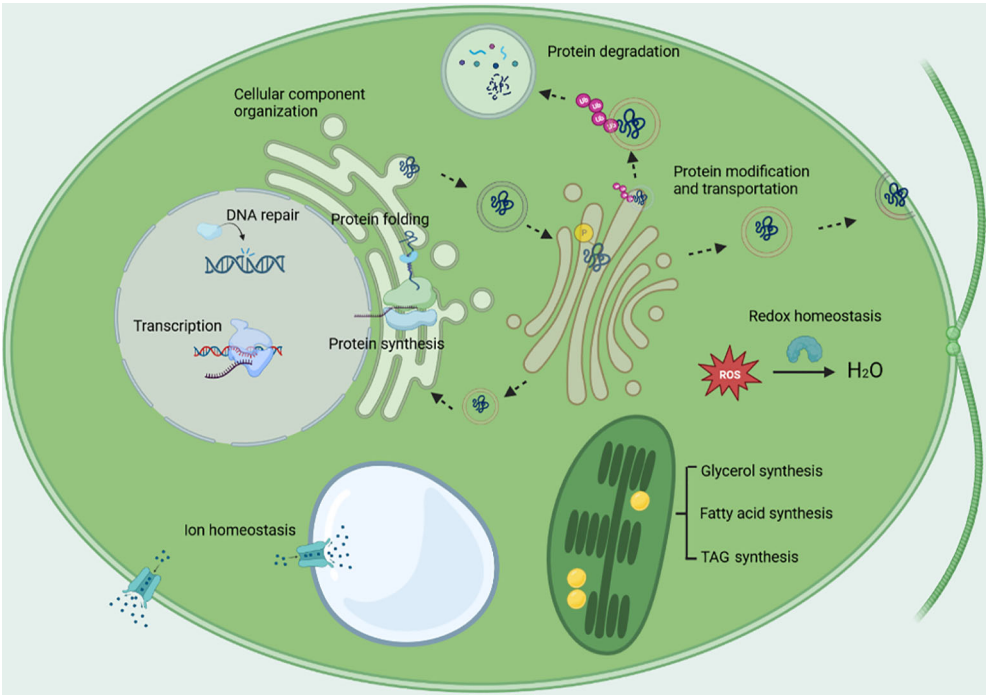

FIGURE 5
The major biological processes being regulated under salt stress. The biological processes include transcription, protein synthesis, protein degradation, protein folding, protein modification, protein transport, cellular component organization, cell redox homeostasis, DNA repair, glycerol synthesis, energy metabolism, lipid metabolism, and ion homeostasis.

expressions of their homologs in *Arabidopsis thaliana* under salt stress (Wu et al., 1996; Shi et al., 2000; Yokoi et al., 2002), which might suggest that these genes are responsible for ion homeostasis.

Finally, what light on the expression profile is the nearly ubiquitous up-regulation of the genes involved in protein folding, DNA repair, and cell redox homeostasis, which suggests that the three biological processes were strongly enhanced under salt stress, in reverse, it also implicates that we can improve plants salt tolerance by enhancing the activities of the three biological processes. Modulating the signal transduction pathways that control the three biological processes might be a promising way to improve salt tolerance. Considering that salt tolerance is a high energy and resource costing process, fine tuning is very important to achieve the balance between growth rate and degree of salt tolerance.

5 Conclusion

The major cellular biological processes that being regulated in response to salt stress, are shown in Figure 5. The GO term of transcription was enriched, the regulation of transcription occurred at pre-initiation, initiation, and post transcription level; protein synthesis and protein degradation were enhanced at the same time, which implicates the acceleration of protein turnover; protein modification was enriched included a lot of protein kinases, which implicates protein phosphorylation plays an important role in response to salt stress; protein transport was enriched, the vesicle-mediated protein transport was enhanced; cellular component organization, which plays an essential role in vesicle-mediated protein transport, cytoskeleton dynamics, autophagy, was enriched; glycerol synthesis was enhanced, the energy for glycerol synthesis might be provided by starch catabolism through glycolysis, pentose phosphate pathway, TCA cycle and oxidative phosphorylation; the synthesis of fatty acids and TAG were enhanced, while desaturation of lipids was also enhanced; the up-regulation of the plasma membrane-type Na^+/H^+ antiporter and the vacuolar-type Na^+/H^+ exchanger together with the vacuolar-type proton ATPase and the pyrophosphate-energized vacuolar membrane proton pump might aid in ion homeostasis; protein folding, cell redox homeostasis, and DNA repair were greatly enhanced as indicated by the nearly ubiquitous up-regulation of the genes involved in the three biological processes, which may confer the algae important mechanisms to survive under salt stress, also implicates that enhancing the activities of the three biological processes are promising strategies to improve crop salt tolerance.

Data availability statement

The datasets presented in this study can be found in online repositories. The names of the repository/repositories and accession number(s) can be found below: Sequence Read Archive under accession number SRR8552788, and SRR8543799 to SRR8543810. The genome data is deposited in the Genbank under accession number JAVFKU000000000.

Author contributions

BZ: Data curation, Formal Analysis, Validation, Writing – review & editing. CD: Data curation, Formal Analysis, Validation, Writing – review & editing. SW: Formal Analysis, Investigation, Writing – review & editing. QD: Formal Analysis, Investigation, Writing – review & editing. YC: Formal Analysis, Validation, Writing – review & editing. ZB: Formal Analysis, Validation, Writing – review & editing. AH: Data curation, Formal Analysis, Validation, Writing – review & editing. QZ: Conceptualization, Supervision, Writing – review & editing, Writing – original draft. QH: Conceptualization, Funding acquisition, Methodology, Resources, Supervision, Writing – original draft, Writing – review & editing, Project administration.

Funding

The author(s) declare financial support was received for the research, authorship, and/or publication of this article. Funds was provided by Natural Science Foundation of Sichuan province (2022NSFSC0244).

Acknowledgments

The authors are grateful to Southwest Minzu University for providing the necessary facilities and support. The authors also would like to express their gratitude for the funding provided by Natural Science Foundation of Sichuan province and Innovation funds for postgraduates, Southwest Minzu University.

Conflict of interest

The authors declare that the research was conducted in the absence of any commercial or financial relationships that could be construed as a potential conflict of interest.

Publisher's note

Supplementary material

The Supplementary Material for this article can be found online at: https://www.frontiersin.org/articles/10.3389/fpls.2023.1278954/full#supplementary-material

References

Agarwal, P. K., Shukla, P. S., Gupta, K., and Jha, B. (2013). Bioengineering for salinity tolerance in plants: state of the art. *Mol. Biotechnol.* 54 (1), 102–123. doi: 10.1007/s12033-012-9538-3

Allakhverdiev, S. I., Kinoshita, M., Inaba, M., Suzuki, I., and Murata, N. (2001). Unsaturated fatty acids in membrane lipids protect the photosynthetic machinery against salt-induced damage in Synechococcus. *Plant Physiol.* 125 (4), 1842–1853. doi: 10.1104/pp.125.4.1842

Anders, S., and Huber, W. (2010). Differential expression analysis for sequence count data. *Genome Biol.* 11 (10), R106. doi: 10.1186/gb-2010-11-10-r106

Anders, S., Pyl, P. T., and Huber, W. (2015). HTSeq–a Python framework to work with high-throughput sequencing data. *Bioinformatics* 31 (2), 166–169. doi: 10.1093/bioinformatics/btu638

Baek, D., Jiang, J., Chung, J. S., Wang, B., Chen, J., Xin, Z., et al. (2011). Regulated AtHKT1 gene expression by a distal enhancer element and DNA methylation in the promoter plays an important role in salt tolerance. *Plant Cell Physiol.* 52 (1), 149–161. doi: 10.1093/pcp/pcq182

Bassham, D. C. (2007). Plant autophagy–more than a starvation response. *Curr. Opin. Plant Biol.* 10 (6), 587–593. doi: 10.1016/j.pbi.2007.06.006

Bassil, E., Ohto, M. A., Esumi, T., Tajima, H., Zhu, Z., Cagnac, O., et al. (2011). The Arabidopsis intracellular Na+/H+ antiporters NHX5 and NHX6 are endosome associated and necessary for plant growth and development. *Plant Cell* 23 (1), 224–239. doi: 10.1105/tpc.110.079426

Ben-Amotz, A., and Avron, M. (1973). The role of glycerol in the osmotic regulation of the halophilic alga dunaliella parva. *Plant Physiol.* 51 (5), 875–878. doi: 10.1104/pp.51.5.875

Chapin, F. S.III (1991). Integrated Responses of Plants to Stress: A centralized system of physiological responses. *BioScience* 41 (1), 29–36. doi: 10.2307/1311538

Chitlaru, E., and Pick, U. (1989). Selection and characterization of dunaliella salina mutants defective in haloadaptation. *Plant Physiol.* 91 (2), 788–794. doi: 10.1104/pp.91.2.788

Chung, K. P., Zeng, Y., and Jiang, L. (2016). COPII paralogs in plants: functional redundancy or diversity? *Trends Plant Sci.* 21 (9), 758–769. doi: 10.1016/j.tplants.2016.05.010

Conesa, A., Götz, S., García-Gómez, J. M., Terol, J., Talón, M., and Robles, M. (2005). Blast2GO: a universal tool for annotation, visualization and analysis in functional genomics research. *Bioinformatics* 21 (18), 3674–3676. doi: 10.1093/bioinformatics/bti610

Denks, K., Vogt, A., Sachelaru, I., Petriman, N. A., Kudva, R., and Koch, H. G. (2014). The Sec translocon mediated protein transport in prokaryotes and eukaryotes. *Mol. Membr Biol.* 31 (2-3), 58–84. doi: 10.3109/09687688.2014.907455

Dittmore, A., Silver, J., Sarkar, S. K., Marmer, B., and Neuman, K. C. (2016). Internal strain drives spontaneous periodic buckling in collagen and regulates remodeling. *Proc. Natl. Acad. Sci. U.S.A.* 113 (30), 8436–8441. doi: 10.1073/pnas.1523228113

El Arroussi, H., Benhima, R., Bennis, I., El Mernissi, N., and Wahby, I. (2015). Improvement of the potential of Dunaliella tertiolecta as a source of biodiesel by auxin treatment coupled to salt stress. *Renewable Energy* 77, 15–19. doi: 10.1016/j.renene.2014.12.010

Ferguson, D. L., Guikema, J. A., and Paulsen, G. M. (1990). Ubiquitin pool modulation and protein degradation in wheat roots during high temperature stress 1. *Plant Physiol.* 92 (3), 740–746. doi: 10.1104/pp.92.3.740

Foyer, C. H., and Noctor, G. (2005). Redox homeostasis and antioxidant signaling: a metabolic interface between stress perception and physiological responses. *Plant Cell* 17 (7), 1866–1875. doi: 10.1105/tpc.105.033589

Frank, J., Kaulfürst-Soboll, H., Rips, S., Koiwa, H., and von Schaewen, A. (2008). Comparative analyses of Arabidopsis complex glycan1 mutants and genetic interaction with staurosporin and temperature sensitive3a. *Plant Physiol.* 148 (3), 1354–1367. doi: 10.1104/pp.108.127027

Gao, F., Nan, F., Feng, J., Lü, J., Liu, Q., Liu, X., et al. (2021). Transcriptome profile of Dunaliella salina in Yuncheng Salt Lake reveals salt-stress-related genes under different salinity stresses. *J. Oceanology Limnology* 39 (6), 2336–2362. doi: 10.1007/s00343-021-0164-4

Garcia-Mata, C., Wang J Fau - Gajdanowicz, P., Gajdanowicz P Fau - Gonzalez, W., Gonzalez W Fau - Hills, A., Hills A Fau - Donald, N., Donald N Fau - Riedelsberger, J., et al. (2010). A minimal cysteine motif required to activate the SKOR K+ channel of Arabidopsis by the reactive oxygen species H2O2. *J. Biol. Chem.* 285 (38), 29286–29294. doi: 10.1074/jbc.M110.141176

Goyal, A. (2007). Osmoregulation in Dunaliella, Part I: Effects of osmotic stress on photosynthesis, dark respiration and glycerol metabolism in Dunaliella tertiolecta and its salt-sensitive mutant (HL 25/8). *Plant Physiol. Biochem.* 45 (9), 696–704. doi: 10.1016/j.plaphy.2007.05.008

Grune, T., Reinheckel, T., and Davies, K. J. A. (1997). Degradation of oxidized proteins in mammalian cells. *FASEB J.* 11 (7), 526–534. doi: 10.1096/fasebj.11.7.9212076

Harrathi, J., Hosni, K., Karray-Bouraoui, N., Attia, H., Marzouk, B., Magné, C., et al. (2011). Effect of salt stress on growth, fatty acids and essential oils in safflower (Carthamus tinctorius L.). *Acta Physiologiae Plantarum* 34 (1), 129–137. doi: 10.1007/s11738-011-0811-z

Haus, M., and Wegmann, K. (1984). Glycerol-3-phosphate dehydrogenase (EC 1.1.1.8) from Dunaliella tertiolecta. I. Purification and kinetic properties. *Physiologia Plantarum* 60 (3), 283–288. doi: 10.1111/j.1399-3054.1984.tb06063.x

He, M., and Ding, N.-Z. (2020). Plant unsaturated fatty acids: multiple roles in stress response. *Front. Plant Sci.* 11. doi: 10.3389/fpls.2020.562785

He, Q., Lin, Y., Tan, H., Zhou, Y., Wen, Y., Gan, J., et al. (2020a). Transcriptomic profiles of Dunaliella salina in response to hypersaline stress. *BMC Genomics* 21 (1), 115. doi: 10.1186/s12864-020-6507-2

He, Q., Toh, J. D., Ero, R., Qiao, Z., Kumar, V., Serra, A., et al. (2020b). The unusual di-domain structure of Dunaliella salina glycerol-3-phosphate dehydrogenase enables direct conversion of dihydroxyacetone phosphate to glycerol. *Plant J.* 102 (1), 153–164. doi: 10.1111/tpj.14619

Hershko, A., and Ciechanover, A. (1992). *The ubiquitin system for protein degradation.* 61 (1), 761–807. doi: 10.1146/annurev.bi.61.070192.003553

Ho, L.-W., Yang, T., Shieh, S.-S., Edwards, G. E., and Yen, H. E. (2010). Reduced expression of a vesicle trafficking-related ATPase SKD1 decreases salt tolerance in Arabidopsis. *Funct. Plant Biol.* 37 (10), 962–973. doi: 10.1071/Fp10049

Hu, Z., Cools, T., and De Veylder, L. (2016). Mechanisms used by plants to cope with DNA damage. *Annu. Rev. Plant Biol.* 67 (1), 439–462. doi: 10.1146/annurev-arplant-043015-111902

Jungnickel, B., Rapoport, T. A., and Hartmann, E. (1994). Protein translocation: common themes from bacteria to man. *FEBS Lett.* 346 (1), 73–77. doi: 10.1016/0014-5793(94)00367-x

Kang, J. S., Frank, J., Kang, C. H., Kajiura, H., Vikram, M., Ueda, A., et al. (2008). Salt tolerance of Arabidopsis thaliana requires maturation of N-glycosylated proteins in the Golgi apparatus. *Proc. Natl. Acad. Sci. U.S.A.* 105 (15), 5933–5938. doi: 10.1073/pnas.0800237105

Kang, W. H., Sim, Y. M., Koo, N., Nam, J. Y., Lee, J., Kim, N., et al. (2020). Transcriptome profiling of abiotic responses to heat, cold, salt, and osmotic stress of Capsicum annuum L. *Sci. Data* 7 (1), 17. doi: 10.1038/s41597-020-0352-7

Konishi, T., Shinohara, K., Yamada, K., and Sasaki, Y. (1996). Acetyl-CoA carboxylase in higher plants: most plants other than gramineae have both the prokaryotic and the eukaryotic forms of this enzyme. *Plant Cell Physiol.* 37 (2), 117–122. doi: 10.1093/oxfordjournals.pcp.a028920

Kowalski, S. P., Lan, T. H., Feldmann, K. A., and Paterson, A. H. (1994). Comparative mapping of Arabidopsis thaliana and Brassica oleracea chromosomes reveals islands of conserved organization. *Genetics* 138 (2), 499–510. doi: 10.1093/genetics/138.2.499

Leshem, Y., Seri L Fau - Levine, A., and Levine, A. (2007). Induction of phosphatidylinositol 3-kinase-mediated endocytosis by salt stress leads to intracellular production of reactive oxygen species and salt tolerance. *Plant J.* 51 (2), 185–197. doi: 10.1111/j.1365-313X.2007.03134.x

Levine, B., and Klionsky, D. J. (2004). Development by self-digestion: molecular mechanisms and biological functions of autophagy. *Dev. Cell* 6 (4), 463–477. doi: 10.1016/s1534-5807(04)00099-1

Li, L., Zhang, X., He, N., Wang, X., Zhu, P., and Ji, Z. (2019). Transcriptome profiling of the salt-stress response in the halophytic green alga dunaliella salina. *Plant Mol. Biol. Rep.* 37 (5), 421–435. doi: 10.1007/s11105-019-01168-z

Lieberman-Aiden, E., van Berkum, N. L., Williams, L., Imakaev, M., Ragoczy, T., Telling, A., et al. (2009). Comprehensive mapping of long-range interactions reveals folding principles of the human genome. *Science* 326 (5950), 289–293. doi: 10.1126/science.1181369

Liu, J. X., and Howell, S. H. (2016). Managing the protein folding demands in the endoplasmic reticulum of plants. *New Phytol.* 211 (2), 418–428. doi: 10.1111/nph.13915

Liu, J. X., Srivastava, R., Che, P., and Howell, S. H. (2010). Salt stress responses in Arabidopsis utilize a signal transduction pathway related to endoplasmic reticulum stress signaling. *Plant J.* 51 (5), 897–909. doi: 10.1111/j.1365-313X.2007.03195.x

Liu, Y., and Bassham, D. C. (2012). Autophagy: pathways for self-eating in plant cells. *Annu. Rev. Plant Biol.* 63, 215–237. doi: 10.1146/annurev-arplant-042811-105441

Livak, K. J., and Schmittgen, T. D. (2001). Analysis of relative gene expression data using real-time quantitative PCR and the 2(-Delta Delta C(T)) Method. *Methods* 25 (4), 402–408. doi: 10.1006/meth.2001.1262

López-Pérez, L., Martínez-Ballesta, M., Maurel, C., and Carvajal, M. (2009). Changes in plasma membrane lipids, aquaporins and proton pump of broccoli roots, as an adaptation mechanism to salinity. *Phytochemistry* 70 (4), 492–500. doi: 10.1016/j.phytochem.2009.01.014

Luo, L., Zhang, P., Zhu, R., Fu, J., Su, J., Zheng, J., et al. (2017). Autophagy is rapidly induced by salt stress and is required for salt tolerance in arabidopsis. *Front. Plant Sci.* 8). doi: 10.3389/fpls.2017.01459

Lv, H., Kim, M., Park, S., Baek, K., Oh, H., Polle, J. E. W., et al. (2021). Comparative transcriptome analysis of short-term responses to salt and glycerol hyperosmotic stress in the green alga Dunaliella salina. *Algal Res.* 53, 102147. doi: 10.1016/j.algal.2020.102147

Mangelsen, E., Kilian, J., Harter, K., Jansson, C., Wanke, D., and Sundberg, E. (2011). Transcriptome analysis of high-temperature stress in developing barley caryopses: early stress responses and effects on storage compound biosynthesis. *Mol. Plant* 4 (1), 97–115. doi: 10.1093/mp/ssq058

Mao, X., Cai, T., Olyarchuk, J. G., and Wei, L. (2005). Automated genome annotation and pathway identification using the KEGG Orthology (KO) as a controlled vocabulary. *Bioinformatics* 21 (19), 3787–3793. doi: 10.1093/bioinformatics/bti430

Marco, F., Alcázar, R., Tiburcio, A. F., and Carrasco, P. (2011). Interactions between polyamines and abiotic stress pathway responses unraveled by transcriptome analysis of polyamine overproducers. *Omics* 15 (11), 775–781. doi: 10.1089/omi.2011.0084

Møller, I. S., and Tester, M. (2007). Salinity tolerance of Arabidopsis: a good model for cereals? *Trends Plant Sci.* 12 (12), 534–540. doi: 10.1016/j.tplants.2007.09.009

Moriya, Y., Itoh, M., Okuda, S., Yoshizawa, A. C., and Kanehisa, M. (2007). KAAS: an automatic genome annotation and pathway reconstruction server. *Nucleic Acids Res.* 35 (Web Server issue), W182–W185. doi: 10.1093/nar/gkm321

Nagashima, Y., von Schaewen, A., and Koiwa, H. (2018). Function of N-glycosylation in plants. *Plant Sci.* 274, 70–79. doi: 10.1016/j.plantsci.2018.05.007

Nakamura, Y., Tsuchiya, M., and Ohta, H. (2007). Plastidic phosphatidic acid phosphatases identified in a distinct subfamily of lipid phosphate phosphatases with prokaryotic origin. *J. Biol. Chem.* 282 (39), 29013–29021. doi: 10.1074/jbc.M704385200

Neelam, S., and Subramanyam, R. (2013). Alteration of photochemistry and protein degradation of photosystem II from Chlamydomonas reinhardtii under high salt grown cells. *J. Photochem. Photobiol. B: Biol.* 124, 63–70. doi: 10.1016/j.jphotobiol.2013.04.007

Nieves-Cordones, M., López-Delacalle, M., Ródenas, R., Martínez, V., Rubio, F., and Rivero, R. M. (2019). Critical responses to nutrient deprivation: A comprehensive review on the role of ROS and RNS. *Environ. Exp. Bot.* 161, 74–85. doi: 10.1016/j.envexpbot.2018.10.039

Nyathi, Y., Wilkinson, B. M., and Pool, M. R. (2013). Co-translational targeting and translocation of proteins to the endoplasmic reticulum. *Biochim. Biophys. Acta* 1833 (11), 2392–2402. doi: 10.1016/j.bbamcr.2013.02.021

Ohlrogge, J., and Browse, J. (1995). Lipid biosynthesis. *Plant Cell* 7 (7), 957–970. doi: 10.1105/tpc.7.7.957

Oren, A. (2005). A hundred years of Dunaliella research: 1905-2005. *Saline Syst.* 1, 2. doi: 10.1186/1746-1448-1-2

Pacifici, R. E., Salo, D. C., and Davies, K. J. (1989). Macroxyproteinase (M.O.P.): A 670 kDa Proteinase complex that degrades oxidatively denatured proteins in red blood cells. *Free Radic. Biol. Med.* 7 (5), 521–536. doi: 10.1016/0891-5849(89)90028-2

Paez Valencia, J., Goodman, K., and Otegui, M. S. (2016). Endocytosis and endosomal trafficking in plants. *Annu. Rev. Plant Biol.* 67, 309–335. doi: 10.1146/annurev-arplant-043015-112242

Panahi, B., and Hejazi, M. A. (2021). Weighted gene co-expression network analysis of the salt-responsive transcriptomes reveals novel hub genes in green halophytic microalgae Dunaliella salina. *Sci. Rep.* 11 (1), 1607. doi: 10.1038/s41598-020-80945-3

Pandit, P. R., Fulekar, M. H., and Karuna, M. S. L. (2017). Effect of salinity stress on growth, lipid productivity, fatty acid composition, and biodiesel properties in Acutodesmus obliquus and Chlorella vulgaris. *Environ. Sci. Pollut. Res.* 24 (15), 13437–13451. doi: 10.1007/s11356-017-8875-y

Pierrugues, O., Brutesco, C., Oshiro, J., Gouy, M., Deveaux, Y., Carman, G. M., et al. (2001). Lipid phosphate phosphatases in Arabidopsis. Regulation of the AtLPP1 gene in response to stress. *J. Biol. Chem.* 276 (23), 6896–6901. doi: 10.1074/jbc.M009726200

Roth, M. G. (2004). Phosphoinositides in constitutive membrane traffic. *Physiol. Rev.* 84 (3), 699–730. doi: 10.1152/physrev.00033.2003

Sandalio, L. M., Espinosa, J., Shabala, S. A.-O., León, J., and Romero-Puertas, M. C. (2023). Reactive oxygen species- and nitric oxide-dependent regulation of ion and metal homeostasis in plants. *J. Exp. Bot.* 74 (19), 5970–5988. doi: 10.1093/jxb/erad349

Segami, S., Asaoka, M., Kinoshita, S., Fukuda, M., Nakanishi, Y., and Maeshima, M. (2018). Biochemical, structural and physiological characteristics of vacuolar H+-pyrophosphatase. *Plant Cell Physiol.* 59 (7), 1300–1308. doi: 10.1093/pcp/pcy054

Shi, H., Ishitani, M., Kim, C., and Zhu, J.-K. (2000). The Arabidopsis thaliana salt tolerance gene SOS1 encodes a putative Na+/H+ antiporter. *Proc. Natl. Acad. Sci. U.S.A.* 97 (12), 6896–6901. doi: 10.1073/pnas.120170197

Smalle, J., and Vierstra, R. D. (2004). The ubiquitin 26s proteasome proteolytic pathway. *Annu. Rev. Plant Biol.* 55 (1), 555–590. doi: 10.1146/annurev.arplant.55.031903.141801

Stryer, L. (1995). *Biochemistry*. (New York: Freeman Company).

Sui, N., and Han, G. (2014). Salt-induced photoinhibition of PSII is alleviated in halophyte Thellungiella halophila by increases of unsaturated fatty acids in membrane lipids. *Acta Physiologiae Plantarum* 36 (4), 983–992. doi: 10.1007/s11738-013-1477-5

Takagi, M., Karseno, and Yoshida, T. (2006). Effect of salt concentration on intracellular accumulation of lipids and triacylglyceride in marine microalgae Dunaliella cells. *J. Biosci. Bioeng.* 101 (3), 223–226. doi: 10.1263/jbb.101.223

Trapnell, C., Williams, B. A., Pertea, G., Mortazavi, A., Kwan, G., van Baren, M. J., et al. (2010). Transcript assembly and quantification by RNA-Seq reveals unannotated transcripts and isoform switching during cell differentiation. *Nat. Biotechnol.* 28 (5), 511–515. doi: 10.1038/nbt.1621

Vabulas, R. M., Raychaudhuri, S., Hayer-Hartl, M., and Hartl, F. U. (2010). Protein folding in the cytoplasm and the heat shock response. *Cold Spring Harb. Perspect. Biol.* 2 (12), a004390. doi: 10.1101/cshperspect.a004390

Van Dijk, E. L., Jaszczyszyn, Y., Naquin, D., and Thermes, C. (2018). The third revolution in sequencing technology. *Trends Genet.* 34 (9), 666–681. doi: 10.1016/j.tig.2018.05.008

Wang, W., Vinocur, B., Shoseyov, O., and Altman, A. (2004). Role of plant heat-shock proteins and molecular chaperones in the abiotic stress response. *Trends Plant Sci.* 9 (5), 244–252. doi: 10.1016/j.tplants.2004.03.006

Wang, X., Xu, M., Gao, C., Zeng, Y., Cui, Y., Shen, W., et al. (2020). The roles of endomembrane trafficking in plant abiotic stress responses. *J. Integr. Plant Biol.* 62 (1), 55–69. doi: 10.1111/jipb.12895

Wang, F., Yang, Y., Wang, Z., Zhou, J., Fan, B., and Chen, Z. (2015). A critical role of lyst-interacting protein5, a positive regulator of multivesicular body biogenesis, in plant responses to heat and salt stresses. *Plant Physiol.* 169 (1), 497–511. doi: 10.1104/pp.15.00518

Wu, S. J., Ding, L., and Zhu, J. K. (1996). SOS1, a genetic locus essential for salt tolerance and potassium acquisition. *Plant Cell* 8 (4), 617–627. doi: 10.1105/tpc.8.4.617

Yang, Y., and Guo, Y. (2018). Elucidating the molecular mechanisms mediating plant salt-stress responses. *New Phytol.* 217 (2), 523–539. doi: 10.1111/nph.14920

Yin, H. L., and Janmey, P. A. (2003). Phosphoinositide regulation of the actin cytoskeleton. *Annu. Rev. Physiol.* 65, 761–789. doi: 10.1146/annurev.physiol.65.092101.142517

Yokoi, S., Quintero, F. J., Cubero, B., Ruiz, M. T., Bressan, R. A., Hasegawa, P. M., et al. (2002). Differential expression and function of Arabidopsis thaliana NHX Na+/H+ antiporters in the salt stress response. *Plant J.* 30 (5), 529–539. doi: 10.1046/j.1365-313x.2002.01309.x

Young, M. D., Wakefield, M. J., Smyth, G. K., and Oshlack, A. (2010). Gene ontology analysis for RNA-seq: accounting for selection bias. *Genome Biol.* 11 (2), R14. doi: 10.1186/gb-2010-11-2-r14

Yu, F., Lou, L., Tian, M., Li, Q., Ding, Y., Cao, X., et al. (2016). ESCRT-I component VPS23A affects ABA signaling by recognizing ABA receptors for endosomal degradation. *Mol. Plant* 9 (12), 1570–1582. doi: 10.1016/j.molp.2016.11.002

Zeng, Y., Li, B., Ji, C., Feng, L., Niu, F., Deng, C., et al. (2021). A unique AtSar1D-AtRabD2a nexus modulates autophagosome biogenesis in Arabidopsis thaliana. *Proc. Natl. Acad. Sci. U.S.A.* 118 (17), e2021293118. doi: 10.1073/pnas.2021293118

Zheng, M., Liu, X., Lin, J., Liu, X., Wang, Z., Xin, M., et al. (2019). Histone acetyltransferase GCN5 contributes to cell wall integrity and salt stress tolerance by altering the expression of cellulose synthesis genes. *Plant J.* 97 (3), 587–602. doi: 10.1111/tpj.14144

Zhu, J.-K. (2003). Regulation of ion homeostasis under salt stress. *Curr. Opin. Plant Biol.* 6 (5), 441–445. doi: 10.1016/s1369-5266(03)00085-2

frontiers | Frontiers in Plant Science

TYPE Original Research
PUBLISHED 14 December 2023
DOI 10.3389/fpls.2023.1313113

OPEN ACCESS

EDITED BY
Zulfiqar Ali Sahito,
Zhejiang University of Technology, China

REVIEWED BY
Daisuke Todaka,
RIKEN Yokohama, Japan
Tabassum Hussain,
University of Karachi, Pakistan

*CORRESPONDENCE
Bingzhe Fu
Fbzhe19@163.com

RECEIVED 10 October 2023
ACCEPTED 24 November 2023
PUBLISHED 14 December 2023

CITATION
Song W, Gao X, Li H, Li S, Wang J, Wang X, Wang T, Ye Y, Hu P, Li X and Fu B (2023) Transcriptome analysis and physiological changes in the leaves of two *Bromus inermis* L. genotypes in response to salt stress. *Front. Plant Sci.* 14:1313113. doi: 10.3389/fpls.2023.1313113

Transcriptome analysis and physiological changes in the leaves of two *Bromus inermis* L. genotypes in response to salt stress

Wenxue Song[1], Xueqin Gao[1,2], Huiping Li[1], Shuxia Li[1,2], Jing Wang[1], Xing Wang[1], Tongrui Wang[1], Yunong Ye[1], Pengfei Hu[1], Xiaohong Li[1] and Bingzhe Fu[1,2,3]*

[1]College of Forestry and Prataculture, Ningxia University, Yinchuan, Ningxia, China, [2]Ningxia Grassland and Animal Husbandry Engineering Technology Research Center, Yinchuan, Ningxia, China, [3]Key Laboratory for Model Innovation in Forage Production Efficiency, Ministry of Agriculture and Rural Affairs, Yinchuan, Ningxia, China

Soil salinity is a major factor threatening the production of crops around the world. Smooth bromegrass (*Bromus inermis* L.) is a high-quality grass in northern and northwestern China. Currently, selecting and utilizing salt-tolerant genotypes is an important way to mitigate the detrimental effects of salinity on crop productivity. In our research, salt-tolerant and salt-sensitive varieties were selected from 57 accessions based on a comprehensive evaluation of 22 relevant indexes, and their salt-tolerance physiological and molecular mechanisms were further analyzed. Results showed significant differences in salt tolerance between 57 genotypes, with Q25 and Q46 considered to be the most salt-tolerant and salt-sensitive accessions, respectively, compared to other varieties. Under saline conditions, the salt-tolerant genotype Q25 not only maintained significantly higher photosynthetic performance, leaf relative water content (RWC), and proline content but also exhibited obviously lower relative conductivity and malondialdehyde (MDA) content than the salt-sensitive Q46 ($p < 0.05$). The transcriptome sequencing indicated 15,128 differentially expressed genes (DEGs) in Q46, of which 7,885 were upregulated and 7,243 downregulated, and 12,658 DEGs in Q25, of which 6,059 were upregulated and 6,599 downregulated. The Kyoto Encyclopedia of Genes and Genomes (KEGG) analysis showed that the salt response differences between Q25 and Q46 were attributed to the variable expression of genes associated with plant hormone signal transduction and MAPK signaling pathways. Furthermore, a large number of candidate genes, related to salt tolerance, were detected, which involved transcription factors (zinc finger proteins) and accumulation of compatible osmolytes (glutathione *S*-transferases and pyrroline-5-

carboxylate reductases), etc. This study offers an important view of the physiological and molecular regulatory mechanisms of salt tolerance in two smooth bromegrass genotypes and lays the foundation for further identification of key genes linked to salt tolerance.

KEYWORDS

Bromus inermis L., salt stress, accessions evaluation, physiological analysis, transcriptome analysis

Introduction

Soil salinity is one of the major factors threatening agricultural production on a global scale (Wang et al., 2020). A high concentration of salt inhibits the growth of plants via osmotic stress and ion imbalance in plant cells (Zhao et al., 2022). What is worse, soil salinization is accelerated by irrational use and exploitation of land, and by 2050, half the world's arable land will be lost (Zhu, 2016; Albaladejo et al., 2018). If these saline soils are fully utilized for agricultural production, the problems of the demand for food caused by the expanding population and the growth of spendable income can be alleviated. However, as the majority of the crops are sensitive to salinity, it is not feasible to cultivate the varieties currently used in saline–alkaline lands (Van Bezouw et al., 2019; Ganie et al., 2021). It is vital to enhance a plant's tolerance to salinity so as to support plant growth and yield. Hence, it is necessary to analyze the genes and molecular mechanisms related to salinity responses for the purpose of enhancing the ability to resist salt stress, which would then make significant contributions to the genetic engineering and food production of plants in salt-affected areas.

Currently, the salt tolerance of Gramineae is the focus of many studies (Van Bezouw et al., 2019; Yu S., et al., 2020; Ganie et al., 2021). Highly saline conditions disturb the homeostasis of water potential and ion distribution, leading to hyperosmotic stress, ion disequilibrium, and oxidative damage, which ultimately threaten plants (Liang et al., 2018; Lv et al., 2019). However, plants have also developed several pathways to respond to high salt stress, including stress-sensing regulatory genes and proteins (Bhattarai et al., 2020). Second messengers, such as Ca^{2+}, reactive oxygen species (ROS), and phytohormones were created at a rapid rate in the cytoplasm under salt stress, which progressively decipher and amplify the salt stress signal, enabling a variety of stress signaling receptors found on the cell membrane to rapidly detect changes in the surroundings (Fahad et al., 2015; Steinhorst and Kudla, 2019). These signals modulate downstream transcription factors (TFs) via a cascade response to further alter the transcript levels of a large number of TFs, including WRKY, AP2/ERF, and MYB (Zhao et al., 2020). Then, the expression of a large number of genes, such as *ZFP179* (zinc-finger protein 179) (Sun et al., 2010), *S1CBL10* (calcineurin B-like protein 10) (Egea et al., 2018), *GsPRX9* (a peroxidase gene) (Jin et al., 2019), *SbNHXLP* (a Na^+/H^+ antiporter-like protein) (Kumari et al., 2017), and *MsFLS13* (saline–alkaline-induced flavonol synthase gene) (Zhang et al., 2023), are eventually affected, resulting in the development of the salt tolerance in the plants. In addition, many salt tolerance-related transporters or channels, including the plasma membrane Na^+/H^+ antiporter (SOS1), have been identified in Gramineae. K^+ transporter 1 (AKT1), K^+ uptake transporter (KUP1), Na^+/H^+ antiporter (NHX), and high-affinity K^+ transporter (HKT) have been identified in Gramineae (Zhu, 2016; Bailey-Serres et al., 2019; Gong et al., 2020; Wang et al., 2021).

Smooth bromegrass is considerable forage with excellent feed value, good palatability, and strong adaptability (Li et al., 2022). It is widely cultivated in northern and northwestern China for grazing and sand binding (Li et al., 2022). However, the combination of climate change and agricultural mismanagement exacerbates soil salinization in these areas, limiting its wide use (Wang and Li, 2013; Wang et al., 2021). Li et al. (2022) found that the physiological characteristics, function of the gene, and mechanism of adaptation have undergone changes under salt stress in smooth bromegrass. Hence, it is necessary to explore the physiological and molecular mechanisms of smooth bromegrass response to salt stress, which will make a significant contribution to forage production in saline–alkaline land.

In the research, the evaluation of salt tolerance was performed in 57 smooth bromegrass accessions by analyzing the indexes during the germination and seedling stages. The salt-tolerant variety Q25 and salt-sensitive Q46 were then screened, and their response mechanisms to salt stress were further investigated by transcriptome analysis. Our objective is to gain a broad understanding of the transcriptional expression of genes related to the response to salt stress and to uncover the candidate genes and mechanisms in smooth bromegrass.

Materials and methods

Plant materials

For the evaluation of salt tolerance, a total of 57 smooth bromegrass accessions were used. Among them, one genotype was from commercial cultivars, obtained from Inner Mongolia

Agricultural University; two accessions were collected from Romania and the United States, obtained from the Institute of Grassland Research; and the others were collected from China (Supplementary Table 1).

Plant growth and treatments

Based on preliminary experiments, the optimal salt concentrations for screening germplasm during the germination and seedling stages were 150 mM and 300 mM, respectively. However, the data from the preliminary experiments were not presented.

In the germination stage, seeds with uniform size were selected from each germplasm, disinfected with 75% ethanol for 30 s, and rinsed six times with distilled water. Fifty sterile seeds were germinated at 25°C/20°C under a light–dark photoperiod of 12/12 h on Petri dishes containing two layers of filter paper moistened with 5 ml of distilled water or 150 mM NaCl solution. Three biological replicates were performed. The filter paper was changed every 2 days, and the number of germinated seeds and moldy seeds was recorded. The indexes were determined when there were no germinated seeds under salt stress (12 days).

The 10-day-old seedlings were moved to a plastic basin filled with sand and kept in the growth chamber at a 12/12 h (light/dark) photoperiod at 25°C ± 2°C with a light intensity of 200 $\mu mol \cdot m^{-2} \cdot s^{-2}$. Three times a week, the seedlings were watered with 1× Hoagland's solution. After 15 days, seedlings were divided into two groups: a control group and an experimental group. The control group was watered with Hoagland's solution every day, and the experimental group was watered with Hoagland's solution amended with 300 mM NaCl (approximately 31.5 $ms \cdot cm^{-1}$) every day. To avoid the accumulation of salt in the sand media, the pot was manually irrigated daily until free drainage occurred. Determination of indexes was performed when there were significant differences between different genotypes under salt stress (13 days). For the determination of further physiological parameters and gene expression analysis, smooth bromegrass leaves were harvested, immediately frozen in liquid nitrogen, and stored at −80°C.

Measurement of evaluation indicators and comprehensive evaluation of accessions

The number of seeds was counted to measure germination rate and germination vigor. Radicle length and embryo length were measured using a ruler. Root bud ratio, germination index, and vitality index were determined through a calculation method. Plant height was measured using a ruler. Fresh weight and biomass were measured using an electronic balance. The leaf morphology indexes were measured using the Li-3100C instrument. The root morphology indexes were measured using Epson Perfection V12000 Photo. To eliminate genetic differences, the salt tolerance coefficient was calculated based on measured indicators, and then correlation and principal component analysis were used to perform a comprehensive evaluation using the membership function.

Measurement of physiological indicators

On the basis of the phenotype of smooth bromegrass plants, each treatment group was photographed on days 1, 5, 9, and 13 of salt treatment. Relative water content (RWC) was measured according to Ahmad et al. (2019). Chlorophyll content (Soil Plant Analysis Development (SPAD)) was measured using the SPAD-502 chlorophyll meter (China) (Li et al., 2022). Relative conductivity (REL) was measured following the method of a previous study (Wu et al., 2017). The parameters of malondialdehyde (MDA), proline (Pro), soluble protein, and soluble sugar were determined using kits from Solarbio (Beijing, China). Three biological replicates were performed.

RNA extraction and sequencing

An RNAprep Pure Plant Kit (Tiangen, Beijing, China) was used to extract total RNA. The quality of the RNA was determined using a NanoPhotometer spectrophotometer (IMPLEN, CA, USA), Qubit 2.0 Fluorometer (Life Technologies, Carlsbad, CA, USA), and an Agilent Bioanalyzer 2100 system (Agilent Technologies, Santa Clara, CA, USA). AMPure XP Beads were used to screen the cDNA (~200 bp). After amplifying and purifying, the cDNA libraries were obtained and sequenced using the Illumina HiSeq™ 2000 System (Illumina, San Diego, CA, USA) of Metware Biotechnology Co., Ltd. (Wuhan, China). Three biological replicates were performed to sequence transcription.

De novo assembly and functional annotation

The raw data were filtered using FASTP (v 0.23.2). Reads containing adapter sequences were eliminated. Paired reads were discarded if the percentage of N bases in either of the sequencing reads exceeded 10% of the total bases. Additionally, paired reads were also removed if the number of low-quality bases ($Q \leq 20$) in either of the sequencing reads exceeded 50% of the total bases. Transcriptome assembly was performed using Trinity (v 2.13.2). The TransDecoder (v 5.3.0) was employed to predict coding sequence (CDS) from the transcripts assembled using Trinity. The following database was used for functional annotation of assembled unigenes: non-redundant protein sequences (Nr), non-redundant nucleotide sequences (Nt), protein family (Pfam), eukaryotic Ortholog Groups/Clusters of Orthologous Groups of proteins (KOG/COG), and a manually annotated and reviewed protein sequence database (Swiss-Prot). The annotation of the Kyoto Encyclopedia of Genes and Genomes (KEGG) pathway analysis was performed using the KEGG Automatic Annotation Server (KAAS). The Gene Ontology (GO) annotation of unigenes

was performed using clusterProfiler (v 4.6.0) according to the Nr and Pfam annotation results.

Differential unigene expression analysis

RSEM (v 1.3.1) was used to estimate gene expression levels. Based on the gene length, the fragments per kilobase of transcripts per million (FPKM) value of each gene were computed. Comparative analysis was performed according to DESeq2 v 1.22.2. The criteria for screening differentially expressed genes (DEGs) were $|\log_2(\text{Fold Change})| \geq 2$ and p-value < 0.01. The GO and KEGG enrichment analyses were performed based on a hypergeometric test. TF analysis was performed using iTAK (1.7a).

Quantitative real-time PCR analyses

Nine DEGs were randomly selected for qRT-PCR analysis to verify the accuracy of the sequencing results. TRIzol Total RNA Extraction Kit (Sangon Biotech, Shanghai, China) was used to extract RNA. RNA was reverse-transcribed using an Evo M-MLV RT Mix Kit with gDNA Clean (Accurate Biotechnology, Hunan, China). The primers are shown in Supplementary Table 2. qRT-PCR was performed using a BioEasy Master Mix (SYBR Green) Kit (Bioer, Hangzhou, China) and a C1000 TouchChihermal Cycler system (Bio-Rad, Hercules, CA, USA). The reference gene *Actin* was used to normalize all transcripts tested. Relative transcript levels were calculated using the $2^{-\Delta\Delta Ct}$ method with three biological replications (Livak and Schmittgen, 2001).

Statistical analysis

The data were sorted using Excel 2010 (Microsoft Inc., Redmond, WA, USA). The data were analyzed by one-way ANOVA using Origin 2023 (Electronic Arts Inc., San Francisco, CA, USA), followed by Tukey's significant difference test ($p < 0.01$ or $p < 0.05$). *t*-Test was performed using SPSS 22 (SPSS Inc., Chicago, IL, USA). The figures were made using Origin 2023 (Electronic Arts Inc., San Francisco, CA, USA).

Results

Salinity effects on 57 smooth bromegrass growth traits

After treatment with NaCl, seedlings of the 57 smooth bromegrass genotypes were significantly suppressed (Supplementary Table 3). In the germination stage, the results showed that salt stress significantly reduced germination potential, germination rate, radicle length, embryo length, root bud ratio, germination index, and vitality index compared with control (Supplementary Table 3). In the seedling stage, NaCl significantly decreased plant height, leaf length, leaf width, leaf area, fresh weight above ground, fresh weight underground, dry weight above ground, dry weight underground, root-to-shoot ratio, root length, root project area, root surface area, average diameter, root volume, and root tips (Supplementary Table 3). Under the treatment of salt, there were significant differences in the growth indexes of 57 smooth bromegrass accessions, and the index values showed obvious normal distribution characteristics. Under salt treatment, the growth traits of 57 varieties were centered in a relatively small range of phenotypic values (Supplementary Figure 1).

Correlation analysis of growth traits among smooth bromegrass germplasm resources under salinity

Relative values of growth characteristics of smooth bromegrass under salinity were calculated using Pearson's correlation coefficient. These results displayed that, during the germination and seedling stages, there were 47 positive correlations ($p < 0.01$) and six negative correlations ($p < 0.01$) in the comparative values of all characteristics under salt stress (Supplementary Figure 2). In the germination stage, the root bud ratio did not correlate with other traits except for embryo length, showing that the root bud ratio was not a good evaluation index for smooth bromegrass. During the seedling stage, there was no significant positive correlation between average root diameter and other traits except for root volume, but a significant negative correlation with root tip and root length. From the results above, it was suggested that 20 traits could be used for the principal component analysis (PCA).

Principal component analysis of growth traits of 57 smooth bromegrass accessions under salinity conditions

The evaluation of 57 smooth bromegrass accessions was performed by principal component analysis of the indexes among the bud stage and seedling stage. Based on the extraction method using eigenvalues greater than 1, six principal components were extracted, with the cumulative contribution rate as high as 84.515% (Supplementary Table 4). The screen plot clearly indicated that the first six factors were significantly higher eigenvalues (Supplementary Figure 3). By extracting these six factors, indicators with similar effects were grouped together, transforming the original indicators into new mutually independent composite indicators for fuzzy membership function analysis. By analyzing the principal component loading matrix, the contribution of each indicator to the composition of the principal components was observed (Supplementary Table 5). In the first principal component, the variables with the highest absolute loading values were root surface area and root projection area. In

the second principal component, the variables with the highest absolute loading values were the germination index and germination rate. In the third principal component, the variables with the highest absolute loading values were leaf area and leaf width. In the fourth principal component, the variables with the highest absolute loading values were embryo root length and root length. In the fifth principal component, the variables with the highest absolute loading values were embryo length and radicle length. In the sixth principal component, the variables with the highest absolute loading values were radicle length and aboveground biomass.

As shown in Supplementary Figure 4, there was a high concentration of indicators in the germination and seedling stages. Combined with the component loading values in Supplementary Table 5, the important roles of the germination stage and seedling stage indicators in salt tolerance principal component analysis of smooth bromegrass were indicated. There may be a certain correlation between salt tolerances in these two stages. The salt tolerance of different smooth bromegrass accessions can be reflected more comprehensively by considering the indexes of the germination stage and seedling stage.

Evaluation of salt tolerance among 57 smooth bromegrass germplasms

In this study, the salt tolerance of 57 accessions was ranked based on the Switching Function Vector Analysis (SFVA) and D values (Figure 1). As can be seen in Figure 1, the top five genotypes with a higher salt tolerance than other accessions in the sequences were Q25, Q6, Q18, Q8, and Q24; less tolerant to salt than the other varieties were Q46 (least) and Q3 (last but one).

Physiological analysis of smooth bromegrass seedlings under salt stress

After 9 days of exposure to salt stress, although the leaves of the two genotypes showed different degrees of wilting, the level of wilting in the salt-tolerant genotype (ST) was lower than that in the salt-sensitive variety (SS). After 13 days of exposure to salt stress, the leaves of the SS experienced withering and eventual death (Figure 2). On the first day, the physiological indexes did not show any significant difference between the SS and the ST under the salt treatment. On the fifth day, there was no significant difference between SS and ST except for RWC, SPAD, and Pro under salt stress. Salt stress significantly decreased the RWC and SPAD of smooth bromegrass on the ninth day compared to the control. Under salt stress, ST had a lower content of the relative conductivity and MDA and higher contents of RWC and SPAD than SS (Figures 3A–D). Thus, after 9 days of salt treatment, ST showed better growth. Furthermore, in response to salt stress, salt treatment resulted in a significant increase in proline, soluble protein, and soluble sugar contents. The ST exhibited significantly higher proline and soluble protein contents compared to the SS (Figures 3E–G). The result showed that a key point in the level of salt treatment was reflected by 9 days of the smooth bromegrass seedlings. Hence, we selected the smooth bromegrass leaves treated with SS and ST under control and salt treatments at 9 days (serious salt stress) for transcriptome analysis.

Transcriptome sequencing and assembly

Twelve cDNA libraries of two different genotypes of smooth bromegrass were sequenced. The clean reads of each library were

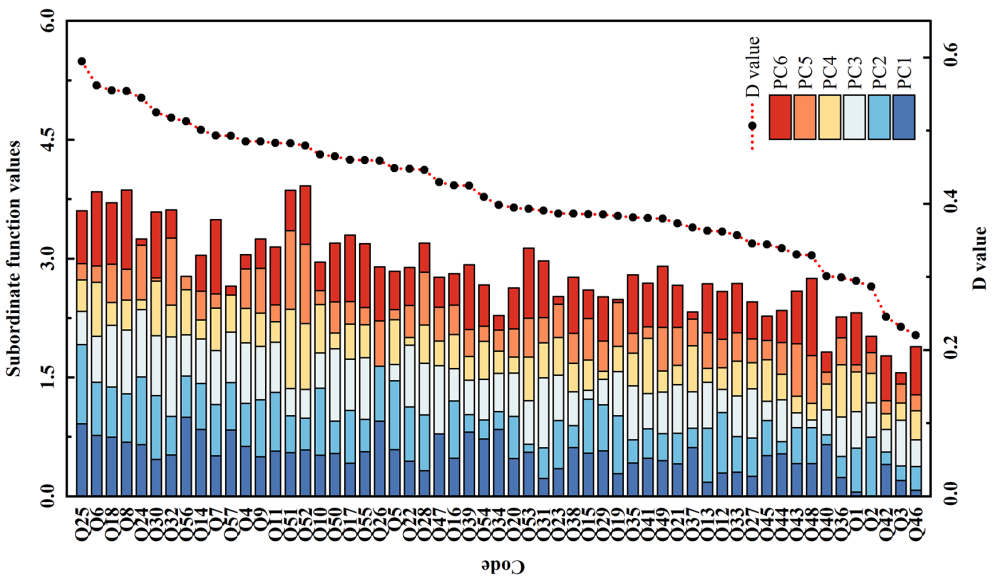

FIGURE 1
The subordinate function values analysis for comprehensive evaluation of salt tolerance among 57 smooth bromegrass accessions. Subordinate function values: the value was calculated based on the switching function vector analysis. D value: the value of weighted membership function; the higher the D value, the stronger the salt tolerance of the genotype.

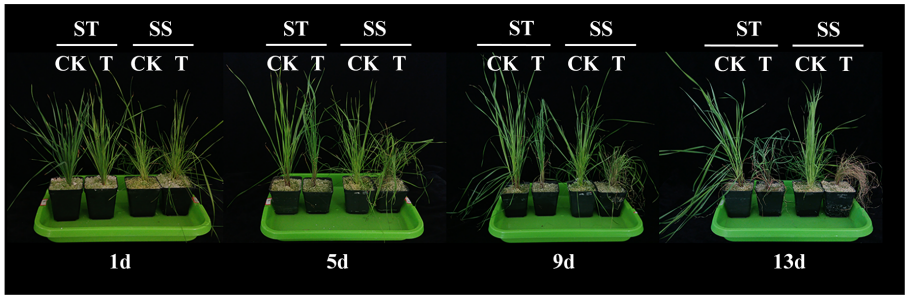

FIGURE 2
Effects of 300 mM NaCl on phenotype of smooth bromegrass seedlings under different salt stress times. ST, salt-tolerant genotype; SS, salt-sensitive genotype; CK, control treatment; T, salt treatment.

obtained. The raw reads, clean reads, clean base, error rate, Q20, Q30, and GC content are shown in Supplementary Table S6. A total of 91.15 Gb of clean data was obtained. Each sample was 6 Gb of clean data, with a Q30 base percentage of 93% or above. A total of 360,627 transcripts with a mean length of 932 bp, an N50 of 1,446 bp, and an N90 of 392 bp, and 194,490 unigenes with a mean length of 1,197 bp, an N50 of 1,667 bp, and an N90 of 561 bp from the 12 sequenced libraries were obtained (Supplementary Table 7). Transcripts and genes were grouped by length as shown in Supplementary Figure 5.

Analysis of gene function annotation

To explore the functionality of unigenes, the sequences of all obtained unigenes were compared using databases such as Nr, Pfam, KOG, SwissProt, KO, NT, and GO, and annotation information for all unigenes was obtained. Annotated unigenes numbers and percentages of the total are listed in Supplementary Table S8. A total of 138,481 assembled unigenes, 71.2% of the total, were annotated in at least one databank. It was found that all unigenes showed the highest homology with *Triticum aestivum* by the analysis of 134,652 unigenes annotated in the Nr database, indicating a close relationship with *T. aestivum* (Supplementary Figure 6).

Expression and cluster analysis of the unigenes

The samples were divided into four groups—salt-sensitive and salt-tolerant samples under control (S-0 and T-0) and salt-sensitive and salt-tolerant samples under stress (S-9 and T-9)—to analyze the transcriptome differences. To analyze the expression level of genes, the read counts of the smooth bromegrass transcriptome were converted to FPKM. Some of the gene expression levels in the T-9 were higher than in S-9 (Figures 4A, B). The gene expression density diagram of samples at different genotypes after salt exposure indicated a similar trend in gene abundance and gene expression density. Moreover, the $\log_2$FPKM values were concentrated in the [−2, 2] interval for all transcripts of the samples (Figure 4A). Correlation heat map analysis of gene expression levels between samples showed a high degree of agreement between each group of samples to ensure the reliability of subsequent differential gene analysis (Supplementary Figure 7). PCA showed that the significant difference between salt and control stress was mainly caused by PC1 (24.42%), while the difference between genotypes was mainly caused by PC2 (18.24%) (Figure 4C).

Differential expression analysis of genes

The four groups (S-0_vs_S-9, T-0_vs_S-0, T-0_vs_T-9, and T-9_vs_S-9) had 15,128, 6,744, 12,658, and 6,115 DEGs, respectively; 7,885, 3,382, 6,059, and 3,232 genes, respectively, were upregulated, and 7,243, 3,362, 6,599, and 2,883 genes, respectively, were downregulated (Figure 5A and Supplementary Table 9). This displayed that, under salt stress, the gene expression levels were significantly changed between salt-tolerant and salt-sensitive varieties. In T-9 and S-9, 1,889 common unigenes were upregulated and 1,810 were downregulated in the Venn diagram analysis (Figure 5B). T-9 had 4,170 unique upregulated DEGs, and S-9 had 5,996 unique downregulated DEGs. These upregulated DEGs, unique to T-9, may have a role in salinity resistance, while the upregulation of DEGs may have a correlation with salt stress susceptibility in S-9. For the two comparisons of T-9_vs_S-9 and T-0_vs_S-0, 3,190 unique genes were specifically upregulated in T-9 and may contribute to salt stress resistance (Figure 5C). In the current study, thousands of DEGs were discovered, which can be attributed to the complex genetic background. All DEGs were divided into 10 subclasses by K-means clustering analysis, among which subclass 7 was the largest, containing 6,603 DEGs, and subclass 4 was the smallest, containing 1,270 DEGs (Figure 5D).

Transcription factor analysis

Further investigation was conducted on the transcripts of TF-encoding genes to explore the regulatory mechanisms of salt stress on smooth bromegrass. A total of 567 TF-encoding genes from 59 different families in T-0_vs_T-9 were identified. As shown in

10.3389/fpls.2023.1313113

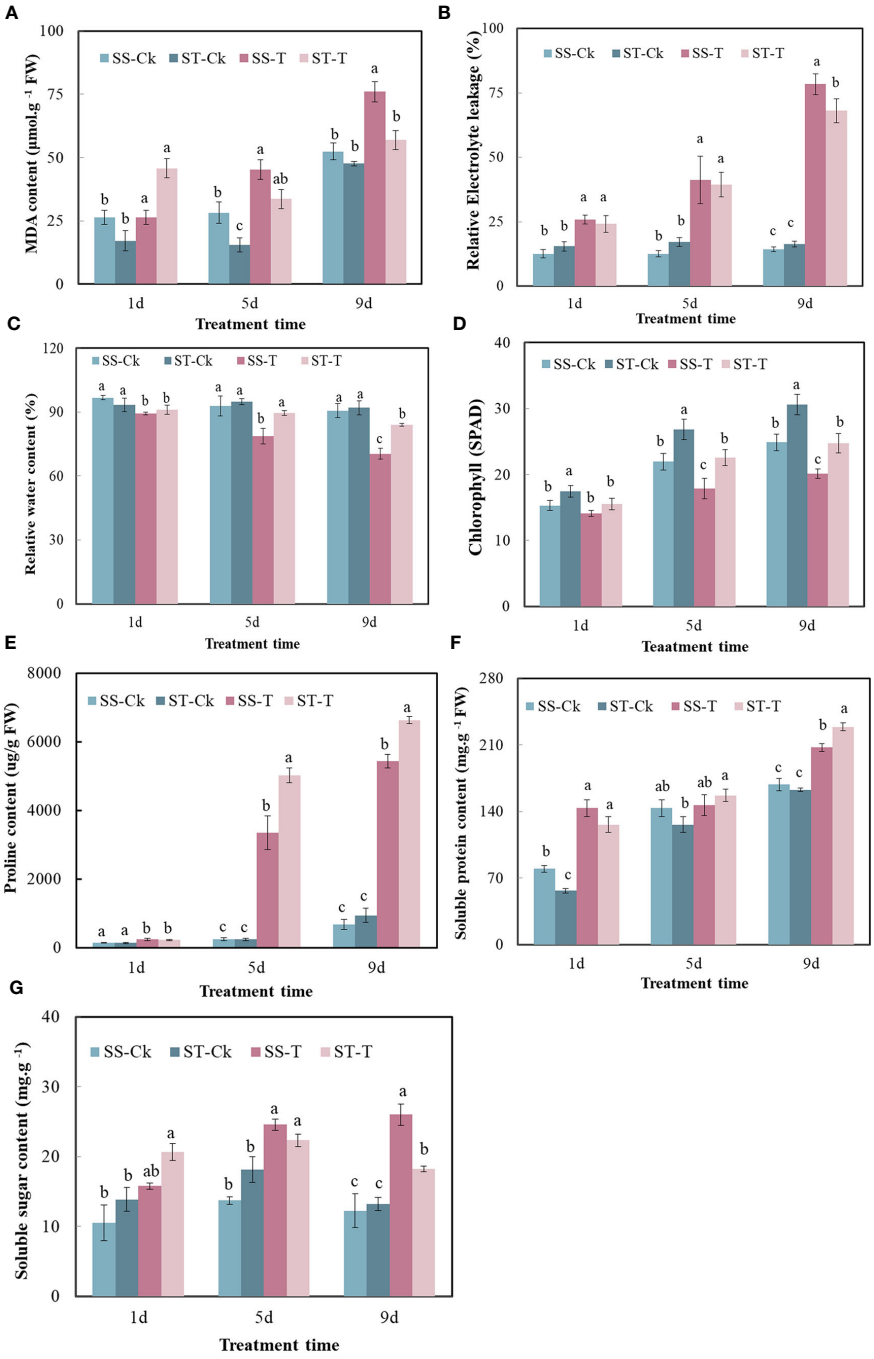

FIGURE 3
Effects of stress on physiological indexes of smooth bromegrass seedlings under different salt stress times. **(A)** MDA content. **(B)** Relative electrolyte leakage. **(C)** Relative water content. **(D)** Chlorophyll content (SPAD). **(E)** Proline content. **(F)** Soluble protein content. **(G)** Soluble sugar content. Significantly different means are shown with different letters, calculated using Tukey's test ($p < 0.05$). ST, salt-tolerant genotype; SS, salt-sensitive genotype; CK, control treatment; T, salt treatment; MDA, malondialdehyde; SPAD, Soil Plant Analysis Development.

Figure 6 and Supplementary Table 10, the top four DEGs in numerical order were 58 in the AP2/ERF-ERF family, 52 in the bHLH family, 44 in the WRKY family, and 34 in MYB-related families. A total of 622 TF-encoding genes were identified from 62 different families in S-0_vs_S-9. The top four were arranged in ascending order of quantity: 54 in the AP2/ERF-ERF family, 49 in the bHLH family, 42 in the MYB-related family, and 42 in the WRKY family. In two varieties, the most represented TFs were AP2/ERF-ERF, and a total of 112 AP2/ERF-ERF-related genes were enriched in these two genotypes.

10.3389/fpls.2023.1313113

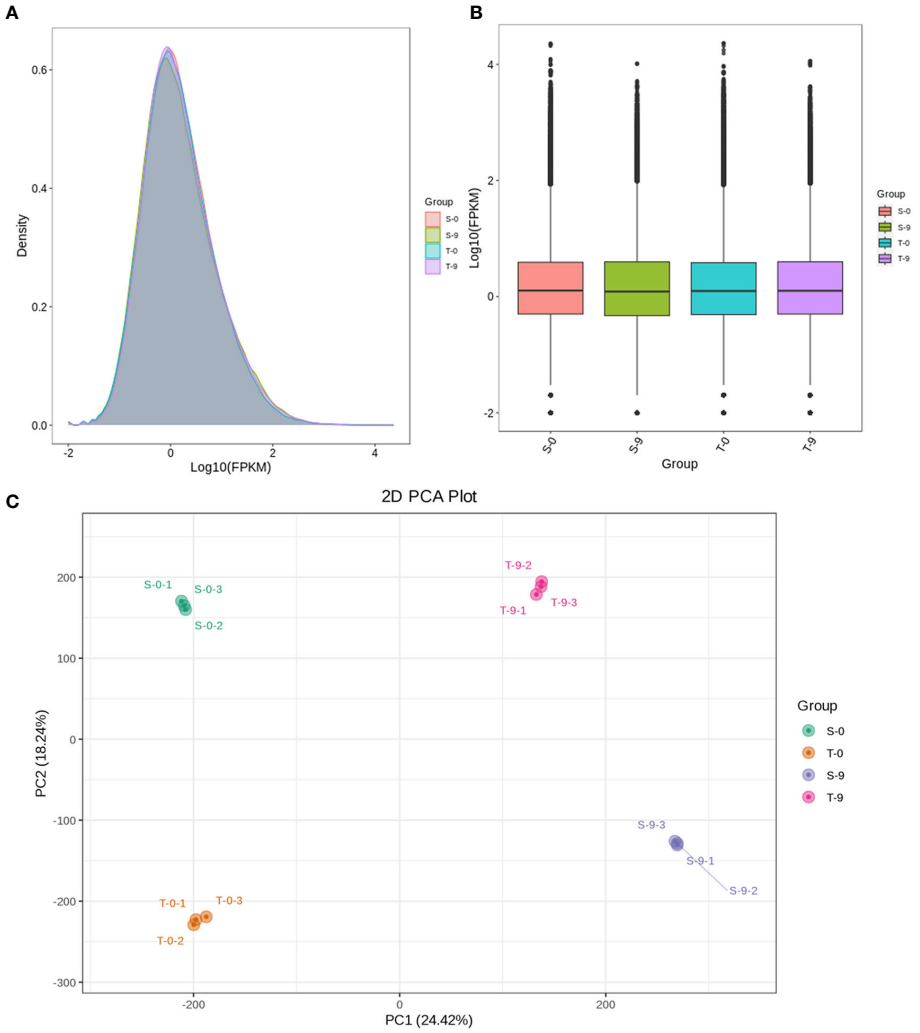

FIGURE 4
Comparison of DEG expression levels of different treatments and PCA with different treatments in smooth bromegrass. **(A)** Density map: the horizontal axis is the log10 (FPKM) value of the gene, and the vertical axis is the distribution density of the gene corresponding to the expression amount. **(B)** FPKM distribution: the middle horizontal line of the box is the median, the upper and lower edges of the box are 75%, and the upper and lower limits are 90%. The external shape is the kernel density estimation. **(C)** PCA. DEG, differentially expressed gene; PCA, principal component analysis.

Functional annotation and enrichment analysis of DEGs

The expression of DEGs in different samples was identified by comparative analysis and enrichment analysis. Using bioinformatics databases such as the GO and KEGG can acquire the most relevant biological pathways and DEGs. In the GO database, DEGs in S-0_vs_S-9 and T-0_vs_T-9 were significantly enriched in "fructosyltransferase activity", "sucrose 1F-fructosyltransferase activity", and "photosystem I" (Figure 7 and Supplementary Table 11). In the comparisons of S-9_vs_T-9, "endochitinase activity" was highly enriched (Figure 7 and Supplementary Table 11). In the KEGG database, enrichment analysis of DEGs indicated that there were 14 common pathways between S-0_vs_S-9 and T-0_vs_T-9, among which "Photosynthesis-antenna proteins" and "Photosynthesis" were the most enriched (Figure 8 and Supplementary Table 12). In addition, in the comparisons of S-9_vs_T-9, the phosphonate and phosphinate pathways were highly enriched. Compared with S-0_vs_S-9, six significant enrichment pathways were uniquely found in T-0_vs_T-9: "plant hormone signal transduction", "MAPK signaling pathway—plant", "Galactose metabolism", "Linoleic acid metabolism", "Cysteine and methionine metabolism", and "Arginine and proline metabolism". The profile of DEGs enriched in the KEGG pathways compared to S-0_vs_T-0 was similar to S-9_vs_T-9. Two common enriched pathways, "plant hormone signal transduction" and "MAPK signaling pathway—plant", were obtained among the three comparisons of T-0_vs_T-9, S-0_vs_T-0, and S-9_vs_T-9.

10.3389/fpls.2023.1313113

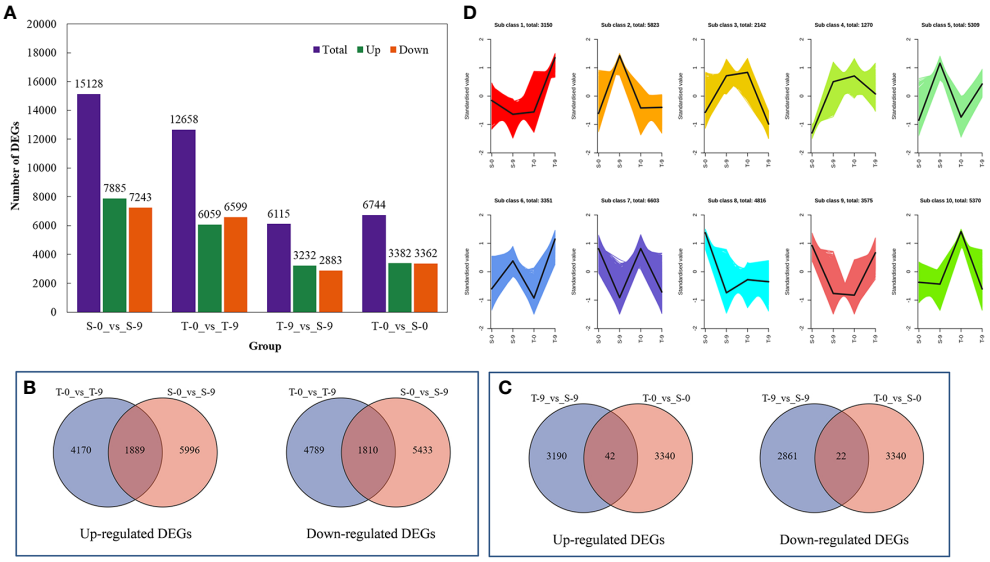

FIGURE 5
The comprehensive description of the transcriptome analysis of the salt stress response of smooth bromegrass. **(A)** Bar charts of up- and downregulated genes in groups. **(B)** Venn diagram of upregulated and downregulated DEGs in the comparison group of T-0_vs_T-9 and S-0_vs_S-9. **(C)** Venn diagram of upregulated and downregulated DEGs in the comparison group of T-9_vs_S-9 and T-0_vs_S-0. **(D)** K-mean cluster analysis. DEGs, differentially expressed genes.

Analysis of DEGs associated with plant hormone signal transduction and MAPK signaling pathway—plant pathways

In order to ensure the reliability and representativeness of the selected DEGs, the filtering standard was defined as p-value < 0.01 and $|\log_2(\text{Fold Change})| \geq 4$. Then, two enriched KEGG pathways, "plant hormone signal transduction" and "MAPK signaling pathway—plant", were further compared.

Under salt stress, several DEGs related to plant hormone signal transduction were found to be enriched in the two genotypes, such as ABA, IAA, and ETH. Most of the DEGs were involved in ABA, auxin, and ETH signaling pathways as shown in Figure 9 and Supplementary Table 13. For the ABA signal, two SNF-related protein kinase 2 (*SnRK2*) were upregulated in the salt-sensitive variety, three genes were upregulated in the salt-tolerance variety, and one *ABF* gene was upregulated and one was downregulated in the salt-sensitive variety. Moreover, two *PYR/PYL* genes were downregulated in the salt-sensitive variety, and one was downregulated in the salt-tolerant variety. For the auxin signal, the four DEGs encoding AUX1 and one encoding TIR1 were upregulated in salt-sensitive variety. One DEG encoding AUX/IAA was downregulated in the salt-sensitive variety and upregulated in the salt-tolerant variety. In addition, six genes encoding auxin response factor (*ARF*) were induced in the salt-tolerance genotype but three in the salt-sensitive variety. For the ETH signal, serine/threonine-protein kinase (*CTR1*) was upregulated in two genotypes, whereas the

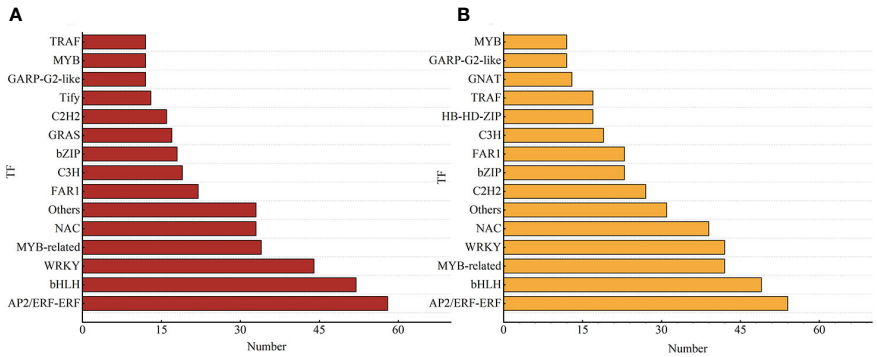

FIGURE 6
Different TFs of smooth bromegrass in response to salt stress. **(A)** T-0_vs_T-9. **(B)** S-0_vs_S-9. The chart shows the different kinds of transcription factors (TFs) on the vertical axis and the quantity of transcription factors on the horizontal axis.

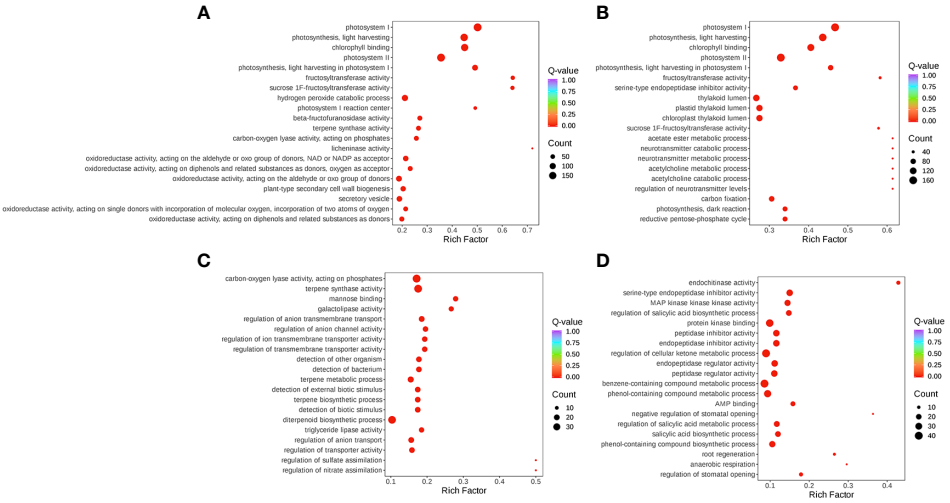

FIGURE 7
GO pathway enrichment plot for gene expression during salt stress. **(A)** T-0_vs_T-9. **(B)** S-0_vs_S-9. **(C)** S-0_vs_T-0. **(D)** S-9_vs_T-9. The size and color of the circle indicate the number of transcripts and the significance value (*p*-value) of the rich factor, respectively. GO, Gene Ontology.

ethylene-responsive transcription factor 1B (*ERF1B*) was downregulated in the salt-sensitive variety under salt stress. Disease resistance and ROS scavenging have been linked to the MAPK pathway. Two DEGs were downregulated and two DEGs were upregulated encoding SnRK2 in the salt-sensitive variety, whereas two DEGs were downregulated and three DEGs were upregulated encoding SnRK2 in the salt-tolerant variety (Figure 10 and Supplementary Table 14). A respiratory burst oxidase gene (*Rboh D*) is downregulated in the salt-sensitive variety, and another was upregulated in the salt-tolerance variety. Five CAT1-related genes were all upregulated in salt-sensitive and salt-tolerance accessions. Interestingly, five MEKK1-related genes were downregulated to enhance salt tolerance.

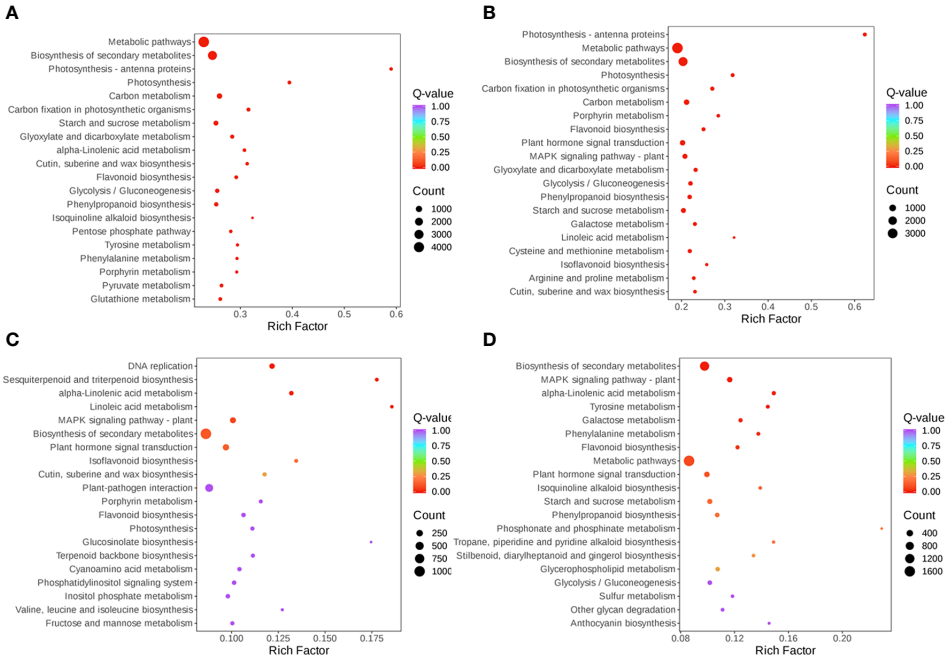

FIGURE 8
Scatterplot of KEGG pathway enrichment for DEGs under salt stress. **(A)** S-0_vs_S-9. **(B)** T-0_vs_T-9. **(C)** S-0_vs_T-0. **(D)** S-9_vs_T-9. The size and color of the circle indicate the number of transcripts and the significance value (*p*-value) of the rich factor, respectively. KEGG, Kyoto Encyclopedia of Genes and Genomes; DEG, differentially expressed gene.

10.3389/fpls.2023.1313113

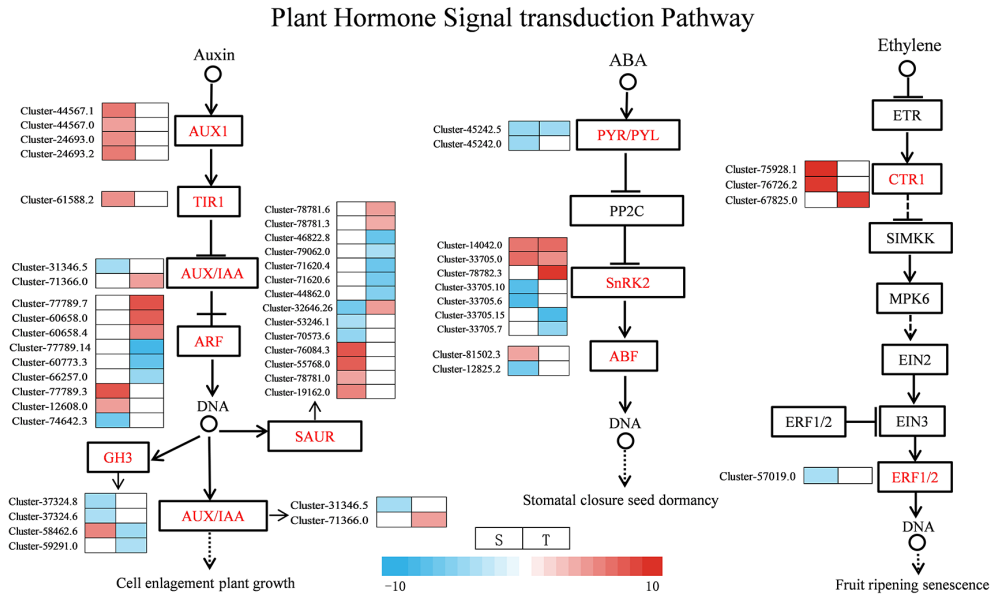

FIGURE 9
Expression map of genes related to plant hormone signaling transduction. S, salt-sensitive genotype; T, salt-tolerant genotype.

Analysis of DEGs associated with photosynthesis and other specific interest pathways

Through DEG annotation analysis, 39 genes that encode photosynthesis-related proteins were identified (Figure 11 and Supplementary Table 15). There were 14 DEGs involving the photosystem II protein of differential varieties that were downregulated under salt stress, while one gene was upregulated in a salt-sensitive genotype, and two were in another. Five genes encoding photosynthetic electron transport were upregulated in the salt-sensitive variety, while two genes were upregulated in the salt-tolerant genotype. In addition, one gene encoding cytochrome b6-f complex iron–sulfur subunit protein (Pet C) was upregulated in the salt-tolerant genotype. In addition, the following were identified: DEGs associated with antioxidant enzymes (*SOD*, *CAT*, *PEX10*, *PEX14*, and *MPV17*), proline synthase (*P5CRs* and *P4HA*), and ABC transporters (*ABCA3*, *ABCB1*, *ABCB10*, *ABCC1*, *ABCG2*, and *PDR5*). They were all regulated with different levels under NaCl stress (Figure 11 and Supplementary Table 16). In our research, there were 10 genes encoding these three types of zinc finger proteins, five of which were upregulated in the salt-tolerant

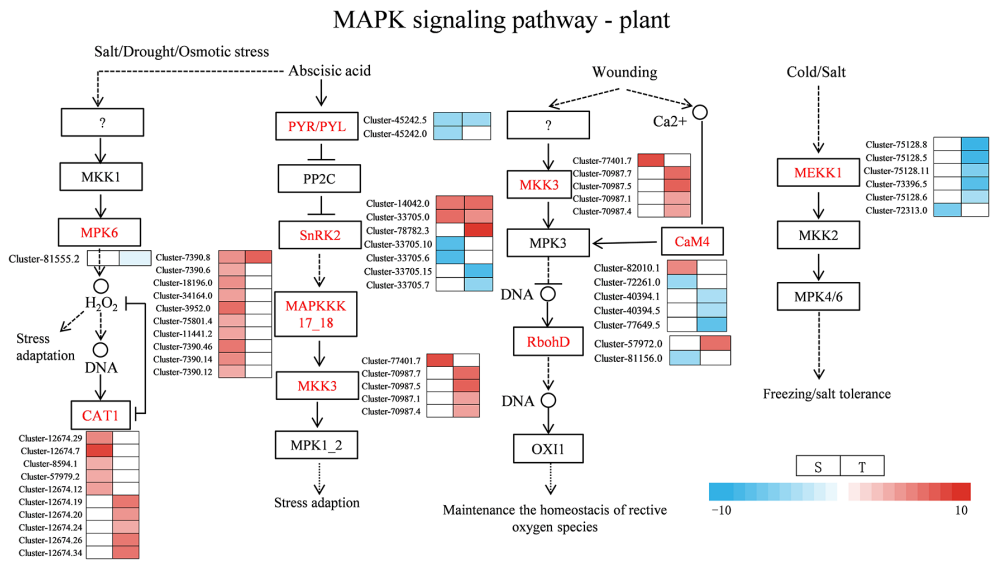

FIGURE 10
Heat map of gene expression related to MAPK signal pathway—plant. S, salt-sensitive genotype; T, salt-tolerant genotype.

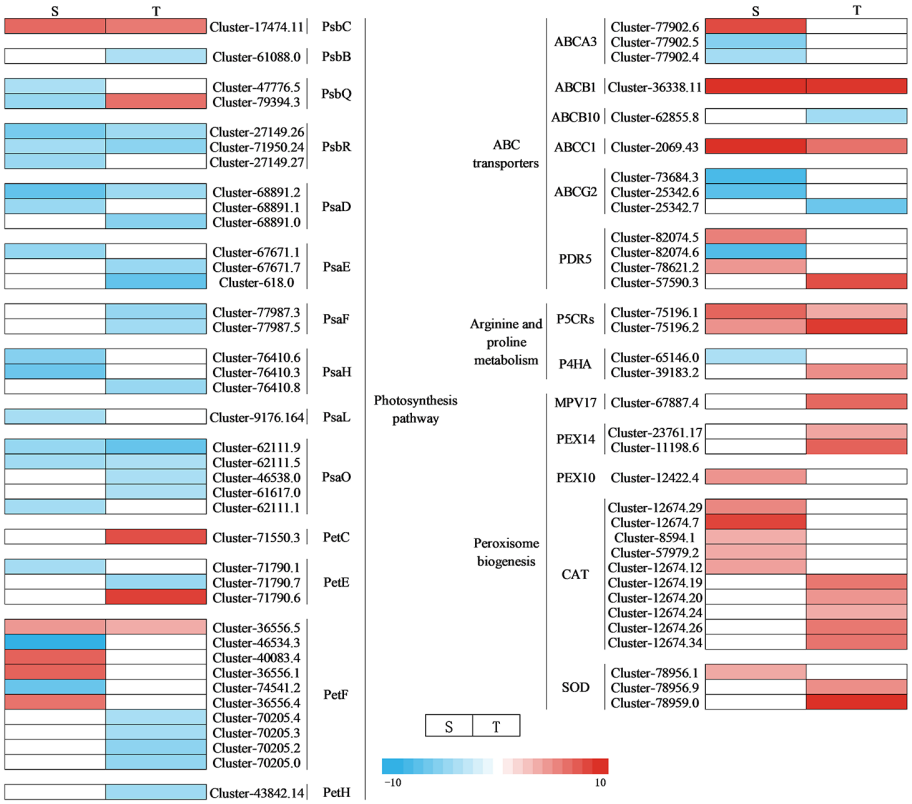

FIGURE 11
Heat map of DEG expression associated with photosynthetic, antioxidant, ROS, and ABC transport pathways under NaCl stress. S, salt-sensitive genotype; T, salt-tolerant genotype; DEG, differentially expressed gene; ROS, reactive oxygen species.

genotype. One gene encoding glutathione was upregulated in the salt-tolerant genotype. Twenty glutathione *S*-transferase, N-terminal domain-related genes were identified to be regulated under salt stress. Three pyridine nucleotide-disulfide oxidoreductase-, one calcium-dependent channel-, one voltage-gated chloride channel-, and two DELLA protein-related genes were identified under salt stress, indicating the key genes responsible for salt tolerance in two genotypes.

RNA-seq data validation with qRT-PCR

The trend of qRT-PCR expression was consistent with the trend of RNA-seq (FPKM) (Supplementary Figure 8A). Meanwhile, qRT-PCR data displayed a strong correlation with the RNA-seq in both SS (R^2 = 0.9185) and ST (R^2 = 0.9511) (Supplementary Figure 8B, C), confirming the high accuracy of the RNA-seq expression pattern. These results confirmed the reproducibility and reliability of RNA-seq data.

Discussion

Salinity can inhibit plant growth, disrupt cell structure, increase mortality rates, and prevent the completion of the life cycle (Sharifi, 2010; Zhang and Shi, 2013). Yin et al. (2022) found that salt stress affected the growth of bermudagrass by increasing relative electrolytic leakage, decreasing chlorophyll content, and increasing Na^+ accumulation. Similarly, the shoot and root growth of seven genotypes of zoysiagrass (*Zoysia* spp.) with different tolerance to salt stress were reduced, and the leaf senescence was accelerated (Hooks et al., 2022). In our research, the growth and development of smooth bromegrass seedlings was retarded due to the reduction of RWC and SPAD and the accretion of MDA content. Meanwhile, compared to the salt-sensitive variety, our results also found that the relative water content and chlorophyll SPAD content of the salt-tolerant variety were higher, the accumulation of relative conductivity and MDA content were lower, and the contents of soluble protein and proline were higher when exposed to salt stress (Figures 3A–F). These results suggested that the salt-tolerant genotype possessed stronger osmotic regulation and photosynthetic regulation ability to cope with adversity.

It is difficult for a single trait to reflect the salt tolerance of a plant, as it is a comprehensive, quantitative, and complex trait influenced by multiple environmental and genetic factors (Al-Ashkar et al., 2020). However, PCA and membership function methods have generally been regarded as relatively reliable methods for evaluating salt tolerance (Baksh et al., 2021). Zhang et al. (2022) conducted a salt tolerance evaluation of 100 oat germplasm samples by measuring 10 parameters including chlorophyll content and root/shoot ratio (fresh and dray water). Furthermore, they

employed PCA and membership functions to comprehensively assess and screen for salt-tolerant and salt-sensitive germplasms (Zhang et al., 2022). There are currently few studies evaluating salt tolerance combined with germinating and seedling stages. In this work, the comparison among 57 accessions suggested that there were large differences among 22 traits under salt stress (Supplementary Table 3). Pearson's correlation coefficients for growing traits among 57 smooth bromegrass accessions suggested that 20 traits could be recognized as evaluation traits for salt tolerance by PCA (Supplementary Figure 2). Q25 and Q46 were classified as the most salt-tolerant accession and salt-sensitive accession to explore their salt response mechanisms by transcriptome profiling.

Transcriptome data from this study showed that stress up- and downregulated a great number of DEGs, resulting in the activation of DEGs to resist stress (Li et al., 2022). The salt-sensitive genotype had 2,470 DEGs more than the salt-tolerant genotype, which may be attributed to an increased demand for the salt-sensitive genotype to activate a large number of genes in response to salt-induced stress (Figure 5A). We also found that the photosynthesis pathway was enriched by KEGG and GO enrichment analyses (Figures 7, 8). Similarly, for the salt-tolerant genotype, plants improved photosynthesis under salt stress due to the related DEGs enriched in the photosynthetic processes (Supplementary Table 15). This finding was consistent with a previous study showing that under salt stress transgenic rice increased the rate of photosynthesis due to the enrichment of DEGs involved in photosynthesis (Boonchai et al., 2018). In contrast, "plant hormone signal transduction" and "MAPK signaling pathway—plant" pathways may correlate with smooth bromegrass resistance to salt stress (Figure 8).

Plant hormones, especially auxins, are important for regulating plant development in coping with salt stress (Li et al., 2022). The auxin-responsive genes can be divided into three main classes of genes: *Aux/IAA*, *GH3*, and *SAUR* (Hagen and Guilfoyle, 2002). Through the transcription of *Aux/IAA* genes, stress pathways interact with the auxin gene regulatory network (Shani et al., 2017). In this research, for the salt-tolerant variety, stress induced the expression of *Aux/IAA* and *ARF3*, which may be the reason for the salt-tolerant genotype, and had the ability to endure the salt stress. ABA is one of the key hormones in plant stress response and regulates intracellular water balance through stomatal closure (Morgil et al., 2019). A previous study showed that when PYR/PYL/RCAR bind to ABA, the complex reduces the inhibitory activity of SNF1-associated kinases (SnRKs) interacting with PP2C and activating its downstream transcription factors (Yang et al., 2019). In the regulation of plant responses to osmotic stress, SnRK2s play a crucial role under stress (Di et al., 2018). The closure of the stomata of tomato is positively regulated by DELLA proteins (Sukiran et al., 2020). Among the DELLA protein, there were two gene expressions in the salt-tolerant genotype (Figure 12). Their effect was strengthened by ABA, which plays an important role in the mediation of resistance (Sukiran et al., 2020). In this study, the salt-tolerant genotype adapted to the stress by accumulating ABA and upregulating DELLA protein under salt stress, leading to the regulation of cells and reduction of water loss to cope with salt stress. These findings were consistent with physiological observations (Figure 3C). The accumulation of ethylene under salt stress plays a crucial role in salt response, and the negative regulation of *CTR1* leads to enhanced salt tolerance (Yu Z., et al., 2020). The ERFs have been identified as the most important downstream regulators of the ETH signaling pathway in the stress response, and the *ERF1B* has been identified as a positive regulator of salt stress tolerance (Gao et al., 2015). In this study, there were two CTR1-related genes upregulated and one ERF1B-related gene downregulated. Therefore, it was inferred that the salt-tolerant genotype might enhance their salt tolerance by regulating key genes involved in ethylene regulation.

Salt stress also increased the accumulation of Na^+ of cells in photosystem II, thereby reducing the photosynthesis of salt-sensitive chickpea (Khan et al., 2016; Kotula et al., 2019). Psb Q and Psb P play an important role in the photosystem in response to abiotic stress (Vani et al., 2001; Adams et al., 2013). In our study, one Psb Q-related gene was upregulated to cope with salt stress. Ferredoxin (Pet F), a catalytic enzyme in the electron transfer chain of the photosynthetic system, actively participates in the process of carbon assimilation (Fukuyama, 2004). In this study, genes related to Pet F were upregulated, suggesting that the sensitive genotype was subjected to damage under salt stress, and the disruption of the electron transfer system increased the production of proteins required to maintain photosynthesis. Studies have indicated that plastocyanin, a copper-containing protein, plays an important part in electron transfer. It actively participates in homeostatic regulation and exhibits antioxidant functions (Zhou et al., 2018). This study observed that the gene encoding cytochrome b6-f complex iron–sulfur subunit protein (*Pet C*) upregulated in the salt-tolerant genotype. This was in line with our finding: salt stress decreased the content of chlorophyll considerably, and the salt-tolerant genotype had significantly more chlorophyll than the salt-sensitive genotype.

MAPK balances the production of reactive oxygen species (Matsuoka et al., 2018). Under stomatal adaptation stress, the MAPK pathway was involved in the ABA signaling pathway, with ROS acting as a second messenger in this pathway (Matsuoka et al., 2018). NaCl may be responsible for inducing *Rboh D* overexpression, as a response element to release H_2O_2 in the respiratory burst, triggering the expression of relevant genes by eliminating H_2O_2 to keep intracellular homeostasis intact (Dietz et al., 2016). It has been discovered that in the fight against salt stress, GATA zinc finger proteins were closely linked to ABA signaling and ROS scavenging (Gupta et al., 2017). In our research, salt stress induced the transcription levels of genes related to Rboh D (Figure 10) and GATA zinc finger protein (Figure 12) in the salt-tolerant genotype to cope with salt stress. Physiological data suggested that stress-induced oxidative damage led to a significant decrease in chlorophyll content and RWC and elevated relative conductivity. Hence, by modulating the levels of osmoprotectants (proline, soluble protein, and sugar), smooth bromegrass activated its antioxidant defense system (Figure 3). The transcriptome data also revealed the molecular level activation of the antioxidant defense system in response to NaCl stress. The KEGG analysis showed enrichment of arginine and proline metabolism pathways and hormone signaling following

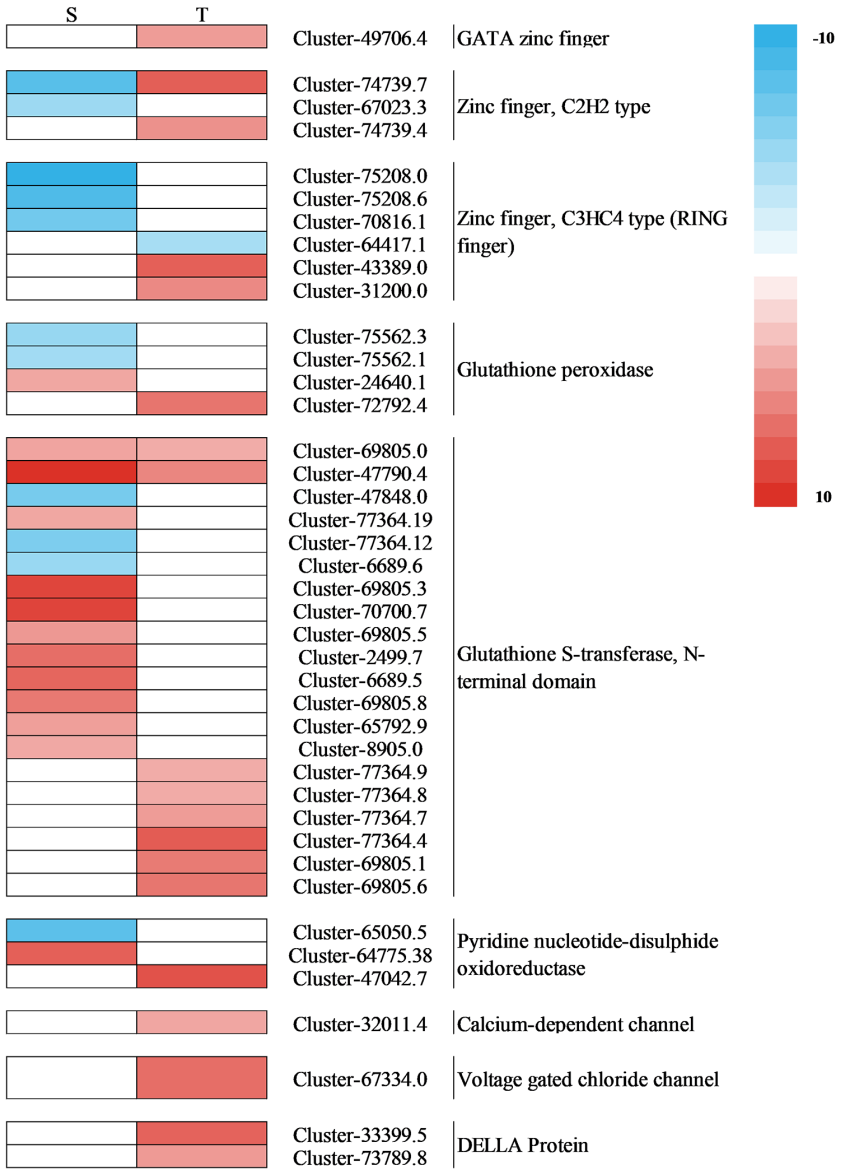

FIGURE 12
Heat map of the expression of the DEGs associated with interested pathways under salt stress. S, salt-sensitive genotype; T, salt-tolerant genotype; DEGs, differentially expressed genes.

NaCl treatment (Figure 8). Furthermore, the number of DEGs associated with antioxidant enzymes (*SOD* and *CAT*) and proline synthesis enzymes (*P5CRs* and *P4HA*) was also modulated under NaCl stress and induced overexpression in salt-tolerant variety (Figure 11). These physiological indicators were correlated with transcriptome data, strongly indicating that these related DEGs play a crucial role in response to stress and subsequent protection against ROS damage.

In plants, the negative electric forces triggered by salt stress could be controlled by sodium entering through ion channels or other membrane transport proteins that increase the movement of sodium across the plasma membrane (Ma et al., 2022). Studies found that ABC transporters play a crucial role in transporting substances across biological membranes in plants, using energy from ATP to move them in and out (Kang et al., 2010; Nguyen et al., 2014). In our research, salt stress induced the transcription levels of genes related to ABC transporters to cope with stress to decrease the passage and transfer of sodium (Figure 11). Meanwhile, we also discovered a gene encoding a calcium-dependent channel and a voltage-gated chloride channel (CLC) gene in the salt-tolerant genotype. The upregulation changes observed in the salt-tolerant genotype showed that these genes were involved in the salt tolerance of smooth bromegrass (Figure 12). Furthermore, we also identified several key genes. *ZFP179*, which encodes a C2H2-type zinc figure protein in rice, has been used to cope with salt stress (Sun et al., 2010), and *BrRZFP1*, which encodes a C3HC4-type protein in *Brassica rapa*, has been used for stress adaptation (Jung et al., 2013). Glutathione (GSH) is a crucial component that is involved in antioxidant defense under stress (Sun et al., 2023). Glutathione *S*-transferases (GSTs) are important and common enzymes that play

an important role in the detoxification of cells under stress. Sharma et al. (2014) showed that *GST* overexpression significantly reduced ROS production and oxidative damage. In addition, the upregulation of pyridine nucleotide-disulfide oxidoreductase genes may display a higher expression of the glutathione reductase (GR) transcripts, resulting in improving GR activity and antioxidant capacity against salt stress (Trivedi et al., 2013; Mudalkar et al., 2017). The results obtained in this research confirmed these findings where four genes involved in these two types of zinc finger proteins, a gene involved in GSH, eight genes involved in GSTs, and a gene involved in pyridine nucleotide-disulfide oxidoreductase were identified to be regulated in salt-tolerant genotype under NaCl stress (Figure 12).

TFs are commonly known to be key genes that respond to stress. TFs, such as AP2/ERF, WRKY, and bHLH, regulate the expression of salt-responsive genes and ultimately determine the level of salt tolerance in the plant (Zhang et al., 2009; Liang et al., 2017). In this study, the AP2/ERF-ERF was the most represented transcription factor among the two genotypes (Figure 6 and Supplementary Table 10). AP2/ERF has been shown to play an important role in the response to biotic and abiotic stresses and is one of the largest families of transcription factors in the plant genome (Zhu et al., 2023). ERFs were important regulators of abiotic stress responses, especially ethylene and salt stress (Li et al., 2020). The WRKY transcription factor is essential for stress resistance (Wang et al., 2023). Yu et al. (2023) showed that *OsWRKY53* could negatively regulate *OsMKK10.2* and *OsHKT1;5* to coordinate the regulation of saline–alkaline stress in rice. In this study, WRKY played a certain role in salt stress. Interestingly, most WRKY transcription factors in the salt-tolerant genotype were downregulated to cope with salt stress, while most were upregulated in the salt-sensitive genotype, suggesting that this might better enhance the resistance of smooth bromegrass.

Conclusion

The salt tolerance and sensitivity of 57 smooth bromegrass genotypes were evaluated during the germination and seedling stages. Among them, Q25 exhibited the highest salt tolerance, while Q46 was identified as the most salt-sensitive variety compared to others. Under salt stress, Q25 not only maintained lower relative conductivity and MDA content ($p < 0.05$) but exhibited substantially better performance than Q46; the contents of leaf RWC, chlorophyll, and proline were also significantly higher than Q46 ($p < 0.05$). A large number of candidate genes have been identified that were associated with salt tolerance in smooth bromegrass. DEGs participated in the phytohormone signaling pathway, transcription factors, modulation of osmoprotectants, photosynthesis, and so on, contributing to salt stress adaptation in smooth bromegrass. This result has provided genetic resources and a theoretical basis for future salt tolerance breeding, as well as provided useful information for understanding the molecular regulations related to salt tolerance in smooth bromegrass.

Data availability statement

The data presented in the study are deposited in the National Center of Biotechnology Information (NCBI) repository, accession number Bioproject PRJNA1017383.

Author contributions

WS: Writing – original draft, Writing – review & editing. XG: Writing – review & editing. HL: Writing – review & editing. SL: Writing – review & editing. JW: Writing – original draft. XW: Writing – original draft. TW: Writing – original draft. YY: Writing – original draft. PH: Writing – original draft. XL: Writing – original draft. BF: Writing – review & editing.

Funding

The author(s) declare financial support was received for the research, authorship, and/or publication of this article. This work was supported by the Ningxia Agricultural Breeding Special Project (2019NYYZ0403).

Conflict of interest

The authors declare that the research was conducted in the absence of any commercial or financial relationships that could be construed as a potential conflict of interest.

Publisher's note

Supplementary material

The Supplementary Material for this article can be found online at: https://www.frontiersin.org/articles/10.3389/fpls.2023.1313113/full#supplementary-material

References

Adams, W. W., Muller, O., Cohu, C. M., and Demmig-Adams, B. (2013). May photoinhibition be a consequence, rather than a cause, of limited plant productivity? *Photosynth. Res.* 117, 31–44. doi: 10.1007/s11120-013-9849-7

Ahmad, S., Kamran, M., Ding, R., Meng, X., Wang, H., Ahmad, I., et al. (2019). Exogenous melatonin confers drought stress by promoting plant growth, photosynthetic capacity and antioxidant defense system of maize seedlings. *Peer J.* 7, e7793. doi: 10.7717/peerj.7793

Al-Ashkar, I., Alderfasi, A., Ben Romdhane, W., Seleiman, M. F., El-Said, R. A., and Al-Doss, A. (2020). Morphological and genetic diversity within salt tolerance detection in eighteen wheat genotypes. *Plants* 9, 287. doi: 10.3390/plants9030287

Albaladejo, I., Egea, I., Morales, B., Flores, F. B., Capel, C., Lozano, R., et al. (2018). Identification of key genes involved in the phenotypic alterations of *res* (*restored cell structure by salinity*) tomato mutant and its recovery induced by salt stress through transcriptomic analysis. *BMC Plant Biol.* 18, 1–19. doi: 10.1186/s12870-018-1436-9

Bailey-Serres, J., Parker, J. E., Ainsworth, E. A., Oldroyd, G. E. D., and Schroeder, J. I. (2019). Genetic strategies for improving crop yields. *Nature* 575, 109–118. doi: 10.1038/s41586-019-1679-0

Baksh, S. K. Y., Donde, R., Kumar, J., Mukherjee, M., Meher, J., Behera, L., et al. (2021). Genetic relationship, population structure analysis and phenomolecular characterization of rice (*Oryza sativa* L.) cultivars for bacterial leaf blight resistance and submergence tolerance using trait specific STS markers. *Physiol. Mol. Biol. Plants* 27, 543–562. doi: 10.1007/s12298-021-00951-1

Bhattarai, S., Biswas, D., Fu, Y., and Biligetu, B. (2020). Morphological, physiological, and genetic responses to salt stress in alfalfa: a review. *Agronomy* 10, 577. doi: 10.3390/agronomy10040577

Boonchai, C., Udomchalothorn, T., Sripinyowanich, S., Comai, L., Buaboocha, T., and Chadchawan, S. (2018). Rice overexpressing *OsNUC1-S* reveals differential gene expression leading to yield loss reduction after salt stress at the booting stage. *Int. J. Mol. Sci.* 19, 3936. doi: 10.3390/ijms19123936

Di, F., Jian, H., Wang, T., Chen, X., Ding, Y., Du, H., et al. (2018). Genome-wide analysis of the *PYL* gene family and identification of *PYL* genes that respond to abiotic stress in *Brassica napus*. *Genes* 9, 156. doi: 10.3390/genes9030156

Dietz, K., Turkan, I., and Krieger-Liszkay, A. (2016). Redox- and reactive oxygen species-dependent signaling into and out of the photosynthesizing chloroplast. *Plant Physiol.* 171, 1541–1550. doi: 10.1104/pp.16.00375

Egea, I., Pineda, B., Ortiz-Atienza, A., Plasencia, F. A., and Drevensek, S. (2018). The S1CBL10 calcineurin b-like protein ensures plant growth under salt stress by regulating Na^+ and Ca^{2+} homeostasis. *Plant Physiol.* 2, 1676–1693. doi: 10.1104/pp.17.01605

Fahad, S., Hussain, S., Matloob, A., Khan, F. A., Khaliq, A., Saud, S., et al. (2015). Phytohormones and plant responses to salinity stress: a review. *Plant Growth Regul.* 75, 391–404. doi: 10.1007/s10725-014-0013-y

Fukuyama, K. (2004). Structure and function of plant-type ferredoxins. *Photosynth. Res.* 81, 289–301. doi: 10.1023/B:PRES.0000036882.19322.0a

Ganie, S. A., Wani, S. H., Henry, R., and Hensel, G. (2021). Improving rice salt tolerance by precision breeding in a new era. *Curr. Opin. Plant Biol.* 60, 101996. doi: 10.1016/j.pbi.2020.101996

Gao, C., Li, P., Song, A., Wang, H., Wang, Y., Ren, L., et al. (2015). Isolation and characterization of six *AP2/ERF* transcription factor genes in *Chrysanthemum nankingense*. *Int. J. Mol. Sci.* 16, 2052–2065. doi: 10.3390/ijms16012052

Gong, Z., Xiong, L., Shi, H., Yang, S., Herrera-Estrella, L. R., Xu, G., et al. (2020). Plant abiotic stress response and nutrient use efficiency. *Sci. China Life Sci.* 63, 635–674. doi: 10.1007/s11427-020-1683-x

Gupta, P., Nutan, K. K., Singla-Pareek, S. L., and Pareek, A. (2017). Abiotic stresses cause differential regulation of alternative splice forms of GATA transcription factor in rice. *Front. Plant Sci.* 8. doi: 10.3389/fpls.2017.01944

Hagen, G., and Guilfoyle, T. (2002). Auxin-responsive gene expression: genes, promoters and regulatory factors. *Plant Mol. Biol.* 49, 373–385. doi: 10.1023/A:1015207114117

Hooks, T., Masabni, J., Ganjegunte, G., Sun, L., Chandra, A., and Niu, G. (2022). Salt tolerance of seven genotypes of zoysiagrass (*zoysia* spp.). *Technol. Horticult.* 2, 1–7. doi: 10.48130/TIH-2022-0008

Jin, T., Sun, Y., Zhao, R., Shan, Z., Gai, J., and Li, Y. (2019). Overexpression of peroxidase gene *GsPRX9* confers salt tolerance in soybean. *Int. J. Mol. Sci.* 20, 3745. doi: 10.3390/ijms20153745

Jung, Y. J., Lee, I. H., Nou, I. S., Lee, K. D., Rashotte, A. M., and Kang, K. K. (2013). *BrRZFP1* a *Brassica rapa* C3HC4-type Ring zinc finger protein involved in cold, salt and dehydration stress. *Plant Biol. (Stuttg)* 15, 274–283. doi: 10.1111/j.1438-8677.2012.00631.x

Kang, J., Hwang, J., Lee, M., Kim, Y., Assmann, S. M., Martinoia, E., et al. (2010). PDR-type ABC transporter mediates cellular uptake of the phytohormone abscisic acid. *Proc. Natl. Acad. Sci.* 107, 2355–2360. doi: 10.1073/pnas.0909222107

Khan, H. A., Siddique, K. H. M., and Colmer, T. D. (2016). Salt sensitivity in chickpea is determined by sodium toxicity. *Planta* 244, 623–637. doi: 10.1007/s00425-016-2533-3

Kotula, L., Clode, P. L., Jimenez, J. D. L. C., and Colmer, T. D. (2019). Salinity tolerance in chickpea is associated with the ability to 'exclude' Na from leaf mesophyll cells. *J. Exp. Bot.* 70, 4991–5002. doi: 10.1093/jxb/erz241

Kumari, P. H., Kumar, S. A., Sivan, P., Katam, R., Suravajhala, P., Rao, K. S., et al. (2017). Overexpression of a plasma membrane bound Na^+/H^+ antiporter-like protein (*SbNHXLP*) confers salt tolerance and improves fruit yield in tomato by maintaining ion homeostasis. *Front. Plant Sci.* 7. doi: 10.3389/fpls.2016.02027

Li, P., Chai, Z., Lin, P., Huang, C., Huang, G., Xu, L., et al. (2020). Genome-wide identification and expression analysis of AP2/ERF transcription factors in sugarcane (*Saccharum spontaneum* L.). *BMC Genomics* 21, 1–17. doi: 10.1186/s12864-020-07076-x

Li, Q., Song, J., Zhou, Y., Chen, Y., Zhang, L., Pang, Y., et al. (2022). Full-length transcriptomics reveals complex molecular mechanism of salt tolerance in *Bromus inermis* L. *Front. Plant Sci.* 13. doi: 10.3389/fpls.2022.917338

Li, S., Wang, Y., Gao, X., Lan, J., and Fu, B. (2022). Comparative physiological and transcriptome analysis reveal the molecular mechanism of melatonin in regulating salt tolerance in alfalfa (*Medicago sativa* L.). *Front. Plant Sci.* 13. doi: 10.3389/fpls.2022.919177

Liang, W., Ma, X., Wan, P., and Liu, L. (2018). Plant salt-tolerance mechanism: a review. *Biochem. Bioph. Res. Co.* 495, 286–291. doi: 10.1016/j.bbrc.2017.11.043

Liang, Q. Y., Wu, Y. H., Wang, K., Bai, Z. Y., Liu, Q. L., Pan, Y. Z., et al. (2017). Chrysanthemum WRKY gene *DgWRKY5* enhances tolerance to salt stress in transgenic chrysanthemum. *Sci. Rep.* 7, 4799. doi: 10.1038/s41598-017-05170-x

Livak, K. J., and Schmittgen, T. D. (2001). Analysis of relative gene expression data using real-time quantitative pcr and the $2^{-\Delta\Delta CTCT}$ method. *Methods* 25, 402–408. doi: 10.1006/meth.2001.1262

Lv, X., Chen, S., and Wang, Y. (2019). Advances in understanding the physiological and molecular responses of sugar beet to salt stress. *Front. Plant Sci.* 10. doi: 10.3389/fpls.2019.01431

Ma, D., Cai, J., Ma, Q., Wang, W., Zhao, L., Li, J., et al. (2022). Comparative time-course transcriptome analysis of two contrasting alfalfa (*Medicago sativa* L.) genotypes reveals tolerance mechanisms to salt stress. *Front. Plant Sci.* 13. doi: 10.3389/fpls.2022.1070846

Matsuoka, D., Soga, K., Yasufuku, T., and Nanmori, T. (2018). Control of plant growth and development by overexpressing *MAP3K17*, an ABA-inducible MAP3K, in *Arabidopsis*. *Plant Biotechnol. Nar.* 35, 171–176. doi: 10.5511/plantbiotechnology.18.0412a

Morgil, H., Tardu, M., Cevahir, G., and Kavakli, I. H. (2019). Comparative RNA-seq analysis of the drought-sensitive lentil (*Lens culinaris*) root and leaf under short- and long-term water deficits. *Funct. Integr. Genomic.* 19, 715–727. doi: 10.1007/s10142-019-00675-2

Mudalkar, S., Sreeharsha, R. V., and Reddy, A. R. (2017). Involvement of glyoxalases and glutathione reductase in conferring abiotic stress tolerance to *Jatropha curcas* L. *Environ. Exp. Bot.* 134, 141–150. doi: 10.1016/j.envexpbot.2016.11.011

Nguyen, V. N. T., Moon, S., and Jung, K. (2014). Genome-wide expression analysis of rice ABC transporter family across spatio-temporal samples and in response to abiotic stresses. *J. Plant Physiol.* 171, 1276–1288. doi: 10.1016/j.jplph.2014.05.006

Shani, E., Salehin, M., Zhang, Y., Sanchez, S. E., Doherty, C., Wang, R., et al. (2017). Plant stress tolerance requires Auxin-sensitive Aux/IAA transcriptional repressors. *Curr. Biol.* 27, 437–444. doi: 10.1016/j.cub.2016.12.016

Sharifi, P. (2010). Evaluation on sixty-eight rice germplasms in cold tolerance at germination stage. *Rice Sci.* 17, 77–81. doi: 10.1016/S1672-6308(08)60107-9

Sharma, R., Sahoo, A., Devendran, R., and Jain, M. (2014). Over-expression of a rice tau class glutathione s-transferase gene improves tolerance to salinity and oxidative stresses in Arabidopsis: e92900. *PloS One* 9, e92900. doi: 10.1371/journal.pone.0092900

Steinhorst, L., and Kudla, J. (2019). How plants perceive salt. *Nature* 572, 318–320. doi: 10.1038/d41586-019-02289-x

Sukiran, N. A., Steel, P. G., and Knight, M. R. (2020). Basal stomatal aperture is regulated by GA-DELLAs in arabidopsis. *J. Plant Physiol.* 250, 153182. doi: 10.1016/j.jplph.2020.153182

Sun, S. J., Guo, S. Q., Yang, X., Bao, Y. M., Tang, H. J., Sun, H., et al. (2010). Functional analysis of a novel Cys2/His2-type zinc finger protein involved in salt tolerance in rice. *J. Exp. Bot.* 61, 2807–2818. doi: 10.1093/jxb/erq120

Sun, K., Mehari, T. G., Fang, H., Han, J., Huo, X., Zhang, J., et al. (2023). Transcriptome, proteome and functional characterization reveals salt stress tolerance mechanisms in upland cotton (*Gossypium hirsutum* L.). *Front. Plant Sci.* 14. doi: 10.3389/fpls.2023.1092616

Trivedi, D. K., Gill, S. S., Yadav, S., and Tuteja, N. (2013). Genome-wide analysis of glutathione reductase (GR) genes from rice and Arabidopsis. *Plant Signal Behav.* 8, e23021. doi: 10.4161/psb.23021

Van Bezouw, R. F. H. M., Janssen, E. M., Ashrafuzzaman, M., Ghahramanzadeh, R., Kilian, B., Graner, A., et al. (2019). Shoot sodium exclusion in salt stressed barley (*Hordeum vulgare* L.) is determined by allele specific increased expression of *HKT1; 5*. *J. Plant Physiol.* 241, 153029. doi: 10.1016/j.jplph.2019.153029

Vani, B., Saradhi, P., and Mohanty, P. (2001). Alteration in chloroplast structure and thylakoid membrane composition due to invivoheat treatment of rice seedlings: correlation with the functional changes. *J. Plant Physiol.* 158, 583–592. doi: 10.1078/0176-1617-00260

Wang, H., Chen, W., Xu, Z., Chen, M., and Yu, D. (2023). Functions of WRKYs in plant growth and development. *Trends Plant Sci.* 28, 630–645. doi: 10.1016/j.tplants.2022.12.012

Wang, Y., and Li, Y. (2013). Land exploitation resulting in soil salinization in a desert-oasis ecotone. *Catena* 100, 50–56. doi: 10.1016/j.catena.2012.08.005

Wang, X., Li, X., Cai, D., Lou, J., Li, D., and Liu, F. (2021). Salinification and salt transports under aeolian processes in potential desertification regions of China. *Sci. Total Environ.* 782, 146832. doi: 10.1016/j.scitotenv.2021.146832

Wang, W., Liu, Y., Duan, H., Yin, X., Cui, Y., Chai, W., et al. (2020). Sshkt1; 1 is coordinated with sssos1 and ssnhx1 to regulate Na^+ homeostasis in *Suaeda salsa* under saline conditions. *Plant Soil* 449, 117–131. doi: 10.1007/s11104-020-04463-x

Wu, W., Zhang, Q., Ervin, E. H., Yang, Z., and Zhang, X. (2017). Physiological mechanism of enhancing salt stress tolerance of perennial ryegrass by 24-epibrassinolide. *Front. Plant Sci.* 8. doi: 10.3389/fpls.2017.01017

Yang, Y., Gao, S., Su, Y., Lin, Z., Guo, J., Li, M., et al. (2019). Transcripts and low nitrogen tolerance: regulatory and metabolic pathways in sugarcane under low nitrogen stress. *Environ. Exp. Bot.* 163, 97–111. doi: 10.1016/j.envexpbot.2019.04.010

Yin, Y. L., Xu, Y. N., Li, X. N., Fan, S. G., Wang, G. Y., Fu, J. M., et al. (2022). Physiological integration between Bermudagrass ramets improves overall salt resistance under heterogeneous salt stress. *Physiol. Plantarum* 174, e13655. doi: 10.1111/ppl.13655

Yu, Z., Duan, X., Luo, L., Dai, S., Ding, Z., and Xia, G. (2020). How plant hormones mediate salt stress responses. *Trends Plant Sci.* 25, 1117–1130. doi: 10.1016/j.tplants.2020.06.008

Yu, S., Wu, J., Wang, M., Shi, W., Xia, G., Jia, J., et al. (2020). Haplotype variations in QTL for salt tolerance in chinese wheat accessions identified by marker-based and pedigree-based kinship analyses. *Crop J.* 8, 1011–1024. doi: 10.1016/j.cj.2020.03.007

Zhang, M., Bai, R., Nan, M., Ren, W., Wang, C., Shabala, S., et al. (2022). Evaluation of salt tolerance of oat cultivars and the mechanism of adaptation to salinity +. *J. Plant Physiol.* 273, 153708. doi: 10.1016/j.jplph.2022.153708

Zhang, G., Chen, M., Li, L., Xu, Z., Chen, X., Guo, J., et al. (2009). Overexpression of the soybean *GmERF3* gene, an AP2/ERF type transcription factor for increased tolerances to salt, drought, and diseases in transgenic tobacco. *J. Exp. Bot.* 60, 3781–3796. doi: 10.1093/jxb/erp214

Zhang, J., and Shi, H. (2013). Physiological and molecular mechanisms of plant salt tolerance. *Photosynth. Res.* 115, 1–22. doi: 10.1007/s11120-013-9813-6

Zhang, L., Sun, Y., Ji, J., Zhao, W., Guo, W., Li, J., et al. (2023). Flavonol synthase gene *MsFLS13* regulates saline-alkali stress tolerance in alfalfa. *Crop J.* 11, 1218–1229. doi: 10.1016/j.cj.2023.05.003

Zhao, Y., Zhang, F., Mickan, B., Wang, D., and Wang, W. (2022). Physiological, proteomic, and metabolomic analysis provide insights into *Bacillus* sp. -Mediated salt tolerance in wheat. *Plant Cell Rep.* 41, 95–118. doi: 10.1007/s00299-021-02788-0

Zhao, C., Zhang, H., Song, C., Zhu, J. K., and Shabala, S. (2020). Mechanisms of plant responses and adaptation to soil salinity. *Innovation (Camb)* 1, 100017. doi: 10.1016/j.xinn.2020.100017

Zhou, X., Wang, F., Ma, Y., Jia, L., Liu, N., Wang, H., et al. (2018). Ectopic expression of SsPETE2, a plastocyanin from *Suaeda salsa*, improves plant tolerance to oxidative stress. *Plant Sci.* 268, 1–10. doi: 10.1016/j.plantsci.2017.12.006

Zhu, J. (2016). Abiotic stress signaling and responses in plants. *Cell* 167, 313–324. doi: 10.1016/j.cell.2016.08.029

Zhu, J., Wei, X., Yin, C., Zhou, H., Yan, J., He, W., et al. (2023). ZmEREB57 regulates OPDA synthesis and enhances salt stress tolerance through two distinct signalling pathways in *Zea mays*. *Plant Cell Environ.* 46, 2867–2883. doi: 10.1111/pce.14644

frontiers | Frontiers in Plant Science

TYPE Original Research
PUBLISHED 09 January 2024
DOI 10.3389/fpls.2023.1296286

OPEN ACCESS

EDITED BY
Zulfiqar Ali Sahito,
Zhejiang University of Technology, China

REVIEWED BY
Sayed Mohammad Mohsin,
Sher-e-Bangla Agricultural University, Bangladesh
Amany H. A. Abeed,
Assiut University, Egypt

*CORRESPONDENCE
Ahmad Rajabi Dehnavi
Rajabi@umk.pl

RECEIVED 18 September 2023
ACCEPTED 19 December 2023
PUBLISHED 09 January 2024

CITATION
Rajabi Dehnavi A, Zahedi M and Piernik A (2024) Understanding salinity stress responses in sorghum: exploring genotype variability and salt tolerance mechanisms.
Front. Plant Sci. 14:1296286.
doi: 10.3389/fpls.2023.1296286

Understanding salinity stress responses in sorghum: exploring genotype variability and salt tolerance mechanisms

Ahmad Rajabi Dehnavi[1,2]*, Morteza Zahedi[2] and Agnieszka Piernik[1]

[1]Department of Geobotany and Landscape Planning, Faculty of Biology and Veterinary Sciences, Nicolaus Copernicus University in Torun, Torun, Poland, [2]Department of Agronomy and Plant Breeding, College of Agriculture, Isfahan University of Technology, Isfahan, Iran

Salinity, a significant abiotic stressor, adversely affects global plant growth. To address this, monitoring genetic diversity within a plant species germplasm for salt tolerance traits is vital. This study investigates the responses of ten sorghum genotypes to varying salt stress levels (control, 60 mM NaCl, and 120 mM NaCl), aiming to assess genetic diversity. Using a randomized complete block design with three replications and a split-plot arrangement, salt treatments were assigned to main plots, and genotypes were placed in sub-plots. Physiological attributes, including photosynthetic rate, stomatal conductance, CO_2 concentration, leaf area index, chlorophyll concentrations, and antioxidant enzyme activity, were measured during the 50% flowering stage. Fresh forage yield was evaluated at the early dough stage, while dry forage yield and sodium/potassium concentrations were determined post-drying. Salinity induced 10–23% and 21–47% reductions in forage fresh yield at 60 mM and 120 mM NaCl, respectively, across sorghum genotypes. Forage dry yield also declined by 11–33% at 60 mM NaCl and 30–58% at 120 mM NaCl. Increased oxidative stress markers, proline, soluble carbohydrates, and antioxidant enzyme activity accompanied salinity. Genotypes exhibited diverse responses, with Payam showing significant chlorophyll and yield reductions at 60 mM NaCl and notable stress indicators at 120 mM NaCl. Pegah and GS4 demonstrated robust osmoregulation. In stress tolerance indices, Sepideh excelled at 60 mM NaCl, while GS4 outperformed at 120 mM NaCl. Pegah demonstrated high tolerance at 120 mM NaCl. Our findings highlight the importance of combating oxidative stress, managing water-related stress, and maintaining ionic homeostasis for sorghum's salt stress resilience. Key indicators like K/Na ratio, MDA, MSI, SOD, and proline effectively differentiate between tolerant and sensitive genotypes, offering valuable insights for sorghum breeding. Salt-tolerant sorghum genotypes exhibit stable photosynthesis, improved stomatal function, and membrane integrity through efficient osmotic regulation and robust antioxidant enzyme activity. This capability enables them to sustain performance, minimizing final product loss. The results suggest cultivating salt-tolerant sorghum in saline areas for increased sustainable production, with Pegah and GS4 emerging as promising candidates for further testing in salt-affected environments to obtain reliable yield data.

KEYWORDS

antioxidant enzymes, osmotic adjustment, photosynthetic pigments, salinity, sorghum genotypes

1 Introduction

The global agricultural landscape is grappling with a pressing issue known as salinity, which characterized by the accumulation of soluble salts in soil and irrigation water. This condition poses a significant challenge with profound implications for food security (Fadl et al., 2023). Approximately 20% of cultivated lands worldwide are affected by salinity, and this problem is particularly acute in arid and semi-arid regions, characterized by high evaporation rates and suboptimal irrigation practices (Mukhopadhyay et al., 2021). Coastal areas, contending with saltwater intrusion, face an added layer of vulnerability (Epanchin-Niell et al., 2023). The escalation of salinity levels over the past decade is the result of a complex interplay of factors, including climate change, excessive water usage, deforestation, industrial activities, and pollution, which highly affected food security and plant production worldwide (Phour and Sindhu, 2023). Salinity adversely impacts crops through osmotic stress, ion toxicity, mineral deficiencies, and various physiological and biochemical impairments (Balasubramaniam et al., 2023). Furthermore, the excessive salt content triggers the generation of reactive oxygen species (ROS) within plant cells. This oxidative stress leads to membrane damage and exacerbates the detrimental impact of salinity on crops (Hasanuzzaman et al., 2021). Additionally, it disrupts soil structure, impeding root penetration, nutrient uptake, and microbial activity, thereby negatively affecting the overall soil ecosystem (Naorem et al., 2023). Ultimately, these multifaceted effects of salinity stress culminate in reduced crop yields in terms of quality and quantity, underscoring the pressing need for strategies to mitigate the adverse consequences of salinity on agriculture.

Monitoring genetic diversity within a plant species germplasm for salt tolerance traits stands out as a crucial approach to mitigating salt stress (Amombo et al., 2022; Kaur et al., 2023). This method helps pinpoint genotypes that exhibit greater sustainability and superior performance compared to their counterparts (Ashraf et al., 2006). It also serves as a foundational strategy for selecting and developing salt-tolerant varieties that can thrive in saline environments, ultimately contributing to improved crop yields and agricultural sustainability. Numerous studies have consistently documented substantial genotypic variation in salt tolerance across various plant species (Manzoor et al., 2023; Sagar et al., 2023; Shams and Khadivi, 2023). It well documented that salt-tolerant plants employ a diverse array of defense mechanisms in response to salinity stress to ensure their survival and promote growth. One critical aspect of this defense strategy is the maintenance of cellular ion balance, particularly the equilibrium between sodium (Na^+) and potassium (K^+), which is essential for the plant viability in saline conditions (Wakeel et al., 2011; Pantha et al., 2023). In addition, plants have developed intricate defense mechanisms to counteract the detrimental impacts of ROS induced by environmental stress, including salinity (Sachdev et al., 2021). This defense system relies on both non-enzymatic antioxidants and antioxidant enzymes working in tandem to neutralize and eliminate ROS accumulation triggered by salt stress (Lamalakshmi Devi et al., 2017). Furthermore, plants accumulate compatible solutes, such as carbohydrates, amino acids, proline, and proteins, as part of their defense strategy (Garcia-Caparros et al., 2021). These solutes play a crucial role in osmotic regulation, ensuring proper water uptake and cell turgor (Sanders and Arndt, 2012). Ultimately this multifaceted defense system enables plants to adapt and thrive in challenging, saline environments.

Sorghum (*Sorghum bicolor* L.) is the fifth most important cereal crop in the world, which plays an important role in feeding the growing world population (Iqbal, 2015). Sorghum is known for its adaptability to various stressors, including salinity. Generally, sorghum is moderately salt-tolerant and considered to tolerate salinity levels up to 70 mM NaCl (Allen et al., 1998). However, the response to salinity stress can vary among different sorghum genotypes.(Shakeri and Emam, 2018; Rajabi Dehnavi et al., 2020). Investigating these genotype-specific responses is vital for sustainable agriculture and food security by enhancing sustainable sorghum production in salt-affected areas (Hossain et al., 2022). In addition, it can aids in understanding the genetic basis of salt tolerance in sorghum and contributes to breeding programs by uncovering genetic traits and markers associated with salt tolerance (Afzal et al., 2023). However, there is limited knowledge regarding the mechanisms involved in salt-tolerant genotypes.

Thus, building upon our prior research on genetic diversity within sorghum plants germplasm for salt tolerance at germination and seedling stages (Rajabi Dehnavi et al., 2020), this study aims to investigate sorghum genotypes under field conditions. The focus is on forage yield under salt stress and the mechanisms involved in salt tolerance. The experimental objectives are to explore how (1) salinity stress impacts the physiological attributes and forage yield of sorghum genotypes, (2) different sorghum genotypes demonstrate variations in their tolerance to salinity, and (3) salt-tolerant sorghum genotypes exhibit efficient defense mechanisms against salt stress.

2 Materials and methods

2.1 Experimental conditions

The research was conducted in the summer of 2021 at the research farm of Isfahan University of Technology, located in the Larek region of Najaf Abad City, Iran. The study area has a semi-arid climate with dry summers and an elevation of 1630 meters above sea level. The average annual temperature is 15.2°C, with the hottest months being July and August and the coldest months being December, January, and February. The highest recorded temperature was 42.5°C, while the lowest was -18.5°C. The average annual rainfall is 150.9 mm, and during the sorghum growing season, the average maximum and minimum temperatures were 34.2°C and 19.5°C, respectively (Supplementary Figure 1).

The soil texture of the farm was classified as loam-clay, with an apparent specific gravity of 1.3 g cm^{-3} and pH of 7.5. Before conducting the experimental treatments, the soil characteristics were assessed at 0 to 50 cm depth in the field experiment (Table 1).

10.3389/fpls.2023.1296286

2.2 Experimental design

This experiment used a split-plot design within a randomized complete block design with three replications. The main factors included three irrigation water salinity levels (control, 60 mM NaCl, and 120 mM NaCl). The sub-factors consisted of ten genotypes (Pegah, Speed feed, Jumbo, Kimia, Sepideh, and Payam, GS4, KGS29, KGS23, and MGS5) obtained from the Seed and Plant Improvement Institute in Karaj, Iran. These sorghum genotypes show great promise in enhancing sustainable sorghum production in arid and saline regions like Iran. Exhibiting high yields, functional stability, and adaptability to challenging environmental stress conditions, these genotypes have become commercially cultivated by sorghum growers in the region. Their successful adoption underscores their recognized value and practical utility in addressing the specific agricultural challenges posed by aridity and salinity in Iran. Seeds were sown during the last week of June 2021. Each main plot measured 30m × 2.5m, with sub-plots of four rows of crops spaced 75 cm apart.

2.3 Irrigation and salinity application

In this investigation, the irrigation system is configured in a drip tape format, utilizing a flow meter to regulate both the volume and frequency of irrigation. Initially, during the first two weeks after planting, the plants in the field received consistent and uniform irrigation, maintaining soil moisture at 40% of the total available water (TAW) discharge in the non-saline control treatment. Following the complete establishment of the plants, saline irrigation water treatments were introduced and persisted until mid-November 2021. Throughout the entire growth phase of the plants, the irrigation strategy adhered to the soil's moisture curve, tailored to its texture, with the objective of achieving a 55% TAW discharge in the non-saline control treatment.

To determine the required water amount for each plot, TAW in the field was calculated in mm using Equation 1 (Allen et al., 1998).

$$\mathbf{TAW} = (\boldsymbol{\theta}_{\mathbf{FC}} - \boldsymbol{\theta}_{\mathbf{PWP}}) \times 10\boldsymbol{\rho}_{\mathbf{b}} \times \mathbf{D}_{\mathbf{rz}} \quad (1)$$

θ_{FC} =moisture percentage of soil water weight in the field capacity

θ_{PWP} =Moisture percentage of soil water weight at permanent wilting point

$\rho_{b=}$ mass of soil volume(g/m^3)

D_{rz} = depth Development plant (cm)

The readily available water (RAW), representing the fraction of TAW easily absorbed by the plant without stress from the root development zone, was calculated using Equation 2 (Allen et al., 1998).

$$\mathbf{RAW} = \mathbf{Total\ available\ water} \times \boldsymbol{\rho} \quad (2)$$

Here, ρ for the sorghum plant was considered as 55% of TAW discharge (Allen et al., 1998). The irrigation level was strategized according to the percentage of maximum allowable depletion, as outlined by Allen et al. (Allen et al., 1998). This approach guaranteed that irrigation took place following the discharge of 55% of TAW in the non-saline control treatment.

To establish the irrigation timing, the humidity and corresponding suction needed to delineate the soil moisture curve were computed using a pressure plate device. The alteration in soil moisture was tracked using a tensiometer, initiating two days post-irrigation and persisting until the subsequent irrigation event.

The determination of the water volume needed for each irrigation level (TVW), aimed at augmenting water content within the root development area (0.5 m), was accomplished using Equation 3 (Allen et al., 1998).

$$\boldsymbol{TVW} = \frac{\mathbf{RAW} \times \mathbf{Plot\ area}}{\mathbf{Irrigation\ efficiency}} \quad (3)$$

In this context, TAW is measured in cubic meters (m^3), the plot area is in square meters (m^2), and f represents the percentage of moisture discharge from the Total Available Water (TAW) set at 55 percent, delineating the irrigation levels in this experiment. Assuming an irrigation efficiency of 70% during the growing season (Allen et al., 1998), the volume of irrigation water for each plot is calculated. Subsequently, the amount of salt required to achieve the desired salinity levels (60 and 120 mM NaCl) is computed in kilograms per liter (kg/l). The precise salinity treatment is executed through the strip irrigation system connected to the reservoir. To avert osmotic shock to plants, the salt for the salinity treatment is gradually introduced into the plant growth medium in three stages. To prevent the accumulation of salt and maintain soil salinity at an approximately constant level, we adhered to the salinity regulation approach outlined in the Food and Agriculture Organization (FAO) guideline (Ayers and Westcot, 1985). This method focuses on leaching salts out of the root zone before they reach the target soil electrical conductivity (EC). In line with this strategy, we calculated the percentage of drainage as the ratio of total irrigation water, taking into consideration the soil textire, the initial EC of the soil, the volume and EC of the irrigation water, and the targeted final EC of the soil. Prior to each irrigation cycle, we conducted a comprehensive assessment of soil salinity up to the depth of root development (50 cm). The measured soil EC from each evaluation served as the initial soil EC for that particular irrigation round.Throughout the salt treatment process, the EC for the 60 mM NaCl treatment and post-experiment was approximately 6.84 dS/m, while for the 120 mM NaCl treatment, it reached around 12.4 dS/m. These values reflect our commitment to controlling and

TABLE 1 Characteristics of the soil used in the field experiment at a depth of 0 to 50 cm.

EC (dS/m)	Total N (%)	K (mg/kg)	P (mg/kg)	Mg (mg/kg)	Fe (mg/kg)	PWP (%)	FC (%)
2.1	0.1	150	19.1	48	8.5	10	23

10.3389/fpls.2023.1296286

maintaining specific salinity levels in the soil throughout the experiment.

2.4 Traits measured at the 50% flowering stage

A destructive sampling method was employed during the 50% flowering phenological stage to assess the desired traits. Sampling took place from late August to mid-September 2021, with the timing customized for the specific genotypes under investigation.

2.4.1 The relative water content

The flag leaf was harvested in the morning and packed in a nylon bag for preservation. Healthy leaf pieces were selected, weighed, and placed in Petri dishes with distilled water for 4 hours at 23°C. After removing excess moisture, the leaves were weighed again to determine accumulated weight. Next, the leaves were dried at 70°C for 48 hours, and their dry weight was measured. RWC was calculated using Equation 4 (Smart and Bingham, 1974) based on these measurements.

$$\mathbf{RWC} = \left(\frac{\mathbf{leaf\ fresh\ weight\ -leaf\ dry\ weight}}{\mathbf{turgid\ leaf\ weight - leaf\ dry\ weight}}\right) \times 100 \quad (4)$$

2.4.2 Concentration of hydrogen peroxide

H_2O_2 concentration was determined following the Velikova et al. method (Velikova et al., 2000). Plant parts were treated with 0.1% trichloroacetic acid, centrifuged at 4000 rpm for 15 minutes (4°C), and mixed with zinc solution, potassium phosphate buffer, and potassium iodide. Absorbance at 390 nm was measured using a spectrophotometer. H_2O_2 concentration was calculated with an extinction coefficient of 0.28 mM^{-1} cm^{-1} and expressed as µmol/g FW.

2.4.3 Malondialdehyde content

To evaluate lipid peroxidation in cell membranes induced by salinity in sorghum plants, the concentration of MDA was quantified following the Davey et al. method (Davey et al., 2005). Plant extract (0.1 **g**) was homogenized with 0.5 ml of 0.1% TCA, centrifuged, and mixed with 20% Trichloroacetic Acid (TCA) and 0.5% Thiobarbituric Acid (TBA). After heating and cooling, the MDA-TBA complex was measured at 532 nm. The MDA content was calculated using an extinction coefficient of 155 $mM^{-1}cm^{-1}$ and expressed as nM MDA/g FW.

2.4.4 Membrane stability index

Fresh leaves (0.1g) were immersed in 10 ml of double distilled water for the analysis. After 30 minutes at 40°C, the electrical conductivity (EC) was measured using an EC meter (C1). Then, the sample was exposed to 100°C for 15 minutes, and the electrical conductivity was measured again (C2). With these values, the MSI was calculated and expressed as % using Equation 5 (Saqib et al., 2011).

$$\boldsymbol{MSI} = \left(1 - \frac{\mathbf{C1}}{\mathbf{C2}}\right) \times 100 \quad (5)$$

2.4.5 Photosynthetic attributes

The photosynthetic rate (Pn), stomatal conductance (Gs), and intercellular CO_2 concentration (Ci) were measured between 9 a.m. and 11 a.m. using a portable photosynthetic system gas analyzer (LI-COR 6400, LI-COR, Lincoln, NE, USA) and expressed as µmol/(m^2·s).

2.4.6 Leaf area index

A destructive method was employed to determine the leaf area (LA), and an electronic leaf area meter (model Winarea-ut-11, made in Iran) was used. The LA was measured in cm^2/plant. Subsequently, the LAI was calculated, representing the LA (on one side only) relative to the land area occupied by the crop.

2.4.7 Photosynthetic pigments content

Chlorophyll concentration was determined using Lichtenthaler and Buschmann method (Lichtenthaler and Buschmann, 2001). Leaves (0.5 g) were crushed with 10 mL of 80% acetone. The mixture was filtered using Whatman paper until the residue became white. The extract was centrifuged at 5000 rpm for 15 minutes. Each test tube was adjusted to a 10 ml volume with 80% acetone. Absorption was measured at 663 nm, 646 nm, and 470 nm (Lichtenthaler and Buschmann, 2001) wavelengths using a spectrophotometer. Equation 6, 7, and 8 were used to calculate chlorophyll a, b, total and leaf carotenoid concentrations in mg/gFW

$$\boldsymbol{Cholorophyll}(a) = \frac{[(\mathbf{12.21} \times \boldsymbol{Abs}\mathbf{663}) - (\mathbf{2.81} \times \boldsymbol{Abs}\mathbf{646}) \times \boldsymbol{mlAseton}]}{\boldsymbol{mgLeaf}} \quad (6)$$

$$\boldsymbol{Cholorophyll}(\boldsymbol{b}) = \frac{[(\mathbf{20.13} \times \boldsymbol{Abs}\mathbf{646}) - (\mathbf{5.03} \times \boldsymbol{Abs}\mathbf{663}) \times \boldsymbol{mlAseton}]}{\boldsymbol{mgLeaf}} \quad (7)$$

$$\frac{\boldsymbol{Carotenoids} = \left(\left[\frac{1000 \times Abs470 - 3.27(Chla) - 104(Chlb)}{227}\right] \times \boldsymbol{mlAseton}\right)}{\boldsymbol{mgLeaf}} \quad (8)$$

In these Equations, 646 Abs, 663 Abs, and 470 Abs absorb at 646, 663, and 470 nm wavelengths, respectively.

2.4.8 Proline content

To determine the proline content (P), the method of Bates et al. was followed (Bates et al., 1973). Plant tissue (0.5g) was ground with 10ml 3% sulfosalicylic acid, and the extract was centrifuged. Two milliliters of the filtered extract were mixed with ninhydrin reagent and glacial acetic acid. After heating and cooling, toluene was added, and the red-colored upper phase containing P was separated. P standards were prepared, and the absorbance was measured at 520 nm using a spectrophotometer, with toluene as the blank.

2.4.9 The content of soluble carbohydrates

To determine the soluble carbohydrate content (Carbo), the method described by Irigoyen et al. was followed (Irigoyen et al., 1992). Leaf tissue (0.5g) was pounded with 5 ml of 95% ethanol to obtain an alcoholic extract. The upper phase was separated, and sediments were washed with 70% ethanol. The combined upper phase was centrifuged, and a portion of the supernatant was transferred to a test tube. Fresh anthrone solution was added, and after heating and cooling, the absorbance was measured at 625 nm using a spectrophotometer. Glucose standard solutions were prepared for a standard curve.

2.4.10 The activity of antioxidant enzymes

To determine the specific activity of antioxidant enzymes, 100 mg of plant tissue was homogenized with 1 ml of extraction buffer (1% polyvinylpyrrolidone and 0.5% Triton X100 in 100 mM potassium phosphate buffer, pH = 7). The transparent supernatant was collected for enzyme activity measurement after centrifugation at 15,000 rpm and 4°C for 20 minutes.

2.4.10.1 The specific activity of catalase enzyme

The specific activity of the enzyme was measured using a modified method based on Alici and Arabaci (Alici and Arabaci, 2016). The assay involved mixing reaction buffer with enzyme extract and monitoring the change in absorbance at 240 nm over two minutes. The volumetric activity of the enzyme was calculated by dividing the enzyme activity by the reaction mixture's volume. The specific activity of the enzyme was determined by dividing the volumetric activity by the protein concentration, measured using the Bradford method (Bradford, 1976).

2.4.10.2 The specific activity of ascorbate peroxidase enzyme

APX activity was determined based on the Nakano and Asada method (Nakano and Asada, 1981), measuring the absorbance decrease at 290 nm. The reaction mixture comprised reaction buffer enzyme extract, and the change in absorbance at 290 nm was monitored over two minutes. The specific activity of APX can be calculated similarly to the CAT enzyme assay, dividing the volumetric activity by the protein concentration in the extract.

2.4.10.3 The specific activity of superoxide dismutase enzyme

SOD enzyme activity was determined using a modified method by Giannopolitis and Ries (Giannopolitis and Ries, 1977). The activity was measured by inhibiting nitro-blue tetrazolium photoreduction at 560 nm. A reaction solution containing enzyme extract and various components was exposed to light for 15 minutes, and the absorption at 560 nm was measured. The specific activity of SOD can be calculated using the same method as the CAT enzyme assay, dividing the volumetric activity by the protein concentration in the extract.

2.5 Measured traits in the pulping stage of the seeds

2.5.1 Quantitative characteristics of sorghum

To measure the total fodder yield, in the middle of November 2021, the fresh and dry yields were determined by harvesting the middle two rows of each plot, excluding two bushes at the beginning and end. Yields were reported as t/ha to indicate productivity.

2.5.2 Concentration of Na^+ and K^+

Samples were dried, ground, and subjected to high-temperature treatment to convert organic material into ashes. The resulting ashes were dissolved in hydrochloric acid, filtered, and adjusted to a final volume. Concentrations of Na^+ and K^+ were measured using a Flame Photometer. A calibration curve was created using standard solutions to correct the data, and the Na^+ and K^+ concentrations were reported as mg/g DW.

2.6 Stress sensitivity index

The SSI of sorghum plants was calculated using Equation 9 (Fischer and Maurer, 1978). This indice provide quantitative measures of salt stress tolerance. A smaller SSI value indicates higher tolerance (Fischer and Maurer, 1978).

$$\mathbf{SSI} = \left(\frac{1 - \frac{\mathbf{Ys}}{\mathbf{Yp}}}{1 - \frac{\bar{Y}\mathbf{s}}{\bar{Y}\mathbf{p}}} \right) \tag{9}$$

In the equation, Ys represents genotype performance in a stressful environment, Yp represents genotype performance in a stress-free environment, $\bar{Y}$ s is the average performance of all genotypes in a stressful environment, and $\bar{Y}$p is the average performance of all genotypes in a stress-free environment.

2.7 Salinity tolerance index

The salinity tolerance index of sorghum plants was calculated using Equation 10 (Fernandez, 1992). This indice offer quantitative assessments of salt stress tolerance, with a higher STI value indicating a higher level of overall tolerance (Fernandez, 1992).

$$\mathbf{STI} = \frac{\mathbf{Yp} \times \mathbf{Ys}}{(\bar{Y}\mathbf{p})^2} \tag{10}$$

Ys represents genotype performance in a stressful environment, Yp represents genotype performance in a stress-free environment, $\bar{Y}$ s is the average performance of all genotypes in a stressful environment, and $\bar{Y}$p is the average performance of all genotypes in a stress-free environment.

2.8 Statistical analysis

Statistical analysis was performed using SAS version 9.4 (SAS Institute Inc., Cary, NC, USA) with two-way ANOVA to assess treatment variances and determine significance ($p \leq 0.05$). *Post-hoc* analysis was conducted using the HSD test. Principal Components Analysis (PCA) was employed to understand the effects and generate a PCA diagram, utilizing Past software version 4.13. Hierarchical agglomerative cluster analysis was employed to illustrate genotype similarity, utilizing percent similarity as the measure of similarity and the unweighted pair group method for constructing the classification tree. Cluster analysis was performed using Past software version 4.13.

3 Results

3.1 Water relations

Evaluating RWC is crucial in understanding water dynamics and adaptive responses to salinity stress. The study demonstrated significant main effects of both salinity and sorghum genotypes, as well as notable interaction effects, particularly concerning Relative Water Content (RWC) (Supplementary Table 2). Salinity exerted a considerable impact on RWC across all sorghum genotypes, leading to a general reduction. Specifically, exposure to 60 mM NaCl resulted in a 14.6% decline in RWC, while 120 mM NaCl induced a more substantial reduction of 31.4% (Table 2). Furthermore, the main effects of genotypes revealed distinct variations in RWC values. Among all sorghum genotypes studied, GS4 and Pegah exhibited the highest RWC values, suggesting a comparatively better ability to maintain water content under salinity stress. In contrast, genotypes Payam and Sepideh displayed the lowest RWC values, indicating a potentially lower capacity to withstand the deleterious effects of salinity on water retention (Table 2). Furthermore, the interaction effects between salinity and genotypes reveal notable variations among the sorghum genotypes. Specifically, at 60 mM NaCl, Kimia demonstrates the most significant decrease in Relative Water Content (RWC) at 19%, while MGS5 exhibits a more moderate reduction at 9%. Moving to higher salinity levels, at 120 mM NaCl, Payam experiences the most substantial reduction in RWC at 46%, while Jumbo shows a comparatively lesser decrease at 16% (Figure 1A). This decline is attributed to osmotic stress and reduced water availability induced by elevated salinity. The distinct responses underscore the critical role of RWC as a discriminating parameter, shedding light on the unique adaptive mechanisms employed by each genotype to address challenges posed by salinity.

3.2 ROS stress indicators

Our study investigated the impact of salt-induced reactive oxygen species (ROS) on cellular membranes, specifically hydrogen peroxide, along with examining membrane integrity (MSI) and damage levels (MDA). Significant main effects of salinity and genotypes, coupled with noteworthy interaction effects, particularly in relation to hydrogen peroxide, MDA, and MSI, were observed (Supplementary Table 2). Overall, salinity induced a reduction in MSI while elevating H_2O_2 and MDA levels across all sorghum genotypes. Specifically, exposure to 60 mM NaCl resulted in a 13.2% decrease in MSI and an increase of 16.9% in H_2O_2 and 34.1% in MDA (Table 2). At 120 mM NaCl, a more pronounced impact was observed, causing a 30.1% decrease in MSI and increases of 42.5% in H_2O_2 and 65.8% in MDA (Table 2). Main effects of genotypes demonstrated significant variability, with GS4 and Pegah exhibiting the highest MSI levels and the lowest H_2O_2 and MDA levels. In contrast, Payam and Sepideh displayed the lowest MSI levels and the highest H_2O_2 and MDA values (Table 2). Salinity and genotype interactions were significant, showing variations in hydrogen peroxide, MDA, and MSI levels. Under 60 mM NaCl, Payam had the highest percentage increase in hydrogen peroxide (33%), while GS4 had the lowest (4%). Sepideh had the highest increase in MDA (51%), while GS4 had the lowest (20%). The most substantial reduction in MSI was in Payam (20%), while Pegah and GS4 showed the most negligible reduction (9%). Under 120 mM NaCl, Sepideh had the highest percentage increase in hydrogen peroxide (57%), with GS4 having the lowest (20%). Payam showed the highest increase in MDA (91%), while Pegah had the lowest (40%) (Figures 1B–D). These findings underscore genotype-specific responses to salinity-induced stress, revealing significant differences in oxidative stress management and membrane stability.

3.3 Photosynthesis attributes

The study underscores the substantial influence of salinity and genotypes on pivotal physiological parameters, including Pn, Gs, Ci, and LAI in sorghum plants. Notably, both main effects and their interaction were found to be statistically significant (Supplementary Table 2). In general, salinity exerted a discernible impact across all sorghum genotypes, leading to reductions in Pn, Gs, and LAI. Specifically, exposure to 60 mM NaCl resulted in a decrease of 17.2% in Pn, 36.6% in Gs, 27.1% in Ci, and 11.1% in LAI (Table 2). The deleterious effects intensified with 120 mM NaCl, causing a further reduction of 36.6% in Pn, 56.4% in Gs, 47.1% in Ci, and 22.0% in LAI (Table 2). Moreover, when scrutinizing the main effects of genotypes, GS4 and Pegah demonstrated the highest values in Pn, Gs, Ci, and LAI, underscoring their relative resilience to salinity stress. Conversely, Payam and Sepideh exhibited the lowest values among all sorghum genotypes, indicating heightened susceptibility (Table 2). However, the interaction effect between salinity and genotypes shows that the responses to salinity stress varied among sorghum genotypes (Figures 2A–C). At a salinity level of 60 mM NaCl, some genotypes exhibited a more modest decline in Pn (e.g., Payam: 25%) and Gs (e.g., GS4: 27%), indicating their relative tolerance to salinity. In contrast, others were more susceptible, with more significant reductions in these parameters (e.g., Kimia: 44% reduction in LAI). At a higher salinity level of 120 mM NaCl, the differences among genotypes became even more apparent, with some genotypes experiencing substantial reductions in Pn (e.g.,

TABLE 2 Mean comparisons for different parameters of ten Sorghum Genotypes under Three levels of Salinity.

Trait	Salt stress (mM NaCl)			Sorghum Genotypes									
	Control	60	120	GS4	Jumbo	Pegah	KGS23	MGS5	Speed feed	Sepideh	Kimia	KGS29	Payam
RWC (%)	85.6 a	73.1 b	58.7 c	78.7 a	77.8 a	78.2 a	75.9 b	74.5 c	70.7 d	66.45 e	67.3 e	70.1 d	64.9 f
Na (mg/g DW)	0.278 c	0.367 b	0.694 a	0.346 f	0.350 f	0.320 g	0.417 e	0.416 e	0.453 d	0.546 b	0.455 d	0.521 c	0.637 a
K (mg/g DW)	8.72 a	6.55 b	4.89 c	7.76 b	7.58 c	8.27 a	7.41 d	5.97 g	6.62 f	5.33 h	6.92 e	5.89 g	5.47 h
K/Na	32.0 a	18.1 b	8.47 c	25.3 ab	24.2 b	27.4 a	20.1 c	16.7 de	18.4 cd	17.8 ef	17.8 d	16.4 de	14.0 f
H_2O_2 (µmol/g FW)	9.75 c	11.4 b	13.9 a	7.42 h	8.64 g	6.33 i	10.0 f	10.8 e	12.9 d	17.2 a	14.7 c	12.7 d	16.2 b
MDA (nM MDA/g FW)	12.3 c	16.5 b	20.4 a	12.0 e	15.4 c	12.2 e	13.9 d	15.9 c	17.8 b	21.0 a	18.7 b	16.0 c	20.9 a
MSI (%)	80.2 a	69.6 b	56.0 c	75.5 a	72.5 c	73.1 b	70.5 e	73.1 b	71.8 d	62.5 h	64.8 g	66.9 f	55.6 i
Pn (µmol m^{-2} s^{-1})	22.1 a	18.3 b	14.0 c	22.5 a	20.3 c	21.8 b	18.7 d	16.6 e	18.7 d	13.8 h	18.8 d	15.5 f	15.0 g
Gs (µmol m^{-2} s^{-1})	131 a	83 b	57 c	102 a	97 b	101 a	85 d	96 b	89 c	84 e	85 de	89 c	76 f
Ci (µmol m^{-2} s^{-1})	70 a	51 b	37 c	57 a	61 a	58 a	56 ab	60 a	43 d	50 bc	45 cd	50 bc	47 cd
LAI	6.49 a	5.77 b	5.06 c	6.90 a	6.61 ab	6.42 b	6.10 c	5.13 f	5.77 d	5.15 f	5.49 de	5.35 ef	4.82 g
Chl a (mg/g FW))	1.78 a	1.36 b	0.99 c	1.58 b	1.48 c	1.66 a	1.43 d	1.43 d	1.37 e	1.06 h	1.27 f	1.29 f	1.18 g
Chl b (mg/g FW)	0.532 a	0.384 b	0.265 c	0.545 a	0.496 b	0.524 a	0.377 e	0.416 d	0.458 c	0.260 h	0.291 g	0.333 f	0.239 h
Chl T (mg/g FW)	2.27 a	1.75 b	1.25 c	2.13 a	1.98 b	2.18 a	1.80 c	1.84 c	1.83 c	1.32 f	1.44 e	1.62 d	1.42 ef
Car (mg/g FW)	0.323 a	0.262 b	0.211 c	0.366 a	0.320 c	0.330 b	0.284 d	0.271 e	0.244 f	0.203 i	0.221 h	0.236 g	0.177 j
P (µmol/g FW)	10.6 c	15.9 b	19.6 a	24.8 a	17.3 c	24.8 a	19.5 b	13.1 e	14.5 d	7.51 i	11.8 f	10.9 g	9.57 h
Carbo (µmol/g FW)	6.72 c	7.84 b	9.76 a	8.06 d	7.69 e	7.11 g	11.0 a	8.57 c	6.41 h	9.49 b	7.72 e	7.27 f	7.71 e
CAT (U/mg protein)	0.398 c	0.695 b	0.778 a	1.02 b	1.00 c	1.12 a	0.707 d	0.566 e	0.495 f	0.296 i	0.321 h	0.422 g	0.280 j
APX (U/mg protein)	1.44 c	2.32 a	1.71 b	2.83 a	2.66 b	2.66 b	2.17 c	1.73 e	2.02 d	0.923 h	1.14 g	1.35 f	0.748 i
SOD (U/mg protein)	2.49 c	3.89 b	4.80 a	5.62 a	5.38 b	5.43 b	4.64 c	4.24 d	2.88 e	2.05 g	2.33 f	2.78 e	1.94 g
FFY (t/ha)	81.1 a	69.3 b	56.1 c	92.5 a	82.6 c	84.8 b	75.2 d	71.1 e	65.9 f	45.3 j	61.0 h	61.8 g	48.1 i
DFY (t/ha)	27.6 a	22.7 b	15.6 c	27.5 a	25.4 b	26.9 a	24.0 c	21.1 d	24.7 bc	13.0 g	19.8 e	21.2 d	16.2 f

RWC, relative leaf water content; Na, sodium content; K, potassium content; K/Na, K to Na ratios in shoot; H_2O_2, hydrogen peroxide concentration; MDA, malondialdehyde concentration; MSI, membrane stability index; Pn, photosynthetic rate; Gs, stomatal conductance; Ci, intercellular CO_2 concentration; LAI, leaf area index; Chl a, chlorophyll a; Chl b, chlorophyll b; Chl T, total chlorophyll; Car, carotenoids; P, proline; Carbo, soluble carbohydrates; CAT, catalase; APX, ascorbate peroxidise; SOD, superoxide dismutase; FFY, fresh fodder yield; and DFY, day fodder yield. Different letters indicate significant differences by HSD at $p<0.05$.

10.3389/fpls.2023.1296286

10.3389/fpls.2023.1296286

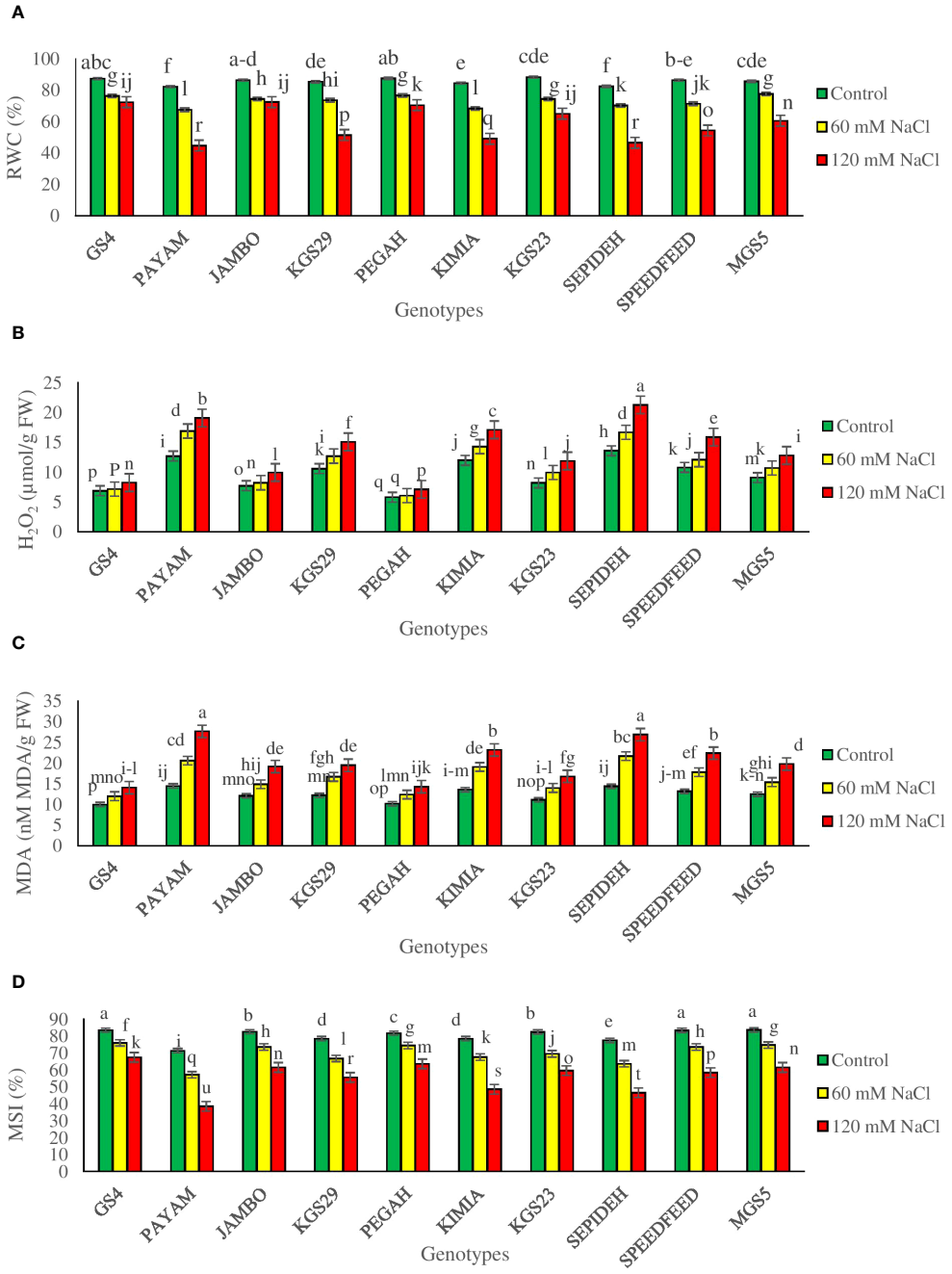

FIGURE 1
(A) relative water content (RWC), **(B)** hydrogen peroxide (H_2O_2), **(C)** malondialdehyde (MDA), and **(D)** membrane stability index (MSI) of sorghum genotypes for interaction of genotypes × salinity (0, 60 and 120 mM NaCl) at fifty percent flowering stage. Different letters indicate significant differences by HSD at $p<0.05$.

Payam: 51%) and Gs (e.g., Payam: 67%), while others exhibited milder declines (e.g., GS4: 30% reduction in Pn).

3.4 Photosynthetic pigments content

The study revealed significant impacts of salinity and genotypes, with notable interactions, on photosynthetic pigment concentrations in sorghum plants (Supplementary Table 2). Salinity notably influenced chlorophyll a (Chl a), chlorophyll b (Chl b), total chlorophyll (Chl T), and carotenoids (Car) across sorghum genotypes. Exposure to 60 mM NaCl resulted in reductions of 23.6% in Chl a, 27.8% in Chl b, 22.9% in Chl T, and 18.9% in Car. At 120 mM NaCl, reductions intensified to 44.3% in Chl a, 50.2% in Chl b, 44.9% in Chl T, and 34.6% in Car (Table 2). Genotypic effects showed GS4 and Pegah with the highest pigment concentrations, while Payam and Sepideh had the lowest values. Noteworthy variations in pigment changes were observed among genotypes. At 60 mM NaCl, Payam displayed the highest chlorophyll reduction (35%), while GS4 had the lowest (13%). Chl b reductions varied, with Payam experiencing the most significant

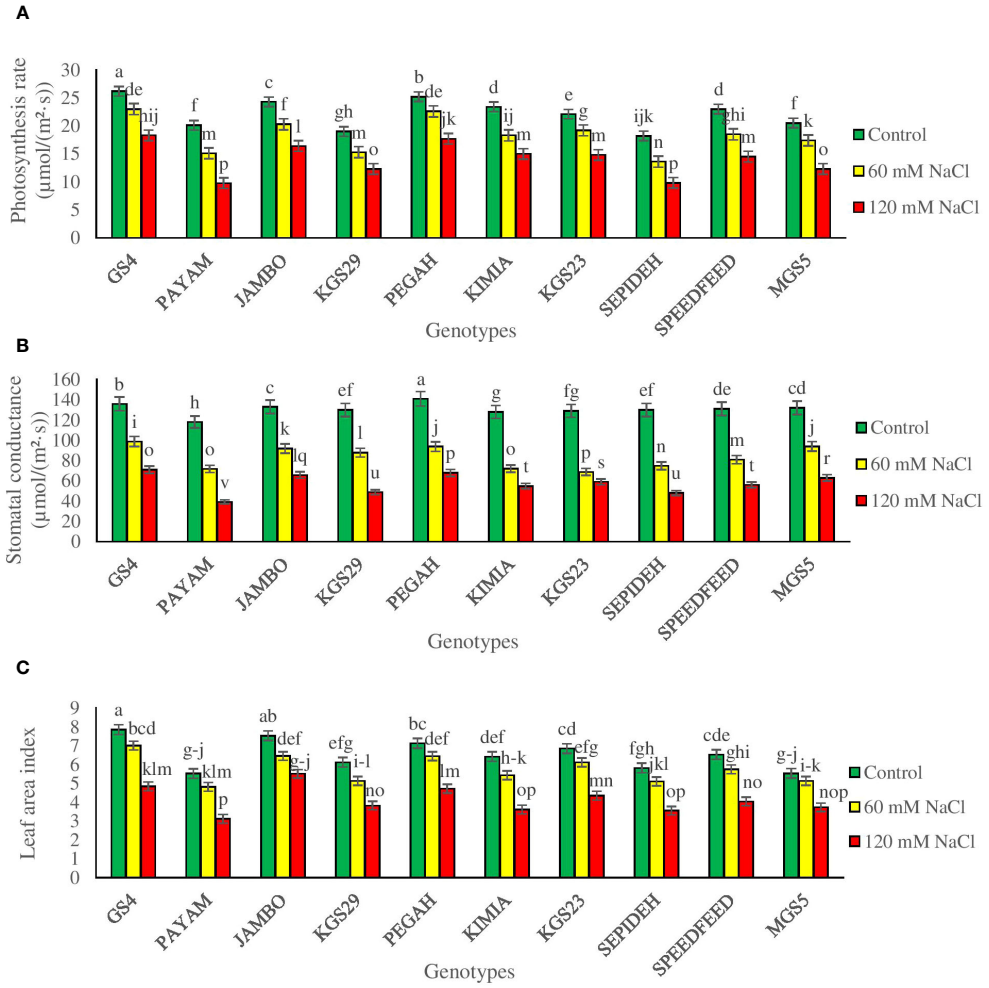

FIGURE 2
(A) photosynthesis rate (Pn), **(B)** stomatal conductance (Gs), and **(C)** leaf area index (LAI) of sorghum genotypes for interaction of genotypes × salinity (0, 60 and 120 mM NaCl) at fifty percent flowering stage. Different letters indicate significant differences by HSD at p<0.05.

decrease (41%) and GS4 the least (17%). Chl T concentration variations were observed, with Payam undergoing the highest reduction (36%) and GS4 the lowest (13%). KGS29 had the most substantial Car reduction (26%), while Jumbo showed the least (9%) at this salinity level. At 120 mM NaCl, Payam showcased the highest chlorophyll reduction (58%), contrasting with GS4's lowest reduction (37%). Chl b reductions varied, with Payam having the highest (62%) and Pegah the lowest (44%). Chl T concentration again saw Payam with the most significant reduction (59%) and Kimia with a relatively lower reduction (35%). Regarding Car, Payam displayed the highest percentage reduction (50%), while Pegah had a less pronounced reduction (29%) (Figures 3A–D). These findings underscore genotype-specific responses to varying salinity levels, emphasizing the intricate interplay between genetic traits and environmental stress.

3.5 Final yield

To assess the impact of salt stress on sorghum genotypes, we measured fresh and dry fodder yields, crucial indicators of crop productivity. The study revealed significant main effects of salinity and genotypes, as well as notable interaction effects, on the final yield (Supplementary Table 2). Salinity significantly influenced both fresh and dry fodder yields in all sorghum genotypes. Exposure to 60 mM NaCl led to a 14.5% reduction in fresh yield and a 17.7% reduction in dry yield, while 120 mM NaCl caused more pronounced decreases of 30.8% in fresh yield and 43.4% in dry yield (Table 2). The main effect of genotypes showed that GS4 and Pegah had the highest values for both fresh and dry fodder yields, while Payam and Sepideh displayed the lowest values (Table 2). This emphasizes the inherent variability among sorghum genotypes in their ability to maintain final yield under salinity stress. The complex interaction between salinity and genotype significantly affected fresh and dry fodder yields. Across various salinity levels, all genotypes experienced consistent reductions in fresh and dry fodder yields. However, the extent of yield reduction varied notably among different sorghum genotypes when subjected to salinity stress. At 60 mM NaCl, the Payam genotype exhibited the most significant decreases in fresh and dry fodder yields, with 23% and 33% reductions, respectively. In contrast, the Pegah genotype showed milder reductions, with declines of 10% in fresh yield and 12% in dry yield.

10.3389/fpls.2023.1296286

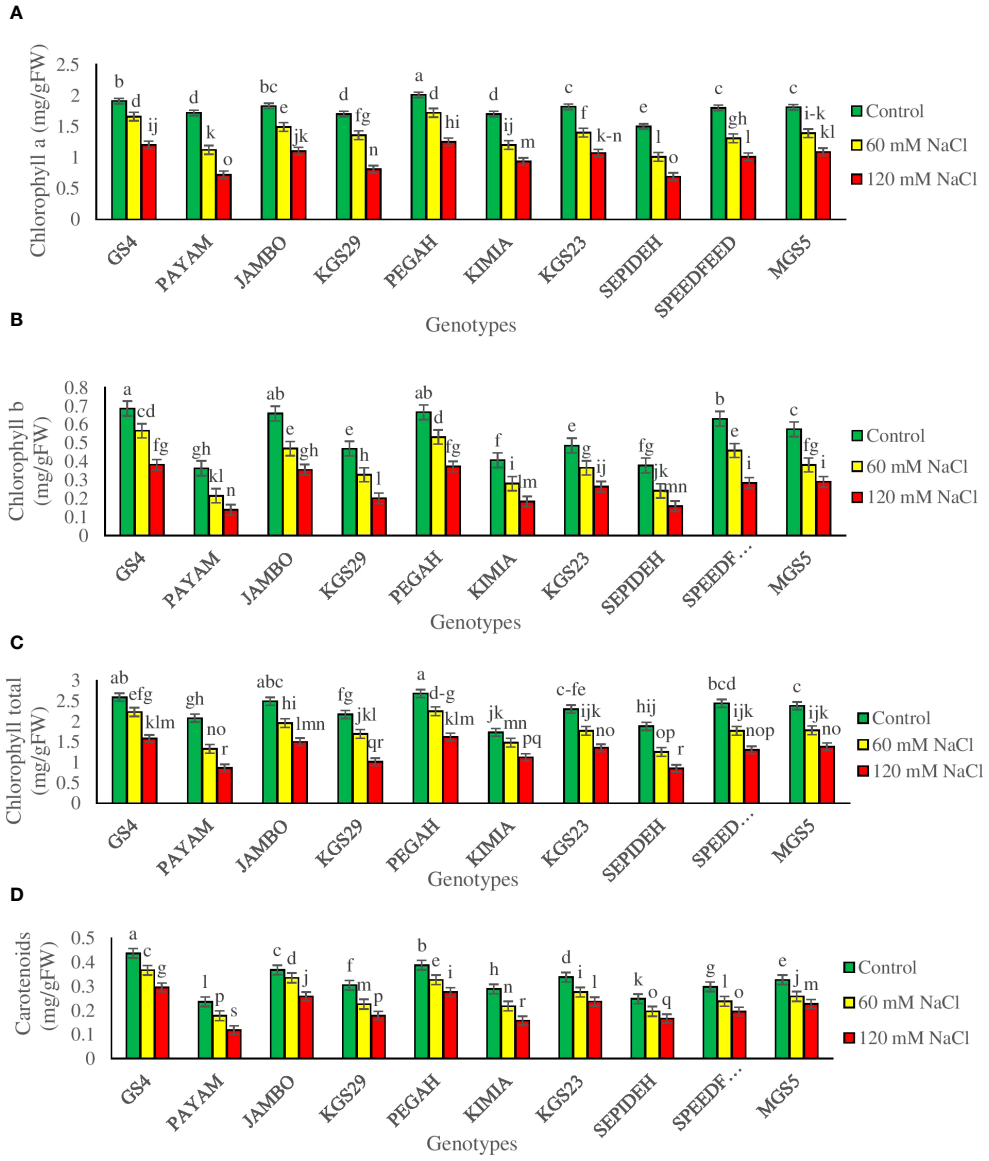

FIGURE 3
The contents of **(A)** chlorophyll a (Chl a), **(B)** chlorophyll b (Chl b), **(C)** total chlorophyll (Chl T) and **(D)** carotenoids (Car) of sorghum genotypes for interaction of genotypes × salinity (0, 60 and 120 mM NaCl) at fifty percent flowering stage. Different letters indicate significant differences by HSD at $p<0.05$.

Upon increasing salinity to 120 mM NaCl, the Payam genotype sustained the highest reductions in both fresh (47%) and dry (58%) fodder yields. Conversely, the Pegah genotype displayed the least reduction, with declines of 21% in fresh yield and 30% in dry yield (Figures 4A, B). These variations in yield responses to salinity stress among sorghum genotypes highlight the intricate interplay between genetic factors and external stressors, providing valuable insights into sorghum's adaptive capabilities in challenging environments.

3.6 Salinity tolerance

In this study, we employed SSI and STI as reliable criteria to assess the salinity tolerance of sorghum genotypes. Dry matter yield was used to calculate these indices (Table 3). At 60 mM NaCl, the Sepideh genotype exhibited the highest SSI value (2.15), whereas the GS4 genotype showed the lowest SSI value (0.605). Conversely, the GS4 genotype displayed the highest STI value (1.25), while the Sepideh genotype had the lowest STI value (0.331). Moving to 120 mM NaCl, the Sepideh genotype demonstrated the highest SSI value (1.57), while the Pegah genotype showed the lowest (0.700). On the other hand, the Pegah genotype exhibited the highest STI value (0.905), and the Sepideh genotype had the lowest STI value (0.169). These findings indicate that the Pegah and GS4 genotypes displayed the highest tolerance to salinity, as evidenced by their lower SSI values and higher STI values. In contrast, the Sepideh and Payam genotypes were the most sensitive among the ten tested genotypes, with higher SSI and lower STI values.

10.3389/fpls.2023.1296286

In addition, based on the classification tree analysis, the genotypes Payam and Sepideh exhibited the highest sensitivity to salt stress, while GS4 and Pegah demonstrated the highest tolerance (Figure 5). Under normal conditions (control), Payam and Sepideh clustered with the other genotypes. However, when exposed to 60 mM NaCl stress, Payam and Sepideh displayed distinct responses and formed a separate cluster (group IV). Notably, the samples grown under 60 mM NaCl were clustered with the genotypes subjected to 120 mM NaCl stress (group IV). Further, Payam and Sepideh under 120 mM NaCl stress constituted a separate cluster (group V), exhibiting the lowest growth parameters. In contrast, GS4 and Pegah clustered with the other genotypes under 60 mM stress and demonstrated better growth performance under 120 mM NaCl stress (cluster III, Figure 5).

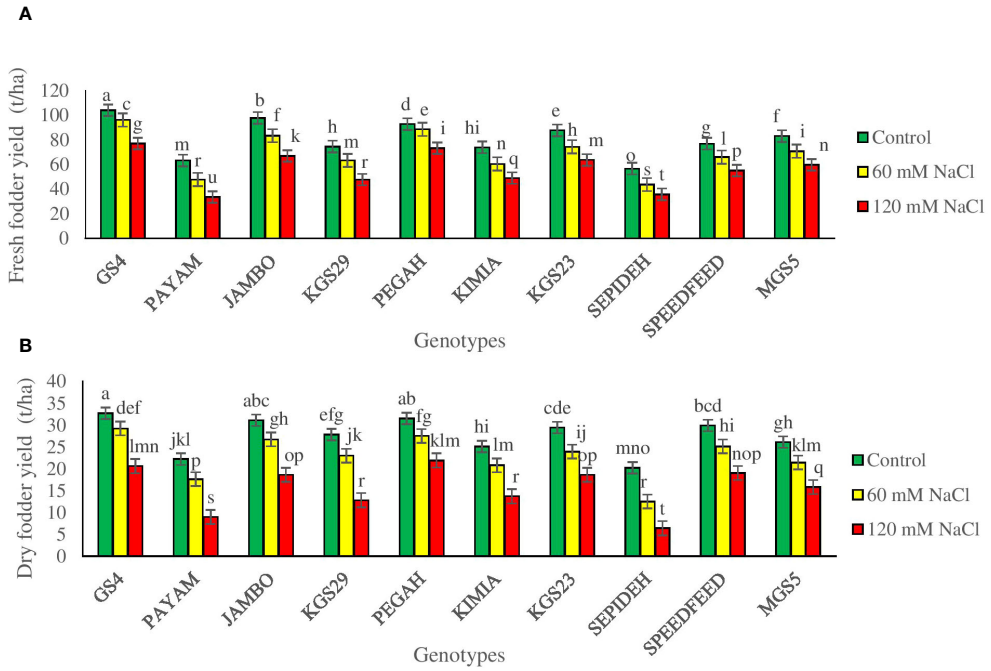

FIGURE 4
(A) Fresh fodder yield (FFY), and **(B)** dry fodder yield (DFY) of sorghum genotypes for the interaction of genotypes × salinity (0, 60, and 120 mM NaCl) at the fifty percent flowering stage. Different letters indicate significant differences by HSD at $p<0.05$.

TABLE 3 SSI and STI indices of sorghum cultivars and genotypes under the influence of different salinity levels.

Index	SSI		STI	
Salinity levels (mM NaCl)	60	120	60	120
Genotypes				
GS4	0.605	0.850	1.25	0.884
PAYAM	1.17	1.37	0.513	0.260
JAMBO	0.799	0.924	1.09	0.759
KGS29	0.975	1.24	0.839	0.467
PEGAH	0.717	0.700	1.14	0.905
KIMIA	0.968	1.04	0.685	0.451
KGS23	1.06	0.844	0.922	0.718
SEPIDEH	2.15	1.57	0.331	0.169
SPEEDFEED	0.907	1.06	0.985	0.746
MGS5	1.02	0.907	0.733	0.541

3.7 Defense mechanisms

3.7.1 Ionic homeostasis

The study emphasized significant main effects of salinity and genotypes, with notable interaction effects, on Na^+ and K^+ concentrations and the K^+/Na^+ ratio (Supplementary Table 2). Salinity consistently reduced K^+ concentrations and the K^+/Na^+ ratio while increasing Na^+ levels across sorghum genotypes. Exposure to 60 mM NaCl resulted in a 24.8% decrease in K^+, a 43.4% reduction in the K^+/Na^+ ratio, and a 32% increase in Na+ (Table 2). At 120 mM NaCl, these effects intensified, causing a 30.8% decrease in K^+, a 43.9% reduction in the K^+/Na^+ ratio, and a substantial 149% increase in Na^+ (Table 2). Examining the main effect of genotypes, GS4 and Pegah had the highest K^+ concentrations and K^+/Na^+ ratio while having the lowest Na^+ levels. Conversely, genotypes Payam and Sepideh displayed the lowest K^+ concentrations and K^+/Na^+ ratio, with the highest Na^+ values. The interaction effect highlighted dynamic responses to salinity stress concerning Na^+ and K^+ concentrations and the K^+/Na^+ ratio. Specifically, the Payam genotype exhibited the most substantial surge in Na content at 60 mM NaCl (69%), while the GS4 genotype showed the least pronounced elevation (8%). At 120 mM NaCl, Payam and Pegah showcased the highest and lowest increments in Na^+ content (283% and 45%, respectively), with similar trends observed in K^+ reduction and the K^+/Na^+ ratio (Figures 6A–C). These findings underscore the genotype-specific nature of responses to salinity stress.

3.7.2 Osmolytes

The study revealed significant main effects of salinity and genotypes on P accumulation and Carbo levels. Salinity consistently increased P and Carbo concentrations across sorghum genotypes (Supplementary Table 2). Exposure to 60 mM NaCl resulted in a 50.0% increase in P and a 16.7% rise in Carbo, while 120 mM NaCl intensified these effects, causing an 84.9% increase in P and a 45.2% rise in Carbo (Table 2). Analyzing the main effect of genotypes showed that GS4 and Pegah had the highest P accumulation and Carbo levels, while Payam and Sepideh exhibited the lowest values for both P accumulation and Carbo levels (Table 2). The investigation revealed a significant interaction between salinity levels and genotypic responses, affecting P accumulation and Carbo levels (Supplementary Table 2). As salinity concentrations increased, a consistent trend emerged across all genotypes, marked by increased P and Carbo concentrations. However, the extent of this increase varied distinctly among genotypes. At 60 mM NaCl, Pegah and GS4 genotypes exhibited notable 71% and 70% increases in P concentration, respectively. In contrast, the Payam genotype showed a more modest 33% increment, and the Sepideh genotype had an 18% elevation in P levels. With 120 mM NaCl exposure, Pegah experienced a substantial 92% rise in P concentration, while GS4 recorded a marked increase of 120%. The Payam genotype demonstrated a 63% increment, and the Sepideh genotype exhibited a 51% elevation in P concentration (Figure 7A). Regarding Carbo, at 60 mM NaCl, Pegah and GS4 genotypes registered 24% and 21% increases, respectively. Under 120 mM NaCl, Pegah demonstrated a heightened increase of 37%, while GS4 showed a substantial 40% rise (Figure 7B). The Payam genotype displayed a 58% increment, and the Sepideh genotype revealed a 49% elevation in Carbo concentration. Notably, Pegah and GS4 genotypes exhibited robust osmoregulation mechanisms, while the Payam and Sepideh genotypes displayed comparatively more restrained responses.

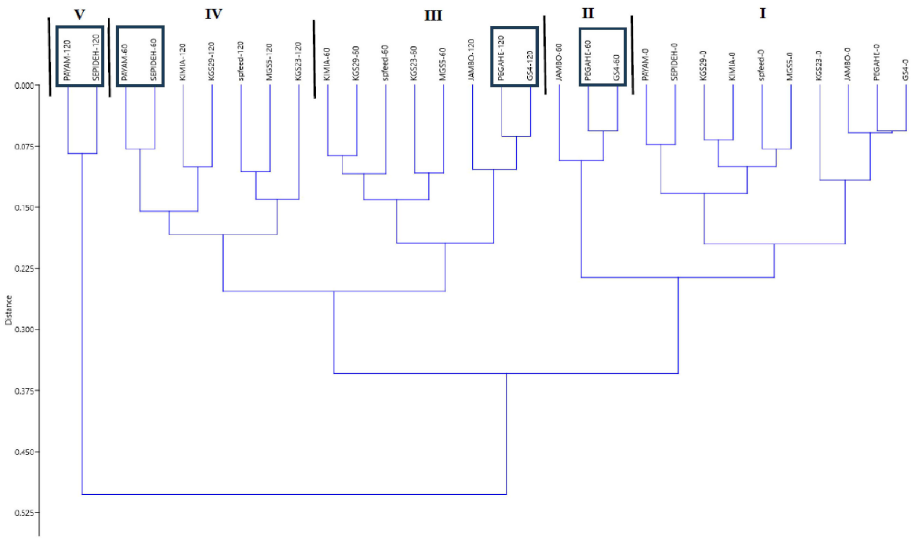

FIGURE 5
The outcomes of the hierarchical agglomerative cluster analysis, considering all traits across the three salt treatments. Clusters I–V are formed based on the similarity observed in all parameters. The samples exhibiting the highest sensitivity to salt stress within each cluster are highlighted within a frame. PEGAH-0 (genotype)–salinity level (mM NaCl).

10.3389/fpls.2023.1296286

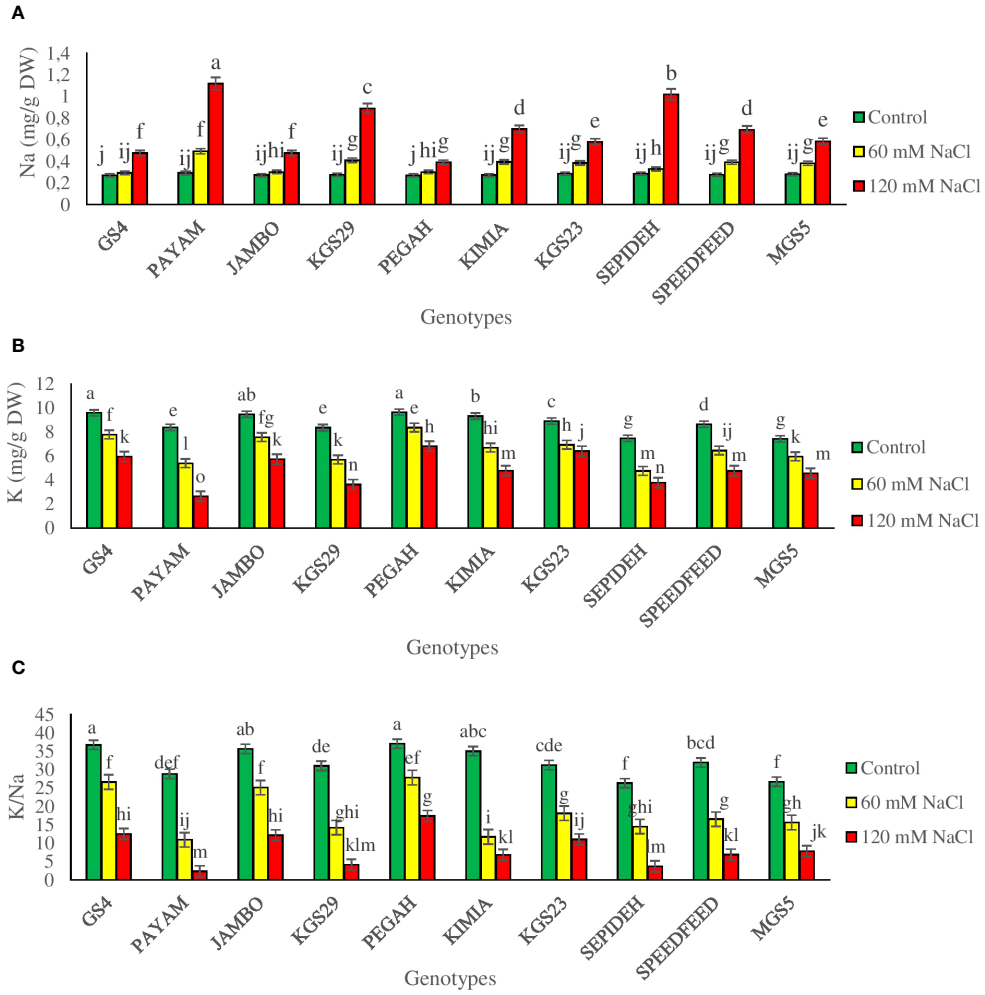

FIGURE 6
(A) sodium concentration (Na), **(B)** potassium concentration (K) and **(C)** potassium to sodium ratio (K/Na) of sorghum genotypes for interaction of genotypes × salinity (0, 60 and 120 mM NaCl) at fifty percent flowering stage. Different letters indicate significant differences by HSD at $p<0.05$.

3.7.3 Antioxidant enzymes activities

The investigation unveiled significant main effects of both salinity and genotypes on antioxidant enzyme activities (Supplementary Table 2). Salinity consistently led to increased catalase (CAT), superoxide dismutase (SOD), and ascorbate peroxidase (APX) activities across all sorghum genotypes. Exposure to 60 mM NaCl resulted in a 74.6% increase in CAT, a 56.2% rise in SOD, and a 61.1% elevation in APX (Table 2). A higher salinity level of 120 mM NaCl intensified these effects, causing a 95.4% increase in CAT, a 92.7% rise in SOD, and a more modest 18.7% increase in APX, which was lower than the lower salt level (Table 2). Analyzing the main effect of genotypes revealed that among all sorghum genotypes, GS4 and Pegah showcased the highest values for CAT, SOD, and APX activities. In contrast, genotypes Payam and Sepideh exhibited the lowest activities for these antioxidant enzymes. These findings highlight the inherent variability among sorghum genotypes in their ability to modulate antioxidant defense mechanisms in response to salinity stress. We also observed a significant interplay between salinity levels and genotypic responses, profoundly impacting the activities of antioxidant enzymes CAT, APX, and SOD (Table 3). Under moderate salinity conditions, all examined genotypes show heightened activities of these enzymes. However, as stress levels escalate, distinct response patterns surface across genotypes (Figure 8). CAT activity varies considerably among genotypes under varying salinity conditions. The Pegah genotype exhibits a marked surge in CAT activity (110%), in contrast to the Sepideh genotype, which shows a modest increment (39%). At the salinity level of 120 mM NaCl, CAT activity responses diverge. Notably, the Pegah genotype displays the most substantial increase (216%), while the Payam genotype demonstrates the most notable reduction (41%) (Figure 8A). APX activity also exhibits significant fluctuations among genotypes. The Pegah genotype showcases a substantial upsurge (98%), while the Payam genotype exhibits a modest increment (5%). At the same salinity level, APX activity varies among genotypes, with Pegah displaying the highest percentage increment (55%) and Payam showing the most considerable decline (50%) (Figure 8B). SOD activity uniformly increases across all genotypes at the salinity level of 120 mM, with notable variations in the magnitude of the increase. The GS4

10.3389/fpls.2023.1296286

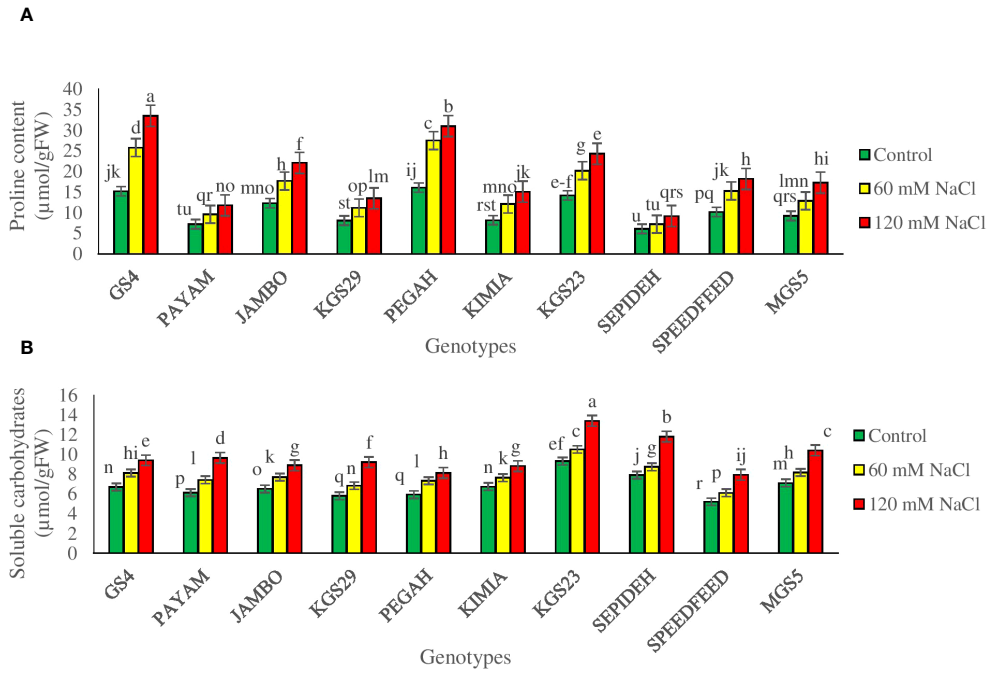

FIGURE 7
The contents of **(A)** proline (P) and **(B)** soluble carbohydrates (Carbo) of sorghum genotypes for the interaction of genotypes × salinity (0, 60, and 120 mM NaCl) at the fifty percent flowering stage. Different letters indicate significant differences by HSD at $p<0.05$.

genotype depicts the highest percentage rise (112%), while the Kimia genotype displays a relatively more modest increment (51%) (Figure 8C). These dynamics underscore the intricate genotypic responses to salinity stress and the potential implications of heightened antioxidant enzyme activities in augmenting salinity tolerance. Significantly, SOD consistently increases, demonstrating enhanced resilience and efficacy under severe stress conditions, while CAT and APX display heightened sensitivity to variations in stress intensity.

3.8 Principal components analysis

Principal Components Analysis (PCA) was employed to enhance the graphical representation of distinct salt-genotype responses, as illustrated in Figure 9. The first principal component (PC1) distinctly accounted for 69.6% of the variance, delineating a salinity gradient across experimental conditions, ranging from right (0 mM NaCl treatments) to left (120 mM NaCl treatments). The second principal component (PC2), governing genotype responses, contributed to 20.2% of the total variance, revealing a hierarchical arrangement of genotypes from lower to upper positions on the diagram. Particularly noteworthy is the spatial distribution of sorghum genotypes under non-saline treatment, predominantly located on the lower right. At the same time, those exposed to 60 mM NaCl exhibited a dual distribution on the upper right and lower left. Genotypes treated with 120 mM NaCl primarily clustered on the left side of the scatter plot. The spatial arrangement on the PCA plot unveiled a correlation between treatments favoring higher growth on the right side and inferior performance under saline conditions on the left. Correlation analysis demonstrated that PC1 correlated positively with various physiological parameters, including K^+, K^+/Na^+, RWC, MSI, Pn, LAI, Chl a, b, T, Car, FFY, FDY, APX, and Gs, while exhibiting negative correlations with H_2O_2, MDA, and Na^+. In contrast, PC2 exhibited positive correlations with P, CAT, APX, and SOD. Furthermore, a positive association was observed between FFY and FDY and the activities of antioxidant enzymes, photosynthetic attributes, pigments, proline content, K^+, and K^+/Na^+, while negative correlations were identified with Na^+, MDA, and H_2O_2. These intricate relationships underscore the multifaceted interplay between salinity levels, sorghum genotypes, and their physiological responses. Notably, genotypes GS4 and Pegah demonstrated superior performance across all salt levels, while genotypes Payam and Sepideh exhibited suboptimal performance under all salinity conditions.

4 Discussion

This study delved into the responses of sorghum plants to salinity, focusing on genotype diversity and the mechanisms behind salt tolerance. In response to salinity, we consistently observed reductions in various crucial parameters such as RWC, K^+ content, K^+/Na^+, MSI, Pn, Gs, Ci, LAI, Chl a, Chl b, Chl T and Car, fresh fodder yield, and dry fodder yield in all sorghum genotypes. Conversely, there were increases in Na^+ content, H_2O_2 concentration, MDA concentration, P, Carbo, CAT, APX, and SOD across all sorghum genotypes. These findings corroborate existing research, highlighting how salinity impacts physiological,

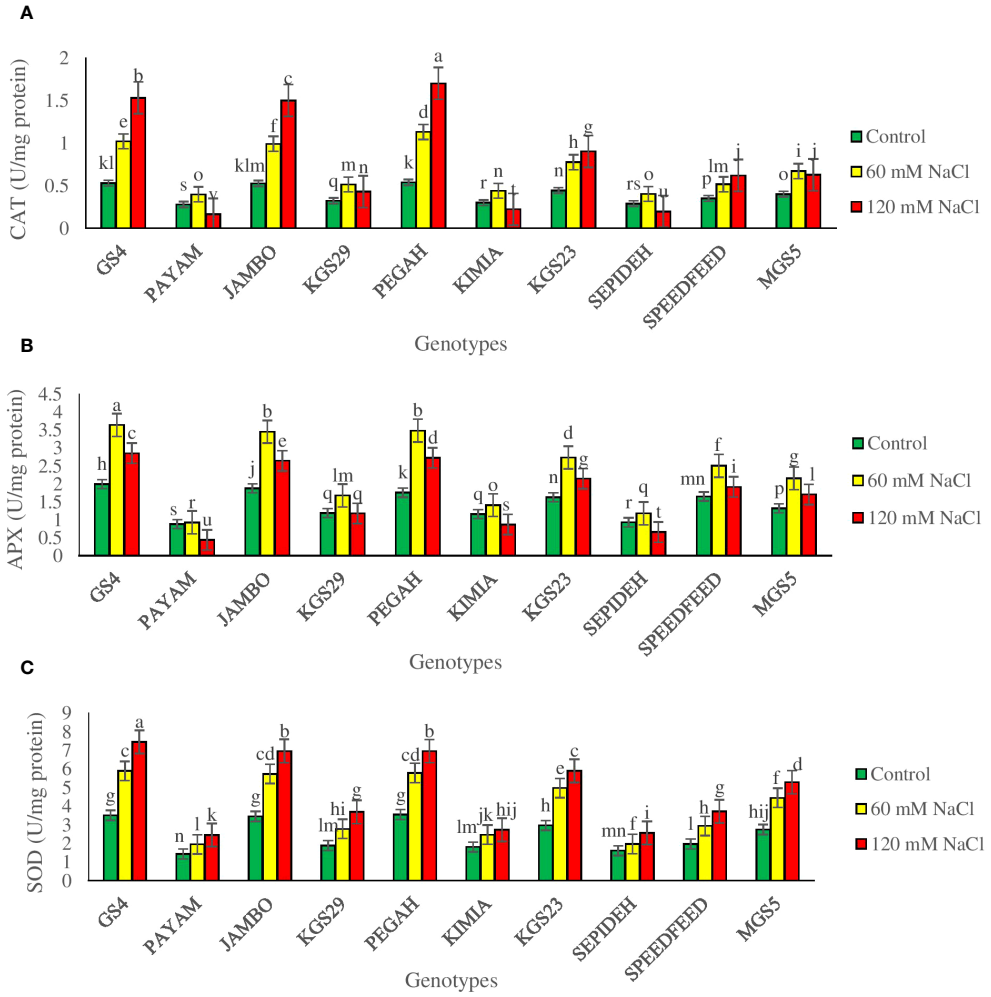

FIGURE 8
The specific activity of antioxidative enzymes **(A)** catalase (CAT), **(B)** ascorbate peroxidase (APX), and **(C)** super-oxide dismutase (SOD) of sorghum genotypes for the interaction of genotypes × salinity (0, 60, and 120 mM NaCl) at fifty percent flowering stage. Different letters indicate significant differences by HSD at $p<0.05$.

biochemical, and growth parameters, ultimately affecting overall yield (Tari et al., 2013; Ali et al., 2022; Rajabi Dehnavi et al., 2022). However, a rich tapestry of responses unfolded beyond this broad trend, exposing the genetic diversity among sorghum genotypes. This dynamic interplay between different salinity levels and genotypes responses underscores the intricate genetic adaptations that equip each genotype to confront adversity. These variations among genotypes are discernible through their unique physiological and biochemical reactions to salt stress, offering valuable insights into the mechanisms governing salt tolerance in sorghum.

Photosynthesis is a fundamental metabolic pathway crucial for regulating plant growth, which emerges as a primary target of salinity stress (Pessarakli, 2018; Pan et al., 2021). Our results show a strong positive correlation between Pn and final fresh and dry yields ($r = 0.92$ and 0.93, respectively) (Supplementary Table 3). Our findings consistently demonstrate a decline in Pn, Gs, and LAI under elevated salinity levels across various sorghum genotypes, emphasizing the common challenges of compromised gas exchange and hindered growth (Sharma et al., 2020; Rajabi Dehnavi et al., 2022). Detrimental effects of salinity on photosynthesis encompass multiple facets, including impacts on stomatal operations, gas exchange, pigments, chloroplast development, membrane structure, electron transport, enzyme activities and photosynthesis surface, ultimately impeding crop production (Ashraf and Harris, 2013; Pan et al., 2021; Amombo et al., 2022). However, our observations reveal that salt-tolerant genotypes (e.g., Pegah and GS4) effectively maintained their Pn and mitigated the negative effects of salt stress on growth. This is evidenced by the minimal reduction in Pn and yields in these genotypes. The preservation of photosynthetic efficiency can be traced through the impact of salinity on stomatal and non-stomatal factors. We noted genotype-specific Gs, LAI and pigment responses, underscoring the adaptive diversity within sorghum genotypes. Salt-tolerant genotypes adeptly retained Gs, LAI and pigments, while salt-sensitive genotypes exhibited greater susceptibility, resulting in a more pronounced decline in photosynthetic activity. This divergence probably results from genotype-specific variations in their ability to handle stress-induced disorders, especially the ability

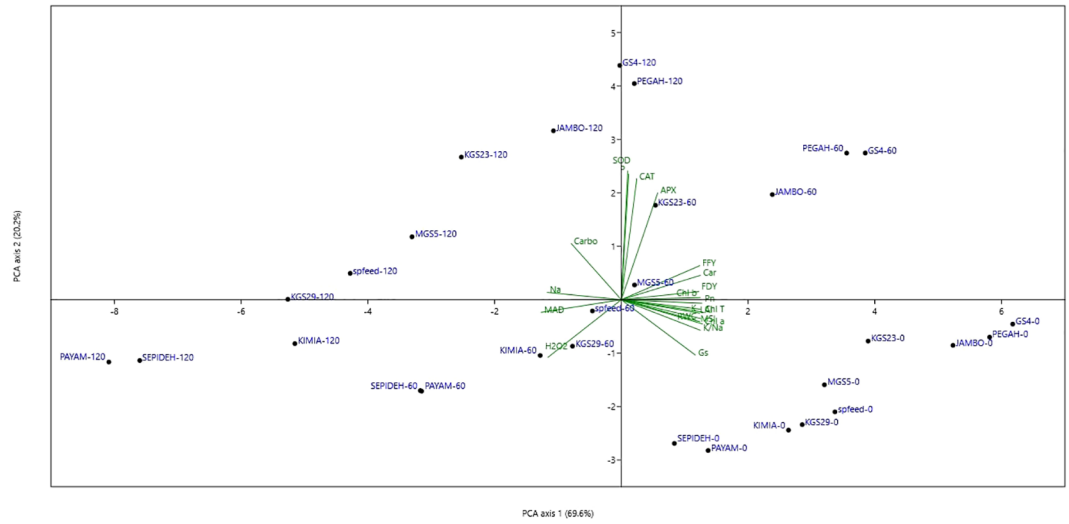

FIGURE 9
Principal components analysis diagram (PCA) of ten sorghum genotypes in three salinity treatments. RWC, relative leaf water content; Na, sodium content; K, potassium content; K/Na, K to Na ratios in the shoot; H_2O_2, hydrogen peroxide concentration; MDA, malondialdehyde concentration; MSI, membrane stability index; Pn, photosynthetic rate; Gs, stomatal conductance; Ci, intercellular CO_2 concentration; LAI, leaf area index; Chl a, chlorophyll a; Chl b, chlorophyll b; Chl T, total chlorophyll; Car, carotenoids; P, proline; Carbo, soluble carbohydrates; CAT, catalase; APX, ascorbate peroxidise; SOD, superoxide dismutase; FFY, fresh fodder yield; DFY, day fodder yield; PEGAH-0–genotype -salinity level Mm NaCl.

of these genotypes to inhibit oxidative stress levels, managing water-related stress and maintenance ionic homeostasis. To prove theses hypothesis, we delved into the intricate dynamics governing cellular membrane responses to oxidative stress induced by salt exposure. In this regard, we used a comprehensive approach that includes the assessment of hydrogen peroxide levels, MSI, and MDA concentrations, which gained deeper insights into the complex interplay involving genetic diversity, salt stress, and cellular reactions. Our findings highlight significant correlations between elevated hydrogen peroxide and MDA levels and the imposition of salt stress, aligning with established knowledge that links increased levels of ROS to subsequent cellular damage. Concurrently, the reduction in MSI values, indicating decreased membrane stability, underscores the susceptibility of cellular membranes to oxidative stress. These patterns are consistent with observations in other plant species, emphasizing the universality of these stress-responsive mechanisms (Youssef et al., 2021; Anwar-ul-Haq et al., 2023). However, our investigation unveils genotype-specific variations, providing insights into the underlying defense mechanisms. The substantial increase in hydrogen peroxide and MDA concentrations in the salt-sensitive genotypes (e.g., Payam and Sepideh), coupled with decreased MSI, signifies its heightened vulnerability to oxidative stress and membrane damage. In contrast, the observed lower levels of hydrogen peroxide and MDA, along with enhanced membrane stability, in the salt-tolerance genotypes (e.g., Pegah and GS4) underscore their superior ability to withstand oxidative stress. These findings emphasize the significance of MDA and MSI as reliable indicators of salt tolerance. These results confirm our hypothesis about the ability of salt-tolerant genotypes to control oxidative stress. However, to understand the mechanism of this ability, we investigated the antioxidant defense system more closely. Our exploration revealed intriguing trends in the activities of CAT, APX, and SOD, presenting a multifaceted view of antioxidant defense responses to salinity stress. The strong positive correlations between sorghum yield and antioxidant enzymes activities highlight the importance of an efficient enzymatic antioxidant defense system in salt-tolerant genotypes (Supplementary Table 3). In addition, we observed that while SOD consistently showed higher activity under stress, CAT and APX exhibited different reactions to varying stress levels. This contrast suggests inherent genetic variability in the efficiency of the enzymatic antioxidant defense system among different sorghum genotypes. SOD enhanced stability and efficacy under severe stress contrast with CAT and APX greater sensitivity to stress intensity variations. These observations underscore the dynamic nature of plant defense mechanisms, which adapt elegantly to the nuances of salinity stress.

In addition, it seems that the orchestration of osmoregulation, along with the modulation of antioxidant enzyme activity, plays a central role in facilitating sorghum plants adaption and resilience to salinity stress. Osmotic regulation plays a crucial role in maintaining water balance and structural integrity. Proline and Carbo, critical players in the osmotic stress response, are vital components of plant adaptive strategies (Alagoz et al., 2023). The positive correlations between P concentration and both fresh (r=0.71) and dry (r=0.70) fodder yield indicated the positive impact of proline accumulation on photosynthesis and cell stability (Supplementary Table 3). Proline, acting as a compatible solute, reinforces cell membrane and protein stability while serving as an effective antioxidant and regulator of cellular processes (Shafi et al., 2019). Simultaneously, soluble carbohydrates sustain turgor pressure and assist water absorption in saline conditions (Singh et al., 2015). It has been documented that under saline conditions, there is an augmentation in the activity of proline synthesis

enzymes, including pyrroline carboxylic acid and glutamyl kinase (Zulfiqar and Ashraf, 2023). Consequently, there is a noticeable elevation in proline content within cells. Furthermore, the observed surge in soluble carbohydrate content is likely a result of disruptions in their synthesis, transport, and utilization pathways. These disruptions inevitably lead to the breakdown of complex sugars (Varshney et al., 2023).

Variations in RWC among different sorghum genotypes subjected to varying salinity levels provide valuable insights into their strategies for managing water-related stress. The consistent reduction in RWC under higher salinity levels underscores the significant impact of osmotic stress, leading to decreased water availability and subsequent adjustments in cellular turgor. These distinct RWC responses across genotypes highlight the complex interplay between genetic traits and environmental conditions, collectively shaping a plant ability to retain water. This observation aligns with previous studies recognizing RWC as an informative marker of stress-induced water deficits (Irigoyen et al., 1992; Zhang et al., 2022). Our findings reveal that salt-tolerant genotypes Pegah and GS4 maintain higher RWC values, indicating their better ability to preserve water under salinity-induced stress. Conversely, salt-sensitive genotypes Payam and Sepideh exhibit lower RWC values, suggesting their reduced capacity to retain water in high salinity conditions. This difference in RWC responses highlights the ability of salt-tolerant genotypes to counteract salt-induced water deficits, possibly due to osmoregulation ability and improved cell wall integrity (Irigoyen et al., 1992; Zhang et al., 2022).

In addition, our findings strongly reinforce the critical significance of K^+/Na^+ ratio as a key indicator of salt tolerance (Basu et al., 2021; Balasubramaniam et al., 2023). A higher K^+/Na^+ ratio serves as a hallmark of effective ion management, reducing the influx of harmful ions while promoting the retention of essential nutrients. This phenomenon aligns with salt-tolerant plants, which naturally possess an enhanced ability to maintain an elevated K^+/Na^+ ratio, limiting Na^+ absorption and enhancing K^+ assimilation (Saqib et al., 2011; Amombo et al., 2022; Balasubramaniam et al., 2023). The distinct responses exhibited by salt-tolerant sorghum genotypes, particularly exemplified by Pegah and GS4, in maintaining an optimal K^+/Na^+ ratio underscore their adaptability to saline conditions. These genotypes likely employ a range of strategies, including restricted Na^+ uptake, increased K^+ acquisition, and coordinated regulation of ion transport, to enhance their performance under salt-induced stress. This finding emphasizes the well-established importance of ion homeostasis in unraveling the intricate mechanisms of salt tolerance (Amtmann and Sanders, 1998; Nieves-Cordones et al., 2016; Mansour et al., 2021; Balasubramaniam et al., 2023).

Our investigation delves into the genotype-specific modulation of salinity responses, as discerned through the comprehensive analysis of the Principal Components Analysis (PCA) diagram. Under control conditions, the sorghum genotypes exhibited uniform behavior, indicating a baseline consistency in their responses. However, the introduction of salt stress unveiled distinctive and significant shifts in their responses. Notably, the salt-tolerant genotypes, prominently represented by GS4 and Pegah, showcased a superior and adaptive performance under salt stress, particularly in the challenging conditions of high salinity (120 mM NaCl). Remarkably, the performance of these salt-tolerant genotypes rivaled that of other genotypes subjected to a lower level of salinity (60 mM NaCl), emphasizing their robust and versatile response mechanisms. The observed high positive correlation between the salt-tolerant genotypes and key physiological parameters, including antioxidant enzymes and osmolytes, serves as compelling evidence supporting our conclusions on the intricate mechanisms underpinning the salt tolerance of these sorghum genotypes. This correlation highlights the orchestrated interplay of various biochemical and physiological pathways that contribute to the enhanced adaptability of genotypes to salt-induced stress. Conversely, the salt-sensitive genotypes, Payam and Sepideh, exhibited the lowest performance across both salt levels. The strong negative correlations identified with Na^+, MDA, and H_2O_2 underscore the limited efficiency of the defense mechanisms in these genotypes against salt stress. This vulnerability suggests a compromised ability to regulate ion homeostasis and manage oxidative stress, crucial aspects in mitigating the impact of salinity. These findings provide valuable insights into the complex relationships between salinity levels, specific sorghum genotypes, and the intricate physiological responses that govern their adaptation to salt stress. Such nuanced understanding is crucial for informing targeted strategies in crop breeding and management practices to enhance salt stress resilience in sorghum cultivation.

In summary, the highlighted defense mechanisms enabled salt-tolerant genotypes to effectively counteract ionic toxicity, maintain a favorable K^+/Na^+ ratio, sustain optimal photosynthesis, improve stomatal function, preserve membrane integrity, and ensure sufficient levels of photosynthetic pigments. This resulted in the maintenance of photosynthetic capacity, improved growth conditions, and stable performance under salt stress. In contrast, sensitive genotypes struggled to deploy these defenses efficiently, rendering them highly susceptible to salinity stress. Additionally, the study delved into the nuanced specificity of sorghum genotypes, revealing diverse reactions across physiological and biochemical parameters. Salinity's significant impact spanned Relative Water Content (RWC), photosynthetic pigments, physiological parameters (Pn, Gs, Ci, LAI), ion concentrations (Na^+, K^+), final yield (FFY, DFY), and antioxidant enzyme activities (CAT, SOD, APX). In terms of RWC, GS4 and Pegah excelled in water retention, contrasting with the lower resilience of Payam and Sepideh to salinity-induced water stress. Analysis of photosynthetic pigments underscored GS4 and Pegah's ability to maintain higher concentrations, highlighting their vitality compared to the vulnerability of Payam and Sepideh. Physiological parameters emphasized GS4 and Pegah's enhanced photosynthetic efficiency and overall resilience, while Payam and Sepideh faced challenges in mitigating salinity's impact. Ion concentrations further showcased GS4 and Pegah's adaptability with higher K^+ concentrations and K^+/Na^+ ratios, along with lower Na^+ levels, differentiating them from the more susceptible Payam and Sepideh. Final yield evaluation confirmed GS4 and Pegah's resilience with higher FFY and DFY values, indicating suitability for saline environments. Analysis of antioxidant enzyme activities solidified GS4 and

Pegah's robust defense mechanisms against salinity stress, contrasting with the weaker response of Payam and Sepideh.

5 Conclusion

This study explored salinity stress responses in sorghum, focusing on genotype variations and salt tolerance mechanisms. Salt-tolerant sorghum genotypes demonstrated effective osmotic regulation, strong antioxidant enzyme activity, and a maintained K^+/Na^+ ratio, ensuring stable photosynthesis, stomatal function, and membrane integrity. These mechanisms contributed to performance maintenance and reduced yield loss. The study identified key indicators such as K^+/Na^+ ratio, MDA, MSI, SOD, and proline for distinguishing between tolerant and sensitive genotypes, offering valuable insights for sorghum breeding. The findings support the potential cultivation of salt-tolerant sorghum in saline areas, enhancing sustainable sorghum production for food security in challenging environments. Pegah and GS4 emerged as promising candidates for salt-affected environments, warranting further testing across different locations and years for reliable yield assessments.

Data availability statement

The raw data supporting the conclusions of this article will be made available by the authors, without undue reservation.

Author contributions

ARD: Conceptualization, Data curation, Formal analysis, Investigation, Methodology, Software, Validation, Visualization, Writing – original draft. MZ: Conceptualization, Methodology, Supervision, Validation, Visualization, Writing – review & editing. AP: Formal analysis, Validation, Visualization, Writing – review & editing.

Funding

The author(s) declare financial support was received for the research, authorship, and/or publication of this article. The publication fee for this research was supported by the IDUB publishing competition at Nicolaus Copernicus University in Toruń, Poland.

Acknowledgments

This study was supported by funds for the science of Isfahan University of Technology, Iran and Nicolaus Copernicus University in Toruń, Poland.

Conflict of interest

The authors declare that the research was conducted in the absence of any commercial or financial relationships that could be construed as a potential conflict of interest.

Publisher's note

Supplementary material

The Supplementary Material for this article can be found online at: https://www.frontiersin.org/articles/10.3389/fpls.2023.1296286/full#supplementary-material

References

Afzal, M., Hindawi, S. E. S., Alghamdi, S. S., Migdadi, H. H., Khan, M. A., Hasnain, M. U., et al. (2023). Potential breeding strategies for improving salt tolerance in crop plants. *J. Plant Growth Regul.* 42 (6), 3365–3387. doi: 10.1007/s00344-022-10797-w

Alagoz, S. M., Lajayer, B. A., and Ghorbanpour, M. (2023). "Proline and soluble carbohydrates biosynthesis and their roles in plants under abiotic stresses," in *Plant stress mitigators* (London, United Kingdom: Academic Press Elsevier), 169–185.

Ali, A. Y. A., Ibrahim, M. E. H., Zhou, G., Zhu, G., Elsiddig, A. M. I., Suliman, M. S. E., et al. (2022). Interactive impacts of soil salinity and jasmonic acid and humic acid on growth parameters, forage yield and photosynthesis parameters of sorghum plants. *S. Afr. J. Bot.* 146, 293–303. doi: 10.1016/j.sajb.2021.10.027

Alici, E. H., and Arabaci, G. (2016). Determination of SOD, POD, PPO and cat enzyme activities in Rumex obtusifolius L. *Annu. Res. Rev. Biol.* 11 (3), 1–7. doi: 10.9734/ARRB/2016/29809

Allen, R. G., Pereira, L. S., Raes, D., and Smith, M. (1998). Crop evapotranspiration-Guidelines for computing crop water requirements-FAO Irrigation and drainage paper 56. *Fao Rome* 300 (9), D05109.

Amombo, E., Ashilenje, D., Hirich, A., Kouisni, L., Oukarroum, A., Ghoulam, C., et al. (2022). Exploring the correlation between salt tolerance and yield: Research advances and perspectives for salt-tolerant forage sorghum selection and genetic improvement. *Planta* 255 (3), 71. doi: 10.1007/s00425-022-03847-w

Amtmann, A., and Sanders, D. (1998). "Mechanisms of Na+ uptake by plant cells," in *Adv. Bot. Res.* (London, United Kingdom: Academic Press Elsevier) 29, 75–112.

Anwar-ul-Haq, M., Iftikhar, I., Akhtar, J., and Maqsood, M. (2023). Role of Exogenous osmolyte supplementation in ameliorating osmotic and oxidative stress and promoting growth in salinity-stressed soybean genotypes. *J. Soil Sci. Plant Nutr.* 23 (3), 1–13. doi: 10.1007/s42729-023-01289-1

Ashraf, M., and Harris, P. J. (2013). Photosynthesis under stressful environments: An overview. *Photosynthetica* 51, 163–190. doi: 10.1007/s11099-013-0021-6

Ashraf, M. Y., Akhtar, K., Hussain, F., and Iqbal, J. (2006). Screening of different accessions of three potential grass species from Cholistan desert for salt tolerance. *Pak. J. Bot.* 38 (5), 1589–1597.

Ayers, R. S., and Westcot, D. W. (1985). *Water quality for agriculture* (Food and Agriculture Organization of the United Nations Rome) 29, 174.

Balasubramaniam, T., Shen, G., Esmaeili, N., and Zhang, H. (2023). Plants' Response mechanisms to salinity stress. *Plants* 12 (12), 2253. doi: 10.3390/plants12122253

Basu, S., Kumar, A., Benazir, I., and Kumar, G. (2021). Reassessing the role of ion homeostasis for improving salinity tolerance in crop plants. *Physiol. Plant* 171 (4), 502–519. doi: 10.1111/ppl.13112

Bates, L. S., Waldren, R. A., and Teare, I. (1973). Rapid determination of free proline for water-stress studies. *Plant Soil* 39, 205–207. doi: 10.1007/BF00018060

Bradford, M. M. (1976). A rapid and sensitive method for the quantitation of microgram quantities of protein utilizing the principle of protein-dye binding. *Anal. Biochem.* 72, 248–254. doi: 10.1016/0003-2697(76)90527-3

Davey, M., Stals, E., Panis, B., Keulemans, J., and Swennen, R. (2005). High-throughput determination of malondialdehyde in plant tissues. *Anal. Biochem.* 347 (2), 201–207. doi: 10.1016/j.ab.2005.09.041

Epanchin-Niell, R. S., Thompson, A., Han, X., Post, J., Miller, J., Newburn, D., et al. (2023). "Coastal agricultural land use response to sea level rise and saltwater intrusion," in *Agricultural and applied economics Association*.

Fadl, M. E., Jalhoum, M. E., AbdelRahman, M. A., Ali, E. A., Zahra, W. R., Abuzaid, A. S., et al. (2023). Soil Salinity assessing and mapping using several statistical and distribution techniques in arid and semi-arid ecosystems, Egypt. *Agronomy* (Shanhua, Taiwan AVRDC World Vegetable Center, Taiwan (AVRDC)) 13 (2), 583. doi: 10.3390/agronomy13020583

Fernandez, G. C. (1992). "Effective selection criteria for assessing plant stress tolerance," in *Proceeding of the international symposium on adaptation of vegetables and other food crops in temperature and water stress*(Shanhua, Taiwan), 257–270. (Year).

Fischer, R., and Maurer, R. (1978). Drought resistance in spring wheat cultivars. I. Grain yield responses. *Aust. J. Agric. Res.* 29 (5), 897–912.

Garcia-Caparros, P., De Filippis, L., Gul, A., Hasanuzzaman, M., Ozturk, M., Altay, V., et al. (2021). Oxidative stress and antioxidant metabolism under adverse environmental conditions: a review. *Bot. Rev.* 87, 421–466. doi: 10.1007/s12229-020-09231-1

Giannopolitis, C. N., and Ries, S. K. (1977). Superoxide dismutases: I. Occurrence in higher plants. *Plant Physiol.* 59 (2), 309–314. doi: 10.1104/pp.59.2.309

Hasanuzzaman, M., Raihan, M. R. H., Masud, A. A. C., Rahman, K., Nowroz, F., Rahman, M., et al. (2021). Regulation of reactive oxygen species and antioxidant defense in plants]\ Cvx nder salinity. *Int. J. Mol. Sci.* 22 (17), 9326. doi: 10.3390/ijms22179326

Hossain, M. S., Islam, M. N., Rahman, M. M., Mostofa, M. G., and Khan, M. A. R. (2022). Sorghum: A prospective crop for climatic vulnerability, food and nutritional security. *J. Agric. Food Res.* 8, 100300. doi: 10.1016/j.jafr.2022.100300

Iqbal, M. A. (2015). Agronomic management strategies elevate forage sorghum yield: A Review. *J. Adv. Bot. Zoo.* 3, 1–6. doi: 10.5281/zenodo.918335

Irigoyen, J., Einerich, D., and Sánchez-Díaz, M. (1992). Water stress induced changes in concentrations of proline and total soluble sugars in nodulated alfalfa (Medicago sativa) plants. *Physiol. Plant* 84 (1), 55–60. doi: 10.1111/j.1399-3054.1992.tb08764.x

Kaur, M., Gupta, N., Kaur, N., Sohu, R., Mahal, A. K., and Choudhary, A. (2023). Preliminary screening of sorghum (Sorghum bicolor L.) germplasm for salinity stress tolerance at the early seedling stage. *Cereal Res. Commun.* 51 (3), 603–613. doi: 10.1007/s42976-022-00327-5

Lamalakshmi Devi, E., Kumar, S., Basanta Singh, T., Sharma, S. K., Beemrote, A., Devi, C. P., et al. (2017). Adaptation strategies and defence mechanisms of plants during environmental stress. *Medicinal Plants Environ. challenges*, 359–413. doi: 10.1007/978-3-319-68717-9_20

Lichtenthaler, H. K., and Buschmann, C. (2001). Chlorophylls and carotenoids: measurement and characterization by UV-VIS spectroscopy. *Curr. Protocol. Food Anal. Chem.* 1 (1), F4.3.1–F4.3.8. doi: 10.1002/0471142913.faf0403s01

Mansour, M. M. F., Emam, M. M., Salama, K. H. A., and Morsy, A. A. (2021). Sorghum under saline conditions: Responses, tolerance mechanisms, and management strategies. *Planta* 254, 1–38. doi: 10.1007/s00425-021-03671-8

Manzoor, M., Naz, S., Muhammad, H. M. D., and Ahmad, R. (2023). Smart reprogramming of jujube germplasm against salinity tolerance through molecular tools. *Funct. Integr. Genomics* 23 (3), 222. doi: 10.1007/s10142-023-01140-x

Mukhopadhyay, R., Sarkar, B., Jat, H. S., Sharma, P. C., and Bolan, N. S. (2021). Soil salinity under climate change: Challenges for sustainable agriculture and food security. *J. Environ. Manage.* 280, 111736. doi: 10.1016/j.jenvman.2020.111736

Nakano, Y., and Asada, K. (1981). Hydrogen peroxide is scavenged by ascorbate-specific peroxidase in spinach chloroplasts. *Plant Cell Physiol.* 22 (5), 867–880. doi: 10.1093/oxfordjournals.pcp.a076232

Naorem, A., Jayaraman, S., Dang, Y. P., Dalal, R. C., Sinha, N. K., Rao, C. S., et al. (2023). Soil constraints in an arid environment—challenges, prospects, and implications. *Agronomy* 13 (1), 220. doi: 10.3390/agronomy13010220

Nieves-Cordones, M., Al Shiblawi, F. R., and Sentenac, H. (2016). Roles and transport of sodium and potassium in plants. *alkali metal ions: Their role Life* 16, 291–324. doi: 10.1007/978-3-319-21756-7_9

Pan, T., Liu, M., Kreslavski, V. D., Zharmukhamedov, S. K., Nie, C., Yu, M., et al. (2021). Non-stomatal limitation of photosynthesis by soil salinity. *Crit. Rev. Environ. Sci. Technol.* 51 (8), 791–825. doi: 10.1080/10643389.2020.1735231

Pantha, P., Oh, D.-H., Longstreth, D., and Dassanayake, M. (2023). Living with high potassium: balance between nutrient acquisition and K-induced salt stress signaling. *Plant Physiol.* 191 (2), 1102–1121. doi: 10.1093/plphys/kiac564

Pessarakli, M. (Ed.) (2018). *Handbook of photosynthesis* (Boca Raton: CRC press). doi: 10.1201/9781315372136

Phour, M., and Sindhu, S. S. (2023). "Soil salinity and climate change: Microbiome-Based Strategies for Mitigation of Salt Stress to Sustainable Agriculture," in *Climate change and microbiome dynamics: carbon cycle feedbacks* (Cham: Springer International Publishing), 191–243.

Rajabi Dehnavi, A., Zahedi, M., Ludwiczak, A., Cardenas Perez, S., and Piernik, A. (2020). Effect of salinity on seed germination and seedling development of sorghum (Sorghum bicolor (L.) Moench) genotypes. *Agronomy* 10 (6), 859. doi: 10.3390/agronomy10060859

Rajabi Dehnavi, A., Zahedi, M., Ludwiczak, A., and Piernik, A. (2022). Foliar application of salicylic acid improves salt tolerance of sorghum (Sorghum bicolor (L.) Moench). *Plants* 11 (3), 368. doi: 10.3390/plants11030368

Sachdev, S., Ansari, S. A., Ansari, M. I., Fujita, M., and Hasanuzzaman, M. (2021). Abiotic stress and reactive oxygen species: Generation, signaling, and defense mechanisms. *Antioxidants* 10 (2), 277. doi: 10.3390/antiox10020277

Sagar, A., Hossain, A., Uddin, N., Tajkia, J. E., Mia, A., et al. (2023). Genotypic divergence, photosynthetic efficiency, sodium extrusion, and osmoprotectant regulation conferred salt tolerance in sorghum. *Phyton-International Journal of Experimental Botany* 92 (8), 2349–2368. doi: 10.32604/phyton.2023.028974

Sanders, G. J., and Arndt, S. K. (2012). "Osmotic adjustment under drought conditions," in R. Aroca *Plant responses to drought stress: From morphological to molecular features* (Berlin, Heidelberg: Springer), 199–229. doi: 10.1007/978-3-642-32653-0_8

Saqib, Z. A., Akhtar, J., Saqib, M., and Ahmad, R. (2011). Contrasting leaf Na+ uptake and transport rates conferred differences in salt tolerance of wheat genotypes. *Acta Agric. Scand. Sect B* 61 (2), 129–135. doi: 10.1080/09064710903571709

Shafi, A., Zahoor, I., and Mushtaq, U. (2019). "Proline accumulation and oxidative stress: Diverse roles and mechanism of tolerance and adaptation under salinity stress," in *Salt stress, microbes, and plant interactions: mechanisms and molecular approaches*. Ed. M. Akhtar (Singapore: Springer), 269–300.

Shakeri, E., and Emam, Y. (2018). Selectable traits in sorghum genotypes for tolerance to salinity stress. *J. Agr. Sci. Tech.* 19, 1319-1332.

Shams, M., and Khadivi, A. (2023). Mechanisms of salinity tolerance and their possible application in the breeding of vegetables. *BMC Plant Biol.* 23 (1), 139. doi: 10.1186/s12870-023-04152-8

Sharma, A., Kumar, V., Shahzad, B., Ramakrishnan, M., Singh Sidhu, G. P., Bali, A. S., et al. (2020). Photosynthetic response of plants under different abiotic stresses: a review. *J. Plant Growth Regul.* 39, 509–531. doi: 10.1007/s00344-019-10018-x

Singh, M., Kumar, J., Singh, S., Singh, V. P., and Prasad, S. M. (2015). Roles of osmoprotectants in improving salinity and drought tolerance in plants: a review. *Rev. Environ. Sci. Bio/Technol.* 14, 407–426. doi: 10.1007/s11157-015-9372-8

Smart, R. E., and Bingham, G. E. (1974). Rapid estimates of relative water content. *Plant Physiol.* 53 (2), 258–260. doi: 10.1104/pp.53.2.258

Tari, I., Laskay, G., Takács, Z., and Poór, P. (2013). Response of sorghum to abiotic stresses: A review. *J. Agron. Crop Sci.* 199 (4), 264–274. doi: 10.1111/jac.12017

Varshney, V., Singh, J., and Salvi, P. (2023). "Sugar signaling and their interplay in mitigating abiotic stresses in plant: A molecular perspective," in D. Sharma, S. Singh, S.K. Sharma and R. Singh (eds) *Smart plant breeding for field crops in post-genomics era.* (Singapore: Springer), 369–393. doi: 10.1007/978-981-19-8218-7_12

Velikova, V., Yordanov, I., and Edreva, A. (2000). Oxidative stress and some antioxidant systems in acid rain-treated bean plants: protective role of exogenous polyamines. *Plant Sci.* 151 (1), 59–66. doi: 10.1016/S0168-9452(99)00197-1

Wakeel, A., Farooq, M., Qadir, M., and Schubert, S. (2011). Potassium substitution by sodium in plants. *Crit. Rev. Plant Sci.* 30 (4), 401–413. doi: 10.1080/07352689.2011.587728

Youssef, M. H., Raafat, A., El-Yazied, A. A., Selim, S., Azab, E., Khojah, E., et al. (2021). Exogenous application of alpha-Lipoic acid mitigates salt-induced oxidative damage in sorghum plants through regulation growth, leaf pigments, ionic homeostasis, antioxidant enzymes, and expression of salt stress responsive genes. *Plants* 10 (11), 2519. doi: 10.3390/plants10112519

Zhang, H., Zhu, J., Gong, Z., and Zhu, J.-K. (2022). Abiotic stress responses in plants. *Nat. Rev. Genet.* 23 (2), 104–119. doi: 10.1038/s41576-021-00413-0

Zulfiqar, F., and Ashraf, M. (2023). Proline alleviates abiotic stress induced oxidative stress in plants. *J. Plant Growth Regul.* 42 (8), 4629–4651. doi: 10.1007/s00344-022-10839-3

frontiers | Frontiers in Plant Science

TYPE Original Research
PUBLISHED 16 January 2024
DOI 10.3389/fpls.2023.1284480

OPEN ACCESS

EDITED BY
Zulfiqar Ali Sahito,
Zhejiang University of Technology, China

REVIEWED BY
Muhammad Ahsan Asghar,
Aarhus University, Denmark
Hamid Manzoor,
Bahauddin Zakariya University, Pakistan
Meilong Xu,
Ningxia Academy of Agriculture and Forestry Sciences, China

*CORRESPONDENCE
Li Zhang
lilizhang324@163.com
Long Yang
lyang@sdau.edu.cn

RECEIVED 28 August 2023
ACCEPTED 29 December 2023
PUBLISHED 16 January 2024

CITATION
Xu J, Wang T, Sun C, Liu P, Chen J, Hou X, Yu T, Gao Y, Liu Z, Yang L and Zhang L (2024) Eugenol improves salt tolerance via enhancing antioxidant capacity and regulating ionic balance in tobacco seedlings. *Front. Plant Sci.* 14:1284480. doi: 10.3389/fpls.2023.1284480

Eugenol improves salt tolerance via enhancing antioxidant capacity and regulating ionic balance in tobacco seedlings

Jiaxin Xu[1], Tingting Wang[1], Changwei Sun[2], Peng Liu[1], Jian Chen[3], Xin Hou[1], Tao Yu[1], Yun Gao[1], Zhiguo Liu[1], Long Yang[1]* and Li Zhang[1]*

[1]College of Plant Protection, Shandong Agricultural University, Taian, China, [2]College of Horticulture, Nanjing Agricultural University, Nanjing, China, [3]Institute of Food Quality and Safety, Jiangsu Academy of Agricultural Sciences, Nanjing, China

Salt stress inhibits plant growth by disturbing plant intrinsic physiology. The application of exogenous plant growth regulators to improve the plant tolerance against salt stress has become one of the promising approaches to promote plant growth in saline environment. Eugenol (4-allyl-2- methoxyphenol) is the main ingredient in clove oil and it is known for its strong antioxidant and anti-microbial activities. Eugenol also has the ability of inhibiting several plant pathogens, implying the potential use of eugenol as an environmental friendly agrichemical. However, little is known about the possible role of eugenol in the regulation of plant tolerance against abiotic stress. Therefore, here we investigated the effectiveness of phytochemical eugenol in promoting salt tolerance in tobacco seedlings through physiological, histochemical, and biochemical method. The seedling roots were exposed to NaCl solution in the presence or absence of eugenol. Salt stress inhibited seedling growth, but eugenol supplementation effectively attenuated its effects in a dose-dependent manner, with an optimal effect at 20 μM. ROS (reactive oxygen species) accumulation was found in seedlings upon salt stress which was further resulted in the amelioration of lipid peroxidation, loss of membrane integrity, and cell death in salt-treated seedlings. Addition of eugenol highly suppressed ROS accumulation and reduced lipid peroxidation generation. Both enzymatic and non-enzymatic antioxidative systems were activated by eugenol treatment. AsA/DHA and GSH/GSSG were also enhanced upon eugenol treatment, which helped maintain redox homeostasis upon salinity. Eugenol treatment resulted in an increase in the content of osmoprotectants (e.g. proline, soluble sugar and starch) in salt-treated seedlings. Na^+ levels decreased significantly in seedlings upon eugenol exposure. This may result from the upregulation of the expression of two ionic transporter genes, *SOS1* (salt-hypersensitive 1) and *NHX1* (Na^+/H^+ anti-transporter 1). Hierarchical cluster combined correlation analysis uncovered that eugenol induced salt tolerance was mediated by redox homeostasis and maintaining ionic balance in tobacco

seedlings. This work reveals that eugenol plays a crucial role in regulating plant resistant physiology. This may extend its biological function as a novel biostimulant and opens up new possibilities for improving crop productivity in the saline agricultural environment.

KEYWORDS

eugenol, oxidative stress, reactive oxygens species, redox homeostasis, salt stress, tobacco

1 Introduction

Soil salinity is one of the important environmental problems worldwide (Al-Turki et al., 2023; Xiao and Zhou, 2023). About 20% of the world's irrigated land is affected by salinity (Wang et al., 2023b). Poor irrigation and industrial pollution continue to exacerbate soil salinization (Yu et al., 2020; Ge et al., 2023). It has been estimated that about 50% of the world's arable land would be salinized in 2050 (Shrivastava and Kumar, 2015). Salt stress inhibits crop growth, leading to the decrease in crop yield (Guijarro-Real et al., 2020). Salt stress-induced phytotoxicity involves various plant physiological disorders. High salinity results in plant dehydration by inducing osmotic stress. Plants activate osmotic adjustment to combat salt stress (van Zelm et al., 2020). Plant cells tend to accumulate carbohydrates (e.g. sugar and starch) to maintain cell turgor under saline conditions (Wang et al., 2021). Proline is another important osmotic regulator (Patani et al., 2023). Proline accumulation plays vital roles in adjusting osmotic potential in plant cells upon salt stress (Mansour and Ali, 2017).

ROS (reactive oxygen species) overaccumulation is one of the typical consequences of salinity-induced phytotoxicity (Wang et al., 2023a). Basically, ROS comprises non-radical form (e.g. hydrogen peroxide, H_2O_2) and free radical form (e.g. superoxide radical, $O_2^{\cdot-}$) (Gill and Tuteja, 2010). Salinity-induced ROS frequently attacks macromolecules in plant cells, resulting in oxidative stress and cell death (Liu et al., 2023). Accordingly, plants detoxify excessive ROS by deploying endogenous antioxidative systems, such as enzymatic system including a set of antioxidative enzymes (e.g. superoxide dismutase, SOD; peroxidase, POD; catalase, CAT; and ascorbate peroxidase, APX) and non-enzymatic system including various antioxidants (e.g. AsA, ascorbic acid; GSH, glutathione; and proline) (Hasanuzzaman et al., 2021). GSSG and DHA (dehydroascorbic Acid) are the oxidized form of GSH and AsA, respectively (Luo et al., 2023). The redox balance can be modulated by GSH/GSSG and AsA/DHA, which play a role in plant responses to abiotic stress (Kumari et al., 2023). Promoting plant salt tolerance has been closely associated with the enhancement of antioxidant capacity and the maintenance of redox status (Gao et al., 2022).

Plant salt tolerance is also involved in maintaining intracellular ionic homeostasis (Song et al., 2021; Zhang et al., 2023b). In saline conditions, excessive solidum (Na^+) in cytosol are toxic to plant cells (Xiao and Zhou, 2023). Plants activate SOS (Salt Overly Sensitive) pathway to prevent Na^+ accumulation in cytosol. In this pathway, *SOS1* is a Na^+ transporter localized in plasma membrane (Ma et al., 2022). *SOS1* excludes Na^+ out of cells to detoxify Na^+. *SOS2-SOS3* kinase complex can phosphorylate and activate *SOS1* (Ali et al., 2023). Plant cells also have another strategy to lower Na^+ concentration in cytosol through Na^+ sequestration in vacuole. For example, *NHX1* (*Na^+/H^+ antiporter 1*) encodes a transporter localized in tonoplast. It can compartmentalize Na^+ into vacuole in order to alleviate Na^+ toxicity in cytosol (Zhang et al., 2017). In Arabidopsis, *NHX1* also has the ability to transport K^+ for plant K^+ uptake to regulate cell turgor upon salt stress (Barragán et al., 2012). Maintaining the proper balance between Na^+ and K^+ is vital for plant tolerance against salinity (Negrão et al., 2017).

Applying exogenous regulators to promote plant salt tolerance has been considering as a promising approach to improve the performance of crops in saline environment (Quamruzzaman et al., 2021). Eugenol ($C_{10}H_{12}O_2$, 4-allyl-2-methoxyphenol) is the main constituent of essential oil obtained from clove (Jia et al., 2020). Eugenol can also be produced by other plants (e.g. strawberry sweet basil and petunia), contributing to aroma (Koeduka et al., 2006; Aragüez et al., 2013). The clinical relevance of eugenol has been associated with its anti-inflammatory activity and antimicrobial activity (Taleuzzaman et al., 2021). As a natural bioactive compound, eugenol can be used as food preservative in food antisepsis field (Hu et al., 2018b). Eugenol inhibits the growth of several agricultural pathogens (Morcia et al., 2011; Olea et al., 2019), implying the potential application of eugenol in agriculture. There are limited reports for eugenol-regulated plant physiology. Several recent studies suggest that eugenol has the ability to modulate plant resistant physiology against abiotic stresses. Eugenol confers drought tolerance in tea plant and heavy metal tolerance in *Brassica rapa* by modulating antioxidant defense through hydrogen sulfide- and abscisic acid-mediated signaling, respectively (e.g. heavy metal, drought, and cold) (Hu et al., 2018a; Zhao et al., 2022). These reports imply the potentiality of using eugenol as an environmental-friendly agrichemical to induce plant tolerance. Till now, little is known about the possible role of eugenol in regulating plant physiology against salinity stress. Mining the capability and mechanism of eugenol-conferred plant

salt tolerance would help extend the biological function of eugenol in agriculture.

Tobacco is not only an importantly economic crop but also one of the model plants to study plant physiological adaptation under environmental stimuli (including salt stress). Tobacco plant activates salt tolerant responses by deploying antioxidative system, ion transport system (Na^+ and K^+ transporters), and osmotic regulation. In addition, some transcription factors (TFs) are involved in salt tolerant responses in tobacco. These TFs consist of AP2/ERF, WRKY, and zinc finger proteins, working on the regulation of the expression of genes that help decrease ROS and adjust osmotic response. CDPKs (calcium-dependent protein kinase) and MAPK (mitogen-activated protein kinases) are also play a role in modulating salinity stress by regulating ROS and hormonal signaling in tobacco plants (Sun et al., 2020). In this work, we detected the ability of eugenol in alleviating salt stress in tobacco seedlings. Then we studied the possible role of eugenol in antioxidation, osmotic adjudgment, and ionic balancing in tobacco seedlings upon salt stress. Finally, we discussed the possible mechanism of eugenol driving these physiological processes and their significance.

2 Materials and methods

2.1 Plant culture and treatment

The seeds of tobacco (K326) were provided by the Germplasm Resources Laboratory of Shandong Agricultural University. Tobacco seeds were rinsed with distilled water followed by sterilized with potassium permanganate (0.2%) for 10 min. Then the seeds were washed with distilled water again for three times. The seeds were placed on moistened triple-layer filter paper in Petri dishes for germination and growth. All the seedlings were cultured in a plant growth cabinet with light intensity of 5000 lx, photoperiod of 12 h, relative air humidity of 50%, and temperature at 26°C. Sixty identical seedlings (4-days old) with root length of 0.5 cm were selected and transferred into a new Petri dish with different concentrations of NaCl (sodium chloride) (0, 50, 100, 150, 200, and 250 mM). Eugenol (0, 5, 10, 20, 40, and 80 μM) was added to the treatment solution according to different treatment groups. The seedlings were harvested for physiological analysis after treatment for 3 days. For the time-course experiment, the seedling samples were analyzed at 0, 12, 24, 36, 48, 60, and 72 h, respectively.

2.2 Measurement of root elongation and fresh weight

We measured the root length of seedlings before and after treatment, respectively. The root elongation was calculated as the difference between these two values. The average root elongation was obtained based on 10-20 replicates for each treatment. The seedlings after treatment were surface-dried gently with filter paper before weighing. Ten seedlings were weighed together as one replicate. The average fresh weight (per 10 seedlings) was obtained based on three replicates for each treatment.

2.3 ROS measurement

Seedlings after treatment were harvested and washed with distilled water. Then the seedlings were used for determining the content of ROS quantified by measuring H_2O_2 and $O_2^{\cdot-}$. The seedling samples were ground and homogenized with cold sodium phosphate buffer (50 mM, pH 7.4), followed by centrifuging at 12, 000 g at 4°C for 20 min. Then the supernatant was collected for the quantification of H_2O_2 and $O_2^{\cdot-}$. A commercial Kit (BC3595, Beijing Solarbio Science & Technology Co., Ltd., Beijing, China) was used to determine H_2O_2 content based on spectrophotometric measurement of the product from the reaction between H_2O_2 and titanium sulfate ($OD_{415\ nm}$). Another commercial kit (BC1290, Solarbio) was used to determine $O_2^{\cdot-}$ content based on spectrophotometric measurement of reaction between $O_2^{\cdot-}$ and hydroxylamine hydrochloride (producing NO_2^- to further react with sulfanilamide and N-ethylenediamine) ($OD_{530\ nm}$) (Sun et al., 2022).

Total ROS in root tips were detected histochemically by using specific fluorescent probe DCFH-DA (2′,7′-dichlorofluorescein diacetate) based on our previously published method (Ye et al., 2017). The roots after treatment were incubated in DCFH-DA solution (10 μM) at 25°C for 20 min in darkness. Then the roots were washed with distilled water for the observation of DCF fluorescence by using a fluorescence microscope (ECLIPSE, TE2000-S, Nikon, Melville, NY, USA).

The $O_2^{\cdot-}$ in leaves were stained with NBT (nitro-blue tetrazolium) (Ye et al., 2016). The leaves were harvested and incubated in NBT solution (6 mM) for 3 h under light at 25°C. NBT can react with $O_2^{\cdot-}$ in leaves to produce formazan compound that is navy blue. Then the leaves were washed with distilled water followed by transferring to boiling ethanol for 20 min to remove the chlorophyll background. A stereoscopic microscope (SteREO Discovery.V8, ZEISS) was applied to observe and to photograph the leaves.

2.4 Thiobarbituric acid reactive substances measurement

A TBARS Content Assay Kit (BC0025, Beijing Solarbio Science & Technology Co., Ltd., Beijing, China) was used to determine TBARS content in seedlings based on spectrophotometric assay of the reaction between TBA (1,3-diethyl-2-thiobarbituric acid) and TBARS in the presence of TCA (trichloroacetic acid) (Sun et al., 2022). The TBARS in root tips was also evaluated histochemically by using specific fluorescent probe C11-BODIPY(581/591) (a lipid peroxidation sensor) (Drummen et al., 2002). The roots were incubated in C11-BODIPY(581/591) solution (10 μM) at 25°C in darkness for 10 min, followed by washing with distilled water and photographing C11-BODIPY fluorescence under a fluorescence microscope (ECLIPSE, TE2000-S, Nikon, Melville, NY, USA).

2.5 Detection of membrane integrity and cell death

Loss of membrane integrity in root tips was detected by using Evans blue staining (Ye et al., 2017). The roots were incubated in 0.025% Evans blue solution at 25°C for 60 min, followed by photographing under stereoscopic microscope (SteREO Discovery.V8, ZEISS).

Cell death in root tips were detected with specific fluorescent probe PI (propidium iodide) (Kellermeier et al., 2013). The roots were incubated in PI solution (20 μM) at 25°C in darkness for 15 min, followed by visualization and photographing under fluorescent microscope (ECLIPSE, TE2000-S, Nikon, Melville, NY, USA).

Trypan blue staining was used to detect cell death in leaves (Ye et al., 2016). The leaves were incubated in Trypan blue solution (10 mg/mL) for 3 h under light at 25°C. Then the leaves were washed with distilled water followed by transferring to boiling ethanol for 20 min to remove the chlorophyll, allowing the appearance of blue. Then the leaves were observed and photographed by using a stereoscopic microscope (SteREO Discovery.V8, ZEISS).

2.6 Assay of the activity of antioxidative enzymes

About 0.1 g of fresh seedling samples were homogenized with 2 mL of cold phosphate buffer (50 mM, pH 7.0). Then the mixture was centrifuged at 12, 000 g for 15 min (4°C). The supernatant was collected for the determination of enzymatic activity. The SOD activity was determined spectrophotometrically ($OD_{560\ nm}$) using a commercial kit (BC0170, Solarbio) based on the quantification of the inhibition of photochemical reaction of NBT (nitro-blue tetrazolium) in a reaction system with methionine and riboflavin. The CAT activity was determined spectrophotometrically ($OD_{240\ nm}$) using a commercial kit (BC0205, Solarbio) based on the decomposition of H_2O_2. The POD activity was determined spectrophotometrically ($OD_{470\ nm}$) using a commercial kit (BC0090, Solarbio) based on the oxidation rate of guaiacol in the presence of H_2O_2. The APX activity was determined spectrophotometrically ($OD_{290\ nm}$) using a commercial kit (BC0220, Solarbio) based on the oxidation rate of AsA in the presence of H_2O_2 (Chen et al., 2020b).

2.7 Measurement of metabolites

A commercial kit (BC1230, Solarbio) was applied to determine AsA content based on the oxidation rate of AsA catalyzed by AAO (ascorbic acid oxidase) (spectrophotometric measurement at $OD_{265\ nm}$). A commercial kit (BC1240, Solarbio) was applied to determine DHA content based on the production rate of AsA from DHA by DTT (1,4-dithiothreitol) (spectrophotometric measurement at $OD_{265\ nm}$). A commercial kit (BC1170, Solarbio) was applied to determine GSH content based on spectrophotometric measurement of the product from the reaction between GSH and DTNB (5,5'-dithiobis-2-nitrobenoic acid) ($OD_{265\ nm}$). A commercial kit (BC1180, Solarbio) was applied to determine GSSG content based on the production rate of GSH (measurement of $OD_{265\ nm}$ for the reaction between GSH and DTNB) from GSSG catalyzed by GR (GSH reductase). A commercial kit (BC0290, Solarbio) was applied to determine proline content based on spectrophotometric measurement of the product from the reaction between proline and ninhydrin ($OD_{520\ nm}$). A commercial kit (BC0035, Solarbio) was applied to determine plant soluble sugar content based on anthrone colorimetric method ($OD_{620\ nm}$). A commercial kit (BC0700, Solarbio) was applied to determine starch content based on the separation of starch with 80% ethanol and acid hydrolyzation to glucose, followed by anthrone colorimetric method ($OD_{620\ nm}$) (Chen et al., 2020b).

2.8 Measurement of Na^+ and K^+ in seedlings

Dried seedling samples were digested with H_2SO_4 (with 10% H_2O_2) using microwave digestion system (MARS6, CEM Corporation, Matthews, NC, USA). Then the content of Na^+ and K^+ were determined by using atomic absorption spectrometer (PinAAcle 900T, PerkinElmer, Hopkinton, Massachusetts, USA).

2.9 Gene expression analysis

Total RNA was extracted from seedling samples using a plant RNA extraction kit (RNE05, Nobelab Biotech. Co., Ltd, Beijing, China). The first cDNA strand was synthesized from 1 μg of total RNA by using RescriptTM II RT SuperMix Reverse Transcriptase (Nobelab Biotech. Co., Ltd, Beijing, China). The qPCR (real-time quantitative polymerase chain reaction) was performed on a CFX96 Touch Real-Time PCR System (Bio-Rad, CA, USA) by using 2 × SYBR Premix UrTaq II (Nobelab Biotech. Co., Ltd, Beijin, Beijing, China). The relative abundance of *NtActin* was determined as internal standard to normalize the expression level of target genes. The primers used for amplifying the genes are as follows: *NtSOS1*, forward 5′-TGGAGGAAGCGACCGATTC-3′ and reverse 5′-CGATAACGAGAAGAGCGACAG-3′; *NtNHX1*, forward 5′-AAGAAGGTCATACTCAGTT-3′ and reverse 5′- GGTAGCAAT AGTCTAATCAAT-3′; *NtActin*, forward 5′-GAAGAAGGTCCC AAGGGTTC-3′ and reverse 5′-TCTCCCTTTAACACCAACGG-3′.

2.10 Data analysis

Each result was shown as the mean ± standard deviation (SD) of 3 to 10 replicates. LSD (least significant difference) test was performed on the original data following ANOVA (one-way analysis of variance) tests to analyze the significant difference at $p<0.05$ among different treatments (SPSS 25.0, SPSS Inc., Chicago, IL, USA). The heatmap for hierarchical cluster analysis was generated by using TBtools (Chen et al., 2020a). Pearson correlation analysis was performed by using the package "corrplot" in R (Wei and Simko, 2017).

3 Results

3.1 Eugenol rescued the growth of tobacco seedlings under salt stress

Salt stress inhibited the root elongation of tobacco seedlings in time- and dose- dependent manner. NaCl at 50-250 mM began to inhibit root elongation at 12 h, followed with continuous decrease in the growth speed of roots (Figure 1A). Compared to the control group, the root elongation significantly decreased by 13.7%, 33.1%, 51.3%, 69.6%, and 79.1% upon NaCl exposure at 50, 100, 150, 200, and 250 mM, respectively, at the end of the exposure (72 h) (Figures 1A, B). We selected NaCl at 150 mM in the following experiments as it inhibited root elongation about half of control.

Compared to NaCl treatment alone, adding eugenol at 5-40 μM significantly rescued root elongation under NaCl treatment. Eugenol at 20 μM showed the greatest effect on root growth, resulting in significant increase in root elongation by 57.1% as compared to NaCl treatment alone (Figures 1C, D). Eugenol at 20 μM began to promote root elongation after treatment for 12 h, followed by enhanced growth speed of roots as compared to NaCl treatment alone (Figure 1E). Eugenol at 20 μM also significantly enhanced the fresh weight of seedlings under NaCl stress (Figure 1F). Eugenol treatment alone slightly affect the growth of tobacco seedlings (Figures 1D–F).

3.2 Eugenol alleviates salt-induced oxidative injury in tobacco seedlings

Salinity always induces ROS accumulation in plants. NaCl exposure significantly increased the content of H_2O_2 and $O_2^{\cdot-}$ increased by 43.7% and 101.9%, respectively, in tobacco seedlings. Adding eugenol resulted in significant decrease in the content of H_2O_2 and $O_2^{\cdot-}$ by 22.3% and 41.1%, respectively, in NaCl-treated seedlings (Figures 2A, B). Then we measured TBARS content, a typical indicator of ROS-induced oxidative injury. Eugenol decreased TBARS content in seedlings by 22.3% as compared to NaCl treatment alone than induced TBARS accumulation (Figure 2C).

We performed a set of *in vivo* detection to further verify eugenol-alleviated oxidative injury in tobacco seedlings. Salt stress induced extensive DCF fluorescence (indicating total ROS) and C11-BODIPY (indicating TBARS) in roots. Adding eugenol effectively decreased the fluorescence of these two probes, suggesting the decrease in the content of ROS and TBARS in roots (Figures 3A, B). ROS-induced lipid peroxidation results in membrane damage. The loss of membrane integrity was indicated by Evans blue staining. Adding eugenol decreased the staining of Evans blue in NaCl-treated root, suggesting that eugenol attenuated NaCl-induced membrane damage in root (Figures 3C, D). Superoxide radical (one typical ROS) in leaves was stained with

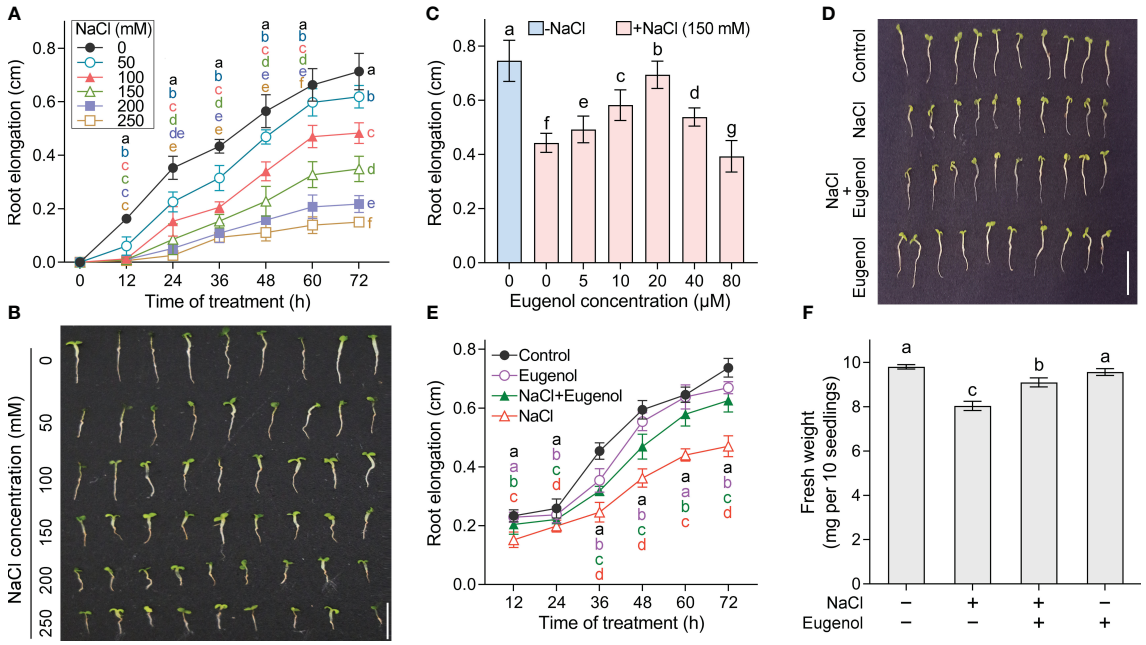

FIGURE 1
Effect of eugenol on the growth of tobacco seedlings upon NaCl exposure. **(A)** Time-course monitoring of root elongation under NaCl stress (0-250 mM). n = 9. **(B)** The seedling photograph taken after NaCl treatment for 72 hours. **(C)** Effect of eugenol (0-80 μM) on root elongation under NaCl (150 mM) stress for 72 h. n = 10. **(D)** Effect of eugenol at 20 μM on the seedling growth under NaCl (150 mM) stress for 72 h. **(E)** Time-course monitoring of root elongation under NaCl (150 mM) + eugenol (20 μM) treatment. n = 20. **(F)** Effect of eugenol at 20 μM on seedling fresh weight growth under NaCl (150 mM) stress for 72 h. n = 3. Different lowercase letters indicate significant difference among different treatments ($p < 0.05$, LSD).

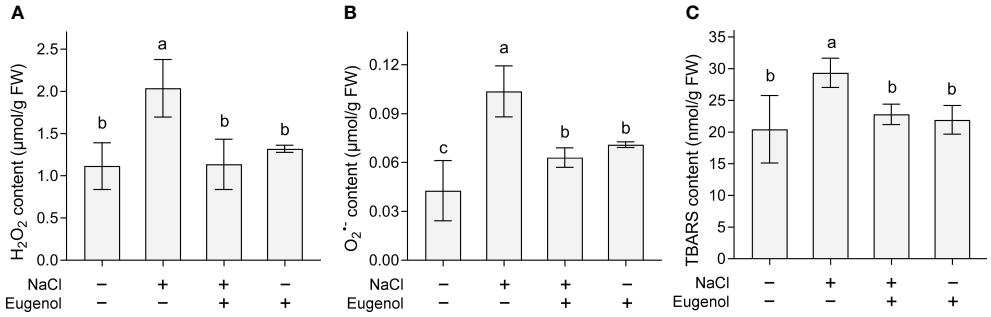

FIGURE 2
Effect of eugenol on the content of H_2O_2, $O_2^{\bullet-}$, and TBARS contents in tobacco seedlings under salt stress. **(A)** H_2O_2 content. **(B)** $O_2^{\bullet-}$ content. **(C)** TBARS content. Different lowercase letters indicate significant difference among different treatments (n = 3, $p < 0.05$, LSD).

NBT. Salt stress induced extensive NBT staining in leaf. Addition of eugenol showed slight NBT staining in the leaf of seedlings under salt stress (Figure 3E). Eugenol was able to attenuated salt-induced cell death in leaf indicated by Trypan blue staining (Figure 3F). All of these results suggested that eugenol alleviated NaCl-induced oxidative injury in tobacco seedlings.

3.3 Eugenol enhanced antioxidative capacity in tobacco seedlings under salt stress

Four typical antioxidative enzymes (SOD, POD, CAT and APX) were measured in tobacco seedlings. The activities of these enzymes were enhanced upon NaCl exposure. Compared to NaCl treatment alone, adding eugenol further significantly increased the activity of SOD, POD, CAT and APX by 11.2%, 74.0%, 44.9%, and 78.8%, respectively (Figure 4). Treatment with eugenol alone was able to increase the activities of SOD, POD, and CAT as compared to the control (Figures 4A–C).

AsA and GSH are two important antioxidants, belonging to non-enzymatic antioxidative system. Compared to NaCl treatment alone, adding eugenol significantly enhanced the content of AsA and GSH by 30.6% and 19.8%, respectively, in tobacco seedlings (Figures 5A, B). DHA and GSSG are the oxidized forms of AsA and GSH, respectively. Compared to NaCl treatment alone, adding eugenol significantly decreased the content of DHA and GSSG by 26.9% and 24.9%, respectively, in tobacco seedlings (Figures 5C, D). In addition, salt stress remarkably decreased the ratio of AsA/DHA and GSH/GSSG in tobacco seedlings, but adding eugenol significantly increased them by 78.3% and 58.9%, respectively (Figures 5E, F).

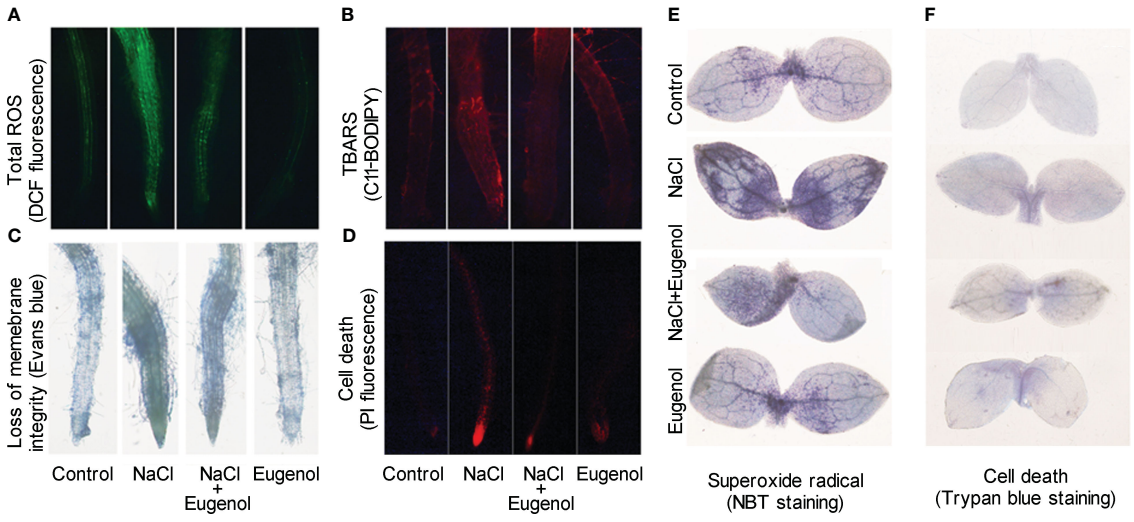

FIGURE 3
Histochemical detection of ROS and oxidative injury in tobacco seedlings upon NaCl and Eugenol treatment. **(A)** Total ROS in roots indicated by DCF fluorescence. **(B)** TBARS in roots indicated by C11BODYPI fluorescence. **(C)** Loss of membrane integrity in roots indicated by staining of Evans blue. **(D)** Cell death in roots indicated by PI fluorescence. **(E)** H_2O_2 content in leaves indicated by DAB staining. **(F)** Cell death in leaves indicated by Trypan blue staining.

10.3389/fpls.2023.1284480

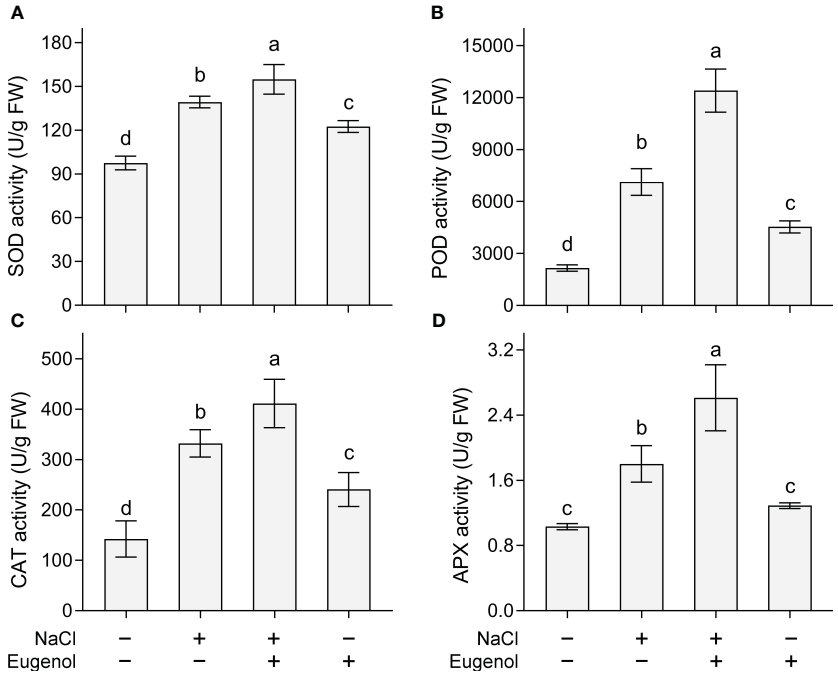

FIGURE 4
Effect of eugenol on the activities of antioxidant enzymes on tobacco seedlings under salt stress. **(A)** SOD activity. **(B)** POD activity. **(C)** CAT activity. **(D)** APX activity. Different lowercase letters indicate significant difference among different treatments (n = 3, $p < 0.05$, LSD).

3.4 Eugenol enhanced the content osmotic metabolites in tobacco seedling under salt stress

In plant cells, proline is a metabolite regulating osmotic adaption induced by salt stress. Proline content increased proline in tobacco seedlings upon salt stress. Adding eugenol further enhanced proline content by 15.9% (Figure 6A). Compared to control, salt stress decreased the content of starch and soluble sugar in seedlings. Adding eugenol significantly the content of starch and soluble sugar by 26.9% and 24.9% (Figures 6B, C), respectively, as compared to NaCl-treatment alone.

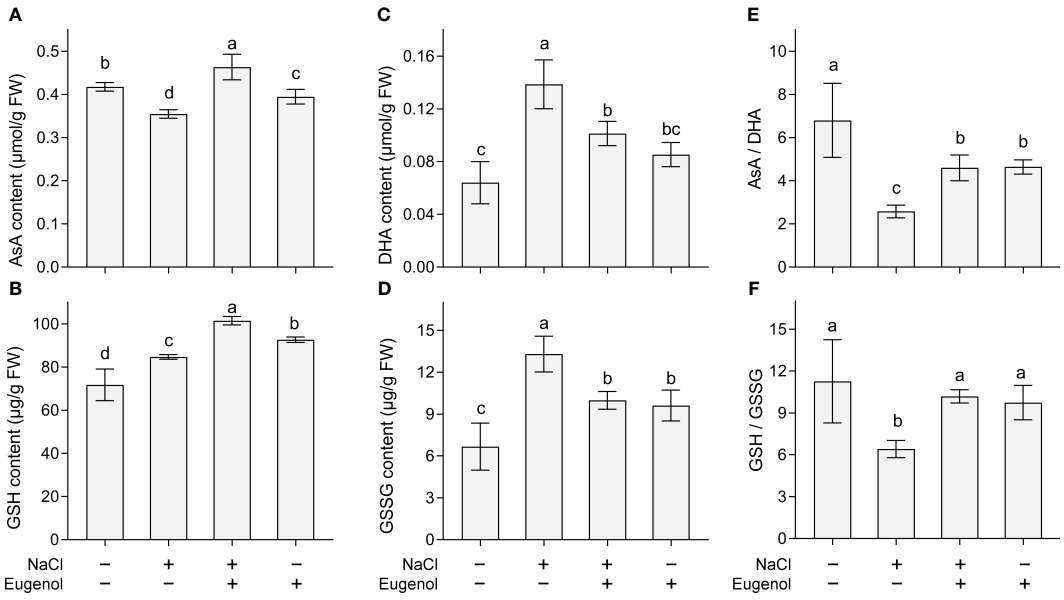

FIGURE 5
Effect of eugenol on antioxidants in tobacco seedlings under salt stress. **(A)** AsA content. **(B)** GSH content. **(C)** DHA content. **(D)** GSSG content. **(E)** The ratio of AsA to DHA. **(F)** The ratio of GSH to GSSG. Different lowercase letters indicate significant difference among different treatments (n = 3, $p < 0.05$, LSD).

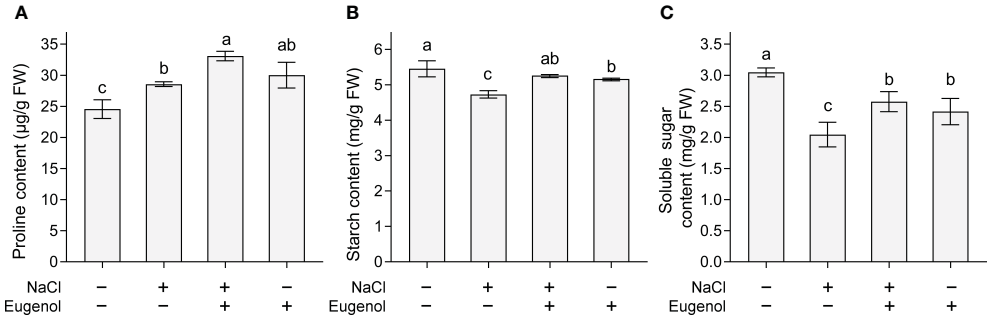

FIGURE 6
Effect of eugenol on the metabolites in tobacco seedlings under salt stress. **(A)** Proline content. **(B)** Starch content. **(C)** Soluble sugar content. Different lowercase letters indicate significant difference among different treatments (n = 3, $p < 0.05$, LSD).

3.5 Eugenol modulated ionic balance in tobacco seedlings under salt stress

Na^+ and K^+ play negative and positive roles, respectively, in regulating plant growth under salt stress. Adding eugenol significantly decreased Na^+ content by 20.2% and increased K^+ content by 12.8% in NaCl-treated tobacco seedlings (Figures 7A, B). Salt stress decreased the ratio of K^+/Na^+, but adding eugenol significantly increased the ratio by 41.0% in NaCl-treated seedlings (Figure 7C).

SOS1 and *NHX1* are two important transporters maintaining ionic homeostasis in plant cells under salt stress. Compared to NaCl treatment alone, treatment with NaCl + eugenol resulted in significant increase in the expression of *NtSOS1* and *NtNHX1* by 57.2% and 135.9%, respectively, in tobacco seedlings (Figure 8).

3.6 Hierarchical cluster analysis of eugenol-regulated physiological changes

The hierarchical cluster analysis was performed to fully understand the changes of physiological parameters obtained above. All the parameters were clustered to three groups (I, II, and III) under the treatment of NaCl and eugenol (Figure 9A). The group I consisted of biomass indexes (root length and fresh weight), the content of starch and soluble sugar, AsA/DHA, GSH/GSSG, and *NtNHX1* expression. All of these parameters were beneficial for plant tolerance against salt stress. In group I, NaCl treatment resulted in the decrease in these parameters while adding eugenol enhanced them in NaCl-treated seedlings. The group II consisted of TBARS, H_2O_2, and $O_2^{\cdot-}$, all of which were injury indexes. In group II, NaCl treatment enhanced all these three parameters while adding eugenol decreased them in NaCl-treated seedlings. Group III consisted of SOD, POD, CAT, APX, proline, and *NtSOS1* expression. All of these parameters were beneficial for plant growth under salt stress. All of these parameters were beneficial for plant tolerance against salt stress. In group III, NaCl treatment increased these parameters while adding eugenol further enhanced them in NaCl-treated seedlings (Figure 9A).

Pearson correlation analysis was performed to help understand the relationships among different parameters during eugenol-conferred salt tolerance (Figure 9B). The biomass indexes (root length and fresh weight) were positively correlated to K^+/Na^+, K^+, GSH/GSSG, AsA/DHA, starch, and soluble sugar, respectively. This suggested that these parameters contributed to eugenol-promoted plant growth under salt stress. The biomass indexes were negatively correlated to Na^+, GSSG, DHA, TBARS, H_2O_2, and $O_2^{\cdot-}$, suggesting that these parameters contributed to salt-induced phytotoxicity. Na^+ was positively correlated to GSSG, DHA, TBARS, H_2O_2, and $O_2^{\cdot-}$, respectively. This suggested that Na^+ accumulation led to

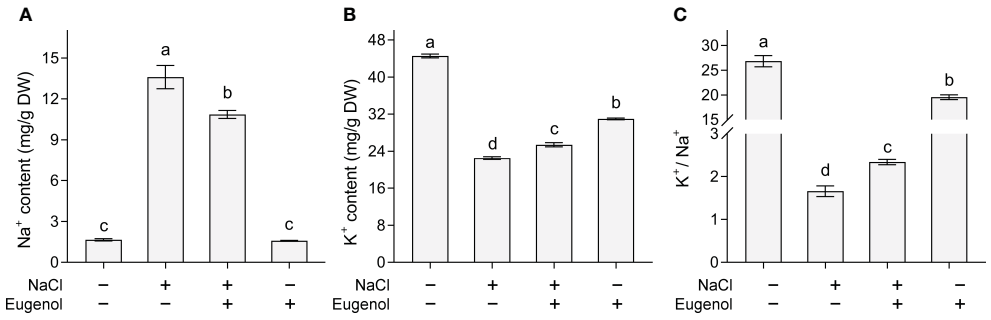

FIGURE 7
Effect of eugenol on ionic balance in tobacco seedlings under salt stress. **(A)** Na^+ content. **(B)** K^+ content. **(C)** The ratio of K^+ to Na^+. Different lowercase letters indicate significant difference among different treatments (n = 3, $p < 0.05$, LSD).

10.3389/fpls.2023.1284480

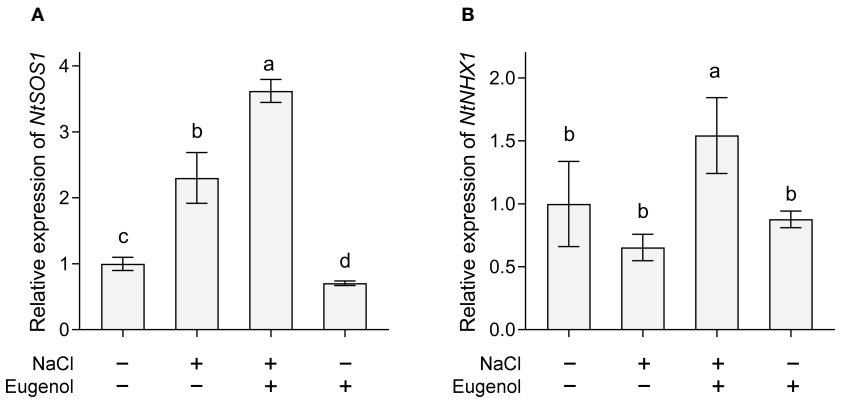

FIGURE 8
Effect of eugenol on the expression of *NtSOS1* **(A)** and *NtNHX1* **(B)** in tobacco seedlings under salt stress. Different lowercase letters indicate significant difference among different treatments (n = 3, $p < 0.05$, LSD).

oxidative injury by damaging redox balance, an effect that could be reversed by adding eugenol. *NtSOS1* was positively correlated to Na^+, suggesting the role of *NtSOS1* in detoxifying excessive Na^+.

4 Discussion

Seeking effective biostimulants with the ability of conferring plant salt tolerance is a promising approach to help crops combat salinity (Ahmad et al., 2022). Eugenol is natural compound derived from plants. Eugenol has broad antimicrobial activity (Marchese et al., 2017), but the role of eugenol in modulating plant physiology is rarely known. In this study, we revealed the novel role of eugenol in inducing salt tolerance in plants. Eugenol triggered salt tolerance by activating antioxidative capacity, adjusting osmotic balance, and modulating ionic homeostasis in tobacco seedlings.

4.1 Eugenol reduces ROS accumulation under salt stress

Plant cells maintain low level of ROS working as signaling molecule to regulate cell functions and plant development, but over-

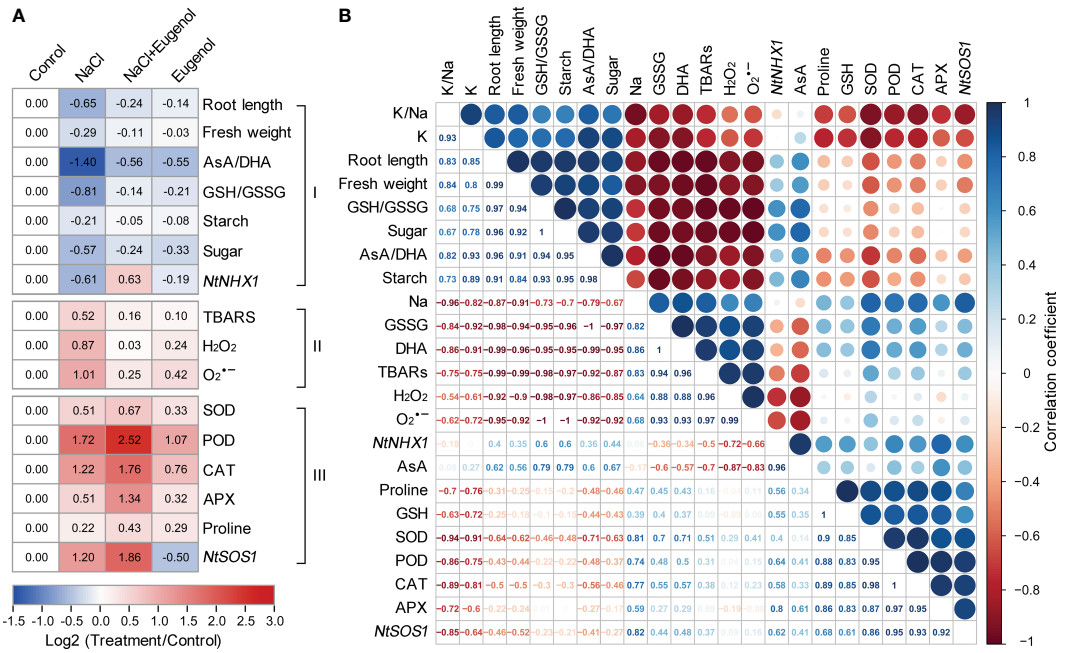

FIGURE 9
Cluster and correlation analysis among physiological parameters in tobacco seedlings under treatment of NaCl, NaCl + Eugenol, and Eugenol. **(A)** Hierarchical cluster analysis. **(B)** Pearson correlation analysis.

accumulated ROS are detrimental to plants under stress conditions (Hasanuzzaman et al., 2020). Salt stress often induces ROS accumulation, leading top membrane lipid peroxidation and cell death (Zhao et al., 2021). Eugenol promoted seedlings growth was linked to the alleviation of oxidative injury and cell death. This mainly due to the decrease in the level of cellular ROS (including both H_2O_2 and $O_2^{\cdot-}$) in tobacco seedlings. Eugenol-restricted ROS may resulted from the enhancement of the activity of antioxidative enzymes in NaCl-treated seedlings. $O_2^{\cdot-}$ is easily generated with only one electron transferred to oxygen. Therefore, $O_2^{\cdot-}$ is often considered as the first ROS generated in plant cells upon stress conditions (Larosa and Remacle, 2018). SOD acts as the scavenger of $O_2^{\cdot-}$ by catalyzing $O_2^{\cdot-}$ to H_2O_2 that can be further metabolized to H_2O by CAT, POD, and APX (Choudhury et al., 2017). Exogenous regulation of salt tolerance has been associated with the activation of antioxidant enzymes in tomato and lettuce (Patani et al., 2023; El-Salam Shalaby, 2024). In the present study, we found that salt stress induced slight increase in the activity of these enzymes. The possible reason was that salt-induced ROS accumulation act as signal to initiate enzymatic antioxidative system (Yang and Guo, 2018). However, the increase in these enzymes may not enough to scavenge large amounts of ROS induced by salt. Adding eugenol further enhanced the activity of these enzymes, which may helped further decrease ROS level in tobacco seedlings under salt stress. It has been reported that eugenol acts as antioxidant agent protecting oxidative injury by activating antioxidative enzymes in liver and lung (Yogalakshmi et al., 2010; Huang et al., 2015). It seems that eugenol can activate enzymatic antioxidative system in both plant and mammalian cells upon stress conditions.

AsA and GSH are two important components of non-enzymatic antioxidative system in plants. AsA and GSH can scavenge ROS directly through transferring electron (Briviba et al., 1997; Smirnoff, 2000). The role of GSH and AsA in inhibiting plant ROS accumulation has been identified in salt acclimation (Kumari et al., 2023). Eugenol increased the content of these two antioxidants, which helped tobacco seedlings lower endogenous ROS level under salinity stress. AsA/DHA and GSH/GSSG has been termed as redox managers for maintaining the redox balance in plant cells. Plant cells tend to maintain a favorable cellular environment at a reduced state with relatively high AsA/DHA and GSH/GSSG under normal growth conditions. Stress conditions may disrupt the redox balance to make a shift to oxidized state, which is harmful for cell function and plant development (Debolt et al., 2007; Zechmann, 2017). Eugenol significantly enhanced both AsA/DHA and GSH/GSSG in salt-treated tobacco seedlings, indicating the capability of eugenol in maintaining cell reduced state in order to combat ROS-induced oxidative stress. In addition, AsA-GSH cycle is an important pathway by coupling the transformation of AsA-DHA and GSH-GSSG. AsA-GSH pathway is one of the major pathways of antioxidative defense for detoxifying ROS in plant cells (Hasanuzzaman et al., 2019). Further studies maybe needed to possible regulation of AsA-GSH cycling by eugenol under salt stress.

It has been suggested that eugenol itself can quench ROS directly *in vitro*. And this ability has been associated with eugenol-reduced radicals in mammalian cells (Gülçin, 2011; Pérez-Rosés et al., 2016). Therefore, apart from activating antioxidative system, we speculate that the eugenol entered into plant cells may directly quench cellular ROS upon salt stress. This hypothesis should be confirmed by detecting the uptake and distribution of eugenol in plants and the *in vivo* interaction between eugenol and ROS in the future.

4.2 Eugenol regulates osmotic balance upon salt stress

Osmotic stress is a typical consequences of salt stress in plants. Carbohydrates (such as sugars and starch) and proline are important primary metabolites acting as osmoprotectants to combat salt-induced osmotic stress (Patel et al., 2020). Induction of these osmoregulatory metabolites has been linked to the enhancement of salt tolerance in citrus and cotton plants (Lu et al., 2023; Zhang et al., 2023a). Plant extracts could be used as potential biostimulants with the ability of inducing plant salt tolerance by priming the synthesis of soluble carbohydrates or proline (Ghezal et al., 2016; Pehlivan, 2018; Lorenzo et al., 2019; Rady et al., 2019; Desoky et al., 2020). Salt stress led to an increase in proline content and a decrease in soluble sugar and starch content in tobacco seedlings, suggesting the occurrence of osmotic stress upon salt exposure. Addition of eugenol induced the accumulation of these osmoregulatory substances in NaCl-treated seedlings, indicating the activation of osmotic adjustment. Eugenol-induced high levels of these metabolites may result from the maintenance of cell membrane integrity. Salt stress caused cell membrane damage and the leakage of these metabolite, whereas eugenol stabilized the integrity of cell membrane to prevent metabolite leakage under salt stress. Plant extracts-triggered biosynthesis of osmotic metabolites to improve salinity acclimation via modulating hormonal signaling and metabolic reprogramming (Bulgari et al., 2015; Rehman et al., 2021). In the present study, induction of osmotic metabolites accumulation is one the important strategies for eugenol-conferred salt tolerance. However, how eugenol regulates the biosynthesis and the metabolism of osmoprotectants against salt stress needs further investigation.

4.3 Eugenol regulates ionic balance under salt stress

Maintaining ionic balance inside of cells is important for plants' adaption to salt stress. *SOS1*, a regulatory star of salt tolerance, works on Na^+ detoxification by performing Na^+ efflux out of cells (Núñez-Ramírez et al., 2012). *NHX1* has been identified as a

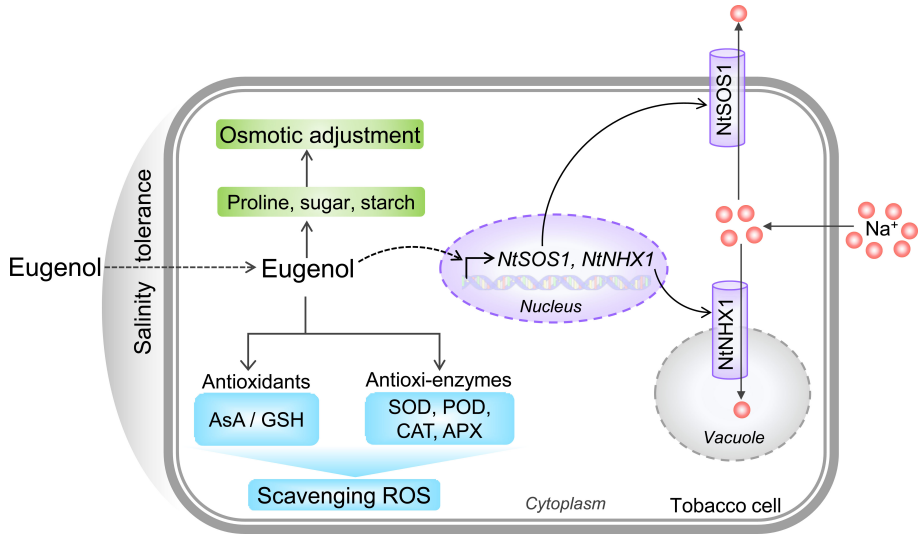

FIGURE 10
Schematic model for eugenol-facilitated three strategies that confer salinity tolerance in tobacco cells. Purple, green, and blue module represents eugenol-regulated ionic balance, osmotic adjustment, and antioxidative capacity, respectively.

tonoplast-located Na^+/H^+ antiporter, detoxifying cytosolic Na^+ through compartmentalizing Na^+ in vacuole (Wu et al., 2019). Thymol can inhibit Na^+ inward flow and reduces Na^+ content in tobacco seedlings by activating *NtSOS1* and *NtNHX1* (Xu et al., 2022). The upregulation of *NtSOS1* expression may contribute to eugenol-induced decrease in Na^+ content in salt-treated tobacco seedlings. In addition, eugenol also up-regulated the expression of *NtNHX1*, which may facilitate the influx of Na^+ into vacuole inside of tobacco cells. However, the distribution of Na^+ in different organelles should be further investigated in order to confirm the possible function of eugenol in distributing intracellular Na^+. Ca^{2+} is an essential regulator of SOS pathway that is a signaling cascade comprising SOS1, SOS2, and SOS3. The SOS3 can be activated through binding to Ca^{2+}. Then Ca^{2+} activated SOS3 recruits and interacts with SOS2 to activate SOS1 (Wang et al., 2022). The Ca^{2+}-SOS3-SOS2 module can also positively regulate vacuolar NHX (Zhao et al., 2021). Eugenol has been reported as an activator of Ca^{2+} channel TRPV1 (transient receptor potential vanilloid channel 1) in mammals. Eugenol can increase intercellular Ca^{2+}, further activating Ca^{2+} signaling cascade in mammalian cells (Jiang et al., 2022). Therefore, it is of interest to further investigate whether eugenol regulates cytosolic Na exclusion and vacuolar Na^+ sequestration in plants by regulating Ca^{2+} signaling.

Plant salt tolerance also involves intrinsic gaseous signaling molecules, such as H_2S (hydrogen sulfide) and NO (nitric oxide). Both H_2S and NO can help plants reestablish redox homeostasis and ionic balance to combat salinity (Wang et al., 2012; Lai et al., 2014). The anti-inflammatory potential of eugenol has been associated with the regulation of endogenous NO in mammals (Barboza et al., 2018). Eugenol can intensify endogenous H_2S in rice plants against heavy metal stress (Hu et al., 2018a). Therefore, further studying the possible involvement of H_2S and NO in eugenol-conferred salt tolerance would help reveal eugenol-primed signaling network for plant salt tolerance.

5 Conclusion

In sum, the present study demonstrates that phytochemical eugenol has the ability of stimulating plant salt tolerance. Eugenol deploys three strategies to ameliorate the detrimental effect of salinity on the growth of tobacco seedlings (Figure 10). First, eugenol detoxifies intracellular Na^+ by upregulating *NtSOS1* (Na^+ efflux) and *NtNHX1* (Na^+ sequestration in vacuole). Second, eugenol promotes osmotic adjustment by inducing the accumulation of metabolites (proline, sugar, and starch). Third, eugenol enhances antioxidative capacity by activating both antioxidants and antioxidative enzymes. The detailed molecular mechanism for eugenol-mediated reestablishment cellular redox homeostasis and ionic balance largely unknown, but our current data propose the novel function of eugenol in regulating plant salinity tolerance. These results would help develop new biostimulant for crop production in saline area, which is important for both applied and fundamental research.

Data availability statement

The original contributions presented in the study are included in the article/supplementary material. Further inquiries can be directed to the corresponding authors.

Author contributions

JX: Conceptualization, Investigation, Methodology, Writing – original draft. TW: Investigation, Writing – review & editing. CS: Investigation, Writing – review & editing. LP: Investigation, Writing – review & editing. JC: Data curation, Investigation, Methodology, Writing – review & editing. XH: Investigation,

Writing – review & editing. TY: Investigation, Writing – review & editing. YG: Investigation, Writing – review & editing. ZL: Investigation, Writing – review & editing. LY: Conceptualization, Writing – review & editing. LZ: Conceptualization, Data curation, Investigation, Writing – review & editing.

Funding

The author(s) declare financial support was received for the research, authorship, and/or publication of this article. This research was funded by Foundation of "Modern Agricultural Technology Industry of Shandong Province System, grant number SDAIT-25-01".

Conflict of interest

The authors declare that the research was conducted in the absence of any commercial or financial relationships that could be construed as a potential conflict of interest.

Publisher's note

References

Ahmad, A., Blasco, B., and Martos, V. (2022). Combating salinity through natural plant extracts based biostimulants: A review. *Front. Plant Sci.* 13. doi: 10.3389/fpls.2022.862034

Ali, A., Petrov, V., Yun, D. J., and Gechev, T. (2023). Revisiting plant salt tolerance: novel components of the SOS pathway. *Trends Plant Sci.* S1360-1385 (23), 1060–1069. doi: 10.1016/j.tplants.2023.1004.1003

Al-Turki, A., Murali, M., Omar, A. F., Rehan, M., and Sayyed, R. Z. (2023). Recent advances in PGPR-mediated resilience toward interactive effects of drought and salt stress in plants. *Front. Microbiol.* 14. doi: 10.3389/fmicb.2023.1214845

Aragüez, I., Osorio, S., Hoffmann, T., Rambla, J. L., Medina-Escobar, N., Granell, A., et al. (2013). Eugenol production in achenes and receptacles of strawberry fruits is catalyzed by synthases exhibiting distinct kinetics. *Plant Physiol.* 163 (2), 946–958. doi: 10.1104/pp.113.224352

Barboza, J. N., da Silva Maia Bezerra Filho, C., Silva, R. O., Medeiros, J. V. R., and de Sousa, D. P. (2018). An overview on the anti-inflammatory potential and antioxidant profile of eugenol. *Oxid. Med. Cell. Longev.* 2018, 3957262. doi: 10.1155/2018/3957262

Barragán, V., Leidi, E. O., Andrés, Z., Rubio, L., De Luca, A., Fernández, J. A., et al. (2012). Ion exchangers NHX1 and NHX2 mediate active potassium uptake into vacuoles to regulate cell turgor and stomatal function in. *Arabidopsis. Plant Cell* 24 (3), 1127–1142. doi: 10.1105/tpc.111.095273

Briviba, K., Klotz, L. O., and Sies, H. (1997). Toxic and signaling effects of photochemically or chemically generated singlet oxygen in biological systems. *Biol. Chem.* 378 (11), 1259–1265.

Bulgari, R., Cocetta, G., Trivellini, A., Vernieri, P., and Ferrante, A. (2015). Biostimulants and crop responses: a review. *Biol. Agric. Hortic.* 31 (1), 1–17. doi: 10.1080/01448765.2014.964649

Chen, C., Chen, H., Zhang, Y., Thomas, H. R., Frank, M. H., He, Y., et al. (2020a). TBtools: An integrative toolkit developed for interactive analyses of big biological data. *Mol. Plant* 13 (8), 1194–1202. doi: 10.1016/j.molp.2020.06.009

Chen, H., Lai, L., Li, L., Liu, L., Jakada, B. H., Huang, Y., et al. (2020b). AcoMYB4, an *Ananas comosus* L. MYB transcription factor, functions in osmotic stress through negative regulation of ABA signaling. *Int. J. Mol. Sci.* 21 (16), 5727. doi: 10.3390/ijms21165727

Choudhury, F. K., Rivero, R. M., Blumwald, E., and Mittler, R. (2017). Reactive oxygen species, abiotic stress and stress combination. *Plant J.* 90 (5), 856–867. doi: 10.1111/tpj.13299

Debolt, S., Melino, V., and Ford, C. M. (2007). Ascorbate as a biosynthetic precursor in plants. *Ann. Bot.* 99 (1), 3–8. doi: 10.1093/aob/mcl236

Desoky, E.-S. M., El-Maghraby, L. M. M., Awad, A. E., Abdo, A. I., Rady, M. M., and Semida, W. M. (2020). Fennel and ammi seed extracts modulate antioxidant defence system and alleviate salinity stress in cowpea (*Vigna unguiculata*). *Sci. Hortic.* 272, 109576. doi: 10.1016/j.scienta.2020.109576

Drummen, G. P., van Liebergen, L. C., Op den Kamp, J. A., and Post, J. A. (2002). C11-BODIPY(581/591), an oxidation-sensitive fluorescent lipid peroxidation probe: (micro)spectroscopic characterization and validation of methodology. *Free Radic. Biol. Med.* 33 (4), 473–490. doi: 10.1016/s0891-5849(02)00848-1

El-Salam Shalaby, O. A. (2024). Moringa leaf extract increases tolerance to salt stress, promotes growth, increases yield, and reduces nitrate concentration in lettuce plants. *Sci. Hortic-Amsterdam* 325, 112654. doi: 10.1016/j.scienta.2023.112654

Gao, Z., Zhang, J., Zhang, J., Zhang, W., Zheng, L., Borjigin, T., et al. (2022). Nitric oxide alleviates salt-induced stress damage by regulating the ascorbate-glutathione cycle and Na^+/K^+ homeostasis in *Nitraria tangutorum* Bobr. *Plant Physiol. Biochem.* 173, 46–58. doi: 10.1016/j.plaphy.2022.01.017

Ge, L., Yang, X., Liu, Y., Tang, H., Wang, Q., Chu, S., et al. (2023). Improvement of seed germination under salt stress via overexpressing *Caffeic Acid O-methyltransferase 1 (SlCOMT1)* in *Solanum lycopersicum* L. *Int. J. Mol. Sci.* 24 (1), 734. doi: 10.3390/ijms24010734

Ghezal, N., Rinez, I., Sbai, H., Saad, I., Farooq, M., Rinez, A., et al. (2016). Improvement of *Pisum sativum* salt stress tolerance by bio-priming their seeds using *Typha angustifolia* leaves aqueous extract. *S. Afr. J. Bot.* 105, 240–250. doi: 10.1016/j.sajb.2016.04.006

Gill, S. S., and Tuteja, N. (2010). Reactive oxygen species and antioxidant machinery in abiotic stress tolerance in crop plants. *Plant Physiol. Biochem.* 48 (12), 909–930. doi: 10.1016/j.plaphy.2010.08.016

Guijarro-Real, C., Adalid-Martinez, A. M., Gregori-Montaner, A., Prohens, J., Rodriguez-Burruezo, A., and Fita, A. (2020). Factors affecting germination of *Diplotaxis erucoides* and their effect on selected quality properties of the germinated products. *Sci. Hortic-Amsterdam* 261, 109013. doi: 10.1016/j.scienta.2019.109013

Gülçin, İ. (2011). Antioxidant activity of eugenol: A structure–activity relationship study. *J. Med. Food* 14 (9), 975–985. doi: 10.1089/jmf.2010.0197

Hasanuzzaman, M., Bhuyan, M. H. M. B., Anee, T. I., Parvin, K., Nahar, K., Mahmud, J. A., et al. (2019). Regulation of ascorbate-glutathione pathway in mitigating oxidative damage in plants under abiotic stress. *Antioxidants* 8 (9), 384. doi: 10.3390/antiox8090384

Hasanuzzaman, M., Bhuyan, M., Parvin, K., Bhuiyan, T. F., Anee, T. I., Nahar, K., et al. (2020). Regulation of ROS metabolism in plants under environmental stress: A review of recent experimental evidence. *Int. J. Mol. Sci.* 21 (22), 8695. doi: 10.3390/ijms21228695

Hasanuzzaman, M., Raihan, M. R. H., Masud, A. A. C., Rahman, K., Nowroz, F., Rahman, M., et al. (2021). Regulation of reactive oxygen species and antioxidant defense in plants under salinity. *Int. J. Mol. Sci.* 22 (17), 9326. doi: 10.3390/ijms22179326

Hu, L., Li, H., Huang, S., Wang, C., Sun, W.-J., Mo, H.-Z., et al. (2018a). Eugenol confers cadmium tolerance via intensifying endogenous hydrogen sulfide signaling in *Brassica rapa*. *J. Agric. Food Chem.* 66 (38), 9914–9922. doi: 10.1021/acs.jafc.8b03098

Hu, Q., Zhou, M., and Wei, S. (2018b). Progress on the antimicrobial activity research of clove oil and eugenol in the food antisepsis field. *J. Food Sci.* 83 (6), 1476–1483. doi: 10.1111/1750-3841.14180

Huang, X., Liu, Y., Lu, Y., and Ma, C. (2015). Anti-inflammatory effects of eugenol on lipopolysaccharide-induced inflammatory reaction in acute lung injury via regulating inflammation and redox status. *Int. Immunopharmacol.* 26 (1), 265–271. doi: 10.1016/j.intimp.2015.03.026

Jia, C., Cao, D., Ji, S., Zhang, X., and Muhoza, B. (2020). Tannic acid-assisted cross-linked nanoparticles as a delivery system of eugenol: The characterization, thermal degradation and antioxidant properties. *Food Hydrocolloid.* 104, 105717. doi: 10.1016/j.foodhyd.2020.105717

Jiang, Y., Feng, C., Shi, Y., Kou, X., and Le, G. (2022). Eugenol improves high-fat diet/streptomycin-induced type 2 diabetes mellitus (T2DM) mice muscle dysfunction by alleviating inflammation and increasing muscle glucose uptake. *Biochem. Biophys. Res. Commun.* 9. doi: 10.3389/fnut.2022.1039753

Kellermeier, F., Chardon, F., and Amtmann, A. (2013). Natural variation of arabidopsis root architecture reveals complementing adaptive strategies to potassium starvation. *Plant Physiol.* 161 (3), 1421–1432. doi: 10.1104/pp.112.211144

Koeduka, T., Fridman, E., Gang, D. R., Vassão, D. G., Jackson, B. L., Kish, C. M., et al. (2006). Eugenol and isoeugenol, characteristic aromatic constituents of spices, are biosynthesized via reduction of a coniferyl alcohol ester. *Proc. Natl. Acad. Sci. U.S.A.* 103 (26), 10128–10133. doi: 10.1073/pnas.0603732103

Kumari, S., Kaur, H., Jain, A., Hussain, S. J., Siddiqui, M. H., and Khan, M. I. R. (2023). Hydrogen sulfide modulates ascorbate-glutathione system, osmolytes production, nutrient content and yield responses under salt stress in wheat. *S. Afr. J. Bot.* 160, 295–308. doi: 10.1016/j.sajb.2023.07.022

Lai, D., Mao, Y., Zhou, H., Li, F., Wu, M., Zhang, J., et al. (2014). Endogenous hydrogen sulfide enhances salt tolerance by coupling the reestablishment of redox homeostasis and preventing salt-induced K^+ loss in seedlings of *Medicago sativa*. *Plant Sci.* 225, 117–129. doi: 10.1016/j.plantsci.2014.06.006

Larosa, V., and Remacle, C. (2018). Insights into the respiratory chain and oxidative stress. *Biosci. Rep.* 38 (5), BSR20171492. doi: 10.1042/bsr20171492

Liu, M. H., Lv, Y., Cao, B. L., Chen, Z. J., and Xu, K. (2023). Physiological and molecular mechanism of ginger *Zingiber officinale* Roscoe) seedling response to salt stress. *Front. Plant Sci.* 14. doi: 10.3389/fpls.2023.1073434

Lorenzo, P., Souza-Alonso, P., Guisande-Collazo, A., and Freitas, H. (2019). Influence of *Acacia dealbata* Link bark extracts on the growth of *Allium cepa* L. plants under high salinity conditions. *J. Sci. Food Agric.* 99 (8), 4072–4081. doi: 10.1002/jsfa.9637

Lu, K., Yan, L., Riaz, M., Babar, S., Hou, J., Zhang, Y., et al. (2023). "Exogenous boron alleviates salt stress in cotton by maintaining cell wall structure and ion homeostasis". *Plant Physiol. Bioch* 201, 107858. doi: 10.1016/j.plaphy.2023.107858

Luo, S. L., Liu, Z. C., Wan, Z. L., He, X. X., Lv, J., Yu, J. H., et al. (2023). Foliar spraying of NaHS alleviates cucumber salt stress by maintaining Na^+/K^+ balance and activating salt tolerance signaling pathways. *Plants-Basel* 12 (13), 2450. doi: 10.3390/plants12132450

Ma, L., Liu, X. H., Lv, W. J., and Yang, Y. Q. (2022). Molecular mechanisms of plant responses to salt stress. *Front. Plant Sci.* 13. doi: 10.3389/fpls.2022.934877

Mansour, M. M. F., and Ali, E. F. (2017). Evaluation of proline functions in saline conditions. *Phytochemistry* 140, 52–68. doi: 10.1016/j.phytochem.2017.04.016

Marchese, A., Barbieri, R., Coppo, E., Orhan, I. E., Daglia, M., Nabavi, S. F., et al. (2017). Antimicrobial activity of eugenol and essential oils containing eugenol: A mechanistic viewpoint. *Crit. Rev. Microbiol.* 43 (6), 668–689. doi: 10.1080/1040841X.2017.1295225

Morcia, C., Malnati, M., and Terzi, V. (2011). *In vitro* antifungal activity of terpinen-4-ol, eugenol, carvone, 1,8-cineole (eucalyptol) and thymol against mycotoxigenic plant pathogens. *Food Addit. Contam. Part A* 29 (3), 415–422. doi: 10.1080/19440049.2011.643458

Negrão, S., Schmöckel, S. M., and Tester, M. (2017). Evaluating physiological responses of plants to salinity stress. *Ann. Bot.* 119 (1), 1–11. doi: 10.1093/aob/mcw191

Núñez-Ramírez, R., Sánchez-Barrena, M. J., Villalta, I., Vega, J. F., Pardo, J. M., Quintero, F. J., et al. (2012). Structural insights on the plant Salt-Overly-Sensitive 1 (SOS1) Na^+/H^+ antiporter. *J. Mol. Biol.* 424 (5), 283–294. doi: 10.1016/j.jmb.2012.09.015

Olea, A. F., Bravo, A., Martínez, R., Thomas, M., Sedan, C., Espinoza, L., et al. (2019). Antifungal activity of eugenol derivatives against *Botrytis cinerea*. *Molecules* 24 (7), 1239. doi: 10.3390/molecules24071239

Patani, A., Prajapati, D., Ali, D., Kalasariya, H., Yadav, V. K., Tank, J., et al. (2023). Evaluation of the growth-inducing efficacy of various *Bacillus* species on the salt-stressed tomato (Lycopersicon esculentum Mill.). *Front. Plant Sci.* 14. doi: 10.3389/fpls.2023.1168155

Patel, M. K., Kumar, M., Li, W., Luo, Y., Burritt, D. J., Alkan, N., et al. (2020). Enhancing salt tolerance of plants: From metabolic reprogramming to exogenous chemical treatments and molecular approaches. *Cells* 9 (11), 2492. doi: 10.3390/cells9112492

Pehlivan, N. (2018). Salt stress relief potency of whortleberry extract biopriming in maize. *3 Biotech.* 8 (2), 89. doi: 10.1007/s13205-018-1113-6

Pérez-Rosés, R., Risco, E., Vila, R., Peñalver, P., and Cañigueral, S. (2016). Biological and nonbiological antioxidant activity of some essential oils. *J. Agric. Food Chem.* 64 (23), 4716–4724. doi: 10.1021/acs.jafc.6b00986

Quamruzzaman, M., Manik, S. M. N., Shabala, S., and Zhou, M. (2021). Improving performance of salt-grown crops by exogenous application of plant growth regulators. *Biomolecules* 11 (6), 788. doi: 10.3390/biom11060788

Rady, M. M., Desoky, E. S. M., Elrys, A. S., and Boghdady, M. S. (2019). Can licorice root extract be used as an effective natural biostimulant for salt-stressed common bean plants? *S. Afr. J. Bot.* 121, 294–305. doi: 10.1016/j.sajb.2018.11.019

Rehman, H.U., Alharby, H. F., Bamagoos, A. A., Abdelhamid, M. T., and Rady, M. M. (2021). Sequenced application of glutathione as an antioxidant with an organic biostimulant improves physiological and metabolic adaptation to salinity in wheat. *Plant Physiol. Biochem.* 158, 43–52. doi: 10.1016/j.plaphy.2020.11.041

Shrivastava, P., and Kumar, R. (2015). Soil salinity: A serious environmental issue and plant growth promoting bacteria as one of the tools for its alleviation. *Saudi J. Biol. Sci.* 22 (2), 123–131. doi: 10.1016/j.sjbs.2014.12.001

Smirnoff, N. (2000). Ascorbic acid: metabolism and functions of a multi-facetted molecule. *Curr. Opin. Plant Biol.* 3 (3), 229–235. doi: 10.1016/S1369-5266(00)80070-9

Song, R. F., Li, T. T., and Liu, W. C. (2021). Jasmonic acid impairs arabidopsis seedling salt stress tolerance through MYC2-Mediated repression of *CAT2* expression. *Front. Plant Sci.* 12. doi: 10.3389/fpls.2021.730228

Sun, G., Geng, S., Zhang, H., Jia, M., Wang, Z., Deng, Z., et al. (2022). Matrilineal empowers wheat pollen with haploid induction potency by triggering postmitosis reactive oxygen species activity. *New Phytol.* 233 (6), 2405–2414. doi: 10.1111/nph.17963

Sun, H., Sun, X., Wang, H., and Ma, X. (2020). Advances in salt tolerance molecular mechanism in tobacco plants. *Hereditas* 157, 5. doi: 10.1186/s41065-020-00118-0

Taleuzzaman, M., Jain, P., Verma, R., Iqbal, Z., and Mirza, A. M. (2021). Eugenol as a potential drug candidate: A review. *Curr. Top. Med. Chem.* 21 (20), 1804–1815. doi: 10.2174/1568026621666210701141433

van Zelm, E., Zhang, Y., and Testerink, C. (2020). Salt tolerance mechanisms of plants. *Annu. Rev. Plant Biol.* 71 (1), 403–433. doi: 10.1146/annurev-arplant-050718-100005

Wang, C.-F., Han, G.-L., Yang, Z.-R., Li, Y.-X., and Wang, B.-S. (2022). Plant salinity sensors: Current understanding and future directions. *Front. Plant Sci.* 13. doi: 10.3389/fpls.2022.859224

Wang, Y., Li, L., Cui, W., Xu, S., Shen, W., and Wang, R. (2012). Hydrogen sulfide enhances alfalfa (*Medicago sativa*) tolerance against salinity during seed germination by nitric oxide pathway. *Plant Soil* 351 (1), 107–119. doi: 10.1007/s11104-011-0936-2

Wang, B. K., Wang, J., Yang, T., Wang, J. X., Dai, Q., Zhang, F. L., et al. (2023a). The transcriptional regulatory network of hormones and genes under salt stress in tomato plants (*Solanum lycopersicum* L.). *Front. Plant Sci.* 14. doi: 10.3389/fpls.2023.1115593

Wang, Z., Zhang, W., Huang, W., Biao, A., Lin, S., Wang, Y., et al. (2023b). Salt stress affects the fruit quality of *Lycium ruthenicum* Murr. *Ind. Crop Prod.* 193, 116240. doi: 10.1016/j.indcrop.2023.116240

Wang, B., Zhang, J., Pei, D., and Yu, L. (2021). Combined effects of water stress and salinity on growth, physiological, and biochemical traits in two walnut genotypes. *Physiol. Plant* 172 (1), 176–187. doi: 10.1111/ppl.13316

Wei, T., and Simko, V. (2017). *"R package "corrplot": Visualization of a correlation matrix (Version 0.84)"*. Available at: https://github.com/taiyun/corrplot.

Wu, H., Shabala, L., Zhou, M., Su, N., Wu, Q., Ul-Haq, T., et al. (2019). Root vacuolar Na^+ sequestration but not exclusion from uptake correlates with barley salt tolerance. *Plant J.* 100 (1), 55–67. doi: 10.1111/tpj.14424

Xiao, F., and Zhou, H. P. (2023). Plant salt response: Perception, signaling, and tolerance. *Front. Plant Sci.* 13. doi: 10.3389/fpls.2022.1053699

Xu, L., Song, J. Q., Wang, Y. L., Liu, X. H., Li, X. L., Zhang, B., et al. (2022). Thymol improves salinity tolerance of tobacco by increasing the sodium ion efflux and enhancing the content of nitric oxide and glutathione. *BMC Plant Biol.* 22 (1), 31. doi: 10.1186/s12870-021-03395-7

Yang, Y., and Guo, Y. (2018). Unraveling salt stress signaling in plants. *J. Integr. Plant Biol.* 60 (9), 796–804. doi: 10.1111/jipb.12689

Ye, X., Ling, T., Xue, Y., Xu, C., Zhou, W., Hu, L., et al. (2016). Thymol mitigates cadmium stress by regulating glutathione levels and reactive oxygen species homeostasis in tobacco seedlings. *Molecules* 21 (10), 1339. doi: 10.3390/molecules21101339

Ye, X.-F., Xue, Y., Ling, T., Wang, Y., Yu, X.-N., Cheng, C., et al. (2017). Cinnamaldehyde ameliorates cadmium-inhibited root elongation in tobacco seedlings via decreasing endogenous hydrogen sulfide production. *Molecules* 22 (1), 15. doi: 10.3390/molecules22010015

Yogalakshmi, B., Viswanathan, P., and Anuradha, C. V. (2010). Investigation of antioxidant, anti-inflammatory and DNA-protective properties of eugenol in thioacetamide-induced liver injury in rats. *Toxicology* 268 (3), 204–212. doi: 10.1016/j.tox.2009.12.018

Yu, Z., Duan, X., Luo, L., Dai, S., Ding, Z., and Xia, G. (2020). How plant hormones mediate salt stress responses. *Trends. Plant Sci.* 25 (11), 1117–1130. doi: 10.1016/j.tplants.2020.06.008

Zechmann, B. (2017). Diurnal changes of subcellular glutathione content in *Arabidopsis thaliana*. *Biol. Plant* 61 (4), 791–796. doi: 10.1007/s10535-017-0729-4

Zhang, W. B., He, X. L., Chen, X. J., Han, H. W., Shen, B. R., Diao, M., et al. (2023b). Exogenous selenium promotes the growth of salt-stressed tomato seedlings by regulating ionic homeostasis, activation energy allocation and CO_2 assimilation. *Front. Plant Sci.* 14. doi: 10.3389/fpls.2023.1206246

Zhang, M. M., Li, X. Y., Wang, X. L., Feng, J. P., and Zhu, S. P. (2023a). Potassium fulvic acid alleviates salt stress of citrus by regulating rhizosphere microbial community, osmotic substances and enzyme activities. *Front. Plant Sci.* 14. doi: 10.3389/fpls.2023.1161469

Zhang, W. D., Wang, P., Bao, Z., Ma, Q., Duan, L. J., Bao, A. K., et al. (2017). SOS1, HKT1;5, and NHX1 synergistically modulate Na^+ homeostasis in the halophytic grass *Puccinellia tenuiflora*. *Front. Plant Sci.* 8. doi: 10.3389/fpls.2017.00576

Zhao, M. Y., Jin, J. Y., Wang, J. M., Gao, T., Luo, Y., Jing, T. T., et al. (2022). Eugenol functions as a signal mediating cold and drought tolerance via UGT71A59-mediated glucosylation in tea plants. *Plant J.* 109 (6), 1489–1506. doi: 10.1111/tpj.15647

Zhao, S., Zhang, Q., Liu, M., Zhou, H., Ma, C., and Wang, P. (2021). Regulation of plant responses to salt stress. *Int. J. Mol. Sci.* 22 (9), 4609. doi: 10.3390/ijms22094609

frontiers | Frontiers in Plant Science

TYPE Original Research
PUBLISHED 24 January 2024
DOI 10.3389/fpls.2023.1342219

OPEN ACCESS

EDITED BY
Zulfiqar Ali Sahito,
Zhejiang University of Technology, China

REVIEWED BY
Akanksha Sehgal,
Agricultural Research Service (USDA), United States
Wenhuai Li,
Inner Mongolia University, China
Junhui Cheng,
Xinjiang Agricultural University, China

*CORRESPONDENCE
Jia Mi
jiami@sxu.edu.cn

†These authors have contributed equally to this work

RECEIVED 21 November 2023
ACCEPTED 29 December 2023
PUBLISHED 24 January 2024

CITATION
Mi J, Ren X, Shi J, Wang F, Wang Q, Pang H, Kang L and Wang C (2024) An insight into the different responses to salt stress in growth characteristics of two legume species during seedling growth.
Front. Plant Sci. 14:1342219.
doi: 10.3389/fpls.2023.1342219

An insight into the different responses to salt stress in growth characteristics of two legume species during seedling growth

Jia Mi [1,2,3*†], Xinyue Ren [1†], Jing Shi [4], Fei Wang [1], Qianju Wang [1], Haiyan Pang [1], Lifang Kang [5] and Changhui Wang [3,6,7]

[1]Shanxi Key Laboratory of Ecological Restoration on Loess Plateau, Institute of Loess Plateau, Shanxi University, Taiyuan, China, [2]Field Scientific Observation and Research Station of the Ministry of Education for Subalpine Grassland Ecosystem in Shanxi, Ningwu, China, [3]Shanxi Key Laboratory of Grassland Ecological Protection and Native Grass Germplasm Innovation, Shanxi Agricultural University, Taigu, China, [4]College of Environment and Resources Sciences, Shanxi University, Taiyuan, China, [5]Key Laboratory of Plant Resources and Beijing Botanical Garden, Institute of Botany, Chinese Academy of Sciences, Beijing, China, [6]College of Grassland Science, Shanxi Agricultural University, Taigu, China, [7]Observation and Research Station for Grassland Ecosystem in the Loess Plateau, Shanxi Agricultural University, Taigu, China

Legumes play a crucial role in the restoration and utilization of salinized grassland. To explore the physiological response mechanism of *Astragalus membranaceus* and *Medicago sativa* seedlings to salt stress, salt stress culture experiments with five NaCl concentration treatments (0 mmol/L, 50 mmol/L, 100 mmol/L, 200 mmol/L, and 300 mmol/L) were conducted on these two legume seedlings. Morphological characteristics, physiological features, biomass, and the protective enzyme system were measured for both seedlings. Correlation analysis, principal component analysis (PCA), and membership function analysis (MFA) were conducted for each index. Structural equation modeling (SEM) was employed to analyze the salt stress pathways of plants. The results indicated that number of primary branches (PBN), ascorbate peroxidase (APX) activity in stems and leaves, catalase (CAT) activity in roots, etc. were identified as the primary indicators for evaluating the salt tolerance of *A. membranaceus* during its seedling growth period. And CAT and peroxidase (POD) activity in roots, POD and superoxide dismutase (SOD) activity in stems and leaves, etc. were identified as the primary indicators for evaluating the salt tolerance of *M. sativa* during its growth period. Plant morphological characteristics, physiological indexes, and underground biomass (UGB) were directly affected by salinity, while physiological indexes indirectly affected the degree of leaf succulence (LSD). Regarding the response of the protective enzyme system to salt stress, the activity of POD and APX increased in *A. membranaceus*, while the activity of CAT increased in

M. sativa. Our findings suggest that salt stress directly affects the growth strategies of legumes. Furthermore, the response of the protective enzyme system and potential cell membrane damage to salinity were very different in the two legumes.

KEYWORDS

salt stress, legume, seedling, morphological and physiological characteristics, protective enzyme system, structural equation modeling

1 Introduction

In the context of global climate change, the threat of soil salinization is escalating. Globally, approximately 1.1 billion hectares of salt-affected land are considered unsuitable for growing crops, constituting 7% of the world's land surface (Wicke et al., 2011). Soil salinization is a primary contributor to the shortage of land resources and the deterioration of the ecological environment. Therefore, it is necessary to utilize saline-alkali land to enhance agricultural production. In China, the area affected by saline-alkali soil is approximately 36 million hectares (Wang et al., 2021). Soil salinization is a critical adverse environmental factor that adversely affects seed germination, plant growth, and productivity, causing significant harm to the biosphere and ecological structure (Li and Li, 2022). Salt-tolerant plants play an active role in utilizing salinized soil, and the study of plant stress resistance under salt stress has become a focal point for botanists (van Zelm et al., 2020). Currently, the saline soil area in China is continuing to increase, and the cultivation of salt-tolerant crops, along with the development and utilization of salt-tolerant plant resources, represents feasible strategies to resist salt stress (Liu and Wang, 2021). Planting salt-tolerant crops can help address the inevitable global shortage of freshwater resources and the threat of soil salinization (Zhang et al., 2021).

Understanding the adaptive mechanisms of plants to saline–alkali stress and investigating the physiological and biochemical responses of plants under such stress are crucial endeavors for researchers. This exploration is essential for comprehending the intricate mechanisms of saline–alkali stress and enhancing the saline–alkali tolerance of plants (Fang et al., 2021). Salt stress exerts various influences on plants. For instance, plants subjected to salt stress undergo a series of physiological and biochemical changes aimed at regulating ion and water balance, thereby sustaining normal photosynthesis (Muchate et al., 2016). The effect of salt stress extends to seed germination, growth, photosynthetic pigments, photosynthesis, ion and nutrient balance, as well as overall productivity (Farooq et al., 2017; Zhou et al., 2023). In response to environmental challenges, plants activate regulatory mechanisms to mitigate salt-induced damage. Osmotic regulation, activation of antioxidant enzymes, and application of exogenous substances represent effective strategies employed by plants to alleviate salt stress (Feng et al., 2023).

Salt stress is a prominent abiotic factor significantly affecting plant growth, development, and yield. In saline-alkali soil, the symbiotic relationship between leguminous herbs and rhizobia not only facilitates salt reduction but also substantially enhances soil fertility during saline–alkali soil amelioration. Research on broad common beans subjected to salt stress revealed that elevated NaCl levels led to a reduction in plant height (PH), leaf area, and leaf number (Torche et al., 2018). Similarly, a 7-day salt stress treatment on soybeans demonstrated that NaCl inhibited overall plant growth (Ning et al., 2018). Studies in peas indicated that salt stress influenced sodium distribution in roots and buds, thereby inhibiting seedling growth and development (Tokarz et al., 2020). Most legumes are sensitive to high salt levels in the soil, and the oil salt content affects almost all parameters of plant development (Shrivastava and Kumar, 2015). Investigations on mung beans underscored the inhibitory effect of salt stress on plant growth (Lim et al., 2022). Consequently, there is a need to intensify research on the growth characteristics of leguminous herbs under salt stress to establish a scientific foundation for assessing plant salt tolerance and understanding the underlying mechanisms.

While existing studies contribute significantly to unraveling the effect of salt on plants, the diverse evaluation indices for legume salt tolerance introduce complexity and hinder the establishment of a standardized index system. Furthermore, the underlying mechanisms driving legume characteristics' response to salt stress remain unclear. Our research aims to address these gaps by exploring a method to screen the salt tolerance index system of legumes. And the response of legume varieties to salt stress along with the associated mechanisms of salt tolerance will be elucidated. We focused on two legume species, *Astragalus membranaceus* and *Medicago sativa*, conducting seedling growth experiments with varying NaCl concentrations. *A. membranaceus* is a medicinal plant with salt-resistance potential and economic value, and *M. sativa* is a high-yield forage plant with high salt tolerance. The objective was to observe changes in the physiological and biochemical characteristics of legume seedlings under NaCl stress, thereby comprehending the response process of the two legume

types to salt stress and revealing the salt tolerance mechanism underpinning legumes' response to salt stress.

2 Materials and methods

2.1 Legume plant species

Two legume species, namely *A. membranaceus* and *M. sativa*, were subjects of experimentation.

2.2 Experimental methods and procedures

2.2.1 Cultivation of seedlings

Plant seedlings were grown in a well-ventilated plant culture laboratory at a temperature of 25 (± 1)°C and a humidity of 40%. The culture substrate of soil consisted of 20% vermiculite, 20% perlite, 10% humus, and 50% sand. The pots with a height of 85 mm and a diameter of 100 mm used in this experiment, in each pot, approximately 80–100 seeds were added. Six pots of each of the five gradients of the two plants were set up for seedling establishment. During the initial 30 days of plant growth, the Hoagland nutrient solution was applied every 5 days. Full-spectrum LED plant growth lamps were used to provide light. The light intensity was 3200 lx for 12 hours of light and 12 hours of dark per day. Upon reaching a seedling height of 8–10 cm, thinning was performed, ten plant individuals of similar height, leaf size, and leaf number were retained in each pot. One week post-thinning, the salt stress experiment commenced.

2.2.2 Salt stress treatment

The experiment involved five levels of salt concentration treatment, and each treatment was replicated three times. Three plant individuals were selected as replicates for the determination of growth and physiological parameters. The designated salt treatment levels were as follows: 0 mmol/L (control check), 50 mmol/L, 100 mmol/L, 200 mmol/L, and 300 mmol/L. We set salt concentrations based on previous studies (Campanelli et al., 2013; Tani et al., 2018). To eliminate the interference of micro-environmental variations from the experimental results, the positioning of the cultivation basin was randomly changed frequently. Empirical observations were conducted over a 14-day period.

2.3 Parameter measurement

2.3.1 Determination of seedling growth index

On the 13th day of treatment, the number of primary branches (PBN) of the main stem and the PH of each potted plant were recorded. Harvesting occurred on the 14th day, with measurements taken for leaf area (LA), the weight of fresh stem and leaf. Roots were washed and weighed fresh after removing sediment and excess water with absorbent paper. Stems, leaves, and roots were dried at 65°C until a constant dry weight was achieved. The root-to-shoot ratio (R/S) and the degree of leaf succulence (LSD) were calculated, representing the ratio of the dry weight of the root to the dry weight of the stem and leaf, and the ratio of fresh weight to the dry weight of leaves, respectively.

2.3.2 Determination of seedling physiological indexes

Malondialdehyde (MDA) levels in plant seedlings were determined using thiobarbituric acid oxidation colorimetry, and the activity of superoxide dismutase (SOD) was determined using the WST-8 method. The activity of peroxidase (POD), ascorbate peroxidase (APX), and catalase (CAT) was determined using guaiacol colorimetry, AsA colorimetry, and ammonium molybdate colorimetry, respectively.

2.4 Statistical analysis

Microsoft Excel 2016 and SPSS 24.0 were utilized for statistical data analysis. A correlation model was established, and Origin 2022 was employed for creating figures. Principal component analysis (PCA) was used to obtain the magnitude of each indicator's contribution and eigenvectors, and the data to compare the magnitude of each indicator's influence on plant salt tolerance. The salt tolerance of the two legumes was comprehensively evaluated by membership function analysis (MFA).

The relative biomass was calculated using the following formula:

$$\text{Relative biomass} = \frac{SB - CB}{CB} \times 100\,\% \tag{1}$$

where *SB* is the biomass of the salt treatment group, and *CB* is the biomass of the control group.

The salt tolerance coefficient (ω) is the ratio of the average measured value between the salt treatment group and the control group.

The membership function value of each Comprehensive index was calculated using the following formula:

$$\mu\,(X_j) = \frac{X_j - X_{min}}{X_{max} - X_{min}} \tag{2}$$

$$\text{or } \mu\,(X_j) = \frac{X_{max} - X_j}{X_{max} - X_{min}} \tag{3}$$

where $\mu\,(X_j)$ represents the membership function value of the comprehensive index of j, X_j represents the comprehensive index value of j, and X_{min} indicates the minimum value of j. X_{max} indicates the maximum value of j. The positive correlation between the indexes and salt tolerance was calculated using MFA (Formula 2). The negative correlation between the indexes and salt tolerance was calculated using MFA (Formula 3).

The weight value (W) of each composite indicator was calculated using the following formula:

$$W_j = \frac{V_j}{\sum_{j=1}^{m} V_j} \quad (4)$$

where: W_j denotes the weight of the composite indicator j among all composite indicators; V_j denotes the contribution percentage of each part of the composite indicator j of the material obtained through PCA.

The salt tolerance index (D) was calculated using the following formula:

$$D = \sum_{j=1}^{n} \mu(X_j) \times W_j \quad (5)$$

The membership function value of each comprehensive index (μ), the weight value (W) and the salt tolerance index (D) of each composite indicator were calculated with reference to the methods of Chen et al. (Chen et al., 2023).

Structural equation modeling (SEM) was employed to analyze the effects of salt stress on plant growth index, physiological index, and protective enzyme system. Before the SEM procedure, variables dimensionality reduction was conducted of by PCA. The parameters of the first principal component were then used in the SEM model. During SEM analyses, the data were fitted to the models using the maximum likelihood estimation method by comparing the model-implied variance–covariance matrix against the observed variance–covariance matrix. All SEM analyses were performed using Amos version 17.0.2 (Amos Development Corporation, Chicago, IL, USA). Model fit was assessed using the chi-square (χ^2) test, comparative fit index (CFI), root square mean error of approximation (RSMEA), and goodness of fit index (GFI) (Mi et al., 2015).

3 Results and analysis

3.1 Effects of NaCl stress on morphological characteristics of two legume species seedlings

With increasement of NaCl concentration, the PBN of both legume species gradually decreased (Figure 1A). The primary branch numbers of *A. membranaceus* and *M. sativa* showed no significant difference compared to the control group at NaCl concentrations of 50 mmol/L and 100 mmol/L. However, a considerable difference emerged at 200 mmol/L and 300 mmol/L NaCl concentrations (P<0.05). The variation in PBN among treatments was attributed to NaCl concentration (P<0.001). *A. membranaceus* exhibited the highest PH at 50 mmol/L and the lowest at 200 mmol/L (Figure 1B). The PH of *M. sativa* decreased with increasing concentration, showing no significant difference at 50 mmol/L compared to the control group. However, at NaCl concentrations of 100 mmol/L, 200 mmol/L, and 300 mmol/L, there were significant differences from the control group (P<0.05). The differences in PH among treatments were influenced by species (P<0.01) and NaCl concentration (P<0.001).

The LA of both plants initially increased and then decreased with rising salt concentration (Figure 1C), reaching its maximum at 50 mmol/L. At this concentration, the LA of *M. sativa* significantly differed from the control group (P<0.05). The LA of *A. membranaceus* decreased by 22.55% compared with the control group at 200 mmol/L and 300 mmol/L NaCl concentrations (P<0.05) and 31.99% (P<0.05). The LA of *M. sativa* decreased by

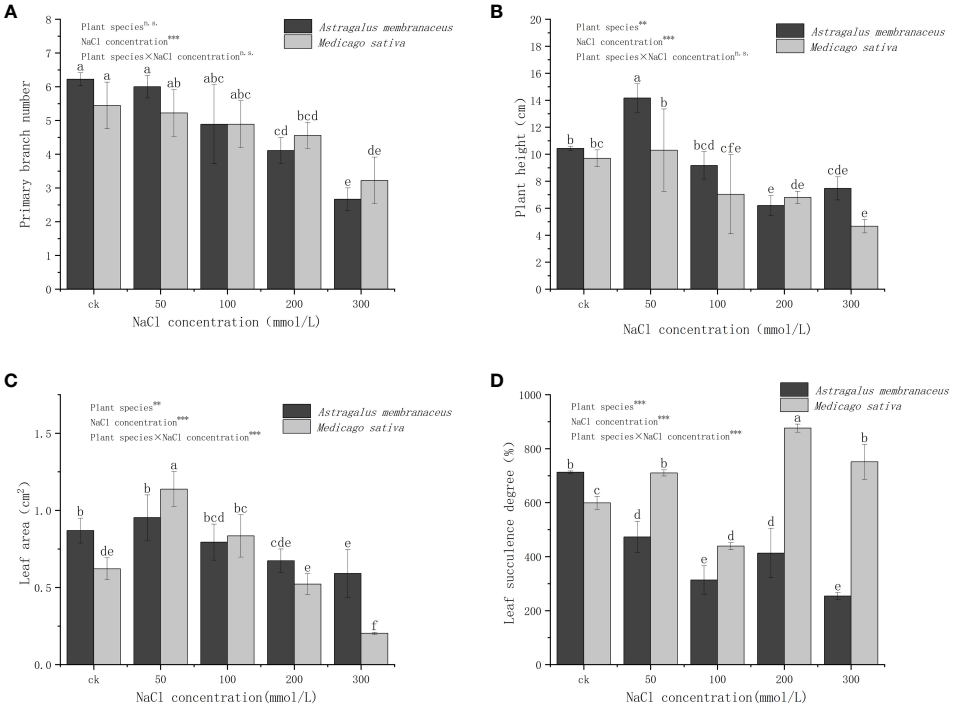

FIGURE 1
Changes in the **(A)** primary branches number, **(B)** plant height, **(C)** leaf area, and **(D)** leaf succulence degree of the two legume species under NaCl stress. Different lowercase letters indicate significant differences between treatments (P<0.05). Through the two-way analysis of variance, the significance of the effect of factors on the indicators is marked as ***(P<0.001), **(P<0.01), *(P<0.05) and n.s. (P>0.05), the same below.

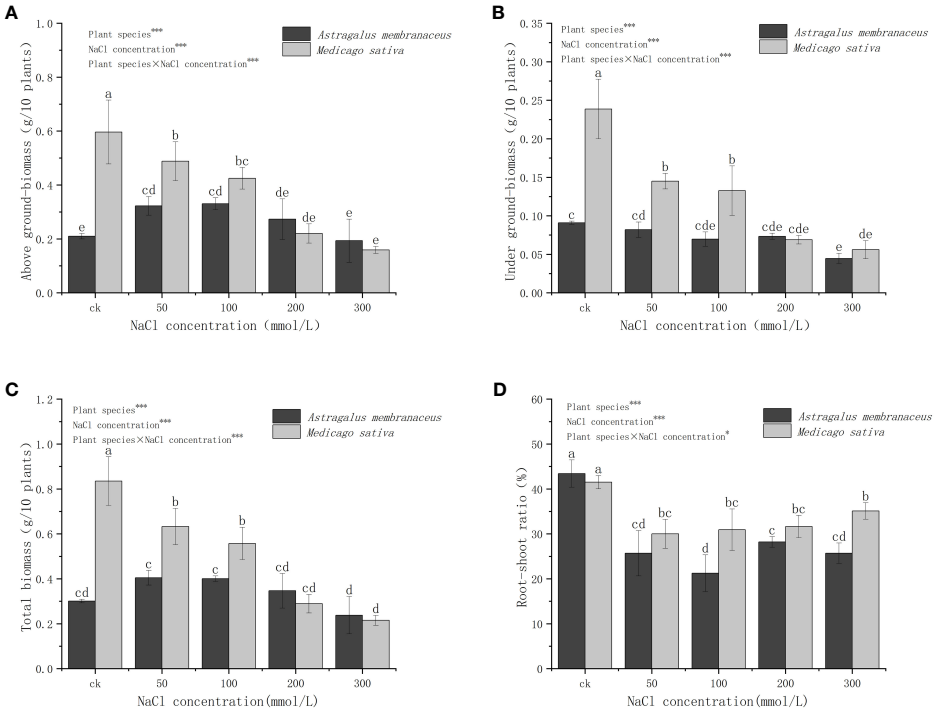

FIGURE 2
Changes in the **(A)** above ground biomass, **(B)** under ground biomass, **(C)** total biomass, and **(D)** root-shoot ratio of the two legume species under NaCl stress.

12.49% ($P<0.05$) and 65.96% ($P<0.05$) at 200 mmol/L and 300 mmol/L salt concentrations, respectively. The differences in LA among treatments were influenced by species ($P<0.01$), NaCl concentration ($P<0.001$), and their interactions ($P<0.001$). The LSD of *A. membranaceus* in all salt treatment groups was significantly lower than that in the control group ($P<0.05$; Figure 1D). Under all of salt treatments, *M. sativa's* LSD was significantly higher than that of *A. membranaceus* ($P<0.05$). At 100 mmol/L salt concentration, the LSD of *M. sativa* was the lowest and significantly lower than that of control group ($P<0.05$). At 50 mmol/L, 200 mmol/L, and 300 mmol/L salt concentrations, it was significantly higher than the control group ($P<0.05$). The differences in LSD among treatments were influenced by species ($P<0.001$), NaCl concentration ($P<0.001$), and their interactions ($P<0.001$).

3.2 Effects of NaCl stress on seedling biomass of the two legume species

The results indicate varying trends in the overall change of different legumes under different salt concentrations (Figure 2). Specifically, the aboveground biomass (AGB) of *A. membranaceus* initially increased and then decreased with rising salt concentration, whereas the underground biomass (UGB) showed insignificant changes. In contrast, both AGB and UGB of *M. sativa* gradually decreased with increasing salt concentration, significantly dropping at 50 mmol/L and 100 mmol/L concentrations ($P<0.05$), and exhibiting higher levels in the 50 mmol/L and 100 mmol/L treatment groups compared to the stress of 200 mmol/L and 300 mmol/L. Total biomass and AGB trends were similar between the two legume species. The R/S of *A. membranaceus* and *M. sativa* in all NaCl-treated groups was significantly lower than in the control ($P<0.05$), with no significant differences among various salt concentration treatment groups. The variations in AGB, UGB, total biomass, and R/S among treatments were influenced by species ($P<0.001$), NaCl concentration ($P<0.001$), and their interactions ($P<0.05$).

Figure 3 illustrates the different trends in the relative biomass (Formula 1) of the two legume seedlings under NaCl stress. The relative AGB of *A. membranaceus* was significantly higher than that of the control, except at 300 mmol/L salt concentration, while the UGB was lower than that of the control group. In contrast, the aboveground and UGB of *M. sativa* was consistently lower than that of the control. The trend in total relative biomass of the two species mirrored that of AGB. *A. membranaceus* exhibited increased total biomass under 50 mmol/L, 100 mmol/L, and 200 mmol/L salt stress (34.44%, 33.00%, and 51.17% higher than the control, respectively), but under 300 mmol/L salt stress, total biomass decreased by 20.93% compared to the control. *M. sativa* showed a decrease in total biomass at 50 mmol/L, 100 mmol/L, 200 mmol/L, and 300 mmol/L NaCl concentrations (24.19%, 33.21%, 65.39%, and 74.25% lower than the control, respectively).

3.3 Effects of NaCl stress on physiological indexes and defense system enzymes of two legume seedlings

Figure 4 reveals significant differences in the MDA content in the aboveground parts of the two legumes. Specifically, at 50 mmol/L and

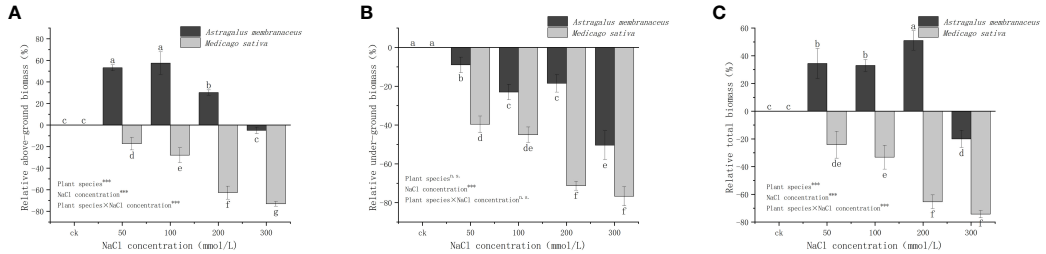

FIGURE 3
Relative changes in the **(A)** above ground biomass, **(B)** under ground biomass, and **(C)** total biomass of the two legume species under NaCl stress.

100 mmol/L salt concentrations, *M. sativa* had a higher MDA content than *A. membranaceus*. At 300 mmol/L salt concentration, the MDA content of *A. membranaceus* was significantly higher than that of *M. sativa*, while the content of *A. membranaceus* did not significantly differ at 0–100 mmol/L salt concentration. There were notable differences in the content of MDA in the underground parts of the two plants. The MDA content of *A. membranaceus* showed no significant difference at 50 mmol/L and 100 mmol/L salt concentrations, but it increased exponentially at 200 mmol/L and 300 mmol/L salt concentrations. The underground MDA content of *M. sativa* was significantly higher at 200 mmol/L and 300 mmol/L salt concentrations than at 50 mmol/L and 100 mmol/L salt concentrations, and the trend of plant MDA content was similar above and below ground.

With an elevation in NaCl concentration, the SOD activity in the aboveground organs of *A. membranaceus* gradually diminishes (Figure 5A). At a concentration of 50 mmol/L, the SOD activity in the aboveground parts of plants exhibits no significant deviation from that in the control group and is notably higher than that in other salt treatment groups. *M. sativa* records the lowest SOD activity at a concentration of 100 mmol/L. Under diverse salt concentrations of *A. membranaceus*, SOD activity in the underground parts of plants progressively diminishes with the escalating salt concentration (Figure 5B), displaying no significant distinctions at 100 mmol/L, 200 mmol/L, and 300 mmol/L salt concentrations ($P>0.05$). The SOD activity of *M. sativa* roots in the treatment group surpasses that in the control group, reaching its peak at a concentration of 200 mmol/L.

POD activity in the aboveground part of *A. membranaceus* systematically rises with the escalating salt concentration, reaching its zenith at 200 mmol/L (Figure 5C). The POD activity of *M. sativa* stems and leaves gradually increases but remains significantly lower than that of the control group ($P<0.05$). POD activity of *A. membranaceus* roots is significantly lower than that of the control group at concentrations of 50 mmol/L and 100 mmol/L ($P<0.05$; Figure 5D). The POD activity of *M. sativa* roots is notably lower than that of the control group at a concentration of 50 mmol/L ($P<0.05$). The POD activity of *M. sativa* roots at 100 mmol/L and 200 mmol/L (reaching the highest value) is significantly higher than that of the control group ($P<0.05$).

The aboveground APX activities in all salt-treated groups of *A. membranaceus* are significantly higher than those in the control group ($P<0.05$; Figure 5E). The APX activity of stems and leaves of *M. sativa* is notably lower than that of the control group only at a 300 mmol/L salt concentration ($P<0.05$). The root APX activity of *A. membranaceus* is significantly higher than that of the control group at concentrations of 100 mmol/L, 200 mmol/L, and 300 mmol/L ($P<0.05$; Figure 5F). The root APX activity of *M. sativa* at concentrations of 100 mmol/L, 200 mmol/L, and 300 mmol/L is significantly lower than that of the control group ($P<0.05$).

The CAT activity of stems and leaves of *A. membranaceus* under all salt treatments was significantly higher than that of the control group ($P<0.05$; Figure 5G). The CAT activity reached its peak value at a 200 mmol/L salt concentration. Similarly, the CAT activity of the stems and leaves of *M. sativa* treated with all salt

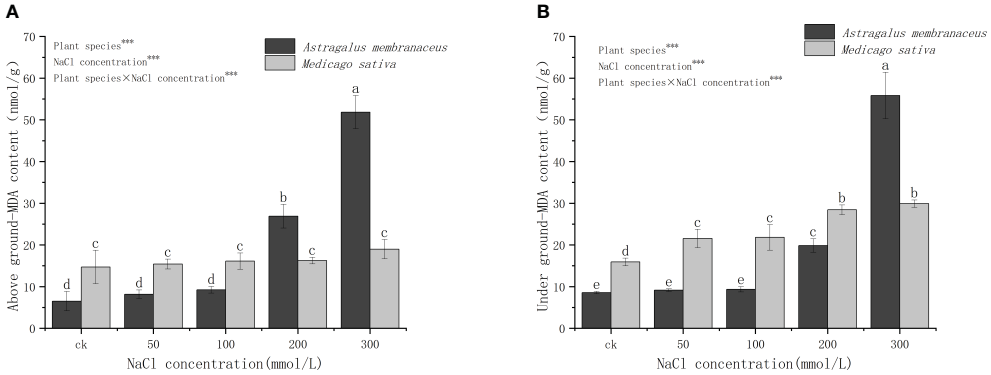

FIGURE 4
Changes in **(A)** above ground MDA content and **(B)** under ground MDA content in the two legume species under NaCl stress.

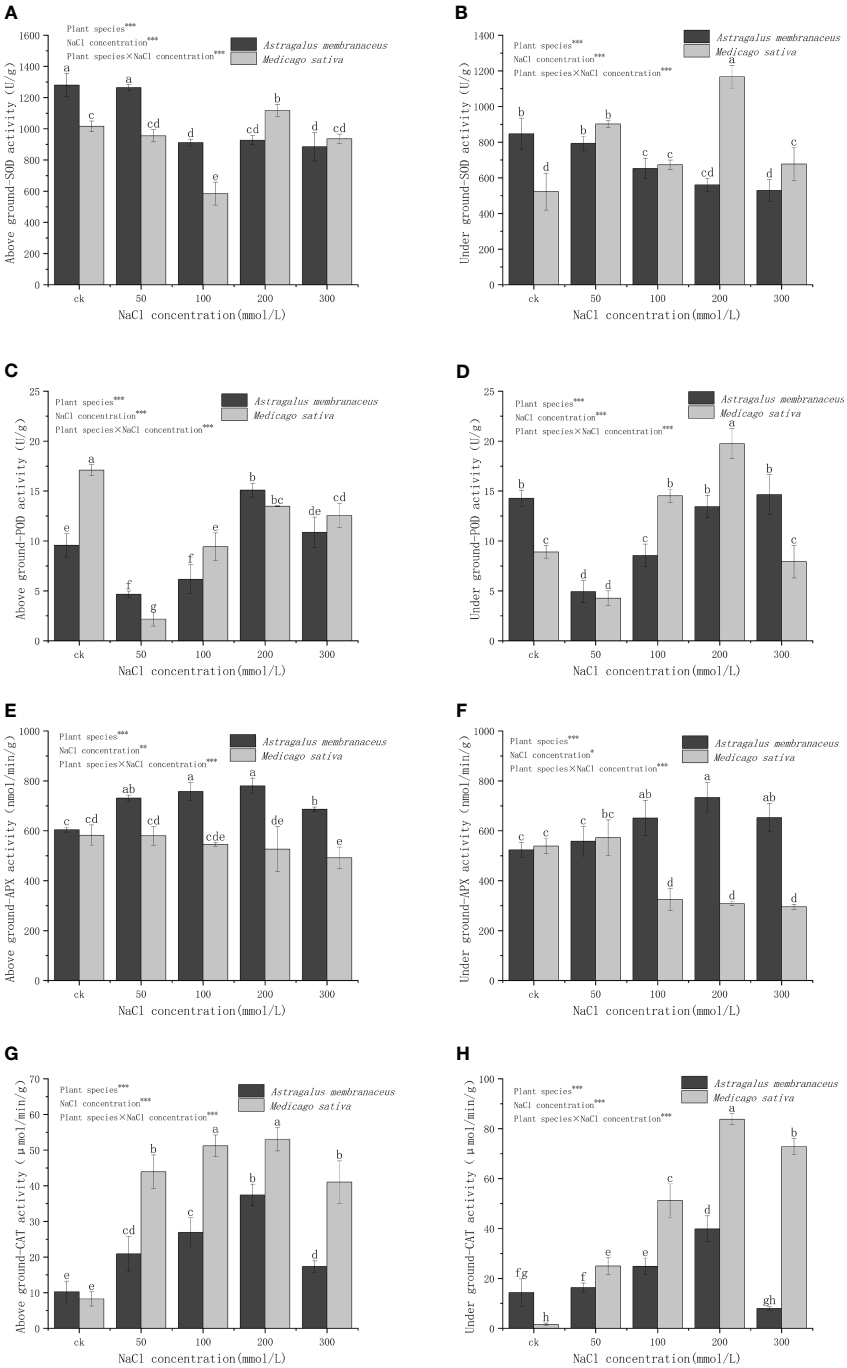

FIGURE 5
Changes in **(A)** above ground SOD activity, **(B)** under ground SOD activity, **(C)** above ground POD activity, **(D)** under ground POD activity, **(E)** above ground APX activity, **(F)** under ground APX activity, **(G)** above ground CAT activity, and **(H)** under ground CAT activity of two legume species under NaCl stress.

concentrations was significantly higher than that of the control group (P<0.05), with the highest values observed at 200 mmol/L concentration. Generally, after salt treatment, the CAT activity of *M. sativa* stems and leaves was significantly higher than that of *A. membranaceus*. The CAT activity of *A. membranaceus* root was significantly higher than that of the control group at 100 mmol/L and 200 mmol/L salt concentrations (P<0.05; Figure 5H). The maximum value was reached at the 200 mmol/L salt concentration. The root CAT activity of *M. sativa* under all salt concentrations was also significantly higher than that of the control group (P<0.05), reaching its peak at 200 mmol/L salt concentration.

3.4 Correlation analysis among parameters

Correlation analyses were conducted on seedling stage indexes of *A. membranaceus* (Supplementary Figure 1A), revealing

significant associations. The PBN exhibited a noteworthy correlation with UGB, plant SOD activity, and LSD ($P<0.05$). Additionally, UGB showed a significant correlation with the MDA content of plants ($P<0.05$). LA demonstrated significant correlations with SOD activity in roots, MDA content in stems and leaves, and PH ($P<0.05$). The R/S was also found to be significantly correlated with LSD ($P<0.05$). Furthermore, plant SOD activity exhibited a significant correlation with root APX activity ($P<0.05$), and plant CAT activity was significantly correlated with stems and leaves APX activity ($P<0.05$).

In the case of *M. sativa* seedling stage (Supplementary Figure 1B), each index was subjected to correlation analysis. The PBN was significantly correlated with PH, biomass, MDA content, and APX activity stems and leaves ($P<0.05$). Biomass displayed significant correlations with plant APX activity, plant CAT activity, and plant MDA content ($P<0.05$). PH exhibited significant correlations with AGB, MDA content in stems and leaves, and APX activity ($P<0.05$). The R/S showed a significant correlation with CAT activity of the stems and leaves ($P<0.05$). Moreover, the MDA content, APX activity, and CAT activity of roots were significantly correlated with each other ($P<0.05$).

3.5 Principal component analysis and membership function analysis of indices of two legume plants under salt stress

The PCA load chart depicts the correlation coefficients between the original variables and the principal components. For *A. membranaceus* seedlings, the first three eigenvalues were 47.38%, 26.31%, and 13.78%, respectively, resulting in a cumulative contribution rate of 87.47% (Supplementary Table 5, Supplementary Figure 2). The eigenvector of the load diagram of the PCA and the contribution rate of each principal component revealed that PBN, SOD activity in plant stems, leaves, and roots exhibited higher loads on the first principal component. The second principal component was characterized by APX activity in stems and leaves, AGB, total biomass. The third principal component was associated with CAT activity in roots, POD activity in stems and leaves, and R/S had higher loads (Supplementary Table 6).

According to the load diagram of PCA of *M. sativa* seedlings, the first four eigenvalues were 46.54%, 17.43%, 13.24%, and 8.80%, leading to a cumulative contribution rate was 85.63% (Supplementary Table 5, Supplementary Figures 3A, B). Therefore, the four principal components were selected as comprehensive indexes to evaluate *M. sativa*. According to the eigenvector of the load diagram of PCA and the contribution rate of each principal component, the load diagram indicates that root CAT activity, total biomass, UGB, had higher loads on the first principal component. POD activity in stems and leaves, R/S and LA contributed more to the second principal component. SOD activity of stems and leaves, LSD, and PH exhibited higher loads in the third principal component. POD activity in plant stems, leaves and roots and MDA activity of stems and leaves contributed more to the fourth principal component. Extracting these four principal components could effectively represent the information from all indicators, allowing the use of four new variables to replace the original eighteen variables (Supplementary Table 6). However, each load vector represents only the correlation coefficient between the principal component and the corresponding variable, not the coefficient corresponding to each index in each principal component.

The highest salt tolerance index (*D*) (Formula 5) values were observed at control for both legume plants, indicating that salt treatment reduced the salt tolerance of the plants (Table 1). In the four salt treatment groups, the highest *D* values of *A. membranaceus* and *M. sativa* occurred at concentrations of 50 mmol/L and 200 mmol/L, respectively. The salt tolerance of *M. sativa* was higher than that of *A. membranaceus* under each concentration treatment in the comprehensive evaluation.

TABLE 1 Comprehensive index value, membership function value and salt tolerance evaluation value of seedling stage under different salt concentration treatments.

	Comprehensive index value				Membership function value				*D*
	x1	x2	x3	x4	μ1	μ2	μ3	μ4	
AM CK	-0.178	-0.512	1.964	0.597	0.402	0.140	1.000	0.724	0.486
AM 50	-0.555	-0.379	1.124	-1.296	0.283	0.185	0.735	0.051	0.307
AM 100	-0.626	-0.261	-0.403	-1.178	0.261	0.223	0.254	0.093	0.225
AM 200	-0.768	-0.403	-0.557	0.248	0.216	0.176	0.205	0.600	0.258
AM 300	-1.453	-0.936	-1.209	0.647	0.000	0.000	0.000	0.742	0.107
MS CK	-0.637	2.085	0.515	1.373	0.257	1.000	0.543	1.000	0.629
MS 50	0.555	0.924	-0.018	-1.439	0.633	0.616	0.375	0.000	0.488
MS 100	0.889	1.028	-1.149	-0.318	0.739	0.650	0.019	0.399	0.529
MS 200	1.717	-0.909	0.270	0.450	1.000	0.009	0.466	0.672	0.570
MS 300	1.055	-0.636	-0.536	0.914	0.791	0.099	0.212	0.837	0.492

AM mean *A. membranaceus* and MS mean *M. sativa*. D mean the salt tolerance index.

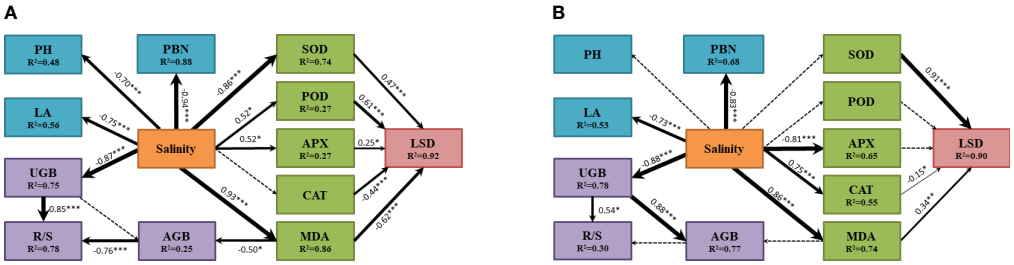

FIGURE 6
The influence pathway of plant morphological characteristics, biomass, antioxidant enzyme system and MDA of two legume species under salt stress fitted by SEM analysis (A for *Astragalus membranaceus* and B for *Medicago sativa*). The results of model fitting were (**A**: χ^2 = 206.859, df=62, *P*=0.242; **B**: χ^2 = 181.459, df=62, *P*=0.138). The arrows represent the action path relationship between the factors. The thickness of the solid arrow represents the standardized path coefficient, and the significance is marked as ***(*P*<0.001), **(*P*<0.01) and *(*P*<0.05). The dashed lines represent insignificant hypothetical regression relationships between the factors. R^2 values indicate the proportion of variation explained by the relationships with other variables. Values associated with solid arrows represent standardized paths coefficients. PH mean plant height, LA mean leaf area, PBN mean number of primary branches, AGB mean above-ground biomass, UGB mean under-ground biomass, R/S mean root-shoot ratio, LSD mean degree of leaf succulence, SOD mean superoxide dismutase, POD mean peroxidase, APX mean ascorbate peroxidase, CAT mean Catalase, MDA mean malondialdehyde.

3.6 Structural equation modeling analysis of pathways of the two legume plants under salt stress

SEM of *A. membranaceus* indicated a high fit (χ^2 = 206.859, df=62, *P*=0.242; Figure 6A). The results showed that salinity significantly negatively affected PBN, PH, and LA, explaining 88%, 48%, and 56% of their variances, respectively. Salinity had a significant positive effect on MDA, POD, and APX and adversely affected SOD. SOD, POD, APX, CAT, and MDA significantly influenced LSD, with MDA and CAT negatively affecting LSD and SOD, POD, and APX positively affecting LSD. Finally, salinity indirectly affected AGB through MDA, where MDA had an adverse effect on AGB, and Salinity directly negatively affected UGB. Both AGB and UGB significantly influenced R/S, with the negative effect of AGB and the positive effect of UGB together explaining 78% of the total variance of R/S.

SEM of *M. sativa* also demonstrated a high fit (χ^2 = 181.459, df=62, *P*=0.138; Figure 6B). Salinity adversely affected PBN and LA, explaining 68% and 53% of their variances, respectively. Salinity directly affected MDA, APX, and CAT, with significant positive effects on MDA and CAT and an adverse effect on APX. Additionally, salinity significantly influenced LSD only through SOD, CAT, and MDA, which together explained 90% of the total variance of LSD. Salinity directly and adversely affected UGB, explaining 78% of its variance. Salinity indirectly affected AGB through UGB, where UGB positively affected AGB, explaining 77% of its variance. In this model, only UGB had a positive effect on R/S.

4 Discussion

4.1 Effects of salt stress on morphological characteristics of seedlings

The tolerance of plants to saline environments is often evident in their growth characteristics (Munns and Tester, 2008; Verma et al., 2023). Under adverse conditions, plants adapt through changes in morphological characteristics and growth state (Miryeganeh, 2021). In our study, morphological traits such as PBN, PH, and LA exhibited a downward trend to varying degrees under salt stress (Figure 1). High level of salt stress had significant and negative effect on plant growth. Plants readjust their resource allocation patterns to cope with stress under high salinity conditions (Zhang et al., 2020). Leaf fleshy refers to the enlargement of parenchyma tissue in plant organs, leading to the dilution of cell fluid, aiding plants in dealing with salt stress (Ottow et al., 2005). Results indicated that under different salt stress treatments, the LSD varied significantly between the two plants, suggesting that *M. sativa* had better water absorption and storage capacity than *A. membranaceus* under salt stress (Figure 1), ensuring water demand for average plant growth (Ogburn and Edwards, 2010).

4.2 Effects of salt stress on seedling biomass

Plants under salt stress maintain growth by adjusting biomass energy distribution, primarily by reducing carbon assimilation and altering osmotic energy consumption (Zhang et al., 2020). Generally, in saline-alkali environments, plant individual development is shortened, growth is slowed or stopped, and biomass accumulation is reduced. However, for some salt-tolerant plants, low-concentration salt stress can promote growth (Ogburn and Edwards, 2010). Our study indicated that both legumes were affected by salt stress to varying degrees, with the AGB of *A. membranaceus* slightly increasing under low salt concentrations (Figure 2). Slight salt stress could sometimes stimulate plant growth (Yu et al., 2020). Conversely, *M. sativa* exhibited a clear downward trend with increasing salt concentration (Figure 2). With increasing stress factors, plants tend to preserve the biomass of the underground part, reflected in the increase in the R/S (Rabhi et al., 2010). The underground parts of plants bear the brunt of environmental stress caused by salt, prompting many plants to adjust root morphology in response to salt stress (Zhang et al., 2023). Some

plants inhibit the growth of the underground part in salt environments to avoid excessive exposure to high salt (Zhao et al., 2020). In our experiment, the biomass of the underground portion relative to the aboveground part increased at a salt concentration of 300 mmol/L. More allocation of root biomass and an increase in the R/S may have a greater potential for plant uptake of soil water under salinity stress conditions. (Figures 2, 3).

4.3 Effects of salt stress on plasma membrane peroxidation and protective enzyme activities of seedlings

When the salt content in the plant growing environment increases, it induces changes in the cell membrane function due to salt damage. This results in an elevated rate of electrolyte exosmosis in the cell, leading to a corresponding increase in relative conductivity (Khatri and Rathore, 2022). The imbalance in free radical metabolism in the body causes an increase in the content of certain free radicals (Heyno et al., 2011; Hasanuzzaman et al., 2021). Specifically, superoxide free radicals can trigger lipid peroxidation of unsaturated fatty acids in membrane lipids, causing serious damage to the biofilm system. MDA, a membrane lipid peroxide produced in this process, serves as an indicator reflecting the strength of plant resistance under stress conditions (de Azevedo Neto et al., 2006). Various plants exhibit different levels of antioxidant enzyme activity in relation to their salt stress tolerance (Costa et al., 2010). Our study demonstrated significant differences in MDA content in *A. membranaceus*, showing an increasing trend with higher salt concentrations (Figure 4). Generally, under stress conditions such as salt, heavy metals, mechanical damage, and high temperature, MDA content in plants tends to increase (Tang et al., 2015). Notably, there was no significant difference in *M. sativa* for MDA content, possibly due to its high salt tolerance, which mitigates MDA changes through osmotic regulation (Figure 4). With increasing salt concentration, SOD activity, as the first line of defense against reactive oxygen species damage, usually increases rapidly and significantly (Xu et al., 2013). In our study, CAT and POD activities exhibited similar trends to SOD but with varying degrees of enhancement, and the change in SOD activity was not significant (Figure 5). The activities of CAT, POD, and APX all increased to different extents, suggesting the plant's ability to perform ion regionalization through self-regulation and the mutual influence of osmoregulatory substances, thereby alleviating high salt stress (Malakar and Chattopadhyay, 2021).

4.4 Comprehensive evaluation of salt stress on salt tolerance of seedlings

The extent of tissue damage in plants responding to salt stress is often reflected in apparent morphological indexes (Xiao and Zhou, 2022). NaCl inhibits plant growth, and this study identified different degrees of damaged morphological characteristics on the fifth day of salt stress treatment. PCA revealed highly significant correlations among the indicators, indicating a certain degree of overlap and crossover in the information reflected by them. A single index was insufficient to gauge salt tolerance (Munns and Tester, 2008). Through PCA, we simplified the data structure, identified which key variables should be retained or excluded to analyze the relationship between each index and salt tolerance, determined reliable salt tolerance evaluation indicators, and adjusted the one-sidedness of a single index. Higher loading values of the indicator for each principal factor indicated a stronger correlation with its principal factors (Chen et al., 2023). In our study, the results of PCA revealed that the morphological parameters (PBN, PH and LA) for *A. membranaceu* and the biomass parameters (TB, AGB and UGB) for *M. sativa* was present in the first principal component and had a large load (Supplementary Table 6). In general, the parameters of morphology and biomass were the most apparent changes under salt stress (Kumar et al., 2021).

SEM for two legumes illustrated the response pathway among indices under salt stress. Salinity directly influenced the PBN, PH, and LA of the main stem. Under low-concentration salt stress, the biomass of *A. membranaceus* increased, maintaining the plant's normal physiological function through a protective enzyme system (Figure 6). AGB slightly increased by reducing PH, while UGB remained relatively stable. Typically, UGB is less affected by salt stress, allowing more nutrients to be allocated to AGB, providing additional energy for stress resistance (Loudari et al., 2022). However, in our study, the increase in salt concentration did not affect the PH of *M. sativa*, and the inhibiting effect of salinity on both aboveground and UGB was synchronized (Figure 6). Variations in stress-tolerant growth strategies among species led to different responses to apparent traits, particularly interspecific variation and environmentally controlled biomass allocation processes (Poorter et al., 2012; Tang et al., 2022). Based on the results of comprehensive salt tolerance analysis, the *D* value decreased with an increase in salt stress concentration, indicating a rise in salt stress and a decrease in plant salt tolerance (Table 1). Simultaneously, the *D* value of *M. sativa* exhibited a slight rebound at 100–200 mmol/L. The comprehensive evaluation of salt tolerance results suggested that under the stimulation of a specific threshold salt concentration, plants would gradually establish a tolerance mechanism through a physiological response (Sohrabi et al., 2012). However, our experimental results may have some potential limitations, including the typicality of legume species, the selected parameters, and the control of soil nutrient conditions, etc. We will continue to investigate the salt tolerance mechanism of legumes in future studies.

5 Conclusion

Salt stress significantly affected the PBN, PH, LA, and LSD of the two legume plants. Salt stress directly affected the energy distribution of plant roots, stems, and leaves. Under salt stress, the two legumes exhibited different response strategies in protective enzyme system and potential cell membrane damage. Two simplified evaluation index systems for the two legumes seedling growth salt tolerance were screened and identified. The primary evaluation parameters for *A. membranaceus* seedlings were PBN, APX and CAT, whereas for *M. sativa* were CAT, POD and SOD. *M. sativa* was more salt tolerant than *A. membranaceus* based on salt tolerance integration scores.

Data availability statement

The original contributions presented in the study are included in the article/Supplementary Material. Further inquiries can be directed to the corresponding author.

Author contributions

JM: Methodology, Project administration, Supervision, Writing – original draft, Writing – review & editing. XR: Data curation, Investigation, Writing – original draft. JS: Writing – review & editing. FW: Investigation, Writing – original draft. QW: Investigation, Writing – original draft. HP: Investigation, Writing – original draft. LK: Formal Analysis, Writing – review & editing. CW: Writing – review & editing.

Funding

The author(s) declare financial support was received for the research, authorship, and/or publication of this article. This project was supported by the Natural Science Foundation of China (32271632, U22A20576), Fundamental Research Program of Shanxi Province (202203021211303, 202203021221014).

Acknowledgments

We thank Jianhao Yu, Chengman She and Yi Qin for their technical assistance with the laboratory work.

Conflict of interest

The authors declare that the research was conducted in the absence of any commercial or financial relationships that could be construed as a potential conflict of interest.

Publisher's note

Supplementary material

The Supplementary Material for this article can be found online at: https://www.frontiersin.org/articles/10.3389/fpls.2023.1342219/full#supplementary-material

References

Campanelli, A., Ruta, C., Morone-Fortunato, I., and De Mastro, G. (2013). Alfalfa (*Medicago sativa* L.) clones tolerant to salt stress: in *vitro* selection. *Cent. Eur. J. Biol.* 8, 765–776. doi: 10.2478/s11535-013-0194-1

Chen, X., Gao, Y., Zhang, D., Gao, Y., Song, Y., Wang, H., et al. (2023). Evaluation of salinity resistance and combining ability analysis in the seedlings of mulberry hybrids (*Morus alba* L.). *Physiol. Mol. Biol. Plants* 29, 543–557. doi: 10.1007/s12298-023-01304-w

Costa, A., Drago, I., Behera, S., Zottini, M., Pizzo, P., Schroeder, J. I., et al. (2010). H_2O_2 in plant peroxisomes: an in *vivo* analysis uncovers a Ca^{2+}-dependent scavenging system. *Plant J.* 62, 760–772. doi: 10.1111/j.1365-313X.2010.04190.x

de Azevedo Neto, A. D., Prisco, J. T., Enéas-Filho, J., CEBd, A., and Gomes-Filho, E. (2006). Effect of salt stress on antioxidative enzymes and lipid peroxidation in leaves and roots of salt-tolerant and salt-sensitive maize genotypes. *Environ. Exp. Bot.* 56, 87–94. doi: 10.1016/j.envexpbot.2005.01.008

Fang, S., Hou, X., and Liang, X. (2021). Response mechanisms of plants under saline-alkali stress. *Front. Plant Sci.* 12. doi: 10.3389/fpls.2021.667458

Farooq, M., Gogoi, N., Hussain, M., Barthakur, S., Paul, S., Bharadwaj, N., et al. (2017). Effects, tolerance mechanisms and management of salt stress in grain legumes. *Plant Physiol. Biochem.* 118, 199–217. doi: 10.1016/j.plaphy.2017.06.020

Feng, D., Gao, Q., Liu, J., Tang, J., Hua, Z., and Sun, X. (2023). Categories of exogenous substances and their effect on alleviation of plant salt stress. *Eur. J. Agron.* 142, 126656. doi: 10.1016/j.eja.2022.126656

Hasanuzzaman, M., Raihan, M. R. H., Masud, A. A. C., Rahman, K., Nowroz, F., Rahman, M., et al. (2021). Regulation of reactive oxygen species and antioxidant defense in plants under salinity. *Int. J. Mol. Sci.* 22, 9326. doi: 10.3390/ijms22179326

Heyno, E., Mary, V., Schopfer, P., and Krieger-Liszkay, A. (2011). Oxygen activation at the plasma membrane: relation between superoxide and hydroxyl radical production by isolated membranes. *Planta* 234, 35–45. doi: 10.1007/s00425-011-1379-y

Khatri, K., and Rathore, M. S. (2022). Salt and osmotic stress-induced changes in physio-chemical responses, PSII photochemistry and chlorophyll a fluorescence in peanut. *Plant Stress* 3, 100063. doi: 10.1016/j.stress.2022.100063

Kumar, S., Li, G., Yang, J., Huang, X., Ji, Q., Liu, Z., et al. (2021). Effect of salt stress on growth, physiological parameters, and ionic concentration of water dropwort (*Oenanthe javanica*) cultivars. *Front. Plant Sci.* 12, 660409. doi: 10.3389/fpls.2021.660409

Li, Y., and Li, G. (2022). Mechanisms of straw biochar's improvement of phosphorus bioavailability in soda saline-alkali soil. *Environ. Sci. pollut. R.* 29, 47867–47872. doi: 10.1007/s11356-022-20489-3

Lim, I., Kang, M., Kim, B. C., and Ha, J. (2022). Metabolomic and transcriptomic changes in mungbean (*Vigna radiata* (L.) R. Wilczek) sprouts under salinity stress. *Front. Plant Sci.* 13, 1030677. doi: 10.3389/fpls.2022.1030677

Liu, L., and Wang, B. (2021). Protection of halophytes and their uses for cultivation of saline-alkali soil in China. *Biol. (Basel).* 10, 353. doi: 10.3390/biology10050353

Loudari, A., Mayane, A., Zeroual, Y., Colinet, G., and Oukarroum, A. (2022). Photosynthetic performance and nutrient uptake under salt stress: Differential responses of wheat plants to contrasting phosphorus forms and rates. *Front. Plant Sci.* 13, 1038672. doi: 10.3389/fpls.2022.1038672

Malakar, P., and Chattopadhyay, D. (2021). Adaptation of plants to salt stress: The role of the ion transporters. *J. Plant Biochem. Biotechnol.* 30, 668–683. doi: 10.1007/s13562-021-00741-6

Mi, J., Li, J., Chen, D., Xie, Y., and Bai, Y. (2015). Predominant control of moisture on soil organic carbon mineralization across a broad range of arid and semiarid ecosystems on the Mongolia plateau. *Landscape Ecol.* 30, 1683–1699. doi: 10.1007/s10980-014-0040-0

Miryeganeh, M. (2021). Plants' epigenetic mechanisms and abiotic stress. *Genes (Basel).* 12, 1106. doi: 10.3390/genes12081106

Muchate, N. S., Nikalje, G. C., Rajurkar, N. S., Suprasanna, P., and Nikam, T. D. (2016). Plant salt stress: adaptive responses, tolerance mechanism and bioengineering for salt tolerance. *Bot. Rev.* 82, 371–406. doi: 10.1007/s12229-016-9173-y

Munns, R., and Tester, M. (2008). Mechanisms of salinity tolerance. *Annu. Rev. Plant Biol.* 59, 651–681. doi: 10.1146/annurev.arplant.59.032607.092911

Ning, L., Kan, G., Shao, H., and Yu, D. (2018). Physiological and transcriptional responses to salt stress in salt-tolerant and salt-sensitive soybean (*Glycine max* [L.] Merr.) seedlings. *Land. Degrad. Dev.* 29, 2707–2719. doi: 10.1002/ldr.3005

Ogburn, R. M., and Edwards, E. J. (2010). "The ecological water-use strategies of succulent plants," in *Advances in botanical research*. Eds. J.-C. Kader and M. Delseny (San Diego, CA, USA: Academic Press), 179–225.

Ottow, E. A., Brinker, M., Teichmann, T., Fritz, E., Kaiser, W., Brosché, M., et al. (2005). Populus euphratica displays apoplastic sodium accumulation, osmotic

adjustment by decreases in calcium and soluble carbohydrates, and develops leaf succulence under salt stress. *Plant Physiol.* 139, 1762–1772. doi: 10.1104/pp.105.069971

Poorter, H., Niklas, K. J., Reich, P. B., Oleksyn, J., Poot, P., and Mommer, L. (2012). Biomass allocation to leaves, stems and roots: meta-analyses of interspecific variation and environmental control. *New Phytol.* 193, 30–50. doi: 10.1111/j.1469-8137.2011.03952.x

Rabhi, M., Ferchichi, S., Jouini, J., Hamrouni, M. H., Koyro, H.-W., Ranieri, A., et al. (2010). Phytodesalination of a salt-affected soil with the halophyte *Sesuvium portulacastrum* L. @ to arrange in advance the requirements for the successful growth of a glycophytic crop. *Bioresour. Technol.* 101, 6822–6828. doi: 10.1016/j.biortech.2010.03.097

Shrivastava, P., and Kumar, R. (2015). Soil salinity: A serious environmental issue and plant growth promoting bacteria as one of the tools for its alleviation. *Saudi. J. Biol. Sci.* 22, 123–131. doi: 10.1016/j.sjbs.2014.12.001

Sohrabi, Y., Heidari, G., Weisany, W., Golezani, K. G., and Mohammadi, K. (2012). Changes of antioxidative enzymes, lipid peroxidation and chlorophyll content in chickpea types colonized by different Glomus species under drought stress. *Symbiosis* 56, 5–18. doi: 10.1007/s13199-012-0152-8

Tang, X., Mu, X., Shao, H., Wang, H., and Brestic, M. (2015). Global plant-responding mechanisms to salt stress: physiological and molecular levels and implications in biotechnology. *Crit. Rev. Biotechnol.* 35, 425–437. doi: 10.3109/07388551.2014.889080

Tang, L., Zhou, Q. S., Gao, Y., and Li, P. (2022). Biomass allocation in response to salinity and competition in native and invasive species. *Ecosphere* 13, e3900. doi: 10.1002/ecs2.3900

Tani, E., Sarri, E., Goufa, M., Asimakopoulou, G., Psychogiou, M., Bingham, E., et al. (2018). Seedling growth and transcriptional responses to salt shock and stress in *Medicago sativa* L., *Medicago arborea* L., and their hybrid (Alborea). *Agronomy* 8, 231. doi: 10.3390/agronomy8100231

Tokarz, B., Wójtowicz, T., Makowski, W., Jędrzejczyk, R. J., and Tokarz, K. M. (2020). What is the difference between the response of grass pea (*Lathyrus sativus* L.) to salinity and drought stress?—A physiological study. *Agronomy* 10, 833. doi: 10.3390/agronomy10060833

Torche, Y., Blair, M., and Saida, C. (2018). Biochemical, physiological and phenological genetic analysis in common bean (*Phaseolus vulgaris* L.) under salt stress. *Annu. Agr. Sci.* 63, 153–161. doi: 10.1016/j.aoas.2018.10.002

van Zelm, E., Zhang, Y., and Testerink, C. (2020). Salt tolerance mechanisms of plants. *Annu. Rev. Plant Biol.* 71, 403–433. doi: 10.1146/annurev-arplant-050718-100005

Verma, K., Kumar, R., Kumar, A., Bhardwaj, A. K., and Verma, R. C. (2023). Host plant regulates growth processes, ion homeostasis, and salinity tolerance of sandalwood (*Santalum album* L.). *J. Plant Growth Regul.* 42, 4423–4435. doi: 10.1007/s00344-023-10906-3

Wang, Z., Tan, W., Yang, D., Zhang, K., Zhao, L., Xie, Z., et al. (2021). Mitigation of soil salinization and alkalization by bacterium-induced inhibition of evaporation and salt crystallization. *Sci. Total. Environ.* 755, 142511. doi: 10.1016/j.scitotenv.2020.142511

Wicke, B., Smeets, E., Dornburg, V., Vashev, B., Gaiser, T., Turkenburg, W., et al. (2011). The global technical and economic potential of bioenergy from salt-affected soils. *Energ. Environ. Sci.* 4, 2669–2681. doi: 10.1039/d0ee90035d

Xiao, F., and Zhou, H. (2022). Plant salt response: Perception, signaling, and tolerance. *Front. Plant Sci.* 13, 1053699. doi: 10.3389/fpls.2022.1053699

Xu, R., Yamada, M., and Fujiyama, H. (2013). Lipid peroxidation and antioxidative enzymes of two turfgrass species under salinity stress. *Pedosphere* 23, 213–222. doi: 10.1016/S1002-0160(13)60009-0

Yu, Z., Duan, X., Luo, L., Dai, S., Ding, Z., and Xia, G. (2020). How plant hormones mediate salt stress responses. *Trends Plant Sci.* 25, 1117–1130. doi: 10.1016/j.tplants.2020.06.008

Zhang, X., He, P., Guo, R., Huang, K., and Huang, X. (2023). Effects of salt stress on root morphology, carbon and nitrogen metabolism, and yield of Tartary buckwheat. *Sci. Rep.* 13, 12483. doi: 10.1038/s41598-023-39634-0

Zhang, M., Liu, Y., Han, G., Zhang, Y., Wang, B., and Chen, M. (2021). Salt tolerance mechanisms in trees: research progress. *Trees-Struct. Funct.* 35, 717–730. doi: 10.1007/s00468-020-02060-0

Zhang, H., Zhao, Y., and Zhu, J.-K. (2020). Thriving under stress: How plants balance growth and the stress response. *Dev. Cell* 55, 529–543. doi: 10.1016/j.devcel.2020.10.012

Zhao, C., Zhang, H., Song, C., Zhu, J.-K., and Shabala, S. (2020). Mechanisms of plant responses and adaptation to soil salinity. *Innovation* 1, 100017. doi: 10.1016/j.xinn.2020.100017

Zhou, H., Shi, H., Yang, Y., Feng, X., Chen, X., Xiao, F., et al. (2023). Insights into plant salt stress signaling and tolerance. *J. Genet. Genomics* 23, 00179. doi: 10.1016/j.jgg.2023.08.007

frontiers | Frontiers in Plant Science

TYPE Original Research
PUBLISHED 14 February 2024
DOI 10.3389/fpls.2024.1283912

OPEN ACCESS

EDITED BY
Zulfiqar Ali Sahito,
Zhejiang University, China

REVIEWED BY
Dhananjaya Pratap Singh,
Indian Institute of Vegetable Research (ICAR), India
Lu Gan,
National Key Facility for Crop Gene Resources and Genetic Improvement, Institute of Crop Sciences, Chinese Academy of Agricultural Sciences (CAAS), China
Wuwei Ye,
Institute of Cotton Research, Chinese Academy of Agricultural Sciences, China

*CORRESPONDENCE
Guoqing Sun
sunguoqing02@caas.cn
Jianbo Zhu
zjbshz@126.com

RECEIVED 27 August 2023
ACCEPTED 30 January 2024
PUBLISHED 14 February 2024

CITATION
Ma P, Li J, Sun G and Zhu J (2024) Comparative transcriptome analysis reveals the adaptive mechanisms of halophyte *Suaeda dendroides* encountering high saline environment.
Front. Plant Sci. 15:1283912.
doi: 10.3389/fpls.2024.1283912

Comparative transcriptome analysis reveals the adaptive mechanisms of halophyte *Suaeda dendroides* encountering high saline environment

Panpan Ma[1,2], Jilian Li[3], Guoqing Sun[4,5]* and Jianbo Zhu[1]*

[1]College of Life Sciences, Shihezi University, Shihezi, China, [2]Xinjiang Production & Construction Group Key Laboratory of Crop Germplasm Enhancement and Gene Resources Utilization, Biotechnology Research Institute, Xinjiang Academy of Agricultural and Reclamation Sciences, Shihezi, China, [3]Key Laboratory of Cotton Biology and Genetic Breeding in Northwest Inland Region of the Ministry of Agriculture (Xinjiang), Institute of Cotton Research, Xinjiang Academy of Agricultural and Reclamation Sciences, Shihezi, China, [4]Biotechnology Research Institute, Chinese Academy of Agricultural Sciences, Beijing, China, [5]Western Research Institute, Chinese Academy of Agricultural Sciences, Changji, China

Suaeda dendroides, a succulent euhalophyte of the Chenopodiaceae family, intermittently spread around northern Xinjiang, China, has the ability to grow and develop in saline and alkali environments. The objective of this study was therefore to investigate the underlying molecular mechanisms of S. dendroides response to high salt conditions. 27 sequencing libraries prepared from low salt (200 mM NaCl) and high salt (800 mM NaCl) treated plants at 5 different stages were sequenced using Illumina Hiseq 2000. A total of 133,107 unigenes were obtained, of which 4,758 were DEGs. The number of DEGs in the high salt group (3,189) was more than the low salt treatment group (733) compared with the control. GO and KEGG analysis of the DEGs at different time points of the high salt treatment group showed that the genes related to cell wall biosynthesis and modification, plant hormone signal transduction, ion homeostasis, organic osmolyte accumulation, and reactive oxygen species (ROS) detoxification were significantly expressed, which indicated that these could be the main mechanisms of *S. dendroides* acclimate to high salt stress. The study provides a new perspective for understanding the molecular mechanisms of halophytes adapting to high salinity. It also provides a basis for future investigations of key salt-responsive genes in *S. dendroides*.

KEYWORDS

halophyte, *Suaeda dendroides*, salt stress, transcriptome, adaptive mechanism

1 Introduction

Soil salinization has emerged as one of the principal abiotic stresses that threaten plant growth and development and restrict the sustainable development of modern agriculture (Lesk et al., 2016; Kopecka et al., 2023). The adverse effects of excessive soil salinity on plants mainly include osmotic and ion stress. Osmotic stress reduces water absorption of plants, resulting in water leakage. A high concentration of salt ions affects the plasma membrane and changes its permeability, which leads to excessive salt ion absorption by plants and excludes the absorption of other nutrient elements. Imbalanced ion absorption causes nutritional imbalance, inhibits growth, and produces single-salt toxicity, causing metabolic disorders (Yang and Guo, 2018; Zhao et al., 2020; Zhang et al., 2022). Understanding the physiological, biochemical, and molecular mechanisms of plant adaptation to salt stress and exploring the genes related to salt tolerance in nature is beneficial for germplasm innovation and cultivating plant varieties with improved salt tolerance. *Arabidopsis* is widely used in gene functional research and is a model plant for studying molecular mechanisms under various biotic and abiotic stresses. Much effort has been made to breed salt-tolerance crops for agricultural demand, however, the salt tolerance of these crops is limited in their systems. In contrast, halophytes, naturally grown under high salinity conditions, have evolved a series of strategies to adapt to extreme saline environments (Flowers et al., 2015; Calone et al., 2021; Rahman et al., 2021). Learning the mechanisms of salt resistance in halophytic plants and mining key salt-responsive genes are of great significance for cultivating crops with improved salt tolerance.

Halophytes are a kind of plant species that grow and complete their life cycle in saline environments where the salt concentration is greater than 200 mM NaCl, which accounts for about 1% of the world flora (Flowers and Colmer, 2008). Euhalophytes, accumulate excessive Na^+ in their succulent leaves and stems and compartmentalize into vacuoles, enabling them to cope with high salt stress (Flowers et al., 2015). The genus *Suaeda* is a typical euhalophyte, an annual or perennial herb or sub-herb of Chenopodiaceae. It is usually distributed in coastal areas, intertidal zones, deserts, inland salt lakes, and various saline and alkali environments around the world (Wang and Song, 2019; Wang et al., 2022). The *suaeda* plants grow well with 200 mM NaCl and complete their life cycle in environments where salt and drought co-exist (Song et al., 2009; Guo et al., 2017; Guo et al., 2020). Moreover, the potential of several high salt responsive genes like transporters (*NHX1* and *HKT1*), ion channel (*AKT1*, *TPCA1*, *SLAC1*, aquaporins), antioxidant (*APX*, *CAT1*, *GST*) and osmotic (*CMO*, *BADH* and *P5CS*) have been identified and cloned (Mishra and Tanna, 2017), and some of these genes were explored for developing stress tolerance in the glycophyte (Lv et al., 2008; Wu et al., 2008; Shao et al., 2014; Himabindu et al., 2016; He et al., 2017; Hao et al., 2020). In addition, studies have increasingly found that halophytes can be economical and environmentally friendly candidate species for phytoremediation; excessive salt and heavy metals can be removed from salt and contaminated soils through various strategies to support plant growth (Liang and Shi, 2021; Wang L. et al., 2021). The above research shows that halophytes have important ecological and economic values. A comprehensive study on salt tolerance mechanism of halophytes is crucial for excavating key genes and cultivating stress-resistant varieties, as well as phytoremediation, which is conducive to promoting the sustainable development of agricultural economy in saline-alkali areas.

Suaeda plants can adapt to high concentration saline soil and act as ideal model plants for investigating complicated physiological and molecular mechanisms of salt tolerance. To explore the molecular mechanism of *S. dendroides* adapting to salt stress conditions, two groups of *de novo* assembled data were generated from mRNA sequencing of shoot samples from low salt and high salt treated seedlings. Bioinformatics analyses were adopted to compare changes at mRNA levels. These data would contribute to elucidating the molecular mechanisms of *S. dendroides* acclimate to high salt stress. Furthermore, the transcript information of *S. dendroides* under high salt treatment was obtained comprehensively, which provided a basis for studying gene expression levels, discovering new transcripts, and exploring the functions of key salt-tolerant genes.

2 Materials and methods

2.1 Plant materials and NaCl treatment

The seeds of *S. dendroides* were collected from saline soil in Fuhai, Xinjiang Uygur Autonomous Region, China. *S. dendroides* seeds were sown in plastic pots (12×12 cm), filled with mixed matrix (sand:vermiculite:nutritive soil = 10:1:2, w/w/w) and irrigated with tap water, placed in a plant culture room, maintained a day/night thermoperiod of 25/20°C, a photoperiod of 16 h light/8 h dark, relative humidity of (50 ± 10)%. 10 seedlings with uniform growth were maintained per pot after germination and irrigated with tap water once a week. After one month of incubation, the seedlings were irrigated with 0, 200, 400, 600, 800, and 1,000 mM NaCl solutions. 150 mL of the NaCl solution was applied in salt treatments, while the control pots were irrigated with the same volume of tap water. Throughout the experimental process, water was replenished daily through weighing methods to ensure that the water content of each pot was maintained at 50%.

2.2 Determination of morphological and physiological characters

According to the growth and phenotype of the *S. dendroides* seedlings under different concentrations of salt stress, the physiological and biochemical parameters were determined after treatment for 10 days. Each variable was determined in three biological replicates.

The shoot samples were taken for biomass and ion content analyses. The fresh weight (FW) of aerial tissues was measured immediately after harvest. The dry weight (DW) was determined by

10.3389/fpls.2024.1283912

putting the FW samples in an oven at 105 °C for 10 min, then drying for 48 h at 85°C until the mass was constant. Relative water content (RWC) was calculated using the formula: RWC = (FW-DW)/FW×100%. In order to know the salt absorption of *S. dendroides* plants, Na content in the seedlings under salt treatment was detected. Briefly, 100 mg dried powder from the shoot of each treatment sample was weighed and digested with 5 mL HNO_3 overnight and incubated at 80°C for 1~2 h, 120°C for 1~2 h, then 160°C for 4 h, cooling to room temperature, after filtering the extracts, Na and K content was determined by inductively coupled plasma atomic emission spectroscopy (ICP-AES/OES/MS).

Fresh leaf samples were taken for physiological and biochemical parameters analyses, such as chlorophyll content, ribulose-1,5-bisphosphate carboxylase/oxygenase (Rubisco) activity, malondialdehyde (MDA) content, proline content, soluble sugar content. All the above variables were assayed as the instructions of the reagent kit (Solarbio, China), and the absorbance was measured using a UV2300 ultraviolet visible spectrophotometer (Tianmei, China).

2.3 RNA sequencing and bioinformatics analysis

Based on our preliminary physical investigations, 200 mM NaCl is the optimal salt concentration, and 800 mM NaCl is the highest salt concentration for the growth of *S. dendroides* seedlings (Figure 1). Consequently, the shoot samples were harvested at 0 (before the treatment, marked as C), 1, 5, 10, and 15 days after 200 (marked as L1, L5, L10, and L15) and 800 mM NaCl treatments (marked as H1, H5, H10, and H15) for RNA- sequencing and QPCR. Total RNA extraction from 27 shoot tissues of *S. dendroides* was according to the manufacturer's procedure of the EASYspin Plus Plant RNA Kit (Aidlab, China). Qubit® RNA Assay Kit in Qubit® 2.0 Fluorometer (Life Technologies, USA) was used to detect RNA concentration, and RNA Nano 6000 Assay Kit of Agilent Bioanalyzer 2100 system (Life Technologies, USA) was used to evaluate RNA integrity. NEBNext® Ultra™ RNA Library Prep Kit of Illumina® (NEB, USA) was used to generate sequencing libraries following the manufacturer's recommendations, and library quality was evaluated by the Agilent

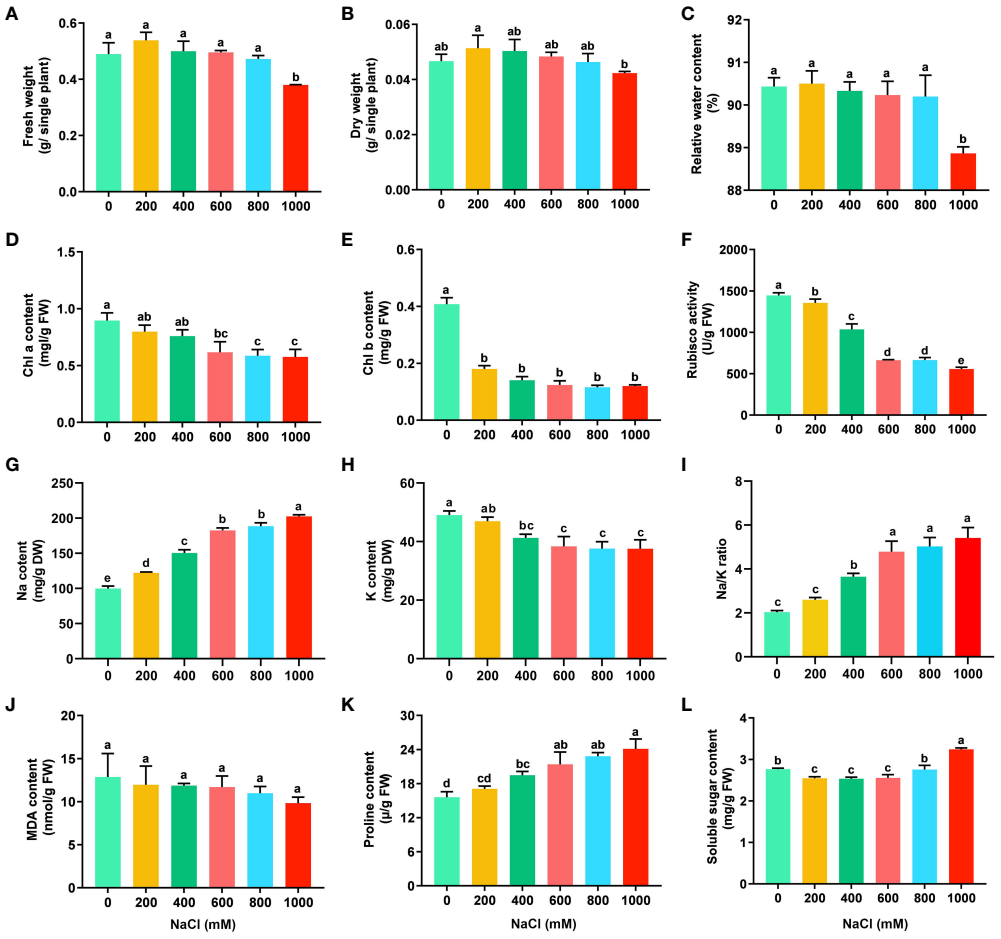

FIGURE 1
Physiological variables of *S. dendroides* under salt stress. **(A)** Fresh weight, **(B)** Dry weight, **(C)** Relative water content, **(D)** Chl a content. **(E)** Chl b content, **(F)** Rubisco activity, **(G)** Na content, **(H)** K content, **(I)** Na/K ratio, **(J)** MDA content, **(K)** Proline content, **(L)** Soluble sugar content. X-axis means the concentration of NaCl (mM). Statistical analysis was conducted using SPSS 20.0 software, the significant difference between different treatments was obtained through Tukey's test of one-way ANOVA analysis. Values are presented as the mean ± the standard error (SE) with three biological replicates. The different letters above the bars indicate the least significant differences between treatments at $p < 0.05$.

Bioanalyzer 2100 system. The libraries were sequenced on an Illumina Hiseq platform, and paired-end reads were generated. After filtering adaptor sequences, duplicated sequences, low-quality bases, and undetermined bases, the high-quality clean reads were assembled using Trinity software (Grabherr et al., 2011). Function annotation of the assembled unigenes was carried out through NCBI non-redundant protein sequences (Nr), NCBI non-redundant nucleotide sequences (Nt), Protein family (Pfam), Clusters of Orthologous Groups of proteins (KOG/COG), A manually annotated and reviewed protein sequence database (Swiss-Prot), KEGG Ortholog database (KO) and Gene Ontology (GO) databases.

2.4 DEG selection and functional enrichment analysis

The transcription level of the assembled unigenes was evaluated according to FPKM to identify DEGs between L1 vs C, L5 vs C, L10 vs C, L15 vc C, H1 vs C, H5 vs C, H10 vs C, H15 vs C, H1vs L1, H5 vs L5, H10 vs L10, and H15 vs L15 compares. Differential expression analysis of two conditions/groups was carried out by DESeq2 software (Love et al., 2014). The negative binomial Wald test was used as a statistical test, and then the Benjamini-Hochberg correction was used to obtain the false discovery rate (FDR) (Benjamini and Hochberg, 1995; Love et al., 2014). FDR < 0.05 and |log2FC| > 1 were set as the thresholds for screening of significantly differential expressed genes. VENNY 2.1 (https://bioinfogp.cnb.csic.es/tools/venny/), a free online platform, was used to draw Venn diagrams. TBtools v1.120 was used to construct the heatmaps for gene expression. GO and KEGG enrichment analysis of DEGs were performed using GOseq R packages based on Wallenius non-central hyper-geometric distribution (Young et al., 2010) and KOBAS software (Mao et al., 2005). The sequences of the target DEGs were aligned to the protein sequence of the reference species contained in the STRING database (http://string-db.org/) by using blasx, and an interaction network was constructed by using the protein-protein interaction (PPI) relationship of the reference species. The PPI network of the DEGs was visualized and edited by Cytoscape software v3.9.1 (Shannon et al., 2003).

2.5 Gene expression validation using quantitative real-time PCR

10 putative DEGs involved in salt conditions were randomly selected for validation of differential expression using QPCR. The primers for the selected genes were designed according to the sequences assembled by *S. dendroides* RNA sequencing and are listed in Supplementary Table S1. 18S gene of *Anabasis aphylla* was used as the reference for quantitative expression analysis. 1 ug RNA of 27 samples was reverse transcribed into cDNA with oligo (dT) primers, and the cDNA libraries were used for QPCR. A total of 20μL fluorescent quantitative reaction system contains 10 μL of 2 × PerfectStart® Green qPCR SuperMix (TransGen, China), 2 μL of cDNA template, 0.8 μL of 10 mM primers and 0.4 μL of 50 × ROX Reference Dye. QPCR was performed on an ABI 7500 platform, and the settings were as follows: step 1 95°C, 30 s; step 2 95°C, 5 s, 60°C, 34 s, 40 cycles, followed by the melting curve analysis. Each DEG was analyzed in three biological samples, and each biological sample was repeated three times. $2^{-\Delta\Delta CT}$ method was used to calculate the relative expression levels of the target genes (Livak and Schmittgen, 2001).

2.6 Statistical analysis

Statistical analysis was conducted using SPSS 20.0 software, the significant differences were analyzed by one-way ANOVA and Tukey's test ($p < 0.05$). The images were visualized using GraphPad Prism software (v. 8.3.0.538), and the data was shown as the mean ± standard deviation (SD) value of at least three biological replicates.

3 Results

3.1 Phenotypic and physiological indicators of *S. dendroides* under salt stress

The physiological and biochemical features of *S. dendroides* seedlings under different salt concentrations were performed to estimate the optimal and highest salt concentration for their growth. The seedlings of *S. dendroides* did not show symptoms of salinity injury after being treated with 200, 400, and 600 mM NaCl treatment compared with the control. The seedlings showed wilting symptoms under 800 and 1,000 mM NaCl treatment and began to recover after 5 days and recovered after 10 days, then gradually returned to normal growth. Under 1000mM NaCl stress, although some seedlings died, most seedlings survived, and the wilting symptoms slowly recovered (Supplementary Figure S1). The fresh weight, dry weight, and relative water content of seedlings showed the highest under 200 mM NaCl treatment, but the difference was not significant compared with the control. However, the fresh weight, dry weight, and relative water content of seedlings treated with 1000 mM NaCl were significantly lower than those of other salt concentrations (Figures 1A-C). The results indicate that a low concentration of NaCl could promote the growth of seedlings. The content of Chl a and Chl b, and Rubisco activity decreased obviously with the increase of NaCl concentration (Figures 1D-F), respectively. Na and K content in the shoots of *S. dendroides* were determined, and the results showed that Na content was significantly increased with the increase of NaCl concentration. When the NaCl concentration reached 400 mM, the accumulation of Na was 1.5 times that of the control (Figure 1G). The content of K decreased obviously with the increase of salt concentration, which was opposite to Na content (Figure 1H). The trend of Na/K ratio was consistent with that of Na accumulation. When the salt concentration increased to 600 mM, the change of Na/K ratio was moderate and kept a relatively stable level (Figure 1I). The results indicated that *S. dendroides* could maintain Na/K balance under high salt stress to avoid ion toxicity.

The physiological parameters, such as MDA, proline, and soluble sugar, are usually used to evaluate salt tolerance of plants. In *S. dendroides*, MDA content decreased gradually with the increase of NaCl concentration, but the difference was not significant (Figure 1J), indicating that salt in this concentration range did not cause the cell membrane lipid peroxidation of *S. dendroides*. The content of free proline in the seedlings of *S. dendroides* was significantly increased with the increase of NaCl concentrations (Figure 1K). The soluble sugar content decreased significantly under 200, 400 and 600 mM NaCl treatment, but it was significantly higher than the control when the salt concentration increased to 1000 mM (Figure 1L).

3.2 RNA-seq, *de novo* assembly and unigene functional annotation

RNA-seq analyses on the *S. dendroides* with water (C), 200 mM NaCl (L), and 800 mM NaCl (H) treatments at different time points (1, 5, 10, and 15 days) were performed. In total, 27 cDNA libraries were generated and sequenced. A total of 211.13 Gb clean data were obtained, and each sample library yielded a mean size of 7.8 Gb clean data, a Q30 percentage higher than 93.65%, and a GC percentage of 42% (Supplementary Table S2). Pearson's coefficient of pairwise biological replicates was greater than 0.85, indicating that the consistency among the replicates was high (Supplementary Figure S2). The data shown above demonstrate that the transcriptome sequencing is of high quality. Since *S. dendroides* has no reference genome, Trinity software was used to do the *de novo* assembly and get the reference sequence for subsequent analysis. 133,107 unigenes were obtained from 27 libraries. The size distribution was shown in Supplementary Figure S3, the sequence of 38,197 unigenes was longer than 1,000 bp, and 12,286 unigenes was longer than 2000 bp, indicating that some candidate genes have obtained nearly full-length sequence. The mean sequence length of all unigenes was 918 bp, and the N50 length was 1,240 bp (Supplementary Table S3).

133,107 unigene sequences of *S. dendroides* were aligned based on similarities to the NR, NT, Pfam, Swiss-Prot, KEGG, GO, and KOG databases. The annotation results were shown in Supplementary Table S4, all 133,107 (100%) unigene sequences were annotated at least in one database, and 6,443 (4.84%) aligned to all seven databases. A total of 58,336 (43.82%), 42,308 (31.78%), and 42,637 (32.03%) unigenes had significant BLAST matches in NR, NT, and Pfam databases, respectively. Moreover, 42,637 (32.03%) unigenes were annotated in at least one term of three GO categories (Supplementary Figure S4), 19,118 (14.36%) unigenes were annotated in the KEGG database and classified into 130 KEGG pathways (Supplementary Figure S5). In addition, 11,489 (8.63%) unigenes were annotated in the KOG database and divided into 25 functional categories (Supplementary Figure S6). By comparing the annotation results with the NR database, the distribution of species on the unigene comparison was statistically analyzed. The result showed that *S. dendroides* transcriptome sequences were well matched with the species of *Chenopodium quinoa* (29.8%), *Beta vulgaris* (27.8%), and *Spinacia oleracea* (19.0%) belonging to Amaranthaceae (Supplementary Figure S7).

3.3 DEGs in *S. dendroides* under salt treatment

DEGs under salt-stressed conditions were defined according to threshold FDR < 0.05 and $|\log_2$ fold change$| > 1$ among different salt-treated samples. A total of 733, 3189, and 992 DEGs were detected between L vs C, H vs C, and H vs L pairwise comparisons, respectively. DEGs were analyzed at each time interval after NaCl treatment (Figure 2A). With the extension of salt treatment time, the number of DEGs increased to 444 and 1,796 after 10 days, which was the peak of salt-responsive genes under both NaCl concentrations, indicating that this period was the key time for *S. dendroides* to adapt to the salt environment. Down-regulated DEG numbers were more than up-regulated genes among all the treatments. 130 of the 3,189 DEGs were detected among different times of 800 mM NaCl treatment. In addition, only 4 DEGs were detected among 733 DEGs at different times of 200 mM NaCl treatment (Figure 2B). In addition, the expression profiles of DEGs under each treatment were visualized in the heat map (Figure 2C). The expression patterns of most DEGs of samples H1, H5, and H10 were similar and clustered in one class, while the samples H15, C, L1, L5, L10, and L15 were clustered in another class. The results showed that the expression pattern of DEGs under 200 mM NaCl treatment was similar to the control, while the DEGs under 800 mM NaCl treatment were contrary to the control. These results indicated that the euhalophyte *S. dendroides* gradually adapted to the high salt stress environment, in which the 10 days was a critical time for *S. dendroides* to cope with the high salt stress environment. Consequently, the following analysis focuses on the DEGs of 800 mM NaCl treatment to get a comprehensive understanding of the adaptive mechanisms of *S. dendroides* encountering high salt stress.

GO and KEGG enrichment analyses were carried out on DEGs at different time points with high salt treatment. GO enrichment analysis showed that the DEGs of H1 vs C, H5 vs C, H10 vs C, and H15 vs C comparisons were significantly enriched in 45, 14, 41, and 39 processes (FDR < 0.05), respectively (Supplementary Table S5). The top 30 Go items of different salt time points were shown in Figures 3A-D, the catalytic activity item was notably enriched at each salt time point, and the DEG numbers were the highest. Besides, carbohydrate metabolic, cell metabolic, methionine metabolic, protein phosphorylation and protein kinase were the most enriched items at each salt treatment. KEGG enrichment results showed that the DEGs of H1 vs C, H5 vs C, H10 vs C, and H15 vs C comparisons were significantly enriched (p-value < 0.05) in 11, 9, 13 and 16 pathways, respectively (Supplementary Table S6). Among these, phenylpropane metabolism, plant hormone signal transduction, cysteine and methionine metabolism, glycerophospholipid metabolism, starch and sucrose metabolism, and ribosome pathway at different salt treatment time points were significantly enriched (Figures 4A-D; Supplementary Table S6). In addition, cell wall-related metabolic pathways were also found in this study, such as the galactose metabolic pathway closely related to pectin, the pentose glucuronic acid conversion, and the flavonoid biosynthesis metabolism closely related to lignin, the phenylalanine metabolic pathway, and keratin and wax biosynthesis. Moreover, the key protein-protein interaction (PPI) network of high NaCl treatment for 10 days was predicted. The result showed that DEGs related to cell wall

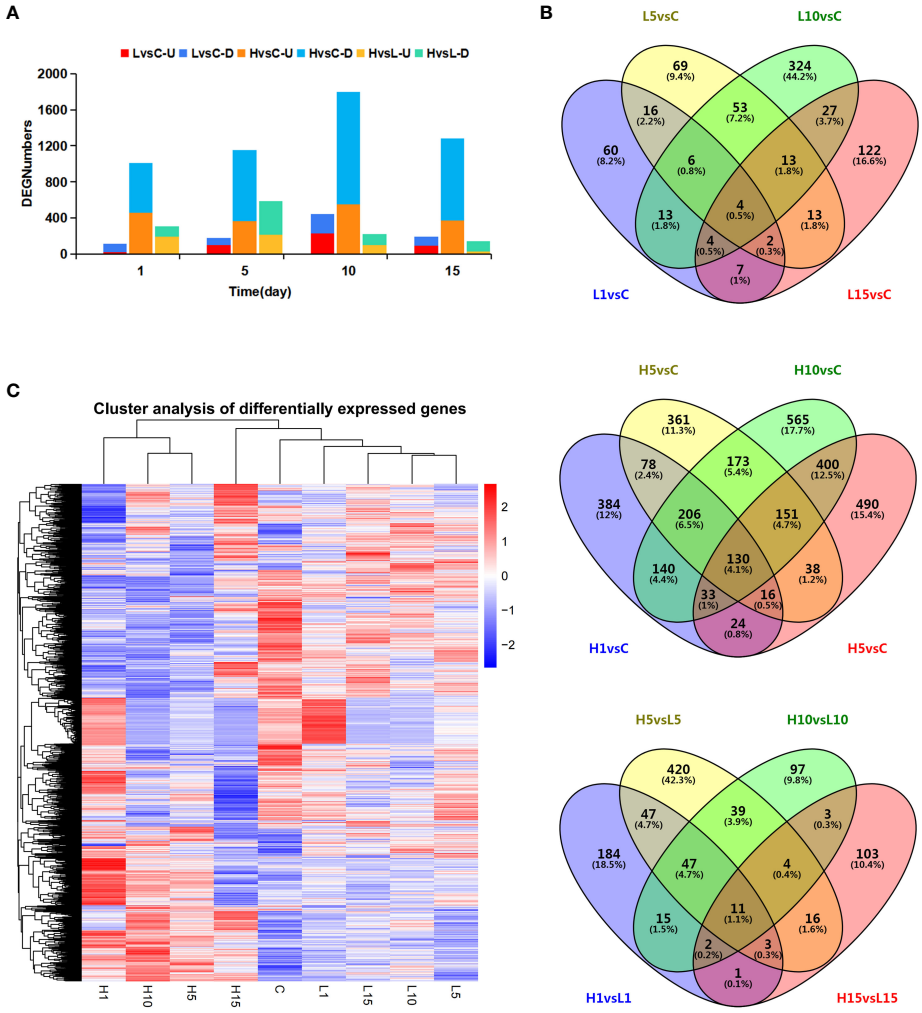

FIGURE 2
The numbers of all DEGs at different salt-stressed time points of two NaCl concentrations. **(A)** Numbers of DEGs in pairwise comparisons at different salt-stressed time points of two NaCl concentrations, **(B)** Venn diagram showed the number of DEGs in different treatment, **(C)** Heatmap diagrams showed the cluster analysis of DEGs among the treatments. Number of DEGs (FDR< 0.05 and |log 2 Fold Change| > 1) under 200mM (L) and 800mM (H) NaCl stress for 1, 5,10 and 15 day as compared to control samples.

synthesis and modification, ABA signaling, ethylene biosynthesis, and organic osmolyte accumulation under high salt treatment, which is consistent with GO and KEGG enrichment results. The above results indicate that cell wall synthesis and modification, ABA signaling, ethylene biosynthesis and signal, organic osmolyte accumulation, and ROS homeostasis might be the main adaptation mechanisms of *S. dendroides* suffering from extreme salt stress.

3.4 DEGs related to cell wall synthesis and modification under high salt treatment

According to GO, KEGG enrichment, and PPI results, the DEGs involved in cell wall metabolism of *S. dendroides* under high saline conditions were analyzed. 13 DEGs involved in cellulose synthesis were induced by 800 mM NaCl stress (Figure 5A; Supplementary Table S7). Among these, 4 predicted cellulose synthase A (*CESA*) genes, including 1 *CESA1* and 3 *CESA3* genes, which produced cellulose in the primary cell wall (PCW), were up-regulated and significantly increased after 10 days of treatment. Moreover, 3 predicted *CESA4*, 2 xylem-specific *CESA7*, and 2 *CESA8* genes involved in the biosynthesis of the secondary cell wall (SCW) were up-regulated and dramatically increased after 10 and 15 days of 800 mM NaCl treatment. In addition, 2 COBRA-like (*COBLs*) genes related to cell wall biosynthesis were up-regulated under 800 mM NaCl treatment and prominently increased after 15 days of the treatment. Moreover, several genes involved in hemicellulose synthesis were detected under high salt stress. 6 glycosyltransferase (GT) family genes involved in the biosynthesis of xylan backbone were identified under high salt treatment (Figure 5A; Supplementary Table S7). Such as glucuronoxylan glucuronosyltransferase (*IRX7*), beta-1,4-xylosyltransferase (*IRX9* and *IRX14*), galacturonosyltransferase-like 1 (*GATL1*), UDP-glucuronate:xylan alpha-glucuronosyltransferase 1 (*GUX1*/*PGSIP*1 and *GUX2*/*PGSIP3*) related to the secondary cell wall biosynthesis, were all significantly increased after 10 days of 800 mM NaCl stress.

10.3389/fpls.2024.1283912

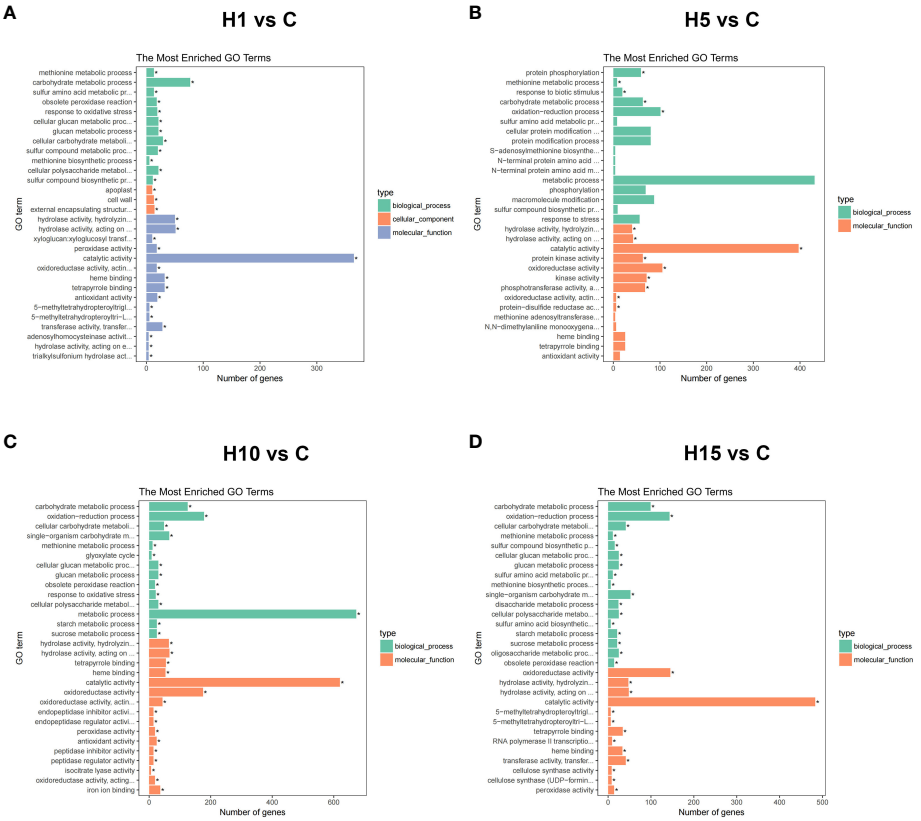

FIGURE 3
GO enrichment analysis of DEGs in **(A)** H1 vs C, **(B)** H5 vs C, **(C)** H10 vs C, **(D)** H15 vs C comparisons of high salt stress. Top 30 GO enrichment terms of differently expressed genes significant p-values ($p < 0.05$). GO terms are mainly divided into three classes: cellular component, molecular function, and biological process. X-axis means the number of DEGs. Y-axis represents GO terms.

Meanwhile, 2 non-glycosyltransferase genes, IRREGULAR XYLEM 1 (*IRX15*) and IRREGULAR XYLEM 1 like (*IRX15L*), related to xylan backbone synthesis were up-regulated under high salt treatment. 2 cellulose synthase-like protein D5 (*CLSD5*) related to the biosynthesis of hemicellulose polysaccharides were detected to be significantly expressed under 800 mM NaCl stress. In addition, 6 laccases (*LAC*) and 30 peroxidases (*PER*) genes related to the polymerization of lignin monolignol were also found under high salt stress (Figures 5A, 6C; Supplementary Table S7).

Interestingly, multiple DEGs involved in cell wall modification and remodeling were identified under 800 mM NaCl stress. 20 xyloglucan endotransglucosylase/hydrolase (*XTH*/*XET*) and 5 expansins/expansins-like (*EXP*/*EXL*) genes that participated in cell wall loosening were identified (Figure 5B; Supplementary Table S7). Several glycosidase encoding DEGs involved in hydrolyzing hemicellulose polysaccharides were obtained, such as 7 β-galactosidase (*BGLU*), 6 β-galactosidase (*BGAL*), and 7 β-D-xylosidases (*BXL*) genes were differentially expressed under 800 mM NaCl stress (Figure 5E; Supplementary Table S7). *XYL* involved in xyloglucan degradation was down-regulated under high salt treatment. Additionally, pectin metabolic enzymes (Figure 5E; Supplementary Table S7), including pectin acetylesterase (*PAE*), pectin methyl esterase (*PME*), polygalacturonase (*PG*), polygalacturonase inhibitor (*PGIP*), and pectate lyase (*PL*) encoding genes involved in cell wall remodeling were obtained under high salt treatment. 4 *PMEs*, 2 *PLs*, 4 *PG1s*, and 1 *PAE* were up-regulated under 800 mM NaCl treatment (Figure 5E; Supplementary Table S7). 5 trichome birefringence-like (*TBL*) genes involved in xylan acetylation were up-regulated, 6 GDSL esterase/lipase (*GSDL*) encoding genes that affecting xylan deacetylation were up-regulated under high salt stress, especially after 10 days, 6 EXORDIUM/EXORDIUM-like (*EXO/EXL*) genes involved in the regulation of secondary cell wall thickening and lignification were significantly increased after 15 days of high salt stress (Figure 5C; Supplementary Table S7). Moreover, several cell wall genes and receptor-like kinase genes were differentially expressed under high salt treatment (Figure 5D; Supplementary Table S7). 6 DEGs encoding FASCICLIN-like arabinogalactan protein (FLA) were notably increased after 15 days of high salt treatment. 1 leucine-rich repeat extensin-like protein (LRX3) decreased at the early stage of high salt treatment and increased after 15 days. 4 FERONIA (*FER*) genes of *Catharanthus roseus* RLK1-like kinase (*CrRLK1L*) family were down-regulated under high salt stress. 9 Wall-associated receptor kinase (*WAK/WAKL*) encoding genes were decreased at the early stage of high salt treatment and increased to varying degrees after 15 days of 800 mM NaCl treatment.

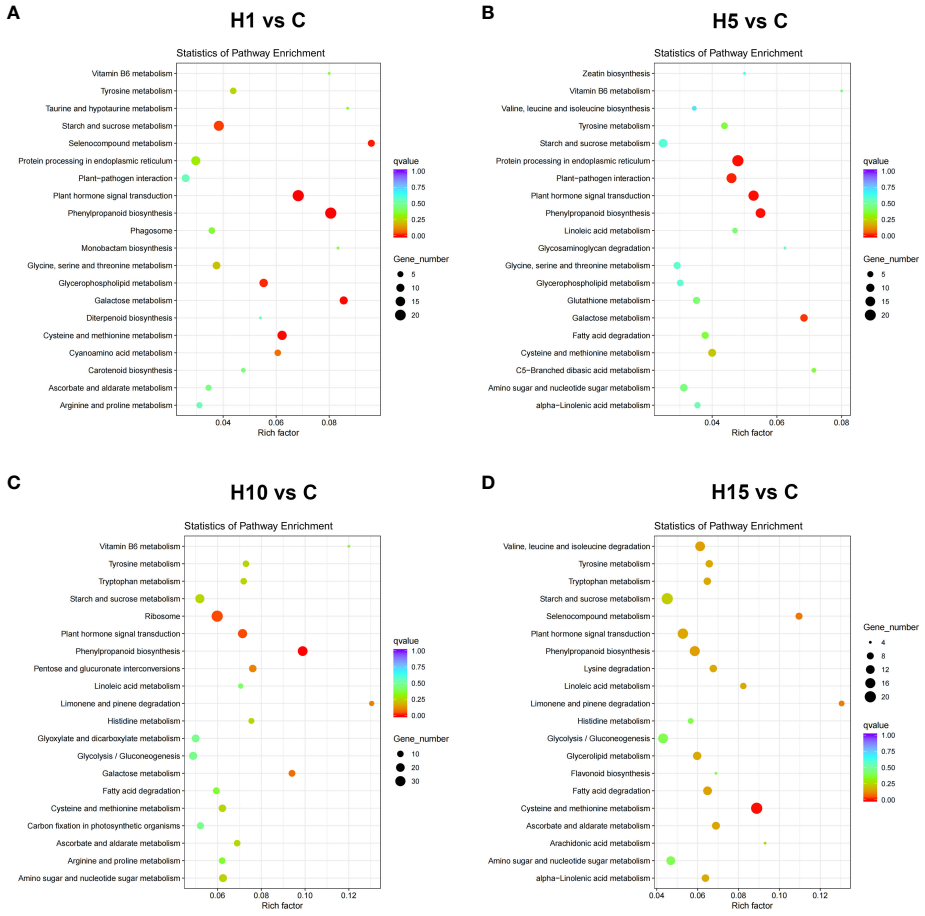

FIGURE 4
KEGG pathway enrichment analysis of DEGs in **(A)** H1 vs C, **(B)** H5 vs C, **(C)** H10 vs C, **(D)** H15 vs C comparisons of high salt stress. Top 20 GO enrichment terms of differently expressed genes significant p-values ($p < 0.05$). X-axis represents Rich factor. Y-axis represents the KEGG pathway.

3.5 DEGs related to ion transport and Ca^{2+} signaling

Several DEGs associated with ion transport were obtained under 800 mM NaCl treatment in the study (Figure 6A; Supplementary Table 7). A sodium/hydrogen exchanger protein NHX1 involved in vacuolar Na^+ transport was significantly up-regulated under 800 mM NaCl treatment. Similarly, a two-pore potassium channel protein TPK3 associated with vacuolar K^+ transport, 2 vacuolar Ca^{2+}/H^+ exchanger (*CAX*) genes were significantly up-regulated. DEGs of plasma membrane ATPase (*PMA*) and vacuolar H^+-pyrophosphatases (*AVP*) were also up-regulated. The results indicated that the up-regulated *NHX*, *PMA*, and *AVP* might be crucial for Na^+ sequestration into the vacuolar of *S. dendroides*. 5 high-affinity K^+ transporter (HKT1) encoding genes involved in Na^+ transport were obtained, the expression level of 3 genes was significantly increased after 1 day, and 2 were increased significantly after 15 days of high salt treatment. Potassium transporter (KUP) was significantly up-regulated after 1 day of 800 mM NaCl treatment. 3 cyclic nucleotide-gated ion channel (*CNGC*) genes were obtained, *CNGC4* was up-regulated, and 2 *CNGC17* genes were down-regulated under high salt treatment. 2 Ca^{2+} influx channel proteins mid1-complementing activity 1 (MCA1) were up-regulated, especially after 10 and 15 days of 800 mM NaCl treatment. The increasing cytoplasmic Ca^{2+} are decoded by a series of Ca^{2+} sensors or binding proteins, such as calcineurin B-like protein (CBL), Ca^{2+}- dependent protein kinases (CPK), Calmodulin (CaM), calmodulin-like proteins (CML), calcium-dependent protein kinase (CIPK) and calreticulin (CRT). 21 DEGs that participated in Ca^{2+} signaling pathway were obtained, as shown in Figure 6A, *CBL4, CIPKs*, *CMLs*, and *CRTs* were induced by high salt stress. Several nitrate transporter 1/peptide transporter, NRT1/PTR family (NPF) encoding genes related to NO^{3-}/Cl^- transport were obtained (Figure 6A). Among these, 8 NPF genes were down-regulated, and 7 were significantly up-regulated after 1 day of high salt stress. Besides, 18 ABC transporters were differently expressed under high salt concentration treatment, in which 3 *ABCC22* genes were notably increased after 1 day, 3 genes were up-regulated at all the treatment times, while the remaining 12 genes were down-regulated at all the treatments.

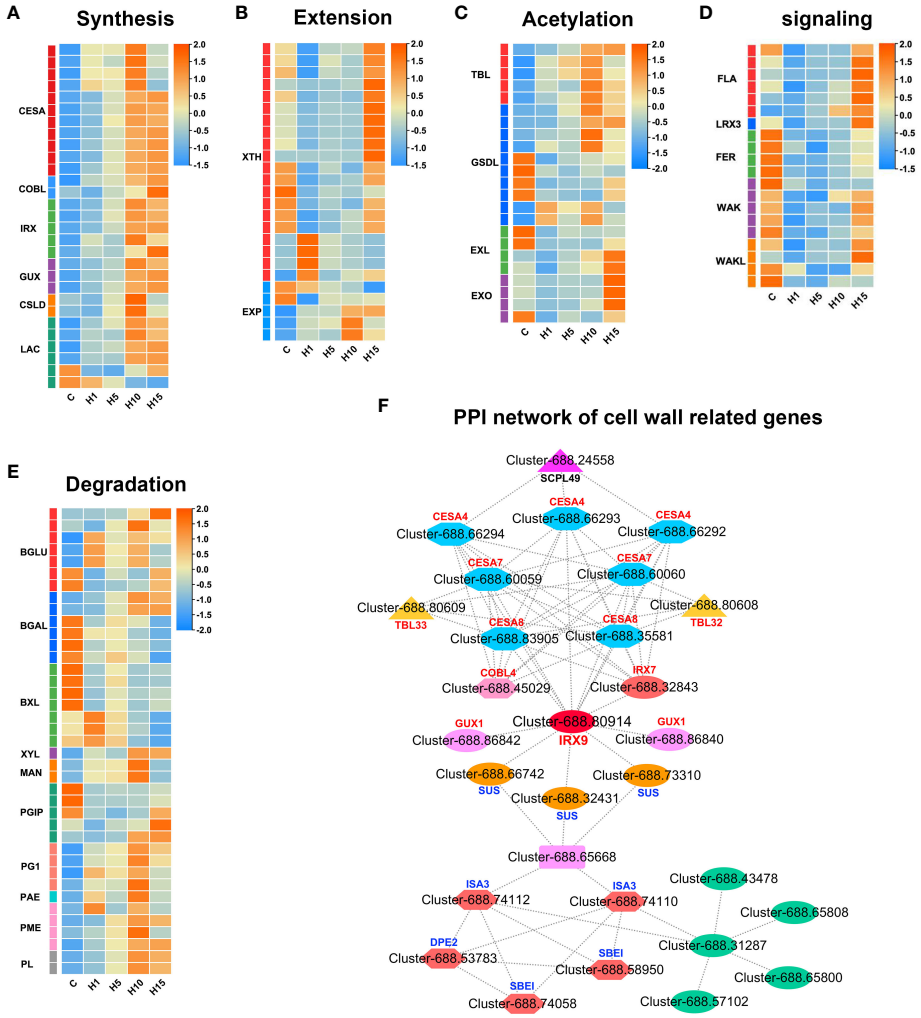

FIGURE 5
Expression profiles of DEGs related to cell wall **(A)** synthesis, **(B)** extension, **(C)** acetylation, **(D)** proteins and signaling, **(E)** degradation, **(F)** PPI network of cell wall related DEGs in *S. dendroides* after 10 days of high salt stress. The column names C, H1, H5, H10, and H15 in each heat map are the samples treated with 800 mM NaCl after 0, 1, 5, 10, and 15 days. The expression level is represented by the mean value of FPKM (n=3), and the color scale in the upper right represents the normalized FPKM value.

3.6 DEGs related to organic osmolyte synthesis and ROS detoxification

The accumulation of organic adjustment substances in succulent leaves is another important reason for *S. dendroides* adapting to high salt environment. In this study, 44 DEGs positively correlated with the synthesis of organic adjustment substances proline, betaine, and soluble sugar were identified (Figure 6B). Among these, 2 delta-1-pyrroline-5-carboxylate synthase (*P5CS*), a key enzyme gene involved in proline synthesis, were significantly up-regulated under 800 mM NaCl treatment. 9 choline monooxygenase (*CMO*) and 3 betaine aldehyde dehydrogenase (*BADH*), key enzyme genes participated in betaine synthesis, were also significantly up-regulated. Moreover, 7 phosphoethanolamine N-methyltransferase (*NMT*) genes were notably up-regulated after 1 day of high salt treatment. Likewise, 5 sucrose synthase (*SUS*) encoding genes and 2 4-alpha-glucanotransferase (*DPE1*) involved in soluble carbohydrate accumulation were significantly up-regulated under 800 mM NaCl treatment. 1 sucrose transport protein SUC and 2 bidirectional sugar transporters (SWEET) were significantly increased under high salt stress. These results showed that the up-regulated DEGs of organic osmolyte synthesis under high salt treatment, including proline, betaine, and soluble sugar, play vital roles in osmoregulation of *S. dendroides*. Antioxidant enzymes and non-enzymatic compounds were crucial for detoxification of ROS under stress conditions. In *S. dendroides*, the genes of ascorbate peroxidase (*APX*), superoxide dismutase (*SOD*), catalase (*CAT*), *PER*, glutathione S-transferase (*GST*), and L-ascorbate oxidase (*AAO*) were significantly enriched and differentially expressed, to avoiding oxidative stress induced by high salinity (Figure 6C). Besides, polyphenol oxidase (*PPO*), primary amine oxidase (*AO*), and ferritin (*Fer*) encoding genes were up-regulated at all time points after 800 mM NaCl treatment. 10 aldehyde dehydrogenase (*ALDH*) encoding genes and 4 alcohol dehydrogenase-like (*ADH*) encoding genes were differently expressed (Figure 6C).

10.3389/fpls.2024.1283912

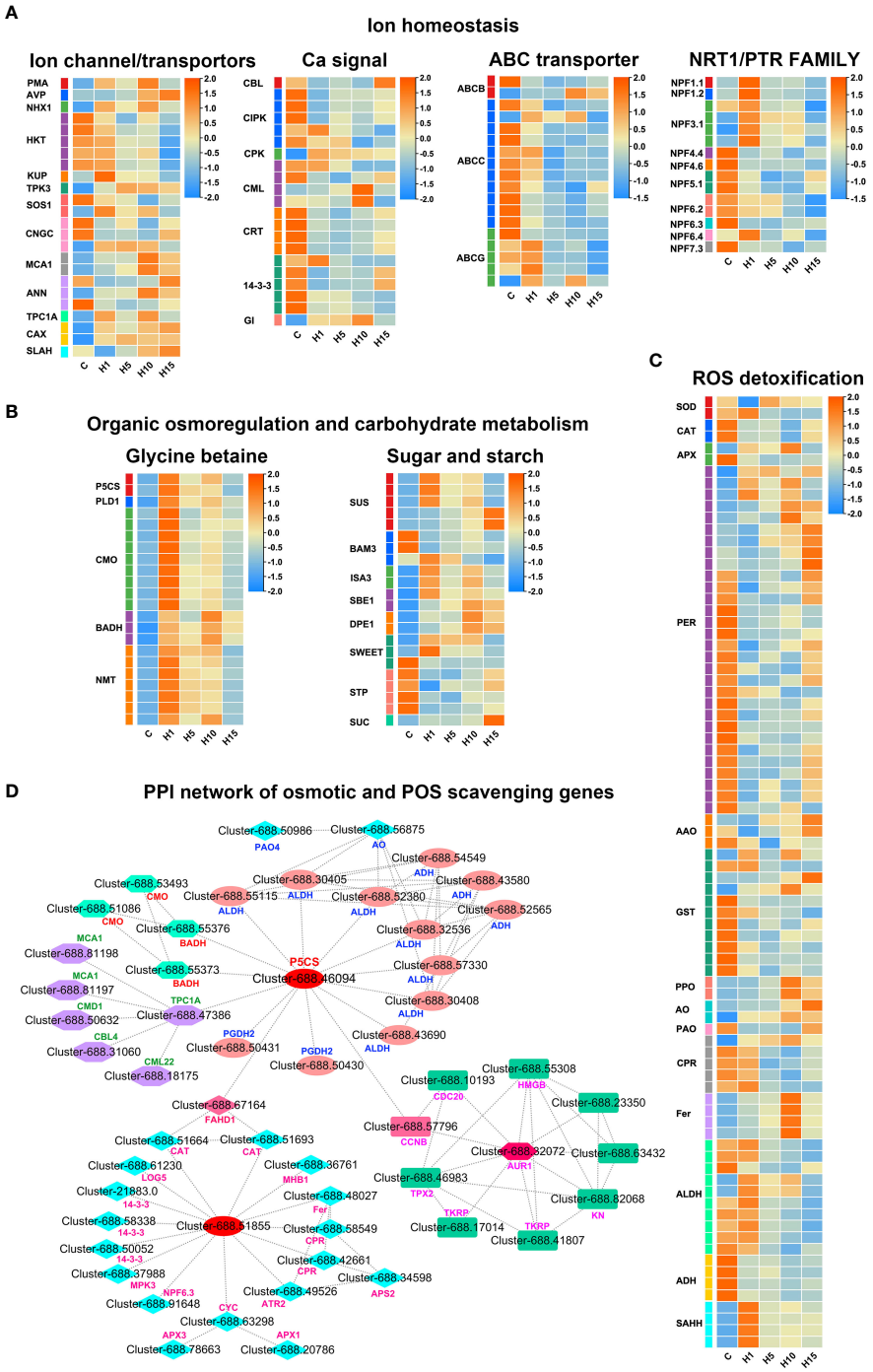

FIGURE 6
Expression profiles of DEGs related to **(A)** Ion homeostasis, **(B)** Organic osmoregulation and carbohydrate metabolism, **(C)** ROS detoxification, **(D)** PPI network of osmotic and ROS scavenging related DEGs in *S. dendroides* after 10 days of high salt stress. The column names C, H1, H5, H10, and H15 in each heat map are the samples treated with 800 mM NaCl after 0, 1, 5, 10, and 15 days. The expression level is represented by the mean value of FPKM (n=3), and the color scale in the upper right represents the normalized FPKM value.

3.7 DEGs related to hormone synthesis and signal transduction in response to high salt stress

GO and KEGG enrichment results showed that the DEGs under high salt stress were significantly enriched in plant hormone signal transduction pathways like ABA and ethylene signal transduction. Several DEGs that participated in ABA signal transduction were differentially expressed under high salt treatment (Figure 7A). 3 9-cis-epoxycarotenoid dioxygenase (*NCED*) encoding genes, involved in ABA synthesis, were rapidly up-regulated after 1 day of high salt treatment. 3 genes encoding ABA receptor *PYLs* were detected, *PYR1* and *PYL4* were rapidly down-regulated under 800 mM NaCl treatment. 9 protein phosphatase 2C (*PP2C*) encoding genes were

prominently up-regulated after 1 day of 800 mM NaCl treatment. 1 SNF1-related protein kinases (*SnRK2*) gene was down-regulated under 800 mM NaCl treatment. 2 ABA-responsive element binding factors (*ABF2*) were increased dramatically after 1 day and declined after 15 days of 800 mM NaCl treatment. 27 DEGs enriched in cysteine and methionine metabolic pathway were mainly associated with ethylene biosynthesis (Figure 7B), such as 5-methyltetrahydropteryltriglutamate homocysteine methyltransferase (*METE*), S-adenosylmethionine synthase (*SAMS*), 1-aminocyclopropane-1-carboxylic acid synthase (*ACS*), 1-aminocyclopropane-1-carboxylic oxidase (*ACO*) and other key enzymes in ethylene biosynthesis. 5 *METE* genes and 3 *SAMS* genes were up-regulated under 800 mM NaCl treatment. 9 *ACO* and *ACO* homologs genes were down-regulated.

3.8 Expression profiling of transcription factors associated with salt tolerance

Transcription factors (TFs) play a key role in regulating plant resistance to abiotic stress. In this study, 1,864 TF members were obtained in the assembly transcriptome sequence of *S. dendroides*, and 120 members were differently expressed under high salt treatment. In addition, 26, 36, 64, and 63 TFs were differently expressed in H1 vs C, H5 vs C, H10 vs C, and H15 vs C comparisons, respectively (Supplementary Table S8). The AP2/ERF family is the most abundant TF family in each comparison, followed by WRKY, MYB, FAR1, NAC, MADS, HB, bHLH, and bZIP (Figure 7C), suggesting that these TFs might be the main regulatory factors of *S. dendroides* plants under high salt treatment.

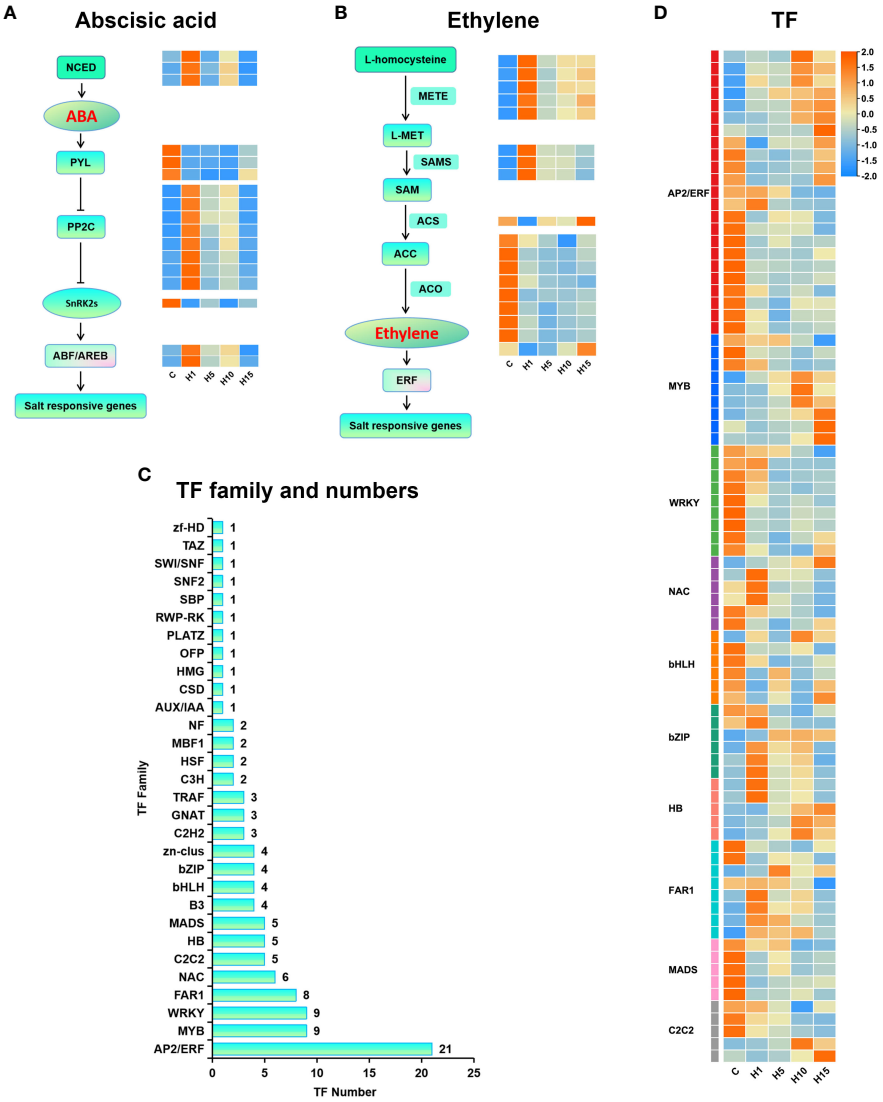

FIGURE 7
Expression profiles of the plant hormone signal transduction genes and TFs of *S. dendroides* in response to high salt treatment. **(A)** ABA synthesis and signal transduction genes, **(B)** ETH synthesis and signal transduction genes, **(C)** The numbers of different transcription factor families, **(D)** Expression profiles of TFs. The column names C, H1, H5, H10, and H15 in each heat map are the samples treated with 800 mM NaCl after 0, 1, 5, 10, and 15 days. The expression level is represented by the mean value of FPKM (n=3), and the color scale in the upper right represents the normalized FPKM value.

The expression profiles of these major TFs under high salt treatment are displayed in Figure 7D.

3.9 QPCR validation of DEGs

In order to verify RNA-seq data, 10 genes involved in different important biological processes were selected for QPCR verification analysis. These 10 genes were involved in ABA signal transduction (Cluster-12993.0 encoding *PP2C* and Cluster-688.5991 encoding Abscisic acid receptor *PYL4*), peroxidase (Cluster-25515.0 encoding peroxidase 44-like), Glycerophospholipid metabolism (Cluster-688.49983 encoding phosphoethanolamine N-methyltransferase), transcription factors (Cluster-688.16078 encoding AP2/ERF-ERF and Cluster-688.2897 encoding C2H2), (Cluster-688.57964 encoding BURP domain-containing protein 5-like), and three genes, Cluster-688.64534, Cluster-688.79365, and Cluster-688.79222, highly expressed at all the treatments without any annotation information. The results of QPCR analysis are shown in Figure 8. Moreover, the expression correlation between RNA-seq data and QPCR was calculated, and the correlation coefficient was 0.8853 (Supplementary Figure S8), suggesting that the reliability of RNA-seq data was high and the DEGs obtained from RNA-seq data should be reliable.

4 Discussion

Soil salinization has become a global ecological problem, especially in arid and semi-arid areas, which affects the establishment, development, and growth of plants and eventually leads to crop yield reduction (Lesk et al., 2016; Kopecka et al., 2023). Halophytes grow well in saline soil with a concentration of about 200 mM NaCl or above and survive in extremely harsh environments (Flowers and Colmer, 2008), which provides valuable resources for us to study the complex physiological and molecular mechanisms of plants adapting to abiotic stress. In this study, the adaptive mechanisms of *S. dendroides* associated with high salt stress were analyzed at the physiological and molecular levels. The fresh weight, dry weight, and relative water content of seedlings showed the highest under 200 mM NaCl treatment (Figures 1A-C), indicating that a low concentration of NaCl could promote the growth of seedlings. Like many succulent euhalophyte species, for example, *Suaeda salsa* grows optimally at 200 mM NaCl, and the optimal growth is accompanied by an increase in succulence and other morphological changes (Song et al., 2009). Under 800 and 1000mM NaCl stress, the seedlings showed wilting symptoms, and some seedlings even died under 1000mM NaCl. However, the wilting symptoms of the seedlings began to recover after 5 days of the treatment, recovered after 10 days and gradually returned to normal growth. After 10 days of NaCl treatment, the content of Na and K in the shoots of *S. dendroides* showed that the change of Na/K ratio was moderate and kept a relatively stable level when the salt concentration increased to 600 mM (Figures 1G-I). These indicate that *S. dendroides* could maintain Na/K balance under high salt stress to avoid ion toxicity. Furthermore, high salt stress can induce the accumulation of proline and soluble sugar, providing osmoprotection and energy for *S. dendroides* plants to adapt to stress environments. The sequencing result showed that the DEG number was the highest after 10 days of high salt treatment (Figure 2A), indicating that this period was a crucial time for *S. dendroides* to adapt to the saline environment. According to the expression level of key genes at different treatment times of high salt treatment, our study indicates that cell wall remodeling, ion homeostasis and compartmentalization, osmotic adjustment, and plant hormone signal transduction regulate the adaptation mechanism of *S. dendroides* suffering from high salt stress (Figure 9).

4.1 Cell wall regulation of *S. dendroides* under high salinity

The plant cell wall is a highly dynamic and complex network, mainly composed of different polysaccharides, lignin, and various structural proteins, which is a barrier to protect plants from the environment (Vaahtera et al., 2019). The cell wall integrity (CWI) maintenance system plays a crucial role in stress sensing and response for plants (Vaahtera et al., 2019; Rui and Dinneny, 2020). At present, a range of plasma membrane-localized receptor-like kinases and cell wall glycoproteins involved in CWI perception and maintenance have been identified. *FER* belongs to *CrRLK1L* family and is regarded as a cell wall sensor, which is necessary to activate Ca^{2+} influx and maintain CWI under salt stress (Feng et al., 2018). Other protein kinase genes, such as *WAK* and *LRX*, are thought to bind to cell wall components and play an important role in regulating cell wall integrity (Decreux and Messiaen, 2005; Herger et al., 2019). In our study, 4 *FER*, 1 *LRX3*, 5 *WAK*, and 4 *WAKL* genes were differently expressed under 800mM NaCl stress (Figure 5D). Several proteins, enzymes, and ions are related to the cell wall modifications in response to abiotic stresses. Generally, salt stress may directly trigger the activation of pectin methyl esterase, which leads to the decrease of pectin methylation degree, thus affecting the characteristics of cell wall (Gigli-Bisceglia et al., 2022). Acetylation is another important pathway of pectin modification (de Souza et al., 2014). Homogalacturonan (HG) is the most abundant pectic polymer, and its remodeling is regulated by special enzymes, such as *PME*, *PAE*, *PG*, or *PLL* (Senechal et al., 2014). In *S. dendroides*, some cell wall modification related genes were identified, 4 *PME*, 5 *PL*, and 4 *PG1* genes were up-regulated under 800 mM NaCl stress (Figure 5E). The result showed that the enzymes involved in pectin modification might be important for *S. dendroides* to adapt to high salt stress. Additionally, cell wall-loosening protein EXPs and XTHs play important roles in coping with high salt stress. *AtXTH30* has a negative effect on salt tolerance (Yan et al., 2019). *AtXTH19* and *AtXTH23* were induced by brassinosteroids, and the double mutant (*atxth19atxth23*) was sensitive to salt stress (Xu et al., 2020). *EXPs* were induced by salt stress, and overexpression of *EXP* gene was helpful to promote plant salt tolerance (Chen et al., 2017; Jadamba et al., 2020). 20 *XTHs* and 3 *EXPAs* in *S. dendroides* were obtained and differently expressed under 800 mM NaCl stress

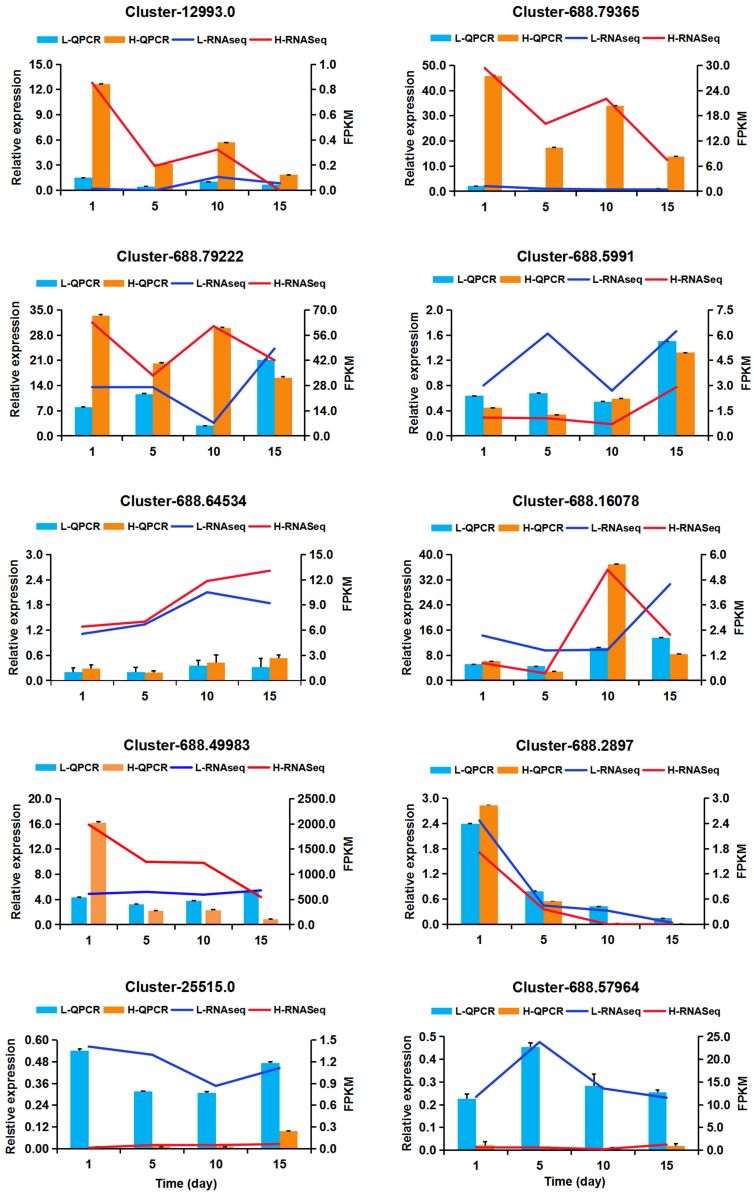

FIGURE 8
Quantitative real-time PCR validation of 10 DEGs. X-axis means NaCl treatment times. The left Y-axis represents the relative expression level of genes and displayed in bar charts, while the right Y-axis represents the PPKM value and showed by fold lines. Values are presented as the mean ± the standard error (SE) with three biological replicates.

(Figure 5B). Thus, cell wall remodeling is particularly important for *S. dendroides* to adapt to a high concentration of Na^+ condition.

SCW is thickened cell walls, mainly consisting of cellulose, hemicellulose, lignin, a minor amount of structural proteins and enzymes, which play an essential role in maintaining plant morphology, providing rigid support and ensuring material transportation, and participating in plant biotic and abiotic stress response as a protective barrier (Cosgrove, 2005; Hamann, 2012). In this study, cellulose synthase genes *CESA4*, *CESA7*, and *CESA8*, related to the SCW synthesis, increased prominently after 10 and 15 days of high salt stress (Figure 5A). PPI analysis showed that the expression of *COBL4* was positively correlated with the expression of cellulose synthesis genes *CESA4*, *CESA7*, and *CESA8* related to SCW (Figure 5F). COBL4 encodes a COBRA-like protein that has typical structural characteristics of a glycosylphosphatidylinositol-anchored protein, like sorghum SbBC1, which is homologous to OsBC1 and AtCOBL4, involved in the biosynthesis of cellulose in SCW and affects the mechanical strength of sorghum plants (Li et al., 2019). The expression level of *CESA4/7/8* and *COBL4* increased significantly under 800 mM NaCl treatment, indicating that high salt stress can promote SCW cellulose synthesis. Xylan is the main component of hemicellulose polysaccharide. Genetic and biochemical analyses revealed that the synthesis of SCW xylan backbone was mediated by *IRX10*/*IRX10L* of the GT47 family, *IRX9*/*IRX9L* and *IRX14*/*IRX14L* of the GT43 family, and *GUXs* of the GT8 family (Zhong et al., 2019). As the result showed in

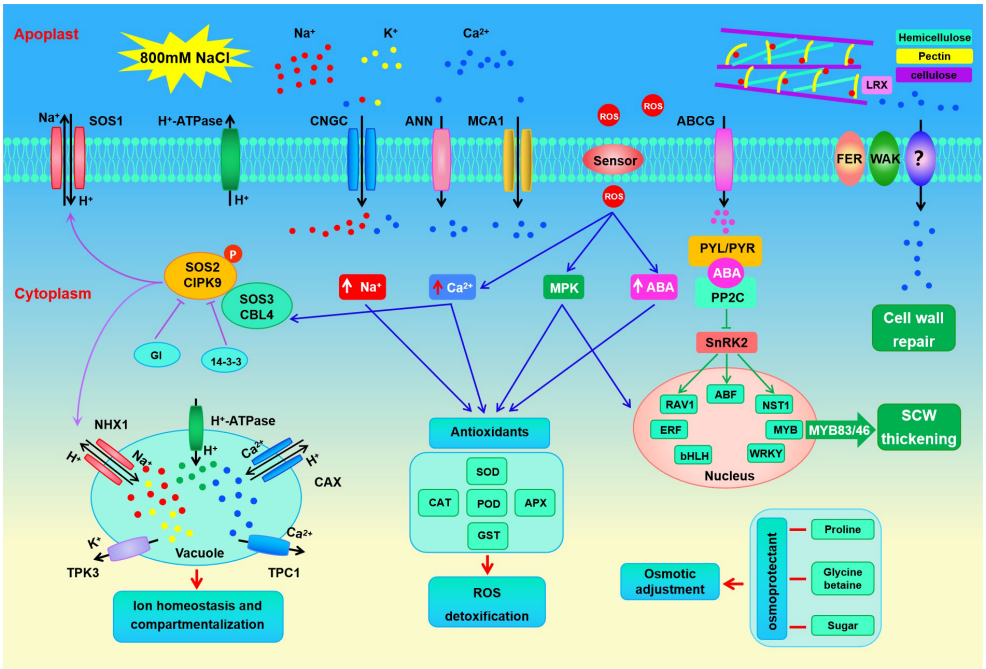

FIGURE 9
Putative mechanisms of halophyte *S. dendroides* plant adapt to high slat stress.

Figure 5A, the DEGs involved in xylan backbone synthesis, such as *IRX9*, *IRX14*, *IRX15*, and *IRX15L*, were up-regulated and significantly increased after 10 and 15 days of 800 mM NaCl stress. Moreover, the expression level of the gene *IRX7* involved in xylan reduction terminal synthesis and the genes *GUX1* and *GUX2* involved in side chain synthesis increased significantly after 10 and 15 days of high salt stress. In addition, 5 *TBL* encoding DEGs were significantly up-regulated after 15 days of 800mM NaCl stress. *TBL32* and *TBL33* are putative acetyltransferases, which participate in acetyl substitutions of 2-O-GlcA-substituted xylosyl residues, playing important roles in xylan acetylation and normal deposition of the SCW (Yuan et al., 2016). Furthermore, PPI network analysis of DEGs at different treatment times under high salt stress showed that the hub gene *IRX9* (Cluster-688.80914) was positively correlated with *GUX1*, *IRX7*, *CSEA4*, *CESA7*, *CESA8* and *SUS3*. These indicated that high salt stress could promote the synthesis of xylan in SCW of *S. dendroides*.

However, the coordinated expression of genes involved in cellulose, xylan, and lignin biosynthesis in SCW is mediated by the NAC-MYB transcriptional network (Nakano et al., 2015). A set of closely related NAC domain TFs acts as the primary switch of plant SCW biosynthesis, activating downstream TFs to regulate the entire network of SCW biosynthesis (Mitsuda et al., 2005; Mitsuda et al., 2007). Most of the R2R3-MYB subfamily TFs function as the second layer-master switches of SCW biosynthesis, such as *MYB26/103* and *MYB46/83* (Xiao et al., 2021). Moreover, the genes involved in ABA synthesis and signal transduction are related to SCW thickening and lignification in *Arabidopsis* (Endler and Persson, 2011; Wang L. et al., 2020). *AtNST1*, a NAC domain family TF that can activate the downstream genes related to SCW biosynthesis. Studies have shown that *AtNST1* is a key phosphorylation substrate of *SnRK2*, which acts as the key positive regulator of ABA signal transduction, which regulates SCW formation and lignin deposition in the stem fiber region of *Arabidopsis thaliana* (Liu et al., 2021). In this study, the expression level of gene *NST1* was significantly increased after 15 days of 800 mM NaCl stress (Figure 7D, Supplementary Table S7). *MYB4*, *MYB86*, and *MYB26/103* were significantly up-regulated after 15 days of high salt stress, and *MYB46/83* was notably up-regulated after 10 days (Figure 7D). Therefore, the genes involved in SCW biosynthesis and thickening may be extremely important for *S. dendroides* adapting to high salt environment. In brief, multiple genes related to cell wall biosynthesis, modification, sensing, and CWI maintenance of *S. dendroides* were significantly expressed under high salt stress. The results indicated that cell wall remodeling and SCW thickening were the key drivers for *S. dendroides* plants adapting to high salt stress.

4.2 An efficient ion transport system is essential for *S. dendroides* response to high salt stress

Succulence is another mechanism for euhalophyte plants to adapt to high salt environments. A large amount of inorganic ions and organic osmotic adjustment substances are accumulated in succulent leaves and stems to maintain osmotic balance (Flowers and Colmer, 2015; Rahman et al., 2021). In this study, a series of genes related to inorganic ion transport, including *SOS1*, *HKT1*, *NHX1*, *TPK3*, *PMA*, and *AVP*, were prominently expressed under 800 mM NaCl treatment (Figure 6A, Supplementary Table S7). The

plasma membrane Na^+/H^+ antiporter *AtSOS1* is located at the root tips, excluding Na^+ from the root, thus reducing Na^+absorption (Shi et al., 2000). Na^+ influx into cells is mediated mainly by non-selective cation channels and the sodium transporter *HKT1*. It has been proved that *AtHKT1* can unload Na^+ from xylem vessels to parenchyma cells and/or control the retrieval of Na^+ from xylem to reduce the amount of Na^+ transported to shoots (Sunarpi et al., 2005). In addition, *SOS1* and *HKT1* mediate opposite Na^+ fluxes, and coordinate the regulation of Na^+ transport and ion homeostasis under salt stress (Wang W.-Y. et al., 2020). Tonoplast located $Na^+(K^+)/H^+$ antiporter *NHX1* has been proven to separate excessive cytoplasmic $Na^+(K^+)$ into vacuoles, which was motivated by the proton motive force produced by vacuolar H^+-ATPase (*VHA*) and H^+-PPase (Yang et al., 2010). The *KT/HAK/KUP* family genes act as K^+/H^+ symporter, and most of them are important for K^+ absorption in plant roots (Wang Y. et al., 2021). Tonoplast localized *AtTPK1* functions in K^+ transport across the tonoplast and plays important roles in many physiological processes (Gobert et al., 2007). As a representative euhalophyte, *S. dendroides* could accumulate a large amount of Na^+ in succulent leaves, and maintain the stability of K^+ by promoting the ability of K^+ transportation under high salt treatment, indicating that *S. dendroides* has the ability to modulate Na^+/K^+ balance. Moreover, it has been found that the concentration of cytosolic Ca^{2+} ($[Ca^{2+}]$ cyt) increases with numerous environmental conditions. Constant $[Ca^{2+}]$cyt is maintained by Ca^{2+} influx through Ca^{2+}-permeable ion channels or transporters located in the plasma membrane or tonoplast, and other membranes. *MCA1* and *MCA2* are responsible for Ca^{2+} influx in *Arabidopsis* cells. Over-expression of *MCA1* driven by a strong promoter can promote the absorption of Ca^{2+} in roots and increase cytoplasmic Ca^{2+} concentration upon hypoosmotic shock (Yamanaka et al., 2010). Two-pore calcium channel protein TPC1 located in the tonoplast acts as a non-selective cation channel, which is co-regulated by voltage and Ca^{2+} to produce a slow vacuolar current (Ye et al., 2021). besides, *CNGC*, located mostly in the plasma membrane, enables the absorption of Na^+, K^+, and Ca^{2+}. *AtCNGC10* is involved in K^+ and Na^+ absorption and long-distance transportation, and *AtCNGC17* mediated the influx of osmotically active K^+ and the second messenger Ca^{2+}, or both (Jarratt-Barnham et al., 2021). In *S. dendroides*, 3 *CNGC* genes were significantly expressed, *CNGC4* was significantly increased, while 2 *CNGC17* genes decreased at all the time points of 800 mM NaCl treatment (Figure 7A, Supplementary Table S7). Furthermore, cytosolic Ca^{2+} binds to calcium sensor protein SOS3/CBL4, and subsequently interacts with protein kinase *SOS2/CIPK24* to form a complex activator that activates SOS1, a Na^+/H^+ antiporter, resulting in Na^+ efflux from the cytosol. The salt overly sensitive (SOS) pathway comprises *CBL4/SOS3*, *CIPK24/SOS2*, and *SOS1*, which has been considered the key mechanism of Na^+ homeostasis and salt tolerance in *Arabidopsis* (Zhu, 2000). Apart from interacting with SOS1 at the plasma membrane, *CIPK24* is also reported to regulate the activity of several tonoplast located transporters by interacting with them, such as Ca^{2+}/H^+ antiporter (Cheng et al., 2004), vacuolar V-ATPase (Batelli et al., 2007), and Na^+/H^+ exchanger (Qiu et al., 2004; Huertas et al., 2012). In this study, *CIPK9*, the closest *SOS2* homolog in *S. dendroides*, functions in a similar manner to *SOS2* in the context of the *SOS3-CIPK9-SOS1* complex to mediate salt tolerance in halophytes *S. dendroides* (Figure 9). These indicate that *S. dendroides* has an efficient Na^+ transport and compartmentalization mechanism to maintain ion homeostasis under high salt environment.

In addition to Na^+/K^+ homeostasis, higher plants need to adjust the balance of various nutrients in saline environments. Several *Arabidopsis* NPF genes were discovered to play a crucial role in nitrate uptake and transport (Corratge-Faillie and Lacombe, 2017), such as *NRT1.1/AtNPF6.3/CHL1* involved in nitrate uptake. *NPF7.3/NRT1.5* plays important roles in K^+ translocation from root to shoot, and it also participates in coordination of K^+/NO_3^- distribution in plants. *NPF2.5* was expressed in the plasma membrane of root cortical cells, functioned in Cl^- efflux from the root, and was up-regulated by NaCl. In the present study, the DEGs involved in the absorption and transportation of some important nutrients were significantly induced by high salt stress. Notably, 15 NPF encoding genes were identified and differently expressed under high salt treatment, in which 7 *NPFs*, including 4 *NPF 3.1* and *NPF 1.1/1.2/6.4*, were significantly increased after 1 day of high salt stress, while 8 NPFs were down-regulated (Figure 6A, Supplementary Table S7). In addition, *NPF4.6/AIT1/NRT1.2* functions as an ABA importer at the site of ABA biosynthesis, plays an important role in regulating the stomatal aperture in inflorescence stems (Kanno et al., 2012). Moreover, it has been found that several members of the ABCG subfamily functioned in ABA transport (Borghi et al., 2015), such as *ABCG25*, which functions as an ABA exporter from the vascular tissue, and *ABCG40* is an ABA uptake transporter in guard cells. A total of 18 ABC family genes were differentially expressed under 800 mM NaCl treatment, including 2 *ABCBs*, 11 *ABCCs*, and 5 *ABCGs*, among which the genes of the ABCC subfamily and the ABCG subfamily were more active under high salt stress (Figure 6A, Supplementary Table S7). Therefore, *S. dendroides* could promote the absorption and transport of various nutrient elements by increasing the transcription lever of transporters/channels.

4.3 Organic osmolyte accumulation is indispensable for *S. dendroides* adaptation to high salinity

PPI analysis showed that *P5CS* interacted with the DEGs encoding *ALDH* and *BADH*, genes involved in Ca^{2+} signaling and antioxidants (Figure 6C). The ALDH superfamily comprises a variety of enzymes involved in endogenous and exogenous aldehyde metabolism (Tola et al., 2021). *P5CS*, a rate-limiting enzyme in proline biosynthesis, is a member of ALDH18 family, and its expression is significantly up-regulated in dehydration reactions (Yoshiba et al., 1997). Studies have shown that the accumulation of proline under salt stress is related to the up regulation of *P5CS* (Mansour and Ali, 2017). Proline plays an essential role in protecting plant growth from unfavorable environmental conditions by osmotic adjustment, working as a molecular chaperone, and protecting the integrity of proteins and enzymes (Ozturk et al., 2021). Nevertheless, phytohormone ABA is

a crucial component in integrating multiple signals, controlling downstream stress responses, and influencing proline synthesis and accumulation by regulating the expression of *P5CS* and *P5CR* in plants (Verslues and Bray, 2006). The interaction of ABA and the Ca^{2+} signaling pathway can also regulate proline accumulation in plants under stress conditions. In this study, several DEGs encoding *TPC1A*, *MCA1*, *CBL4*, and *CML22* involved in Ca^{2+} signaling pathway were directly or indirectly related to *P5CS* (Figure 6C). In addition, proline can also stabilize the antioxidant system and protect the integrity of cell membranes through osmotic adjustment, thereby reducing the influence of ROS and overcoming or repairing stress injury (Banu et al., 2009). In *S. dendroides*, the major antioxidant enzymes, including *SOD*, *CAT*, *APX*, *CPR*, and *Fer*, obviously expressed under high salt stress, may interact with the genes involved in osmoregulation (Figure 6C). *BADH*, also known as *ALDH10* family genes, has been widely studied for its role in stress responses and the production of the osmoprotectant GB (Tola et al., 2021). In plants, *PEAMT* is the rate-limiting enzyme for synthesizing choline, the precursor of betaine (Nuccio et al., 2000), while CMO and BADH are the key enzymes involved in betaine biosynthesis. It was found that the tolerance of gene *CMO* and *BADH* over-expressed plants was enhanced (Shirasawa et al., 2006; Wu et al., 2008). In our study, several key genes involved in GB synthesis were significantly up-regulated under 800 mM NaCl stress, like *CMO*, *BADH*, and *PEAMT* encoding genes were continuously expressed under 800 mM NaCl treatment for 1, 5, 10, and 15 days (Figure 6B). The result above suggests that *S. dendroides* could synthesize and accumulate a large number of osmoprotectants to protect the plants from high salt stress by regulating the expression patterns of key genes involved in the biosynthesis of compatible solutes.

5 Conclusion

This study identified potential genes showing a possible adaptation mechanism of halophytic *S. dendroides* encountering a high salt condition, mainly involved in cell wall metabolism, inorganic ion transport, and organic osmolyte synthesis (Figure 9). A large number of DEGs encoding cell wall sensing, modification, and secondary wall thickening were prominently increased under 800 mM NaCl treatment, which might be important for cell wall repair and integrity maintenance under high salt concentrations. Moreover, the DEGs encoding Na^+, K^+, Ca^{2+}, and Cl^-/NO_3^- transporters/channels were significantly increased under 800 mM NaCl treatment, which might be beneficial to promote the absorption and transport of nutrient elements under high salt stress. Notably, some genes involved in Na^+/K^+ transport (such as *SOS1*, *HKT1*, *NHX*, and *TPK3*) might play important roles in Na^+ transporting and sequestering, maintaining ion homeostasis under high saline conditions. Moreover, several genes involved in the synthesis of organic regulators were significantly up-regulated under 800 mM NaCl treatment, suggesting that *S. dendroides* possesses an effective mechanism to accumulate more osmoprotectants to enhance salt tolerance. Our results contribute a new perspective for understanding the molecular mechanisms of halophytes adapting to high salinity and provide a basis for genetic improvement of salt tolerance in important plants by using excellent genes from halophytic *S. dendroides*.

Data availability statement

The datasets presented in this study can be found in online repositories. The names of the repository/repositories and accession number(s) can be found below: SRA, and the accession numbers PRJNA1018260.

Author contributions

PM: Conceptualization, Methodology, Supervision, Writing – original draft, Writing – review & editing, Formal Analysis, Investigation. JL: Methodology, Writing – review & editing. GS: Methodology, Conceptualization, Project administration, Writing – review & editing, Funding acquisition, Investigation, Resources, Supervision. JZ: Conceptualization, Methodology, Project administration, Writing – review & editing.

Funding

The author(s) declare financial support was received for the research, authorship, and/or publication of this article. This research was funded by the Key Research and Development Task and Special Project of Xinjiang Uygur Autonomous Region (Grant No. 2022B02052-2), the Applied Basic Research Program of Xinjiang Production and Construction Corps (Grant No. 2016AG005), and the Project of Innovation Team Building in Key Areas of Xinjiang Production and Construction Corps (Grant No. 2019CB008).

Conflict of interest

The authors declare that the research was conducted in the absence of any commercial or financial relationships that could be construed as a potential conflict of interest.

Publisher's note

Supplementary material

The Supplementary Material for this article can be found online at: https://www.frontiersin.org/articles/10.3389/fpls.2024.1283912/full#supplementary-material

References

Banu, M. N. A., Hoque, M. A., Watanabe-Sugimoto, M., Matsuoka, K., Nakamura, Y., Shimoishi, Y., et al. (2009). Proline and glycinebetaine induce antioxidant defense gene expression and suppress cell death in cultured tobacco cells under salt stress. *J. Plant Physiol.* 166, 146e156. doi: 10.1016/j.jplph.2008.03.002

Batelli, G., Verslues, P. E., Agius, F., Qiu, Q. S., Fujii, H., Pan, S. Q., et al. (2007). SOS2 promotes salt tolerance in part by interacting with the vacuolar H^+-ATPase and upregulating its transport activity. *Mol. Cell. Biol.* 27, 7781–7790. doi: 10.1128/MCB.00430-07

Benjamini, Y., and Hochberg, Y. (1995). Controlling the false discovery rate: a practical and powerful approach to multiple testing. *J. R. Stat. Soc B.* 57, 289–300. doi: 10.1111/j.2517-6161.1995.tb02031.x

Borghi, L., Kang, J., Ko, D., Lee, Y., and Martinoia, E. (2015). The role of ABCG-type ABC transporters in phytohormone transport. *Biochem. Soc Trans.* 43, 924–930. doi: 10.1042/BST20150106

Calone, R., Bregaglio, S., Sanoubar, R., Noli, E., Lambertini, C., and Barbanti, L. (2021). Physiological adaptation to water salinity in six wild halophytes suitable for mediterranean agriculture. *Plants* 10, 309. doi: 10.3390/plants10020309

Chen, Y.-H., Han, Y.-Y., Kong, X.-Z., Kang, H.-H., Ren, Y.-Q., and Wang, W. (2017). Ectopic expression of wheat expansin gene *TaEXPA2* improved the salt tolerance of transgenic tobacco by regulating Na^+/K^+ and antioxidant competence. *Physiol. Plant* 159, 161–177. doi: 10.1111/ppl.12492

Cheng, N. H., Pittman, J. K., Zhu, J.-K., and Hirschi, K. D. (2004). The protein kinase *SOS2* activates the Arabidopsis H^+/Ca^{2+}antiporter CAX1 to integrate calcium transport and salt tolerance. *J. Biol. Chem.* 279, 2922–2926. doi: 10.1074/jbc.M309084200

Corratge-Faillie, C., and Lacombe, B. (2017). Substrate (un)specificity of arabidopsis NRT1/PTR FAMILY (NPF) proteins. *J. Exp. Bot.* 68, 3107–3013. doi: 10.1093/jxb/erw499

Cosgrove, D. J. (2005). Growth of the plant cell wall. *Nat. Rev. Mol. Cell Biol.* 6, 850–861. doi: 10.1038/nrm1746

Decreux, A., and Messiaen, J. (2005). Wall-associated kinase *WAK1* interacts with cell wall pectins in a calcium-induced conformation. *Plant Cell Physiol.* 46, 268–278. doi: 10.1093/pcp/pci026

de Souza, A., Hull, P. A., Gille, S., and Pauly, M. (2014). Identification and functional characterization of the distinct plant pectin esterases *PAE8* and *PAE9* and their deletion mutants. *Planta* 240, 1123–1138. doi: 10.1007/s00425-014-2139-6

Endler, A., and Persson, S. (2011). Cellulose synthases and synthesis in *arabidopsis*. *Mol. Plant* 4, 199–211. doi: 10.1093/mp/ssq079

Feng, W., Kita, D., Peaucelle, A., Cartwright, H. N., Doan, V., Duan, Q.-H., et al. (2018). The FERONIA receptor kinase maintains cell-wall integrity during salt stress through Ca^{2+} Signaling. *Curr. Biol.* 28, 666–675.e5. doi: 10.1016/j.cub.2018.01.023

Flowers, T. J., and Colmer, T. D. (2008). Salinity tolerance in halophytes. *New Phytol.* 179, 945–963. doi: 10.1111/j.1469-8137.2008.02531.x

Flowers, T. J., and Colmer, T. D. (2015). Plant salt tolerance: adaptations in halophytes. *Ann. Bot.* 115, 327–331. doi: 10.1093/aob/mcu267

Flowers, T. J., Munns, R., and Colmer, T. D. (2015). Sodium chloride toxicity and the cellular basis of salt tolerance in halophytes. *Ann. Bot.* 115, 419–431. doi: 10.1093/aob/mcu217

Gigli-Bisceglia, N., van Zelm, E., Huo, W.-Y., Lamers, J., and Testerink, C. (2022). *Arabidopsis* root responses to salinity depend on pectin modification and cell wall sensing. *Development* 149, dev200363. doi: 10.1242/dev.200363

Gobert, A., Isayenkov, S., Voelker, C., Czempinski, K., and Maathuis, F. J. M. (2007). The two-pore channel *TPK1* gene encodes the vacuolar K^+ conductance and plays a role in K^+ homeostasis. *Proc. Natl. Acad. Sci. U.S.A.* 104, 10726–10731. doi: 10.1073/pnas.0702595104

Grabherr, M. G., Haas, B. J., Yassour, M., Levin, J. Z., Thompson, D. A., Amit, I., et al. (2011). Full-length transcriptome assembly from RNA-Seq data without a reference genome. *Nat. Biotechnol.* 29, 644–652. doi: 10.1038/nbt.1883

Guo, J.-R., Du, M., Tian, H.-Y., and Wang, B.-S. (2020). Exposure to high salinity during seed development markedly enhances seedling emergence and fitness of the progeny of the extreme halophyte *Suaeda salsa*. *Front. Plant Sci.* 11. doi: 10.3389/fpls.2020.01291

Guo, J.-R., Li, Y.-D., Han, G.-L., Song, J., and Wang, B.-S. (2017). NaCl markedly improved the reproductive capacity of the euhalophyte *Suaeda salsa*. *Funct. Plant Biol.* 45, 350–361. doi: 10.1071/FP17181

Hamann, T. (2012). Plant cell wall integrity maintenance as an essential component of biotic stress response mechanisms. *Front. Plant Sci.* 3. doi: 10.3389/fpls.2012.00077

Hao, X.-Y., Li, J.-P., Gao, S.-Q., Tuerxun, Z., Chang, X.-C., Hu, W.-R., et al. (2020). *SsPsaH*, a H subunit of the photosystem I reaction center of *Suaeda salsa*, confers the capacity of osmotic adjustment in tobacco. *Genes Genom.* 42, 1455–1465. doi: 10.1007/s13258-020-00970-4

He, R., Yu, G.-H., Han, X.-R., Han, J., Li, W., Wang, B., et al. (2017). *ThPP1* gene, encodes an inorganic pyrophosphatase in *Thellungiella halophila*, enhanced the tolerance of the transgenic rice to alkali stress. *Plant Cell Rep.* 36, 1929–1942. doi: 10.1007/s00299-017-2208-y

Herger, A., Dunser, K., Kleine-Vehn, J., and Ringli, C. (2019). Leucine-rich repeat extensin proteins and their role in cell wall sensing. *Curr. Biol.* 29, R851–R858. doi: 10.1016/j.cub.2019.07.039

Himabindu, Y., Chakradhar, T., Reddy, M. C., Kanygin, A., Redding, K. E., and Chandrasekhar, T. (2016). Salt-tolerant genes from halophytes are potential key players of salt tolerance in glycophytes. *Environ. Exp. Bot.* 124, 39–63. doi: 10.1016/j.envexpbot.2015.11.010

Huertas, R., Olias, R., Eljakaoui, Z., Galvez, F. J., Li, J., De Morales, P. A., et al. (2012). Overexpression of *SlSOS2* (*SlCIPK24*) confers salt tolerance to transgenic tomato. *Plant Cell Environ.* 35, 1467–1482. doi: 10.1111/j.1365-3040.2012.02504.x

Jadamba, C., Kang, K., Paek, N. C., Lee, S. I., and Yoo, S. C. (2020). Overexpression of rice *expansin 7* (*Osexpa7*) confers enhanced tolerance to salt stress in rice. *Int. J. Mol. Sci.* 21, 454. doi: 10.3390/ijms21020454

Jarratt-Barnham, E., Wang, L.-M., Ning, Y.-Z., and Davies, J. M. (2021). The complex story of plant cyclic nucleotide-gated channels. *Int. J. Mol. Sci.* 22, 874. doi: 10.3390/ijms22020874

Kanno, Y., Hanada, A., Chiba, Y., Ichikawa, T., Nakazawa, M., Matsui, M., et al. (2012). Identification of an abscisic acid transporter by functional screening using receptor complex as a sensor. *Proc. Natl. Acad. Sci. U.S.A.* 109, 9653–9658. doi: 10.1073/pnas.1203567109

Kopecka, R., Kameniarova, M., Cerny, M., Brzobohaty, B., and Novak, J. (2023). Abiotic stress in crop production. *Int. J. Mol. Sci.* 24, 6603. doi: 10.3390/ijms24076603

Lesk, C., Rowhani, P., and Ramankutty, N. (2016). Influence of extreme weather disasters on global crop production. *Nature* 529, 84–87. doi: 10.1038/nature16467

Li, P., Liu, Y.-R., Tan, W.-Q., Chen, J., Zhu, M.-J., Lv, Y., et al. (2019). Brittle culm 1 encodes a cobra-like protein involved in secondary cell wall cellulose biosynthesis in sorghum. *Plant Cell Physiol.* 60, 788–801. doi: 10.1093/pcp/pcy246

Liang, J.-P., and Shi, W.-J. (2021). Cotton/halophytes intercropping decreases salt accumulation and improves soil physicochemical properties and crop productivity in saline-alkali soils under mulched drip irrigation: A three-year field experiment. *Field Crop Res.* 262, 108027. doi: 10.1016/j.fcr.2020.108027

Liu, C., Yu, H., Rao, X. L., Li, L. G., and Dixon, R. A. (2021). Abscisic acid regulates secondary cell-wall formation and lignin deposition in *Arabidopsis thaliana* through phosphorylation of *NST1*. *Proc. Natl. Acad. Sci. U.S.A.* 118, e2010911118. doi: 10.1073/pnas.2010911118

Livak, K. J., and Schmittgen, T. D. (2001). Analysis of relative gene expression data using real-time quantitative PCR and the 2(-Delta Delta C(T)) Method. *Methods* 25, 402–408. doi: 10.1006/meth.2001.1262

Love, M. I., Huber, W., and Anders, S. (2014). Moderated estimation of fold change and dispersion for RNA-seq data with DESeq2. *Genome Biol.* 15, 550. doi: 10.1186/s13059-014-0550-8

Lv, S.-L., Zhang, K.-W., Gao, Q., Lian, L.-J., Song, Y.-J., and Zhang, J.-R. (2008). Overexpression of an H^+-PPase gene from *Thellungiella halophila* in cotton enhances salt tolerance and improves growth and photosynthetic performance. *Plant Cell Physiol.* 49, 1150–1164. doi: 10.1093/pcp/pcn090

Mansour, M. M. F., and Ali, E. F. (2017). Evaluation of proline functions in saline conditions. *Phytochemistry* 140, 52–68. doi: 10.1016/J.Phytochem.2017.04.016

Mao, X.-Z., Cai, T., Olyarchuk, J. G., and Wei, L.-P. (2005). Automated genome annotation and pathway identification using the KEGG Orthology (KO) as a controlled vocabulary. *Bioinformatics* 21, 3787–3793. doi: 10.1093/bioinformatics/bti430

Mishra, A., and Tanna, B. (2017). Halophytes: potential resources for salt stress tolerance genes and promoters. *Front. Plant Sci.* 8. doi: 10.3389/fpls.2017.00829

Mitsuda, N., Iwase, A., Yamamoto, H., Yoshida, M., Seki, M., Shinozaki, K., et al. (2007). NAC transcription factors, *NST1* and *NST3*, are key regulators of the formation of secondary walls in woody tissues of *Arabidopsis*. *Plant Cell* 19, 270–280. doi: 10.1105/tpc.106.047043

Mitsuda, N., Seki, M., Shinozaki, K., and Ohme-Takagi, M. (2005). The NAC transcription factors *NST1* and *NST2* of *Arabidopsis* regulate secondary wall thickenings and are required for anther dehiscence. *Plant Cell* 17, 2993–3006. doi: 10.1105/tpc.105.036004

Nakano, Y., Yamaguchi, M., Endo, H., Rejab, N. A., and Ohtani, M. (2015). NAC-MYB-based transcriptional regulation of secondary cell wall biosynthesis in land plants. *Front. Plant Sci.* 6. doi: 10.3389/fpls.2015.00288

Nuccio, M. L., McNeil, S. D., Ziemak, M. J., Hanson, A. D., Jain, R. K., and Selvaraj, G. (2000). Choline import into chloroplasts limits glycine betaine synthesis in tobacco: analysis of plants engineered with a chloroplastic or a cytosolic pathway. *Metab. Eng.* 2, 300–311. doi: 10.1006/mben.2000.0158

Ozturk, M., Unal, B. T., Garcia-Caparros, P., Khursheed, A., Gul, A., and Hasanuzzaman, M. (2021). Osmoregulation and its actions during the drought stress in plants. *Physiol. Plant* 172, 1321–1335. doi: 10.1111/ppl.13297

Qiu, Q.-S., Guo, Y., Quintero, F. J., Pardo, J. M., Schumaker, K. S., and Zhu, J.-K. (2004). Regulation of vacuolar Na^+/H^+ exchange in *Arabidopsis thaliana* by the SOS pathway. *J. Biol. Chem.* 279, 207–215. doi: 10.1074/jbc.M307982200

Rahman, M. M., Mostofa, M. G., Keya, S. S., Siddiqui, M. N., Ansary, M. M. U., Das, A. K., et al. (2021). Adaptive mechanisms of halophytes and their potential in improving salinity tolerance in Plants. *Int. J. Mol. Sci.* 22, 10733. doi: 10.3390/ijms221910733

Rui, Y., and Dinneny, J. R. (2020). A wall with integrity: surveillance and maintenance of the plant cell wall under stress. *New Phytol.* 225, 1428–1439. doi: 10.1111/nph.16166

Senechal, F., Wattier, C., Rusterucci, C., and Pelloux, J. (2014). Homogalacturonan-modifying enzymes: structure, expression, and roles in plants. *J. Exp. Bot.* 65, 5125–5160. doi: 10.1093/jxb/eru272

Shannon, P., Markiel., A., Ozier, O., Baliga, N. S., Wang, J. T., Ramage, D., et al. (2003). Cytoscape: a software environment for integrated models of biomolecular interaction networks. *Genome Res.* 13, 2498–2504. doi: 10.1101/gr.1239303

Shao, Q., Han, N., Ding, T.-L., Zhou, F., and Wang, B.-S. (2014). *SsHKT1;1* is a potassium transporter of the C3 halophyte *Suaeda salsa* that is involved in salt tolerance. *Funct. Plant Biol.* 41, 790–802. doi: 10.1071/FP13265

Shi, H.-Z., Ishitani, M., Kim, C., and Zhu, J.-K. (2000). The *Arabidopsis thaliana* salt tolerance gene *SOS1* encodes a putative Na^+/H^+ antiporter. *Proc. Natl. Acad. Sci. U.S.A.* 97, 6896–6901. doi: 10.1073/pnas.120170197

Shirasawa, K., Takabe, T., Takabe, T., and Kishitani, S. (2006). Accumulation of glycinebetaine in rice plants that overexpress choline monooxygenase from spinach and evaluation of their tolerance to abiotic stress. *Ann. Bot.* 98, 565–571. doi: 10.1093/aob/mcl126

Song, J., Chen, M., Feng, G., Jia, Y.-H., Wang, B.-S., and Zhang, F.-S. (2009). Effect of salinity on growth, ion accumulation and the roles of ions in osmotic adjustment of two populations of *Suaeda salsa*. *Plant Soil* 314, 133–141. doi: 10.1007/s11104-008-9712-3

Sunarpi,, Horie, T., Motoda, J., Kubo, M., Yang, H., Yoda, K., et al. (2005). Enhanced salt tolerance mediated by *AtHKT1* transporter-induced Na^+unloading from xylem vessels to xylem parenchyma cells. *Plant J.* 44, 928–938. doi: 10.1111/j.1365-313X.2005.02595.x

Tola, A. J., Jaballi, A., Germain, H., and Missihoun, T. D. (2021). Recent development on plant aldehyde dehydrogenase enzymes and their functions in plant development and stress signaling. *Genes* 12, 51. doi: 10.3390/genes12010051

Vaahtera, L., Schulz, J., and Hamann, T. (2019). Cell wall integrity maintenance during plant development and interaction with the environment. *Nat. Plants* 5, 924–932. doi: 10.1038/s41477-019-0502-0

Verslues, P. E., and Bray, E. A. (2006). Role of abscisic acid (ABA) and *Arabidopsis thaliana* ABA-insensitive loci in low water potential-induced ABA and proline accumulation. *J. Exp. Bot.* 57, 201e212. doi: 10.1093/jxb/erj026

Wang, Y., Chen, Y.-F., and Wu, W.-H. (2021). Potassium and phosphorus transport and signaling in plants. *J. Integr. Plant Biol.* 63, 34–52. doi: 10.1111/jipb.13053

Wang, L., Hart, B. E., Khan, G. A., Cruz, E. R., Persson, S., and Wallace, I. S. (2020). Associations between phytohormones and cellulose biosynthesis in land plants. *Ann. Bot.* 126, 807–824. doi: 10.1093/aob/mcaa121

Wang, W.-Y., Liu, Y.-Q., Duan, H.-R., Yin, X.-X., Cui, Y.-N., Chai, W.-W., et al. (2020). *SsHKT1;1* is coordinated with *SsSOS1* and *SsNHX1* to regulate Na^+ homeostasis in Suaeda salsa under saline conditions. *Plant Soil* 449, 117–131. doi: 10.1007/s11104-020-04463-x

Wang, X.-Y., Shao, X.-T., Zhang, W.-J., Sun, T., Ding, Y.-L., Lin, Z., et al. (2022). Genus *Suaeda*: advances in phytology, chemistry, pharmacology and clinical application, (1895-2021). *Pharmacol. Res.* 179, 106203. doi: 10.1016/j.phrs.2022.106203

Wang, F.-L., and Song, N.-N. (2019). Salinity-induced alterations in plant growth, antioxidant enzyme activities, and lead transportation and accumulation in *suaeda salsa*: implications for phytoremediation. *Ecotoxicology* 28, 520–527. doi: 10.1007/s10646-019-02048-8

Wang, L., Wang, X., Jiang, L., Zhang, K., Tanveer, M., Tian, C.-Y., et al. (2021). Reclamation of saline soil by planting annual euhalophyte *Suaeda salsa* with drip irrigation: A three-year field experiment in arid northwestern China. *Ecol. Eng.* 159, 106090. doi: 10.1016/j.ecoleng.2020.106090

Wu, W., Su, Q., Xia, X.-Y., Wang, Y., Luan, Y.-S., and An, L.-J. (2008). The *Suaeda liaotungensis* kitag betaine aldehyde dehydrogenase gene improves salt tolerance of transgenic maize mediated with minimum linear length of DNA fragment. *Euphytica* 159, 17–25. doi: 10.1007/s10681-007-9451-1

Xiao, R.-X., Zhang, C., Guo, X.-R., Li, H., and Lu, H. (2021). MYB Transcription factors and its regulation in secondary cell wall formation and lignin biosynthesis during xylem development. *Int. J. Mol. Sci.* 22, 3560. doi: 10.3390/ijms22073560

Xu, P.-P., Fang, S., Chen, H.-Y., and Cai, W.-M. (2020). The brassinosteroid-responsive xyloglucan endotransglucosylase/hydrolase 19 (*XTH19*) and *XTH23* genes are involved in lateral root development under salt stress in *Arabidopsis*. *Plant J.* 104, 59–75. doi: 10.1111/tpj.14905

Yamanaka, T., Nakagawa, Y., Mori, K., Nakano, M., Imamura, T., Kataoka, H., et al. (2010). MCA1 and MCA2 that mediate Ca^{2+} uptake have distinct and overlapping roles in Arabidopsis. *Plant Physiol.* 152, 1284–1296. doi: 10.1104/pp.109.147371

Yan, J.-W., Huang, Y., He, H., Han, T., Di, P.-C., Sechet, J., et al. (2019). Xyloglucan endotransglucosylase hydrolase 30 negatively affects salt tolerance in *Arabidopsis*. *J. Exp. Bot.* 70, 5495–5506. doi: 10.1093/jxb/erz311

Yang, Y.-Q., and Guo, Y. (2018). Elucidating the molecular mechanisms mediating plant salt-stress responses. *New Phytol.* 217, 523–539. doi: 10.1111/nph.14920

Yang, M.-F., Song, J., and Wang, B.-S. (2010). Organ-specific responses of vacuolar H^+-ATPase in the shoots and roots of C-3 halophyte *Suaeda salsa* to NaCl. *J. Integr. Plant Biol.* 52, 308–314. doi: 10.1111/j.1744-7909.2010.00895.x

Ye, F., Xu, L.-Y., Li, X.-X., Zeng, W.-Z., Gan, N.-H., Zhao, C., et al. (2021). Voltage-gating and cytosolic Ca^{2+} activation mechanisms of Arabidopsis two-pore channel *AtTPC1*. *Proc. Natl. Acad. Sci. U.S.A.* 118, e2113946118. doi: 10.1073/pnas.2113946118

Yoshiba, Y., Kiyosue, T., Nakashima, K., Yamaguchi-Shinozaki, K., and Shinozaki, K. (1997). Regulation of levels of proline as an osmolyte in plants under water stress. *Plant Cell Physiol.* 38, 1095–1102. doi: 10.1093/oxfordjournals.pcp.a029093

Young, M. D., Wakefield, M. J., Smyth, G. K., and Oshlack, A. (2010). Gene ontology analysis for RNA-seq: accounting for selection bias. *Genome Bio.* 11, R14. doi: 10.1186/gb-2010-11-2-r14

Yuan, Y.-X., Teng, Q., Zhong, R.-Q., Haghighat, M., Richardson, E. A., and Ye, Z.-H. (2016). Mutations of *Arabidopsis TBL32* and *TBL33* affect xylan acetylation and secondary wall deposition. *PloS One* 11, e0146460. doi: 10.1371/journal.pone.0146460

Zhang, H.-M., Zhu, J.-H., Gong, Z.-Z., and Zhu, J.-K. (2022). Abiotic stress responses in plants. *Nat. Rev. Genet.* 23, 104–119. doi: 10.1038/s41576-021-00413-0

Zhao, C.-Z., Zhang, H., Song, C.-P., Zhu, J.-K., and Shabala, S. (2020). Mechanisms of plant responses and adaptation to soil salinity. *Innov.* 1, 100017. doi: 10.1016/j.xinn.2020.100017

Zhong, R.-Q., Cui, D.-T., and Ye, Z.-H. (2019). Secondary cell wall biosynthesis. *New Phytol.* 221, 1703–1723. doi: 10.1111/nph.15537

Zhu, J.-K. (2000). Genetic analysis of plant salt tolerance using *Arabidopsis thaliana*. *Plant Physiol.* 124, 941–948. doi: 10.1104/pp.124.3.941

frontiers | Frontiers in Plant Science

TYPE Original Research
PUBLISHED 05 March 2024
DOI 10.3389/fpls.2024.1364826

OPEN ACCESS

EDITED BY
Zulfiqar Ali Sahito,
Zhejiang University, China

REVIEWED BY
Jianxiong Jiang,
Jiangsu University, China
Mohamed El Gharous,
Mohammed VI Polytechnic University, Morocco
Gang Nie,
Sichuan Agricultural University, China

*CORRESPONDENCE
Liang Xiao
xiaoliang@hunau.edu.cn
Zili Yi
yizili@hunau.net

RECEIVED 03 January 2024
ACCEPTED 21 February 2024
PUBLISHED 05 March 2024

CITATION
Tang Y, Li S, Zerpa-Catanho D, Zhang Z, Yang S, Zheng X, Xue S, Kuang X, Liu M, He X, Yi Z and Xiao L (2024) Salt tolerance evaluation and mini-core collection development in *Miscanthus sacchariflorus* and *M. lutarioriparius*.
Front. Plant Sci. 15:1364826.
doi: 10.3389/fpls.2024.1364826

Salt tolerance evaluation and mini-core collection development in *Miscanthus sacchariflorus* and *M. lutarioriparius*

Yanmei Tang[1], Shicheng Li[1], Dessireé Zerpa-Catanho[2], Zhihai Zhang[3], Sai Yang[4], Xuying Zheng[2], Shuai Xue[1], Xianyan Kuang[5], Mingxi Liu[6], Xiong He[7], Zili Yi[1]* and Liang Xiao[1]*

[1]College of Bioscience and Biotechnology, Hunan Agricultural University, Changsha, Hunan, China, [2]Department of Crop Sciences, University of Illinois at Urbana-Champaign, Champaign, IL, United States, [3]Institute for Sustainability, Energy, and Environment, University of Illinois at Urbana-Champaign, Champaign, IL, United States, [4]Orient Science & Technology College of Hunan Agricultural University, Changsha, Hunan, China, [5]Department of Biological and Environmental Sciences, Alabama A&M University, Huntsville, AL, United States, [6]Department of Grassland Science, College of Agronomy, Hunan Agricultural University, Changsha, Hunan, China, [7]Hunan Heyi Crop Science Co., Ltd., Changsha, Hunan, China

Marginal lands, such as those with saline soils, have potential as alternative resources for cultivating dedicated biomass crops used in the production of renewable energy and chemicals. Optimum utilization of marginal lands can not only alleviate the competition for arable land use with primary food crops, but also contribute to bioenergy products and soil improvement. *Miscanthus sacchariflorus* and *M. lutarioriparius* are prominent perennial plants suitable for sustainable bioenergy production in saline soils. However, their responses to salt stress remain largely unexplored. In this study, we utilized 318 genotypes of *M. sacchariflorus* and *M. lutarioriparius* to assess their salt tolerance levels under 150 mM NaCl using 14 traits, and subsequently established a mini-core elite collection for salt tolerance. Our results revealed substantial variation in salt tolerance among the evaluated genotypes. Salt-tolerant genotypes exhibited significantly lower Na^+ content, and K^+ content was positively correlated with Na^+ content. Interestingly, a few genotypes with higher Na^+ levels in shoots showed improved shoot growth characteristics. This observation suggests that *M. sacchariflorus* and *M. lutarioriparius* adapt to salt stress by regulating ion homeostasis, primarily through enhanced K^+ uptake, shoot Na^+ exclusion, and Na^+ sequestration in shoot vacuoles. To evaluate salt tolerance comprehensively, we developed an assessment value (D value) based on the membership function values of the 14 traits. We identified three highly salt-tolerant, 50 salt-tolerant, 127 moderately salt-tolerant, 117 salt-sensitive, and 21 highly salt-sensitive genotypes at the seedling stage by employing the D value. A mathematical evaluation model for salt tolerance was established for *M. sacchariflorus* and *M. lutarioriparius* at the seedling stage. Notably, the mini-core collection

containing 64 genotypes developed using the Core Hunter algorithm effectively represented the overall variability of the entire collection. This mini-core collection serves as a valuable gene pool for future in-depth investigations of salt tolerance mechanisms in *Miscanthus*.

KEYWORDS

***Miscanthus sacchariflorus*, *Miscanthus lutarioriparius*, seedling stage, salt tolerance, comprehensive evaluation, ion homeostasis, core collection**

1 Introduction

Salinity is a significant abiotic stress factor that inhibits plant growth and reduces crop yield (Munns and Gilliham, 2015). Soil salinization is a devastating global environmental issue, affecting over 833 million hectares and accounting for more than 8.7% of the world's land area (FAO, 2021). In China, the distribution of saline land is extensive, with approximately 99.13 million hectares located mainly in northern, northwestern, northeastern, and coastal areas (Wu et al., 2019). Saline land is generally unsuitable for most crops and leads to reduced production and plant mortality. There is an urgent global ecological need to find practical approaches to improve and utilize these salty lands (Wang et al., 2019). The most promising strategy is screening and developing salt-tolerant crop species and varieties (Ashraf et al., 2012).

Plant response to salt stress is a complex genetic and physiological mechanism controlled by multiple quantitative trait loci (QTL) (Flowers, 2004). Salt stress induces osmotic pressure, ion toxicity, and nutritional imbalances, which reduce cell growth and alter metabolite levels (Munns and Tester, 2008). Higher plants have developed various adaptive mechanisms in response to salt stress, which are generally categorized into three groups: tolerance to osmotic stress, Na^+ exclusion through leaves, and tissue tolerance (Munns, 2005). Under salt stress, plants regulate osmotic pressure through the synthesis of organic regulators and accumulation of inorganic ions. Among these ions, K^+, Na^+, and Cl^- are crucial for 80-95% of cellular osmoregulation (Munns, 2005). K^+, in particular, is essential for maintaining vital cellular functions and has been emphasized for the critical role it plays in plant salt tolerance (Cuin et al., 2008). Additionally, plants possess mechanisms for external Na^+ exclusion or ion segregation within cells (with ions accumulating in vesicles) to maintain ion homeostasis and stable plant growth under salt stress. Plant roots activate specific ion transporters, such as HKT (high-affinity K^+ transporters), NHX (Na^+/H^+ antiporters), SOS (salt overly sensitive genes), HAK (high-affinity K^+), potassium channels (AKT), and H^+ pumping, to facilitate Na^+ transport, compartmentation, or elimination under salt stress (Zhu, 2016).

Miscanthus is a perennial, rhizomatous, tall C4 grass that has been deemed a promising energy crop and is currently being developed to produce lignocellulosic biomass as a sustainable alternative to fossil fuels and as an eco-industrial crop (Shavyrkina et al., 2023). Growing *Miscanthus* on marginal land for biomass production could contribute to food security and efficient land use (Xue et al., 2016). Additionally, it has the potential to enhance soil carbon sequestration with long-term benefits for the recovery of marginal land by improving soil structure and fertility (Xu et al., 2021). *M. lutarioriparius* and *M. sacchariflorus* are closely related subspecies that are distributed in different habitats belonging to Poaceae, *Miscanthus* Anderson. *M. sacchariflorus*, characterized by high genetic diversity and adaptation (Sun et al., 2010), can be an alternative for ecological landscape restoration in coastal saline areas (Sun and Chen, 2015). Furthermore, *M. lutarioriparius*, a species endemic to Central China, exhibits the highest biomass production (Sun et al., 2010). Studies have shown that the seeds of *M. sacchariflorus* and *M. lutarioriparius* are more salt-tolerant than those of *M. sinensis* (Zheng et al., 2015). On marginal land (salinity level of 2.7 dS/m) in the Yellow River Delta, *M. sacchariflorus* demonstrated stable yields, whereas the biomass yield of *M. lutarioriparius* surpassed that of switchgrass (Zheng et al., 2019). Thus, *M. sacchariflorus* and *M. lutarioriparius* are biomass crops with a high potential for sustainable production in saline soils (Zheng et al., 2022). However, further research is required to fully understand the salt tolerance mechanisms of *M. sacchariflorus* and *M. lutarioriparius*. Previous evaluations of the salt tolerance of the seeds and seedlings of both species were performed using small sample sizes (Zong et al., 2013; Sun and Chen, 2015; Zheng et al., 2015; Chen et al., 2017; Duan et al., 2018). Similarly, transcriptomic approaches have shed light on some responsive genes in *M. lutarioriparius* under long-term salt stress. However, these represent only a fraction of the overall mechanisms underlying salt tolerance in *M. lutarioriparius* (Song et al., 2017; Wang et al., 2019; Yu et al., 2023). Therefore, the genetic diversity and mechanisms underlying salt tolerance in *M. sacchariflorus* and *M. lutarioriparius* remain largely unknown and require further investigation.

Studying the mechanism of salt tolerance using a large number of genotypes in *M. sacchariflorus* and *M. lutarioriparius* is time-consuming, labor-intensive, and expensive. To improve efficiency, it is necessary to establish a core library of salt tolerance that captures the entire range of genetic variability with minimal redundancy, by reducing the size and increasing the diversity of the germplasm set.

This core set can provide a starting point for enhancing genetic gains and employing phenomic and genomic tools in less time (Tripathi et al., 2022). An economical, time-effective, and labor-saving approach for studying physiological or molecular response mechanisms using phenotypic traits of the core collection or trait-marker associations has been widely used (Guo et al., 2022; Wang et al., 2022).

In this study, we assessed the salt tolerance of 318 genotypes of *M. sacchariflorus* and *M. lutarioriparius* in a hydroponic system using 14 salt-tolerance traits. The objectives of this study were: (1) to determine the optimal salt concentration for evaluating salt tolerance in *M. sacchariflorus* and *M. lutarioriparius*; (2) to explore the genetic diversity and physiological mechanisms of salt tolerance in these species; (3) to develop a mathematical evaluation model for studying salt tolerance in *M. sacchariflorus* and *M. lutarioriparius*; and (4) to establish a core collection for salt tolerance in *M. sacchariflorus* and *M. lutarioriparius*. This study provides a better understanding of salt-tolerant *Miscanthus* variety breeding and improvement, as well as the optimum utilization of marginal lands.

2 Materials and methods

2.1 Plant materials

The study material comprised 318 *Miscanthus* genotypes, including 230 *M. lutarioriparius*, 87 *M. sacchariflorus*, and one *M.* × *giganteus* (Mxg), a natural allotriploid hybrid between *M. sacchariflorus* and *M. sinensis*. The genotypes were collected from a range of regions in China and cultivated in *Miscanthus* Germplasm Nursery of Hunan Agricultural University (N28.18°, E113.07°) in Changsha, Hunan, China. Figure 1 and Supplementary Table S1 show the geocoordinates of each collection site mapped using geographic information system (GIS) tools with the Krasovsky_1940 datum and geographic projection system. For each genotype, clones were subjected to vegetative propagation by dividing the rhizomes.

2.2 Determination of optimal salt stress concentration

A preliminary experiment was performed to determine the optimal salt-stress concentration. Ten genotypes (M87, M112, M129, M164, M228, M229, M245, M253, M275, and Mxg) were randomly selected from the 318 genotypes and used to determine the optimal salt concentration across a range of NaCl concentrations (0, 100, 150, 200, and 250 mM). To prepare the plant materials, rhizomes of each genotype were divided into small cuttings, with each cutting carrying 1-2 buds (approximately eight cuttings per treatment), and placed into plug trays filled with peat soil. After one month of growth in the greenhouse, plants of uniform height and growth were selected for each genotype. The plants were transferred to a hydroponic system following the removal of the attached soil and were subjected to a one-week acclimation period. The hydroponic system comprised a 24-hole floating planting plate (4 cm in diameter per hole), measuring 60 × 40 × 3 cm. This plate, which held a planting plug and a planting basket, was placed within a square plastic tray (61 × 42 × 9.5 cm) designed to accommodate up to 24 plants. A half-strength modified version of Hoagland's solution was added to the square trays for growth support and was replaced every five days. Each container included eight genotypes in three replicates, totaling 24 plants. After one week of acclimation, NaCl was incrementally added to the nutrient solution at daily increments of 20, 30, 40, and 50 mM until the desired corresponding concentrations of 100, 150, 200, and 250 mM were reached, except for the 0 mM NaCl control.

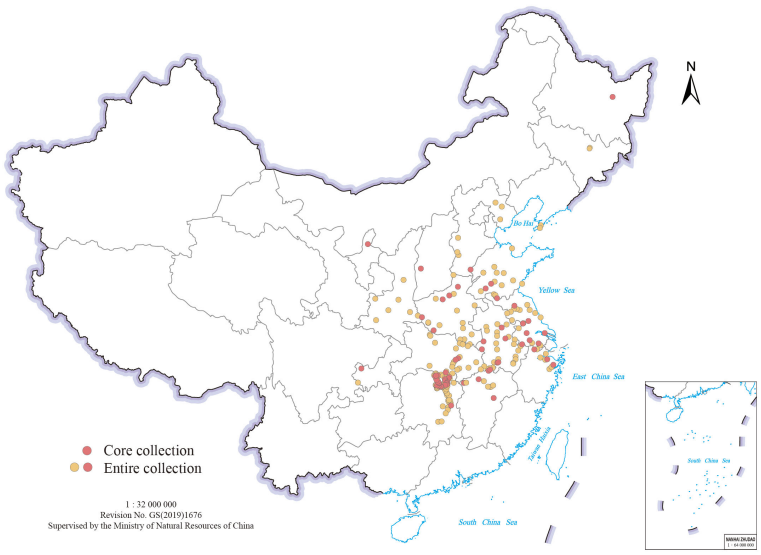

FIGURE 1
Collection sites of 318 *M. sacchariflorus* and *M. lutarioriparius* genotypes (excluding *M.* × *giganteus*) from different regions of China.

10.3389/fpls.2024.1364826

Thehydroponic salt stress experiments were conducted in a growth chamber set at a constant temperature of 25°C, a relative humidity of 70%, and a light intensity of 650 μmol·m^{-2}·s^{-1} (16 h light/8 h dark).

After 17 days of salt treatment, the plants from both the salt and control treatments were evaluated for 14 traits (Table 1): shoot growth rate (GR), leaves increased number (NIL), leaf expansion rate (LER), leaf senescence scale (Sen), shoot water content (SWC), root water content (RWC), shoot Na^+ concentration (SNC), root Na^+ concentration (RNC), the ratio of shoot Na^+ concentration to root Na^+ concentration (SN/RN), shoot K^+ concentration (SKC), root K^+ concentration (RKC), the ratio of shoot K^+ concentration to root K^+ concentration (SK/RK), the ratio of shoot K^+ concentration to shoot Na^+ concentration (SK/N), and the ratio of root K^+ concentration to root Na^+ concentration (RK/N).

TABLE 1 Description of abbreviations.

Code	Descriptors	Code	Descriptors
GR	Shoot growth rate	SKC	Shoot K^+ concentration
GR_CK	Shoot growth rate under control	RKC	Root K^+ concentration
GR_S	Shoot growth rate under 150 mM NaCl	SK/RK	The ratio of shoot K^+ concentration to root K^+ concentration
RGR	Salt-tolerance index of shoot growth rate	SK/N	The ratio of shoot K^+ concentration to shoot Na^+ concentration
NIL	Leaves increased number	RK/N	The ratio of root K^+ concentration to root Na^+ concentration
NIL_CK	Leaves increased number under control	STI	Salt tolerance index
NIL_S	Leaves increased number under 150 mM NaCl	SII	Salt-injury index
RNIL	Salt-tolerance index of leaves increased number	DAS	Day after starting the stress treatment
LER	Leaf expansion rate	MFV	Membership function value
LER_CK	Leaf expansion rate under control	HST	Highly salt tolerant
LER_S	Leaf expansion rate under 150 mM NaCl	ST	Salt tolerant
RLER	Salt-tolerance index of leaf expansion rate	MST	Moderately salt tolerant
Sen	Leaf senescence scale	SS	Salt sensitive
SWC	Shoot water content	HSS	Highly salt sensitive
RWC	Root water content	CR%	Coincidence rate of range between the entire and core collections
SNC	Shoot Na^+ concentration	VR%	Variable rate between the entire and core collections
RNC	Root Na^+ concentration	VD%	Variance difference percentage between the entire and core collections
SN/RN	The ratio of shoot Na^+ concentration to root Na^+ concentration	MD %	Mean difference percentage between the entire and core collections

The salt tolerance index (STI) for GR, NIL, and LER was calculated for each as the ratio of the value of stressed plants to the value of the control plants. For instance, the relative GR (RGR) was calculated as RGR = GR under salt stress/GR under control conditions. These ratios are referred to as RGR, Relative NIL (RNIL), and Relative LER (RLER), respectively. Additionally, salt-injury index (SII) is defined as SII = 1-STI, which quantifies the degree of injury from salt stress (Wu et al., 2019). The SII for GR, NIL and LER were calculated for the 10 genotypes at each concentration. The optimum stress concentration of NaCl was determined at the level where the SII was 50% of the control's value and the diversity of Sen was the greatest.

2.3 Main experiment design

Following the above-mentioned methods, plants derived from a pool of 318 genotypes were vegetative propagation, washed, and transferred to a hydroponic system in a growth chamber for evaluation. Each treatment had three biological replicates and was treated with the optimal NaCl concentration (150 mM NaCl) and 0 mM NaCl (control). The growth chamber conditions were identical to those used in the preliminary experiment. After four days of acclimation in the hydroponics system, NaCl was added to the stress treatment group at 75 mM daily increments until the final concentration reached 150 mM NaCl. Treatments were carried out for 17 d, during which GR, NIL, and LER were determined under control and salt stress conditions, and STI was calculated for these traits (RGR, RNIL, and RLER). In addition, Sen, SWC, RWC, SNC, RNC, SN/RN, SKC, RKC, SK/RK, SK/N, and RK/N were determined under the salt treatment. The experiment was repeated three times.

2.4 Assessment of growth traits

Plant height, leaf expansion, and leaf number were recorded for all plants under control and saline conditions. Plant height (cm) was measured from the base of the plant to the tip of the tallest leaf on the second day after starting the stress treatment (DAS) and at 7 and 17 DAS. The GR, NIL, LER, Sen, SWC, and RWC were assessed according to the protocol described by Chen et al. (2017). GR was evaluated as the daily increase in height, with the unit of centimeters per day (cm/day); it was calculated as the mean of the daily increase in height between 7 and 2 DAS and between 17 and 2 DAS. Similarly, NIL (leaf) was obtained by subtracting the number of leaves at 1 DAS from the number of leaves at 17 DAS. For leaf expansion measurements, the youngest leaf of each plant was marked at 1 DAS and its length measured at 2, 7, and 12 DAS. LER was evaluated as the mean of the daily leaf expansion between 7 and 2 DAS and between 12 and 2 DAS (cm/day). Sen was measured by visually scoring all leaves of each plant under salt stress at 17 DAS, using a 1 to 9 scale according to the percentage of senesced area (1 = no

senescence, 3 = 1-30% senesced area, 5 = 30-60% senesced area, 7 = 60-90% senesced areas, 9 = >90% senesced area). At harvest (17 DAS), all plants from the control and salt treatment groups were thoroughly washed, blotted dry, cut, and separated into shoots and roots. The fresh weights of the shoots and roots were then separately measured immediately. Subsequently, both plant parts were dried separately in a forced- air oven at 80°C for 3-4 days, and their dry weights were recorded to calculate the SWC (%) and RWC (%).

2.5 Measurement of Na^+ and K^+ concentrations

To determine the ion concentrations in the shoots and roots, three replicate samples of either shoots or roots for each genotype were pooled after the dry weights were measured. The samples were then processed by shearing and grinding to a fine powder using a sample grinder, followed by sieving with a 0.15 mm sieve. A 0.1 g sample of this dry powder was digested on a graphite digester using the H_2SO_4-H_2O_2 digestion method. Distilled water was added to the digested solution to obtain a final volume of 50 mL. The sample solutions were then filtered through a filter with a pore size of 0.22 μm, and the filtered solutions were diluted 160-fold for shoot samples and 100-fold for root samples before the Na^+ and K^+ content was assessed for each genotype's root and leaf samples using a flame atomic absorption spectrophotometer (AA-7000, SHIMADZU, Japan).

2.6 Salt tolerance evaluation

The salt tolerance of *M. sacchariflorus* and *M. lutarioriparius* was evaluated by calculating the membership function value (MFV) of STI and traits such as RGR, RNIL, RLER, Sen, SWC, RWC, SNC, RNC, SN/RN, SKC, RKC, SK/RK, SK/N, and RK/N using a fuzzy comprehensive evaluation method. The MFV of salt tolerance was calculated using the following equation (Wassie et al., 2019; Weng et al., 2021; Wang et al., 2023):

$$F_{ij} = (X_{ij} - X_{jmin})/(X_{jmax} - X_{jmin}) \quad (1)$$

$$F_{ij} = 1 - (X_{ij} - X_{jmin})/(X_{jmax} - X_{jmin}) \quad (2)$$

$$D_i = \frac{1}{n}\sum_{j=1}^{n} F_{ij} \quad (3)$$

Where F_{ij} is the MFV of indicator (j) for genotype (i) for salt tolerance. X_{ij} is the value of indicator (j) for genotype (i). X_{jmax} and X_{jmin} are the maximum and minimum values of the indicator (j), respectively. The membership function reflects the positive correlation between a particular indicator variable and salt stress, as expressed in Equation 1, whereas Equation 2 expresses a negative correlation. D_i is the mean MFV of the 14 salt tolerance traits of genotype (i) by Equation 3 for salt tolerance. Higher values of D indicate higher salt tolerance.

2.7 Hierarchical cluster analysis

Hierarchical cluster analysis based on the Euclidean distance of D values was also used to evaluate salt tolerance. Salt tolerance was clustered into five different levels: highly salt tolerant (HST), salt tolerant (ST), moderately salt tolerant (MST), salt sensitive (SS), and highly salt sensitive (HSS).

Multiple regression analysis was performed on the 303 genotypes' D values (taking as dependent variable Y) and indicator values (taking as independent variable X_i). A mathematical evaluation model for salt tolerance was established as follows: $Y = \mu+\beta_1X_1+\beta_2X_2+\beta_3X_3+\beta_4X_4+\beta_5X_5+\beta_6X_6+\beta_7X_7$, where Y is the D_i, X_1 is SNC, X_2 is RNIL, X_3 is RWC, X_4 is RGR, X_5 is RKC, X_6 is Sen, X_7 is RNC, β is the B of unstandardized coefficient, and μ is constant (random error). For model validation, another 15 genotypes were used, with three genotypes selected from each of the five salt tolerance levels.

2.8 Development and validation of mini-core collection

A mini-core collection was developed using 14 traits of salt tolerance (RGR, RNIL, RLER, Sen, SWC, RWC, SNC, RNC, SN/RN, SKC, RKC, SK/RK, SK/N, and RK/N) and the distance-based Core Hunter approach. Gower's distance measure (Gower, 1971) was employed in the CH3 method (De Beukelaer et al., 2018) to calculate the pairwise distances between genotypes as entry-to-nearest-entry (E-NE) and access-to-nearest-entry (A-NE). The core set, which accounted for 20% of the entire collection, was generated by optimizing both E-NE (maximizing) and A-NE (minimizing) with equal weighting. The optimization process used the default parallel tempering search algorithm, which was terminated when no improvement was observed for 30 s.

To compare the mean, variance, median, and representativeness of the entire and core collections for the 14 traits, we applied the Newman-Keuls procedure (Newman, 1939; Keuls, 1952), Levene's test (Levene, 1960), Wilcoxon rank-sum non-parametric test (Wilcoxon, 1945), and the Shannon-Weaver diversity index (Shannon and Weaver, 1949), respectively. In addition, we assessed the quality of the developed mini-core collection using various criteria proposed by Hu et al. (2000) and Kim et al. (2007). These criteria included the estimation of the mean difference percentage (MD %), variance difference percentage (VD %), coincidence rate of range (CR %), and variable rate (VR %) between the entire and core collections. The mini core collection was considered well represented by the entire collection if MD % was below 20%, VD % and VR % were sufficiently large, and CR % exceeded 80% (Hu et al., 2000). The similarity in genetic traits between the entire and core collections was also compared using correlation analysis. The contributions of different descriptor traits to multivariate polymorphisms and conservation in the core collection were assessed using principal component analysis (PCA).

2.9 Statistical analysis

Data are presented as means. The statistics and summarization of the data were conducted using Excel 365. All subsequent data analysis and visualization were performed by R 4.3.0, with the exception of generating the distribution map of germplasm using GIS. Specifically, the core collection tests were performed using the *EvaluateCore* package in R (Aravind et al., 2022).

3 Results

3.1 Determination of optimal salt concentration

We evaluated the GR, NIL, LER, Sen, SWC, RWC, SNC, RNC, SN/RN, SKC, RKC, SK/RK, SK/N, and RK/N of the genotypes at 17 DAS, as detailed in Supplementary Table S2, Supplementary Figure S1. The SII of GR, NIL, and LER were calculated from the data in Supplementary Tables S2 and S3. Linear regression analysis was conducted on the mean values of the three SII across the ten genotypes. The results indicated that according to the linear regression fitting, the SII for NIL would decrease to 50% of the control's value at a NaCl concentration of 144.48 mM NaCl (Figure 2A), and the SII for LER would decrease to 50% of the control's value at the predicted 153.70 mM (Figure 2B). Notably, Sen exhibited considerable variability under 150 mM NaCl treatment, indicating its suitability as a criterion for evaluating salt tolerance across different genotypes (Figure 2C). Therefore, 150 mM NaCl was used for the evaluation of the salt tolerance for the 318 genotypes in the present study.

3.2 Phenotypic variations for salt tolerance-related traits

Salt tolerance of the 318 genotypes at the seedling stage was evaluated using 150 mM NaCl, as detailed in Supplementary Table S4 and Figure 3. Descriptive statistics for the salt tolerance traits, including RG, RGR, NIL, RNIL, LER, RLER, Sen, SWC, RWC, SNC, RNC, SN/RN, SKC, RKC, SK/RK, SK/N, and RK/N, are presented in Table 2 and Supplementary Figure S2. Continuous variation was observed across all traits with approximately normal distributions, as seen in Supplementary Figure S3. The 318 genotypes exhibited a wide variation in response to the 150 mM NaCl treatment. A Kruskal-Wallis test applied to salt tolerance-related traits indicated significant differences (P<0.001) among genotypes, suggesting that genetic effects explained a large proportion of the phenotypic variance. Significant differences in GR, NIL, and LER between the control and salt treatment (P<0.001) were also noted (Supplementary Figure S2). Furthermore, to account for background differences, salt tolerance indices of GR, NIL, and LER (RGR, RNIL, and RLER, respectively) were used to evaluate the salt stress response in *M. sacchariflorus* and *M. lutarioriparius*. RGR, RNIL, and RLER showed variations ranging from 0.03 to 1.77, 0.00 to 0.94, and 0.19 to 1.09, respectively, with RGR exhibiting the most significant coefficient of variation at 53%. The water content of the plants was affected by salt stress, leading to SWC varying from 4.37% to 28.78% and RWC from 3.57% to 22.62%. Sen exhibited a mean value of 6.33 with a range of variability from 3.67 to 8.78 across different genotypes, highlighting the diverse response of *M. sacchariflorus* and *M. lutarioriparius* genotypes to salt stress.

The 318 genotypes showed significant differences (P<0.001) in their Na^+ and K^+ responses to salt stress (Figure 4, Table 2, Supplementary Table S4). Specifically, SNC ranged from 53.20 mg/g (in genotype M192) to 220.31 mg/g (in genotype M88), RNC ranged from 23.97 mg/g (in genotype M338) to 82.13 mg/g (in genotype M301), and SN/RN was notably high at 3.13, suggesting a greater accumulation of Na^+ in the shoots of *M. sacchariflorus* and *M. lutarioriparius* under salt stress. In contrast, the range of K^+ concentration was narrower; SKC was 44.32 mg/g (in genotype M19) - 104.75 mg/g (in genotype M122), and RKC was 12.83 mg/g (M203) - 39.50 mg/g (M349), but SK/RK also reached 2.94. Regarding the K^+ to Na^+ ratio, SK/N ranged from 0.33 (in genotype M126) to 1.33 (in genotype M192), and RK/N ranged from 0.26 (in genotype M123) to 1.22 (in genotype M405). Notably, a decline in SKC and RKC was not observed despite increased SNC, indicating the capacity of *M. sacchariflorus* and *M. lutarioriparius*

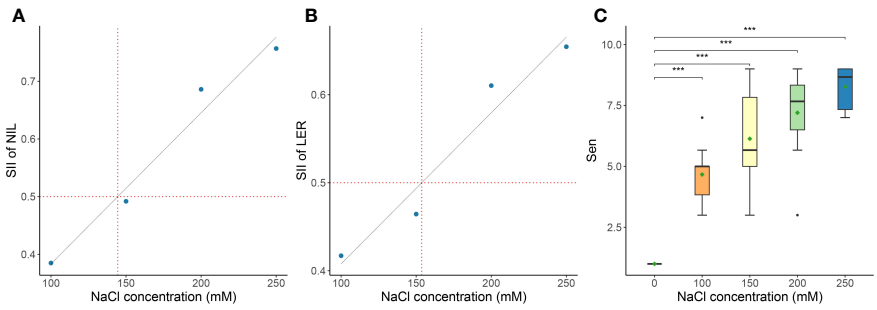

FIGURE 2
Determination of the optimal NaCl concentration for evaluating salt tolerance. The NaCl concentration of the salt-injury index (SII) is 0.5 of leaves increased number (NIL) **(A)**, leaf expansion rate (LER) **(B)** of ten *Miscanthus* genotypes under different NaCl concentrations, as well as the effect on leaf senescence scale (Sen) (significance of the t-test: ***P<0.001) **(C)**. Data in the figure are means of ten *Miscanthus* genotypes for each trait under each concentration of NaCl.

10.3389/fpls.2024.1364826

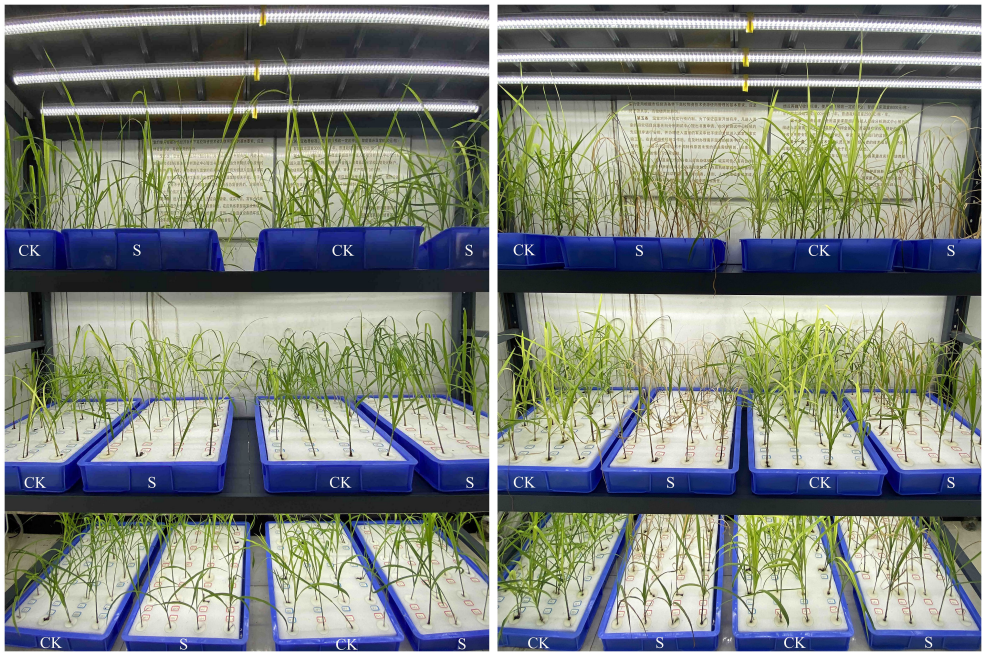

FIGURE 3
Plants were subjected to 150 mM NaCl (S) and control (CK) conditions for 0 (left panel) and 17 days (right panel). Each group of two adjacent hydroponic containers, from left to right, was used to represent the CK and S conditions, respectively. The position of each plant in these two hydroponic containers was matched one-to-one.

to enhance K^+ uptake under salt stress conditions. Additionally, among the 20 genotypes with the highest SNC, genotypes M283 and M349 exhibited Sen values lower than 7, specifically 6.56. Genotype M283 also displayed relatively high levels of RNIL, RLER, and SWC; M349 also exhibited relatively high RGR and SWC, and slightly higher average RNIL. These results suggest that these genotypes may utilize a tissue tolerance mechanism, possibly through the accumulation of Na^+ in shoot vacuoles.

TABLE 2 Descriptive statistics of all traits for 318 *M. sacchariflorus* and *M. lutarioriparius* genotypes.

Traits	Min	Max	Mean	SE	CV	Skewness	Kurtosis
GR_CK (cm/day)	0.06	0.96	0.39	0.01	0.39	0.64	0.42
GR_S (cm/day)	0.01	0.59	0.16	0.01	0.55	1.30	3.14
RGR	0.03	1.77	0.49	0.01	0.53	1.09	2.29
NIL_CK (leaf)	0.78	3.33	2.30	0.02	0.18	-0.39	0.41
NIL_S (leaf)	0.00	2.11	1.06	0.02	0.34	0.10	-0.04
RNIL	0.00	0.94	0.47	0.01	0.33	0.18	0.07
LER_CK (cm/day)	0.56	2.46	1.22	0.02	0.26	0.60	0.65
LER_S (cm/day)	0.17	1.63	0.69	0.01	0.35	0.86	1.12
RLER	0.19	1.09	0.61	0.01	0.28	0.19	-0.27
SWC (%)	4.37	28.78	15.57	0.25	0.29	0.42	-0.36
RWC (%)	3.57	22.62	11.10	0.20	0.32	0.56	-0.03
Sen	3.67	8.78	6.33	0.06	0.16	-0.06	-0.32
SNC (mg/g)	53.20	220.31	126.00	1.45	0.21	0.33	0.35
RNC (mg/g)	23.97	82.13	45.22	0.60	0.24	0.47	-0.20
SN/RN	1.17	5.68	3.13	0.04	0.24	0.11	0.16

(Continued)

10.3389/fpls.2024.1364826

TABLE 2 Continued

Traits	Min	Max	Mean	SE	CV	Skewness	Kurtosis
SKC (mg/g)	44.32	104.75	68.39	0.45	0.12	0.22	0.88
RKC (mg/g)	12.83	39.50	26.20	0.30	0.21	0.15	-0.31
SK/RK	1.60	6.03	2.94	0.05	0.28	1.13	1.58
SK/N	0.33	1.33	0.59	0.01	0.26	1.51	3.49
RK/N	0.26	1.22	0.63	0.01	0.30	0.48	-0.06

SE, standard error; CV, coefficient of variation.

GR_CK, Shoot growth rate under control; GR_S, Shoot growth rate under 150 mM NaCl; RGR, salt-tolerance index of shoot growth rate; NIL_CK, leaves increased number under control; NIL_S, leaves increased number under 150 mM NaCl; RNIL, salt-tolerance index of leaves increased number; LER_CK, leaf expansion rate under control; LER_S, leaf expansion rate under 150 mM NaCl; RLER, salt-tolerance index of leaf expansion rate; Sen, leaf senescence scale; SWC, shoot water content; RWC, root water content; SNC, shoot Na^+ concentration; RNC, root Na^+ concentration; SN/RN, the ratio of shoot Na^+ concentration to root Na^+ concentration; SKC, shoot K^+ concentration; RKC, root K^+ concentration; SK/RK, the ratio of shoot K^+ concentration to root K^+ concentration; SK/N, the ratio of shoot K^+ concentration to shoot Na^+ concentration; RK/N, the ratio of root K^+ concentration to root Na^+ concentration.

3.3 Correlation and principal component analysis of seedling traits under salt stress

Correlation analyses were conducted to examine the relationships among various parameters under NaCl stress, including RGR, RNIL, RLER, Sen, SWC, RWC, SNC, RNC, SN/RN, SKC, RKC, SK/RK, SK/N, and RK/N (Figure 5). Significant positive correlations were found between RGR, RLER, RNIL, and SWC as well as between SKC, SK/RK, and SK/N. The highest positive correlation coefficient was observed between SWC and RWC (0.73), followed by SNC and Sen (0.66). Significant positive correlations were also noted between SN/RN and SNC (0.58), Sen (0.55), and RK/N (0.53). Notably, both SKC and RKC showed significant positive correlations with SNC. Conversely, significant negative correlations existed between Sen, SNC, and SN/

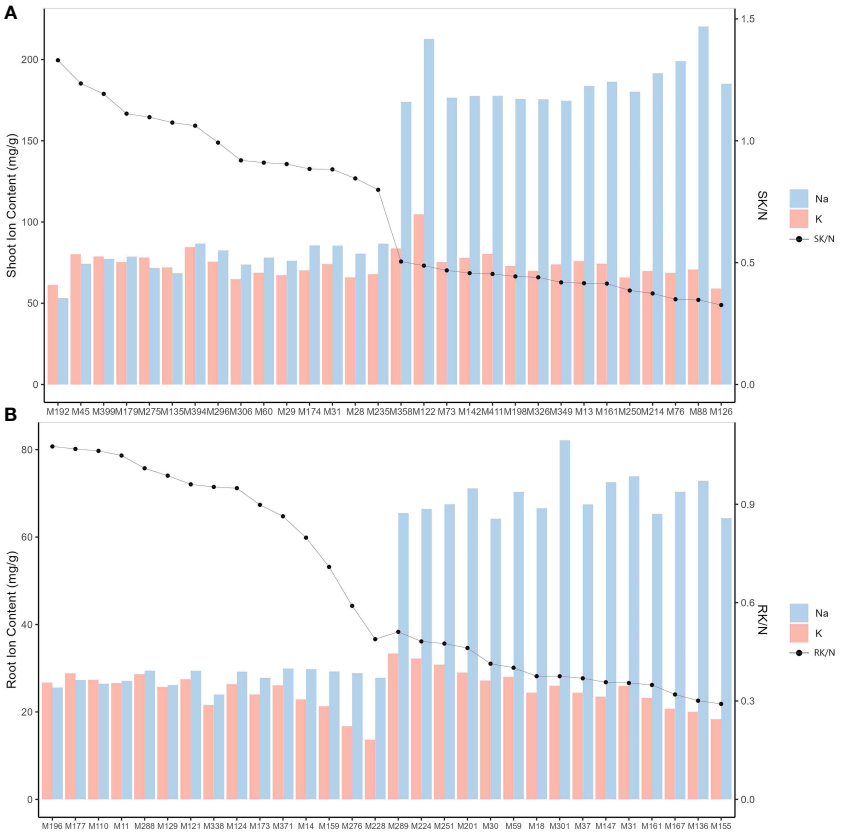

FIGURE 4
Na^+ and K^+ concentrations and K^+/Na^+ ratios in *M. sacchariflorus* and *M. lutarioriparius* under 150 mM NaCl. Ion concentrations for 15 genotypes with the highest shoot Na^+ concentration (SNC) and 15 genotypes with the lowest shoot Na^+ concentration **(A)**, and ion concentrations for 15 genotypes with the highest root Na^+ concentration (RNC) and 15 genotypes with the lowest root Na^+ concentration **(B)**. SK/N and RK/N are K^+/Na^+ ratios in shoots and roots, respectively.

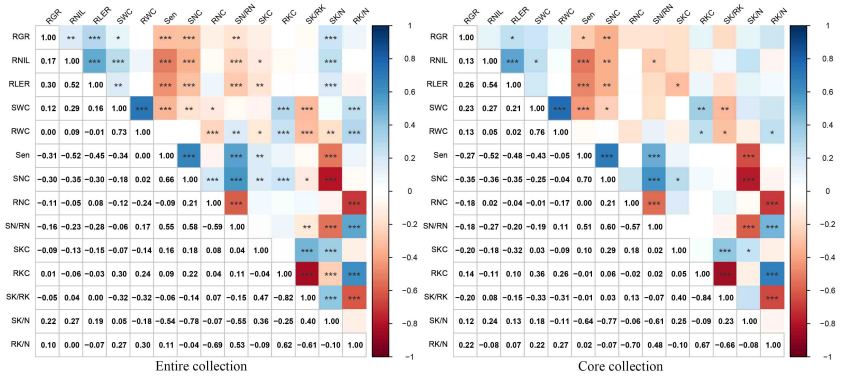

FIGURE 5
Pearson correlation analysis between 14 traits of the entire and core collections. *, **, and *** indicate significance at P<0.05, P<0.01, and P<0.001, respectively. Salt-tolerance index of leaves increased number (RNIL), salt-tolerance index of leaf expansion rate (RLER), leaf senescence scale (Sen), shoot water content (SWC), root water content (RWC), shoot Na^+ concentration (SNC), root Na^+ concentration (RNC), the ratio of shoot Na^+ concentration to root Na^+ concentration (SN/RN), shoot K^+ concentration (SKC), root K^+ concentration (RKC), the ratio of shoot K^+ concentration to root K^+ concentration (SK/RK), the ratio of shoot K^+ concentration to shoot Na^+ concentration (SK/N), and the ratio of root K^+ concentration to root Na^+ concentration (RK/N).

RN with RGR, RNIL, RLER, and SK/N. The correlation coefficient between Sen and SK/N had the largest absolute value at -0.54, followed by that between Sen and RNIL at -0.52, and that between Sen and RLER at -0.45.

PCA was used to synthesize these 14 normalized traits. Based on eigenvalues greater than one, five principal components (PCs) were extracted, which accounted for a cumulative variance contribution rate of 81.42% (Table 3, Figure 6). PC1 (27.75%) mainly reflected

TABLE 3 Principal component analysis of the entire and core sets showing the contributions of each trait to the variation in the germplasm.

Traits	Entire set					Core set				
	PC1	PC2	PC3	PC4	PC5	PC1	PC2	PC3	PC4	PC5
RGR	-0.02	0.06	0.02	-0.04	0.01	0.08	-0.06	-0.03	-0.02	0.00
RNIL	-0.04	**0.10**	0.01	0.00	0.06	0.03	**-0.13**	-0.03	0.00	0.09
RLER	-0.06	**0.11**	-0.02	-0.03	**0.12**	0.08	**-0.13**	-0.04	-0.07	**0.13**
SWC	0.05	**0.13**	-0.01	**0.10**	-0.02	**0.15**	-0.08	0.08	**0.12**	0.00
RWC	0.09	0.08	0.01	**0.13**	-0.01	**0.14**	0.01	0.07	**0.17**	0.03
Sen	0.09	**-0.14**	0.00	0.01	0.02	-0.06	**0.19**	0.03	0.00	0.02
SNC	0.07	**-0.10**	-0.05	0.03	0.05	-0.05	**0.14**	0.06	0.01	0.05
RNC	-0.08	-0.03	**-0.16**	0.02	-0.01	**-0.11**	-0.07	**0.21**	-0.05	0.03
SN/RN	**0.11**	-0.06	0.08	0.01	0.06	0.03	**0.17**	-0.08	0.04	0.05
SKC	-0.02	-0.03	0.02	0.01	-0.05	-0.04	0.01	0.03	0.04	-0.08
RKC	**0.14**	0.06	-0.09	-0.06	-0.04	**0.19**	0.05	**0.10**	-0.09	-0.05
SK/RK	**-0.14**	-0.07	0.08	0.05	0.00	**-0.19**	-0.05	-0.07	0.09	-0.01
SK/N	-0.09	0.06	0.05	-0.03	-0.08	0.00	**-0.15**	-0.04	0.01	**-0.12**
RK/N	**0.16**	0.07	0.07	-0.06	-0.02	**0.20**	0.09	-0.07	-0.03	-0.04
Eigenvalues	0.12	0.10	0.06	0.04	0.03	0.19	0.17	0.09	0.07	0.06
% of Variance	27.75	23.18	12.87	9.82	7.79	26.79	23.91	13.21	10.20	8.78
Cumulative %	27.75	50.93	63.80	73.62	81.42	26.79	50.70	63.91	74.11	82.90

Bold numbers indicate eigenvalues are significant ≥|0.1|.
RGR, salt-tolerance index of shoot growth rate; RNIL, salt-tolerance index of leaves increased number; RLER, salt-tolerance index of leaf expansion rate; Sen, leaf senescence scale; SWC, shoot water content; RWC, root water content; SNC, shoot Na^+ concentration; RNC, root Na^+ concentration; SN/RN, the ratio of shoot Na^+ concentration to root Na^+ concentration; SKC, shoot K^+ concentration; RKC, root K^+ concentration; SK/RK, the ratio of shoot K^+ concentration to root K^+ concentration; SK/N, the ratio of shoot K^+ concentration to shoot Na^+ concentration; RK/N, the ratio of root K^+ concentration to root Na^+ concentration.

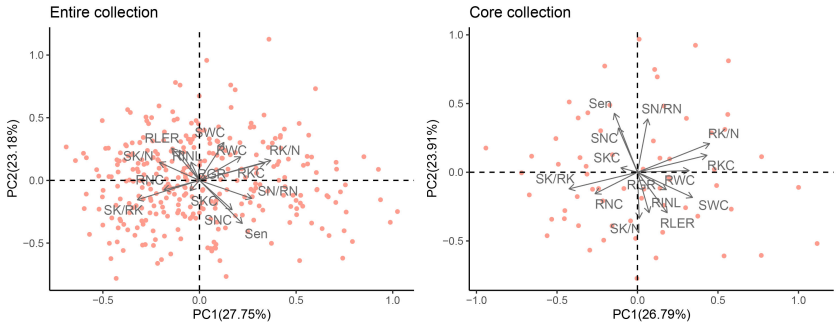

FIGURE 6
Principal component analysis plot of the entire and mini-core sets of *M. sacchariflorus* and *M. lutarioriparius* based on 14 traits. The angles captained by any of the two arrows less than 90° imply the two indices have a positive correlation, otherwise they represent a negative correlation between the two indices. Salt-tolerance index of shoot growth rate (RGR), salt-tolerance index of leaves increased number (RNIL), salt-tolerance index of leaf expansion rate (RLER), leaf senescence scale (Sen), shoot water content (SWC), root water content (RWC), shoot Na^+ concentration (SNC), root Na^+ concentration (RNC), the ratio of shoot Na^+ concentration to root Na^+ concentration (SN/RN), shoot K^+ concentration (SKC), root K^+ concentration (RKC), the ratio of shoot K^+ concentration to root K^+ concentration (SK/RK), the ratio of shoot K^+ concentration to shoot Na^+ concentration (SK/N), and the ratio of root K^+ concentration to root Na^+ concentration (RK/N).

the effect of 150 mM NaCl stress on RK/N, RKC, SN/RN (positive loading), and SK/RK (negative loading), which are traits related to ion content. PC2 (23.18%) was significantly correlated with the growth traits of SWC, RLER, RNIL (positive loading), and Sen (negative loading) as well as the ion content-related traits of SNC (negative loading). PC3 (12.87%) was primarily associated with RNC, showing a significantly negative loading. PC4 (9.82%) included SWC and RWC, with positive loadings. Finally, PC5 (7.79%) mainly consisted of RLER with a positive loading.

3.4 Comprehensive evaluation of salt stress tolerance

Based on the results of the pre-experiment for the ten genotypes and the subsequent correlation analysis, it was found that Sen, SNC, RNC, SN/RN, SKC, and RKC exhibited higher levels under salt stress than under the control conditions and that these traits showed a negative correlation with salt stress (Supplementary Figure S1, Figure 5). Consequently, Equation 2 was employed to calculate the MFV for Sen, SNC, RNC, SN/RN, SKC, and RKC, whereas Equation 1 was used for the remaining eight traits. The mean MFV (D value) was calculated for each genotype (see Supplementary Table S5). Hierarchical cluster analysis based on the D values was used to assess the salt tolerance of 318 *M. sacchariflorus* and *M. lutarioriparius* genotypes (Figure 7). Salt tolerance was classified into five levels at a Euclidean distance of 0.12: highly salt tolerant (HST), salt tolerant (ST), moderately salt tolerant (MST), salt sensitive (SS), and highly salt sensitive (HSS). Among the genotypes analyzed, three were classified as HST, 50 as ST, 127 as MST, 117 as SS, and 21 as HSS. Across these categories, a trend was observed whereas the level of salt tolerance decreased from HST to HSS, the values of RGR, RLER, and SK/N decreased, whereas Sen, SNC, RNC, and SN/RN exhibited an increasing trend. Notably, SNC was over two times as high in the HSS group (176.6 mg/g) compared to the HST (72.52 mg/g), as detailed in Supplementary Table S6. Genotypes classified in the higher salt tolerance categories exhibited superior growth characteristics, reduced leaf senescence, and lower Na^+ content.

To screen and evaluate salt tolerance traits in *M. sacchariflorus* and *M. lutarioriparius*, the D values of 303 genotypes were used as a dependent variable and the values of the 14 traits as independent variables to develop the most predictive regression equation for salt tolerance. The random error term was 0.6895. The unstandardized coefficients for SNC, RNIL, RWC, RGR, RKC, Sen, and RNC were -0.0012, 0.1242, 0.0057, 0.0516, -0.0023, -0.0202, and -0.0010, respectively. The optimal regression equation is as follows: Y=0.6895-0.0012SNC+0.1242RNIL+0.0057RWC+0.0516RGR-0.0023RKC-0.0202Sen-0.0010RNC (R^2 = 0.962, P<0.001) (Table 4).

To verify the predictability of the mathematical evaluation model for salt tolerance in *M. sacchariflorus* and *M. lutarioriparius*, three genotypes from each cluster were randomly selected and their corresponding Y values were calculated (Table 5). These results demonstrated that this formula can effectively evaluate the salt tolerance of *M. sacchariflorus* and *M. lutarioriparius* at the seedling stage. For instance, for genotype M411 which was classified as HSS, it had a Y value of 0.3167 (Y= 0.6895-0.0012*177.6243 + 0.1242*0.2667 + 0.0057*8.4277 + 0.0516*0.0350-0.0023*29.2614-0.0202*7.0000-0.0010*33.9501), which closely matched its D value of 0.317; for genotype M333 which was categorized as MST, it had a Y value of 0.4496, aligning well with its D value of 0.4513; for genotype M135 which was under the HST group, its Y value is 0.6504, which is very close to its D value of 0.6528. The close correspondence between the D and Y values indicates the reliability of our model and its applicability in predicting salt tolerance in *M. sacchariflorus* and *M. lutarioriparius* at the seedling stage.

10.3389/fpls.2024.1364826

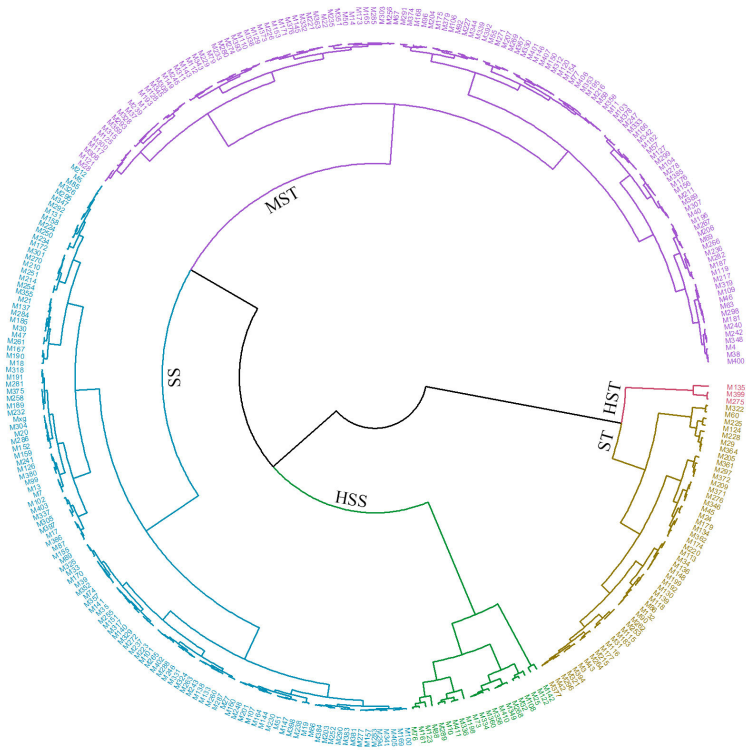

FIGURE 7
Hierarchical cluster analysis based on the Euclidean distance to evaluate the salt tolerance of 318 *M. saccharifloru*s and *M. lutarioriparius*. HST, highly salt tolerant; ST, salt tolerant; MST, moderately salt tolerant; SS, salt sensitive; and HSS, highly salt sensitive.

3.5 Development and validation of the mini-core collection

The mini-core collection displayed strong representativeness of the entire collection, as determined by the Core Hunter algorithm. Of the 318 genotypes used for the entire collection, 64 (20%) were selected to constitute the mini-core collection (Supplementary Table S4). The CR % was high for all studied traits except for RWC and RNC, which fell slightly below 80%. CR % values were 100% for Sen, SNC, and RK/N. The mean CR % was calculated to be 94.28% (Table 6). The VR % values for all studied traits were high, ranging from 101.32% for RWC to 175.87% for RGR, with an average VR % value of 141.16. The highest and lowest VD % values were observed for the RGR and RWC, respectively. The MD % analysis indicated a minimal difference (0.18-8.69%) between the mini-core and entire collections for all the traits. The Newman-

TABLE 4 Multiple linear regression analysis of the comprehensive evaluation value of salt tolerance (D value) on seven traits.

	Unstandardized coefficients		Standardized coefficients		
Variables	B	Standard error	Beta	*t*	Sig.
(Constant)	0.6895	0.0108		63.58	0.00
SNC	-0.0012	0.0000	-0.4140	-25.48	0.00
RNIL	0.1242	0.0062	0.2689	20.17	0.00
RWC	0.0057	0.0002	0.2912	23.82	0.00
RGR	0.0516	0.0033	0.1884	15.63	0.00
RKC	-0.0023	0.0002	-0.1793	-14.90	0.00
Sen	-0.0202	0.0013	-0.2791	-16.06	0.00
RNC	-0.0010	0.0001	-0.1601	-12.39	0.00

SNC, shoot Na^+ concentration; RNIL, salt-tolerance index of leaves increased number; RWC, root water content; RGR, salt-tolerance index of shoot growth rate; RKC, root K^+ concentration; Sen, leaf senescence scale; RNC, root Na^+ concentration.

10.3389/fpls.2024.1364826

TABLE 5 Verification of salinity tolerance values (Y value) from multiple regression analysis with the comprehensive evaluation value of salt tolerance (D value).

Category	Genotype	SNC (mg/g)	RNIL	RWC (%)	RGR	RKC (mg/g)	Sen	RNC (mg/g)	D value	Y value
HST	M135	68.5235	0.6722	10.6811	1.3153	21.8653	4.1111	35.7473	0.6528	0.6504
HST	M399	77.2951	0.5873	9.6401	0.4770	17.0181	4.7778	42.9012	0.6321	0.5707
HST	M275	71.7442	0.5595	7.4736	1.0119	15.0141	4.3333	42.2869	0.6307	0.6034
ST	M29	76.0937	0.7806	7.5559	1.0206	24.2159	3.6667	57.0360	0.5981	0.6041
ST	M372	109.2919	0.6699	19.1205	0.2283	24.4107	4.7778	44.9874	0.5663	0.5647
ST	M42	101.2471	0.6257	10.9623	0.7333	17.8049	5.2222	54.8780	0.5376	0.5447
MST	M235	86.6145	0.4393	6.5162	0.4582	20.1583	5.0000	53.5684	0.5143	0.5000
MST	M333	143.8789	0.5833	9.5685	0.4326	25.8235	5.6667	42.7207	0.4513	0.4496
MST	M166	128.6327	0.2922	15.0708	0.4771	29.3749	6.5556	43.3426	0.4477	0.4386
SS	M160	120.8193	0.4180	7.0272	0.4324	22.1833	7.2222	30.6579	0.4331	0.4312
SS	M397	135.6414	0.0000	6.0231	0.8124	23.4249	6.3333	42.5636	0.3975	0.3786
SS	M318	155.5016	0.4563	10.2639	0.4746	26.3178	7.8889	41.0854	0.3845	0.3816
HSS	M268	148.0509	0.0741	9.1441	0.4711	28.2644	7.0000	55.8626	0.3481	0.3352
HSS	M336	161.1194	0.2323	8.8758	0.1580	22.0328	7.6667	50.8735	0.3180	0.3273
HSS	M411	177.6243	0.2667	8.4277	0.0350	29.2614	7.0000	33.9501	0.3172	0.3167

HST, highly salt tolerant; ST, salt tolerant; MST, moderately salt tolerant; SS, salt sensitive; HSS, highly salt sensitive.
SNC, shoot Na^+ concentration; RNIL, salt-tolerance index of leaves increased number; RWC, root water content; RGR, salt-tolerance index of shoot growth rate; RKC, root K^+ concentration; Sen, leaf senescence scale; RNC, root Na^+ concentration.

TABLE 6 Evaluation parameters of the core collection.

Traits	CR %	VR %	VD %	MD %	Shannon-Weiner diversity index[a]	Newman-Keuls test	Levene's test	Wilcoxon rank-sum test
RGR	99.97%	175.87%	43.14%	8.69%	3.97 (5.63)	0.22 ns	0.03*	0.59 ns
RNIL	91.18%	128.54%	22.20%	3.57%	4.09 (5.70)	0.43 ns	0.22 ns	0.43 ns
RLER	94.08%	137.70%	27.38%	2.38%	4.10 (5.72)	0.54 ns	0.08 ns	0.62 ns
SWC	92.25%	132.98%	24.80%	4.48%	4.10 (5.72)	0.30 ns	0.20 ns	0.24 ns
RWC	79.34%	101.32%	1.30%	5.60%	4.10 (5.71)	0.23 ns	0.79 ns	0.22 ns
Sen	100.00%	131.25%	23.81%	0.18%	4.14 (5.75)	0.94 ns	0.42 ns	0.90 ns
SNC	100.00%	142.09%	29.62%	0.30%	4.13 (5.74)	0.92 ns	0.21 ns	0.88 ns
RNC	79.75%	121.40%	17.63%	0.45%	4.13 (5.73)	0.89 ns	0.15 ns	0.94 ns
SN/RN	99.58%	157.12%	36.35%	0.64%	4.11 (5.73)	0.85 ns	0.03*	0.57 ns
SKC	94.49%	145.92%	31.47%	1.86%	4.15 (5.76)	0.25 ns	0.12 ns	0.40 ns
RKC	94.93%	137.77%	27.41%	0.56%	4.13 (5.74)	0.85 ns	0.07 ns	0.83 ns
SK/RK	96.39%	146.88%	31.92%	3.29%	4.11 (5.73)	0.39 ns	0.12 ns	0.71 ns
SK/N	97.92%	172.77%	42.12%	4.64%	4.11 (5.73)	0.19 ns	0.09 ns	0.64 ns
RK/N	100.00%	144.69%	30.89%	0.77%	4.10 (5.72)	0.86 ns	0.05*	0.86 ns

[ns]$P>0.05$, *$P<0.05$; [a]Values in parentheses are the Shannon-Weiner diversity index of the entire collection.
CR %, VR %, VD %, and MD % are coincidence rate of range, variable rate, variance difference percentage, and mean difference percentage for 14 traits between the entire and mini-core collections, respectively.
RGR, salt-tolerance index of shoot growth rate; RNIL, salt-tolerance index of leaves increased number; RLER, salt-tolerance index of leaf expansion rate; Sen, leaf senescence scale; SWC, shoot water content; RWC, root water content; SNC, shoot Na^+ concentration; RNC, root Na^+ concentration; SN/RN, the ratio of shoot Na^+ concentration to root Na^+ concentration; SKC, shoot K^+ concentration; RKC: root K^+ concentration; SK/RK, the ratio of shoot K^+ concentration to root K^+ concentration; SK/N, the ratio of shoot K^+ concentration to shoot Na^+ concentration; RK/N, the ratio of root K^+ concentration to root Na^+ concentration.

Keuls test and Wilcoxon rank-sum test showed no significant differences in the means and medians between the entire and core collections for the studied traits. Furthermore, Levene's test results indicated that there were no significant differences (P>0.05) between the core and entire collections for all traits except RGR, SN/RN, and RK/N, demonstrating that the central tendency and variability of phenotypic traits in the mini-core collection closely matched those in the entire collection. The Shannon-Weaver diversity index, which measures the diversity of individual phenotypic traits, ranged from 3.97 to 4.15 in the mini-core collection and from 5.63 to 5.76 in the entire collection, averaging 4.10 and 5.72, respectively. These results imply a moderate loss of diversity, about 28.32%, in the core collection, which could be attributed to missing genetic data.

In the mini-core collection of *M. sacchariflorus* and *M. lutarioriparius*, significant positive correlations were observed between SWC and RWC (r=0.76, r=0.73 in the entire set), as well as between Sen and SNC (r=0.70, r=0.66 in the entire set). Additionally, significant positive correlations were found between SKC and SNC, whereas the correlation between RKC and SNC was insignificant. Sen exhibited a significantly negative correlation with RNIL (r=-0.52, r=-0.52 in the entire set) and RLER (r=-0.48, r=-0.45 in the entire set). The correlation trends between traits in the core set resembled those observed in the entire set (Figure 5). Furthermore, the PCA conducted on the core set resulted in the extraction of five PCs, which explained 82.90% of the total variation in the mini core set. PC1, PC2, PC3, PC4, and PC5 accounted for 26.79%, 23.91%, 13.21%, 10.20%, and 8.78% of total variation, respectively (Table 3). PC1 displayed significant correlations with RK/N, RKC, SWC, RWC (positive loading), SK/RK and RNC (negative loading), whereas PC2 primarily included Sen, SN/RN and SNC with a positive loading, and SK/N, RNIL and RLER with a negative loading (Figure 6). These values were comparable to those obtained for the entire set.

4 Discussion

4.1 Screening system

The susceptibility of plants to environmental conditions during the seedling stage highlights the importance of evaluating salt tolerance based on plant responses at the seedling stage as a crucial screening criterion. However, the genetic diversity of salt tolerance in these species remains largely unknown due to the self-incompatibility of *Miscanthus* (Jiang et al., 2017) and the high heterozygosity of their genetic background. This complicated the use of plants at the seedling stage for stress experiments in subsequent genomic studies, as it is costly to obtain plants through asexual propagation (O'Loughlin et al., 2018). Previous studies by Chen et al. (2017) explored salt tolerance of 70 *Miscanthus* genotypes at the seedling stage (including 57 *M. sinensis*, 5 *M. sacchariflorus*, and 8 hybrids) using an indoor hydroponic system. The present study represents the first attempt to assess the genetic diversity of salt tolerance in *M. sacchariflorus* and *M. lutarioriparius* at the seedling stage using a large sample size of 318 genotypes. Our methodology involved planting rhizomes, each with 1-2 buds of a specific genotype, in plug trays prior to stress application. Hydroponics offer a favorable alternative for maintaining consistent screening conditions within a large population by providing uniform root environments and accommodating a high capacity of different genotypes (Tavakkoli et al., 2012; Nguyen et al., 2013). Single plants of similar heights from each genotype were selected and transferred to a homemade hydroponic setup after thorough root cleaning to ensure the uniformity of the tested plant materials. It is reported that employing such a similar system has allowed for successful assessment of salt tolerance and cadmium accumulation in different rapeseed germplasms, with related QTLs identified (Wan et al., 2017; Chen et al., 2018). Moreover, to account for the inherent differences among genotypes, our methodology also adopted the usage of relative values of growth traits, a widely-used approach (Wu et al., 2019; Luo et al., 2021), to evaluate the performance of different *M. sacchariflorus* and *M. lutarioriparius* genotypes under salt stress.

4.2 Mechanisms of salt tolerance

Studies have demonstrated that high concentrations of soil salts damage plants by causing ion (mainly Na^+) toxicity and osmotic stress (Munns and Tester, 2008). Therefore, osmotic tolerance and ion exclusion need to be considered together when improving salt tolerance in plants (Genc et al., 2010). Low Na^+ concentrations in shoots have been successfully used as selection criteria for breeding salt-tolerant cultivars of durum wheat (Munns et al., 2012), barley (Nguyen et al., 2013), and rice (Lin et al., 2004). Our results indicated that salt-tolerant genotypes exhibited significantly lower SNC, which is consistent with previous studies on salt tolerance in *M. sinensis* (Sun et al., 2014; Chen et al., 2017; Sun et al., 2021), *M.* × *giganteus* (Plazek et al., 2014; Stavridou et al., 2020), and polyploid *M. lutarioriparius* (Duan et al., 2018). These findings suggested that the mechanisms of Na^+ exclusion utilized to improve salt tolerance in cereals were also employed by *M. sacchariflorus* and *M. lutarioriparius*. Notably, our study revealed that two genotypes (M283 and M349) exhibited lower Sen and higher RGR, RNIL, RLER, and SWC despite having high shoot Na^+ concentrations. This observation may indicate the existence of a tissue tolerance mechanism, with Na^+ being compartmentalized within vacuoles to prevent toxic concentrations in the cytoplasm (Munns and James, 2003).

However, under salt stress, high Na^+ concentrations interfere with K^+ uptake and function (Shabala and Cuin, 2008). Maintaining a high K^+ concentration is another important mechanism in response to relatively high Na^+ levels under salt stress (Munns and James, 2003; Krishnamurthy et al., 2007). In the present study, the evaluation of ten genotypes based on different salt concentrations showed that most genotypes had higher SKC and RKC under salt stress than under the control. Moreover, our evaluation of 318 genotypes under 150 mM NaCl revealed that genotypes with high Na^+ concentrations displayed higher K^+ concentrations than those with low Na^+ concentrations.

These results can be attributed to the adaptive response of *M. sacchariflorus* and *M. lutarioriparius* to excessive Na^+ levels in their surrounding environments, leading to increased uptake and transport of K^+ possibly through the enhanced activity of K^+ channels in the cell membrane and transporter proteins. This response allows the maintenance of stable levels of intracellular K^+ and Na^+, ultimately enabling normal growth and metabolic functions. Previous studies have reported a higher K^+ content under salt stress than under the control in *M.* × *giganteus* (Plazek et al., 2014; Stavridou et al., 2020) and polyploid *M. lutarioriparius* (Duan et al., 2018). Plazek et al. (2014) concluded that a high accumulation of K^+ in leaves reduces the Na^+ effect and determines the salinity tolerance of *Miscanthus*. Our study showed a strong positive correlation between the ability of plants to retain K^+ after exposure to NaCl and salinity tolerance, which is consistent with previous reports in a wide range of plants, including wheat (Cuin et al., 2008), Hami melon (Xiong et al., 2018), *Nitraria sibirica* (Tang et al., 2018), pumpkin (Huang et al., 2019) and *Puccinellia nuttalliana* (Vaziriyeganeh et al., 2022).

4.3 Evaluation of salt tolerance of *M. sacchariflorus* and *M. lutarioriparius* by multivariate analysis

The stress resistance capacity of plants results from their responses to adverse environmental conditions and long-term evolution. As it is a quantitative trait controlled by multiple genes, using a single index to evaluate the stress resistance of plants is unreliable. For a more comprehensive assessment of plant stress resistance, employing multidimensional indices is considered more scientifically sound (Wu et al., 2019; Weng et al., 2021). Membership function analysis has gained a wider use in recent years for evaluating plant stress tolerance in that it addresses the limitations of selecting plant varieties based on a single index (Wassie et al., 2019; Weng et al., 2021; Wang et al., 2023). In the present study, through membership function analysis, 14 individual indicators were integrated into a comprehensive evaluation index of salt tolerance (D value) for different genotypes of *M. sacchariflorus* and *M. lutarioriparius* at the seedling stage, with a higher D value indicating stronger salt tolerance ability. Cluster analysis based on the D value would lead to a more objective selection of three HST, 50 ST, 127 MST, 117 SS and 21 HSS genotypes. This outcome diverges from what would be obtained if any single indicator were used, suggesting that salt tolerance evaluation of *M. sacchariflorus* and *M. lutarioriparius* could not rely on a single indicator. All genotypes of *M. sacchariflorus* and *M. lutarioriparius* were evaluated for salt tolerance for the first time. Further studies are needed to compare differences in physiological indicators among genotypes of *M. sacchariflorus* and *M. lutarioriparius* with different salt tolerance levels and their performance in saline soils. Our findings may provide materials with extreme salt tolerance for further studies on the mechanisms of *M. sacchariflorus* and *M. lutarioriparius* in response to salt stress using comparative transcriptome and selective sweep analysis.

Determining the salt tolerance of one or some *M. sacchariflorus* and *M. lutarioriparius* genotypes is challenging without a large number of other genotypes for comparison. Assessing 14 traits and calculating the D value for salt tolerance evaluation is laborious and complicated. To evaluate the salt tolerance of *M. sacchariflorus* and *M. lutarioriparius* in a more convenient and reliable manner, a mathematical evaluation model for the salt tolerance was established using multiple regression analysis. The larger the Y value, the higher the salt tolerance. As a result, it is only necessary to measure seven traits: SNC, RNIL, RWC, RGR, RKC, Sen, and RNC to calculate the Y value for estimating salt tolerance in any genotypes of *M. sacchariflorus* and *M. lutarioriparius*. To our best knowledge, this is the first time a mathematical evaluation model is established to predict the salt tolerance of *M. sacchariflorus* and *M. lutarioriparius* during the seedling stage.

4.4 Development of a mini-core collection

This study represents a pioneering effort to establish a core collection for the salt tolerance of *M. sacchariflorus* and *M. lutarioriparius* at the seedling stage. The salt-tolerant traits used were able to generate a mini-core collection that captured the full range of trait variability that existed in the entire collection. This provides the foundation for studying the salt tolerance mechanism through marker-trait associations, which is essential for the conservation of genetic resources and the breeding of salt-tolerant *M. sacchariflorus* and *M. lutarioriparius* lines.

The mini-core collection constituted approximately 20% of the evaluated entire collection, falling within the recommended size range of 10% to 30% for a well-representative core collection (Tchokponhoue et al., 2020; Uba et al., 2023). Additionally, a mini-core collection with a CR % exceeding 80% is deemed suitable for breeding (Hu et al., 2000). High values of VR % and VD % indicate the successful preservation of diversity from the entire set in the core set (Mahmoodi et al., 2019). The MD % for all studied traits was below 20%, indicating that the mini-core collection effectively represented the entire collection. Notably, no significant differences were observed between the core and entire collections in terms of means, variances (for all traits except for RGR, SN/RN, and RK/N), and medians, further validating the representativeness of the mini-core collection.

When establishing a core set, it is crucial to preserve the phenotypic associations within the entire collection to maintain co-adapted genetic complexes and enable efficient germplasm utilization (Tripathi et al., 2022). The results of the Pearson's correlation analysis for the 14 traits showed that the correlation coefficients between all combinations of traits remained similar in both the core and entire sets. This preservation of trait associations in the core set aligns with findings from previous studies on core collection development in various crops, such as turnips (Li et al., 2021), wheat (Phogat et al., 2021), mustards (Nanjundan et al., 2022), and lentils (Tripathi et al., 2022). Furthermore, five PCs were identified in the core and entire sets, which collectively explained 82.90% and 81.42% of the total variation, respectively. This indicates that the mini-core collection established in this study

effectively represents the overall variability of the entire collection. The use of PCA to assess the spatial distribution of entries and to explain the variance serves as an exploratory criterion for evaluating the core set, as has been reported in previous studies (Li et al., 2021; Tripathi et al., 2022).

5 Conclusion

This study established that the optimal NaCl concentration for evaluating the salt tolerance of *M. sacchariflorus* and *M. lutarioriparius* is 150 mM. Significant genotype-dependent differences in salt tolerance were observed at the seedling stage in both species. *M. sacchariflorus* and *M. lutarioriparius* adapt to salt stress by regulating ion homeostasis primarily through enhanced K^+ uptake, shoot Na^+ exclusion, and Na^+ sequestration in shoot vacuoles. A total of 318 genotypes were evaluated, resulting in the identification of three HST, 50 ST, 127 MST, 117 SS, and 21 HSS genotypes of *M. sacchariflorus* and *M. lutarioriparius* at the seedling stage. A mathematical evaluation model was proposed to assess salt tolerance by using fourteen traits in the 318 *M. sacchariflorus* and *M. lutarioriparius* genotypes, leading to the development of a representative mini core set of 64 genotypes. These findings significantly contribute to the evaluation and breeding of salt-tolerant *M. sacchariflorus* and *M. lutarioriparius*. Moreover, these also provide valuable resources for an in-depth understanding of the adaptive mechanisms and molecular regulatory networks of *M. sacchariflorus* and *M. lutarioriparius* in response to salt stress, thereby offering scientific support for future efforts to enhance salt tolerance and improve stress resilience in plants. This study is of great implication for the utilization and improvement of marginal lands.

Data availability statement

The original contributions presented in the study are included in the article/Supplementary Material. Further inquiries can be directed to the corresponding authors.

Author contributions

YT: Conceptualization, Data curation, Formal Analysis, Investigation, Methodology, Software, Visualization, Writing – original draft, Writing – review & editing. SL: Investigation, Software, Writing – original draft. DZ: Writing – review & editing. ZZ: Writing – review & editing. SY: Resources, Writing – original draft. XZ: Writing – review & editing. SX: Resources, Writing – original draft. XK: Writing – review & editing. ML: Methodology, Writing – original draft. XH: Investigation, Writing – original draft. ZY: Conceptualization, Funding acquisition, Resources, Writing – review & editing. LX: Project administration, Supervision, Writing – review & editing, Writing – original draft.

Funding

The author(s) declare financial support was received for the research, authorship, and/or publication of this article. This research was supported by the National Natural Science Foundation of China (Grant No. 31871693) and Foundation for the Construction of Innovative Hunan (Grant No. 2019NK2011).

Acknowledgments

The authors thank Jian Tang, Hongge Qian, Weihong Du, Peng Zhu, Ning Peng, Songtao Guo, Miaomiao Peng, Jie Li, Manti Li, Tianzhuo Fu, Lan Gu, Xianghui Li, and Kejia Zhu for their assistance with experiments. We also thank the reviewers.

Conflict of interest

Author XH is employed by Hunan Heyi Crop Science Co., Ltd., Changsha, Hunan, China.

The remaining authors declare that the research was conducted in the absence of any commercial or financial relationships that could be construed as a potential conflict of interest.

Publisher's note

Supplementary material

The Supplementary Material for this article can be found online at: https://www.frontiersin.org/articles/10.3389/fpls.2024.1364826/full#supplementary-material

References

Aravind, J., Kaur, V., Wankhede, D. P., and Nanjundan, J. (2022). *EvaluateCore: Quality Evaluation of Core Collections* (R package version 0.1.3). Available at: https://aravind-j.github.io/EvaluateCore/, https://CRAN.R-project.org/package=EvaluateCore.

Ashraf, M. Y., Awan, A. R., and Mahmood, K. (2012). Rehabilitation of saline ecosystems through cultivation of salt tolerant plants. *Pak. J. Bot.* 44, 69–75.

Chen, C.-L., van der Schoot, H., Dehghan, S., Kamei, C. L. A., Schwarz, K.-U., Meyer, H., et al. (2017). Genetic diversity of salt tolerance in *Miscanthus.* Front. *Plant Sci.* 8. doi: 10.3389/fpls.2017.00187

Chen, L. L., Wan, H. P., Qian, J. L., Guo, J. B., Sun, C. M., Wen, J., et al. (2018). Genome-wide association study of cadmium accumulation at the seedling stage in rapeseed (*Brassica napus* L.). *Front. Plant Sci.* 9. doi: 10.3389/fpls.2018.00375

Cuin, T. A., Betts, S. A., Chalmandrier, R., and Shabala, S. (2008). A root's ability to retain K^+ correlates with salt tolerance in wheat. *J. Exp. Bot.* 59, 2697–2706. doi: 10.1093/jxb/ern128

De Beukelaer, H., Davenport, G. F., and Fack, V. (2018). Core Hunter 3, flexible core subset selection. *BMC Bioinform.* 19, 203. doi: 10.1186/s12859-018-2209-z

Duan, J. Y., Shi, Y. L., Lin, Y. H., Huang, H. M., Liu, Q. B., Yi, Z. L., et al. (2018). Characteristics of inorganic salt ion absorption of *Miscanthus lutarioriparius* polyploid under NaCl stress. *Pratacultural Sci.* 35, 2893–2902. doi: 10.11829/j.issn.1001-0629.2018-0432

FAO. Global Soil Partnership (2021) World map of salt-affected soils launched at virtual conference. Available online at: https://www.fao.org/global-soil-partnership/resources/highlights/detail/en/c/1445579/ (Accessed October 20, 2021).

Flowers, T. J. (2004). Improving crop salt tolerance. *J. Exp. Bot.* 55, 307–319. doi: 10.1093/jxb/erh003

Genc, Y., Oldach, K., Verbyla, A. P., Lott, G., Hassan, M., Tester, M., et al. (2010). Sodium exclusion QTL associated with improved seedling growth in bread wheat under salinity stress. *Theor. Appl. Genet.* 121, 877–894. doi: 10.1007/s00122-010-1357-y

Gower, J. C. (1971). A general coefficient of similarity and some of its properties. *Biometrics* 27, 857–871. doi: 10.2307/2528823

Guo, Y. Y., Kuang, L. H., Xu, Y., Yan, T., Jiang, L. X., Dong, J., et al. (2022). Construction of a worldwide core collection of rapeseed and association analysis for waterlogging tolerance. *Plant Growth Regul.* 98, 321–328. doi: 10.1007/s10725-022-00862-5

Hu, J., Zhu, J., and Xu, H. M. (2000). Methods of constructing core collections by stepwise clustering with three sampling strategies based on the genotypic values of crops. *Theor. Appl. Genet.* 101, 264–268. doi: 10.1007/s001220051478

Huang, Y., Cao, H. S., Yang, L., Chen, C., Shabala, L., Xiong, M., et al. (2019). Tissue-specific respiratory burst oxidase homolog-dependent H_2O_2 signaling to the plasma membrane H^+-ATPase confers potassium uptake and salinity tolerance in Cucurbitaceae. *J. Exp. Bot.* 70, 5879–5893. doi: 10.1093/jxb/erz328

Jiang, J. X., Guan, Y. F., McCormick, S., Juvik, J., Lubberstedt, T., and Fei, S. Z. (2017). Gametophytic self-incompatibility is operative in *Miscanthus sinensis* (Poaceae) and is affected by pistil age. *Crop Sci.* 57, 1948–1956. doi: 10.2135/cropsci2016.11.0932

Keuls, M. (1952). The use of the studentized range in connection with an analysis of variance. *Euphytica* 1, 112–122. doi: 10.1007/BF01908269

Kim, K. W., Chung, H. K., Cho, G. T., Ma, K. H., Chandrabalan, D., Gwag, J. G., et al. (2007). PowerCore, a program applying the advanced M strategy with a heuristic search for establishing core sets. *Bioinformatics* 16, 2155–2162. doi: 10.1093/bioinformatics/btm313

Krishnamurthy, L., Serraj, R., Hash, C. T., Dakheel, A. J., and Reddy, B. V. S. (2007). Screening sorghum genotypes for salinity tolerant biomass production. *Euphytica* 156, 15–24. doi: 10.1007/s10681-006-9343-9

Levene, H. (1960). ""Robust tests for equality of variances,"," in *contributions to probability and statistics, essays in honor of harold hoteling.* Ed. I. Olkin (Stanford University Press, Stanford, CA), 278–292.

Li, R. R., Zhou, F. Y., Gao, Y. Y., Liu, C. L., Yu, S. B., Zhao, K., et al. (2021). Genetic diversity and primary core collection construction of turnip (*Brassica rapa* L. ssp. *rapifera* Matzg) landraces in tibet revealed via morphological and SSR markers. *Agron. J.* 11, 1901. doi: 10.3390/agronomy11101901

Lin, H. X., Zhu, M. Z., Yano, M., Gao, J. P., Liang, Z. W., Su, W. A., et al. (2004). QTLs for Na^+ and K^+ uptake of the shoots and roots controlling rice salt tolerance. *Theor. Appl. Genet.* 108, 253–260. doi: 10.1007/s00122-003-1421-y

Luo, M. J., Zhang, Y. X., Li, J. N., Zhang, P. P., Chen, K., Song, W., et al. (2021). Molecular dissection of maize seedling salt tolerance using a genome-wide association analysis method. *Plant Biotechnol. J.* 19, 1937–1951. doi: 10.1111/pbi.13607

Mahmoodi, R., Dadpour, M. R., Hassani, D., Zeinalabedini, M., Vendramin, E., Micali, S., et al. (2019). Development of a core collection in Iranian walnut (*Juglans regia* L.) germplasm using the phenotypic diversity. *Sci. Hortic.* 249, 439–448. doi: 10.1016/j.scienta.2019.02.017

Munns, R. (2005). Genes and salt tolerance, bringing them together. *New Phytol.* 167, 645–663. doi: 10.1111/j.1469-8137.2005.01487.x

Munns, R., and Gilliham, M. (2015). Salinity tolerance of crops - what is the cost? *New Phytol.* 208, 668–673. doi: 10.1111/nph.13519

Munns, R., and James, R. A. (2003). Screening methods for salinity tolerance, a case study with tetraploid wheat. *Plant Soil.* 253, 201–218. doi: 10.1023/A:1024553303144

Munns, R., James, R. A., Xu, B., Athman, A., Conn, S. J., Jordans, C., et al. (2012). Wheat grain yield on saline soils is improved by an ancestral Na^+ transporter gene. *Nat. Biotechnol.* 30, 360–364. doi: 10.1038/nbt.2120

Munns, R., and Tester, M. (2008). Mechanisms of salinity tolerance. *Annu. Rev. Plant Biol.* 59, 651–681. doi: 10.1146/annurev.arplant.59.032607.092911

Nanjundan, J., Aravind, J., Radhamani, J., Singh, K. H., Kumar, A., Thakur, A. K., et al. (2022). Development of Indian mustard [*Brassica juncea* (L.) Czern.] core collection based on agro-morphological traits. *Genet. Resour. Crop Evol.* 69, 145–162. doi: 10.1007/s10722-021-01211-7

Newman, D. (1939). The distribution of range in samples from a normal population expressed in terms of an independent estimate of standard deviation. *Biometrika* 31, 20–30. doi: 10.1093/biomet/31.1-2.20

Nguyen, V. L., Ribot, S. A., Dolstra, O., Niks, R. E., Visser, R. G. F., and van der Linden, C. G. (2013). Identification of quantitative trait loci for ion homeostasis and salt tolerance in barley (*Hordeum vulgare* L.). *Mol. Breed.* 31, 137–152. doi: 10.1007/s11032-012-9777-9

O'Loughlin, J., McDonnell, K., and Finnan, J. (2018). Quantifying the economic and greenhouse gas balance advantages of establishing *Miscanthus* from stem cuttings. *Biomass Bioenergy* 109, 147–154. doi: 10.1016/j.biombioe.2017.12.010

Phogat, B. S., Kumar, S., Kumari, J., Kumar, N., Pandey, A. C., Singh, T. P., et al. (2021). Characterization of wheat germplasm conserved in the Indian National Genebank and establishment of a composite core collection. *Crop Sci.* 61, 604–620. doi: 10.1002/csc2.20285

Plazek, A., Dubert, F., Koscielniak, J., Tatrzanska, M., Maciejewski, M., Gondek, K., et al. (2014). Tolerance of *Miscanthus* × *giganteus* to salinity depends on initial weight of rhizomes as well as high accumulation of potassium and proline in leaves. *Ind. Crops Prod.* 52, 278–285. doi: 10.1016/j.indcrop.2013.10.041

Shabala, S., and Cuin, T. A. (2008). Potassium transport and plant salt tolerance. *Physiol. Plant* 133, 651–669. doi: 10.1111/j.1399-3054.2007.01008.x

Shannon, C. E., and Weaver, W. (1949). *The mathematical theory of communication* (Champaign, IL: The University of Illinois Press).

Shavyrkina, N. A., Budaeva, V. V., Skiba, E. A., Gismatulina, Y. A., and Sakovich, G. V. (2023). Review of current prospects for using *Miscanthus*-based polymers. *Polymers* 15, 3097. doi: 10.3390/polym15143097

Song, Z. H., Xu, Q., Lin, C., Tao, C. C., Zhu, C. Y., Xing, S. L., et al. (2017). Transcriptomic characterization of candidate genes responsive to salt tolerance of *Miscanthus* energy crops. *GCB Bioenergy* 9, 1222–1237. doi: 10.1111/gcbb.12413

Stavridou, E., Webster, R. J., and Robson, P. R. H. (2020). The effects of moderate and severe salinity on composition and physiology in the biomass crop *Miscanthus* × *giganteus. Plant* 9, 1266. doi: 10.3390/plants9101266

Sun, P., and Chen, Y. Y. (2015). Physiological response of *Triarrherca sacchariflora* under heavy saline-alkali stress in coastal region. *Periodical Ocean Univ. China* 45, 115–120. doi: 10.16441/j.cnki.hdxb.20130369

Sun, Q., Lin, Q., Yi, Z. L., Yang, Z. R., and Zhou, F. S. (2010). A taxonomic revision of *Miscanthus* s.l. (Poaceae) from China. *Bot. J. Linn. Soc* 164, 178–220. doi: 10.1111/boj.2010.164.issue-2

Sun, Q., Yamada, T., Han, Y. L., and Takano, T. (2021). Differential responses of *NHX1* and *SOS1* gene expressions to salinity in two *Miscanthus sinensis* Anderss. accessions with different salt tolerance. *Phyton-Int. J. Exp. Bot.* 90, 827–836. doi: 10.32604/phyton.2021.013805

Sun, Q., Yamada, T., and Takano, T. (2014). Salinity effects on germination, growth, photosynthesis, and ion accumulation in wild *Miscanthus sinensis* Anderss. populations. *Crop Sci.* 54, 2760–2771. doi: 10.2135/cropsci2013.09.0636

Tang, X. Q., Yang, X. Y., Li, H. Y., and Zhang, H. X. (2018). Maintenance of K^+/Na^+ balance in the roots of *Nitraria sibirica* Pall. in response to NaCl stress. *Forests* 9, 601. doi: 10.3390/f9100601

Tavakkoli, E., Fatehi, F., Rengasamy, P., and McDonald, G. K. (2012). A comparison of hydroponic and soil-based screening methods to identify salt tolerance in the field in barley. *J. Exp. Bot.* 63, 3853–3867. doi: 10.1093/jxb/ers085

Tchokponhoue, D. A., Achigan-Dako, E. G., N'Danikou, S., Nyadanu, D., Kahane, R., Houéto, J., et al. (2020). Phenotypic variation, functional traits repeatability and core collection inference in *Synsepalum dulcificum* (Schumach & Thonn.) Daniell reveals the Dahomey Gap as a center of diversity. *Sci. Rep.* 10, 19538. doi: 10.1038/s41598-020-76103-4

Tripathi, K., Kumari, J., Gore, P. G., Mishra, D. C., Singh, A. K., Mishra, G. P., et al. (2022). Agro-morphological characterization of lentil germplasm of Indian national genebank and development of a core set for efficient utilization in lentil improvement programs. *Front. Plant Sci.* 12. doi: 10.3389/fpls.2021.751429

Uba, C. U., Oselebe, H. O., Tesfaye, A. A., Mekonen, G. S., and Abtew, W. G. (2023). Exploring phenotypic variation of diverse bambara groundnut (*Vigna subterranea* L) origin and development of mini-core collection for future breeding. *Food Energy Secur.* 12, e460. doi: 10.1002/fes3.460

Vaziriyeganeh, M., Carvajal, M., Du, N., and Zwiazek, J. J. (2022). Salinity tolerance of halophytic grass *Puccinellia nuttalliana* is associated with enhancement of aquaporin-mediated water transport by sodium. *Int. J. Mol. Sci.* 23, 5732. doi: 10.3390/ijms23105732

Wan, H. P., Chen, L. L., Guo, J. B., Li, Q., Wen, J., Yi, B., et al. (2017). Genome-wide association study reveals the genetic architecture underlying salt tolerance-related traits in rapeseed (*Brassica napus* L.). *Front. Plant Sci.* 8. doi: 10.3389/fpls.2017.00593

Wang, Q., Kan, L. F., Lin, C., Song, Z. H., Tao, C. H., Liu, W., et al. (2019). Transcriptomic evaluation of *Miscanthus* photosynthetic traits to salinity stress. *Biomass Bioenergy* 125, 123–130. doi: 10.1016/j.biombioe.2019.03.005

Wang, X. L., Li, J. Q., Sun, J., Gu, S., Wang, J. B., Su, C., et al. (2022). Mining beneficial genes for salt tolerance from a core collection of rice landraces at the seedling stage through genome-wide association mapping. *Front. Plant Sci.* 13. doi: 10.3389/fpls.2022.847863

Wang, Y., Liu, K., Liang, G., Jia, Z. F., Ju, Z. L., Ma, X., et al. (2023). Comprehensive evaluation of low nitrogen tolerance in oat (*Avena sativa* L.) seedlings. *Agronomy* 13, 604. doi: 10.3390/agronomy13020604

Wassie, M., Zhang, W. H., Zhang, Q., Ji, K., and Chen, L. (2019). Effect of heat stress on growth and physiological traits of alfalfa (*Medicago sativa* L.) and a comprehensive evaluation for heat tolerance. *Agronomy* 9, 597. doi: 10.3390/agronomy9100597

Weng, J. Y., Li, P. L., Rehman, A. S., Wang, L. K., Gao, X., and Niu, Q. L. (2021). Physiological response and evaluation of melon (*Cucumis melo* L.) germplasm resources under high temperature and humidity stress at seedling stage. *Sci. Hortic.* 288, 110317. doi: 10.1016/j.scienta.2021.110317

Wilcoxon, F. (1945). Individual comparisons by ranking methods. *Biometrics* 1, 80–83. doi: 10.2307/3001968

Wu, H., Guo, J., Wang, C., Li, K. L., Zhang, X. W., Yang, Z., et al. (2019). An effective screening method and a reliable screening trait for salt tolerance of *Brassica napus* at the germination stage. *Front. Plant Sci.* 10. doi: 10.3389/fpls.2019.00530

Xiong, M., Zhang, X. J., Shabala, S., Shabala, L., Chen, Y. J., Xiang, C. L., et al. (2018). Evaluation of salt tolerance and contributing ionic mechanism in nine Hami melon landraces in Xinjiang, China. *Sci. Hortic.* 237, 277–286. doi: 10.1016/j.scienta.2018.04.023

Xu, Y., Zheng, C., Liang, L., Yi, Z. L., and Xue, S. (2021). Quantitative assessment of the potential for soil improvement by planting *Miscanthus* on saline-alkaline soil and the underlying microbial mechanism. *GCB Bioenergy* 13, 1191–1205. doi: 10.1111/gcbb.12845

Xue, S., Lewandowski, I., Wang, X. Y., and Yi, Z. L. (2016). Assessment of the production potentials of *Miscanthus* on marginal land in China. *Renew. Sust. Energy Rev.* 54, 932–943. doi: 10.1016/j.rser.2015.10.040

Yu, T., Wang, Y. C., Xu, P. P., Cheng, S. A., Hou, X. W., Geng, G. F., et al. (2023). *MsaH2A.W* is identified response to salt tolerance in *Miscanthus sacchariflorus*. *GCB Bioenergy* 15, 1058–1073. doi: 10.1111/gcbb.13084

Zheng, C., Iqbal, Y., Labonte, N., Sun, G. R., Feng, H., Yi, Z. L., et al. (2019). Performance of switchgrass and *Miscanthus* genotypes on marginal land in the Yellow River Delta. *Ind. Crops Prod.* 141, 111773. doi: 10.1016/j.indcrop.2019.111773

Zheng, C., Yi, Z. L., Xiao, L., Sun, G. R., Li, M., Xue, S., et al. (2022). The performance of *Miscanthus* hybrids in saline-alkaline soil. *Front. Plant Sci.* 13. doi: 10.3389/fpls.2022.921824

Zheng, C., Yi, Z. L., Xiao, L., Yang, S., Chen, Z. Y., and Pang, Z. J. (2015). Effects of NaCl stress on seed germination and seedling growth of *Miscanthus*. *Chin. J. Grassland* 37, 37–42. doi: 10.3969/j.issn.1673-5021.2015.03.007

Zhu, J. K. (2016). Abiotic stress signaling and responses in plants. *Cell* 167, 313–324. doi: 10.1016/j.cell.2016.08.029

Zong, J. Q., Gao, Y. Z., Chen, J. B., Nie, D. Y., and Liu, J. X. (2013). Evaluation of salinity tolerance of *Miscanthus sacchariflorus* Germplasm during Germination Period. *Acta Agrestia Sin.* 21, 1148–1156. doi: 10.11733/j.issn.1007-0435.2013.06.018

frontiers | Frontiers in Plant Science

TYPE Original Research
PUBLISHED 15 April 2024
DOI 10.3389/fpls.2024.1376427

OPEN ACCESS

EDITED BY
Zulfiqar Ali Sahito,
Zhejiang University, China

REVIEWED BY
Lars Hendrik Wegner,
Foshan University, China
Min Chen,
Shandong Normal University, China

*CORRESPONDENCE
Suping Gao
gao_suping@sicau.edu.cn

†These authors have contributed equally to this work

RECEIVED 25 January 2024
ACCEPTED 29 March 2024
PUBLISHED 15 April 2024

CITATION
Duan Y, Jiang L, Lei T, Ouyang K, Liu C, Zhao Z, Li Y, Yang L, Li J, Yi S and Gao S (2024) Increasing Ca^{2+} accumulation in salt glands under salt stress increases stronger selective secretion of Na^+ in *Plumbago auriculata* tetraploids.
Front. Plant Sci. 15:1376427.
doi: 10.3389/fpls.2024.1376427

Increasing Ca^{2+} accumulation in salt glands under salt stress increases stronger selective secretion of Na^+ in *Plumbago auriculata* tetraploids

Yifan Duan[1†], Liqiong Jiang[2†], Ting Lei[1], Keyu Ouyang[1], Cailei Liu[1], Zi'an Zhao[1], Yirui Li[1], Lijuan Yang[1], Jiani Li[1], Shouli Yi[3] and Suping Gao[1*]

[1]College of Landscape Architecture, Sichuan Agricultural University, Chengdu, China, [2]Chengdu Academy of Agriculture and Forestry Sciences, Chengdu, China, [3]College of Fine Art and Calligraphy, Sichuan Normal University, Chengdu, China

Under salt stress, recretohalophyte Plumbago auriculata tetraploids enhance salt tolerance by increasing selective secretion of Na^+ compared with that in diploids, although the mechanism is unclear. Using non-invasive micro-test technology, the effect of salt gland Ca^{2+} content on Na^+ and K^+ secretion were investigated in diploid and tetraploid P. auriculata under salt stress. Salt gland Ca^{2+} content and secretion rates of Na^+ and K^+ were higher in tetraploids than in diploids under salt stress. Addition of exogenous Ca^{2+} increased the Ca^{2+} content of the salt gland in diploids and is accompanied by an increase in the rate of Na^+ and K^+ secretion. With addition of a Ca^{2+} channel inhibitor, diploid salt glands retained large amounts of Ca^{2+}, leading to higher Ca^{2+} content and Na^+ secretion rate than those of tetraploids. Inhibiting H_2O_2 generation and H^+-ATPase activity altered Na^+ and K^+ secretion rates in diploids and tetraploids under salt stress, indicating involvement in regulating Na^+ and K^+ secretion. Our results indicate that the increased Na^+ secretion rate of salt gland in tetraploids under salt stress was associated with elevated Ca^{2+} content in salt gland.

KEYWORDS

recretohalophyte, salt gland, salt stress, selective secretion, tetraploid

Highlight

- The Ca^{2+} content in salt glands and the rate of Na^+ secretion were analyzed in diploid and tetraploid *P. auriculata* under salt stress, and high tetraploid rate of Na^+ secretion was strongly correlated with high salt gland Ca^{2+} accumulation.

1 Introduction

Salt stress is a major abiotic stress that affects plant growth (Ruan et al., 2010). In the early stages of salt stress, high salt concentrations limit plant water uptake, resulting in osmotic stress. With prolonged salt stress, accumulation of excessive salt ions can cause oxidative stress, ion toxicity, and nutrient deficiencies in plants (Munns and Tester, 2008). Plants increase salt tolerance by various mechanisms. In nonsucculent halophytes, one particular adaptation is the secretion of excess salt ions from stem and leaf surfaces, and plants that increase salt tolerance using this pathway are called recretohalophytes (Flowers et al., 2008; Guo et al., 2023). Recretohalophytes can secrete multiple ions, and secretion rates are influenced by rhizosphere ion concentrations (Ding et al., 2010).

The mechanism of salt secretion by the salt glands is still unclear, and only possible paths have been suggested. There are three hypotheses of secretion include (1) the role of the osmotic potential in salt secretion; (2) a transfer system that is similar to liquid flow in animals; (3) salt solution excretion by vesicles in the plasma membrane (Yuan et al., 2016). Secretion rates of Na^+ and Cl^- are usually higher than those of other ions (Yuan et al., 2016), which may be due to the many Na^+ and Cl^- transport channels on the plasma membrane of salt gland cells. However, there are some recretohalophytes, such as those in the family Plumbaginaceae, in which Ca^{2+} is the predominant ion secreted (Faraday and Thomson, 1986; Duan et al., 2023).

The Ca^{2+} ion can be a signaling molecule in plants in response to salt stress. Exogenous addition of Ca^{2+} inhibits Na^+ uptake by roots under salt stress and reduces K^+ loss, thereby maintaining plant Na^+/K^+ ratio (Jin et al., 2017). The ion K^+ is an essential activator of various enzymes in plant metabolic processes, and therefore, maintaining K^+ homeostasis under salt stress is crucial to increase salt tolerance (Horie et al., 2009). The plasma membrane Na^+/H^+ antiporter SOS1 plays a key role in Na^+ efflux from cells and is activated by Ca^{2+} signaling. Salt stress increases cytosolic Ca^{2+} levels, leading to the activation of SOS3, which binds to SOS2 to form the SOS3–SOS2 complex, ultimately phosphorylating and activating SOS1 for Na^+ efflux (Qiu et al., 2002; Zhu, 2016). The SOS1 relies on the activity of plasma membrane H^+-ATPase for ion translocation across the membrane (Chen J. A. et al., 2010; Sanadhya et al., 2015; Che et al., 2019), whereas Ca^{2+} may regulate H^+-ATPase activity (Sun et al., 2010). Hydrogen peroxide (H_2O_2) can be an important signaling molecule in regulating the Na^+/K^+ balance. Under salt stress, H_2O_2 promotes Na^+ efflux by stabilizing the mRNA of SOS1, and inhibiting H_2O_2 production leads to increased K^+ efflux under salt stress (Chung et al., 2008). The Ca^{2+} ion acts as an upstream signal for H_2O_2, suggesting that Ca^{2+} is involved in regulating the Na^+/K^+ balance by modulating H_2O_2 production.

In recretohalophytes, Ca^{2+} is involved in regulating ion secretion from salt glands, and exogenous addition of Ca^{2+} significantly increases Na^+ secretion under salt stress (Ding et al., 2010). Salt gland excretion of ions in recretohalophytes depends on ion transport systems and vesicular transport (Li et al., 2020). The plasma membrane Na^+/H^+ antiporter SOS1 is a crucial pathway for salt gland Na^+ secretion (Guo et al., 2020), and Ca^{2+} acts as an activating signal upstream of SOS1, potentially increasing Na^+ secretion. Addition of Ca^{2+} also increases vesicular transport, promoting Na^+ secretion (Ding et al., 2010).

Research on the ion channels involved in K^+ secretion of recretohalophytes is limited, and currently, K^+ secretion is proposed to primarily occur by a Na^+-K^+-Cl^- cotransporter (Yuan et al., 2016). Under salt stress, plasma membrane depolarization in plant cells leads to activation of outward-rectifying K^+ channels (DA-KORCs) and nonselective cation channels (DA-NSCCs), resulting in K^+ efflux from cells (Shabala and Pottosin, 2014). However, whether DA-KORCs and DA-NSCCs are involved in K^+ secretion in salt glands of recretohalophytes remains unclear. When exogenous Ca^{2+} channel inhibitors are added, which reduce plant Ca^{2+} levels, only the Na^+ secretion rate is inhibited, without significant effects on K^+ secretion rate (Kobayashi et al., 2007). Therefore, in addition to a Na^+-K^+-Cl^- cotransporter, K^+ secretion may also occur through other ion channels.

Plumbago auriculata (Plumbaginaceae) is a typical calcium-secreting plant that has important medicinal value. Under normal growth conditions, Ca^{2+} is the primary ion secreted by *P. auriculata* salt glands. Under NaCl stress in our previous study, tetraploid *P. auriculata* are more salt tolerant than diploids with better ion homeostasis and less morphology damage under saline conditions. The Na^+ secretion rate in whole leaves of tetraploid *P. auriculata* was higher than that in whole leaves of diploids. However, the Ca^{2+} content in tetraploid leaves is significantly lower than that in diploid leaves (Duan et al., 2023). Those results contradict the results of previous studies that suggest Ca^{2+} promotes Na^+ secretion under salt stress. In animals, salt gland secretions indicate that sustained elevation of Ca^{2+} content in salt glands serves as a primary signal for secretion activity (Shuttleworth and Thompson, 1989; Shuttleworth and Hildebrandt, 1999). Therefore, it was hypothesized that *P. auriculata* Na^+ and K^+ secretion rates are regulated by salt gland Ca^{2+} content, not by the overall Ca^{2+} content in leaves. Thus, in this study, changes in Ca^{2+} content in the salt glands of diploid and autotetraploid *P. auriculata* were investigated by adding exogeneous Ca^{2+}, inhibiting Ca^{2+} transport channels, and suppressing the generation of H_2O_2 regulated by Ca^{2+} signaling and H^+-ATPase activity under NaCl stress. Effects of Ca^{2+} and downstream substances on salt gland Na^+ and K^+ secretion rates were also examined. The results provide a new perspective for exploring the reasons behind increased salt tolerance in polyploid recretohalophytes.

10.3389/fpls.2024.1376427

2 Materials and methods

2.1 Plant materials and treatments

Autotetraploid *Plumbago auriculata* Lam. (*2n* = 24) was induced by colchicine treatment of stem segments from diploid *P. auriculata* (*2n* = 12) in the laboratory of the Landscape Architecture Institute at Sichuan Agricultural University (Jiang et al., 2020). Both diploid and tetraploid cytotypes were obtained by tissue culture and were subcultured for 25 d. After root formation, all seedlings were transferred to a climate-controlled growth chamber. A total of 72 plants (36 diploids and 36 tetraploids) of similar size were grown for 3 months in a nutrient substrate composed of soil, vermiculite, and perlite in a 1:1:1 ratio (by volume). The plants were placed in an intelligent biochemical incubator (Ningbo Jiangnan Instrument Factory, Zhejiang, China) under controlled conditions: 25 °C/20 °C (day/night) temperature, 12-h day/12-h night photoperiod, 6,600 Lx light intensity, and 70% relative humidity. Observations on the structure and secretory components of the salt glands of diploids and tetraploids under normal growth conditions prior to salt stress provide a basic reference for analyzing ion secretion from diploid and tetraploid salt glands The sixth mature leaf, counted from the top, was selected from diploid and tetraploid plants for structural observation and analysis of salt gland secretory components.

To determine the effect of salt gland Ca^{2+} content on Na^+ and K^+ secretion in diploid and tetraploid plants under salt stress, plants were transferred to a hydroponic system containing 1/6th-strength Hoagland's solution (pH 6.0 ± 0.2), with the nutrient solution refreshed at 5-d intervals. After 15 d of cultivation in the hydroponic system, diploid and tetraploid plants with similar growth were selected for six different treatments (Table 1). 300 mM NaCl was selected for salt stress treatment based on our preliminary experiments that it is the highest concentration at which both diploids and tetraploids will be stressed, but diploid salt gland secretion will not be inhibited because the stress is too severe. Treatments included $LaCl_3$, used to inhibit Ca^{2+} channels; Na_3VO_4, used to inhibit H^+-ATPase activity; and Diphenyleneiodonium chloride (DPI), used to inhibit plasma membrane NADPH oxidase. The $CaCl_2$ and the inhibitors $LaCl_3$, DPI, and Na_3VO_4 were pre-treated 20 min before the salt stress treatment. Salt stress treatment duration was 2 d, with six plants per treatment for each ploidy level.

2.2 Leaf sample preparation for scanning electron microscopy

Leaf samples were prepared following the method described by Ding et al. (2010) with slight modifications. Fresh leaves of diploid and tetraploid *P. auriculata* were cut into small pieces of 0.5 cm × 0.5 cm from the leaf margin to the middle position of the leaf vein using a razor blade. Leaf pieces were fixed in 2.5% glutaraldehyde solution at room temperature for 24 h. After fixation, leaf samples were washed with 0.05 mM HNO_3 to remove salt crystals on leaf surfaces, followed by rinsing with distilled water. Leaves were gently dried with absorbent paper and then dehydrated in a graded ethanol series (30%, 50%, 70%, 80%, 90%, and 95% ethanol). Dehydration time for the 30% to 90% ethanol series was 20 min, whereas it was 1 h for 95% ethanol. After dehydration, samples were dried using a critical point dryer (Leica, Nussloch, Germany). Dried samples were observed and photographed using a scanning electron microscope (SEM; Carl Zeiss, Oberkochen, **Germany**), and the area of salt glands was measured using ImageJ software. Twenty salt glands from six individual plants were measured for both diploid and tetraploid *P. auriculata*.

2.3 Salt gland density and area measurement

Leaf samples were prepared following the method described by Yuan et al. (2013). Fresh leaves of diploid and tetraploid *P. auriculata* were cut into small pieces as previously described. Leaf pieces (0.5 cm × 0.5 cm) were fixed in Carnoy's fixative (ethanol:acetone = 3:1) and then washed with 0.05 mM HNO_3 to remove salt crystals on leaf surfaces. Leaves were rinsed with distilled water, gently dried with absorbent paper, and then decolorized in 70% ethanol. Decolorized leaves were mounted with Hoyer's solution, making temporary slides. To measure density and area of salt glands, slides were observed and photographed using a fluorescence microscope (Olympus, Tokyo, Japan) under UV excitation light (330–380 nm) at 20× magnification. Twenty different fields of view from six leaves were measured for both diploid and tetraploid *P. auriculata*.

2.4 Histological cross section of salt glands

Fresh leaves of diploid and tetraploid *P. auriculata* were cross-sectioned in the middle using a sharp blade. Leaf pieces

TABLE 1 Concentration of drugs used in control and treatment groups.

	Control group	NaCl Treatment group	NaCl +$CaCl_2$ Treatment group	NaCl +$LaCl_3$ Treatment group	NaCl +DPI Treatment group	NaCl +Na_3VO_4 Treatment group
Diploid	1/6 Hoagland	1/6 Hoagland +300 mM NaCl	1/6 Hoagland+300 mM NaCl+5 mM $CaCl_2$	1/6 Hoagland+300 mM NaCl+5 mM $LaCl_3$	1/6 Hoagland+300 mM NaCl+0.2 mM DPI	1/6 Hoagland+300 mM NaCl+0.2 mM Na_3VO_4
Tetraploid	1/6 Hoagland	1/6 Hoagland +300 mM NaCl	1/6 Hoagland+300 mM NaCl+5 mM $CaCl_2$	1/6 Hoagland+300 mM NaCl+5 mM $LaCl_3$	1/6 Hoagland+300 mM NaCl+0.2 mM DPI	1/6 Hoagland+300 mM NaCl+0.2 mM Na_3VO_4

(1.0 cm × 1.0 cm) were quickly fixed in formalin-aceto-alcohol (FAA) fixative at room temperature for 24 h. After fixation, leaf tissues were rinsed with distilled water for 10 min, dried with absorbent paper, and then sequentially dehydrated in a gradient series of ethanol (70%, 80%, 90%, 95%, 100%, and 100% ethanol for two times). After dehydration, tissues were cleared with xylene and then embedded in paraffin in a constant-temperature oven at 60 °C. Leaf-containing paraffin blocks were sectioned using a microtome (**Leica,** Nussloch, **Germany)**, producing 4 µm-thick sections. Sections were placed on glass slides coated with glycerol mounting medium and dried in a constant-temperature oven at 50 °C. Following dewaxing with xylene, rehydration with a gradient series of ethanol, and staining with SafraninO/Fast green, sections were dehydrated with ethanol and cleared with xylene. Last, sections were mounted with Canada balsam and air-dried at low temperature. Salt gland anatomical structures were observed and photographed using a fluorescence microscope (Olympus), and the external cuticle layer of salt glands was observed under UV excitation light (330–380 nm) using fluorescence mode. Twenty salt glands from six individual plants were observed for both diploid and tetraploid *P. auriculata*.

2.5 Energy dispersive X-ray analysis of salt gland secretory crystals

Salt gland secretory crystals were observed and photographed using an SEM (Carl Zeiss) equipped with an energy dispersive X-ray (EDX) system. Cross sections of mature leaf portions (0.5 cm × 0.5 cm) from the lower part of *P. auriculata* diploid and tetraploid leaves were cut with a sharp blade. Leaf sections were placed in a vacuum dryer for 1 h, and then, sections were attached to conductive adhesive tape on the SEM stage for EDX analysis of crystals secreted on leaf surfaces. Twenty salt glands from six leaves were analyzed for both diploid and tetraploid *P. auriculata*.

2.6 Measurement of Ca^{2+} content in salt gland cells

After 2-d treatment of diploid and tetraploid *P. auriculata*, mature leaves from the same position were collected and washed with 0.05 mM HNO_3 to remove salt crystals on leaf surfaces. Leaves were rinsed with double-distilled water and quickly dried with absorbent paper to remove surface water. The lower epidermis of leaves was carefully torn off and placed in 0.4 mM Floura-8 Ca fluorescence probe dye solution, with addition of Pluronic F-127 to enhance fluorescence. To ensure sufficient contact between dye and leaf epidermis, a vacuum pump was used for 10 min, followed by incubation at room temperature for 40 min (avoiding light). After incubation, leaf epidermis tissues were thoroughly rinsed with double-distilled water to remove residual dye. Rinsed epidermis tissue was mounted with a fluorescence decay-resistant medium, making temporary slides. The fluorescence of Ca^{2+} in salt glands was observed with a laser scanning confocal microscope (Olympus LSCM) in the FITC channel, and fluorescence intensity was analyzed using ImageJ software. Twenty salt glands from six plants were observed for each treatment.

2.7 Measurement of Na^+ and K^+ secretion rates in salt glands

Instantaneous secretion rates of Na^+ and K^+ from individual salt glands on the abaxial side surface were measured using an NMT system (NMT-100SIM-YG; Younger USA LLC, Amherst, MA, USA) as described by Chen Z. et al. (2010). Leaves from the lower part of the same position of both diploid and tetraploid *P. auriculata* were collected following 2 d of salt stress treatment. The abaxial side epidermis of leaves was gently peeled off using forceps and fixed in a culture dish with the outer surface facing up. Test solutions (Na^+: 1.0 mM NaCl, 0.1 mM KCl, 0.2 mM MES, pH 5.8; K^+: 30 mM NaCl, 0.5 mM KCl, 0.2 mM MES, pH 5.8) were added to the culture dish, and samples were left undisturbed for 30 min before measurement. Under a microscope, a target salt gland was located, and a selective microelectrode (Na^+: XY-SJ-Na; K^+: XY-SJ-K; Xuyue, Beijing, China) was positioned approximately 5 µm above the outer surface of the salt gland without touching it. Each sample was measured for 5 min. Each group included nine replicates. The Na^+ and K^+ flux data were read directly and outputted using imFluxes v3.0 software (Xuyue, Beijing, China). Positive values represented Na^+ and K^+ secretion from a salt gland to the external environment, whereas negative values represented absorption from the external environment into a salt gland.

2.8 Data analyses

Data were analyzed using SPSS 19.0 (SPSS Inc., Chicago, IL, USA) for Windows, and all values are reported as the mean ± standard deviation (SD). Two-way ANOVA and Student's *t*-test were used to compare means of different treatments for each data set at the significance level of $P < 0.05$.

3 Results

3.1 Influence of polyploidization on salt glands of *Plumbago auriculata*

Polyploidization significantly increased salt gland area of *P. auriculata*, with the area of tetraploid salt glands 41.1% larger than that of diploid salt glands. However, salt gland density decreased significantly in tetraploid plants (Figure 1). There were no significant differences in salt gland structure between diploid and tetraploid *P. auriculata* (Figures 2, 3). Salt glands in both cytotypes consisted of 16 salt gland cells, with four collecting cells, four accessory cells, four cup cells, and four secretory cells, each with a secretion pore in the center.

10.3389/fpls.2024.1376427

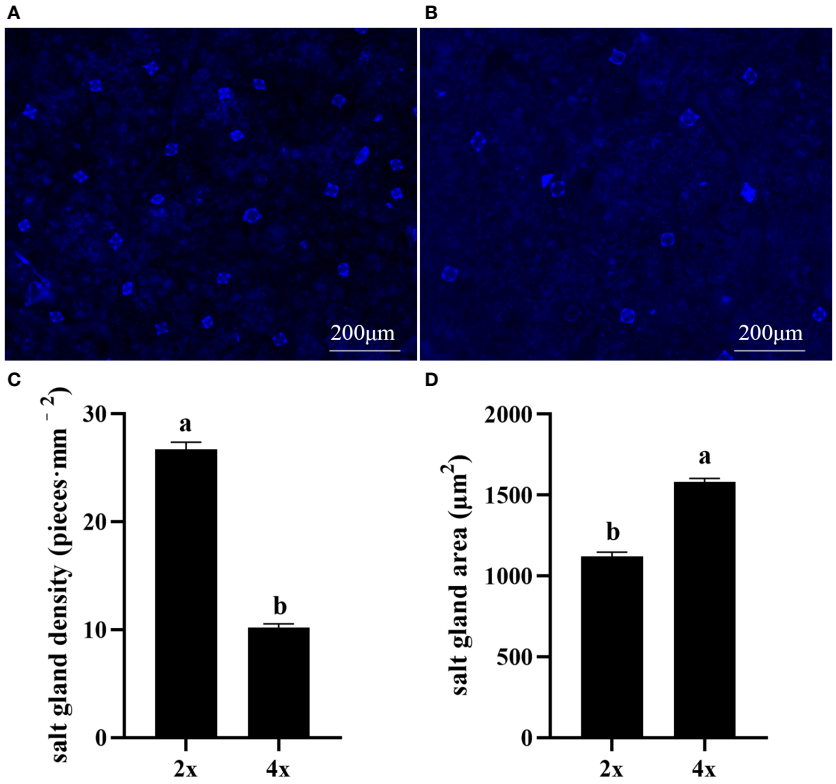

FIGURE 1
Salt gland density and salt gland area in diploid (2x) and tetraploid (4x) *Plumbago auriculata*. **(A)** Diploid salt glands and **(B)** tetraploid salt glands. **(C)** Salt gland density and **(D)** salt gland area of single salt gland in diploids and tetraploids. Different lowercase letters indicate significant differences ($P < 0.05$) between diploids and tetraploids.

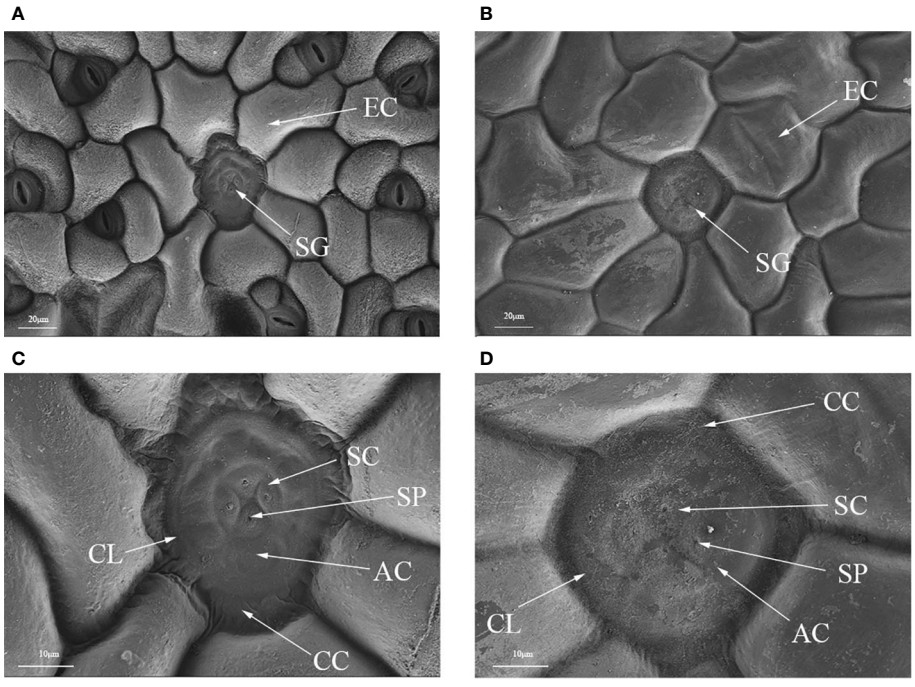

FIGURE 2
Optical microscope and scanning electron microscope images of salt glands in diploid and tetraploid *Plumbago auriculata*. **(A)** Diploid salt gland and **(B)** tetraploid salt gland observed under an optical microscope. **(C)** Diploid salt gland and **(D)** tetraploid salt gland observed under a scanning electron microscope. SG, salt gland; EP, epidermal cell; SC, secretory cell; AC, accessory cell; SP, secretion pore; CC, collecting cell; CL, cuticle layer.

10.3389/fpls.2024.1376427

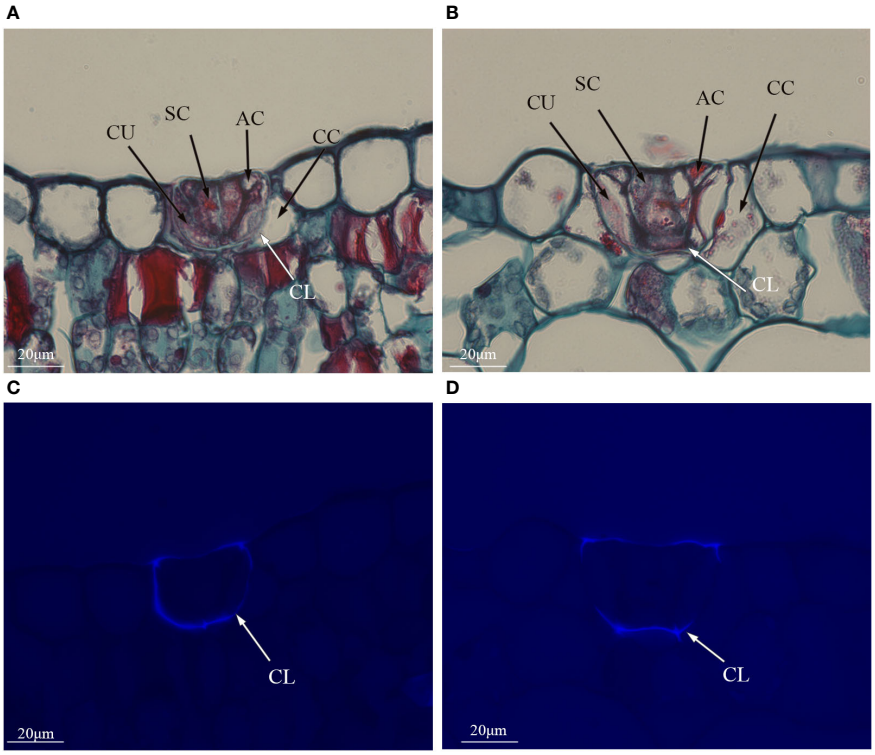

FIGURE 3
Histological cross sections of salt glands in diploid and tetraploid *Plumbago auriculata*. Cross section of **(A)** diploid salt gland and **(B)** tetraploid salt gland. Fluorescence of the cuticle layer in **(C)** diploid salt gland and **(D)** tetraploid salt gland. SC, secretory cell; AC, accessory cell; CC, collecting cell; CU, cup cell; CL, cuticle layer.

In SEM images of secreted salt gland crystals, the volume of salt crystals secreted on leaf surfaces was significantly larger in tetraploids than in diploids, indicating higher secretion capacity of individual salt glands in tetraploids under normal growth conditions. According to the EDX analysis of secreted crystals in diploids and tetraploids, the main ion secreted was Ca^{2+}, followed by Mg^{2+}, whereas the secretion of Na^+ and Cl^- was minimal (Figure 4). This result suggested that polyploidization of *P. auriculata* did not significantly affect composition of salt gland secretions.

3.2 Polyploidization of *Plumbago auriculata* results in significant differences in Ca^{2+} content of salt glands compared with that in diploids

Under control conditions, Ca^{2+} content in salt glands of diploids was significantly higher than that in salt glands of tetraploids, with content in diploids 4.5 times higher (Figure 5). Compared with the control, NaCl stress significantly increased Ca^{2+} accumulation in the salt glands of tetraploid plants, whereas it did not significantly affect Ca^{2+} accumulation in diploid salt glands. After adding $CaCl_2$, Ca^{2+} content in the salt glands of diploids under NaCl stress increased significantly compared with that in the NaCl treatment alone, whereas no significant change was observed in tetraploids, and then, there was no significant difference in Ca^{2+} content between diploid and tetraploid salt glands. The addition of the Ca^{2+} inhibitor $LaCl_3$ suppressed NaCl-induced accumulation of Ca^{2+} in tetraploid salt glands, resulting in no significant difference in Ca^{2+} accumulation compared with the control. Notably, Ca2+ content in the salt glands of diploids increased significantly with $LaCl_3$ treatment, surpassing that of both the NaCl treatment alone and tetraploid salt glands treated with $LaCl_3$. When the H_2O_2 inhibitor DPI or the H^+-ATPase inhibitor Na_3VO_4 was added, Ca^{2+} content in the salt glands of both diploids and tetraploids decreased significantly compared with that in the NaCl treatment alone.

3.3 Polyploidization increases Na^+ secretion rate in salt glands under salt stress, which is significantly inhibited by the Ca^{2+} channel inhibitor $LaCl_3$

Salt stress induces strong and stable Na^+ secretion. After salt stress, Na^+ secretion rate increased significantly in both diploids and tetraploids and was 212.11 and 50.92 times higher, respectively, than that in the control. The Na^+ secretion rate was 5.28 times higher in tetraploids than in diploids (Figures 6A, B). Thus, salt stress activated Na^+ secretion in *P. auriculata*, and Na^+ secretion capacity in individual salt glands under salt stress was greater in tetraploids than in diploids. Addition of $CaCl_2$ significantly increased Na^+ secretion in diploid salt glands under salt stress, with secretion 1.8

10.3389/fpls.2024.1376427

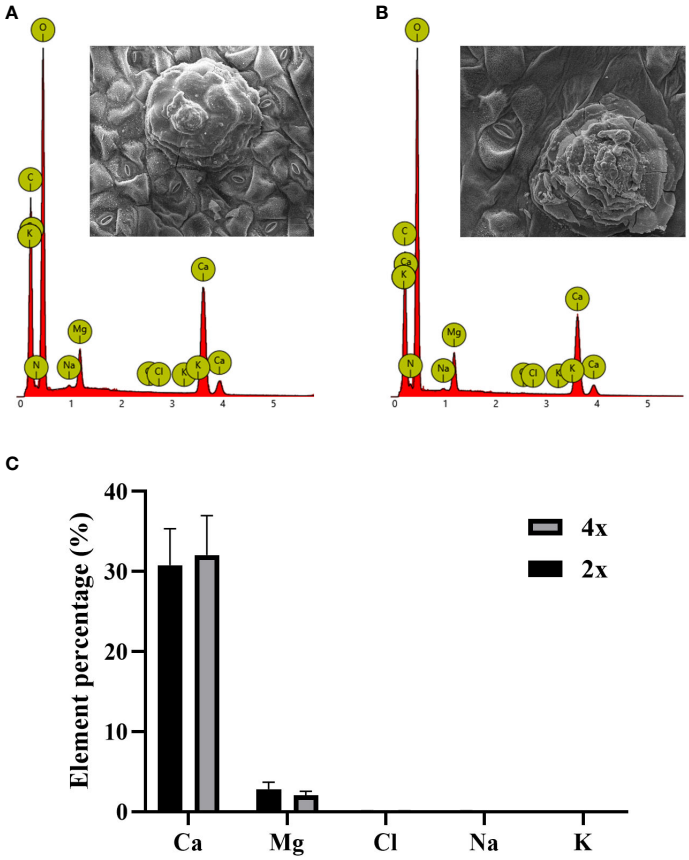

FIGURE 4
Ion composition of crystals secreted by salt glands in diploid and tetraploid *Plumbago auriculata*. Energy dispersive spectroscopy scan of secreted crystals from **(A)** diploid and **(B)** tetraploid salt glands. Element percentage of crystals secreted from the salt glands of **(C)** diploids (2x) and tetraploids (4x).

times higher than that in the NaCl treatment alone. However, $CaCl_2$ addition significantly inhibited Na^+ secretion in tetraploid salt glands, reaching 67.56% of the NaCl treatment alone. Nevertheless, the Na^+ secretion rate in tetraploid salt glands remained significantly higher than that in diploid salt glands (Figure 6C). After addition of the Ca^{2+} channel inhibitor $LaCl_3$, Na^+ secretion in tetraploids was severely inhibited, reaching only 6.5% and 9.68% of that in NaCl and $CaCl_2$ treatments, respectively, and with secretion only 3.26 times higher than that in the control. By contrast, the Na^+ secretion rate in diploid salt glands increased significantly and was 2.60 and 1.44 times higher than that in NaCl and $CaCl_2$ treatments, respectively, and was 7.25 times higher than that in tetraploid salt glands under the same conditions (Figure 6D). Pretreatment with the H^+-ATPase inhibitor (Na_3VO_4) or the H_2O_2 inhibitor (DPI) significantly decreased Na^+ secretion rate under salt stress in both diploids and tetraploids, indicating the important roles of endogenous H^+-ATPase and H_2O_2 in increasing Na^+ secretion rate under salt stress (Figures 6E, F). Overall, the Na^+ secretion rate in tetraploids was lower than that in diploids only in the $LaCl_3$+NaCl treatment, whereas in other treatments, the Na^+ secretion rate was higher in tetraploids than in diploids (Figure 6G).

3.4 Secretion rates of K^+ in salt glands of diploid and tetraploid Plumbago auriculata under different stress treatments

Salt stress induced a significant increase in K^+ secretion rate in individual salt glands of both diploids and tetraploids, with the K^+ secretion rate in tetraploids significantly higher than that in diploids by 3.20 times. However, the Na^+/K^+ secretion rate ratio was also higher in tetraploids, indicating stronger selective secretion of Na^+ in tetraploids than in diploids under salt stress (Figures 7A, B). After addition of $CaCl_2$, K^+ secretion in tetraploid salt glands under salt stress was inhibited, reaching 60.52% of that in the NaCl treatment, whereas K^+ secretion in diploid salt glands increased significantly and was 3.51 times higher than that in the NaCl treatment (Figure 7C).

The K^+ secretion rate was inhibited in tetraploid plants by the addition of $LaCl_3$ compared with NaCl alone due to the inhibitory effect of $LaCl_3$ on K^+ channels (Wegner et al., 1994). However, it increased in diploid plants. This may be due to the fact that in addition to the inhibitory effect of $LaCl_3$ on K^+ channels the presence of large amounts of retained Ca^{2+} in the salt glands increased the overall secretion level including the K^+ secretion

10.3389/fpls.2024.1376427

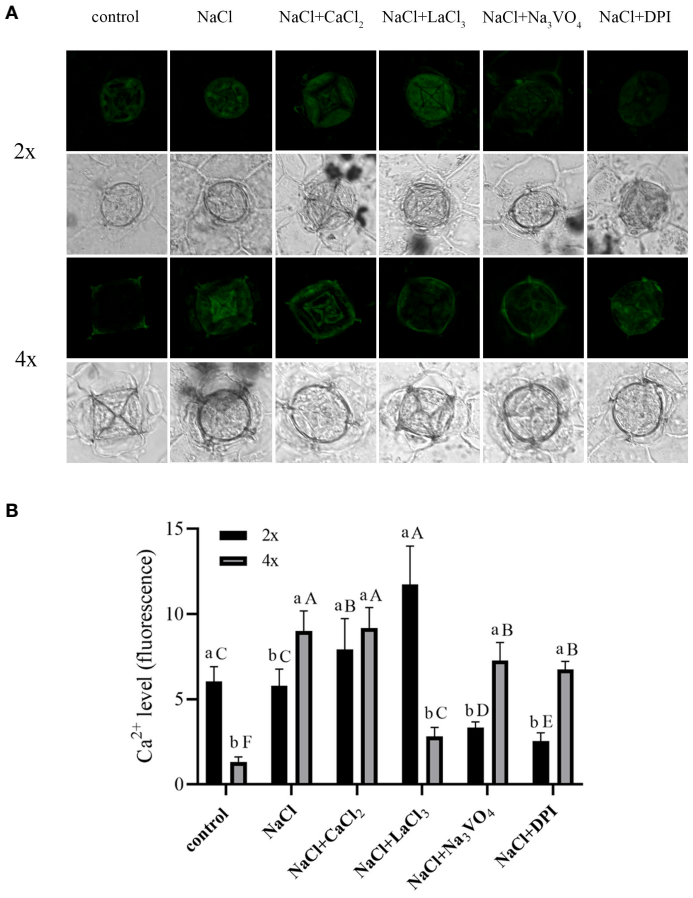

FIGURE 5
Changes in Ca^{2+} accumulation in salt glands of diploid (2x) and tetraploid (4x) *Plumbago auriculata* induced by NaCl stress and effects of $LaCl_3$, Na_3VO_4, and DPI on Ca^{2+} accumulation under NaCl stress. **(A)** Representative graphs showing changes in Ca^{2+} accumulation in (top) diploid and (bottom) tetraploid salt glands before and after salt stress, as well as effects under $LaCl_3$, Na_3VO_4, and DPI treatments. **(B)** Fluorescence intensity values from **(A)** measured by Image J software. For each treatment, nine salt glands from six individual plants were observed and quantified. In **(B)**, different capital letters indicate significant differences ($P < 0.05$) between different treatments of the same ploidy level, whereas different lowercase letters indicate significant differences ($P < 0.05$) between ploidy levels of the same treatment.

rate (Figure 7D). Notably, the addition of the H^+-ATPase inhibitor (Na_3VO_4) or the H_2O_2 inhibitor (DPI) inhibited K^+ secretion in tetraploid salt glands under salt stress, whereas in diploid salt glands, secretion increased significantly (Figures 7E, F). Overall, the K^+ secretion rate in tetraploid salt glands was higher than that in diploid salt glands only in the NaCl treatment, and in other treatments, the rate was lower in tetraploids than in diploids (Figure 7G).

4 Discussion

4.1 Polyploidization promotes secretion of individual salt glands but does not alter components of secretions under normal growth conditions

There may be a positive correlation between salt gland size and secretion rate (Feng et al., 2014; Mi et al., 2021). Polyploidization in *P. auriculata* significantly increased the size of salt glands, and under normal growth conditions, the volume of secreted crystals also increased significantly. It is hypothesized that polyploidization enhances the secretory capacity of individual salt glands of *P. auriculata* under normal growth conditions.

4.2 Polyploidization increases efficiency of Ca^{2+} allocation and increases its transport to salt glands under salt stress

Under control conditions, Ca^{2+} content in tetraploid salt glands was only 22.22% of that in diploid glands, indicating that tetraploids decreased the allocation of Ca^{2+} to salt glands and increased that to leaf mesophyll cells for plant growth and metabolism (Dayod et al., 2010; Gilliham et al., 2011; Nomura and Shiina, 2014). In a previous study, under control conditions, *P. auriculata* had significantly lower Ca^{2+} secretion rates in tetraploid leaves than in diploid leaves, only reaching 33% of the diploid secretion (Duan et al., 2023). Therefore, the decrease in Ca^{2+} allocation to salt glands might be an important factor contributing to the decrease in Ca^{2+} secretion rate in

10.3389/fpls.2024.1376427

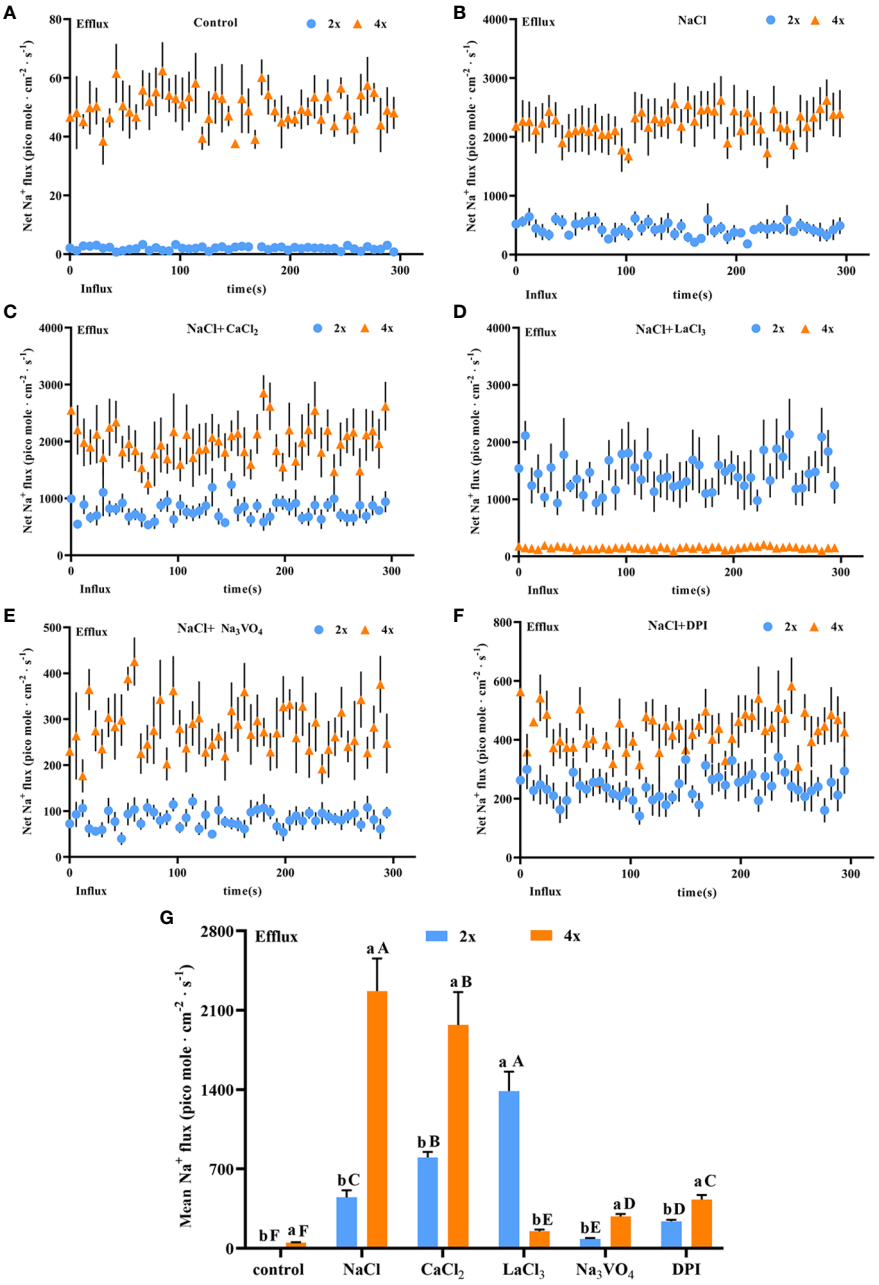

FIGURE 6
Changes in Na^+ instantaneous and average secretion rates in salt glands of diploid (2x) and tetraploid (4x) *Plumbago auriculata* under NaCl stress and effects of $LaCl_3$, Na_3VO_4, and DPI on Na^+ secretion rate under NaCl stress. **(A)** Instantaneous Na^+ secretion rate in salt glands under control conditions. **(B)** Instantaneous Na^+ secretion rate in salt glands under NaCl stress. **(C)** Instantaneous Na^+ secretion rate in salt glands under NaCl stress with exogenous $CaCl_2$ addition. **(D)** Instantaneous Na^+ secretion rate in salt glands under NaCl stress with $LaCl_3$ addition. **(E)** Instantaneous Na^+ secretion rate in salt glands under NaCl stress with Na_3VO_4 addition. **(F)** Instantaneous Na^+ secretion rate in salt glands under NaCl stress with DPI addition. **(G)** Average Na^+ secretion rate (~300 s) in different treatments. Each point represents the mean of the nine salt glands collected from six individual plants.

tetraploids compared with that in diploids under control conditions. Salt stress stimulates Ca^{2+} influx into cells (Dong et al., 2022) but also inhibits root Ca^{2+} uptake (Guo et al., 2022), leading to a decrease in overall Ca^{2+} content in plants (Guo et al., 2015). However, although Ca^{2+} content showed no significant change in diploid salt glands under salt stress, it increased significantly in tetraploid salt glands, indicating that tetraploids significantly increased Ca^{2+} transport to salt glands.

With loss of Ca^{2+}, selective transport of Ca^{2+} to salt glands requires increases in energy consumption (Dassanayake and Larkin, 2017). Under control conditions, tetraploids decreased the allocation of Ca^{2+} to salt glands, thereby reducing the energy expenditure for transport and retaining more Ca^{2+} in leaf mesophyll cells as essential nutrients and signaling molecules for normal plant growth and metabolism (Dayod et al., 2010). Under salt stress, Ca^{2+} promotes Na^+ secretion (Mahajan et al., 2008; Guo et al., 2009), and increased allocation of Ca^{2+}

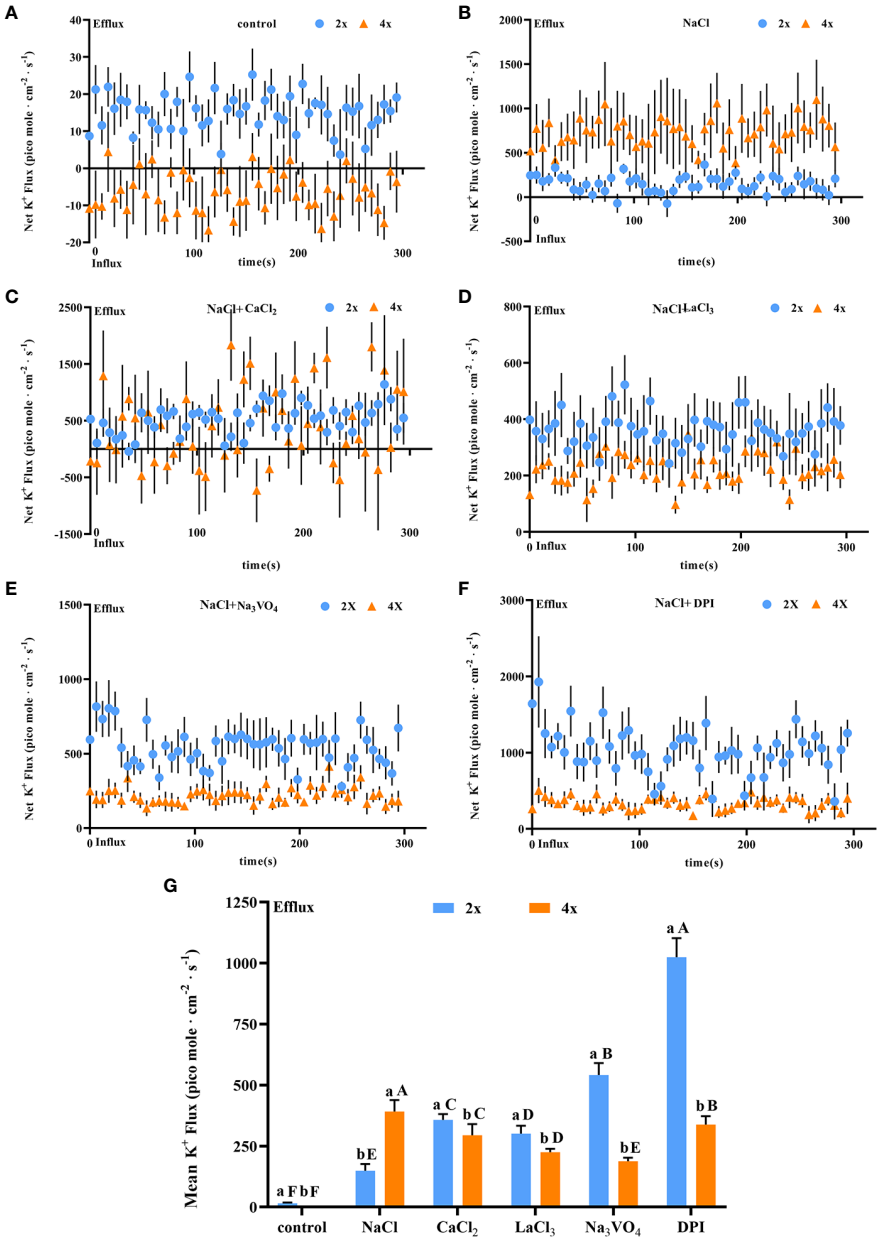

FIGURE 7
Changes in K^+ instantaneous and average secretion rates in salt glands of diploid (2x) and tetraploid (4x) *Plumbago auriculata* induced by NaCl stress and effects of $LaCl_3$, Na_3VO_4, and DPI on K^+ secretion rate under NaCl stress. **(A)** Instantaneous K^+ secretion rate in salt glands under control conditions. **(B)** Instantaneous K^+ secretion rate in salt glands under NaCl stress. **(C)** Instantaneous K^+ secretion rate in salt glands under NaCl stress with exogenous $CaCl_2$ addition. **(D)** Instantaneous K^+ secretion rate in salt glands under NaCl stress with $LaCl_3$ addition. **(E)** Instantaneous K^+ secretion rate in salt glands under NaCl stress with Na_3VO_4 addition. **(F)** Instantaneous K^+ secretion rate in salt glands under NaCl stress with DPI addition. **(G)** Average K^+ secretion rate (~300 s) in different treatments. Each point represents the mean of the nine salt glands collected from six individual plants.

to salt glands might be the reason for higher Na^+ secretion rate in tetraploids (Duan et al., 2023).

Ca^{2+} content in salt glands is affected by both Ca^{2+} transport from the chloroplasts and Ca^{2+} secretion from the salt glands. No direct evidence has been obtained to confirm the pathway of salt transport into the salt gland, but ion carriers or channels, plasmodesmata and vesicles may play an important role in transporting (Yuan et al., 2016). Ca^{2+} influx in plant cells is predominantly mediated by NSCC, and it has been shown that Ca^{2+} channel inhibitors do not only block Ca^{2+} influx but also Ca^{2+} efflux (Zherelova et al., 1994), and La^{3+} can also block outward current (Terry et al., 1992). The diploid salt glands secreted large amounts of Ca^{2+} under control conditions, and the addition of $LaCl_3$ resulted in a significant increase in the Ca^{2+} content of the salt glands, probably due to the inhibition of Ca^{2+} secretion leading to its accumulation in the salt glands. At this time, we found that the Ca^{2+} content in diploid salt glands was significantly higher than that in tetraploids, and the rate of Na^+ secretion from salt glands was

also significantly higher than that in tetraploids, so we hypothesized that the Ca^{2+} content of salt glands was one of the important factors affecting the rate of Na^+ secretion.

4.3 Increased Ca^{2+} content in salt glands increases Na^+ secretion rate in *Plumbago auriculata* under salt stress

It was shown that Ca^{2+} promotes the secretion of Na^+ from salt glands of recretohalophytes (Ding et al., 2010; Maeda, 2019). In our previous study on whole-leaf secretion rates in *P. auriculata* under salt stress, Ca^{2+} content in diploid leaves was higher than that in tetraploid leaves, but the Na^+ secretion rate was lower in diploids than in tetraploids (Duan et al., 2023). Besides, it has been suggested in the other research that K^+ in the salt gland promotes salt gland NaCl secretion (Feng et al., 2015). After salt stress, Ca^{2+} content in diploid salt glands was significantly lower than that in tetraploid salt glands, and the Na^+ secretion rate in individual diploid salt glands was also significantly lower. Therefore, it was hypothesized that Ca^{2+} content in salt glands is a key factor determining salt gland Na^+ secretion rate, not the overall Ca^{2+} content in leaves. Besides, increasing Na^+ secrete rate is companied with increased Ca^{2+} content in salt gland of tetraploid. The plasma membrane Na^+/H^+ antiporter (SOS1) been shown to be involved in Na^+ secretion in recretohalophyte with *SOS1* genes up-regulated after salt treatment and Na^+ secretion rate was decreased when Silencing *SOS1* (Guo et al., 2020; Zhang et al., 2017). The higher secretion rate in tetraploid in salt glands under salt stress might suggested higher *SOS1*gene expression, and the molecular mechanisms require further research.

Notably, although addition of $CaCl_2$ did not significantly affect Ca^{2+} content in tetraploid salt glands, the Na^+ secretion rate in tetraploids was significantly lower than that in the NaCl treatment alone. It was presumed that because Ca^{2+} content of salt glands did not increase, the decrease in Na^+ secretion from salt glands was due to $CaCl_2$ reducing the activation of Na^+ secretion by NaCl stress (Mulaudzi et al., 2020).

The Ca^{2+} ion is an important secondary messenger that regulates H^+-ATPase activity and H_2O_2 generation (Demidchik and Shabala, 2018; Shabala, 2019). In the present study, we found that inhibition of H^+-ATPase activity or H_2O_2 production inhibited both diploid and tetraploid Na^+ secretion rates in *P. auriculata*. Ca^{2+} may also indirectly regulate Na^+ secretion through H^+-ATPase and H_2O_2 (Kong et al., 2016; Wang et al., 2020), and the mechanisms need to be further investigated.

4.4 K^+ efflux channels induced by plasma membrane depolarization might participate in K^+ secretion in *Plumbago auriculata*

Although the mechanism of salt secretion in recretohalophytes remains not fully understood, salt secretion is an active transport process that requires H^+-ATPase to provide energy (Chen JA et al., 2010). Therefore, inhibiting H^+-ATPase activity significantly suppresses ion secretion in salt glands. In this study, inhibiting H^+-ATPase significantly inhibited Na^+ secretion in both diploids and tetraploids. Notably, under salt stress, inhibiting H^+-ATPase activity suppressed K^+ secretion in tetraploids but significantly increased it in diploids. Therefore, it was hypothesized that the K^+ efflux channels DA-KORCs and DA-NSCCs, activated by plasma membrane depolarization, were involved in K^+ secretion in *P. auriculata* salt glands (Shabala et al., 2006; Sun et al., 2009). Therefore, inhibiting H^+-ATPase activity induced severe depolarization of the plasma membrane in diploid salt gland cells, activating DA-KORCs and DA-NSCCs efflux channels (Goncalves et al., 2000) and increasing the rate of K^+ secretion. Additionally, Ca^{2+} inhibits the activation of the K^+ efflux channels DA-KORCs and DA-NSCCs by depolarization, and the decrease in Ca^{2+} content in salt glands after H^+-ATPase inhibition contributed to the increase in K^+ efflux and increased K^+ secretion. Hydrogen peroxide is a signaling molecule that increases H^+-ATPase activity (Lu et al., 2013), and the addition of the NADPH oxidase inhibitor DPI, which inhibits H_2O_2 production, increases the loss of K^+ caused by depolarization of the plasma membrane (Ma et al., 2012). By contrast, the secretion of K^+ was inhibited in tetraploids following inhibition of H^+-ATPase or H_2O_2, suggesting that the effect of depolarization-induced K^+ efflux on tetraploids was relatively minor than diploids.

5 Conclusion

Rates of Na^+ and K^+ secretion in salt glands of the recretohalophyte *P. auriculata* were regulated by Ca^{2+} content in the glands. The high Ca^{2+} content in salt glands was an important factor contributing to higher Na^+ secretion rates in tetraploids than in diploids under salt stress. The downstream signals of Ca^{2+}, H_2O_2 and H^+-ATPase, were also involved in regulating Na^+ and K^+ secretion rates. In addition to directly promoting ion secretion, Ca^{2+} might have indirectly regulated Na^+ and K^+ secretion by modulating H_2O_2 and H^+-ATPase. Inhibiting H_2O_2 production or H^+-ATPase activity significantly increased the rate of K^+ secretion in diploids under salt stress, suggesting the involvement of depolarization-activated K^+ efflux channels (DA-KORCs and DA-NSCCs) in salt stress-induced salt gland K^+ secretion. Overall, polyploidization in *P. auriculata* led to an increase in utilization efficiency of Ca^{2+}, resulting in increased accumulation of Ca^{2+} in salt glands under salt stress. This, in turn, increased Na^+ secretion from salt glands and decreased Na^+ accumulation in plant tissues, thereby mitigating the damage caused by salt stress.

Data availability statement

The original contributions presented in the study are included in the article/supplementary material. Further inquiries can be directed to the corresponding author.

Author contributions

YD: Writing – original draft, Writing – review & editing. LJ: Funding acquisition, Writing – review & editing. TL: Writing – review & editing. KO: Writing – review & editing. CL: Writing – review & editing. ZZ: Writing – review & editing. YL: Writing – review & editing. LY: Writing – review & editing. JL: Writing – review & editing. SY: Writing – review & editing. SG: Writing – review & editing.

Funding

The author(s) declare financial support was received for the research, authorship, and/or publication of this article. This work was supported by the Natural Science Foundation of Sichuan Province (project no. 2022NSFSC0099), the Sichuan Province Science and Technology Support Program (project no. 2021YFYZ0006), the Science and Technology Department of Sichuan Province (project no. 2021YJ0497), the Doctoral Fund of Chongqing Industry Polytechnic College (project no. 2023GZYBSZK2-02).

Conflict of interest

The authors declare that the research was conducted in the absence of any commercial or financial relationships that could be construed as a potential conflict of interest.

Publisher's note

References

Che, B., Cheng, C., Fang, J., Liu, Y., and Yu, B. (2019). The recretohalophyte *Tamarix TrSOS1* gene confers enhanced salt tolerance to transgenic hairy root composite cotton seedlings exhibiting virus-induced gene silencing of *GhSOS1*. *Int. J. Mol. Sci.* 20, 2930. doi: 10.3390/ijms20122930

Chen, Z., Newman, I., Zhou, M., Mendham, N., Zhang, G., and Shabala, S. (2010). Screening plants for salt tolerance by measuring K^+ flux: a case study for barley. *Plant Cell Environ.* 28, 1230–1246. doi: 10.1111/j.1365-3040.2005.01364.x

Chen, J. A., Xiao, Q. A., Wu, F. H., Dong, X. J., He, J. X., Pei, Z. M., et al. (2010). Nitric oxide enhances salt secretion and Na^+ sequestration in a mangrove plant, Avicennia marina, through increasing the expression of H^+-ATPase and Na^+/H^+ antiporter under high salinity. *Tree Physiol.* 30, 1570–1585. doi: 10.1093/treephys/tpq086

Chung, J. S., Zhu, J. K., Bressan, R. A., Hasegawa, P. M., and Shi, H. H. (2008). Reactive oxygen species mediate Na^+-induced *SOS1* mRNA stability in *Arabidopsis*. *Plant J.* 53, 554–565. doi: 10.1111/j.1365-313X.2007.03364.x

Dassanayake, M., and Larkin, J. C. (2017). Making plants break a sweat: the structure, function, and evolution of plant salt glands. *Front. Plant Sci.* 8. doi: 10.3389/fpls.2017.00406

Dayod, M., Tyerman, S. D., Leigh, R. A., and Gilliham, M. (2010). Calcium storage in plants and the implications for calcium biofortification. *Protoplasma* 247, 215–231. doi: 10.1007/s00709-010-0182-0

Demidchik, V., and Shabala, S. (2018). Mechanisms of cytosolic calcium elevation in plants: the role of ion channels, calcium extrusion systems and NADPH oxidase-mediated 'ROS-Ca^{2+} Hub'. *Funct. Plant Biol.* 45, 9–27. doi: 10.1071/FP16420

Ding, F., Chen, M., Sui, N., and Wang, B. S. (2010). Ca^{2+} significantly enhanced development and salt-secretion rate of salt glands of *Limonium bicolor* under NaCl treatment. *South Afr. J. Botany.* 76, 95–101. doi: 10.1016/j.sajb.2009.09.001

Dong, Q. Y., Wallrad, L., Almutairi, B. O., and Kudla, J. (2022). Ca^{2+} signaling in plant responses to abiotic stresses. *J. Integr. Plant Biol.* 64, 287–300. doi: 10.1111/jipb.13228

Duan, Y. F., Lei, T., Li, W. J., Jiang, M. Y., Zhao, Z. A., Yu, X. F., et al. (2023). Enhanced Na^+ and Cl^- sequestration and secretion selectivity contribute to high salt tolerance in the tetraploid recretohalophyte *Plumbago auriculata* Lam. *Planta* 257 (3), 52. doi: 10.1007/s00425-023-04082-7

Faraday, C. D., and Thomson, W. W. (1986). Functional aspects of the salt glands of the Plumbaginaceae. *J. Exp. Botany.* 37, 1129–1135. doi: 10.1093/jxb/37.8.1129

Feng, Z. T., Sun, Q. J., Deng, Y. Q., Sun, S. F., Zhang, J. G., and Wang, B. S. (2014). Study on pathway and characteristics of ion secretion of salt glands of *Limonium bicolor*. *Acta Physiologiae Plantarum* 36, 2729–2741. doi: 10.1007/s11738-014-1644-3

Feng, Z. T., Deng, Y. Q., Zhang, S. C., Liang, X., Yuan, F., Hao, J. L., et al. (2015). K^+ accumulation in the cytoplasm and nucleus of the salt gland cells of *Limonium bicolor* accompanies increased rates of salt secretion under NaCl treatment using NanoSIMS. *Plant Science* 238, 286–296. doi: 10.1016/j.plantsci.2015.06.021

Flowers, T. J., and Colmer, T. D. (2008). Salinity tolerance in halophytes. *New Phytol.* 179, 945–963. doi: 10.1111/j.1469-8137.2008.02531.x

Gilliham, M., Dayod, M., Hocking, B. J., Xu, B., Conn, S. J., Kaiser, B. N., et al. (2011). Calcium delivery and storage in plant leaves: exploring the link with water flow. *J. Exp. Botany.* 62, 22–50. doi: 10.1093/jxb/err111

Goncalves, P. P., Meireles, S. M., Neves, P., and Vale, M. G. (2000). Distinction between Ca^{2+} pump and Ca^{2+}/H^+ antiport activities in synaptic vesicles of sheep brain cortex. *Neurochemist. Int.* 37, 387–396. doi: 10.1016/S0197-0186(00)00009-7

Guo, K. M., Babourina, O., and Rengel, Z. (2009). Na^+/H^+ antiporter activity of the *SOS1* gene: lifetime imaging analysis and electrophysiological studies on *Arabidopsis* seedlings. *Plant Physiol.* 137, 155–165. doi: 10.1111/j.1399-3054.2009.01274.x

Guo, J. X., Lu, X. Y., Tao, Y. F., Guo, H. J., and Min, W. (2022). Comparative ionomics and metabolic responses and adaptive strategies of cotton to salt and alkali stress. *Front. Plant Sci.* 13. doi: 10.3389/fpls.2022.871387

Guo, Q., Meng, L., Han, J. W., Mao, P. C., Tian, X. X., Zheng, M. L., et al. (2020). SOS1 is a key systemic regulator of salt secretion and K^+/Na^+ homeostasis in the recretohalophyte *Karelinia caspia*. *Environ. Exp. Bot.* 177, 104098. doi: 10.1016/j.envexpbot.2020.104098

Guo, Z., Wei, M. Y., Zhong, Y. H., Wu, X., Chi, B. J., Li, J., et al. (2023). Leaf sodium homeostasis controlled by salt gland is associated with salt tolerance in mangrove plant *Avicennia marina*. *BMC Plant Biol.* 43, 817–831. doi: 10.1093/treephys/tpad002

Guo, R., Yang, Z. Z., Li, F., Yan, C. R., Zhong, X. L., Liu, Q., et al. (2015). Comparative metabolic responses and adaptive strategies of wheat (*Triticum aestivum*) to salt and alkali stress. *BMC Plant Biol.* 15, 170. doi: 10.1186/s12870-015-0546-x

Horie, T., Hauser, F., and Schroeder, J. I. (2009). HKT transporter-mediated salinity resistance mechanisms in *Arabidopsis* and monocot crop plants. *Trends Plant Sci.* 12, 660–668. doi: 10.1016/j.tplants.2009.08.009

Jiang, Y. L., Liu, S. L., Hu, J., He, G. T., Liu, Y. Q., Chen, X., et al. (2020). Polyploidization of *Plumbago auriculata* Lam. in *vitro* and its characterization including cold tolerance. *Plant Cell Tissue Organ Culture.* 140, 315–325. doi: 10.1007/s11240-019-01729-w

Jin, J., Cui, H. M., Lv, X. M., Yang, Y. F., Wang, Y., and Lu, X. Y. (2017). Exogenous $CaCl_2$ reduces salt stress in sour jujube by reducing Na^+ and increasing K^+, Ca^{2+}, and Mg^{2+} in different plant organs. *J. Hortic. Sci. Biotechnol.* 92, 98–106. doi: 10.1080/14620316.2016.1228435

Kobayashi, H., Masaoka, Y., and Takahashi, Y. (2007). Ability of salt glands in Rhodes grass (*Chloris gayana Kunth*) to secrete Na^+ and K^+. *Soil Sci. Plant Nutr.* 53, 764–771. doi: 10.1111/j.1747-0765.2007.00192.x

Kong, X. Q., Luo, Z., Dong, H. Z., Eneji, A. E., and Li, W. J. (2016). H_2O_2 and ABA signaling are responsible for the increased Na^+ efflux and water uptake in *Gossypium hirsutum* L. roots in the non-saline side under non-uniform root zone salinity. *J. Exp. Botany.* 67, 2247–2261. doi: 10.1093/jxb/erw026

Li, J. P., Fang, Y., Liu, Y. L., Zhang, M. J., Liu, Y., Zhao, Y., et al. (2020). Exogenous melatonin enhances salt secretion from salt glands by upregulating the expression of ion transporter and vesicle transport genes in *Limonium bicolor*. *BMC Plant Biol.* 20, 493–493. doi: 10.1186/s12870-020-02703-x

Lu, Y. J., Li, N. Y., Sun, J., Hou, P. C., Jing, X. S., Zhu, H. P., et al. (2013). Exogenous hydrogen peroxide, nitric oxide and calcium mediate root ion fluxes in two non-secretor mangrove species subjected to NaCl stress. *Tree Physiol.* 33, 81–95. doi: 10.1093/treephys/tps119

Ma, L. Y., Zhang, H., Sun, L. R., Jiao, Y. H., Zhang, G. Z., Miao, C., et al. (2012). NADPH oxidase AtrbohD and AtrbohF function in ROS-dependent regulation of Na^+/K^+ homeostasis in *Arabidopsis* under salt stress. *J. Exp. Botany.* 63, 305–317. doi: 10.1093/jxb/err280

Maeda, Y. (2019). Effects of calcium application on the salt tolerance and sodium excretion from salt glands in zoysiagrass (*Zoysia japonica*). *Grassland Sci.* 65, 189–196. doi: 10.1111/grs.12234

Mahajan, S., Pandey, G. K., and Tuteja, N. (2008). Calcium- and salt-stress signaling in plants: shedding light on SOS pathway. *Arch. Biochem. Biophys.* 471, 146–158. doi: 10.1016/j.abb.2008.01.010

Mi, P., Yuan, F., Guo, J. R., Han, G. L., and Wang, B. S. (2021). Salt glands play a pivotal role in the salt resistance of four recretohalophyte *Limonium Mill.* Species. *Plant Biol.* 23, 1063–1073. doi: 10.1111/plb.13284

Mulaudzi, T., Hendricks, K., Mabiya, T., Muthevhuli, M., Ajayi, R. F., Mayedwa, N., et al. (2020). Calcium improves germination and growth of *Sorghum bicolor* seedlings under salt stress. *Plants-Basel* 9, 9060730. doi: 10.3390/plants9060730

Munns, R., and Tester, M. (2008). Mechanisms of salinity tolerance. *Annu. Rev. Plant Biol.* 59, 651–681. doi: 10.1146/annurev.arplant.59.032607.092911

Nomura, H., and Shiina, T. (2014). Calcium signaling in plant endosymbiotic organelles: mechanism and role in physiology. *Mol. Plant* 7, 1094–1104. doi: 10.1093/mp/ssu020

Qiu, Q. S., Guo, Y., Dietrich, M. A., Schumaker, K. S., and Zhu, J. K. (2002). Regulation of SOS1, a plasma membrane Na^+/H^+ exchanger in *Arabidopsis thaliana*, by SOS2 and SOS3. *Proc. Natl. Acad. Sci. United States Am.* 99, 8436–8441. doi: 10.1073/pnas.122224699

Ruan, C. J., da Silva, J. A. T., Mopper, S., Qin, P., and Lutts, S. (2010). Halophyte improvement for a salinized world. *Crit. Rev. Plant Sci.* 29, 329–359. doi: 10.1080/07352689.2010.524517

Sanadhya, P., Agarwal, P., Khedia, J., and Agarwal, P. K. (2015). A low-affinity K^+ transporter *AlHKT2; 1* from recretohalophyte *Aeluropus lagopoides* confers salt tolerance in yeast. *Mol. Biotechnol.* 57, 489–498. doi: 10.1007/s12033-015-9842-9

Shabala, S. (2019). Linking ploidy level with salinity tolerance: NADPH-dependent 'ROS-Ca^{2+} Hub' in the spotlight. *J. Exp. Botany.* 70, 1063–1067. doi: 10.1093/jxb/erz042

Shabala, S., Demidchik, V., Shabala, L., Cuin, T. A., Smith, S. J., Miller, A. J., et al. (2006). Extracellular Ca^{2+} ameliorates NaCl-induced K^+ loss from *Arabidopsis* root and leaf cells by controlling plasma membrane K^+-permeable channels. *J. Plant Physiol.* 141, 1653–1665. doi: 10.1104/pp.106.082388

Shabala, S., and Pottosin, I. (2014). Regulation of potassium transport in plants under hostile conditions: implications for abiotic and biotic stress tolerance. *J. Plant Physiol.* 151, 257–279. doi: 10.1111/ppl.12165

Shuttleworth, T. J., and Hildebrandt, J. P. (1999). Vertebrate salt glands: short- and long-term regulation of function. *J. Exp. Zool.* 183, 689–701. doi: 10.1002/(SICI)1097-010X(19990601)283:7<689::AID-JEZ7>3.0.CO;2-T

Shuttleworth, T. J., and Thompson, J. L. (1989). Intracellular Ca^{2+} and inositol phosphates in avian nasal gland cells. *Am. J. Physiol.* 257, C1020–C1029. doi: 10.1152/ajpcell.1989.257.5.C1020

Sun, J., Dai, S. X., Wang, R. G., Chen, S. L., Li, N. Y., Zhou, X. Y., et al. (2009). Calcium mediates root K^+/Na^+ homeostasis in poplar species differing in salt tolerance. *Tree Physiol.* 29, 1175–1186. doi: 10.1093/treephys/tpp048

Sun, J., Wang, M. J., Ding, M. Q., Deng, S. R., Liu, M. Q., Lu, C. F., et al. (2010). H_2O_2 and cytosolic Ca^{2+} signals triggered by the PM H^+-coupled transport system mediate K^+/Na^+ homeostasis in NaCl-stressed *Populus euphratica* cells. *Plant Cell Environ.* 33, 943–958. doi: 10.1111/j.1365-3040.2010.02118.x

Terry, B. R., Findlay, G. P., and Tyerman, S. D. (1992). Direct effects of Ca^{2+}-channel blockers on plasma membrane cation channels of *Amaranthus tricolor* protoplasts. *J. Exp. Botany.* 43, 7–1473. doi: 10.1093/jxb/43.11.1457

Wang, W. L., Xing, L., Xu, K., Ji, D. H., Xu, Y., Chen, C. S., et al. (2020). Salt stress-induced H_2O_2 and Ca^{2+} mediate K^+/Na^+ homeostasis in *Pyropia haitanensis*. *J. Appl. Phycol.* 32, 4199–4210. doi: 10.1007/s10811-020-02284-0

Wegner, L. H., De Boer, A. H., and Raschke, K. (1994). Properties of the K^+ inward rectifier in the plasma membrane of xylem parenchyma cells from barley roots: Effects of TEA^+, Ca^{2+}, Ba^{2+} and La^{3+}. *J. Membrane Biol.* 142, 363–379. doi: 10.1007/BF00233442

Yuan, F., Chen, M., Leng, B. Y., and Wang, B. S. (2013). An efficient autofluorescence method for screening *Limonium bicolor* mutants for abnormal salt gland density and salt secretion. *South Afr. J. Botany.* 88, 110–117. doi: 10.1016/j.sajb.2013.06.007

Yuan, F., Leng, B. Y., and Wang, B. S. (2016). Progress in studying salt secretion from the salt glands in recretohalophytes: how do plants secrete salt? *Frontiers in Plant Science* 7, 977. doi: 10.3389/fpls.2016.00977

Zhang, W. D., Wang, P., Bao, Z. L. T., Ma, Q., Duan, L. J., Bao, A. K., et al. (2017). *SOS1*, *HKT1*; 5, and *NHX1* synergistically modulate Na^+ homeostasis in the halophytic grass *Puccinellia tenuiflora*. *Frontiers in Plant Science* 8, 576. doi: 10.3389/fpls.2017.00576

Zherelova, O. M., Grishchenko, V. M., and Chaylakhyan, L. M. (1994). Blockers of Ca^{2+} channels in the plasmalemma of perfused *Characeae* cells. *Comp. Biochem. Physiol. c-Toxicol. Pharmacol.* 107, 475–480. doi: 10.1016/1367-8280(94)90079-5

Zhu, J. K. (2016). Abiotic stress signaling and responses in plants. *Cell* 167, 313–324. doi: 10.1016/j.cell.2016.08.029

frontiers | Frontiers in Plant Science

TYPE Original Research
PUBLISHED 05 June 2024
DOI 10.3389/fpls.2024.1361422

OPEN ACCESS

EDITED BY
Zulfiqar Ali Sahito,
Zhejiang University, China

REVIEWED BY
Qi Zheng,
Henan Agricultural University, China
Muhammad Anwar,
Hainan University, China
Faheeda Soomro,
The Graduate School, Chinese Academy of Agricultural Sciences, China
Habiba Habiba,
Lehman College, United States

*CORRESPONDENCE
Qilin Tang
tangqilin71@163.com

†These authors have contributed equally to this work

RECEIVED 26 December 2023
ACCEPTED 29 April 2024
PUBLISHED 05 June 2024

CITATION
Li X, Ma Q, Wang X, Zhong Y, Zhang Y, Zhang P, Du Y, Luo H, Chen Y, Li X, Li Y, He R, Zhou Y, Li Y, Cheng M, He J, Rong T and Tang Q (2024) A teosinte-derived allele of ZmSC improves salt tolerance in maize. *Front. Plant Sci.* 15:1361422. doi: 10.3389/fpls.2024.1361422

A teosinte-derived allele of ZmSC improves salt tolerance in maize

Xiaofeng Li[1,2†], Qiangqiang Ma[3†], Xingyu Wang[1], Yunfeng Zhong[1], Yibo Zhang[1], Ping Zhang[4], Yiyang Du[1], Hanyu Luo[1], Yu Chen[1], Xiangyuan Li[1], Yingzheng Li[1], Ruyu He[5], Yang Zhou[1], Yang Li[6], Mingjun Cheng[7], Jianmei He[1], Tingzhao Rong[1] and Qilin Tang[1*]

[1]Maize Research Institute, Sichuan Agricultural University, Chengdu, China, [2]Agricultural Genomics Institute at Shenzhen, Chinese Academy of Agricultural Sciences, Shenzhen, China, [3]Pingliang Academy of Agricultural Sciences, Pingliang, China, [4]Animal Feeding and Management Department, Research Base of Giant Panda Breeding, Chengdu, China, [5]Horticulture Research Institute, Sichuan Academy of Agricultural Sciences, Chengdu, China, [6]School of Urban and Rural Planning and Construction, Mianyang Teachers' College, Mianyang, China, [7]College of Grassland Resources, Southwest Minzu University, Chengdu, China

Maize, a salt-sensitive crop, frequently suffers severe yield losses due to soil salinization. Enhancing salt tolerance in maize is crucial for maintaining yield stability. To address this, we developed an introgression line (IL76) through introgressive hybridization between maize wild relatives *Zea perennis*, *Tripsacum dactyloides*, and inbred Zheng58, utilizing the tri-species hybrid MTP as a genetic bridge. Previously, genetic variation analysis identified a polymorphic marker on *Zm00001eb244520* (designated as ZmSC), which encodes a vesicle-sorting protein described as a salt-tolerant protein in the NCBI database. To characterize the identified polymorphic marker, we employed gene cloning and homologous cloning techniques. Gene cloning analysis revealed a non-synonymous mutation at the 1847th base of $ZmSC^{IL76}$, where a guanine-to-cytosine substitution resulted in the mutation of serine to threonine at the 119th amino acid sequence (using $ZmSC^{Z58}$ as the reference sequence). Moreover, homologous cloning demonstrated that the variation site derived from *Z. perennis*. Functional analyses showed that transgenic *Arabidopsis* lines overexpressing $ZmSC^{Z58}$ exhibited significant reductions in leaf number, root length, and pod number, alongside suppression of the expression of genes in the SOS and CDPK pathways associated with Ca^{2+} signaling. Similarly, fission yeast strains expressing $ZmSC^{Z58}$ displayed inhibited growth. In contrast, the $ZmSC^{IL76}$ allele from *Z. perennis* alleviated these negative effects in both *Arabidopsis* and yeast, with the lines overexpressing $ZmSC^{IL76}$ exhibiting significantly higher abscisic acid (ABA) content compared to those overexpressing $ZmSC^{Z58}$. Our findings suggest that ZmSC negatively regulates salt tolerance in maize by suppressing downstream gene expression associated with Ca2+ signaling in the CDPK and SOS pathways. The $ZmSC^{IL76}$ allele from *Z. perennis*, however, can mitigate this negative regulatory effect. These results provide valuable insights and genetic resources for future maize salt tolerance breeding programs.

KEYWORDS

salt stress, maize, wild relatives, transgenic *Arabidopsis*, CDPK

1 Introduction

Salt stress is one of the major abiotic stresses, that significantly hinder agricultural production and limits the further improvement of crop yield (Zhang et al., 2023). In particular, maize is a glycophytic crop highly susceptible to salt stress. Moreover, most currently available maize germplasm resources lack salt-tolerant traits, and the underlying molecular mechanism of plant responses to salt stress remains unclear. However, the wild relatives of maize, *Zea perennis*, and *Tripsacum dactyloides*, retain beneficial traits that have been eliminated during the domestication process and represent a valuable gene pool for the genetic improvement of maize. Therefore, retrieving the lost alleles and strengthening research on the molecular mechanisms of salt stress response in maize are of great theoretical and practical significance.

Salt stress decreases soil hydraulic conductivity and increases the external osmotic pressure of plant roots (Pingle et al., 2022). Under salt stress, excessive ion uptake in plants leads to significant disruption of the dynamic ion and water balance, resulting in membrane damage and cell death (Zhu, 2016). Consequently, seed water absorption ability is significantly reduced, leading to greatly diminished germination rates, germination potential, and radicle development, making seedling establishment difficult. It has been reported that excessive uptake of Na^+ in plants will compete with potassium ions, resulting in reduced K^+ content, and the unbalanced Na^+/K^+ ratio leads to more severe damage (Rubio et al., 2020). Intensified salt stress can further cause oxidative stress, resulting in the accumulation of toxic compounds such as reactive oxygen species (ROSs). This can ultimately alter membrane functionality, impairing the cell's ability to maintain proper ion and nutrient balances, and negatively affecting plant growth and development (Zhu, 2001; Yang and Guo, 2018).

To cope with salt stress, plants have developed various adaptive mechanisms (Yang et al., 2020). Organic osmoregulatory agents such as proline (Pro), soluble sugar, and glycine betaine (GB), play a pivotal role in preventing water loss in plants. Studies have shown a significant increase in the content of Pro and GB in maize under salt stress (Bano and Fatima, 2009). Additionally, the soluble sugar content of salt-tolerant maize lines has been reported to be higher than that of salt-sensitive lines. To enhance salt tolerance in maize, genes mediating shoot Na^+ exclusion by withdrawing Na^+ from the root xylem flow are known (Zhang et al., 2019, 2023).

Plant hormones play a pivotal role in the stress response, particularly abscisic acid (ABA), which is an endogenous signal molecule involved in regulating abiotic stresses in plants, such as salt stress (Sah et al., 2016; Li et al., 2024). When plants experience salt stress, the activation of the ABA signal pathway leads to the expression of downstream osmotic regulation response genes in *Arabidopsis* (Yu et al., 2020). Under salt stress, the osmotic potential and pre-dawn leaf water potential are reduced, leading to an increase in ABA levels, which consequently decreases the stomatal model parameters, thereby enhancing salt and drought resistance (Song et al., 2023). Furthermore, overexpression of *AtLOS5* promotes ABA biosynthesis in *Arabidopsis*, and the transgenic plant has shown stronger salt tolerance than the wild type (Zhang et al., 2016).

In response to salt stress, plants activate signaling transduction networks. Among these networks, the salt overly sensitive (SOS), calcium-dependent protein kinase (CDPK), and mitogen-activated protein kinase (MAPK) pathways play pivotal roles in transducing environmental cues perceived by plant cell membranes to target genes (Li and Nam, 2002). CDPKs are essential factors in abiotic stress tolerance, and CDPK regulates stress tolerance by modulating ABA signaling and reducing ROS accumulation (Asano et al., 2012). The SOS pathway plays a key role in regulating ion transport under salt stress (Zhou et al., 2022). In the SOS pathway, the cascade activation of *SOS3*, *SOS2*, and *SOS1* triggered by an increase in cellular Ca^{2+} concentration, activates *SOS1*, which promotes Na^+ efflux, and overexpression of *SOS1* significantly enhanced the salt tolerance in *Arabidopsis* (Shi et al., 2003).

Iqbal et al. (2019) reported a tri-species hybrid called MTP (2n = 20M+ 34T + 20P = 74; M, T, and P, stand for autotetraploid maize, *T. dactyloides*, and *Z. perennis*, respectively). MTP has exhibited excellent salt tolerance, and its hybrids with maize are fertile, allowing for the development of a series of MTP-maize introgression lines with high salt tolerance utilizing MTP as the donor and maize inbred line as the recipient (Li et al., 2023). During genetic diversity analysis of MTP-maize introgression lines, a mutated gene *Zm00001eb244520* (designed as *ZmSC*) was detected in a salt-tolerant MTP-maize introgression line 76 (IL76), using its parent Zheng58 (Z58) as a reference. This gene was described as a salt-tolerant protein (Alexandrov et al., 2009), and a previous study showed that overexpression of *TaSC*, a homologous gene of *ZmSC*, could enhance *Arabidopsis* salt tolerance (Huang et al., 2012). In the current study, we aimed to elucidate the effect of the *ZmSC* on salt tolerance in maize under salt stress conditions and preliminarily unravel the regulatory mechanism of *ZmSC* in the salt response. To this end, we conducted experiments to determine the expression pattern of *ZmSC* under salt stress, investigate its molecular function, and identify the source of its variation. Collectively, our research provides valuable insights into the molecular mechanism of salt tolerance and provides genetic resources to facilitate the development of salt-tolerant maize varieties.

2 Materials and methods

2.1 Plant materials and growth conditions

In a previous study, a series of MTP-maize introgression lines were generated by utilizing the tri-species hybrid MTP as a donor and elite inbred line Zheng58 (Z58) as the acceptor through backcrossing and self-crossing, and IL76 (BC_9F_5) was one of the lines. To develop a near-isogenic line carrying the $ZmSC^{IL76}$ allele from IL76(BC_9F_5). the line was backcrossed to Z58 for three generations and then selfed to make it homozygous, resulting in the near-isogenic line NIL^{IL76} ($BC_{12}F_6$). In each generation, molecular markers were used to select for the introgressed $ZmSC^{IL76}$, the molecular marker primers are listed in Supplementary Table 3. Field pollination was conducted in the

experimental field of Sichuan Agriculture University (Chengdu, China) (30°26′N–31°26′N, 102°54′E–104°53′E). All the experiments of salt tolerance identification were performed in the greenhouse of Sichuan Agriculture University with 14 h of light at 28°C and 10 h of darkness at 23°C, and 75% humidity.

2.2 Cloning and bioinformatics analysis of the *ZmSC*

Genomic DNA and total RNA were isolated from inbred line Z58, IL76, wild relatives T. dactyloides, Z. perennis, and MTP. Electrophoresis on 1.5% agarose gels and sequencing were utilized to examine DNA and total RNA. The promoter and full-length *ZmSC* gene were amplified using DNA as a template, with primers designed online at NCBI (https://www.ncbi.nlm.nih.gov/tools/primer-blast/, accessed on 6 March 2023). Total RNA was reverse transcribed to cDNA, followed by amplification of CDS to detect sources of variation. The sequences were aligned using DNAMAN software. All primers were listed in Supplementary Tables 3, 4, the same below.

The Hidden Markov Model (HMM) profile of *ZmSC* domain UPF0220 downloaded from the Pfam database was employed to identify *ZmSC* genes in the maize genome (www.maizegdb.org, accessed on 6 March 2023), using the simple HMM search program of TBtools (Chen et al., 2020). To confirm the *ZmSC* domain, SMART and NCBI conserved Domain Data (CDD) search programs were utilized. ClustalW (Chenna et al., 2003) was utilized to carry out multiple sequence alignment analysis, and the phylogenetic tree was constructed by the neighbor-joining method of MEGA 7.0 with 1000 bootstrap replicates (Kumar et al., 2016).

2.3 *ZmSC* subcellular localization

The Vector pCAMBIA2300-Pro35s::eGFP and BM seamless cloning kit (Biomed) were used for the construction of recombinant vector pCAMBIA2300-Pro35s::ZmSC-eGFP. The recombinant vector was transformed into the *E.coli* DH5α competent cells using a heat shock protocol for propagation and validated by Sanger sequencing. Recombinant plasmids pCAMBIA2300-Pro35s::ZmSC-eGFP were transformed into the *Agrobacterium strain* GV3101 using the freeze-thaw method and infiltrated into four-week-old Tobacco (*Nicotiana. benthamiana*) leaves. For each transformation, three biological replicates were used. ER-mCherry and NLS-mCherry were used as the endoplasmic reticulum and nuclear marker, respectively. The signal was detected using a confocal microscope (Leica, Germany) 72 h after infiltration as described previously (Zou et al., 2018).

2.4 Transformation of *Arabidopsis* and fission yeast

The constructed vector pCAMBIA2300-Pro35s::ZmSC-eGFP was then transformed into the floral tissues of *Arabidopsis thaliana* via Agrobacterium-mediated floral dip method. Following transformation, plants were screened by PCR to confirm the presence of the *ZmSC* gene, resulting in developing three independent transgenic overexpression lines. From these lines, those exhibiting the highest *ZmSC* expression level, as determined by RT-qPCR, were subsequently selected for further experiments, including salt tolerance identification and physiological index measurement under NaCl stress.

Primers containing restriction sites for *SalI* and *BamHI* were used to amplify the target gene region. The digested products were recovered from the agarose gel using a DNA Recovery Kit (TIANGEN Biotech). Plasmid pREP1 was digested with restriction enzymes *SalI* and *BamHI* and connected with digested products using T4 DNA ligase. The method for transforming the recombinant vector into the *E.coli* DH5α competent cells, as well as validation, is the same as the method described in the 2.3 section. To transform the recombinant plasmid DNA into fission yeast (Schizosaccharomyces pombe *SPQ.01*), a mixture of 10 μl Carrier DNA, 1 μg recombinant plasmid DNA, 50 μl fission yeast competent cells, and 500 μl buffer was incubated in a water bath for 30 minutes in a 1.5 ml EP tube, followed by a 15-minute incubation at 42°C. The resulting product was centrifuged at 12,000 rpm for 15 seconds, and the supernatant was discarded. This process was repeated after adding 500 μl sterile ddH_2O for washing. Reconstructed yeast was resuspended in 50 μl ddH_2O and then daubed on MM medium. After 4–6 days of cultivation, the surviving single clones were picked up and expanded at 28°C, 200 rpm for 24h. After bacterial liquid PCR detection, the recombinant yeast was used for further identification of salt tolerance. For salt tolerance identification, positive yeast transformants and empty vector were both diluted to an OD600 of 0.8, and then further diluted to 10^{-2}, 10^{-3}, 10^{-4}, and 10^{-5}. Finally, 4 μl of the diluted cultures was cultured with MM medium containing NaCl.

2.5 RNA extraction and RT-qPCR

The total RNA of roots and leaves was extracted using the EasyPure Plant RNA Kit (TransGen Biotech, Beijing, China). RNA integrity was examined by electrophoresis in 1.5% agarose gel. Reverse transcription was immediately performed using the RevertAid First Strand cDNA Synthesis Kit. Primers were designed using an online tool from NCBI. RT-qPCR was conducted using the "SYBR" Premix Ex TaqTM kit (Takara, Japan) on a Roche LightCycler480 instrument. Glyceraldehyde 3-phosphate dehydrogenase (GAPDH) was used as an internal control. The relative abundance of transcripts was determined using the $2^{-\Delta\Delta CT}$ method (Livak and Schmittgen, 2001).

We defined the relative expression as the ratio of expression levels in the experimental group (T) to that in the control group (CK). Here, T represents conditions of salt stress or the introgression line IL76, while CK represents normal conditions or inbred Z58. Relative expression was calculated using the formula:

$$Relative\ Expression = \frac{Expression\ Level\ (T)}{Control\ Group\ (CK)}$$

All experiments were performed three times to ensure accuracy.

2.6 Physiological indices measurements

Root and leaf samples were collected from 2-week-old seedlings under normal and 200 mM NaCl stress conditions for 7 d. the contents of Na^+, K^+, and Ca^{2+} were determined by atomic absorption spectrometry (Cushman et al., 2020). WinRhizo software (LC4800-II LA2400, Sainte Foy, Canada) was used to analyze the root traits, including total root length, volume, surface area, tip number, and average diameter.

The concentrations of phytohormones, including IAA (Indole acetic acid), GA (Gibberellic acid), JA (Jasmonic acid), ABA (Abscisic acid), and CTK (Cytokinin), were determined using Ruixinbio kits (Ruixin Biological Technology Co., Ltd, Quanzhou, China) by following manufacturer protocols. Each experimental procedure was conducted with three biological replicates.

2.7 Statistical analysis

Excel 2019 (Microsoft, Redmond, USA) and SPSS 27.0 (SPSS, Chicago USA) software were used for data analysis and collation, and OriginLab 2022 (Originlab, MA, USA) was used for plotting. We performed statistical analysis using t-tests and analysis of variance (ANOVA). All of the assays were performed in triplicated and repeated at least three times. Salt tolerance coefficients (STC) were calculated using the formula (Luo et al., 2017):

$$STC = \frac{Value\ under\ salt\ stress\ (T)}{Value\ under\ normal\ condition\ (CK)} \times 100\ \%$$

3 Results

3.1 Single nucleotide mutation leads to ZmSC protein variants

According to the B73 reference genome (APG_V5), *ZmSC* comprises a full length of 2292 bp, consisting of four exons, and encodes a UPF0220 family protein comprising 142 amino acids. Sequence alignment revealed that the CDS of $ZmSC^{Z58}$ was consistent with that of the reference genome (APG_V5), and there were no mutations identified in the promoter region when comparing $ZmSC^{Z58}$ with $ZmSC^{IL76}$ (2 kb upstream of *ZmSC* of ATG). However, six SNP mutations (M1-M6) occurred in the CDS sequence of $ZmSC^{IL76}$ (Figure 1A), and M5 (G to C) at the 356th base resulting in an amino acid change from serine to threonine (S to T) distinguishing $ZmSC^{Z58}$ from $ZmSC^{IL76}$ (Figure 1B). Homologous sequence alignment showed that maize wild relatives *Zea perennis* and MTP carry the C allele at M5 but not in B73 and Z58 (Figure 1C). We conducted further analysis of the frequency of M5 in 36 maize genomes, including the NAM population, and 8 wild maize relatives (5 teosinte and 3 *Tripsacum dactyloides*) downloaded from the maize genome database. The results indicate that the frequency of M5 is 100% in the wild relatives but only 36% in the maize population (Supplementary Figure 1). Unfortunately, we were unable to collect these germplasm resources for salt tolerance identification, however, valuation of salt tolerance demonstrated that IL76 exhibits stronger salt tolerance compared to Z58 (Supplementary Figures 2, 3). Additionally, IL76 exhibited resilience to drought stress (Supplementary Figure 4) and ABA stress (Supplementary Figure 5). These results suggest that M5 is an allele of *Zea perennis*, which is widely prevalent in wild maize relatives, and this allele may have been reintroduced to maize cultivation through genetic bridge MTP, and it could have been lost during maize domestication.

Based on the ortholog of amino acids, ortholog proteins of ZmSC were searched in OrthoDB (https://www.orthodb.org/, accessed on 8 March 2023) (Figure 1D), functional annotation revealed that these proteins are UPF0220 mainly transmembrane protein 50 homolog with a similar function, and five conservative motifs were detected using MEME program (https://meme-suite.org/meme/tools/meme, accessed on 8 March 2023) (Figure 1D). Among these, *TaSC* and *AtSC* have been shown to regulate salt tolerance in wheat (Huang et al., 2012). However, the function of *ZmSC* has not been reported. We further used the online tools (https://bioinformatics.psb.ugent.be/webtools/plantcare/html/, accessed on 8 March 2023) to predict the cis-element of 2 kb upstream of *ZmSC* of ATG, the promoter comprised a variety of functional elements. Including the most basic elements such as TATA-box and CAAT-box, as well as cis-element such as ABRE, AE-box, ARE, CAT-box, CGTCA-motif, G-Box, I-box, MBS, MYC, W-box, MYB, O2-site, TATC-box, TCA-element, TCCC-motif, TGACG-motif, as-1, and GC-motif, which are closely related to plant response to salt, drought, and other abiotic stress (Supplementary Table 1).

To better understand *ZmSC*, we searched the *Zea mays* genome with the UPF0220 domain and validated it in the SMART database. Only one gene (*Zm00001eb100550*) belonging to the *ZmSC* family was identified at chromosome 2. This gene encodes a transmembrane protein 50A and is involved in late endosome to vacuole transport via multivesicular body sorting pathway. Currently, only one study has reported a potential association of this gene with maize grain weight (Zhou et al., 2020), and there is no research on its stress tolerance to date. To confirm the subcellular location of *ZmSC*, the *ZmSC* sequence was fused to green fluorescent protein (GFP) and transiently expressed in tobacco (*Nicotiana benthamiana*) epidermal cells, this revealed that the ZmSC-eGFP protein was primarily localized in the plasma membrane and nuclear membrane (Figure 2).

3.2 Downregulation of $ZmSC^{IL76}$ expression under salt stress

To investigate the expression patterns of *ZmSC*, inbred Z58, and IL76 seedlings (10 days old seedlings after germination) were exposed to salt stress (200 mM NaCl) and 100 μmol/L ABA stress for 48 hours. Leaf and root samples were collected at 0h, 3h, 6h, 9h, 12h, 24h, and 48-hour intervals for RT-qPCR analysis. The comparison of expression levels is conducted by evaluating the ratio of relative expression between $ZmSC^{IL76}$ and $ZmSC^{Z58}$, represented as the expression level of $ZmSC^{IL76}$ to the expression

10.3389/fpls.2024.1361422

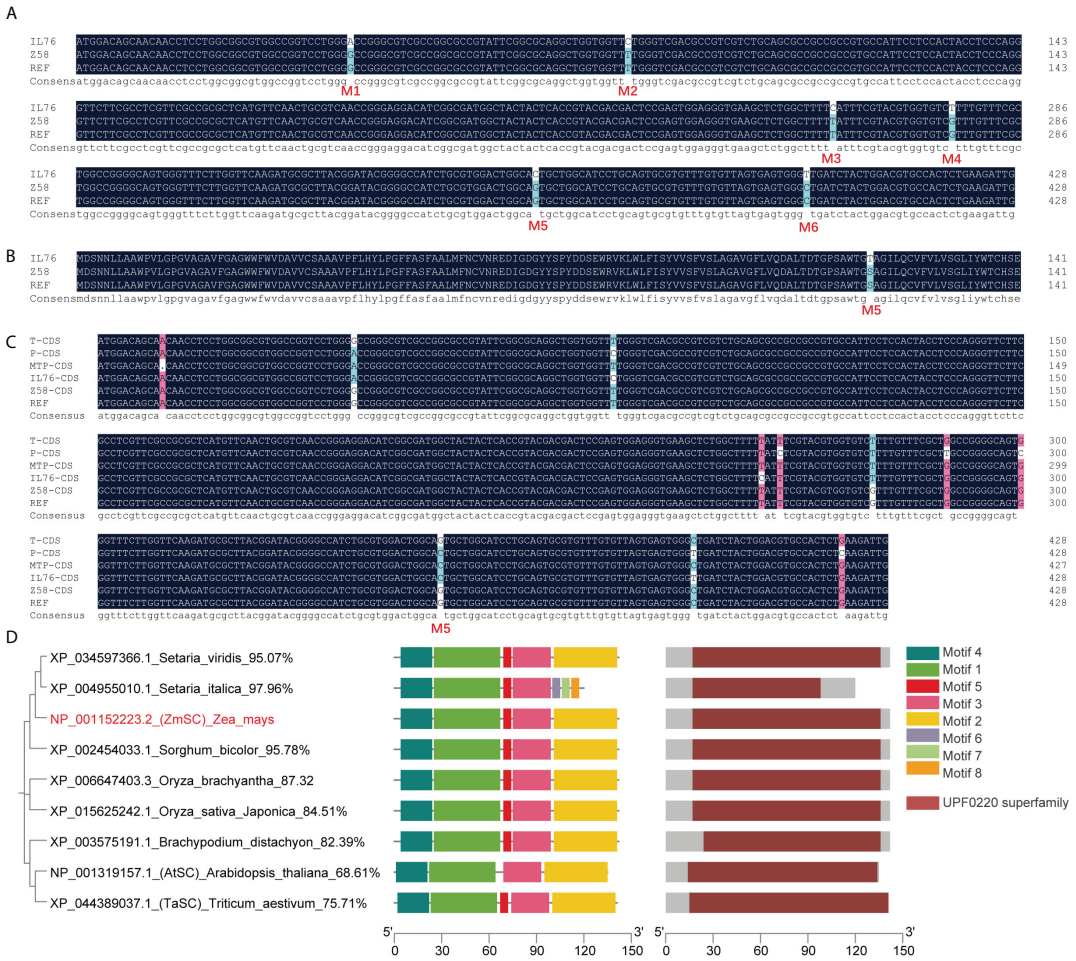

FIGURE 1
Mutation analysis of *ZmSC* coding region in IL76, and Phylogenetic tree and MEME analysis of ZmSC ortholog protein. **(A)** CDS sequence alignment result of *ZmSC* in the IL76, Z58, and B73 reference sequences; **(B)** The amino acid sequence alignment result of *ZmSC* in the IL76, Z58, and B73 reference sequences. **(C)** The results of homologous cloning of *ZmSC* CDS in wild parent *T. dactyloides* (T), *Z. perennis* (P), and MTP. **(D)** Phylogenetic tree, MEME analysis, and conserved domains of ZmSC ortholog protein.

level of $ZmSC^{Z58}$ at each time point (Figure 3). Our results showed that, under salt stress, except for the relative expression at 24h and 48h time points in leaf tissue and 3h time point at in root tissue, all other time points exhibited a ratio less than 1.0, indicating significant differences in the response of $ZmSC^{IL76}$ and $ZmSC^{Z58}$ to salt stress and the expression of $ZmSC^{IL76}$ was suppressed (Figure 3A). Under ABA stress conditions, the expression of $ZmSC^{IL76}$ appears to be suppressed, similar to the situation under salt stress (Figure 3B). These results indicate that compared to $ZmSC^{Z58}$, $ZmSC^{IL76}$ exhibits lower expression levels under salt and ABA stress at most time potions.

3.3 *ZmSC* negatively regulated salt tolerance

To investigate the role of *ZmSC* in stress responses, we constructed the expression vector pREP1-$ZmSC^{Z58}$ and pREP1-$ZmSC^{IL76}$ in fission yeast, while the empty vector pREP1 served as the control. All strains grew normally on MM medium; however, their growth on MM medium supplemented with gradient NaCl was inhibited to varying degrees. Notably, the growth of pREP1-$ZmSC^{Z58}$ strain was severely affected when the NaCl concentration was above 300 mM, followed by pREP1-$ZmSC^{IL76}$, while pREP1 exhibited the least inhibitory effect (Figure 4A). Under mannitol stress, no significant difference was observed among the three strains (Figure 4B). These results indicate that $ZmSC^{Z58}$ and $ZmSC^{IL76}$ play a negative regulatory role in the salt tolerance of yeast, with $ZmSC^{Z58}$ exhibiting a stronger negative effect.

To investigate the role of $ZmSC^{Z58}$ and $ZmSC^{IL76}$ in salt stress responses in detail, Two overexpression vectors, pCAMBIA2300-$Pro35_S$::$ZmSC^{Z58}$-eGFP and pCAMBIA2300-$Pro35_S$::$ZmSC^{IL76}$-eGFP, were constructed. Subsequently, they were transferred into *Arabidopsis thaliana* (WT). As a result, homozygous T3 lines were developed, and lines OE-IL76–1 (OE#$ZmSC^{IL76}$) and OE-Z58–13 (OE#$ZmSC^{Z58}$) showed a high expression level of *ZmSC* (Supplementary Figure 6) compared with WT. Therefore, these two lines were selected for identification of salt tolerance, while the WT was used as a control. After 2 weeks of growth, there were no significant differences among the three plants under normal conditions (1/2 MS medium). However, under salt stress

10.3389/fpls.2024.1361422

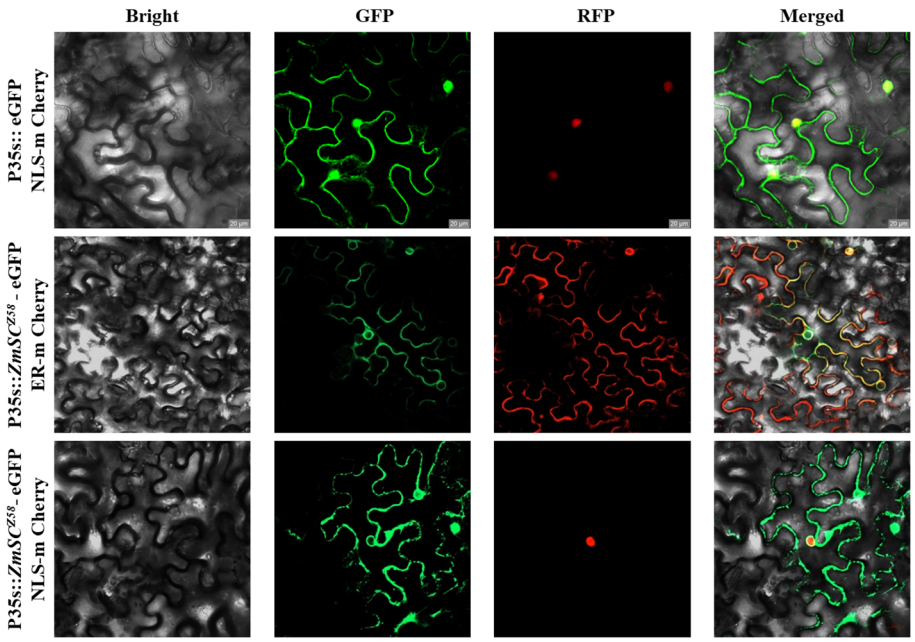

FIGURE 2
Subcellular localization of ZmSC-eGFP represents empty vector, NLS-mCherry (Nucleus marker chrrey), and ER-mChrrey (Endoplasmic reticulum marker chrrey) represents the nucleus and endoplasmic reticulum marker, respectively. Scale bar = 20 um.

conditions, there were noticeable differences, with OE#ZmSC^{Z58} showing more pronounced salt damage at both the seeding stage (Figure 5A) and mature stage (Figure 5B) than OE#ZmSC^{IL76}. Comparative analysis of leaf number (Figure 5C), root length (Figure 5D), and the number of mature pods (Figures 5B, E) has all confirmed this phenomenon. Salt tolerance analysis of the near-isogenic lines NIL^{IL76} ($BC_{12}F_6$), which were constructed through backcrossing with Z58 and self-crossing (see methods 2.1), also showed that NIL^{IL76} had a stronger growth trend compared to Z58 (Supplementary Figure 7). Based on these results, it appears that *ZmSC* has a negative impact on the early growth and development of plants under salt stress, while the *ZmSC* mutation appears to alleviates this negative regulatory impact.

3.4 *ZmSC*^{IL76} promotes ABA accumulation

To determine whether phytohormones are involved in the regulation of *ZmSC*-mediated salt tolerance, we analyzed the level of five levels in Z58 and NIL^{IL76} under salt stress, including GA,

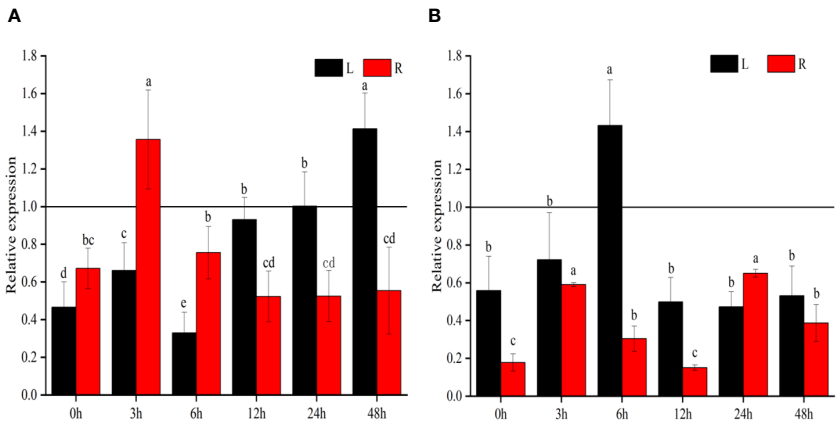

FIGURE 3
The relative expression of *ZmSC* at different time points under salt **(A)** and ABA **(B)** stress. L and R represent leaf and root tissues, respectively, the same as below. Different letters denote significant differences in the relative expression levels of *ZmSC* at different time points with the same tissues at the $P < 0.05$ level (n = 3; error bar = SD).

10.3389/fpls.2024.1361422

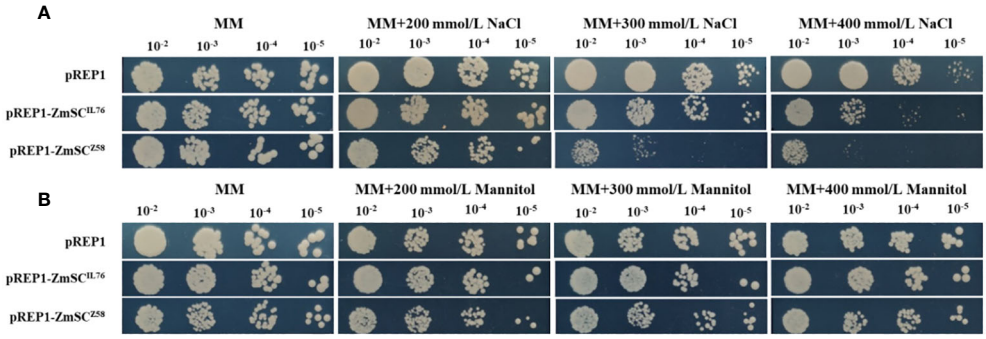

FIGURE 4
Expression of fission yeast transformants on different concentrations of NaCl **(A)** and Mannitol **(B)** MM medium.

ABA, JA, IAA, and CTK. First, NIL^{IL76} was germinated under normal and 200 mM NaCl stress, with phytohormone content measured on days 4, 6, 8, and 10, respectively, with Z58 serving as a control. The result showed that the hormone content of both NIL^{IL76} and Z58 increased to varying degrees as the duration of salt stress increased. Phytohormones such as CTK, IAA, JA, and GA in NIL^{IL76} were significantly lower than Z58 under salt stress, except for ABA, which was higher in NIL^{IL76} than in Z58 under salt stress (Figure 6). And the same result was observed in the ABA content determination assays of overexpression *Arabidopsis*, with OE#ZmSC^{IL76} showing significantly higher levels than OE#ZmSC^{Z58} under salt stress (Supplementary Figure 10). This indicates that *ZmSC^{IL76}* may enhance the accumulation of ABA to response the salt stress.

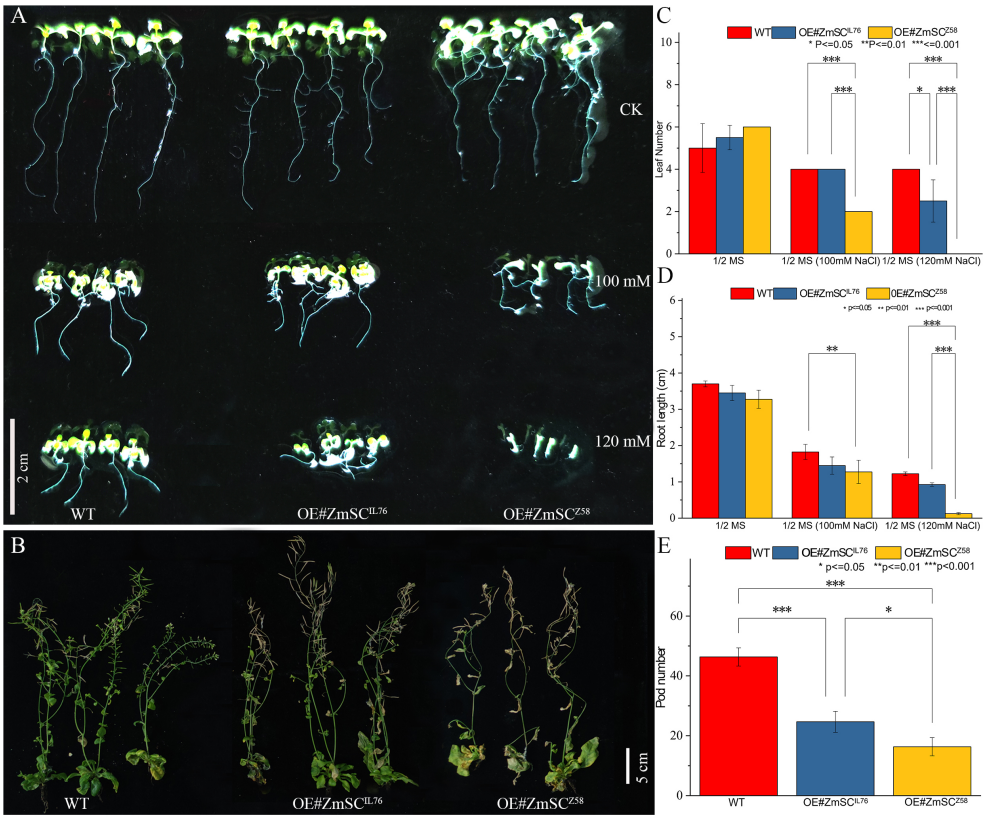

FIGURE 5
Phenotypes and indicators of wild-type (WT) and *ZmSC*-overexpressing (OE) *Arabidopsis* lines under stress conditions. **(A)** Growth of WT and OE seedlings under different stress conditions: 1/2 MS medium (control, CK), 1/2 MS supplemented with 100 mM NaCl, and 120 mM NaCl, Scale bar = 2 cm. Comparative analysis of leaf number and root length is presented in **(C)** and **(D)**, respectively. **(B)** Growth of three-week-old WT and OE plants after four weeks of treatment with 150 mM NaCl. Scale bar = 5 cm. Comparative analysis of pods is shown in **(E)**. Asterisks (*, **, and ***) indicate significant differences at $P < 0.05$, $P < 0.01$, and $P < 0.001$ levels, respectively, (n = 3; error bars = SD).

3.5 The upstream transcription factor of *ZmSC* is associated with stress resistance

To explore the potential molecular regulatory mechanisms of upstream transcription factors of *ZmSC*, we selected the 2 kb sequence upstream of the ATG of ZmSC as the promoter sequence. Using the online tool (http://planttfdb.gao-lab.org/, accessed on 12 October 2022), we predicted 24 putative transcription factors belonging to various gene families, including NAC (11), bZIP (3), TCP (2), BBR-BPC (2), LBD (1), WOX (1), G2-like (1), C2C2-Dof (1), GRAS (1) and MADS (1) (Supplementary Table 2). From the 24 candidate transcription factors, we successfully cloned seven closely associated with abiotic stress responses for subsequent Yeast one-hybrid assay (Y1H), including *ZmNAC-tf79*, *ZmBBR-BPC-tf4*, *ZmC2C2-Dof-tf29*, *ZmBBR-BPC-tf3*, *ZmMADS-tf1*, *ZmNAC-tf112* and *ZmbZIP-obf1*.

The promoter of *ZmSC* was inserted into the pHis2 vector, whereas the CDS of the candidate transcription factors was inserted into the pGADT7-Rec2 vector. The recombinant plasmids His-ZmSC+Rec2-target_gene were independently introduced into the genome of the AH109 yeast strain, with the empty vectors His2 +Rec2 and His2-ZmSC+Rec2 serving as control. All yeast cells were grown successfully on SD/-Leu/-Trip medium, except for His2-ZmSC+Rec2-ZmNAC-tf112, whose growth was inhibited when diluted 1000-fold. For all yeast cells transformed with target genes, growth was observed when placed on the SD/-His/-Leu/-Trip/X-α-Gal medium. When grown in the presence of 100 mM 3-AT on the SD/-His/-Leu/-Trip/X-α-Gal medium, all yeasts grew normally at a concentration of 10^{-1} except for the control and His2-ZmSC+Rec2-ZmBBR-BPC-tf3 which failed to grow. Therefore, we conclude that all transcription factors, except *ZmBBR-BPC-tf3*, interacted with *ZmSC* (Figure 7). The RT-qPCR assays confirmed that all six transcription factors, except for *ZmBBR-BPC-tf4*, exhibited a significant response to salt stress (Supplementary Figure 8). However, transcription activation assays indicated that *ZmNAC-tf79*, *ZmNAC-tf112*, and *ZmbZIP-obf1* possessed transcriptional activation ability (Supplementary Figure 9).

3.6 Overexpression of *ZmSC* in *Arabidopsis* suppressed the expression of the downstream genes in SOS and CDPK pathways

In a previous study, it was demonstrated that the overexpression of *TaSC*, a homolog of *ZmSC*, significantly affected the expression of a series of genes involved in CDPK and SOS pathways in *Arabidopsis* (Huang et al., 2012). In this study, we selected ten genes involved in CDPK and SOS pathway to investigate their response to salt stress in leaves of transgenic *Arabidopsis* lines overexpressing $ZmSC^{Z58}$ and $ZmSC^{IL76}$, with wild-type *Arabidopsis* used as control (Figure 8). To characterize the changes in gene expression under salt stress (150 mM NaCl) compared with normal condition (ddH_2O, CK), we defined the ratio of expression levels under stress conditions (T) to those under control conditions (CK) as the relative expression level (T/CK), The results showed that in the WT line, the expression, of seven genes (*AtFRY1*, *AtADH*, *AtP5CS1*, *AtRD29b*, *AtKIN2*, *AtCDPK1*, *AtSOS2*) were up-regulated under salt stress compared to normal condition (relative expression > 1). However, the most of gene expression in OE#$ZmSC^{Z58}$ and OE#$ZmSC^{IL76}$ were down-regulated and exhibited a consistent trend (relative expression level < 1), such as *AtFRY1*, *AtSAD1*,

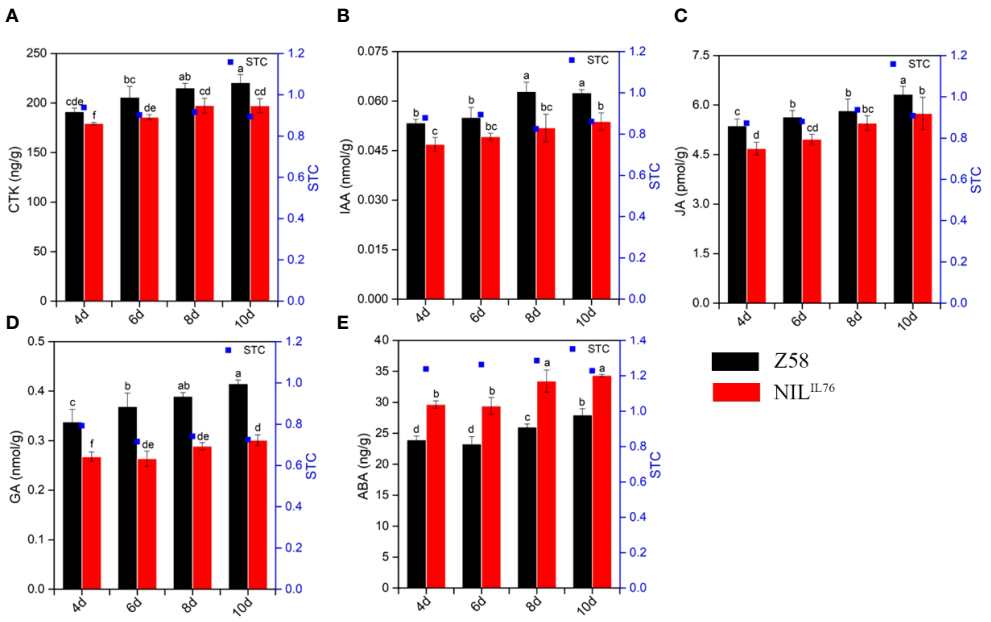

FIGURE 6
Phytohormone content dynamic changes under salt stress of inbred line Z58 and NIL^{IL76}. **(A–E)** represents the GA, ABA, JA, IAA, and CTK phytohormone content, respectively. Different letters indicate significant differences at the $P < 0.05$ level, the same as below.

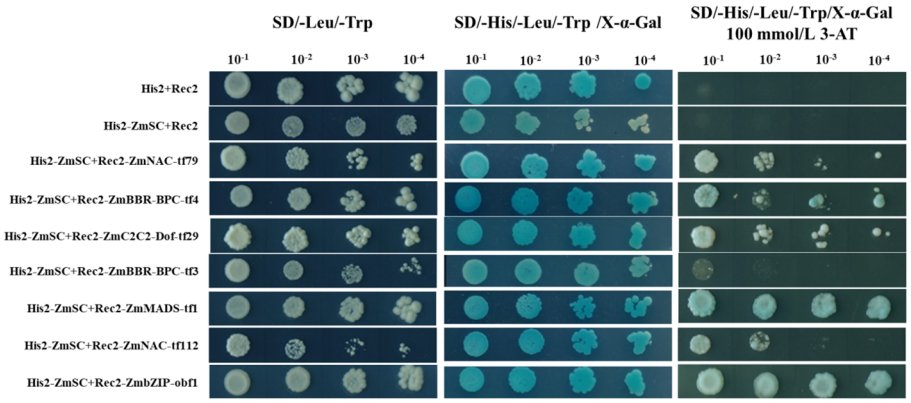

FIGURE 7
Yeast one-hybrid assays of upstream transcription factors of *ZmSC*.

ATCOR15a, *AtRD29b*, *AtKIN2* and *AtSOS3*. Interestingly, under salt stress, the expression of genes *AtP5CS1* and *AtSOS2* appeared to be up-regulated in OE#ZmSC^{IL76}, while being down-regulated in OE#ZmSC^{Z58}. These results suggest that overexpression of *ZmSC*^{Z58} and *ZmSC*^{IL76} in *Arabidopsis* inhibits the expression of these genes in both the CDPK and SOS pathways.

4 Discussion

4.1 MTP is a genetic bridge to retrieve superior alleles from wild species *Zea perennis* and *Tripsacum dactyloides*

Crop wild relatives (CWRs) are a valuable reservoir of genetic resources that can be used to improve the genetic traits of cultivated species. Several studies have demonstrated the potential of maize wild relatives to enhance plant architecture (Tian et al., 2019), resist gray leaf spot (Zhang et al., 2017), increase protein content (Huang et al., 2022), improve yield (Wang et al., 2022), and enhance drought (Kumar et al., 2022). However, progress has been limited in improving salt tolerance in maize using wild species, likely due to the potential salt-tolerant wild relatives of maize being polyploid, such as *T. dactyloides* and *Z. perennis*. Higher ploidy levels may result in barriers that impede the genetic exchange with maize. Fortunately, recent work by Iqbal et al. (2019) and Yan et al. (2020) have reported a new tri-species hybrid MTP, which possesses the genomes of *Z. mays*, *T. dactyloides*, and *Z. perennis*. Li et al. (2023) confirmed that MTP exhibited strong salt tolerance, and a series of salt tolerance introgression lines have been screened from the backcross progeny of MTP with maize, using MTP as a genetic bridge. Cold tolerance introgression lines (He et al., 2023) and novel allotetraploid maize (Iqbal et al., 2023) have also been

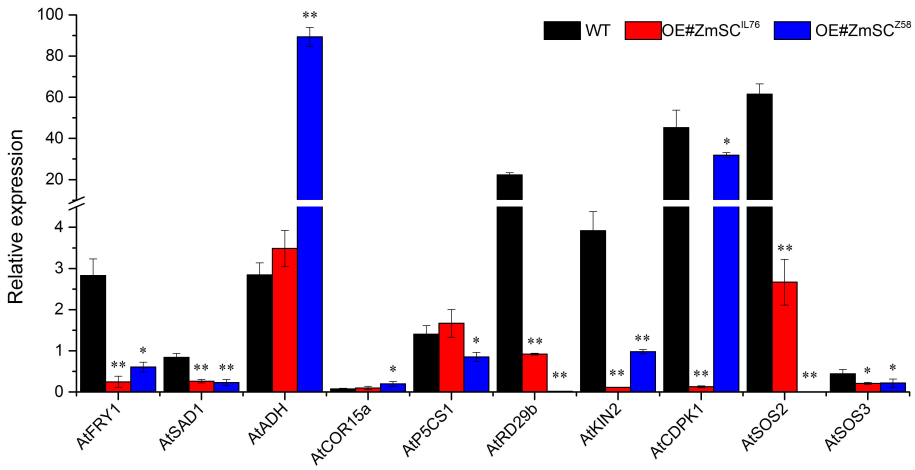

FIGURE 8
Expression of salt tolerance-related genes in *Arabidopsis thaliana* overexpressed by *ZmSC* under salt stress. The six-week-old wild type (WT), OE#ZmSC^{Z58}, and OE#ZmSC^{IL76} plants were exposed to normal and 150 mM NaCl stress for 5 days. Leaf samples were collected for RT-qPCR analysis. The graph presents the mean ± standard deviation of three biological replicates. Asterisks (* and **) indicate significant differences at the $P < 0.05$, and $P < 0.01$ levels, respectively.

created. The introgression line IL76 in this study is one of those introgression lines. Sequence alignment analysis of the homologs revealed that the mutant site of *ZmSC*^{IL76} leads to amino-acid changes present in both *Z. perennis* and MTP (Figure 1C), highlighting the potential of MTP as a gene pool for retrieving superior alleles from wild relatives.

4.2 *ZmSC* negatively regulates salt stress

We expressed *ZmSC* in both *Arabidopsis* and yeast and observed no significant differences in plant and yeast strain growth under normal conditions, suggesting that neither *ZmSC*^{Z58} nor *ZmSC*^{IL76} play a significant role in plant development under normal conditions. However, under salt stress, overexpression of *ZmSC*^{Z58} and *ZmSC*^{IL76} in *Arabidopsis* and yeast resulted in significant inhibition compared to WT (Figures 4, 5). Notably, *ZmSC*^{Z58} transgenic plants and yeasts display even greater salt sensitivity than *ZmSC*^{IL76} transgenic plants and yeasts (Figures 4, 5). These results suggest that *ZmSC*^{Z58} acts as a negative regulator of salt tolerance in both *Arabidopsis* and yeast and that this negative regulatory effect is impeded when the gene is mutated. This conclusion was further supported by salt stress experiments conducted on NIL^{IL76} (Supplementary Figure 7). The intriguing aspect is the contrast between our findings, where overexpression of ZmSC negatively regulates salt tolerance in *Arabidopsis*, and the previous research indicating that the overexpression of the homologous gene *TaSC* had a positive impact on salt tolerance in *Arabidopsis* (Huang et al., 2012). This contrasting phenomenon may be explained by differences in the interaction of overexpressed genes. In our study, overexpression of *ZmSC* appears to inhibit the expression of *AtFRY1*, while overexpression of *TaSC* promotes the expression of *AtFRY1*. Plant domestication and selection are closely linked to environmental adaptations. Cao Y. et al. (2019) reported that an allele conferring an amino acid variant in *ZmHKT2* enhances maize salt tolerance and likely underwent positive selection during maize domestication. Similarly, the allele found in *Z. perennis* in our study suggests that this variant may have experienced negative selection during maize domestication, leading to its loss or reduced prevalence in the maize population (Supplementary Figure 1).

4.3 *ZmSC* participates in salt stress response via ABA pathway

Abscisic acid (ABA) is a crucial hormone involved in stress response, including salt stress. Previous studies in maize have established that salt stress induces ABA synthesis, leading to the activation of the ABA signaling pathway. This activation, in turn, regulates the expression of downstream osmotic stress-related genes, thereby orchestrating the plant's response to stress (Bahrun et al., 2002; Sah et al., 2016). In our study, we conducted Y1H assays and identified significant interactions between gene *ZmSC* and key transcription factors, namely *ZmNAC-tf79*, *ZmNAC-tf112*, and *ZmbZIP-obf1* (Figure 7). Importantly, the binding region of these transcription factors contained cis-element such as ABRE, CGTCA-motif, and TGACG-motif (Supplementary Table 1). Notably, ABRE has been previously demonstrated to play a crucial role in the ABA response (Finkelstein et al., 2005), and previous research has established that these three genes were associated with plant drought stress (Wang et al., 2020a; Cao L. et al. (2019)). Our RT-qPCR assays revealed that these transcription factors were induced by NaCl stress (Supplementary Figure 8). Concurrently, we observed a significantly higher accumulation of ABA in NIL^{IL76} (Figure 6) and OE#ZmSC^{IL76} (Supplementary Figure 10) compared to inbred Z58 and OE#ZmSC^{Z58} under salt stress conditions. *ZmSC* significantly responds to ABA stress and shows the different expression patterns between Z58 and IL76 (Figure 3B). These findings substantiate the potential association between ZmSC and the ABA pathway in the modulation of salt tolerance.

Moreover, recent research has highlighted the role of Sorting Nexin 2 proteins in modulating the trafficking and protein levels of the ABA exporter ABCG25, impacting cellular ABA levels (Liang et al., 2022), and multivesicular body pathway modulate the turnover and activity of ABA receptors and downstream regulators (Wang et al., 2020b). Given that *ZmSC* encodes for a transmembrane 50A-like protein involved in late endosome to vacuole transport via multivesicular body sorting pathway, suggesting a potential essential role for *ZmSC* in regulating salt tolerance by modulating the levels of ABA. Compared to ZmSC^{Z58}, the mutation in ZmSC^{IL76} may result in reduced ABA transport, decreased ABA degradation, and regulated salt tolerance.

4.4 *ZmSC* is involved in the Ca^{2+}-mediated response of salt stress

Ca^{2+} serves the function as a second messenger by interacting with Ca^{2+}-sensing domains of CDPK (Wan et al., 2007). Cellular exposure to salt and other stresses increases Ca^{2+} levels, activating the CDPK and SOS signaling pathway to regulate downstream gene expression in response to stress (Shi et al., 2000; Ludwig et al., 2004). In a previous study, overexpression of *TaSC* enhanced the salt tolerance and increased Ca^{2+} content in *Arabidopsis*, likely due to the Ca^{2+} accumulation in transgenic *Arabidopsis* under salt stress, further activates CDPK pathway gene expression (Huang et al., 2012). The lack of activation in plasma membrane ion-binding channel activity, leading to a failure to release Ca^{2+} (Edel and Kudla, 2016), results in the down-regulation of genes, including downstream genes in the CDPK and SOS pathways.

In our study, under salt stress, the Ca^{2+} content significantly decreased in both IL76 and Z58, with IL76 exhibiting a higher level compared to Z58 (Supplementary Figure 3E). RT-qPCR assays revealed that the expression of genes *AtFRY1*, *AtSAD1*, *AtRD29b*, *AtKIN2*, *AtCDPK1* in the CDPK pathway and *AtSOS2*, *AtSOS3* in the SOS pathway was significantly down-regulated in overexpression *ZmSC*^{Z58} and *ZmSC*^{IL76} *Arabidopsis* compared with WT (Figure 8). This finding contrasts with the result reported by Huang et al. (2012), suggesting that the overexpression of *ZmSC*^{Z58} and *ZmSC*^{IL76} suppresses the expression of downstream salt tolerance-related genes in the CDPK and SOS pathways in *Arabidopsis*.

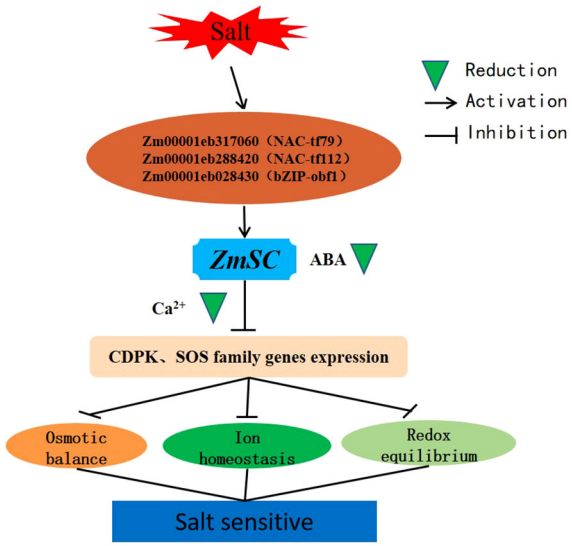

FIGURE 9
Working model of *ZmSC* in response to salt stress.

Given that, we speculate that *ZmSC* expression is activated upon recognition of the ABA signal, followed by transport of ABA to the vacuole through the *ZmSC*-mediated vacuolar sorting pathway, leading to its degradation. Ultimately, gene function in the Ca^{2+}-mediated CDPK and SOS pathways becomes inhibited, leading to the disruption of ion homeostasis, osmotic balance, and oxidative regulation, consequently negatively regulating salt tolerance in plants (Figure 9).

5 Conclusion

In conclusion, our study demonstrated that *ZmSC* is expressed under salt and ABA stresses, functioning as a negative regulator of salt stress by suppressing the activation of genes in CDPK and SOS pathways under salt stress. Additionally, we observed that an allele derived from *Z. perennis* can alleviate this negative regulatory effect and enhance salt tolerance in maize. Therefore, our research establishes a robust foundation and provides valuable material for the molecular design breeding for salt tolerance in maize.

Data availability statement

The original contributions presented in the study are included in the article/Supplementary Material. Further inquiries can be directed to the corresponding author.

Author contributions

XFL: Conceptualization, Writing – original draft, Writing – review & editing, Data curation, Investigation, Visualization. QQM: Conceptualization, Data curation, Software, Visualization, Writing – original draft, Writing – review & editing. XYW: Data curation, Investigation, Writing – review & editing. YFZ: Investigation, Writing – review & editing. YBZ: Writing – review & editing. PZ: Writing – review & editing. YYD: Writing – review & editing. HYL: Writing – review & editing. YC: Writing – review & editing, Investigation. XYL: Writing – review & editing. YZL: Writing – review & editing. RYH: Writing – review & editing. YZ: Writing – review & editing, Investigation. YL: Writing – review & editing. MJC: Writing – review & editing. JMH: Writing – review & editing, Supervision. TZR: Writing – review & editing, Conceptualization. QLT: Writing – review & editing, Conceptualization, Funding acquisition, Project administration, Supervision, Writing – original draft.

Funding

The author(s) declare financial support was received for the research, authorship, and/or publication of this article. This study was supported by the National Natural Science Foundation of China (32272035), the Department of Science and Technology of Sichuan Province (2022NSFSC0167), the Department of Science and Technology of Sichuan Province (2021NZZJ0009), the National Natural Science Foundation of China (31371640), the Department of Science and Technology of Sichuan Province (2020YJ0466) and China Postdoctoral Science Foundation (2023M743850).

Conflict of interest

The authors declare that the research was conducted in the absence of any commercial or financial relationships that could be construed as a potential conflict of interest.

Publisher's note

Supplementary material

The Supplementary Material for this article can be found online at: https://www.frontiersin.org/articles/10.3389/fpls.2024.1361422/full#supplementary-material

References

Alexandrov, N. N., Brover, V. V., Freidin, S., Troukhan, M. E., Tatarinova, T. V., Zhang, H., et al. (2009). Insights into corn genes derived from large-scale cDNA sequencing. *Plant Mol. Biol.* 69, 179–194. doi: 10.1007/s11103-008-9415-4

Asano, T., Hayashi, N., Kikuchi, S., and Ohsugi, R. (2012). CDPK-mediated abiotic stress signaling. *Plant Signaling Behav.* 7, 817–821. doi: 10.4161/psb.20351

Bano, A., and Fatima, M. (2009). Salt tolerance in *Zea mays* (L). following inoculation with Rhizobium and Pseudomonas. *Biol. Fertility Soils* 45, 405–413. doi: 10.1007/s00374-008-0344-9

Bahrun, A., Jensen, C. R., Asch, F., and Mogensen, V. O. (2002). Drought-induced changes in xylem pH, ionic composition, and ABA concentration act as early signals in field-grown maize (*Zea mays L.*). *Journal of experimental botany* 53 (367), 251–263.

Cao, L., Lu, X., Zhang, P., Wang, G., Wei, L., and Wang, T. (2019). Systematic analysis of differentially expressed maize *ZmbZIP* genes between drought and rewatering transcriptome reveals *bZIP* family members involved in abiotic stress responses. *Int. J. Mol. Sci.* 20 (17), 4103. doi: 10.3390/ijms20174103

Cao, Y., Liang, X., Yin, P., Zhang, M., and Jiang, C. (2019). A domestication-associated reduction in K^+-preferring *HKT* transporter activity underlies maize shoot K^+ accumulation and salt tolerance. *New Phytol.* 222, 301–317. doi: 10.1111/nph.15605

Chen, C., Chen, H., Zhang, Y., Thomas, H. R., Frank, M. H., He, Y., et al. (2020). TBtools: an integrative toolkit developed for interactive analyses of big biological data. *Mol. Plant* 13, 1194–1202. doi: 10.1016/j.molp.2020.06.009

Chenna, R., Sugawara, H., Koike, T., Lopez, R., Gibson, T. J., Higgins, D. G., et al. (2003). Multiple sequence alignment with the Clustal series of programs. *Nucleic Acids Res.* 31, 3497–3500. doi: 10.1093/nar/gkg500

Cushman, K. R., Pabuayon, I. C., Hinze, L. L., Sweeney, M. E., and de Los Reyes, B. G. (2020). Networks of physiological adjustments and defenses, and their synergy with sodium (Na^+) homeostasis explain the hidden variation for salinity tolerance across the cultivated *Gossypium hirsutum* germplasm. *Front. Plant Sci.* 11, 588854. doi: 10.3389/fpls.2020.588854

Edel, K. H., and Kudla, J. (2016). Integration of calcium and ABA signaling. *Curr. Opin. Plant Biol.* 33, 83–91. doi: 10.1016/j.pbi.2016.06.010

Finkelstein, R., Gampala, S. S., Lynch, T. J., Thomas, T. L., and Rock, C. D. (2005). Redundant and distinct functions of the ABA response loci *ABA-INSENSITIVE(ABI)5* and *ABRE-BINDING FACTOR(ABF)3*. *Plant Mol. Biol.* 59, 253–267. doi: 10.1007/s11103-005-8767-2

He, R. Y., Yang, T., Zheng, J. J., Pan, Z. Y., Chen, Y., Zhou, Y., et al. (2023). QTL mapping and a transcriptome integrative analysis uncover the candidate genes that control the cold tolerance of maize introgression lines at the seedling stage. *Int. J. Mol. Sci.* 24, 2629. doi: 10.3390/ijms24032629

Huang, X., Zhang, Y., Jiao, B., Chen, G., Huang, S., Guo, F., et al. (2012). Overexpression of the wheat salt tolerance-related gene *TaSC* enhances salt tolerance in Arabidopsis. *J. Exp. Bot.* 63, 5463–5473. doi: 10.1093/jxb/ers198

Huang, Y., Wang, H., Zhu, Y., Huang, X., Li, X., Wu, Y., et al. (2022). THP9 enhances seed protein content and nitrogen-use efficiency in maize. *Nature* 612 (7939), 292–300.

Iqbal, M. Z., Cheng, M., Su, Y., Li, Y., Jiang, W., Li, H., et al. (2019). Allopolyploidization facilitates gene flow and speciation among corn, Zea perennis and Tripsacum dactyloides. *Planta* 249, 1949–1962.

Iqbal, M. Z., Wen, X., Lulu, X., Zhao, Y., Jing, L., Weiming, J., et al. (2023). Multispecies polyploidization, chromosome shuffling, and genome extraction in Zea/Tripsacum hybrids. *Genetics* 223, iyad029. doi: 10.1093/genetics/iyad029

Kumar, A., Singh, V. K., Saran, B., Al-Ansari, N., Singh, V. P., Adhikari, S., et al. (2022). Development of novel hybrid models for prediction of drought-and stress-tolerance indices in teosinte introgressed maize lines using artificial intelligence techniques. *Sustainability* 14, 2287. doi: 10.3390/su14042287

Kumar, S., Stecher, G., and Tamura, K. (2016). MEGA7: molecular evolutionary genetics analysis version 7.0 for bigger datasets. *Mol. Biol. Evol.* 33, 1870–1874. doi: 10.1093/molbev/msw054

Li, C., He, Y. -Q., Yu, J., Kong, J. -R., Ruan, C. -C., Yang, Z. -K., et al. (2024). The rice LATE ELONGATED HYPOCOTYL enhances salt tolerance by regulating Na^+/K^+ homeostasis and ABA signalling. *Plant Cell Environ.* 47, 1625–1639. doi: 10.1111/pce.14835

Li, J., and Nam, K. H. (2002). Regulation of brassinosteroid signaling by a GSK3/SHAGGY-like kinase. *Science* 295, 1299–1301. doi: 10.1126/science.1065769

Li, X., Wang, X., Ma, Q., Zhong, Y., Zhang, Y., Zhang, P., et al. (2023). Integrated single-molecule real-time sequencing and RNA sequencing reveal the molecular mechanisms of salt tolerance in a novel synthesized polyploid genetic bridge between maize and its wild relatives. *BMC Genomics* 24, 1–21. doi: 10.1186/s12864-023-09148-0

Liang, C., Li, C., Wu, J., Zhao, M., Chen, D., Liu, C., et al. (2022). SORTING NEXIN2 proteins mediate stomatal movement and the response to drought stress by modulating trafficking and protein levels of the ABA exporter ABCG25. *Plant J.* 110, 1603–1618. doi: 10.1111/tpj.15758

Livak, K. J., and Schmittgen, T. D. (2001). Analysis of relative gene expression data using real-time quantitative PCR and the $2^{-\Delta\Delta CT}$ method. *methods* 25, 402–408. doi: 10.1006/meth.2001.1262

Ludwig, A. A., Romeis, T., and Jones, J. D. (2004). CDPK-mediated signalling pathways: specificity and cross-talk. *J. Exp. Bot.* 55, 181–188. doi: 10.1093/jxb/erh008

Luo, M., Zhao, Y., Zhang, R., Xing, J., Duan, M., Li, J., et al. (2017). Mapping of a major QTL for salt tolerance of mature field-grown maize plants based on SNP markers. *BMC Plant Biol.* 17, 1–10. doi: 10.1186/s12870-017-1090-7

Pingle, S. N., Suryawanshi, S. T., Pawar, K. R., and Harke, S. N. (2022). The effect of salt stress on proline content in maize (*Zea mays*). *Environ. Sci. Proc.* 16, 64. doi: 10.3390/environsciproc2022016064

Rubio, F., Nieves-Cordones, M., Horie, T., and Shabala, S. (2020). Doing 'business as usual' comes with a cost: evaluating energy cost of maintaining plant intracellular K^+ homeostasis under saline conditions. *New Phytol.* 225, 1097–1104. doi: 10.1111/nph.15852

Sah, S. K., Reddy, K. R., and Li, J. (2016). Abscisic acid and abiotic stress tolerance in crop plants. *Front. Plant Sci.* 7, 571–597. doi: 10.3389/fpls.2016.00571

Shi, H., Ishitani, M., Kim, C., and Zhu, J. K. (2000). The Arabidopsis thaliana salt tolerance gene SOS1 encodes a putative Na^+/H^+ antiporter. *Proc. Natl. Acad. Sci.* 97, 6896–6901. doi: 10.1073/pnas.120170197

Shi, H., Lee, B. H., Wu, S. J., and Zhu, J. K. (2003). Overexpression of a plasma membrane Na^+/H^+ antiporter gene improves salt tolerance in *Arabidopsis thaliana*. *Nat. Biotechnol.* 21, 81–85. doi: 10.1038/nbt766

Song, L., Ding, R., Du, T., Kang, S., Tong, L., Xue, F., et al. (2023). Stomatal conductance parameters of tomatoes are regulated by reducing osmotic potential and pre-dawn leaf water potential via increasing ABA under salt stress. *Environ. Exp. Bot.* 206, 105176. doi: 10.1016/j.envexpbot.2022.105176

Tian, J., Wang, C., Xia, J., Wu, L., Xu, G., Wu, W., et al. (2019). Teosinte ligule allele narrows plant architecture and enhances high-density maize yields. *Science* 365, 658–664. doi: 10.1126/science.aax5482

Wan, B., Lin, Y., and Mou, T. (2007). Expression of rice Ca^{2+}-dependent protein kinases (CDPKs) genes under different environmental stresses. *FEBS Lett.* 581, 1179–1189. doi: 10.1016/j.febslet.2007.02.030

Wang, G., Yuan, Z., Zhang, P., Liu, Z., Wang, T., and Wei, L. (2020a). Genome-wide analysis of NAC transcription factor family in maize under drought stress and rewatering. *Physiol. Mol. Biol. Plants* 26, 705–717. doi: 10.1007/s12298-020-00770-w

Wang, M., Li, X., Luo, S., Fan, B., Zhu, C., and Chen, Z. (2020b). Coordination and crosstalk between autophagosome and multivesicular body pathways in plant stress responses. *Cells* 9, 119. doi: 10.3390/cells9010119

Wang, Q., Liao, Z., Zhu, C., Gou, X., Liu, Y., Xie, W., et al. (2022). Teosinte confers specific alleles and yield potential to maize improvement. *Theor. Appl. Genet.* 135, 3545–3562. doi: 10.1007/s00122-022-04199-5

Yan, X., Cheng, M., Li, Y., Wu, Z., Li, Y., Li, X., et al. (2020). Tripsazea, a Novel Trihybrid of *Zea mays*, *Tripsacum dactyloides*, and *Zea perennis*. *G3: Genes Genomes Genet.* 10, 839–848. doi: 10.1534/g3.119.400942

Yang, Y., and Guo, Y. (2018). Unraveling salt stress signaling in plants. *J. Integr. Plant Biol.* 60, 796–804. doi: 10.1111/jipb.12689

Yang, Z., Li, J. L., Liu, L. N., Xie, Q., and Sui, N. (2020). Photosynthetic regulation under salt stress and salt-tolerance mechanism of sweet sorghum. *Front. Plant Sci.* 10, 1722. doi: 10.3389/fpls.2019.01722

Yu, Z., Duan, X., Luo, L., Dai, S., Ding, Z., and Xia, G. (2020). How plant hormones mediate salt stress responses. *Trends Plant Sci.* 25, 1117–1130. doi: 10.1016/j.tplants.2020.06.008

Zhang, J., Yu, H., Zhang, Y., Wang, Y., Li, M., Zhang, J., et al. (2016). Increased abscisic acid levels in transgenic maize overexpressing *AtLOS5* mediated root ion fluxes and leaf water status under salt stress. *J. Exp. Bot.* 67, 1339–1355. doi: 10.1093/jxb/erv528

Zhang, M., Li, Y., Liang, X., Lu, M., Lai, J., Song, W., et al. (2023). A teosinte-derived allele of an *HKT1* family sodium transporter improves salt tolerance in maize. *Plant Biotechnol. J.* 21, 97–108. doi: 10.1111/pbi.13927

Zhang, M., Liang, X., Wang, L., Cao, Y., Song, W., Shi, J., et al. (2019). A HAK family Na^+ transporter confers natural variation of salt tolerance in maize. *Nat. Plants* 5, 1297–1308. doi: 10.1038/s41477-019-0565-y

Zhang, X., Yang, Q., Rucker, E., Thomason, W., and Balint-Kurti, P. (2017). Fine mapping of a quantitative resistance gene for gray leaf spot of maize (*Zea mays* L.) derived from teosinte (Z. mays ssp. *parviglumis*). *Theor. Appl. Genet.* 130, 1285–1295. doi: 10.1007/s00122-017-2888-2

Zhou, Z., Li, G., Tan, S., Li, D., Weiß, T. M., Wang, X., et al. (2020). A QTL atlas for grain yield and its component traits in maize (*Zea mays*). *Plant Breed.* 139, 562–574. doi: 10.1111/pbr.12809

Zhou, X., Li, J., Wang, Y., Liang, X., Zhang, M., Lu, M., et al. (2022). The classical SOS pathway confers natural variation of salt tolerance in maize. *New Phytol.* 236, 479–494. doi: 10.1111/nph.18278

Zhu, J. K. (2001). Plant salt tolerance. *Trends Plant Sci.* 6, 66–71. doi: 10.1016/S1360-1385(00)01838-0

Zhu, J. K. (2016). Abiotic stress signaling and responses in plants. *Cell* 167, 313–324. doi: 10.1016/j.cell.2016.08.029

Zou, T., Liu, M., Xiao, Q., Wang, T., Chen, D., Luo, T., et al. (2018). *OsPKS2* is required for rice male fertility by participating in pollen wall formation. *Plant Cell Rep.* 37, 759–773. doi: 10.1007/s00299-018-2265-x

Frontiers in
Plant Science

Cultivates the science of plant biology and its applications

The most cited plant science journal, which advances our understanding of plant biology for sustainable food security, functional ecosystems and human health.

Discover the latest Research Topics

See more →

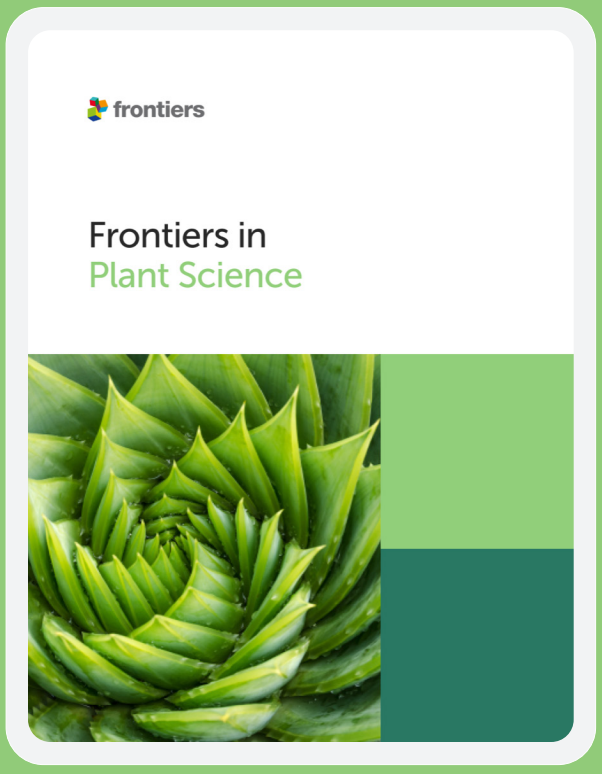

Frontiers

Avenue du Tribunal-Fédéral 34
1005 Lausanne, Switzerland
frontiersin.org

Contact us

+41 (0)21 510 17 00
frontiersin.org/about/contact